

THÈSE

Présentée pour l'obtention du
DOCTORAT DE L'UNIVERSITÉ PIERRE ET MARIE CURIE
-Paris 6-

spécialité: Sciences de la Terre

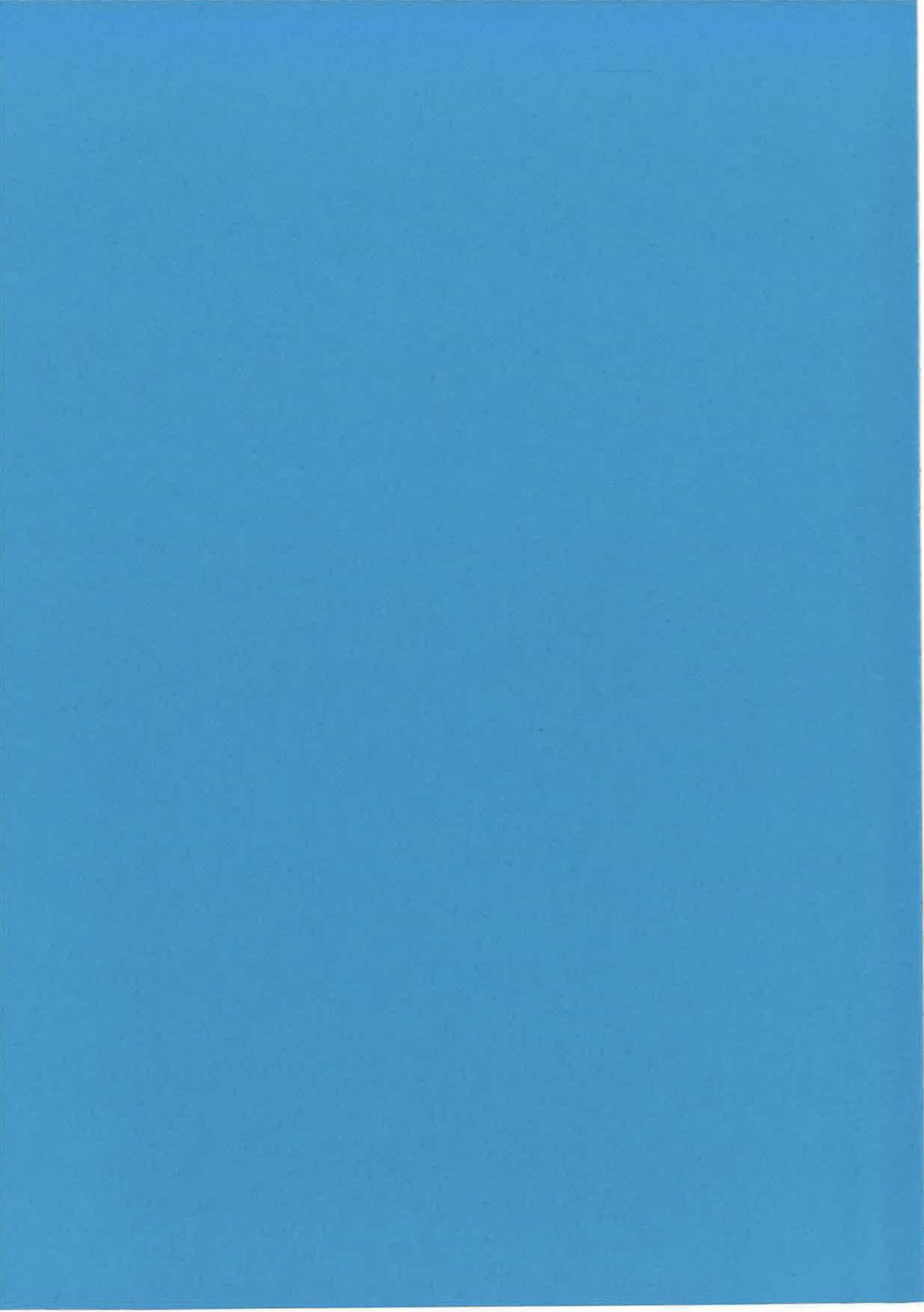
OUVERTURE DE BASSINS MARGINAUX ET DÉFORMATION CONTINENTALE : L'EXEMPLE DE LA MER DU JAPON

par Marc FOURNIER

le 29 - 04 - 1994
devant un jury composé de :

X. LE PICHON	(Collège de France)	Président
J. ANGELIER	(Université P. et M. Curie)	Rapporteur
J. P. CADET	(Université P. et M. Curie)	Examinateur
J. CHARVET	(Université d'Orléans)	Rapporteur
P. DAVY	(Université de Rennes)	Examinateur
J. F. DEWEY	(Université d'Oxford)	Examinateur
L. JOLIVET	(Ecole Normale Supérieure)	Directeur de thèse

Laboratoire de Géologie, Ecole Normale Supérieure, Paris



THÈSE

Présentée pour l'obtention du
DOCTORAT DE L'UNIVERSITÉ PIERRE ET MARIE CURIE
-Paris 6-

spécialité: Sciences de la Terre

OUVERTURE DE BASSINS MARGINAUX ET DÉFORMATION CONTINENTALE : L'EXEMPLE DE LA MER DU JAPON

par Marc FOURNIER

le 29 - 04 - 1994
devant un jury composé de :

X. LE PICHON	(Collège de France)	Président
J. ANGELIER	(Université P. et M. Curie)	Rapporteur
J. P. CADET	(Université P. et M. Curie)	Examinateur
J. CHARVET	(Université d'Orléans)	Rapporteur
P. DAVY	(Université de Rennes)	Examinateur
J. F. DEWEY	(Université d'Oxford)	Examinateur
L. JOLIVET	(Ecole Normale Supérieure)	Directeur de thèse

Laboratoire de Géologie, Ecole Normale Supérieure, Paris

RÉSUMÉ

Ce travail est une étude du mécanisme d'ouverture de la Mer du Japon et de ses rapports avec la déformation continentale de l'Asie consécutive à la collision de l'Inde.

La déformation contemporaine de l'ouverture de la mer du Japon est décrite à Sakhaline et dans le Japon sud-ouest. La déformation décrochante mise en évidence sur la marge orientale de la mer du Japon se suit à l'intérieur du continent asiatique jusqu'à l'extrémité nord de Sakhaline. Elle y est exprimée par des décrochements dextres N-S actifs depuis le Miocène inférieur, des plis en échelon, et des bassins en échelon associés. Le régime de contrainte est transpressif avec une direction de compression NE-SO. A l'échelle de l'ensemble de la zone décrochante est-mer du Japon, le régime de contrainte est transpressif dans la portion continentale au nord, et transtensif au voisinage de la zone de subduction au sud. A Sakhaline, le régime de déformation actuel est identique au régime de déformation miocène, avec peut-être une rotation de la compression vers une direction plus E-O.

Sur la marge sud de la mer du Japon, le champ de contraintes est pratiquement purement extensif avec une direction d'extension NO-SÉ. La synthèse des données de fracturation le long des marges est, sud et ouest de la mer du Japon montre que les directions de contraintes miocènes sont remarquablement cohérentes, NE-SO pour la contrainte maximum horizontale et NO-SÉ pour la contrainte minimum horizontale. Cette cohérence suggère que le champ de contrainte mesuré est postérieur aux rotations différentielles du Japon SO et NE documentées par le paléomagnétisme et achevées à 14 Ma, et qu'il correspond à un stade tardif de l'ouverture (Miocène moyen). La géométrie de l'ouverture suggère cependant qu'il est resté identique pendant toute la durée de l'ouverture.

L'étude de la déformation des formations d'âge Miocène inférieur qui ont subi une rotation horaire dans le Japon sud-ouest permet de mettre en évidence sur un même affleurement des systèmes de blocs limités par des décrochements à plusieurs échelles. Ce type de déformation, qui n'est pas observé dans les formations plus récentes qui n'ont pas tourné, suggère qu'une partie au moins de la rotation du Japon sud-ouest est absorbée par la déformation interne de l'arc et des rotations de blocs à différentes échelles. D'autre part, le champ de contrainte miocène moyen mesuré le long de la dislocation majeure du Japon SO, la Ligne Tectonique Médiane (MTL), est compatible avec un mouvement sénestre et normal le long du plan de faille. La composante sénestre est cohérente avec les rotations dextres si l'on considère la MTL comme une faille de second ordre, tournant et accommodant la rotation horaire de blocs à l'intérieur d'une zone de cisaillement dextre d'échelle plus grande.

Un modèle d'ouverture de la mer du Japon prenant en compte les rotations paléomagnétiques est proposé. La mer du Japon s'ouvre en bassin pull-apart à l'Oligo-Miocène à l'intérieur d'une zone de cisaillement dextre limitée à l'est et à l'ouest par deux zones décrochantes N-S en relais. A l'intérieur de la zone de cisaillement (Japon SO) et le long des zones décrochantes bordières, les blocs tournent dans le sens horaire compatible avec le sens de cisaillement dextre. Le déplacement accommodé le long de la zone décrochante à l'est (± 400 km) est plus important qu'à l'ouest (± 200 km). Une partie (30°) de la rotation horaire du Japon sud-ouest est attribuée à cette différence de mouvements, l'autre partie étant absorbée par la déformation interne du Japon sud-ouest.

Nous décrivons ensuite les résultats d'expériences de modélisation analogique réalisées pour tester l'interaction de la collision et de l'extension dans la déformation continentale. Un modèle rhéologique de lithosphère 3-couches est déformé le long de sa bordure sud par un poinçon rigide progressant vers le nord. L'extension est gouvernée par l'étalement gravitaire du modèle. Ce dispositif est testé pour différentes conditions aux limites. La déformation dans la partie NE du modèle est gouvernée par l'interaction collision-extension, tandis qu'elle est gouvernée par l'étalement gravitaire uniquement dans la partie SE. Un mécanisme reliant l'ouverture de la mer du Japon à la collision Inde-Asie est suggéré par ces expériences. Une large zone de cisaillement sénestre se développe depuis le coin NO du poinçon jusqu'au coin NE du modèle. Elle inclue en bordure NE du modèle des décrochements dextres N-S qui accommodent des rotations anti-horaires de blocs et le long desquels s'ouvrent des bassins. La zone de déformation trans-asiatique Pamir-Baïkal-Stanovoï est comparée à cette zone de cisaillement sénestre (Cobbold et Davy, 1988). La zone de cisaillement dextre de la mer du Japon est incluse dans une zone de cisaillement sénestre plus large limitée au sud et au nord par le Qinling Shan et les Monts Stanovoï. Nous proposons qu'elle accorde la rotation anti-horaire de blocs continentaux de la même façon que les grabens en échelon dextre du Shansi accorde la rotation anti-horaire du bloc Ordos. La rotation anti-horaire du Japon NE est expliquée dans ce contexte.

ABSTRACT

This work is a study of the mechanism of the Japan Sea opening and its relations with the continental deformation of Asia subsequent to the collision of India.

The deformation coeval with the opening of the Japan Sea is described in Sakhalin and SW Japan. We followed the strike-slip zone of the eastern margin of the Japan Sea northward inside the Asian continent, up to Sakhalin. There, the Miocene deformation is expressed by right-lateral N-S trending strike-slip faults associated with en echelon folds and en echelon grabens. The stress regime is transpressional with a direction of compression NE-SW. The same transpressional regime presently prevails in Sakhalin, with possibly a clockwise rotation of the direction of compression from NE-SW to nearly E-W. At the scale of the east Japan Sea strike-slip zone, the stress regime is transpressional to the north in the continental part of the strike-slip zone and transtensional to the south in the vicinity of the subduction zone.

On the southern margin of the Japan Sea, the Early and Middle Miocene stress field is almost purely extensional with a direction of extension NW-SE. Fracture data along the eastern, southern, and western margins of the Japan Sea show remarkably consistent Miocene stress directions: the maximal horizontal stress trends NE-SO and the minimal horizontal stress trends NW-SE. This consistency suggests that we essentially measured a stress field post-dating the differential rotations of NE and SW Japan documented by paleomagnetism before 14 Ma and corresponding to a late stage of opening of the Japan Sea (Middle Miocene). However, the overall geometry of opening suggests that the same stress field likely prevailed during the whole opening.

We describe the deformation in lower Miocene formations of SW Japan which underwent clockwise rotations. Several systems of blocks bounded by strike-slip faults are observed at different scale on the same outcrop. This type of deformation is never observed in younger formations which did not undergo clockwise rotations. At least part of the rotations of SW Japan may have been taken up by the internal deformation of the arc and block rotations at different scales. Moreover, the middle Miocene stress field measured along the main dislocation of SW Japan, the Median Tectonic Line (MTL), is compatible with normal and left-lateral slip along the fault plane. The left-lateral component is compatible with the clockwise rotations of SW Japan, provided that the MTL is considered as a second order fault rotating and accommodating clockwise rotation of blocks.

We propose a model of opening of the Japan Sea accounting for offshore and onland structural data as well as paleomagnetic data. The Japan Sea opened as a pull-apart basin within a right-lateral shear zone bounded to the east and to the west by two N-S trending dextral strike-slip zones en relais. The distribution of paleomagnetic rotations is linked with the strain field: rotations are clockwise in the Neogene right-lateral strike-slip zones and in SW Japan, and counterclockwise in the unstrained blocks of NE Japan. We propose that the rotation of SW Japan is partly (30°) due to the asymmetric opening of the Japan Sea, and partly (15°) due to right-lateral shear in SW Japan and taken up by the internal deformation of the arc. The Median Tectonic Line of SW Japan is a normal and left-lateral second order fault during the opening.

We describe the results of analogue experiments of indentation performed to test the interaction of collision and extension during continental deformation. We used a 3-layer rheological model of lithosphere strained along its southern boundary by a rigid indenter progressing northward. The extension is controlled by gravitational spreading of the model. In the NE part of the model the deformation is controlled by the interaction collision-extension, and in the SE part of the model it is controlled by extension only. A mechanism of deformation relating the opening of the Japan Sea to the India-Asia collision is suggested by these experiments. A wide left-lateral shear zone running NE develops from the NW corner of the indenter. Along the NE boundary of the model it includes N-S trending right-lateral shear zones which accommodate counterclockwise rotations of rigid blocks and the opening of basins. The Pamir-Baikal-Stanovoy deformation zone in Asia is compared to the left-lateral shear zone (Cobbold and Davy, 1988). It accommodates the north-eastward motion of Asia with respect to Siberia. In NE Asia, it is bounded to the south by the Qinling Shan and to the north by the Stanovoy ranges where left-lateral shear was reported. It includes the Japan Sea right-lateral shear zone which accommodates the counterclockwise rotation of continental blocks and the opening of the Japan Sea. The counterclockwise rotation of NE Japan is related to left-lateral shear produced by the collision of India.

INTRODUCTION	1
--------------------	---

PREMIÈRE PARTIE
PRINCIPALES CONTRAINTES CONCERNANT
L'OUVERTURE DE LA MER DU JAPON

I. STRUCTURE CRUSTALE	9
II. ANOMALIES MAGNÉTIQUES	12
III. RESULTATS DES FORAGES ODP.....	12
IV. AGE DE L'OUVERTURE	16
V. CONTEXTE GÉODYNAMIQUE	18
A. LES PLAQUES EN PRÉSENCE.....	18
B. LA FRONTIÈRE NORD AMÉRIQUE-EURASIE	18
C. LA PLAQUE AMOUR	24
VI. LA MARGE OCCIDENTALE DÉCROCHANTE	24
VII. MODÈLES D'OUVERTURE.....	28
VIII. LES MOTEURS DE L'OUVERTURE	30
IX. PERSPECTIVES.....	34

SECONDE PARTIE
DEFORMATION DÉCROCHANTE DE LA MARGE ORIENTALE
DE LA MER DU JAPON

I. DÉFORMATION DÉCROCHANTE NÉOGÈNE À SAKHALINE : article "Neogene strike-slip faulting in Sakhalin and the Japan Sea opening"	41
II. LA ZONE DÉCROCHANTE DE L'EST DE LA MER DU JAPON : article "Cenozoic intracontinental dextral motion in the Okhotsk-Japan Sea region"	97
III. CONCLUSIONS	109

TROISIÈME PARTIE
CHAMP DE CONTRAINTES ET MÉCANISME DE DÉFORMATION
PENDANT L'OUVERTURE DE LA MER DU JAPON :
COMPATIBILITÉ AVEC LES ROTATIONS PALÉOMAGNÉTIQUES

I. INTRODUCTION	113
II. LES DONNÉES PALÉOMAGNÉTIQUES	113
III. CHAMP DE CONTRAINTES ACTUEL	118

IV. CHAMP DE CONTRAINTES NÉOGÈNE ET MÉCANISME DE DÉFORMATION DU JAPON SUD-OUEST : article "Neogene stress field in SW Japan and mechanism of deformation during Japan Sea opening"	125
V. COMPATIBILITÉ DES DONNÉES PALÉOMAGNÉTIQUES ET STRUCTURALES : article "Paleomagnetic rotations and the Japan sea opening"	167
VI. CONCLUSIONS	195

QUATRIÈME PARTIE
OUVERTURE DE BASSINS MARGINAUX
ET DÉFORMATION CONTINENTALE :
APPROCHE ANALOGIQUE

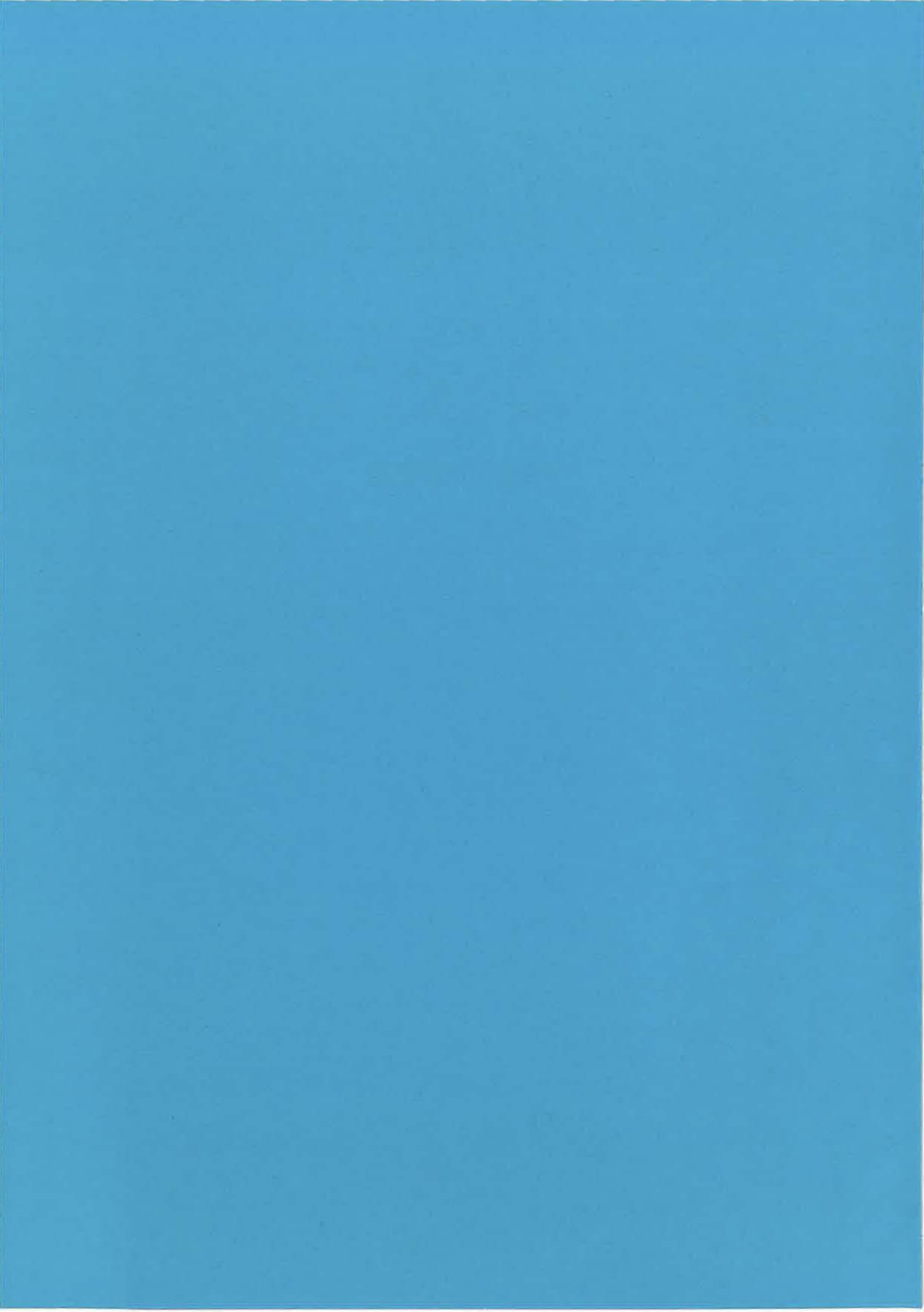
I. INTRODUCTION	199
II. DÉFORMATION DE L'ASIE CONTINENTALE DEPUIS LA COLLISION AVEC L'INDE	200
A. DÉFORMATION ACTIVE EN ASIE	200
1. Convergence et extension en Himalaya et au Tibet	200
a. Cinématique de la convergence en Himalaya.....	200
b. Cinématique de l'extension.....	200
c. Poids de la topographie et extension ductile	205
2. Décrochements sénestres et cisaillement dextre N-S à l'est du Tibet	209
3. Bordures nord et est du plateau du Tibet : extrusion de la Chine du sud ?	212
4. La zone de cisaillement sénestre trans-asiatique.....	214
B. DEFORMATION FINIE EN ASIE.....	216
1. Épaississement	216
2. Extrusion	216
C. CONCLUSION.....	217
III. DÉFORMATION CONTINENTALE ET EXTENSION MARGINALE : article "Role of extension during collision tectonics : an analogue experimental approach" .	218
IV. CONCLUSIONS	275

SYNTHÈSE

I. INTRODUCTION	277
II. MÉCANISME D'OUVERTURE DE LA MER DU JAPON	278
A. ÉVOLUTION DE LA DÉFORMATION LE LONG DE LA ZONE DÉCROCHANTE EST-MER DU JAPON	278
1. Stabilité du champ de contraintes et de la déformation à Sakhaline.....	278

2. Variabilité du champ de contraintes en bordure de la zone de subduction	278
a. Hokkaido	278
b. Honshu.....	281
3. Conclusion	281
B. DÉFORMATION DANS LE JAPON SUD-OUEST ET ROTATIONS PALÉOMAGNÉTIQUES	281
1. Champ de contraintes Miocène inférieur et moyen dans le Japon sud-ouest	282
a. Sur la côte de la mer du Japon	282
b. Le long de la MTL.....	287
2. Âge des rotations paléomagnétiques du Japon sud-ouest et ouverture de la mer du Japon	291
a. Le diachronisme entre océanisation et rotations est-il réel ?	291
b. Les rotations paléomagnétiques du Japon sud-ouest sont-elles liées à l'ouverture de la mer du Japon ?	291
3. Distribution des rotations en fonction de la déformation.....	292
C. MODÈLE D'OUVERTURE DE LA MER DU JAPON	294
III. CAUSES DE L'OUVERTURE DE LA MER DU JAPON : COLLISION ET EXTENSION.....	297
A. DÉFORMATION CONTINENTALE EN ASIE DU NORD-EST GOUVERNÉE PAR LES CONDITIONS AUX LIMITES	297
1. Déformation continentale en Asie du NE et collision.....	297
2. Influence du régime de subduction sur la déformation	298
3. Conclusion	301
B. INTERACTION COLLISION-EXTENSION : APPROCHE ANALOGIQUE.....	301
1. Protocole expérimental	302
2. Géométrie de la déformation.....	302
3. Cinématique de la déformation et champ de failles dans les expériences	303
4. Ouverture des bassins marginaux	303
IV. CONCLUSION	305
CONCLUSIONS	311

INTRODUCTION



INTRODUCTION

On peut se faire une idée de la déformation de l'Asie simplement en regardant une carte topographique (Figure 1) et une carte de la sismicité (Figure 2). La topographie est un enregistrement de la déformation finie, suffisamment fidèle pour les 50 derniers millions d'années, et la sismicité est un instantané de la déformation actuelle. Si l'on considère comme représentative d'une croûte normale et stable l'absence de relief dans la plaine russe au NE de la carte, on isole nettement une zone d'épaississement à altitude positive à l'avant de l'Inde et jusqu'aux Monts Stanovoï, et une zone d'amincissement à altitude négative marquée par les bassins marginaux en bordure de la zone de subduction Pacifique. Ces deux zones sont séparées par une bande d'altitude faible qui court de l'Indochine à la plaine de Chine du nord, en passant par la plaine de Chine du sud. Si en Asie la plus grande part du relief (positif ou négatif) peut être reliée à des structures géologiques majeures, la limite ouest de cette bande de faible altitude, correspondant à la courbe d'altitude 500 m rectilinéaire sur plus de 3500 km, n'est associée à aucune faille importante. Elle correspond dans sa partie nord à la limite ouest de la dépression Quaternaire de Chine du nord. On peut vérifier qu'elle n'est pas non plus soulignée par la sismicité. Il existe cependant des "ponts" topographiques à travers cette bande, qui relient la zone épaisse à la zone amincie. On peut en distinguer deux assez nettement, l'un au niveau des Monts Stanovoï reliant la région du lac Baïkal à la mer d'Okhotsk septentrionale, et l'autre au nord de l'Indochine reliant la province du Yunnan à la mer de Chine du sud.

La carte de la sismicité confirme les enseignements de la carte topographique puisque deux zones sismogéniques peuvent y être différencierées, la zone de collision et son prolongement vers le nord jusqu'aux Monts Stanovoï d'une part, et les zones de subduction d'autre part. On trouve aussi des "ponts" de sismicité entre ces zones de déformation, un très marqué au niveau des Monts Stanovoï rejoignant la subduction Pacifique via Sakhaline, un autre plus tenu au niveau du bassin de Chine du nord (bassin de Bohai) et qui ne traverse pas la péninsule coréenne. Il n'y a pratiquement pas de sismicité en Indochine.

Cette approche simple, sans carte géologique, de la déformation de l'Asie amène tout le propos de ma thèse. Comment les deux moteurs de la déformation que sont la collision Inde-Asie et la subduction interagissent-ils dans la déformation du continent asiatique ? Quels sont les "ponts" entre collision et subduction qui mettent en évidence cette interaction ? Le problème a été abordé d'une part par l'étude au moyen de la géologie de terrain du mécanisme d'ouverture de la mer du Japon, à la suite des travaux de Lallemand et Jolivet (1985), Jolivet et Huchon (1989), et Jolivet et al. (1991), ouverture dont Kimura et Tamaki (1986) et Jolivet et al. (1990) avaient déjà suggéré qu'elle était le résultat de l'interaction de la collision et de la subduction, et d'autre part par une approche analogique de la déformation continentale sous la double dépendance de la collision et de l'extension.

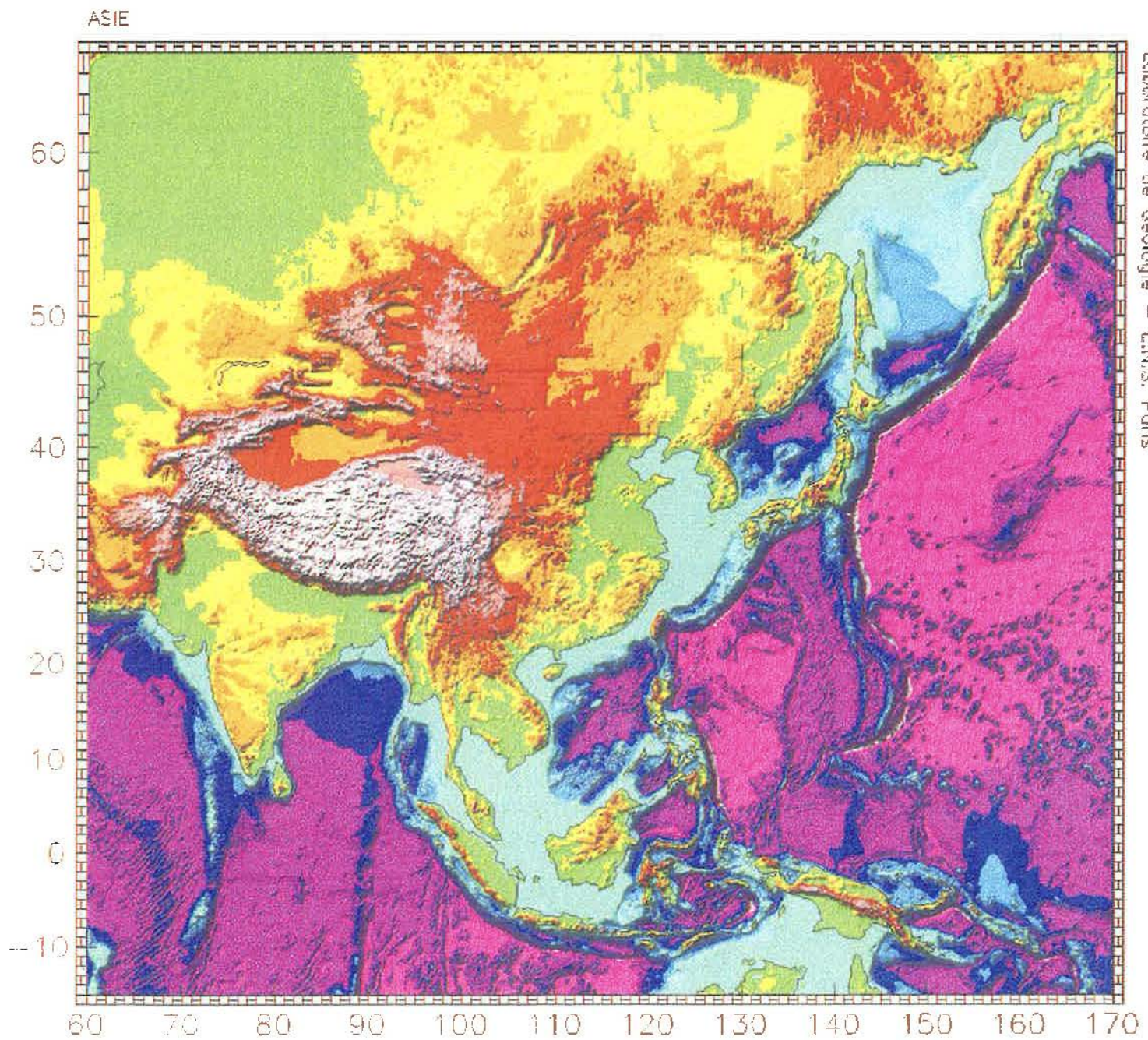
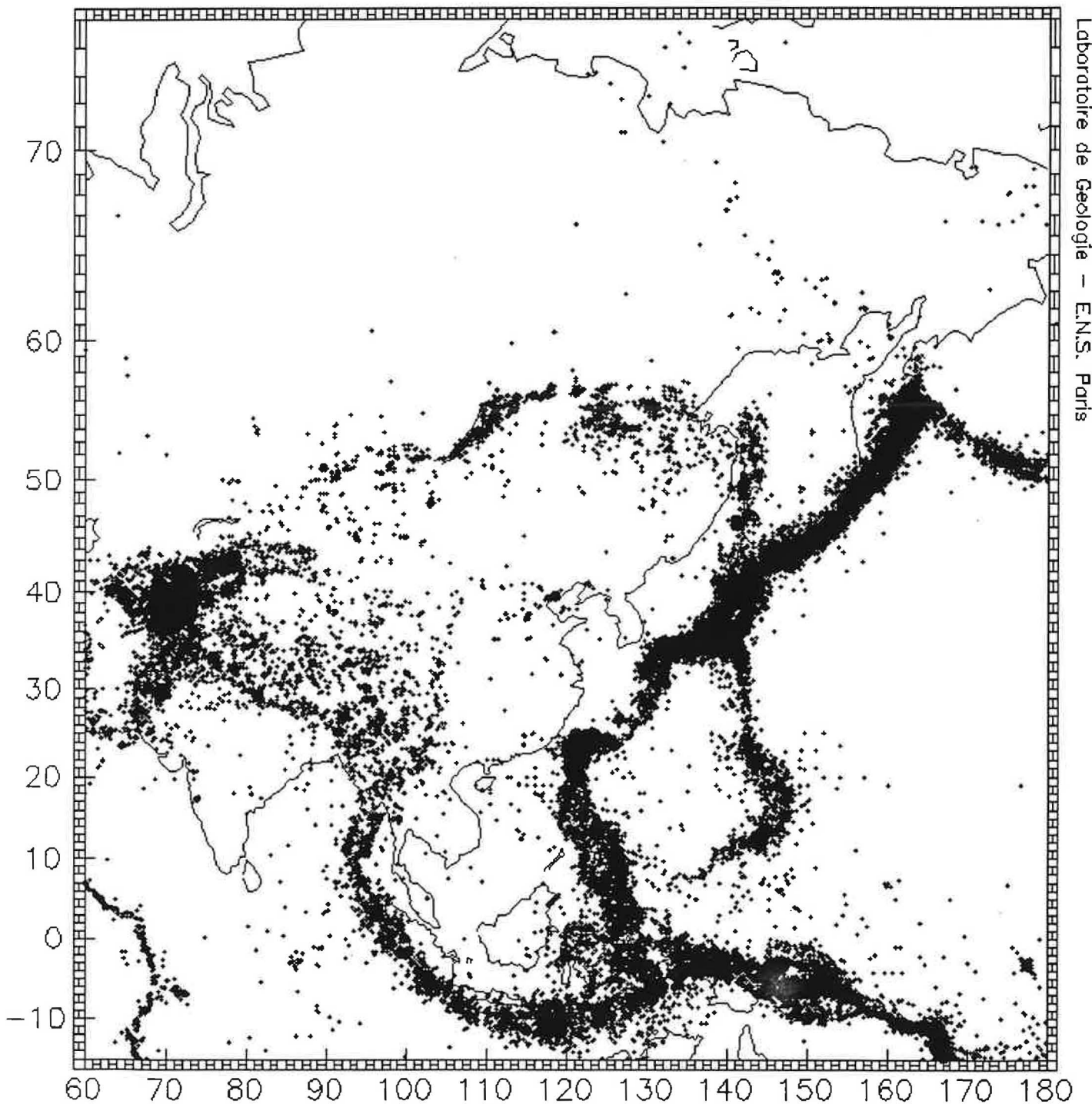


Figure 1. Carte topographique de l'Asie.

SEISMICITY ASIA - Depth < 50 km



Laboratoire de Géologie - E.N.S. Paris

Figure 2. Sismicité en Asie entre 1964 et 1989 (toutes magnitudes; profondeur < 50 km)

(Global Hypocenter Data Base, National Earthquake Information Center, US Geological Survey)

Entre le moment où j'ai débuté ce travail, au début de l'année 1990, et celui où je le termine, les connaissances sur la mer du Japon ont effectué un bond en avant sous l'impulsion des Legs ODP 127 et 128 de l'été 1989, qui pour la première fois ont foré le socle océanique du bassin du Japon. L'âge de l'accrétion, et plus généralement celui de l'ouverture de la mer du Japon, ont ainsi été déterminés avec suffisamment de précision pour trancher en faveur des structuralistes et des géophysiciens le débat qui les opposait aux paléomagnéticiens sur le calendrier d'ouverture : la mer du Japon ne s'est pas ouverte en moins d'un million d'années aux alentours de 15 Ma comme pouvait le laisser croire le calage en temps des rotations paléomagnétiques (Otofuji et al., 1985), mais sur une période courant de 32 à 10 Ma (Tamaki et al., 1992). Les rotations n'en restent pas moins incontournables, elles sont vraisemblablement assez rapides (quelques millions d'années), et il faut les prendre en compte dans tout modèle d'ouverture de la mer du Japon.

A la suite des travaux de Rozhdestvensky (1982), Kimura et al. (1983), Jolivet et Miyashita (1985), Lallemand et Jolivet (1985), Kimura et Tamaki (1986), et Jolivet et Huchon (1989), il est apparu que pendant l'ouverture de la mer du Japon, sa future marge orientale était le siège de mouvements décrochants dextres le long d'accidents N-S. Ce type d'observations, conjuguées à des observations similaires le long de la marge occidentale, inspirèrent à Lallemand et Jolivet (1985) l'idée du modèle d'ouverture en pull-apart. Par la suite, Jolivet et Huchon (1989) et Jolivet et al. (1991) ont décrit l'évolution du régime de contraintes le long de la marge orientale de la mer du Japon pendant son ouverture, de transpressif au nord à transtensif au sud, et conclurent au rôle significatif de la subduction dans la déformation extensive. La synthèse de Kimura et Tamaki (1986) sur la déformation Cénozoïque en Asie du NE, suite aux travaux sur la déformation active de Zonenshain et Savostin (1981) et Savostin et al. (1983), ainsi que les expériences analogiques de Davy et Cobbold (1988) interprétées par Jolivet et al. (1990), suggéraient aussi que la déformation continentale consécutive à la collision Inde-Asie joue un rôle dans l'ouverture de la mer du Japon.

Plusieurs questions étaient donc posées quand j'ai débuté ce travail :

(I) Quelle était la relation entre les rotations paléomagnétiques et les mouvements décrochants dextres ?

(II) Quelle était l'extension à l'intérieur du continent asiatique de la zone décrochante à l'est de la mer du Japon ?

(III) Quelles étaient les contributions respectives de la collision Inde-Asie et de la subduction Pacifique dans la déformation de la marge est-asiatique ?

Cette thèse est une contribution aux réponses à ces questions.

Il était intéressant d'aller étudier à Sakhaline le prolongement nord de la zone décrochante est-mer du Japon. Outre un complément d'information sur la déformation

décrochante pendant l'ouverture de la mer du Japon, on pouvait espérer y trouver le lien entre l'ouverture de la mer du Japon et la déformation continentale de l'Asie. La chaîne des Monts Stanovoï qui se termine à peu près à l'extrême nord de Sakhaline, est en effet en lien direct avec la zone de collision Inde-Asie par l'intermédiaire de la zone de déformation Tertiaire Pamir, Tien Shan, Altaï, Saïan, Baïkal, Stanovoï (Figure 3; Cobbold et Davy, 1988). Si la charnière Stanovoï-Sakhaline n'a pu être étudiée, l'étude que nous avons menée sur le terrain à Sakhaline en parallèle avec les expériences de modélisation analogique, nous ont permis d'intégrer l'ouverture de la mer du Japon dans le cadre général de la déformation de l'Asie. Par ailleurs, j'ai pu lors d'un séjour au Japon mener une étude sur le champ de contraintes contemporain de l'ouverture de la mer du Japon dans le Japon sud-ouest. Cette étude débouche sur des suggestions quant à l'intégration des rotations paléomagnétiques dans le modèle d'ouverture en pull-apart.

Ainsi sont discutés dans cette thèse les mécanismes à différentes échelles qui régissent la déformation pendant l'ouverture de la mer du Japon.

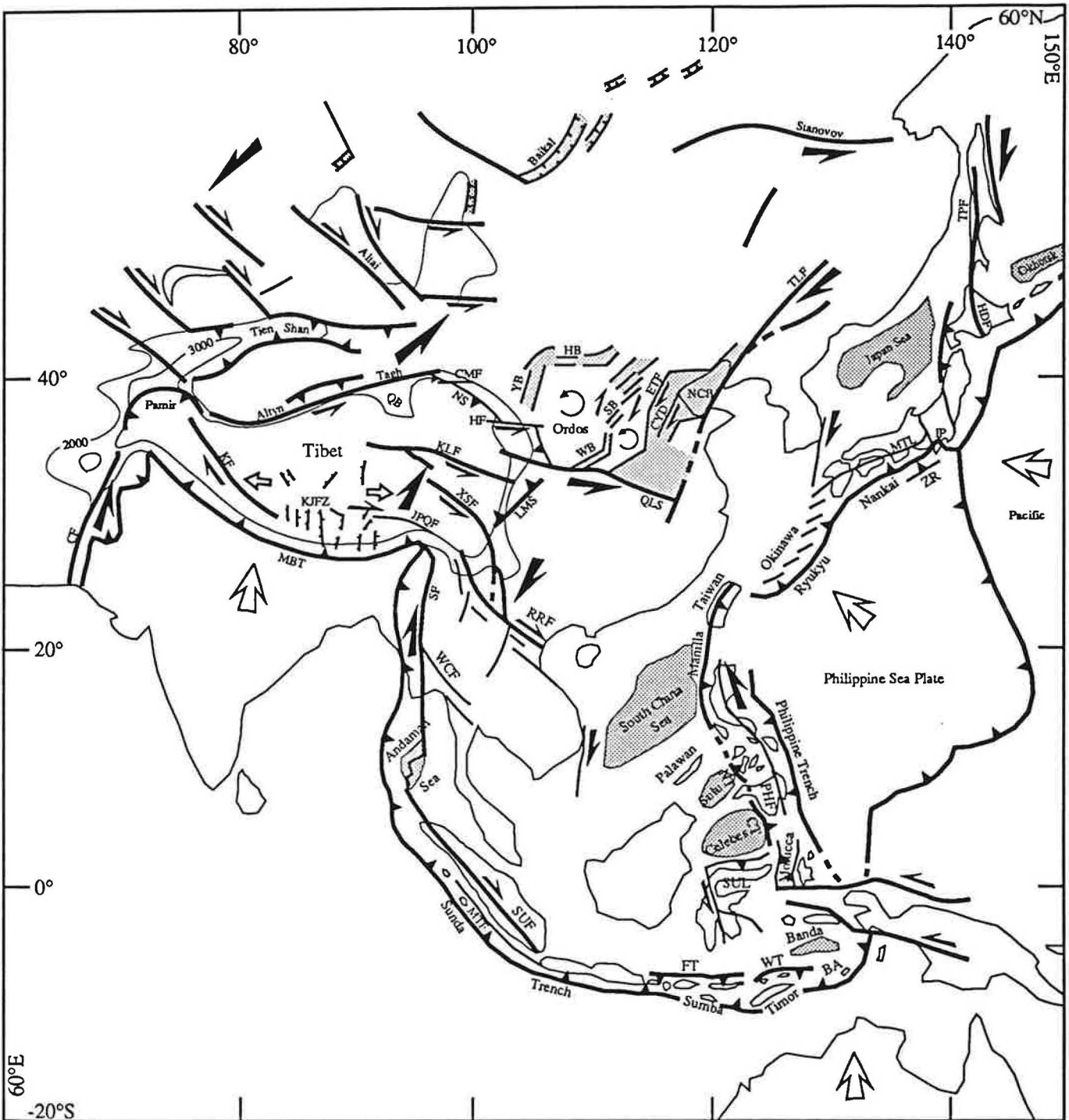
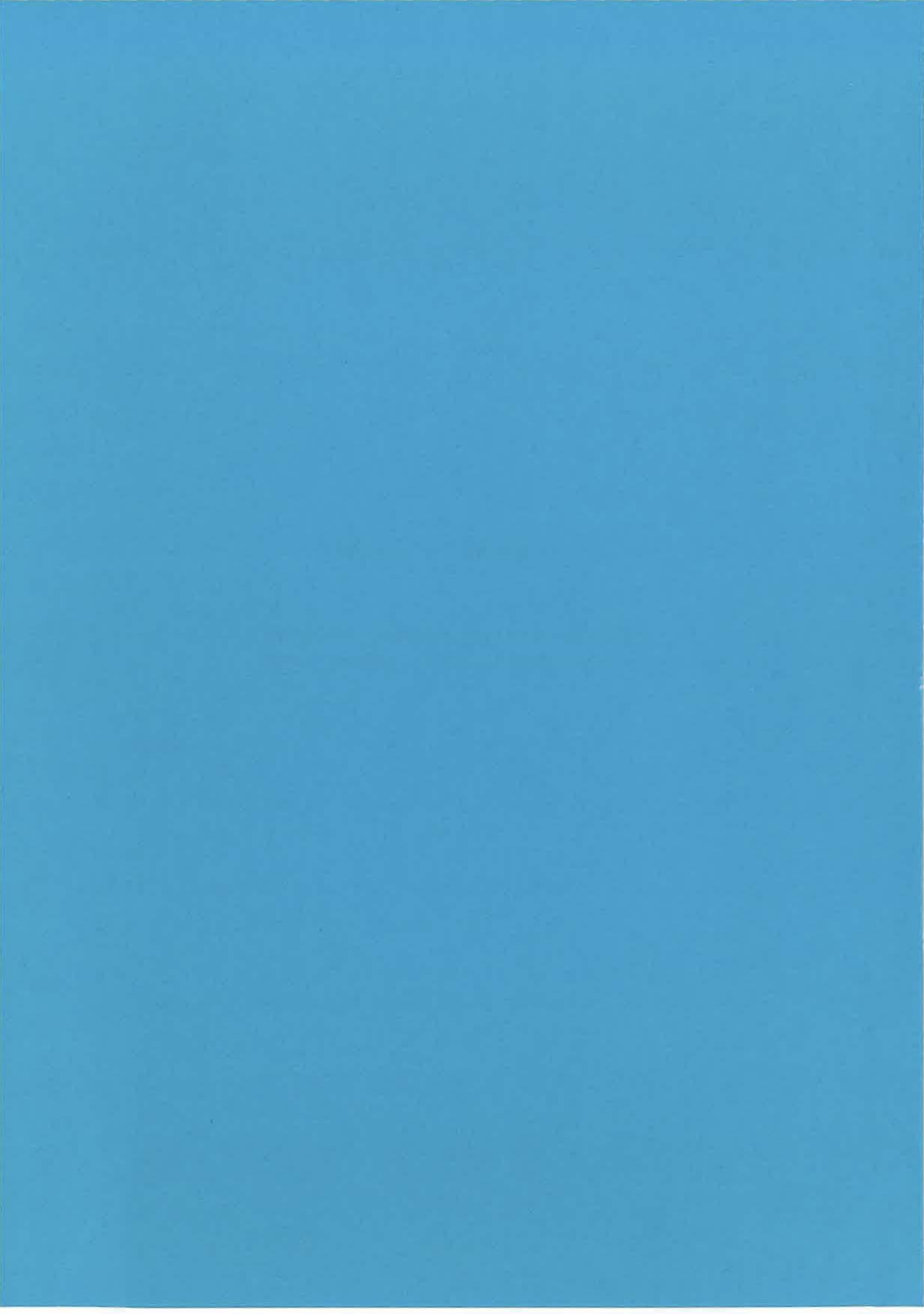


Figure 3. Carte structurale de l'Asie. Les courbes topographiques 2000 et 3000 m sont reportées. BA is Banda Arc, BP is Burma Plate, CF is Chaman Fault, CMF is Chang Ma Fault, CT is Cotobato Trench, CXD is Cang Xian-Dongning Fault system, ETF is East Taihang Fault system, FT is Flores Thrust, HB is Hetao Basins, HDF is Hidaka Fault zone, HF is Haiyuan Fault, IP is Izu Peninsula, KF is Karakorum Fault, KJFZ is Karakorum-Jiali Fault Zone, KLF is Kunlun Fault, LMS is Longmen Shan, MBT is Main Boundary Thrust, MTF is Mentawai Fault, MTL is Median Tectonic Line, NCB is North China Basin, NS is Nan Shan, NT is Negros Trench, PHF is Philippine Fault, QB is Qaidam Basin, QLS is Qinling Shan, SB is Shanxi Basins, SF is Sagaing Fault, SUF is Sumatra Fault, SUL is Sulawesi, TLF is Tan-Lu Fault, TPF is Tym-Poronaysk Fault, WCF Wang Chao (or Mae Ping) Fault, WH is Weihe Basin, WT is Wetar Thrust, XSF is Xianshuihe Fault, YB is Yinshuan Basins, ZR is Zenisu Ridge.

PREMIÈRE PARTIE

PRINCIPALES CONTRAINTES CONCERNANT L'OUVERTURE DE LA MER DU JAPON



PREMIÈRE PARTIE

PRINCIPALES CONTRAINTES CONCERNANT

L'OUVERTURE DE LA MER DU JAPON

Les données de la déformation et les données paléomagnétiques sont brièvement évoquées dans cette première partie. Elles font l'objet d'une description de détail dans les parties suivantes.

I. STRUCTURE CRUSTALE

La Mer du Japon comprend trois bassins : le bassin du Japon, le bassin de Yamato, et le bassin de Tsushima (Figures 4 et 5). La croûte du bassin du Japon est de type océanique : son épaisseur sans les sédiments est de 6-7 km (Ludwig et al., 1975), et sa structure de vitesse sismique est identique à celle d'une croûte océanique normale. Elle est recouverte par 2000 à 3000 m de sédiments. La croûte du bassin de Yamato est deux fois plus épaisse que celle du bassin du Japon, et sa structure de vitesse sismique est identique à celle d'une croûte océanique avec des couches d'épaisseur double (Tamaki et al., 1992). Deux modèles ont été proposés pour l'origine de cette croûte épaisse. Selon Hirata et al. (1989), elle serait due à une remontée asthénosphérique de type Islande alimentant une chambre magmatique de taille anormalement grande qui produirait une croûte océanique anormalement épaisse. Le second modèle est celui d'une croûte d'arc insulaire étirée et amincie (Seno, 1991 ; Tamaki et al., 1992). Deux arguments jouent en faveur du second modèle. Premièrement, aucune anomalie magnétique claire n'a été observée dans le bassin de Yamato ce qui va à l'encontre de l'existence de croûte océanique. Deuxièmement, le flux de chaleur mesuré dans le bassin de Yamato (2,34 HFU, Tamaki, 1988) est trop faible pour rendre compte d'une remontée mantellique.

La structure crustale du bassin de Tsushima est mal connue. Ludwig et al. (1975) n'ont pas détecté de signal de réfraction du Moho, ce qui suggère une croûte plutôt épaisse. D'après leurs données de sismique réflexion, la profondeur du socle est inférieure de 2 km à celle du bassin du Japon, comme dans le bassin de Yamato. La croûte du bassin de Tsushima est donc vraisemblablement analogue à celle du bassin de Yamato. La Figure 6 montre une carte interprétative de la structure crustale de la Mer du Japon d'après Tamaki (1992). Outre la croûte océanique dans la bassin du Japon et la croûte continentale étirée des bassins de Yamato et de Tsushima, des blocs de croûte continentale imagés en sismique (Tamaki, 1988) ont été représentés, en particulier le banc de Yamato au centre de la mer du Japon. Les monts sous-marins volcaniques largement distribués dans la mer du Japon (Tamaki, 1988) n'ont pas été représentés.

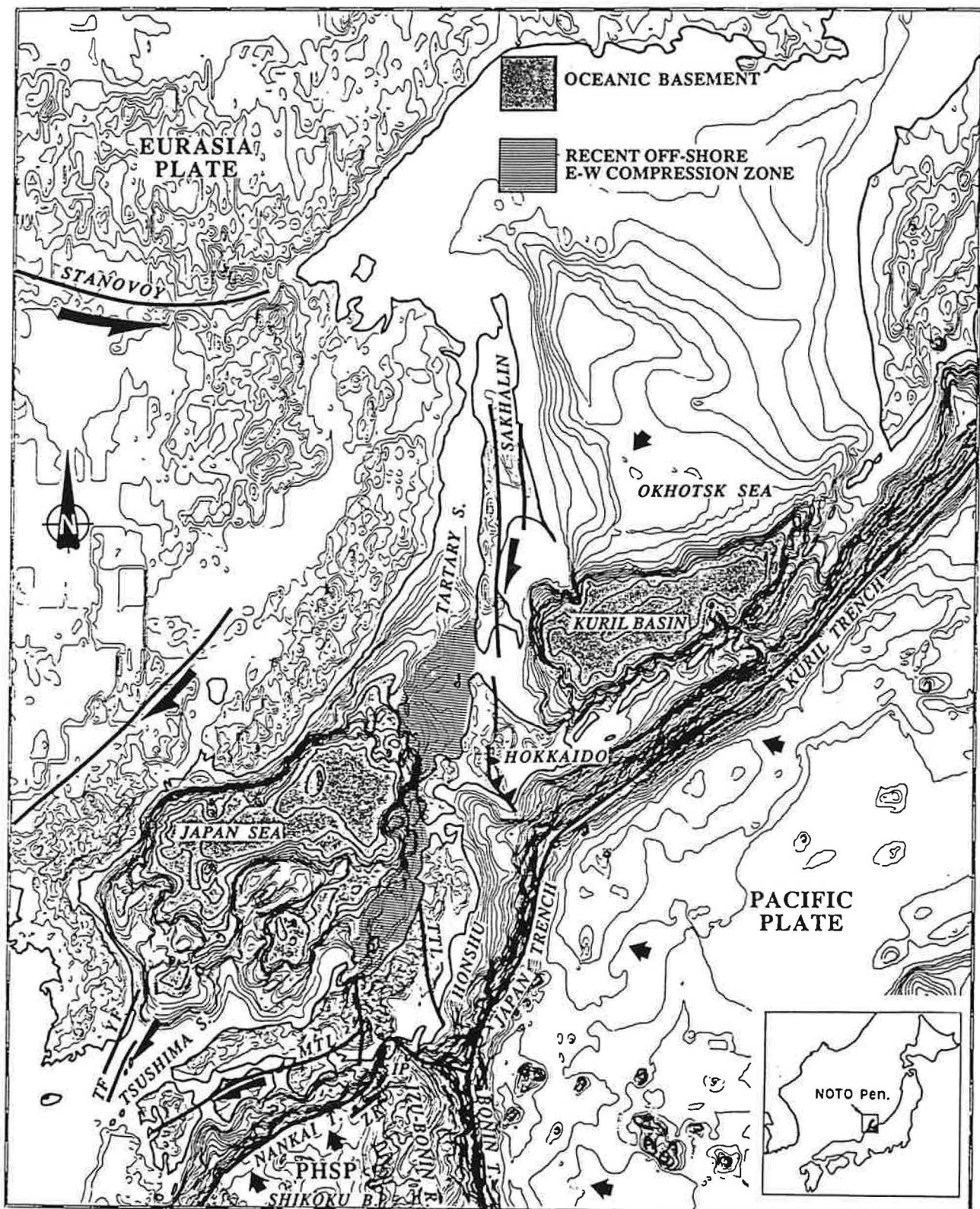


Figure 4. Carte bathymétrique de la région mer du Japon-mer d'Okhotsk. Bathymétrie en mètres.

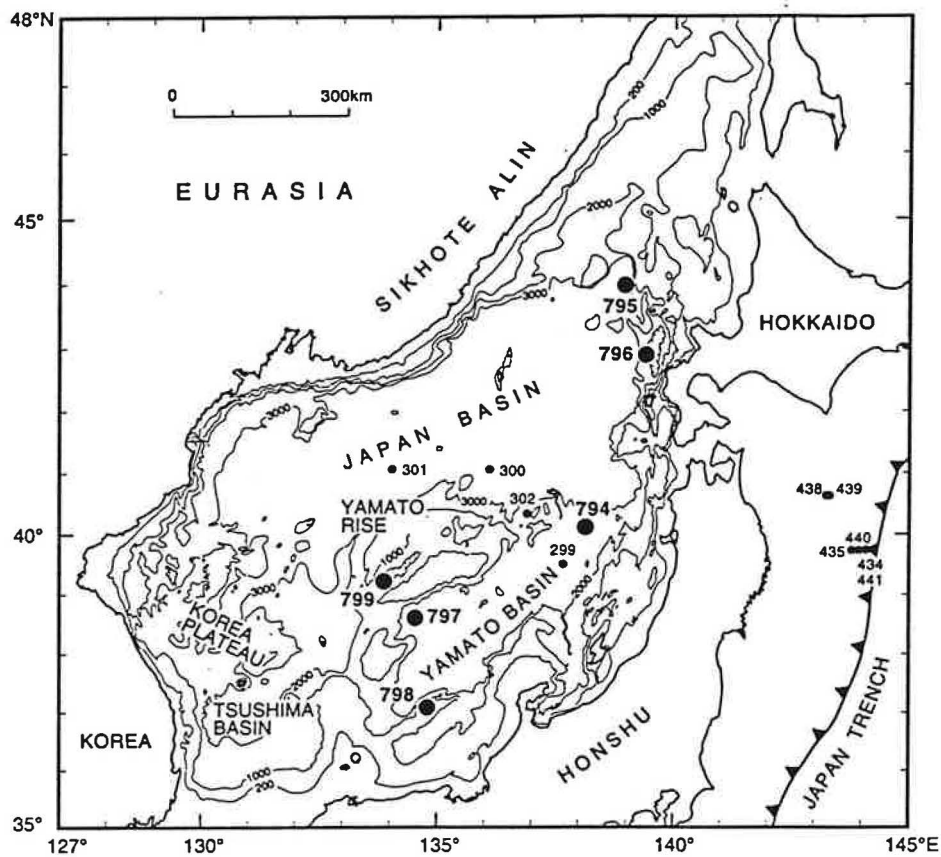


Figure 5. Carte bathymétrique de la mer du Japon avec les sites de forages. Leg 31: sites 299-302. Legs 127/128: sites 794-799. Bathymétrie en mètres (d'après Tamaki et al., 1992).

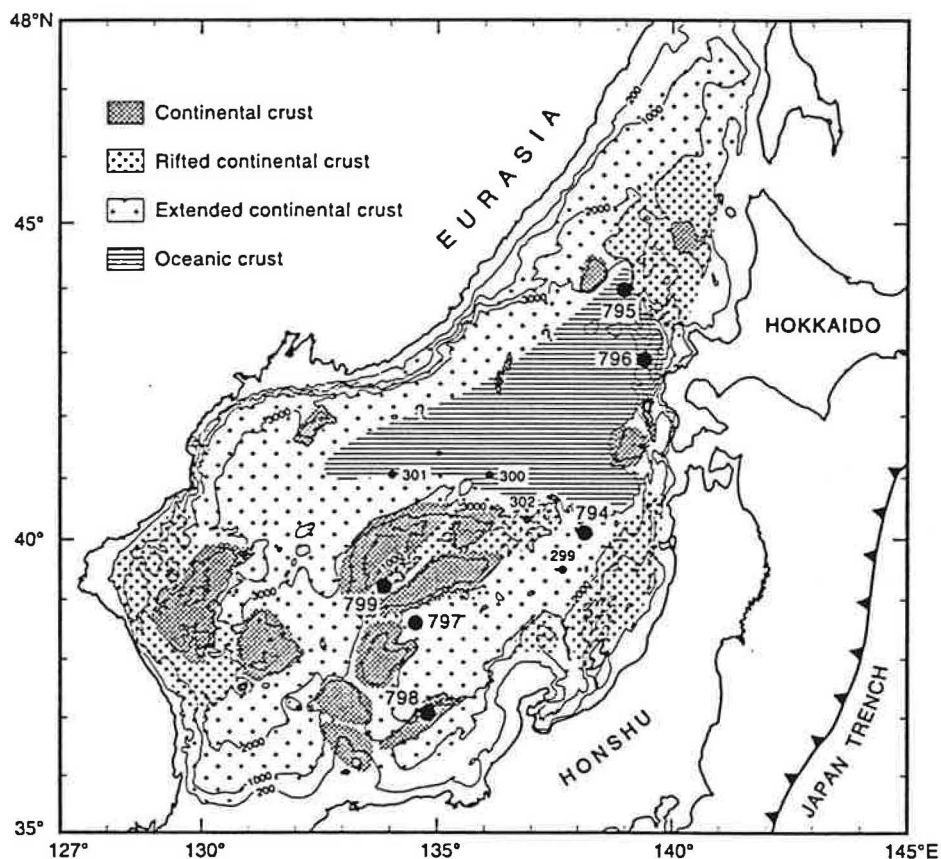


Figure 6. Carte interprétative de la structure crustale de la mer du Japon (d'après Tamaki et al., 1992).

II. ANOMALIES MAGNÉTIQUES

Contrairement à la plupart des bassins marginaux du Pacifique ouest dont l'âge a été déterminé par l'identification d'anomalies magnétiques, la mer du Japon ne présente pas d'anomalies magnétiques bien définies (Figure 7; Isezaki, 1986). Une tentative d'identification des anomalies magnétiques de la partie est du bassin du Japon a cependant été proposée par Tamaki et Kobayashi (1988) : les anomalies 7A (27 Ma) à 5E (19 Ma) de direction N070E auraient été reconnues (Figure 8). La distribution des anomalies magnétiques ainsi que la terminaison en pointe vers l'ouest de la croûte océanique du bassin du Japon, suggèrent une propagation de l'ouverture d'est en ouest (Tamaki et al., 1992). Une étude récente montre que la linéation magnétique centrale de la mer du Japon se prolonge vers l'ouest sur la marge coréenne et jusqu'à terre (Oshida, comm pers., 1993). Ce prolongement à terre de l'anomalie magnétique suggère, selon Oshida, une origine non océanique de l'anomalie (des arguments identiques ont été utilisés par Oshida et al. (1992) pour remettre en question l'existence de croûte océanique dans la partie sud du bassin d'Okinawa).

III. RESULTATS DES FORAGES ODP

Six forages ont été réalisés dans la Mer du Japon lors des Legs ODP 127 et 128 (sites 794 à 799, Figure 5), dont trois ont atteint le socle (sites 794, 795, et 797) (Tamaki et al., 1992). Ces forages ont permis d'échantillonner en continu la colonne sédimentaire du Miocène inférieur au Quaternaire (Figure 9). Aux sites 794 et 797, leurs principales caractéristiques sont :

1. 300 m de sills et de coulées basaltiques datés radiométriquement entre 24 et 17 Ma (Kaneoka, 1992 ; Pouclet et Bellon, 1992) et intercalés avec des grès volcanoclastiques d'âge Miocène inférieur à moyen,
2. 100 à 200 m d'argiles calcaires à phosphates d'âge Miocène moyen intercalées avec d'épais "tufs bleus" (tufs dacitiques),
3. 80 à 150 m de cherts et argiles siliceuses datés du sommet du Miocène moyen à la base du Miocène supérieur,
4. 100 m d'argiles à diatomées d'âge Miocène supérieur,
5. 100 à 150 m de boues à diatomées d'âge fini Miocène à Pliocène,
6. 80 à 100 m de boues d'âge Quaternaire.



Figure 7. Carte des anomalies magnétiques de la mer du Japon (d'après Isezaki, 1986).

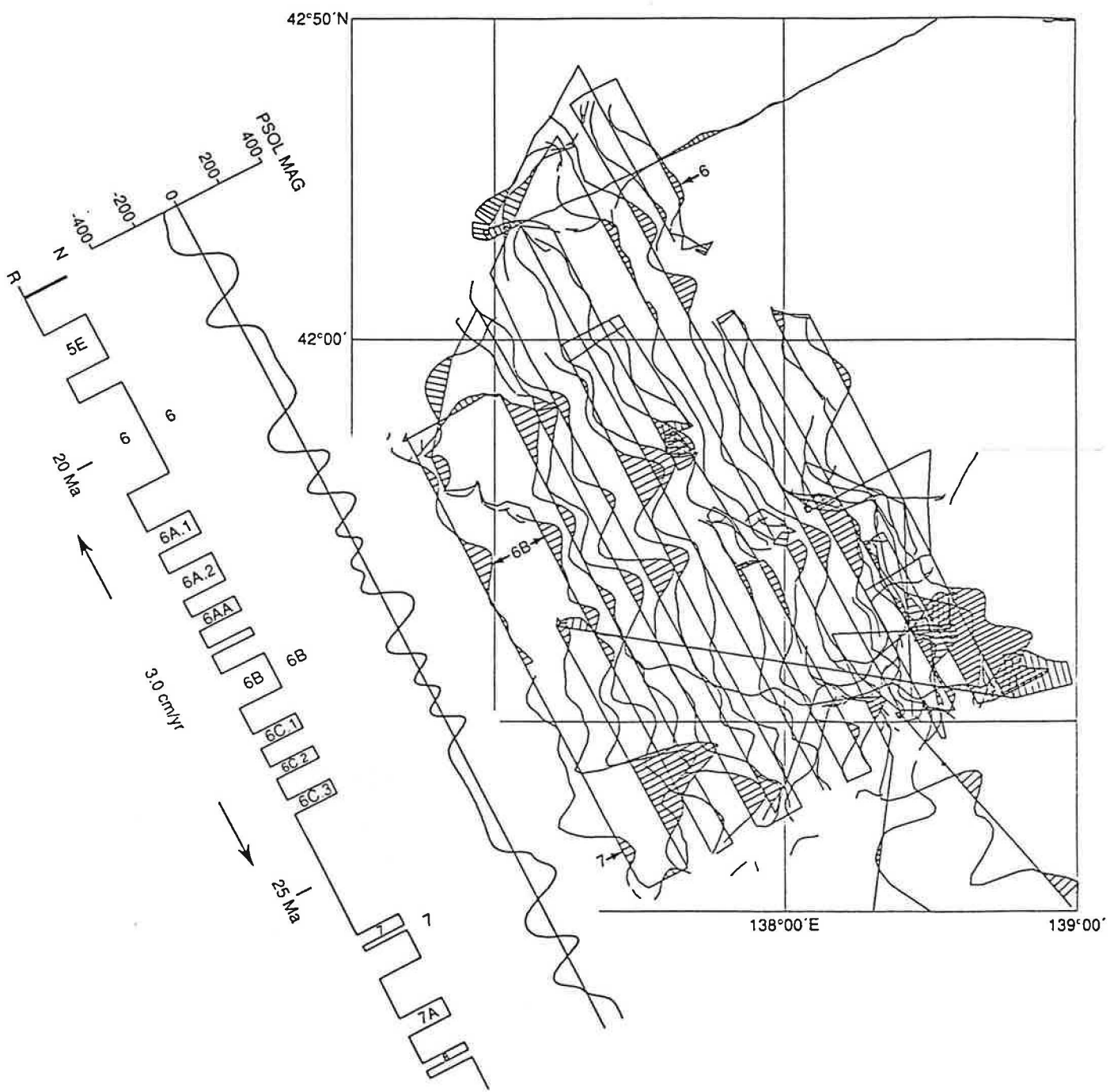


Figure 8. Profils magnétiques dans la partie est du bassin du Japon et corrélation avec les anomalies magnétiques (d'après Tamaki et Kobayashi, 1988).

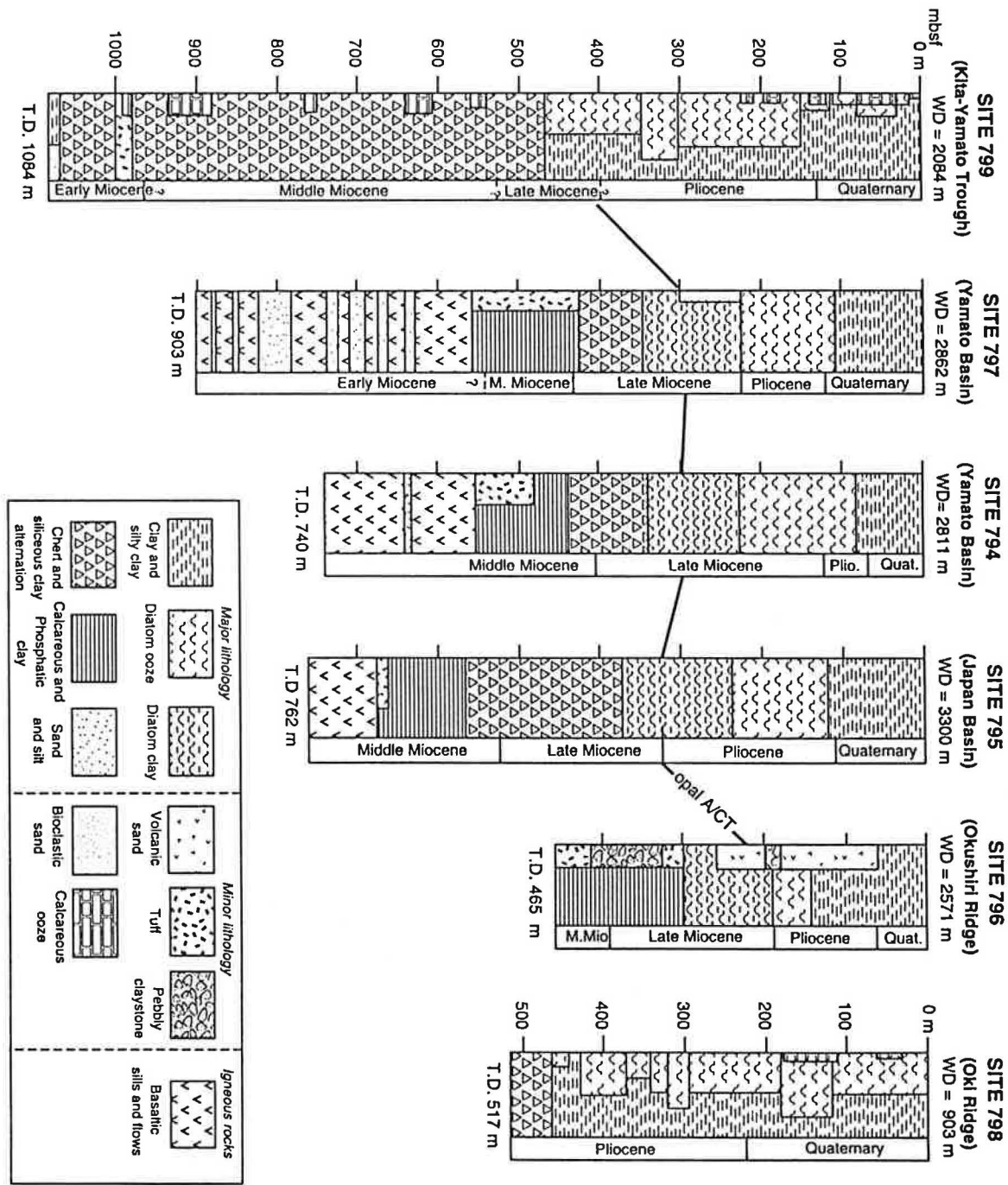


Figure 9. Colonnes sédimentaires des sites de forage ODP, Leg 127 et 128 (d'après Tamaki et al., 1992).

Des courbes de subsidence totale et de subsidence tectonique ont été déterminées pour la Mer du Japon à partir de ces forages et de données à terre (Figure 10; Ingle, 1992). La subsidence s'amorce lentement aux alentours de 32 Ma à des taux faibles comparables aux taux de subsidence "thermique" (Parson et Sclater, 1977; Ingle, 1992). Elle s'accélère entre 23 et 13 Ma, traduisant un contrôle mécanique de la subsidence (Ingle, 1992). Ingle (1992) note que le fort taux de subsidence (900 m/Ma) entre 24-23 Ma et 19 Ma est comparable au taux de subsidence initiale prédict dans les bassins en pull-apart. La subsidence cesse entre 13 et 10 Ma, période à laquelle un soulèvement s'amorce qui s'accélère aux alentours de 5 Ma pour atteindre il y a 2 Ma le taux de surrection actuel du Japon, environ 500 m/Ma.

IV. AGE DE L'OUVERTURE

Les âges ^{39}Ar - ^{40}Ar du socle basaltique de la Mer du Japon déterminés grâce aux forages ODP, et les âges des sédiments qui le recouvrent sont synthétisés en Figure 11 d'après Tamaki et al. (1992). L'âge des basaltes est compris entre 24 et 17 Ma. Kaneoka et al. (1990) avaient auparavant fait une récapitulation de tous les âges radiométriques obtenus sur des roches draguées dans la Mer du Japon. De manière générale, les âges obtenus dans le bassin du Japon et dans le bassin de Yamato sont plus jeunes que 18 Ma. En particulier, les basaltes et les andésites dragués sur les monts sous-marins du bassin de Yamato ont un âge compris entre 17 et 11 Ma. Si ces roches sont l'expression de la dernière activité volcanique liée à l'ouverture, il faut considérer que celle-ci se termine vers 11 Ma dans le bassin de Yamato. Par ailleurs, les courbes de subsidence évoquées précédemment fournissent une limite supérieure à l'âge de l'ouverture en situant le début de l'extension à 32 Ma. Tamaki (1986) avait proposé une estimation de l'âge des bassins de la Mer du Japon à partir de la profondeur du socle océanique et du flux de chaleur. Son estimation pour le bassin du Japon, seul bassin véritablement océanisé, était comprise entre 30 et 15 Ma, ce qui est en accord avec les données précédentes.

Ainsi, on peut raisonnablement caler l'âge de l'ouverture de la Mer du Japon entre 32 et 11 Ma. L'âge de l'océanisation du bassin du Japon n'est pas bien contraint. L'âge le plus ancien, suggéré par les anomalies magnétiques, est 27 Ma, et l'âge le plus récent, fourni par les datations du socle océanique, est 17 Ma. La période commune déterminée par les deux méthodes, magnétique et radiométrique, est comprise entre 24 et 19 Ma et coïncide avec une phase de subsidence rapide entre 23 et 19 Ma (Figure 10; Ingle, 1992). Tamaki et al. (1992) interprètent cette période comme une phase d'océanisation et de propagation rapide de l'ouverture vers l'ouest.

JAPAN SEA

17

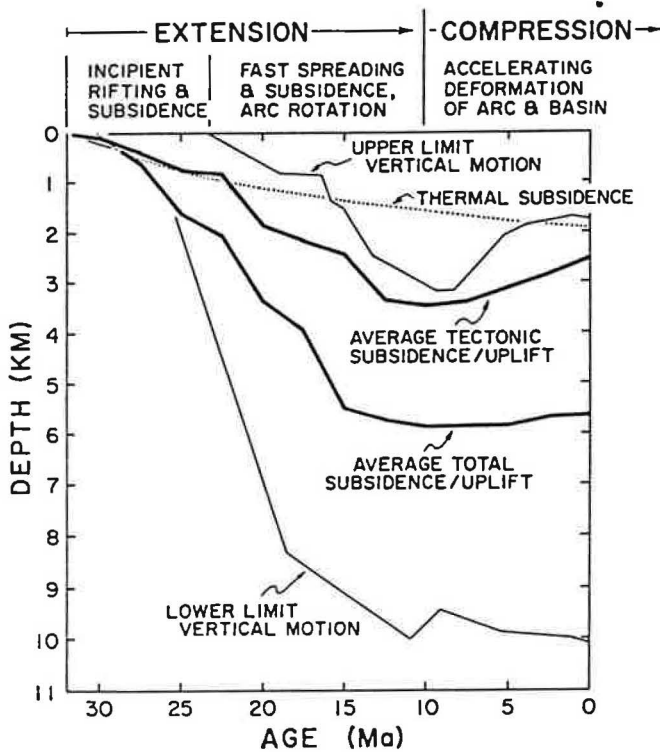


Figure 10. Courbes de subsidence dans la mer du Japon (d'après Ingle, 1992).

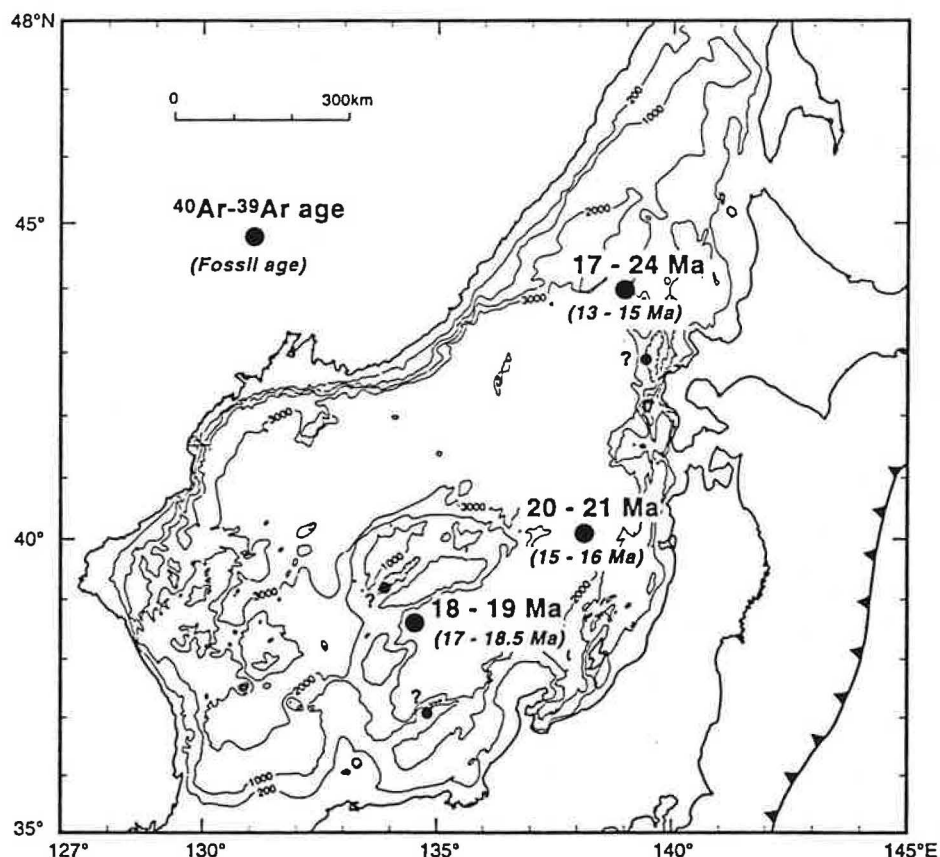


Figure 11. Ages ^{39}Ar - ^{40}Ar du socle basaltique déterminés par Kaneoka et al. (1992), et âges des sédiments recouvrant les basaltes (entre parenthèses) (d'après Tamaki et al., 1992).

V. CONTEXTE GÉODYNAMIQUE

A. LES PLAQUES EN PRÉSENCE

La Mer du Japon est située dans la zone d'interaction des plaques Eurasie, Nord Amérique, Pacifique, et Mer des Philippines (PSP) (Figure 12). Les mouvements relatifs des trois premières sont bien contraints depuis l'Éocène. La croûte océanique d'âge Crétacé (Nakanishi et al., 1992) de la plaque Pacifique passe en subduction vers l'ouest sous l'arc japonais à un taux de 10 cm/an (Seno, 1985). Au sud de l'arc japonais, la croûte océanique d'âge Oligo-Miocène du bassin de Shikoku (plaque Mer des Philippines ; Seno et Maruyama, 1984 ; Chamot-Rooke et al., 1987) passe en subduction dans la fosse de Nankai. La direction de convergence établie à partir des mécanismes au foyer des séismes est N305°E (Ishibashi, 1981), et le taux de subduction varie en fonction des pôles de rotation Pacifique-Philippine utilisés et vaut 3,9 cm/an (Seno, 1977 ; DeMets, 1990), 1,3 cm/an (Ranken et al., 1984), 2,1 cm/an (Huchon, 1986) et 4,0 cm/an (Seno et al., 1993) (Figure 13) au niveau du site KAIKO-NANKAI à l'ouest de la péninsule d'Izu (Le Pichon, Kobayashi et al., 1992 ; Figure 14). A partir de l'inversion de données géodésiques, Yoshioka et al. (1993) ont estimé la direction de convergence à N330°E et le taux à 3,0 cm/an au niveau du site KAIKO-NANKAI (Figure 15), ce qui est proche de la direction de mouvement relatif entre les plaques mer des Philippines et Nord Amérique. Selon les reconstructions paléocinématiques, la subduction de la plaque Mer des Philippines sous le Japon débute au Miocène inférieur (Seno et Maruyama, 1984) ou au sommet du Miocène moyen (Jolivet et al., 1989).

B. LA FRONTIÈRE NORD AMÉRIQUE-EURASIE

La frontière entre les plaques Nord Amérique et Eurasie dans le NE sibérien est mal définie par la sismicité comme le montre la Figure 12. Une guirlande de sismicité peu marquée joint la mer de Laptev, dans le prolongement de la ride médio-océanique arctique, à la zone de subduction Pacifique au niveau de la jonction entre la fosse des Kouriles et la fosse des Aléoutiennes. Cette guirlande débute au sud de la mer de Laptev au niveau de l'embouchure de la Léna, suit le rift de Moma et les Monts Cherski, et passe au nord de la mer d'Okhotsk pour rejoindre la subduction Pacifique (Figure 12). La Figure 16 montre uniquement les séismes utilisés pour déterminer des tenseurs de moment sismique (magnitude supérieure à 5 environ) depuis 1979 (Dziewonski et al., 1981). Elle met en évidence la quasi absence de gros séismes depuis 1979 le long de la frontière Nord Amérique-Eurasie. La faible sismicité peut s'expliquer par la proximité du pôle de mouvement relatif Nord Amérique-Eurasie. Le pôle NUVEL-1 Nord Amérique-Eurasie est situé juste au sud de cette frontière (Figure 12; DeMets et al., 1990). Sa position n'a pas

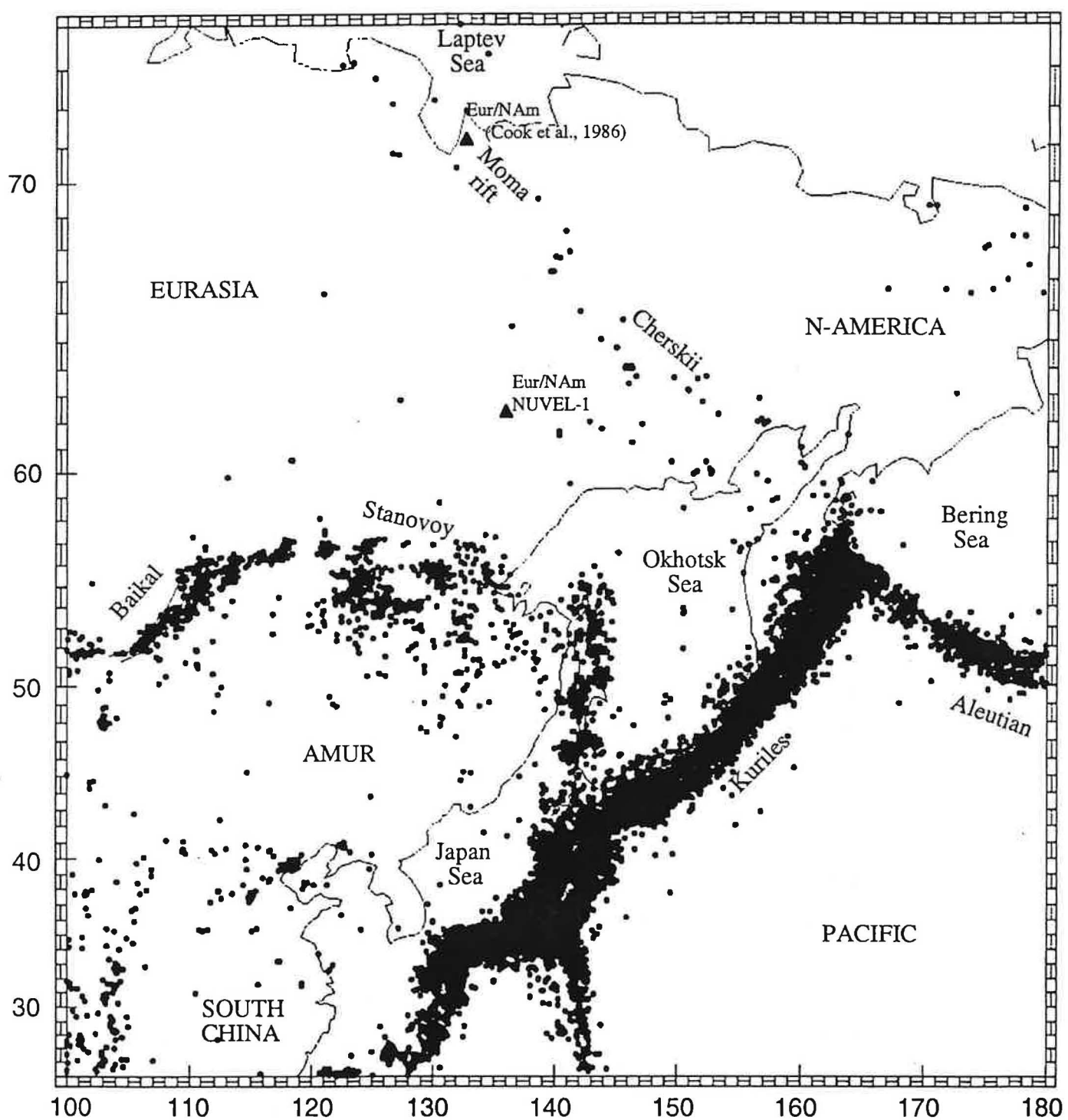


Figure 12. Sismicité en Asie du nord-est entre 1964 et 1989 (toutes magnitudes; profondeur < 50 km)

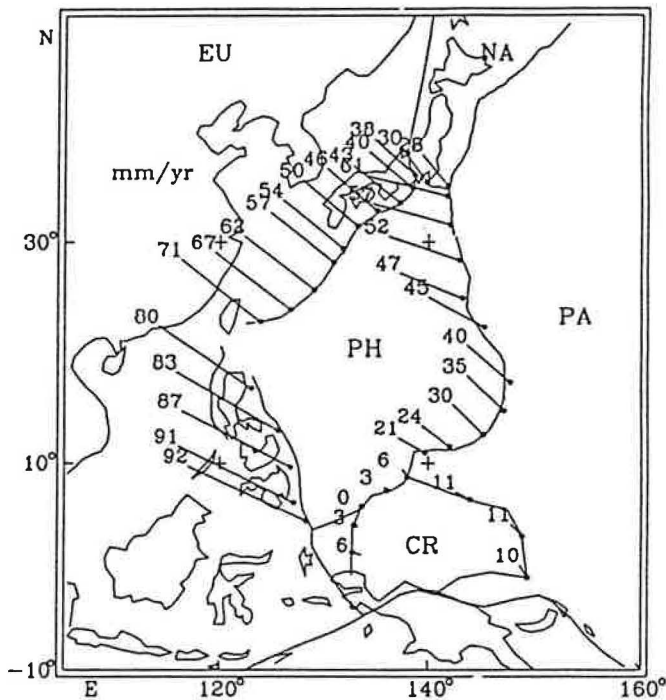


Figure 13. Taux de mouvements relatifs aux limites de la plaque mer des Philippines en mm/an (d'après Seno et al., 1993).

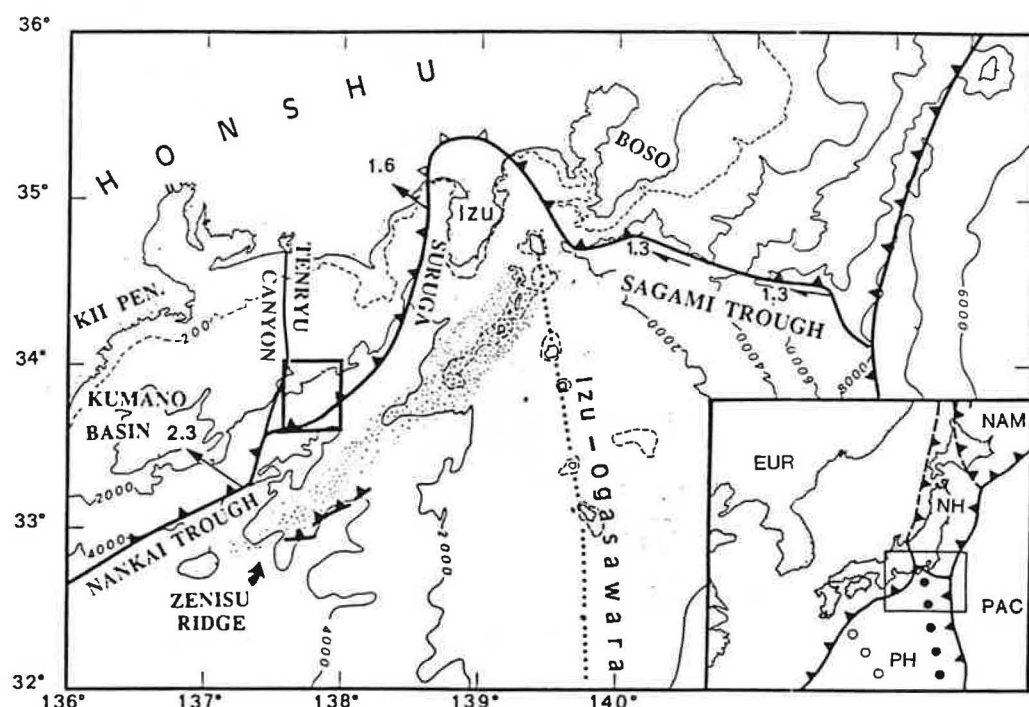


Figure 14. Site KAIKO-NANKAI (encadré) à l'ouest de la zone de collision d'Izu. Les flèches sur les limites de plaques indiquent les taux de mouvements relatifs calculés avec le pôle EUR-PSP de Huchon (1986). La zone de compression de la ride de Zenisu est en pointillés. L'arc d'Izu-Bonin est ombré. Bathymétrie en mètres (d'après Le Pichon, Kobayashi et al., 1992).

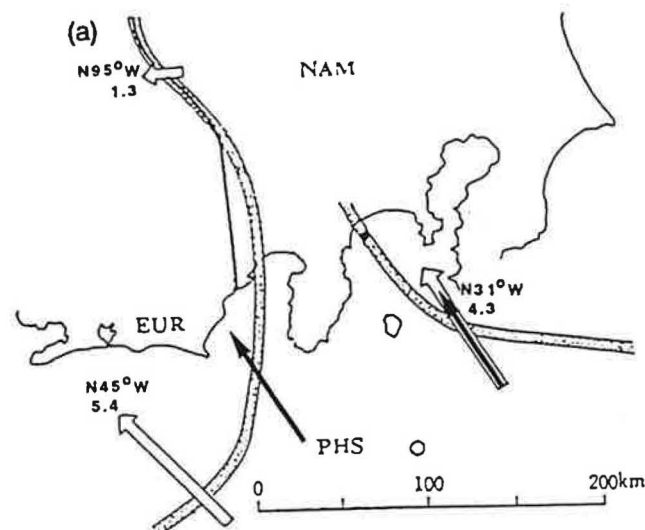


Figure 15. Taux de mouvements relatifs dans la région d'Izu calculés à partir du modèle de Minster et Jordan (1978) (flèches blanches), et de l'inversion de données géodésiques par Yoshioka et al. (1992) (flèches noires) (d'après Yoshioka et al., 1992).

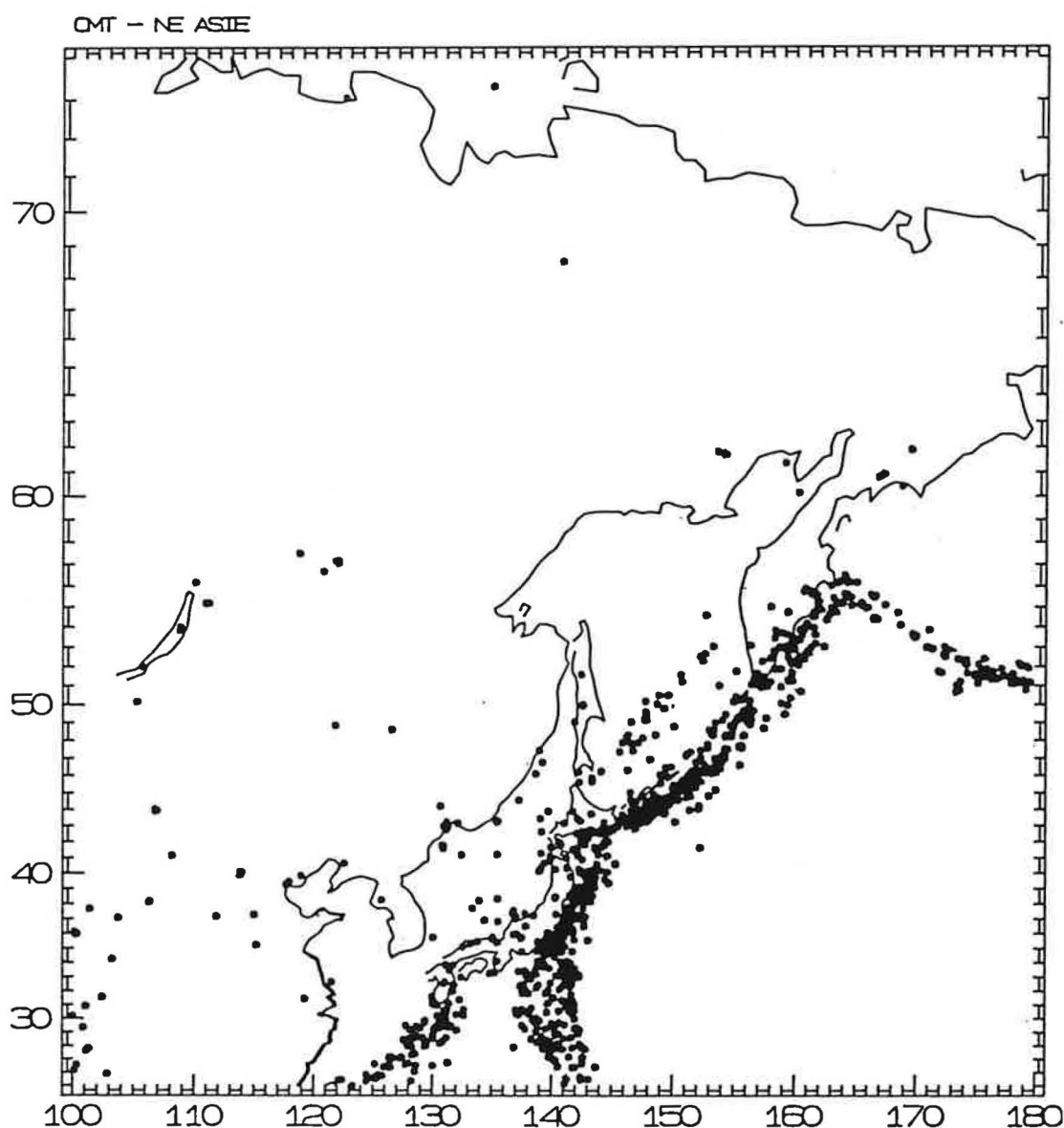


Figure 16. Séismes utilisés pour déterminer les tenseurs de moment sismique (Dziewonski et al., 1881, Dziewonski et Woodhouse, 1983).

beaucoup varié depuis l'Oligocène (Savostin et Karasik, 1981 ; Jolivet, 1986). Cook et al. (1986) ont cependant déterminé des mécanismes au foyer de séismes compressifs au nord-ouest des Monts Cherski incompatibles avec ce pôle, et des structures compressives (plis et failles inverses) post Éocène sont décrites dans la région du rift de Moma (Fujita et al., 1990). L'extension active étant bien documentée dans la mer de Laptev (voir par exemple Fujita et al., 1990), Cook et al. (1986) placent le pôle actuel Nord Amérique-Eurasie à l'embouchure de la Léna, entre la zone en extension et la zone en compression (Figure 12). Le Moma rift étant considéré d'âge Pliocène (Fujita et al., 1990), Cook et al. (1986) suggèrent que le pôle a migré vers le nord aux alentours de 3 Ma, éventuellement à la suite de l'individualisation d'une plaque Okhotsk entre les plaques Nord Amérique et Eurasie. L'existence de la plaque Okhotsk a souvent été discutée (Chapman et Solomon, 1976 ; Zonenshain and Savostin, 1981 ; Savostin et al., 1983 ; Jolivet, 1986 ; Fujita et al., 1990 ; DeMets, 1992 ; Riegel et al., 1993), la principale difficulté étant l'absence totale de sismicité au nord de Sakhaline (DeMets, 1992). La géométrie actuelle des limites de plaques retenue par DeMets (1992) à partir de NUVEL-1 et de données additionnelles de vecteurs glissement le long des fosses du Japon et des Kouriles, est montrée en Figure 17. Elle n'inclut pas de plaque Okhotsk, mais elle inclut une micro-plaque Sud Kouriles en terminaison sud-ouest de la fosse des Kouriles, qui migre vers l'ouest relativement à la plaque Nord Amérique et dont le mouvement de convergence est absorbée par de la compression E-O dans la chaîne centrale d'Hokkaido provoquant le soulèvement rapide du cœur métamorphique de cette chaîne (zone d'Hidaka ; Kimura, 1983).

Hormis cette micro-plaque, la géométrie de DeMets (1992) diffère aussi de celle de Chapman and Solomon (1976) par le fait que la partie nord-est du Honshu est intégrée à la plaque Nord Amérique, la limite de plaque longeant la marge est de la mer du Japon (Figure 17). Cette marge est le siège de forts séismes compressifs le long d'accidents N-S (Fukao et Furumoto, 1975 ; Tamaki et Honza, 1984 ; Seno, 1985) (Figure 18), interprétés par Nakamura (1983) comme résultant de la subduction de la mer du Japon sous l'arc japonais. Tamaki et al. (1992) ont daté le début du soulèvement de la ride d'Okushiri au large d'Hokkaido à 1,8 Ma, et l'ont interprété comme l'âge de l'initiation de cette subduction.

Au sud, la limite de plaque traverse le Japon central le long de l'Itoigawa-Shizuoka Tectonic Line (ISTL) et rejoiit la plaque Philippines au niveau de la zone de collision d'Izu. Il semble cependant que la subduction de la mer du Japon ait lieu aussi au nord de la péninsule de Noto où des séismes compressifs le long d'accident NNE-SSO sont documentés (Figure 18). La limite de plaque Nord Amérique-Eurasie ainsi que la jonction triple NAM-EUR-PSP correspondent vraisemblablement à une zone de déformation diffuse au niveau du Japon central.

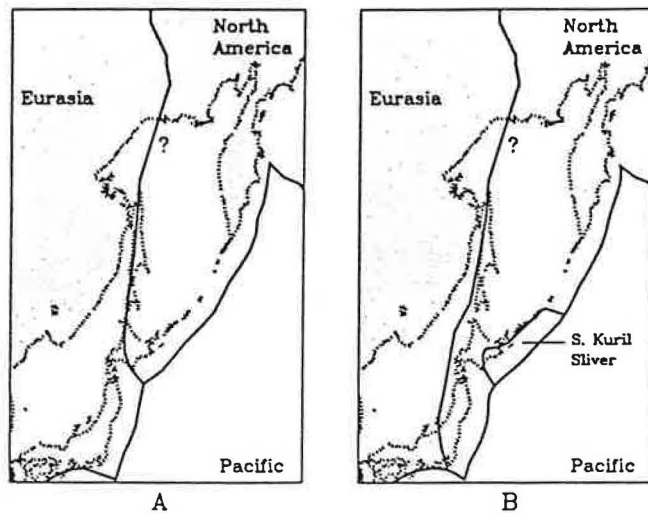


Figure 17. Configuration actuelle des plaques lithosphériques selon (A) Chapman et Solomon (1976) et (B) DeMets (1992) (d'après DeMets, 1992).

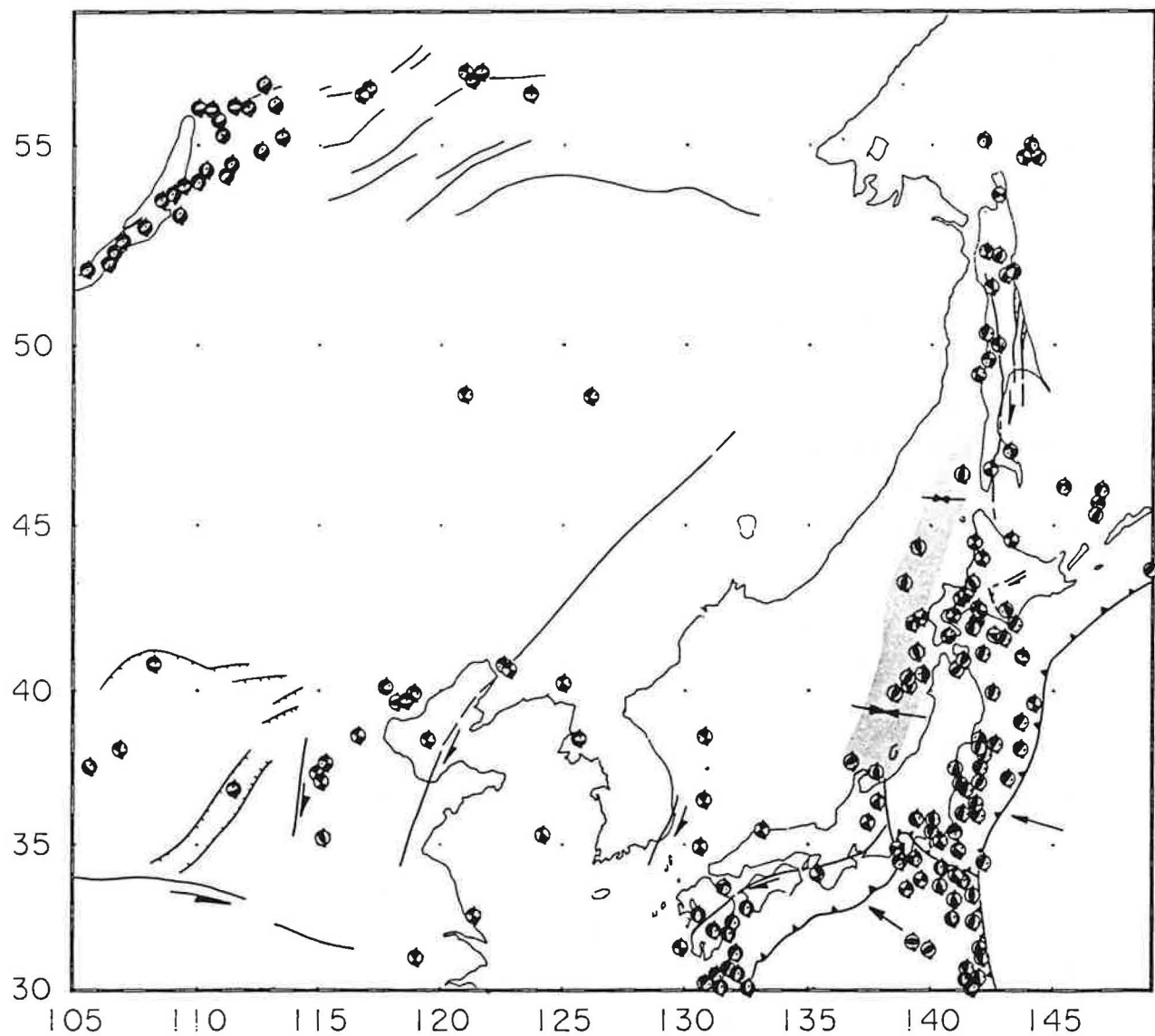


Figure 18. Mécanismes au foyer de séismes crustaux (d'après Jolivet et al., 1992). La zone ombrée représente la zone de compression E-O récente sur la marge est de la mer du Japon.

C. LA PLAQUE AMOUR

A partir de l'étude de la sismicité à terre, l'existence d'une plaque Amour a été proposée par Zonenshain et Savostin (1981) au sud de la zone Baikal-Stanovoï. La sismicité dans les Monts Stanovoï est bien documentée par les réseaux régionaux russes comme le montre la Figure 19; d'après Parfenoy et al. (1987). Zonenshain and Savostin (1981) placent la frontière sud de la plaque Amour au nord du bloc Ordos et au niveau du bassin de Bohai (Figure 20). La ceinture sismique qui relie le bassin d'Hetao, au nord du bloc Ordos, au bassin de Bohai, ne se poursuit pas jusqu'à la zone de subduction d'après la Figure 12, mais la carte de la sismicité en Corée d'après Ishikawa (1992) (Figure 21) montre qu'en réalité ce lien n'est pas à exclure. Ishikawa (1992) montre aussi l'agencement des principaux bassins dans la région (Figure 22), qui pourraient constituer la frontière sud de la plaque Amour. Le lien Baikal-Ordos n'est pas non plus bien marqué par la sismicité.

Zonenshain and Savostin (1981) ont défini un pôle Amour-Eurasie situé entre la zone d'extension Baikal et la zone de compression Stanovoï ($56,95^{\circ}\text{N}$, $117,45^{\circ}\text{E}$) et ont estimé une vitesse angulaire à partir du taux d'ouverture du lac Baikal à $0,1^{\circ}/\text{Ma}$. La frontière est de la plaque Amour traverse Sakhaline longitudinalement, et se poursuit par la zone de compression est-mer du Japon.

VI. LA MARGE OCCIDENTALE DÉCROCHANTE

La marge occidentale de la mer du Japon est structurée par deux décrochements majeurs d'orientation NNE-SSO actifs depuis le Crétacé, la faille de Yangsan et la faille de Tsushima. En Corée, la faille de Yangsan décale dans le sens dextre les formations du groupe Hayang (Aptien-Albien) et des rhyolites Éocène (Hwang, 1992 ; Figure 23). Son rejet horizontal dextre est estimé à 35 km (Chang et al., 1990). Sillitoe (1977) montre de plus que, de part et d'autre du détroit de Tsushima, des ceintures métallogéniques corrélables entre la Corée et le Japon sont décalées en dextre de 200 km, ce décalage étant plus récent que 46 Ma (Figure 24).

Dans le bassin Tertiaire de Pohang, des failles normales en échelon de direction NE-SO sont décrites dans les dépôts Miocène inférieur du groupe Yangbug, scellées par des dépôts d'âge Miocène moyen (groupe Yeonil ; Lee et Pouclet, 1988 ; Lee, 1989). Ces failles fossilisent une phase extensive contemporaine de l'ouverture de la mer du Japon et compatible avec des mouvements décrochants dextres le long de sa marge occidentale. Les tenseurs de contraintes calculés dans le bassin de Pohang à partir des données de fracturation documentent un régime transtensif (Hwang, 1992), avec une contrainte maximale compressive horizontale NE-SO compatible avec un jeu dextre de la faille de Yangsan. Enfin,

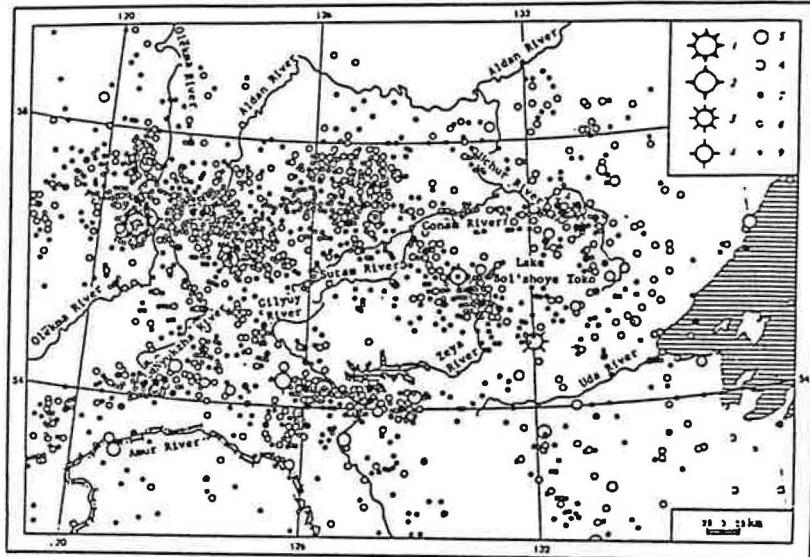


Fig. 1. Map of earthquake epicenters for 1937-1984.
1-9) Earthquake epicenters with magnitude, M: 1) 7.0; 2) 6.5; 3) 6.0; 4) 5.5; 5) 5.0;
6) 4.5; 7) 4.0; 8) 3.0-3.5; 9) M < 2.5.

Figure 19. Sismicité dans les Monts Stanovoï entre 1937 et 1984. La mer d'Okhotsk est montrée en hachuré horizontal (d'après Parfenoy et al., 1987).

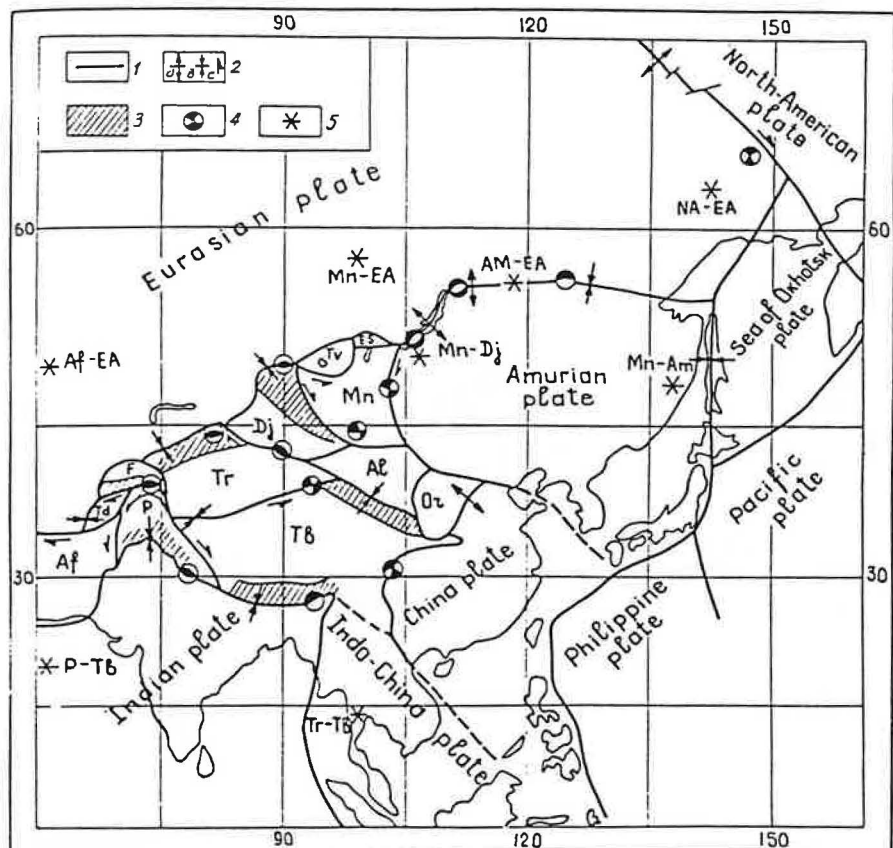


Figure 20. Géométrie des plaques en Asie et directions de mouvements relatifs le long des frontières d'après Zonenshain et Savostin (1981).

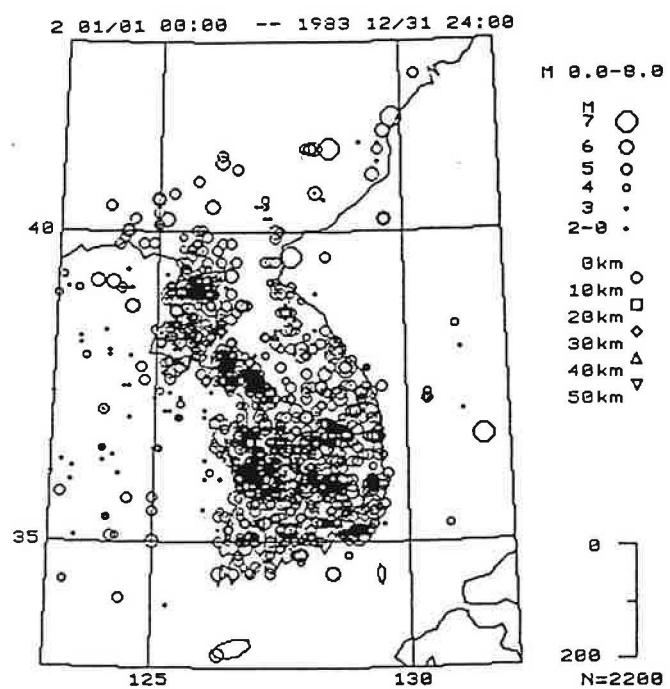


Figure 21. Sismicité en Corée (d'après Ishikawa, 1992)

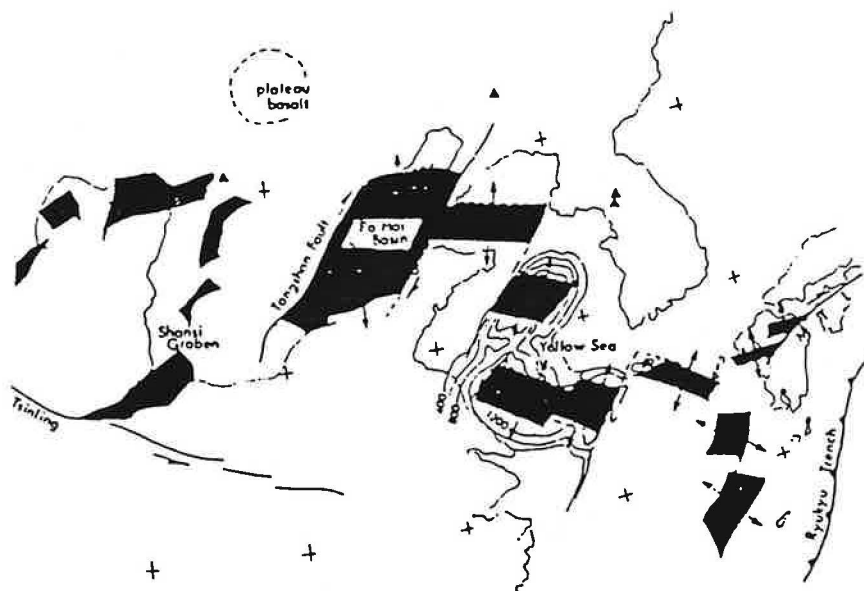


Figure 22. Géométrie des bassins sédimentaires (en noir) entre la Chine du nord et la fosse des Ryukyu (d'après Ishikawa, 1992).

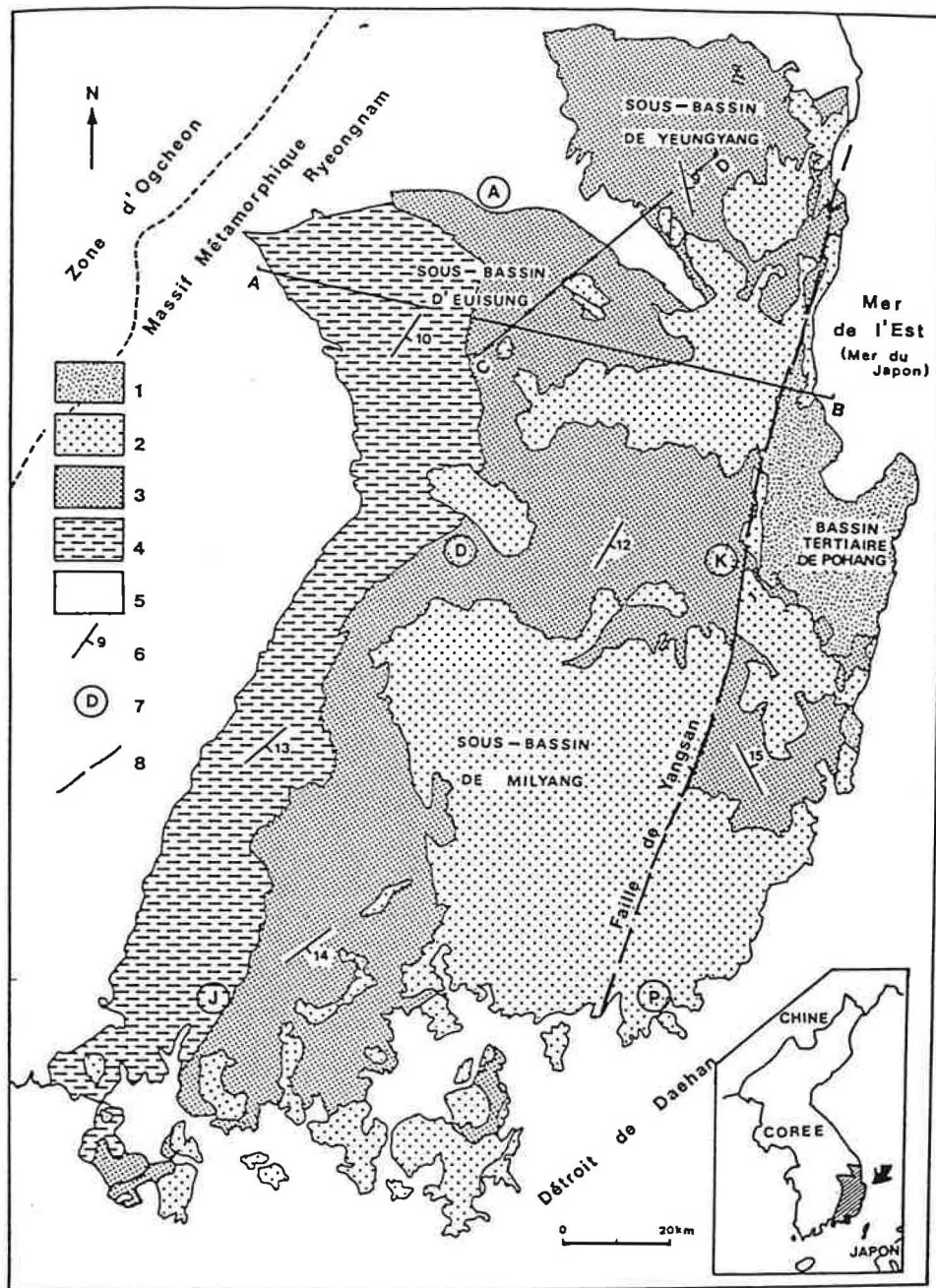


Figure 23. Carte géologique de la Corée du sud-est (d'après Hwang, 1992). 1: Tertiaire. 2: groupe Youcheon. 3: groupe Hayang. 4: groupe Sindong. 5: socle métamorphique.

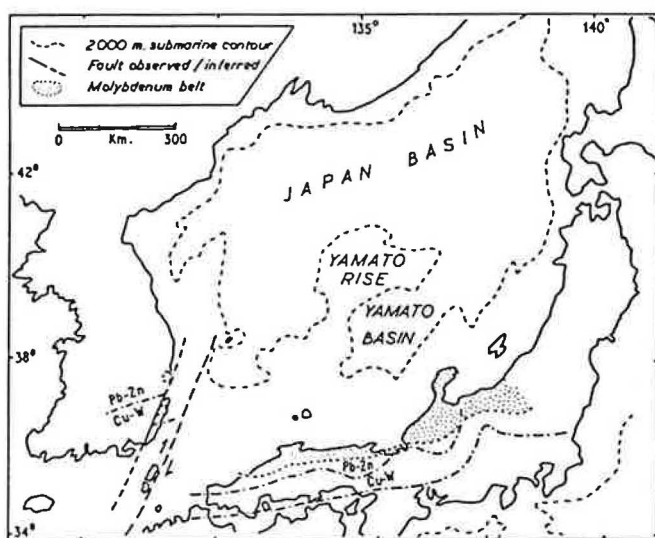


Figure 24. Décalage dextre par le système de failles du détroit de Tsushima des ceintures métallogéniques du Japon et de Corée (d'après Sillitoe, 1977).

les roches miocènes du bassin de Pohang ont subi des rotations horaires (McCabe, comm. pers., 1989 ; Kim et al., 1986) compatibles aussi avec un jeu dextre de la faille de Yangsan.

Il existe cependant des indications de mouvements sénestres dans le détroit de Tsushima. A Tsushima, les formations du Miocène moyen sont affectés par des plis en échelon dont les axes de direction NE-SO se courbent en une sigmoïde sénestre au voisinage de la faille de Tsushima (Fabbri et Charvet, 1994). Ce plissement est reliée à une phase compressive NO-SE documentée par l'analyse de la fracturation à Tsushima, et régionalement connue et datée du Miocène supérieur-Pliocène. D'autre part, les études paléomagnétiques réalisées par Ishikawa et al. (1989) et Ishikawa et Tagami (1991) dans les îles de Tsushima et de Goto mettent en évidence une rotation anti-horaire (20° - 30° à Tsushima) des roches d'âge Miocène moyen inférieur. A Goto, les intrusions granitiques datées de 15 Ma environ n'ont pas subi la rotation. Il est donc impossible de relier cette rotation à la rotation anti-horaire récente (post 6 Ma) documentée dans le sud de l'île de Kyushu (Kodama et al., 1993) et attribuée à l'ouverture du bassin d'Okinawa. Il faut plutôt y voir l'indication de mouvements sénestres dans le détroit de Tsushima.

VII. MODÈLES D'OUVERTURE

Le débat autour de l'ouverture de la mer du Japon s'est cristallisé ces 10 dernières années autour de deux modèles : le modèle d'ouverture quasi instantanée type porte à double battants défendu par les paléomagnéticiens (Kawai et al., 1971 ; Sasajima, 1981 ; Otofuji et al., 1985 ; Celaya and McCabe, 1987), et le modèle d'ouverture en pull-apart proposé par Lallemand et Jolivet (1985) et modifié par Jolivet et al. (1991).

Le modèle en porte à double battants (Figure 25) comprend en guise de charnières un pôle de rotation dans le détroit de Tsushima pour le Japon sud-ouest, et un pôle de rotation au nord-est d'Hokkaido pour le Japon nord-est. Ce modèle rend compte des données paléomagnétiques, à savoir les rotations différentielles du Japon nord-est et sud-ouest entre 21-15 Ma (Tosha et Hamano, 1988) et 16-14 Ma (Otofuji et al., 1991 ; Hayashida et al., 1991) respectivement. Faure et Lalevée (1987) ont déplié les structures anté-ouverture de l'arc japonais pour proposer un modèle d'ouverture similaire. Outre la difficulté que représente le fort taux d'ouverture requis par ce modèle (20 à 50 cm/an) pour faire tourner d'un bloc le Japon sud-ouest presque instantanément, force est de constater qu'il ne rend pas compte des données des forages ODP qui concluent à une ouverture sur plus de 10 millions d'années, pas plus que des données structurales à terre et en mer. D'ailleurs le reproche le plus important que l'on puisse faire à ce modèle est bien celui de ne pas avoir de base structurale. Les données (paléomagnétiques, géométrie des structures anciennes) sont utilisées pour reconstruire une géométrie anté-ouverture sans que les moyens de cette ouverture ne soient

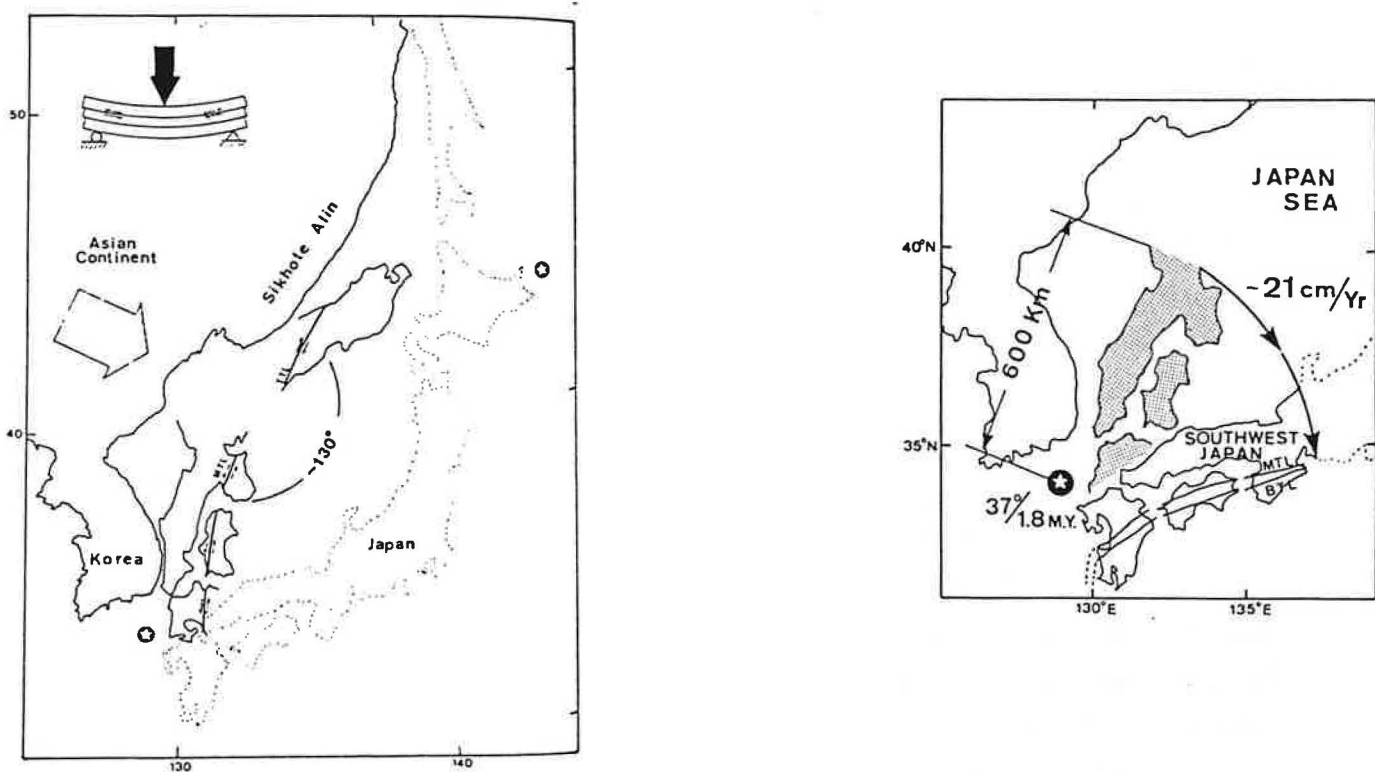


Figure 25. Modèle d'ouverture de la mer du Japon en porte à doubles battants proposé par Otofuji et al.(1985, 1991). Les étoiles représentent les pôles de rotations du Japon sud-ouest et nord-est.

discutés. Ce modèle n'apporte pas de réponse à la question : comment sont accommodés les mouvements pendant l'ouverture ?

Otsuki et Ehiro (1978) sont les premiers à avoir souligné le rôle des mouvements décrochants pendant l'ouverture de la mer du Japon. Le modèle d'ouverture en tiroir qu'ils ont proposé comprend un rail décrochant dextre à l'ouest, la faille de Tsushima, et un rail décrochant sénestre à l'est, la Ligne Tectonique Tanakura (TTL), entre lesquels la mer du Japon s'ouvre. Pour Koshiya (1986), la TTL est cependant un décrochement dextre au Miocène moyen, et les rotations horaires des roches Paléogène à Miocène inférieur documentées par Otofuji et al. (1985) le long de la TTL sont en accord avec cette interprétation.

La déformation décrochante dextre N-S contemporaine de l'ouverture a été décrite à Sakhaline (Rozhdestvensky, 1982), Hokkaido (Kimura et al., 1983 ; Jolivet et Miyashita, 1985), et le long de la marge est de la mer du Japon (Lallemand et Jolivet, 1985), ce qui a conduit Lallemand et Jolivet (1985) à proposer le modèle d'ouverture en pull-apart dextre entre cette zone décrochante à l'est et la zone décrochante du détroit de Tsushima à l'ouest (Figure 26). Pas plus que le modèle d'Otsuki et Ehiro (1978), ce modèle ne rendait compte des rotations paléomagnétiques. Jolivet et al. (1991) ont montré, à partir d'expériences de modélisation analogique de la déformation décrochante, que la déformation en régime transtensif dextre était accommodée par des rotations horaires de blocs rigides susceptibles de rendre compte de la rotation horaire du Japon sud-ouest. La cinématique d'ouverture en pull-apart qu'ils proposent est contrainte en partie par la similarité de forme entre le banc de Yamato et la marge de Corée du nord observable sur la carte bathymétrique (Figure 4) et en partie par la direction de failles de transfert. Elle inclut une rotation horaire du Japon sud-ouest de 30° (Figure 27). Cette rotation est accommodée par un mouvement décrochant fini moins important sur la zone décrochante de Tsushima (150 à 200 km) que sur la zone décrochante est-mer du Japon (environ 400 km).

VIII. LES MOTEURS DE L'OUVERTURE

Mécanisme et causes de l'ouverture sont largement discutés dans les parties qui suivent, en particulier dans le chapitre de description des expériences de modélisation analogique entreprises notamment dans le but de montrer qu'un mécanisme d'ouverture en pull-apart, sous la dépendance à la fois de la collision continentale et de l'extension liée à la subduction, était envisageable.

La Figure 28 d'après Tamaki et Honza (1991) illustre les principaux moteurs de l'ouverture des bassins marginaux invoqués à ce jour (cf. Taylor and Karner, 1983). Les modèles 1 et 2 sont considérés comme "modèles d'ouverture active" parce qu'ils font

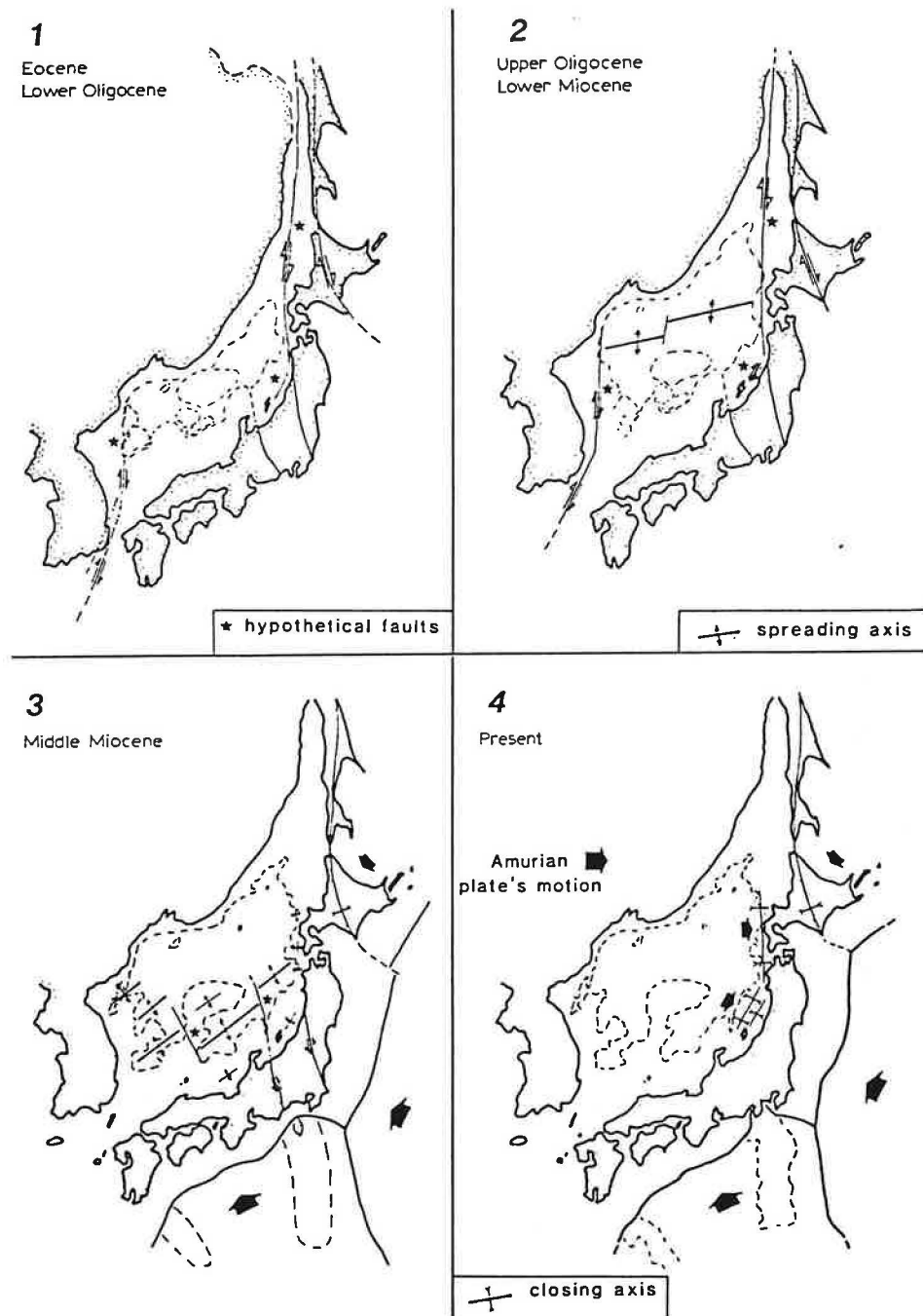


Figure 26. Modèle d'ouverture en pull-apart de la mer du Japon sans rotations, proposé par Lallemand et Jolivet (1985).

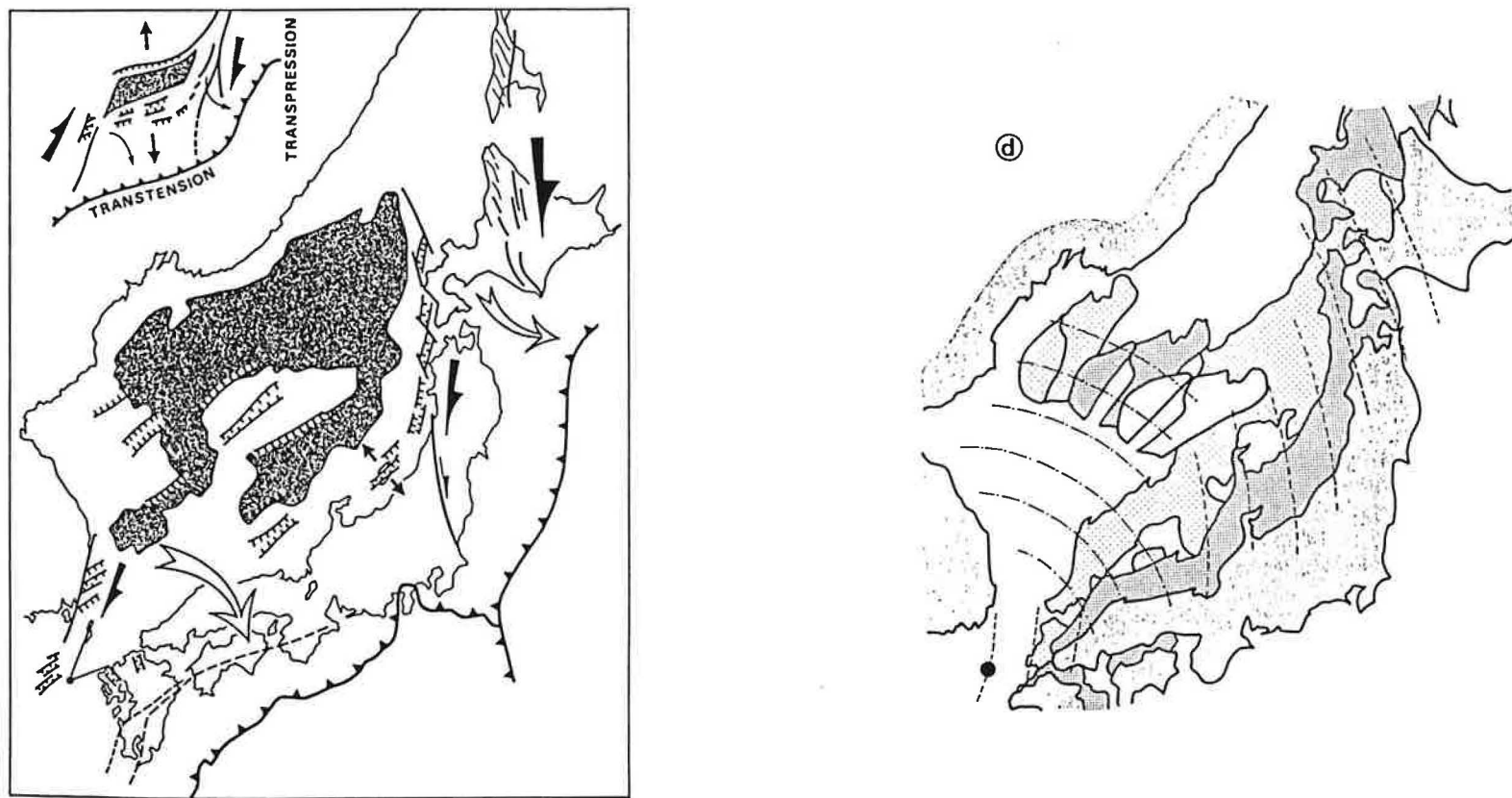
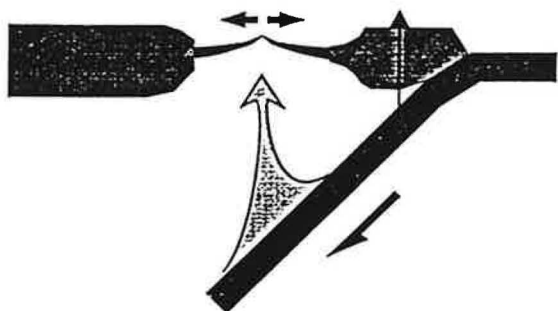


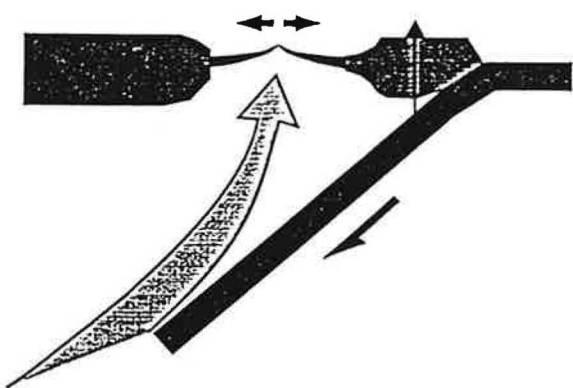
Figure 27. Modèle d'ouverture de la mer du Japon en pull-apart avec rotation du Japon sud-ouest, et cinématique de l'ouverture (d'après Jolivet et al., 1991).

MODELS OF BACKARC SPREADING

Model 1. Slab-induced upwelling model

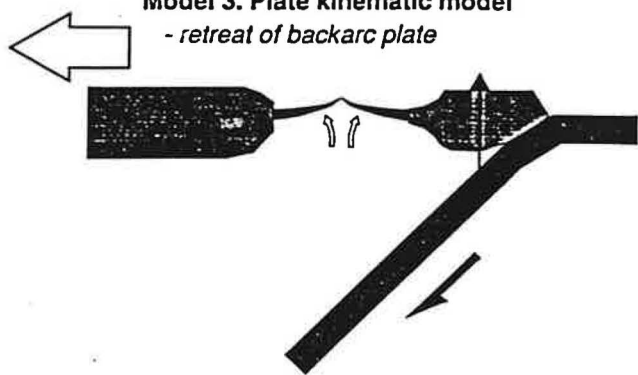


Model 2. Plume injection model



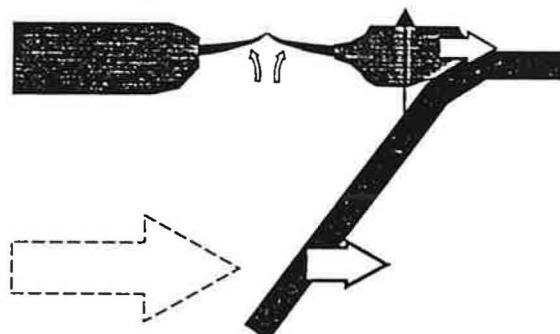
Model 3. Plate kinematic model

- retreat of backarc plate



Model 4. Asthenospheric flow model 1

- trench roll back by eastward asthenospheric current



Model 5. Asthenospheric flow model 2

- trench roll back by instability of downgoing asthenospheric flow

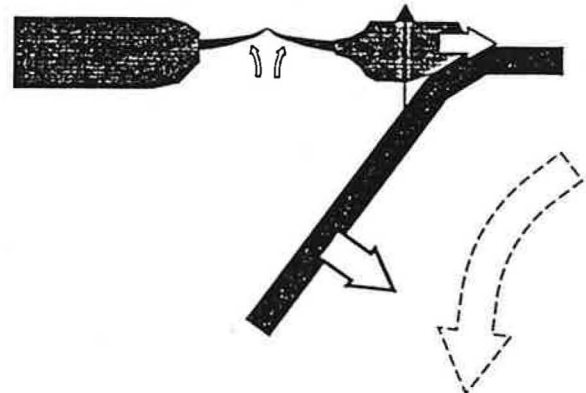


Figure 5.—Models of backarc spreading. See text for discussion.

Figure 28. Modèles d'ouverture arrière-arc (d'après Tamaki et Honza, 1991).

intervenir une remontée asthénosphérique, alors que les modèles 3 à 5 sont considérés comme "modèles d'ouverture passive" parce qu'ils font intervenir uniquement le mouvement des plaques lithosphériques comme cause de l'ouverture.

Modèle 1 : la remontée asthénosphérique est provoquée par le panneau plongeant (génération de chaleur par friction (Karig, 1971), convection secondaire (McKenzie, 1969 ; Sleep and Toksoz, 1971)).

Modèle 2 : la remontée asthénosphérique est liée à un panache mantellique généré par un point chaud (Miyashiro, 1986 ; Tatsumi et al., 1989).

Modèle 3 : modèle cinématique simple qui suppose le retrait de la plaque supérieure loin de la zone de subduction (Chase 1978 ; Dewey, 1980). C'est ce type de modèle qu'ont proposé Kimura et Tamaki (1986) pour rendre compte de l'ouverture de la mer du Japon : celle-ci s'ouvre en réponse au mouvement vers le N-NE de la plaque Amour relativement à la fosse.

Modèles 4 et 5 : ces modèles supposent le retrait de la fosse plutôt que celle de la plaque supérieure, sous l'influence d'un courant asthénosphérique vers l'est dans le modèle 4 (Uyeda et Kanamori, 1979), et de la gravité agissant sur le panneau plongeant dans le modèle 5 (Molnar et Atwater, 1978 ; Glatzmaier et al., 1990).

A partir d'expériences de modélisation analogique d'indentation, Jolivet et al. (1990) ont proposé un modèle d'ouverture du type 3 de Tamaki et Honza (1991) dans lequel la déformation de l'Asie est responsable de l'ouverture. Ce modèle, inspiré des expériences de Davy et Cobbold (1988) (Figure 29), comprend une large zone décrochante sénestre courant du Pamir aux Monts Stanovoï via le Tien Shan, l'Altai et le Baikal. Cette zone est transpressive au sud et transtensive au nord. Dans la partie transtensive, le cisaillement sénestre est accommodé par la rotation anti-horaire de blocs rigides délimités par des décrochements dextres. Le long de ces décrochements s'ouvrent les bassins en pull-apart dextres d'Asie du nord-est : la mer du Japon et le bassin de Bohai. La frontière de subduction est considérée comme une bordure libre n'affectant pas la déformation de l'Asie.

IX. PERSPECTIVES

Le déchiffrage des anomalies magnétiques du bassin du Japon reste à l'ordre du jour. L'équipe de Tamaki à l'ORI a engagé un programme d'identification de ces anomalies au moyen d'un magnétomètre profond (deep-towed magnetometer). Les premiers résultats obtenus pendant l'été 93 lors de la mise au point du magnétomètre ont une résolution des anomalies au moins deux fois supérieure à celle des données antérieures et permettent d'espérer leur identification prochaine (Sayanagi, comm. pers.).

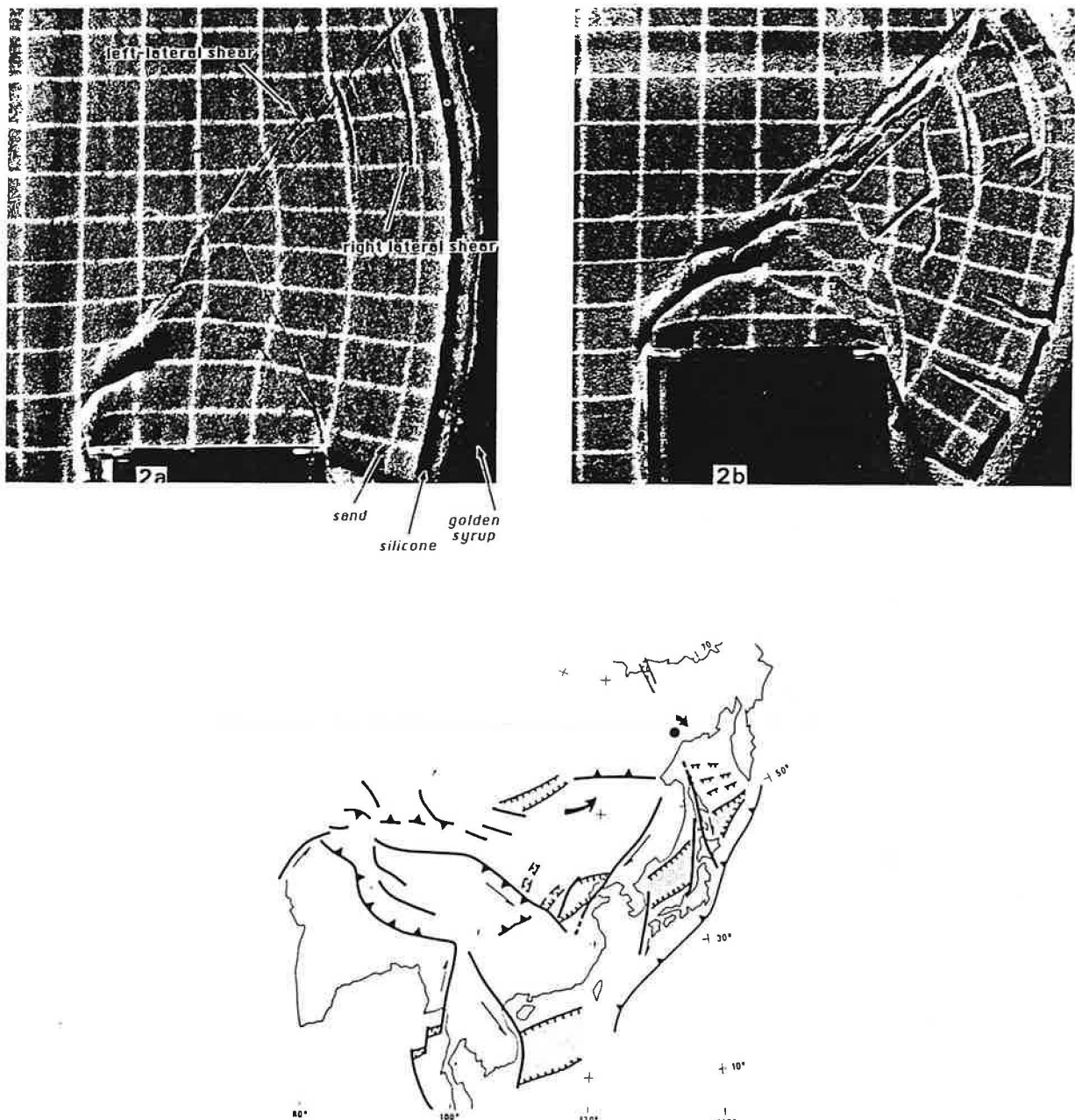


Figure 29. Photographies à deux stades successifs de l'expérience de Davy et Cobbold (1988) utilisé par Jolivet et al. (1990) pour leur modèle d'ouverture des bassins du NE asiatique (d'après Jolivet et al., 1990).

Les autres projets japonais en ce qui concerne la mer du Japon se concentrent essentiellement sur l'étude de la zone de compression active de la marge est de la mer du Japon génératrice de séismes destructeurs (Figure 30). C'est ainsi qu'ont pu être localisées et observées à l'aide du submersible *Shinkai 6500* les ruptures de surface du séisme d'Okushiri du 12 juillet 1993 ($M=7,8$) (Figure 31).

Major quakes, tsunami

The following is a list of major earthquakes and tsunami that have struck Japan. Magnitudes are according to the Richter scale.

- Aug. 14, 1909** — Forty-one people were killed in Shiga and Gifu prefectures, and 978 houses collapsed in a magnitude 6.8 earthquake.
- March 15, 1914** — Ninety-four people were killed in Akita Prefecture in a magnitude 7.1 tremor.
- Sept. 1, 1923** — Fires after the Great Kanto Earthquake, of magnitude 7.9, killed about 140,000 people in Tokyo and Yokohama, and destroyed more than 560,000 homes.
- March 7, 1927** — There were 2,935 people killed in Kyoto Prefecture in this earthquake of magnitude 7.3, whose focal point was right beneath the surface.
- May 23, 1925** — A magnitude 6.8 quake in western Japan killed 428.
- Nov. 26, 1930** — A tremor of magnitude 7.3 and aftershocks killed 272 people in northern Izu, Shizuoka Prefecture.
- March 3, 1933** — Tsunami as high as 27.8 meters killed 3,064 people on the coast of Miyagi Prefecture.
- Dec. 7, 1944** — Tsunami and the initial shock of magnitude 7.9 killed 998 people in Wakayama Prefecture.
- Dec. 21, 1946** — About 1,400 people died, 13,042 buildings collapsed, and 2,598 structures were destroyed by fire when a magnitude 8 earthquake with an epicenter off Shikoku struck western Japan.
- June 28, 1948** — A magnitude 7.1 tremor jolted Fukui Prefecture, killing 3,769 people. Some 36,184 buildings collapsed, and 3,851 were destroyed by fire.
- March 4, 1952** — Thirty-three people died, 815 buildings collapsed and 91 were washed away by tsunami after an magnitude 8.2 quake struck off Hokkaido.
- May 23, 1960** — A tsunami triggered by a magnitude 8.5 quake off Chile killed 142 people and destroyed 1,599 buildings in northeastern Japan.
- June 16, 1964** — Twenty-six people were killed and 1,960 buildings destroyed when a magnitude 7.5 quake rocked Niigata Prefecture.
- May 16, 1968** — Fifty-two people perished and 673 buildings collapsed in a magnitude 7.9 earthquake focused under the seabed off Tokachi, Hokkaido.
- May 9, 1974** — Thirty died and 134 buildings were destroyed in a magnitude 6.9 tremor originating off Izu Peninsula, Shizuoka Prefecture.
- Jan. 14, 1978** — Twenty-five were killed and 94 buildings collapsed in a magnitude 7 quake off Izu Oshima island, Tokyo.
- June 12, 1978** — Twenty-eight perished and 1,183 buildings were destroyed when a magnitude 7.4 quake rocked the seabed off Miyagi.
- May 26, 1983** — A magnitude 7.7 earthquake focused under the Sea of Japan killed 104 people and destroyed 934 buildings when it struck Akita and Aomori prefectures.
- Jan. 15, 1993** — One person was killed and 34 buildings destroyed in a magnitude 7.8 quake centered off Kushiro, Hokkaido.

Figure 30. Liste des principaux séismes et tsunamis au Japon depuis 1900 (*Japan Times*, 14/07/1993).

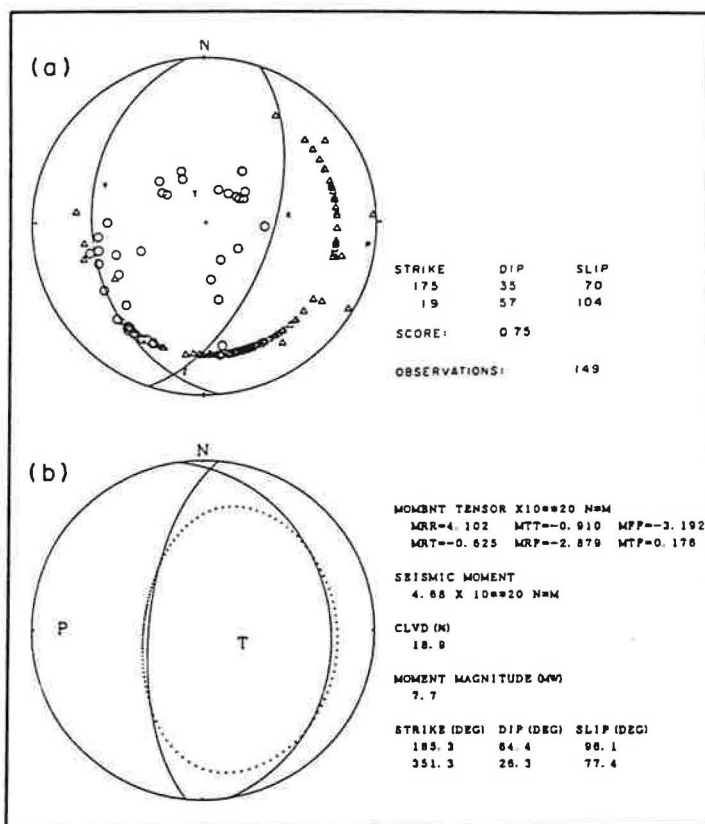
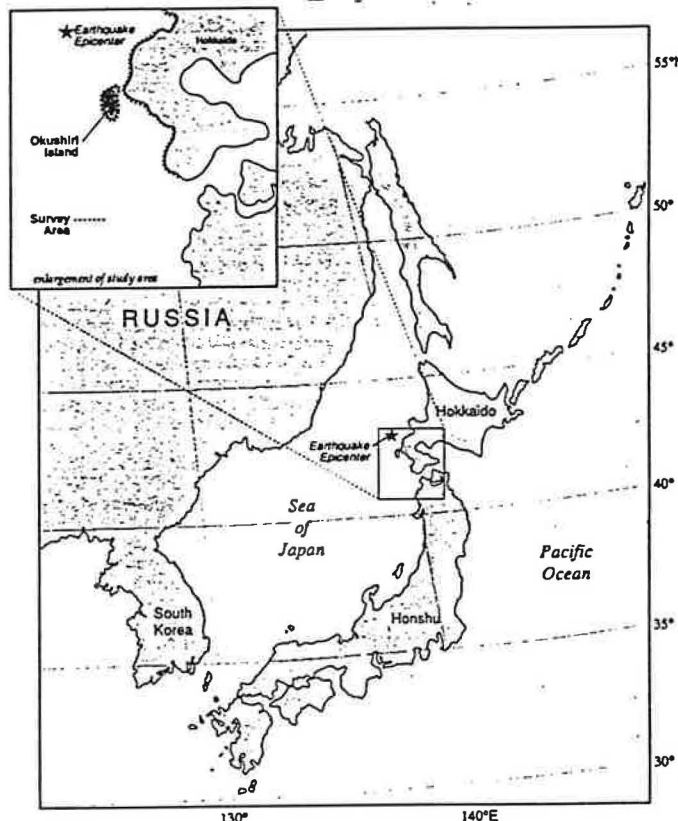
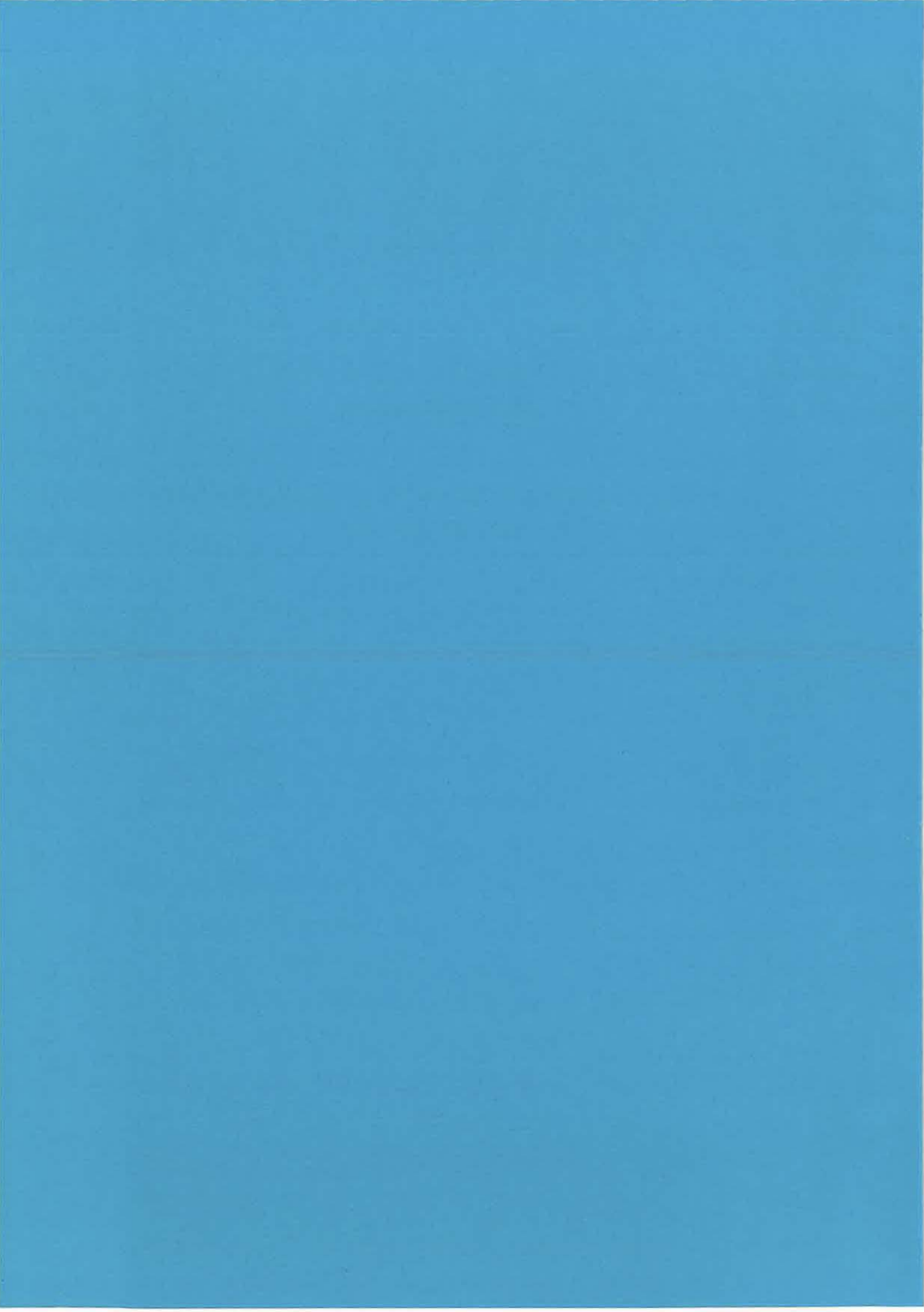


Figure 31. Localisation et mécanisme au foyer du séisme d'Okushiri ($M_s=7,8$) du 12 juillet 1993 (in *Eos*, 24/08/93 et 14/09/93). Ce séisme a fait 197 victimes, le tsunami qu'il a généré a localement dépassé 30 m.

SECONDE PARTIE

DEFORMATION DÉCROCHANTE DE LA MARGE ORIENTALE DE LA MER DU JAPON



SECONDE PARTIE
DEFORMATION DÉCROCHANTE DE LA MARGE ORIENTALE
DE LA MER DU JAPON

I. DÉFORMATION DÉCROCHANTE NÉOGÈNE À SAKHALINE : article "Neogene strike-slip faulting in Sakhalin and the Japan Sea opening"
(J. Geophys. Res., 99, 2701-2725, 1994)

Résumé : Cet article complète la description de la zone décrochante est-mer du Japon réalisée par Jolivet et Miyashita (1985) à Hokkaido, et Lallemand et Jolivet (1985), Jolivet et Huchon (1989), et Jolivet et al. (1991) le long de la côte ouest du Japon NE à terre et en mer. Des données sur la déformation contemporaine de l'ouverture sont décrites aux deux extrémités de la zone décrochante, au nord à Sakhaline, et au sud dans la péninsule de Noto et le bassin de Yatsuo (Japon central). Une large place est faite aux données sur Sakhaline. Cette étude regroupe les données de deux missions de terrain à Sakhaline en septembre 1989 et 1990, et d'une mission de terrain au Japon en Juin 1990.

Les images satellites de Sakhaline (couverture Landsat plus six images SPOT), des données de terrain, et des mécanismes au foyer des séismes sont décrits et interprétés. Depuis le Miocène, la déformation est absorbée à Sakhaline par des décrochements dextres N-S associés à des plis en échelon. Le décrochement majeur, la faille de Tym-Poronaysk (TPF), se suit sur plus de 600 km. Les plis affectant les formations Miocène à l'ouest de la TPF et dans son voisinage immédiat à l'est, sont déformés par le mouvement cisaillant le long de cette faille, et leurs axes courbés en une sigmoïde dextre. Les axes de paléo-contraintes déduits de l'étude de la fracturation dans les formations Miocène montrent une compression NE-SO compatible avec le mouvement dextre sur la faille et perpendiculaire aux axes de plis. Le champ de contraintes tourne dans le sens horaire avec les axes de plis au voisinage de la faille, mettant en évidence le synchronisme du plissement et du champ de contraintes, ainsi que des mouvements décrochants. Plus on remonte dans la série Miocène, moins les formations sont affectées par le plissement, la formation Mio-Pliocène Maruyama n'étant jamais basculée de plus de 30°. La progressivité du plissement au cours du Néogène est ainsi mise en évidence.

A l'est de la TPF, des bassins néogènes étroits en échelon sont observés le long de décrochements dextres NNE-SSO. Ces bassins ont tardivement subi un raccourcissement latéral (\pm E-O). Nous proposons un modèle de formation de ces bassins, équivalents de fentes en échelon, le long de failles normales délimitant des blocs rigides entre deux décrochements majeurs N-S. La déformation cisaillante dextre en régime transpressif a provoqué la rotation anti-horaire des blocs et des bassins qui sont devenus progressivement obliques à la direction de compression et ont subi un raccourcissement latéral.

Une différence de comportement mécanique entre le socle Paléozoïque-Jurassique à l'est de la TPF et la pile de sédiments Crétacé supérieur-Cénozoïque à l'ouest de la TPF est mise en évidence. Le socle Paléozoïque-Jurassique plus compétent est recoupé par des décrochements le long desquels se sont ouverts des bassins Néogènes, tandis que les sédiments Crétacé supérieur-Cénozoïque moins compétents sont déformés de manière homogène par des plis distribués.

La déformation active suit la même logique que la déformation Néogène, comme en témoigne la coexistence de mécanismes au foyer décrochants et compressifs le long d'accidents N-S. Une rotation horaire de la direction de compression vers une orientation plus E-O, comme celle enregistrée à Hokkaido au Miocène supérieur, peut cependant être envisagée. Les mécanismes au foyer des plus gros séismes, celui de Moneron en septembre 1971 (Fukao et Furumoto, 1975) et les deux séismes utilisés par Dziewonski et al. (1985, 1987) pour calculer des tenseurs de moment, sont en effet purement compressifs E-O.

L'étude de la fracturation menée à l'extrême sud de la zone décrochante est-mer du Japon, dans la péninsule de Noto et le bassin de Yatsuo, a permis de mettre en évidence une déformation caractérisée par des failles normales et décrochantes associées, dans les formations datées du Miocène inférieur et moyen. Les formations Miocène supérieur ne sont pas affectées par cette déformation. Les tenseurs de contraintes calculés à partir de ces failles montrent une direction de compression NE-SO, et une direction d'extension NO-SE. Ce régime de contraintes est en accord avec les observations réalisées le long de la côte ouest du Japon NE par Jolivet et Huchon (1989) et Jolivet et al. (1991) dans les formations contemporaines de l'ouverture de la mer du Japon.

L'évolution de la déformation décrochante le long de l'ensemble de la zone décrochante est-mer du Japon est brièvement décrite. Pendant l'ouverture de la mer du Japon, le régime décrochant est transpressif au nord et transtensif au sud. La composante extensive au sud est attribuée à la subduction de la lithosphère océanique ancienne et à un retrait éventuel de la fosse. La composante décrochante est attribuée à la déformation du continent asiatique consécutive à la collision Inde-Asie. L'extrusion d'une plaque Okhotsk pincée entre les plaques Nord Amérique et Eurasie est aussi envisagée.

Neogene Strike-Slip Faulting in Sakhalin and the Japan Sea Opening

MARC FOURNIER, LAURENT JOLIVET, AND PHILIPPE HUCHON

Laboratoire de Géologie, Département Terre Atmosphère Ocean, Ecole Normale Supérieure, Paris

KONSTANTIN F. SERGEYEV AND LEONID S. OSCORBIN

Institute of Marine Geology and Geophysics, Far East Science Center, Yuzhno-Sakhalinsk, Russia

We describe structural data from a 2000 km N-S dextral strike-slip zone extending from northern Sakhalin to the southeast corner of the Japan Sea. Satellite images, field data, and focal mechanisms of earthquakes in Sakhalin are included in the interpretation. Since Miocene time the deformation in Sakhalin has been taken up by N-S dextral strike-slip faults with a reverse component and associated en échelon folds. Narrow en échelon Neogene basins were formed along strike-slip faults and were later folded in a second stage of deformation. We propose a model of basin formation along extensional faults delimitating dominos between two major strike-slip faults, and subsequent counterclockwise rotation of the dominos in a dextral transpressional regime, basins becoming progressively oblique to the direction of maximum horizontal compression and undergoing shortening. The association of both dextral and compressional focal mechanisms of earthquakes indicates that the same transpressional regime still prevails today in Sakhalin. We present fault set measurements undertaken in Noto Peninsula and Yatsuo Basin at the southern end of the Sakhalin-East Japan Sea strike-slip zone. Early and middle Miocene formations recorded the same transtensional regime as observed along the west coast of NE Honshu. During the early and middle Miocene the strike-slip regime was transpressional to the north in Sakhalin and Hokkaido, and transtensional to the south along the west coast of NE Honshu as far as Noto Peninsula and Yatsuo basin. Dextral motion accommodated the opening of the Japan Sea as a pull-apart basin, with the Tsushima fault to the west. The opening of the Japan Sea ceased at the end of the middle Miocene when transtension started to change to E-W compression in the Japan arc. Subduction of the Japan Sea lithosphere under the Japan arc started 1.8 Ma ago. The evolution of the stress regime from transtensional to compressional in the southern part of the strike-slip zone is related to the inception of the subduction of the young Philippine Sea Plate lithosphere under the Japan arc during the late Miocene. Subduction related extension is a necessary condition for the opening of the Japan Sea. Two possible mechanisms can account for dextral shear in this area: (1) counterclockwise rotation of crustal blocks due to the collision of India with Asia, (2) extrusion of the Okhotsk Sea block squeezed between the North America and Eurasia plates.

INTRODUCTION

Deformation resulting from the India-Asia collision is taken up by crustal thickening in the Himalaya-Tibet collision zone and by geometric reorganization of continental blocks accommodated by strike-slip motion along major faults [Molnar and Tapponnier, 1975; Tapponnier and Molnar, 1976; Zonenshain and Savostin, 1981; Cobbold and Davy, 1988; England and Molnar, 1990; Holt et al., 1991]. Along the southeastern limit of Asia, strike-slip faults accommodated the opening of two marginal basins: the Andaman Sea in the prolongation of the Sagaing fault and Shan scarp system [Curray et al., 1979; Tapponnier et al., 1986], and possibly the South China Sea along the extension of the Red River fault [Tapponnier et al., 1982, 1986; Briais et al., 1993].

In northeast Asia, at the end of the Tien Shan-Baikal-Stanovoy deformation zone, the Japan and Okhotsk Seas (Figure 1) opened in the Early and Middle Miocene. The oldest oceanic basalts drilled on the eastern margin of the Japan Sea during Ocean Drilling Program leg 127 have a radiometric ^{40}Ar - ^{39}Ar age of 24 Ma [Tamaki et al., 1992] and the youngest dredged basaltic volcanics were dated 11 Ma [Kaneoka et al., 1990]. These ages are in good agreement with an earlier determination of the age of Japan Sea basement based on geophysical data between 30 and 10 Ma [Tamaki, 1986, 1988]. Similar average heat flow value and basement depth in both Japan and Kuril Basins led Tamaki [1988] to conclude to a simultaneous opening of the two basins in the late Oligocene to middle Miocene. Otsuki and

Ehri [1978] first outlined the role of strike-slip faults in the opening of the Japan Sea and proposed a drawerlike model of opening between the left-lateral Tanakura tectonic line (TTL) to the east and the right-lateral Tsushima fault (TF) to the west. *Kimura et al.* [1983] and *Jolivet and Miyashita* [1985] described onland transpressional deformation associated with N-S dextral strike-slip motion in Sakhalin and Hokkaido during the Oligocene and Miocene. *Lallemand and Jolivet* [1985] proposed a model of opening of the Japan Sea as a simple dextral pull-apart basin between this strike-slip zone to the east, and the Tsushima fault to the west. *Jolivet et al.* [1991], using analogue laboratory modelling, refined the pull-apart model by introducing blocks rotations in the dextral shear zone, that only partly fit the paleomagnetic data. *Jolivet* [1986] associated the dextral motion to southward extrusion of the Okhotsk Sea block squeezed between the North America and the Eurasia plates. *Kimura and Tamaki* [1986] and *Jolivet et al.* [1990] finally related the opening of the Japan and Okhotsk Seas to the motions of Asian microplates as a consequence of the India-Asia collision.

The eastern guide of the Japan Sea dextral pull-apart is a 2000-km-long strike-slip zone extending from the northern end of Sakhalin island to the north, to the southeast corner of the Japan Sea to the south (Figure 2)[*Kimura et al.*, 1983; *Lallemand and Jolivet*, 1985]. The central part of the strike-slip zone from Hokkaido to the west coast of NE Honshu is described by *Lallemand and Jolivet* [1985], *Jolivet and Huchon* [1989] and *Jolivet et al.* [1991]. In Sakhalin, field studies showed that the island is cut by a N-S trending faults system [Zanyukov, 1971; Rozhdestvensky, 1982] which is responsible for the intense shallow seismicity of the island [e.g., *Oskorbin*, 1977; *Savostin et al.*, 1983; *Tarakamov and Kim*, 1983]. Field observations by *Rozhdestvensky* [1982] described dextral Miocene strike-slip motion along the faults. In this paper we describe both the north and the south ends of the strike-slip zone, respectively, in Sakhalin and Central Japan.

We first present a study of the strike-slip zone in Sakhalin based on the structural interpretation of Landsat images, results of field work in 1989 and 1990 along the Tym-Poronaysk fault and in the East Sakhalin Mountains, and fault plane solutions for major earthquakes since 1960 [this study; *Fukao and Furumoto*, 1975; *Dziewonski et al.*, 1985; 1987]. We confirm the conclusions of *Rozhdestvensky* [1982]: the island is a right-lateral strike-slip zone of Neogene age. Dextral motion is inferred from large-scale geological structures observed on the satellite images. Small-scale fault measurements in Neogene deposits provide maximal horizontal stress directions compatible with the dextral motion along the N-S faults. Seismological data show that the dextral motion is still active today. We propose a model of progressive strike-slip deformation with block rotations about vertical axes to explain the later shortening of the Neogene dextral en échelon basins. In a second part we infer the Miocene paleostress field from fault measurements undertaken in Noto peninsula and Yatsuo basin (central Japan, Figure 1) at the southern extremity of the Sakhalin-East Japan Sea strike-slip zone. Miocene formations recorded there the same transtensional

deformation as observed along the west coast of NE Honshu [Jolivet *et al.*, 1991]. We conclude by discussing the evolution of the strike-slip zone from the Miocene to the present, e.g., from the pull-apart opening of the Japan Sea to its present-day incipient closure.

PRESENT-DAY GEODYNAMIC SETTING

The Japan island arc lies above the old Pacific slab to the east which is subducted westward at a high rate of 10 cm/yr, and above the younger slab of the Philippine Sea Plate to the south which underthrusts Japan at a slower rate of a few centimeters per year (Figure 1) [Matsukata *et al.*, 1991]. The Philippine sea plate (PHSP)/Eurasia (EUR) rotation pole is located immediately north of the PHSP/EUR/Pacific (PAC) triple junction [Seno, 1977; Ranken *et al.*, 1984; Huchon, 1985]. The slightly oblique subduction of the PHSP in the Nankai trench is partitioned between compressional deformation in the trench and slow dextral motion along the median tectonic line (MTL) in southwest Japan. A large accretionary prism is progressively built up in the Nankai trench at the expense of trench turbidites [Le Pichon *et al.*, 1987; Le Pichon, Kobayashi *et al.*, 1992]. Close to the triple junction the Bonin arc collides with Central Japan giving rise to active thrusting north of the Izu Peninsula with a fan-shaped stress pattern [Huchon, 1985]. Active compression propagates southward inside the Bonin arc and Shikoku Basin with the formation of crustal scale shortening thrust (Zenisu ridge) [Lallemand *et al.*, 1989; Chamot-Rooke and Le Pichon, 1989].

The Pacific plate is consumed in the Bonin, Japan and Kuril trenches which are almost devoid of turbidites infill, and where fast erosion of the inner wall and tectonic erosion are the major phenomena [Cadet *et al.*, 1987a, 1987b; Von Huene and Lallemand, 1990]. A compressional stress field dominates in northeast Japan with an E-W direction of compression almost parallel to the PAC/EUR motion vector. Active shortening is observed along the eastern margin of the Japan Sea as a zone of shallow seismicity (Figure 1) with large earthquakes ($M>7.5$) evidencing E-W compression [Fukao and Furumoto, 1975] taken up by thrust faults [Tamaki and Honza, 1984; Lallemand and Jolivet, 1985]. This active deformation has been interpreted as the incipient subduction of the young Japan Sea lithosphere under northeast Japan [Nakamura, 1983]. The seismogenic zone extends northward in Sakhalin where both pure compressional and pure strike-slip events are recorded [Chapman and Solomon, 1976; Savostin *et al.*, 1983; this study]. Seismicity activity also occurs in the western part of the Japan Sea displaying dextral strike-slip events along NE trending faults in the Tsushima strait [Jun, 1990]. Within the Asian continent dextral motions along NE trending faults control the formation of pull-apart basins in the Bohai Gulf region [Chen and Nabelek, 1988].

TRANSPRESSIONAL DEFORMATION IN SAKHALIN

In order to get information at the scale of the entire shear zone located east of the Japan Sea, the precise geometry of the whole strike-slip system in Sakhalin has to be known. For this purpose we studied Landsat Thematic Mapper images with natural color on 240-mm paper at the scale of 1/1000000. The mosaic covers the entire island except the northern Schmidt peninsula (Figure 3c). Our map shows geological objects such as sedimentary layers with indication of dips, folds, faults, major volcanic intrusions and sedimentary basins. Despite a dense vegetation cover, the morphological signature of the geological formations allowed simple large-scale mapping. Working with the 1/1000000 geological map of Sakhalin [*Geology of the USSR*, 1970], it was possible to draw a large-scale geologic map consistent with our observations. The results are presented in Figure 3a, the Landsat image mosaic, Figure 3b, a data map showing the structures observed on the images, the paleo-stress field directions measured on the field and the focal mechanisms of earthquakes, and Figure 3c, an interpretative geological map. The geometry of the major dislocation, the Tym-Poronaysk fault, is detailed. Using six SPOT images we studied at a smaller scale three regions located along the Tym-Poronaysk fault (see location in Figure 3c). For each region we present a sketch of two SPOT images with its structural interpretation. In the central region, the geologic map is compiled from *K. F. Sergeyev* (unpublished data, 1980), the geologic map of Sakhalin, and our new observations.

Geological Setting

Sakhalin island is 1000 km long and 30 to 180 km wide. It is structurally divided in two parts by the Tym-Poronaysk fault that bounds to the west a central depression filled with quaternary deposits (see geological map Figure 3c). To the east of the depression, the East Sakhalin Mountains (in the north) and the Susunai metamorphic complex (in the south) display a Paleozoic basement metamorphosed during Mesozoic time, with eclogitic and high-pressure/low-temperature parageneses. The basement is overlain by a pile of Mesozoic (Jurassic-Cretaceous) deep sea sediments consisting of a folded and schistosized tectonic alternation of cherts, blackshales and basalts, described as an ancient accretionary complex [Zonenshain *et al.*, 1990; Kimura *et al.*, 1992]. These formations are cut by N-S trending faults bounding narrow basins in which Neogene sediments were unconformably deposited and later folded. To the west, the Tym-Poronaysk fault bounds the West Sakhalin Mountains, folded strata of Upper Cretaceous to Quaternary age. The thick Upper Cretaceous (Cenomanian to Danian) sequence lays unconformably over a Paleozoic and Mesozoic basement similar to that of the East Sakhalin mountains [Melnikov and Zakharova, 1977; Melnikov, 1987; Melnikov and Rozhdestvensky, 1989]. Three transgressive cycles are recognized during the Late Cretaceous in the northern part of the west Sakhalin basin (Figure

4), with deepening sequences of terrigenous deposits showing successively coal-bearing continental deposits, sandstones and claystones. The base of the Paleogene is marked by a conglomerate of variable thickness (up to 600 m), overlain by two transgressive sequences of terrigenous deposits, with a thick volcanogenic layer at the top (Takaradaï and Maruyama formations). To the east of the Tym-Poronaysk fault (Figure 4) the Neogene deposits lay directly on the Paleozoic-Mesozoic basement as shown by drilling in the central Neogene-Quaternary depression [Rozhdestvensky, 1982]. The Cretaceous sequence to the west and Neogene formations to the east are in contact across the fault. Basic sills and dykes of Neogene age are emplaced in the vicinity of the fault.

An E-W synthetic cross section of Sakhalin island is presented in Figure 5 after Rozhdestvensky [1982], Pushcharovskiy *et al.* [1983], and our field observations (see location of the cross section in Figure 3c). The Tym-Poronaysk fault is localized along the boundary between a Mesozoic accretionary complex to the east and a sedimentary basin of Upper Cretaceous age to the west. The sedimentary Upper Cretaceous and Cenozoic sequence in this basin is about 10 km thick. The Tym-Poronaysk fault might have reworked an inherited Cretaceous structure as a strike-slip reverse fault.

Seismic data show that the off shore structure in the vicinity of the island is similar to the onland structure. Along the east coast of Sakhalin Gnibidenko and Svarichevsky [1984] and Gnibidenko [1985] described N-S trending faults parallel to the Tym-Poronaysk fault. The northeast coast of Sakhalin is limited by off shore faults several hundred kilometers long, bounding narrow basins filled with Cenozoic sediments more than 5000 m thick. The southwest coast is bordered by the West Sakhalin fault parallel to the Tym-Poronaysk fault, and which is observed onland in Boshnyakovo region (Figures 2 and 3c). Along this coast Antipov *et al.* [1979] described en échelon narrow basins with a north-northeast trend filled with 2000-m-thick middle Miocene and younger sediments. Such basins similar to these described by Lallemand and Jolive [1985] along the northwest coast of Honshu may be interpreted as dextral en échelon structures associated with the West Sakhalin fault.

Active Strike-Slip Motion Along the Tym-Poronaysk Fault

The Tym-Poronaysk fault is seismically active and has caused most of the onland main earthquakes of Sakhalin [Oscorbin, 1977; see Chapman and Solomon, 1976; Savostin *et al.*, 1983]. In contrast, the faults cutting through the East Sakhalin Mountains are seismically inactive. Fault plane solutions (Table 1) of shallow earthquakes (depth less than 30 km) determined in this study (by L. S. Oscorbin), Fukao and Furumoto [1975], and centroid moment tensors determined by Dziewonski *et al.* [1985, 1987] are plotted in Figure 3b. The focal mechanisms were determined by utilizing *P* wave first motions detected by a Soviet regional seismological network. The radius of the focal mechanisms is a function of the magnitude (surface waves) of the earthquakes except for those taken from Dziewonski *et al.*

[1985, 1987] which are kept constant in size. When two focal mechanisms were determined for an earthquake and its aftershock, we only plotted the focal mechanism corresponding to the main event. The two centroid moment tensors determined by *Dziewonski et al.* [1985, 1987] correspond to two earthquakes whose fault plane solutions have independently been determined in this study (for simplicity we only indicate our epicenter locations). The *P* axes are almost similar in both cases, and the *T* axes of the *Dziewonski et al.* [1985, 1987] focal mechanisms are steeper so that they indicate compressional motion when ours indicate strike-slip motion.

Most of the mechanisms determined along the Tym-Poronaysk fault evidences dextral strike-slip motion on the fault. The same observation applies to the West Sakhalin fault which parallels the Tym-Poronaysk fault along the western coast. Focal mechanisms of the northern offshore earthquakes are not consistent with onshore focal mechanisms; they are not even internally consistent and are not clearly related to surface structures. *Savostin et al.* [1983] saw evidence of dextral motion along NNW trending faults in this region. At island scales, two categories of focal mechanisms are represented: strike-slip ones essentially located in the vicinity of the Tym-Poronaysk fault and consistent with dextral motion along it, and compressional ones evidencing E-W shortening taken up along N-S trending faults. We therefore conclude that Miocene transpressional dextral strike-slip motion continues at present in Sakhalin.

Assuming that the regional stress field is simple and does not show major local variations of the directions of the principal stress axes, *P* and *T* axes plotted on a stereographic projection may be used to infer a regional stress tensor (Figure 6). Hereafter, σ_1 , σ_2 , and σ_3 will refer to the principal axes of the stress tensor, with $\sigma_1 > \sigma_2 > \sigma_3$. The best *P* and *T* axes directions determined with the right dihedra method [*Angelier and Mechler*, 1977] are assumed to be σ_1 and σ_3 , respectively. The result shows σ_1 almost horizontal and trending ENE-WSW. Directions and dips of σ_2 and σ_3 are poorly constrained as both compressional and strike-slip focal mechanisms co-exist. Though it is questionable in general that a small number of focal mechanisms can be used to compute a mean regional stress tensor, the result we obtain is very similar to the results of fault sets analysis undertaken in Sakhalin and described later, with roughly the same trend of σ_1 though sometimes more northerly. This suggests that both Miocene and present-day seismic deformation patterns were governed by a similar overall stress field. However, there is a possibility that σ_1 rotated slightly clockwise toward a more latitudinal orientation, as we will discuss later.

Neogene Strike-Slip Deformation Along the Tym-Poronaysk Fault

The Tym-Poronaysk fault is the major geological feature of Sakhalin. It is 600 km long and disappears to the north under Quaternary deposits and to the south in the La Pérouse Strait between Sakhalin and Hokkaido. It extends in Hokkaido as the Horonoba fault and the

Hidaka mountains [Kimura *et al.*, 1983; Jolivet and Miyashita, 1985]. In Sakhalin, the fault trends roughly N-S, bracketed between 142°E and 143°E. The fault trace consists of a succession of nearly linear segments, the longer ones trending N160°E to N180°E are shifted dextrally by shorter ones trending N010°E to N045°E (Figures 3b and 3c). The ratio of long and short segments determines the mean trend of the fault: N-NW from north of the island to Poronaysk city in the central part with only three short N010°E to N045°E trending segments (Figure 3c), and N-NE to the south with many dextrally shifting short segments. Bedding traces are parallel to the long segments and are strained by dextral shear along the short ones. This is observed in the Yuzhno-Sakhalinsk region to the south, and in the Poronaysk region in the central part of the island (Figures 3b and 3c). The same geometry is observed with the axes of en échelon folds affecting the whole sedimentary section (upper Cretaceous to upper Miocene) on each side of the fault. The fold axes trend N140°E to N180°E, roughly parallel to the long segments of the fault, and are strained by dextral shear along the short segments. There is a single exception in the Vostochnyy region where a fold trends northwesterly. This fold could be older than the others as it affects only Cretaceous and Paleogene formations. Figure 7 shows a detail of the Landsat image of the southwestern peninsula of the island. Four dextral en échelon folds in Miocene formations are strained by dextral shear along the Tym-Poronaysk fault. Neogene deposits of northern Sakhalin are affected by similar N-NW trending folds [Rozhdestvensky, 1982, 1986]. The fold axes direction provides an east-northeast (N050°E to N090°E) trend of maximal horizontal stress, which is consistent with dextral motion along the Tym-Poronaysk fault, as well as the dextral en échelon pattern of the folds and their sigmoidal shape. In the field, the fault is a steep structure dipping sometimes to the east and to the west, always showing a reverse motion component. This is illustrated in Figure 8 with compressive structures, drag folds, and ramp and flat structures in Cretaceous formations along the fault. The overall structure, a N-S strike-slip fault with a reverse component associated with N140°E to N180°E trending folds, results from deformation in a transpressional regime along the N-S discontinuity, with $\sigma_{Hmax} = \sigma_1$ trending E-NE (σ_{Hmax} is the maximal horizontal stress). The deformation is partitioned between pure compression along the N160°E to N180°E segments, and almost pure strike-slip shear along the N010°E to N045°E segments.

To the north, in the Aleksandrovsk-Sakhalinskiy area, two dextral en échelon Miocene basins trend NNE (Figure 3c). These basins are similar to those described below in the East Sakhalin Mountains and are consistent with Miocene dextral motion along the Tym-Poronaysk fault. As we will see later, the formation of these basins preceded their sublatitudinal shortening. Assuming that they formed parallel to σ_{Hmax} as for extensional cracks, their present trends provide a direction for σ_{Hmax} between N000°E and N030°E. Thus the maximal horizontal stress apparently rotated clockwise during the late Miocene from N000-N030°E to N050-N090°E. The significance of this apparent rotation will be discussed later.

Our interpretation of the SPOT images of the Yuzhno-Sakhalinsk region in the southern part of the fault (location in Figure 3c), is shown in Figure 9. The city is located in the central Quaternary depression (Figure 3c) bounded to the east by the Susunai metamorphic complex and to the west by the Tym-Poronaysk fault. The fault, parallel to bedding traces in its northern part, is twice shifted dextrally by NE trending segments in the vicinity of Yuzhno-Sakhalinsk and obliquely cut Cretaceous formations (Figure 3c). Dextral shear is also observed along a NE trending fault in the Susunai metamorphic complex to the east, where lineaments, probably representing the surface traces of the metamorphic foliation, are curved in a dextral sigmoid.

Figure 10 shows the interpretation of the two northern SPOT images along the fault (see location in Figure 3c). The sharpness of the Tym-Poronaysk fault is pronounced to the south, along the NE trending segment cutting through Lower Late Cretaceous formations. The hanging wall to the west shows degraded triangular facets evidencing recent activity.

Small-scale field work was undertaken in the central region located on the east coast of the island, between Gastello and Vostochnyy (SPOT images detailed in Figures 11a, 11b, and 11c, location on Figure 3c). On the SPOT images, the most prominent feature is the Santonian-Campanian cuesta marked by the thick terrigenous Campanian deposits to the west (see Figure 11c). To the south this limit makes the Vostochnyy fold (NE trending axis) stand out on the images. To the west, the discordance of the Paleogene basal conglomerate (Figure 12a) onto Cretaceous strata is clearly observed on the images: the conglomerate cuts through the underlying Cretaceous bedding traces. Along the east coast the Tym-Poronaysk fault is a sharp feature particularly clear in its southern part where it divides the relief of Miocene terrigenous and volcanic formations to the east from a depression filled with Cretaceous argilites (Bikov formation) to the west. As already noticed on the Landsat images, the Tym-Poronaysk fault consists of long roughly N-S segments dextrally shifted by short NE trending segments. Evidence for dextral Miocene motion along the fault is especially remarkable in the north where three en échelon folds in Miocene formations are strained by dextral shear. A similar fold in the Neogene Kholmsk formation is shown in Figure 12b outcropping along the coast line, south of Yuzhno-Sakhalinsk. Figure 13 shows two cross sections through the Tym-Poronaysk fault (see location of the cross sections in Figure 11c): the folds close to the fault evidence the transverse shortening associated with strike-slip motion (see also Figure 10c showing vertical Miocene sedimentary beds). The upper Miocene and Pliocene deposits are weakly folded and the younger part of the section (the late Miocene-Early Pliocene Maruyama formation) is even less folded with limbs dipping not more than 20°. Thus these folds experienced a continuous deformation during the Miocene and the Pliocene. Three Quaternary terraces are superimposed on the west coast of the island, the highest one (probably 500,000 years old by analogy with Hokkaido) is about 500 m high, and there is only one low terrace or no terrace at all on the east coast. This is an indicator of relative uplift of the west coast with respect to the east coast. The Tym-Poronaysk fault is

likely to localize relative motion between the east and the west coasts, which would imply an intense Quaternary activity with a high reverse component of motion [Zakharov and Yakushko, 1972]. However, it was not possible to observe whether the Quaternary marine terraces are folded or not. In some places the Tym-Poronaysk fault splits in several parallel segments and could be the surface manifestation of a deep compressional flower structure. Volcanic rocks mapped in Figure 11b were emplaced during the Miocene as dykes and sills in the vicinity of the fault, with a NNE trending direction slightly oblique to the fault, compatible with dextral shear along it. Large sills in Cretaceous formations are also mapped in Figure 11a. These sills make the topographic crests and determine the geometry of the hydrographic network. One such sill is shown in Figure 12c in Miocene deposits.

Volcanic rocks recorded well the brittle deformation and are good candidates for stress orientation measurements along the Tym-Poronaysk fault in both Cretaceous and Miocene formations. Four stereograms used to calculate the paleostress field directions plotted in Figure 12c are shown in Figure 14. The tensor analysis follows the method developed by Angelier [1984]. In the field we mostly observed compatible strike-slip and reverse faults. The direction of σ_1 is bracketed between N050°E and N090°E and it is always perpendicular to the fold axes. We therefore assume that the measured stress field is associated with folding. The sites TPF7, TPF8 and TPF9 are located on an almost pure strike-slip segment of the fault, along which the fold axes are curved and suffered at least a 30° clockwise rotation (Figures 12c). The σ_1 rotated clockwise with the fold axes near the fault. Thus the true trend of σ_1 associated with folding is likely to be bracketed between N020°E and N060°E. The superposition of two distinct stress fields discernable chronologically was seldom observed. When observed, it showed that σ_1 was always horizontal and trended first E-W and secondly NE-SW, which can be accommodated by a progressive clockwise rotation of structures under a single stress field with σ_1 trending NE-SW. This NE-SW trend is consistent with dextral strike-slip motion along the Tym-Poronaysk fault.

Paleostress fields inferred from fault measurements undertaken in other parts of the island are plotted in Figure 3b and the corresponding stereo plots are shown in Figure 15. We first focus on the southeast peninsula of the island northeast of Aniwa bay where faults were measured in Jurassic, Cretaceous and Paleogene rocks (see geological map in Figure 3c). Two sites (T3 and T5) have recorded two successive episodes with roughly perpendicular σ_1 (site T4 also recorded two successive episodes but it is disturbed by the emplacement of a Paleogene granite in its vicinity). No obvious chronology has been observed in the field; the chronology given in Figure 3c is based on the study area being analogous to NE Japan [Jolivet et al., 1990]. Figure 15 illustrates phase separation for the three sites T3, T4 and T5. Phase 1 has σ_1 trending N020°E in good agreement with most of the sites of the peninsula, and also with direction of σ_1 determined in the central region (see above). If we generalize these observations to the whole island, it is possible to interpret all the computed paleo-stress-directions in one single stress system with horizontal σ_1 trending NE-SW, and with local

rotations along the Tym-Poronaysk fault. Phase 2 with σ_1 roughly E-W can be related either to late sublatitudinal shortening as observed in Hokkaido [Jolivet et al., 1990] or to local rotations as observed along the Tym-Poronaysk fault.

Geometry of the Neogene Strike-Slip Deformation in the East Sakhalin Mountains

In the East Sakhalin Mountains three parallel submeridian en échelon faults cut through the Paleozoic and Mesozoic basement (Figures 3b and 3c): from west to east they are the Central, Pribrezhnaya (coastal) and Liman (estuarine) faults [Rozhdestvensky, 1982]. These faults are well expressed on the Landsat images in their northern parts (see a detail of the Landsat mosaic in Figure 16) as they put into contact contrasted lithological formations, a high block to the west made of Mesozoic rocks cut by deep valleys, and a low one to the east made of Neogene deposits with smooth topography. The faults are indeed bordered to the east by narrow basins with a NNE trend, filled with Miocene and Pliocene deposits overlying unconformably the Paleozoic and Mesozoic basement [Rozhdestvensky, 1982]. The present trends of the basins (N000°E to N030°E), assumed to be parallel to the maximal horizontal stress direction, and their dextral en échelon pattern are consistent with dextral strike-slip motion along N-S faults. A Neogene pull-apart basin along the Central fault is also an indicator of dextral motion, and to the south the sigmoidal shape of the Mesozoic crests between the Pribrezhnaya and the Liman fault supports dextral shear along these faults. The three faults therefore experienced dextral strike-slip motion with a normal component in Neogene time. An evaluation of the displacement along the Central fault is given by the 25-km offset of the metamorphic complex in the southern part of the fault (Figure 3c). The Langeri graben (Figure 16) is filled with Mio-Pliocene formations up to 600 m thick lying unconformably either on Paleozoic or Mesozoic rocks [Rozhdestvensky, 1982]; the Miocene deposits are folded and stand almost vertically on the east side of the basin. A late sublatitudinal shortening thus affected the Miocene basin. Similar observations are made along the southern coast of the Aniva peninsula to the south, where the Mesozoic basement was thrusted eastward over Paleogene basins folded into synclines (cross sections of Melnikov and Rozhdestvensky [1989], and Rikhter [1986]).

North of the East Sakhalin Mountains, the submeridian Gyrgylan'i-Ossov, Ekhabi-Pil'tun and Okha faults continue the above described structures until the Schmidt Peninsula through Neogene formations. We observed on the Landsat images that the northern part of the Gyrgylan'i-Ossov fault shifts dextrally a ridge for about 10 km (Figure 3b). According to Rozhdestvensky [1982], en échelon folds with sigmoidal bends evidence dextral motion along these faults. In the Schmidt Peninsula the Cretaceous-Neogene contact is dextrally offset by a strike-slip fault for 5.5 km, and another strike-slip fault cut through Neogene sediments with a displacement of up to 7 km [Rozhdestvensky, 1982]. A summation of the strike-slip offsets of

faults from the East Sakhalin Mountains to the Schmidt peninsula therefore gives a minimum value of dextral N-S relative motion of about 50 km since Miocene time.

Discussion: Progressive Strike-Slip Deformation From Miocene to Present

The observations made at all scales reveal the juxtaposition and succession in time and space of pure strike-slip structures, pure compressional structures, and extensional structures. At island scales, the western side of the Tym-Poronaysk fault is characterized by en échelon folds and the fault itself has a thrust component which indicates a transpressional regime along 600 km from south to north. While the Upper Cretaceous to Neogene sediments on the west side of the fault displays a distributed deformation symptomatic of a relatively soft medium, the more competent Mesozoic basement on the eastern side of the fault displays en échelon narrow basins localized along strike-slip faults (in the East Sakhalin Mountains), which had been in turns folded showing an apparent rotation of σ_1 . Small-scale observations shows that compression is always perpendicular to the fold axes and that the E-W compression seen in the microtectonic analyses is the result of clockwise rotations close to the Tym-Poronaysk fault. Thus at this scale, only one stress regime is required. It is possible to reach the same conclusion at the scale of the island with large-scale structures.

The overall structure of the East Sakhalin Mountains can be described as a domino system in a shear zone between two master faults, the Tym-Poronaysk fault to the west and an offshore fault observed on seismic data along the northeast coast of Sakhalin to the east [Gnibidenko and Svarichevsky, 1984; Gnibidenko, 1985], the Central, Pribrezhnaya, and Liman faults being cross faults which bound crustal blocks (Figure 17). Such geometry implies block rotations about vertical axes [Ron et al., 1984; Nur et al., 1986; Scotti et al., 1991]. Assuming that the cross faults appear first as extensional cracks parallel to $\sigma_{H\max}$ and are later rotated, the sense of rotation depends upon the sign of the stress tensor component perpendicular to the plane of the master faults. An overall transtensional stress field would lead to a widening of the shear zone and favors clockwise rotation of blocks accommodated by sinistral motion along the cross faults. Extra space in the shear zone would be accommodated by the formation of grabens along the cross faults. However, if transpression prevails, the shear zone tends to narrow and counterclockwise rotations will be accommodated by dextral motion along the cross faults. E-W shortening will be taken up by counterclockwise rotations of the blocks and compressional structures along their borders. Applying this model to the East Sakhalin Mountains where the stress regime is transpressional and the cross faults are dextral, we should expect counterclockwise rotations of the dominos.

The evolution of the East Sakhalin Mountains can be explained as follows: the narrow basins first formed along the cross faults which were parallel to the maximum horizontal stress and then later progressively rotated in a counterclockwise manner. The trend of the

basins thus becomes oblique to the maximum horizontal stress and they were subjected to shortening and folding. *Takeuchi et al.* [1992] recently presented paleomagnetic results from Hokkaido and southern Sakhalin, including several sites on the western side of the Tym-Poronaysk fault. They obtained Middle to Late Miocene dextral rotations, compatible with the progressive dextral shear of the fold axes along the fault. They unfortunately have no data from the East Sakhalin Mountains, so the block model there cannot be tested with the paleomagnetic results obtained so far. The expected counterclockwise rotations are however small and might not be easily detected.

Figure 17 shows the precise geometry imposed by this model. Figure 17a shows the simplified fault pattern in Sakhalin, which is isolated from the coast lines in Figure 17b. The continuity of geological structures in western Sakhalin shows that this region behaved as a single elongated block between the West Sakhalin fault and the Tym-Poronaysk fault. Continuous strain within the block was accommodated by en échelon folds leading to oblique shortening. In the East Sakhalin mountains, however, the basement was cut by several parallel faults and was divided into several dominos which we predict have rotated counterclockwise. Figure 17c is a simplification of the fault pattern with a block model. The E-W shortening coeval with dextral strike-slip involves a component of thrusting along the blocks boundaries, since the total width of the shear zone decreases. One can see that the counterclockwise rotation of blocks along the dextral cross faults can lead to the distribution of pure strike-slip segments and mostly compressional segments actually observed along the Tym-Poronaysk fault. This geometry can be obtained provided that some of the cross faults can be connected to some of the dextral offsets along the Tym-Poronaysk fault through the basement under the Quaternary depression as shown in Figure 17b.

The observed clockwise rotations of fold axes caused by dextral simple shear along the Tym-Poronaysk fault can explain the E-W direction of compression deduced from fault set analysis: σ_1 was initially NE-trending and has been rotated with the rocks. The block model with counterclockwise rotations in the East Sakhalin Mountains can explain the apparent succession of tectonic stages (basins formation followed by transverse shortening) in the single transpressional stress field [*Scotti et al.*, 1991]. This model integrates in a single stage a succession of superimposed structures of various style and explains the geometry of the Tym-Poronaysk fault, but it still needs to be tested with paleomagnetic data. However, we cannot eliminate the possibility of a change in stress conditions from σ_1 trending NE-SW to nearly E-W (see Figure 2).

TRANSTENSIONAL DEFORMATION IN NOTO PENINSULA AND YATSUO BASIN

We have described Sakhalin Island as a Neogene N-S dextral strike-slip zone. This continues to the south in the Hidaka Mountains (Hokkaido) reworking a major Mesozoic suture zone that localized part of the strain during the Cenozoic [*Kimura et al.*, 1983]. Strike-

slip ductile deformation in high-temperature conditions [*Jolivet and Miyashita*, 1985] during late Oligocene and early Miocene is associated with en échelon folds and thrusts in the upper brittle crust [*Jolivet and Huchon*, 1989]. Fault set analysis in lower and middle Miocene formations provides a direction of horizontal compression compatible with folding that trends NE-SW. The same dextral transpressional stress field therefore characterizes Sakhalin and Hokkaido during the early and middle Miocene.

Further south Miocene strike-slip extends along the eastern margin of the Japan Sea. It is distributed in a transition zone between the oceanic crust of the Japan Sea basin and the continental crust of the Japan arc. It is expressed offshore by dextral en échelon basins with a NNE trend [*Lallemand and Jolivet*, 1985; *Tamaki*, 1988; *Jolivet et al.*, 1991] and onland by the dextral transtensional deformation described by *Otsuki* [1989, 1990] and *Jolivet et al.* [1991], distributed all along the west coast of NE Honshu down to Sado island to the south. *Yamaji* [1990] described basins in the Uetsu district (along the west coast of NE Honshu) formed between 18 and 15 Ma with the same dextral en échelon pattern. To the south the Tanakura Tectonic Line (Figure 2) localized part of the dextral motion during the Miocene [*Otsuki and Ehiro*, 1978; *Koshiya*, 1986].

The transition from transpression to transtension is observed at the latitude of southwest Hokkaido. In order to see the transition between the dextral shear zone and the southern extensional margin of the Japan Sea [*Tamaki*, 1988], we studied the brittle deformation in Noto peninsula and Yatsuo basin (Figure 18) at the southeast corner of the Japan Sea (see location in Figure 1). Volcanic and pyroclastic rocks of Miocene age observed in Noto peninsula and Yatsuo basin lay directly on the Upper Cretaceous basement. Upper Miocene formations did not record any significant brittle deformation. Lower and middle Miocene formations are affected by conjugate strike-slip faults associated with compatible normal faults: fault sets analysis provides a direction of maximal horizontal compression trending N030°E associated with a perpendicular extension (Figure 18). On a regional scale, the Yatsuo basin is bordered to the east and to the south by large normal faults that probably have some strike-slip component in this transtensional context. The middle Miocene transtensional deformation corresponds to a late stage of opening of the Japan Sea.

Our results are in agreement with previously published paleostress fields [*Otsuki*, 1989, 1990; *Jolivet et al.*, 1991] determined along the eastern margin of the Japan Sea from northern Honshu to Sado island: we observed in Noto peninsula and Yatsuo basin the same association of strike-slip and normal faults as in Sado, with similar principal stress directions. The same transtensional conditions prevailed all along the margin during opening of the Japan Sea and the deformation of the strike-slip margin continued during oceanic accretion.

DISCUSSION AND CONCLUSIONS

Nakamura and Uyeda [1980] showed that stress regime evolved in NE Japan during late Miocene from an extensional regime with $\sigma_{Hmax} = \sigma_2$ trending NNE to a compressional regime with $\sigma_{Hmax} = \sigma_1$ trending E-W. The late E-W compression is recorded in late Miocene and Pliocene rocks [*Yamagishi and Watanabe*, 1986; *Jolivet and Huchon*, 1989]: it is related to an uplift of western northeast Japan since 10 Ma [*Sugi et al.*, 1983; *Jolivet and Tamaki*, 1992]. The offshore Miocene extensional structures have been reworked as compressional ones [*Tamaki and Honza*, 1984; *Tamaki*, 1988], and *Tamaki et al.* [1992] showed that thrusting and convergence along the eastern margin began 1.8 Ma ago. The margin is seismically active and focal mechanisms of earthquakes indicate compression along N-S reverse faults [*Fukao and Furumoto*, 1975; *Tamaki*, 1988](see also Figure 3 of *Jolivet et al.* [1992]).

The stress field and the associated deformation evolved along the strike-slip zone (Figure 2). In early and middle Miocene time the stress field was transpressional to the north in Sakhalin and Hokkaido, and transtensional to the south where the Japan Sea opened behind the Pacific subduction zone. During the late Miocene the stress orientation changed: in the south σ_{Hmax} rotated clockwise from NE-SW to E-W (we have seen before that we do not necessarily need a rotation of σ_{Hmax} in Sakhalin), and σ_{Hmax} became σ_1 all along the strike-slip zone. In the Japan arc the recent deformation is purely compressional with folds and reverse faults, while dextral motion is still active in Sakhalin. We therefore observe a different behavior between the northern intra-continental part of the strike-slip zone, transpressional since the Late Oligocene, and the southern part neighboring the subduction zone. The Japan Sea opened in a transtensional regime when the subduction boundary was stress-free. It began to close when subduction imposed a compressional regime perpendicular to the trenches [*Nakamura and Uyeda*, 1980] probably linked with the inception of subduction of the young oceanic lithosphere of the Philippine sea plate under the Japan arc during the late Miocene [e.g., *Jolivet et al.*, 1989]. The geometry of the strike-slip zone is controlled by the variations of stress regime in the back arc region due to changing geodynamic conditions along the subduction zone. Thus the extensional component of the Japan Sea opening is likely to have been provided by back arc rifting probably due to trench retreat [*Chase*, 1978; *Molnar and Atwater*, 1978; *Uyeda and Kanamori*, 1979], and the strike-slip component is linked to some other mechanism such as the India-Asia collision as discussed by *Kimura and Tamaki* [1986] and *Jolivet et al.* [1990] (Figure 19). The model presented by *Jolivet et al.* [1990] is derived from *Davy and Cobbold's* [1988] experiments: it involves a wide left-lateral shear zone connecting the Pamir-Tien Shan ranges to the Baikal-Stanovoy regions which evolves from transpression to transtension. In the transtensional domain left-lateral shear is accommodated by rotation of large-scale dominos and dextral motion between them. An additional component can be added: the North America-Eurasia pole of rotation is located in east Siberia

between the Laptev Sea and the Okhotsk Sea [Chapman and Solomon, 1976; Savostin *et al.*, 1983; Cook *et al.*, 1986] and has always been in this region since the early Eocene. This situation leads to extensional strain north of the rotation pole along the Nansen Ridge and Lena river mouth, and compressional strain south of it. The compression might be partly taken up by the southeastward extrusion of the Okhotsk block producing transpressional dextral shear in Sakhalin [Jolivet, 1986; Riegel *et al.*, 1993].

To conclude, the Sakhalin-NE Japan strike-slip zone is a 2000-km-long crustal scale structure that penetrates inside Asia to the north and has guided the opening of the Japan Sea to the south along the Pacific subduction zone. Jolivet and Tamaki [1992] presented new reconstructions of the opening of the Japan Sea that allow a crude quantification of the finite dextral offset since 25 Ma: at least 400 km of relative motion are necessary to accommodate the opening (Figure 20). It seems unlikely that this large offset has been accommodated only by the Tym-Poronaysk fault: most of the offset was probably taken up by offshore faults in the Tartary strait between Sakhalin and mainland Asia where the crust is the thinnest, and further south along the transition from continental (NE Japan arc) to oceanic crust (Japan basin).

In NE-Asia, dextral motion associated with extension is also evidenced by Chen and Nabelek [1988] along the Tanlu fault in the Bohai Gulf (Figure 19). It is not yet possible to quantify the total amount of dextral offset taken up along the eastern border of Asia at the latitude of Japan during Neogene, but a minimum of 400 to 500 km is likely. This makes this cluster of dextral shear zones a first-order feature of Asia, as important as the Altyn Tagh fault or the Red River fault which accommodated also several hundreds of kilometers of left-lateral offset during Cenozoic (Figure 19) [Tapponnier and Molnar, 1977; Tapponnier *et al.*, 1990]. If the strike-slip deformation is mostly localized along left-lateral faults immediately north and east of Tibet, close to the Indian indenter, it is mostly accommodated by dextral motion along antithetic N-S trending faults far from the indenter near the Pacific subduction. This emphasizes the role played by the Pacific subduction as an active extensional boundary, and implies that the geometry of deformation in Asia is controlled by two equally important lateral conditions: shortening along the Himalaya, and extension along the western Pacific subduction.

Acknowledgments. This work was funded by a CNRS-INSU grant (DBT 5-06) and supported by the Institute of Marine Geology and Geophysics, Yuzhno-Sakhalinsk. We are very grateful to K. Fujita for his constructive review. We thank Jacques Angelier for allowing us to use his brittle deformation analysis software. We are also grateful to O. A. Melnikov and V. S. Rozhdestvensky for their introduction to Sakhalin geology, and especially to Rima Kovalenko and Tania Godounova for their indispensable help in Sakhalin and Moscow. Special thanks are due to G. Marquis who kindly improved the english of the manuscript.

REFERENCES

- Angelier, J., Tectonic analysis of fault slip data sets, *J. Geophys. Res.*, 89, 5835-5848, 1984.
- Angelier, J., and P. Mechler, Sur une méthode graphique de recherche des contraintes principales également utilisable en tectonique et en sismologie, la méthode des dièdres droits, *Bull. Soc. Géol. France*, 19, 1309-1318, 1977.
- Antipov, M. P., V. M. Kovylin, and V. P. Filat'yev, Sedimentary cover of the deepwater basins of Tatar strait and the northern part of the sea of Japan, *Int. Geol. Rev.*, 22(11), 1327-1334, 1979.
- Briais A., P. Patriat and P. Tapponnier, Updated interpretation of magnetic anomalies and seafloor spreading stages in the South China Sea: implications for the tertiary tectonics of southeast Asia, *J. Geophys. Res.*, 98, 6299-6328, 1993.
- Cadet, J. P., et al., Deep scientific dives in the Japan and Kuril trenches, *Earth Planet. Sci. Lett.*, 83, 313-328, 1987a.
- Cadet, J. P., et al., The Japan trench and its juncture with the Kuril trench, cruise results of the Kaiko project, Leg 3, *Earth Planet. Sci. Lett.*, 83, 267-284, 1987b.
- Chamot-Rooke, N., and X. Le Pichon, Zenisu ridge: Mechanical model of formation, *Tectonophysics*, 160, 175-194, 1989.
- Chapman, M.C., and S. C. Solomon, North American-Eurasian plate boundary in northeast Asia, *J. Geophys. Res.*, 81, 921-930, 1976.
- Chase, C. G., Extension behind island arcs and motion relative to hot-spots, *J. Geophys. Res.*, 83, 5385-5387, 1978.
- Chen, W. P., and J. Nabelek, Seismogenic strike-slip faulting and the development of the North China basin, *Tectonics*, 7, 975-989, 1988.
- Cobbold, P.R. and P. Davy, Indentation tectonics in nature and experiments, 2, Central Asia, *Bull. Geol. Instit. Univ. Uppsala*, 14, 143-162, 1988.
- Cook, D.B., K. Fujita, and C. A. Mac Mullen, Present day plate interactions in northeast Asia: North America, Eurasian and Okhotsk plates, *J. Geodyn.*, 6, 33-51, 1986.
- Curry, M. P., D. G. Moore, L. Lawver, F. J. Emmel, R. W. Raitt, M. Henry, and R. Kieckhefer, Tectonics of the Andaman Sea and Burma, Geological and Geophysical Investigations of Continental Margins, edited by J. S. Watkins, L. Montadert, and P. Dickerson, *AAPG Mem.*, 29, 189-198, 1979.
- Davy, P., and P. R. Cobbold, Indentation tectonics in nature and experiments. Experiments scaled for gravity, *Bull. Geol. Instit. Univ. Upsalla*, 14, 129-141, 1988.
- Dziewonski, A. M., J. E. Franzen, and J. H. Woodhouse, Centroid-moment tensor solutions for October-December 1984, *Phys. Earth Planet. Inter.*, 39, 147-156, 1985.
- Dziewonski, A. M., G. Ekstrom, J. E. Franzen, and J. H. Woodhouse, Global seismicity of 1979: centroid-moment tensor solutions for 524 earthquakes, *Phys. Earth Planet. Inter.*, 48, 18-46, 1987.

- England, P. and P. Molnar, Right-lateral shear and rotation as the explanation for strike-slip faulting in eastern Tibet, *Nature*, 344, 140-142, 1990.
- Fukao, Y. and M. Furumoto, Mechanisms of large earthquakes along the eastern margin of the Japan Sea, *Tectonophysics*, 25, 247-266, 1975.
- Geology of the USSR, vol. 33, *Sakhalin Geological Description*, 431 pp., Nedra, Moscow, 1970.
- Gnibidenko, H.S., The Sea of Okhotsk-Kuril islands ridge and Kuril-Kamchatka trench, in *The Ocean Basins and Margins*, vol. 7A, edited by A.E.N. Nairn, F.G. Stehli and S. Uyeda, pp. 377-418, Plenum, New York, 1985.
- Gnibidenko, H.S., and A. S. Svarichevsky, Tectonics of the south Okhotsk deep-sea basin, *Tectonophysics*, 102, 225-244, 1984.
- Holt, E. H., J. F. Ni, T. C. Wallace, and A. J. Haines, The active tectonics of the eastern Himalayan syntaxis and surrounding regions, *J. Geophys. Res.*, 96, 14,595-14,632, 1991.
- Huchon, P., Géodynamique de la zone de collision d'Izu et du point triple du Japon Central, thèse de doctorat, 414 pp., Univ. Pierre et Marie Curie, Paris, 1985.
- Jolivet, L., America-Eurasia plate boundary in eastern Asia and the opening of marginal basins, *Earth Planet. Sci. Lett.*, 81, 282-288, 1986.
- Jolivet, L., and P. Huchon, Crustal scale strike-slip deformation in Hokkaido, Northeast Japan, *J. Struct. Geol.*, 11, 509-522, 1989.
- Jolivet, L., and S. Miyashita, The Hidaka Shear Zone (Hokkaido, Japan): Genesis during a right-lateral strike slip movement, *Tectonics*, 4, 289-302, 1985.
- Jolivet, L., and K. Tamaki, Neogene kinematics in the Japan Sea region and volcanic activity of the northeast -Japan arc, edited by Tamaki et al., *Proc. Ocean Drill. Program, Sci. Results*, 127/128, 1311-1331, 1992.
- Jolivet, L., P. Huchon, and C. Rangin, Tectonic setting of Western Pacific marginal basins, *Tectonophysics*, 160, 23-47, 1989.
- Jolivet, L., P. Davy, and P. Cobbold, Right-lateral shear along the northwest Pacific margin and the India-Eurasia collision, *Tectonics*, 9, 1409-1419, 1990.
- Jolivet, L., P. Huchon, J.P. Brun, N. Chamot-Rooke, X. Le Pichon, and J.C. Thomas, Arc deformation and marginal basin opening, Japan Sea as a case study, *J. Geophys. Res.*, 96, 4367-4384, 1991.
- Jolivet, L., M. Fournier, P. Huchon, V. S. Rozhdestvensky, K. F. Sergeyev, and L. Oscrbin, Cenozoic intracontinental dextral motion in the Okhotsk-Japan Sea region, *Tectonics*, 11, 968-977, 1992.
- Jun, M.S., Source parameters of shallow intraplate earthquakes in and around the Korean peninsula and their tectonic implication, *Acta Univ. Ups. Abstr. Uppsala Diss. Fac. Sci.*, 285, 16, 1990.

- Kaneoka, I., K. Notsu, Y. Takigami, K. Fujioka, and H. Sakai, Constraints on the evolution of the Japan Sea based on 39Ar-40Ar ages and Sr isotopic ratios for volcanic rocks of the Yamato seamount chain in the Japan Sea, *Earth Planet. Sci. Lett.*, 97, 211-225, 1990.
- Kimura, G., and K. Tamaki, Collision, rotation and back arc spreading: The case of the Okhotsk and Japan Seas, *Tectonics*, 5, 389-401, 1986.
- Kimura, G., S. Miyashita, and S. Miyasaka, in *Collision Tectonics in Hokkaido and Sakhalin, Accretion Tectonics in the Circum Pacific Regions*, edited by M. Hashimoto and S. Uyeda, pp. 117-128, Terrapub, Tokyo, 1983.
- Kimura, G., M. Sakakibara, H. Ofuka, H. Ishizuka, S. Miyashita, M. Okamura, O. A. Melnikov, and V. Lushchenko, A deep section of accretionary complex: Susunai complex in Sakhalin island, northwest Pacific margin, *Isl. Arc*, 1, 166-175, 1992.
- Koshiya, S., Tanakura Shear Zone, the deformation process of fault rocks and its kinematics, *J. Geol. Soc. Jpn.*, 92, 15-29, 1986.
- Lallemand, S., and L. Jolivet, Japan Sea: A pull apart basin, *Earth Planet. Sci. Lett.*, 76, 375-389, 1985.
- Lallemand, S., N. Chamot-Rooke, X. Le Pichon, and C. Rangin, Zenisu Ridge: A deep intra-oceanic thrust related to subduction off Southwest Japan, *Tectonophysics*, 160, 151-174, 1989.
- Le Pichon, et al., Nankai trough and the fossil Shikoku ridge: Results of Box 6 Kaiko survey, *Earth Planet. Sci. Lett.*, 83, 186-198, 1987.
- Le Pichon, X., K. Kobayashi, et al., Fluid venting activity within the eastern Nankai trough accretionary wedge: A summary of the 1989 Kaiko-Nankai results, *Earth Planet. Sci. Lett.*, 109, 303-318, 1992.
- Matsuzaka, S., M. Tobita, and Y. Nakahori, Detection of Philippine sea plate motion by very long baseline interferometry, *Geophys. Res. Lett.*, 18, 1417-1419, 1991.
- Melnikov, O. A., *Structure and Geodynamics of the Hokkaido-Sakhalin Folded Region* (in Russian), 94 pp., Nauka, Moscow, 1987.
- Melnikov, O. A., and V. S. Rozhdestvensky, *Guide-Book for Geological Excursions on the Southern Part of Sakhalin Island*, edited by H. S. Gnibidenko, Yuzhno-Sakhalinsk, 1989.
- Melnikov, O. A., and M. A. Zakharova, *Cenozoic Sedimentary and Volcanic-Sedimentary Formations of Sakhalin* (in Russian), 242 pp., Nauka, Moscow, 1977.
- Molnar, P., and T. Atwater, Interarc spreading and cordilleran tectonics as alternates related to the age of the subducted oceanic lithosphere, *Earth Planet. Sci. Lett.*, 41, 330-340, 1978.
- Molnar, P., and P. Tapponnier, Cenozoic tectonics of Asia: Effects of a continental collision, *Science*, 189, 419-426, 1975.
- Nakamura, K., Possible nascent trench along the eastern Japan Sea as the convergent boundary between Eurasian and North American plates (in Japanese), *Bull. Earthquake. Res. Inst. Univ. Tokyo*, 58, 711-722, 1983.

- Nakamura, K., and S. Uyeda, Stress gradient in back arc regions and plate subduction, *J. Geophys. Res.*, 85, 6419-6428, 1980.
- Nur, A., H. Ron, and O. Scotti, Fault mechanics and the kinematics of block rotations, *Geology*, 14, 746-749, 1986.
- Oscorbin, L. S., Seismicity of the Sakhalin island, in *Seismic Regions of the Kuril Islands, Primorja and Priamurjia*, edited by S. L. Solovjev, Vladivostok, 1977.
- Otsuki, K., Reconstruction of Neogene tectonic stress field of Northeast Honshu arc from metalliferous veins, *Mem. Soc. Geol. Jpn.*, 32, 281-304, 1989.
- Otsuki, K., Neogene tectonic stress fields of northeast Honshu Arc and implications for plate boundary conditions, *Tectonophysics*, 181, 151-164, 1990.
- Otsuki, K., and M. Ehiro, Major strike slip faults and their bearing on the spreading of the Japan Sea, *J. Phys. Earth*, 26, suppl., 537-555, 1978.
- Pushcharovskiy, Y. M., V. P. Zinkevich, A. O. Mazarovich, A. A. Peyve, Y. N. Raznitsin, A. V. Rikhter, and N. V. Tsukanov, Overthrusts and imbricate structures of the northwestern Pacific margin, *Geotectonics*, 17, 466-477, 1983.
- Ranken, B., R. K. Cardwell and D. E. Karig, Kinematics of the Philippine sea plate, *Tectonics*, 3, 555-575, 1984.
- Riegel, S.A., K. Fujita, B. M. Koz'min, V. S. Imaev, and D. B. Cook, Extrusion tectonics of the Okhotsk plate, northeast Asia, *Geophys. Res. Lett.*, 20, 607-610, 1993.
- Rikhter, A. V., *Structure and Tectonic Evolution of Sakhalin in the Mesozoic* (in Russian), 90 pp., Nauka, Moscow, 1986.
- Ron, H., R. Freund, Z. Garfunkel, and A. Nur, Block rotation by strike slip faulting, structural and paleomagnetic evidence, *J. Geophys. Res.*, 89, 6256-6270, 1984.
- Rozhdestvensky, V. S., The role of wrench-faults in the structure of Sakhalin, *Geotectonics*, 16, 323-332, 1982.
- Rozhdestvensky, V. S., Evolution of the Sakhalin fold system, *Tectonophysics*, 127, 331-339, 1986.
- Savostin, L., L. Zonenshain, and B. Baranov, Geology and plate tectonics of the Sea of Okhotsk, in *Geodynamics of the Western Pacific-Indonesian Region*, *Geodyn. Ser.*, vol. 11, edited by T. W. C. Hilde and S. Uyeda, pp. 343-354, AGU, Washington, D.C., 1983.
- Scotti, O., A. Nur, and R. Estevez, Distributed deformation and block rotation in three dimensions, *J. Geophys. Res.*, 96, 12,225-12,243, 1991.
- Seno, T., The instantaneous rotation vector of the Philippine sea plate relative to the Eurasian plate, *Tectonophysics*, 42, 209-226, 1977.
- Sugi, N., K. Chinzei and S. Uyeda, Vertical crustal movements of northeast Japan since Middle Miocene, in *Geodynamics of the Western Pacific-Indonesian Region*, *Geodyn. Ser.*, vol. 11, edited by T. W. C. Hilde and S. Uyeda, pp. 317-329, AGU, Washington, D.C., 1983.

- Takeuchi, T., T. Ozawa, and K. Kodoma, Paleomagnetism of the late Cretaceous to Neogene deposits in central Hokkaido, Japan and south Sakhalin of the USSR: multiple rotations caused by transcurrent faults, paper presented at 29th International Geological Congress, Jpn. Geol. Soc., Kyoto, 24 August-3 September 1992.
- Tamaki, K., Age estimation of the Japan Sea on the basis of stratigraphy, basement depth and heat flow data, *J. Geomagn. Geoelectr.*, 38, 427-446, 1986.
- Tamaki, K., Geological structure of the Japan Sea and its tectonic implications, *Bull. Geol. Surv. Jpn.*, 39, 269-365, 1988.
- Tamaki, K., and E. Honza, Incipient subduction and obduction along the eastern margin of the Japan Sea, *Tectonophysics*, 119, 381-406, 1984.
- Tamaki, K., K. Suyehiro, J. Allan, M. McWilliams, et al., Tectonic synthesis and implication of Japan Sea ODP drilling, *Proc. Ocean Drill. Program, Sci. Results*, 127/128, 1333-1348, 1992.
- Tapponnier, P., and P. Molnar, Slip line field theory and large-scale continental tectonics, *Nature*, 264, 319-324, 1976.
- Tapponnier, P., and P. Molnar, Active faulting and tectonics in China, *J. Geophys. Res.*, 82, 2905-2930, 1977.
- Tapponnier, P., G. Peltzer, A. Y. Le Dain, and R. Armijo, Propagating extrusion tectonics in Asia: new insights from simple experiments with plasticine, *Geology*, 10, 611-616, 1982.
- Tapponnier, P., G. Peltzer, and R. Armijo, On the mechanics of the collision between India and Asia, Collision tectonics, edited by M. P. Coward and A. C. Ries, *Geol. Soc. Spec. Publ. London*, 19, 115-157, 1986.
- Tapponnier, P., R. Lacassin, P. H. Leloup, U. Shärer, Zhong Dalai, Wu Haiwei, Liu Xiohan, Ji Shaocheng, Zhang Lianshang, and Zhong Jiayou, The Ailao Shan/Red River metamorphic belt: Tertiary left-lateral shear between Indochina and South China, *Nature*, 343, 431-437, 1990.
- Tarakamov, R. Z., and C. U. Kim, Seismofocal zones and geodynamics of the Kuril-Japan region, in *Geodynamics of the Western Pacific-Indonesian Region*, *Geodyn. Ser.*, vol. 11, edited by T. W. C. Hilde and S. Uyeda, pp. 223-236, AGU, Washington, D.C., 1983.
- Uyeda, S., and H. Kanamori, Back arc opening and the mode of subduction, *J. Geophys. Res.*, 84, 1049-1061, 1979.
- Von Huene, R., and S. Lallemand, Tectonic erosion of the Japan and Peru convergent margins, *Geol. Soc. Am. Bull.*, 102, 704-720, 1990.
- Yamagishi, H., and Y. Watanabe, Change of stress field of Late Cenozoic in Southwest Hokkaido, Japan, Investigation of geologic faults, dykes, ore veins and active faults, *Monogr. Geol. Collabor. Jpn.*, 31, 321-332, 1986.
- Yamaji, A., Rapid intra-arc rifting in Miocene Northeast Japan, *Tectonics*, 9, 365-378, 1990.

- Zakharov, V. K., and G. G. Yakushko, Modern vertical crustal movement in southern Sakhalin as determined by repeated surveying, *Dokl. Akad. Nauk SSSR*, Engl. Transl., 207, 45, 1972.
- Zanyukov, V. N., The central Sakhalin fault and its role in the tectonic evolution of the island (in Russian), *Dokl. Akad. Nauk SSSR*, 196, 913-916, 1971.
- Zonenshain, L.P., and L.A. Savostin, Geodynamics of the Baikal rift zone and plate tectonics of Asia, *Tectonophysics*, 76, 1-45, 1981.
- Zonenshain, L. P., M. I. Kuzmin, and L. M. Natapov, Geology of the USSR: A plate-tectonic synthesis, in *Geodyn. Ser.*, vol. 21, edited by B. M. Page, pp. 242, AGU, Washington, D. C., 1990.

M. Fournier, P. Huchon, and L. Jolivet, Laboratoire de Géologie, Département Terre Atmosphère Océan, Ecole Normale Supérieure, 24 rue Lhomond, 75231 Paris cedex 05, France.

L. S. Oscorbin and K. F. Sergeyev, Institute of Marine Geology and Geophysics, Far East Science Center, Yuzhno-Sakhalinsk, Russia.

(Received April 1, 1992;
revised July 6, 1993;
accepted July 20, 1993.)

Copyright 1993 by the American Geophysical Union.

Paper number 93JB02026.

0148-0227/93/93JB-02026\$05.00

Fig. 1. Simplified structural map of far east Asia with topography and bathymetry. Solid arrows give directions of motions of Pacific and Okhotsk plates relative to Asia. B is basin, IP is Izu Peninsula, MTL is median tectonic line, R is ridge, S is strait, T is trench, TF is Tsushima fault, TTL is Tanakura tectonic line, YF is Yangsan fault, and ZR is Zenisu ridge.

Fig. 2. Tectonic map of the Sakhalin-East Japan Sea strike-slip zone. Solid arrows represent early and middle Miocene main stress field directions, transpressional to the north in Sakhalin and Hokkaido, and transtensional the south along the eastern margin of the Japan Sea (with dextral en échelon basins). Open arrows represent upper Miocene and Pliocene main stress field directions, still transpressional in Sakhalin and purely compressional in the Japan arc. Changes of stress field directions in the south of the strike-slip zone correspond to change of subduction regime from stress-free to compressional during late Miocene. The possible

clockwise rotation of the stress field in Sakhalin is discussed in the text. TTL is Tanakura tectonic line.

Fig. 3. (a) Sketch of Landsat images of Sakhalin. (b) Seismotectonic map of Sakhalin. For fault plane solution (lower hemisphere), *T* quadrants (compressional quadrants) are shown in shaded areas and *P* quadrants (dilatational quadrants) are open areas. Solid *T* quadrants correspond to fault plane solutions determined by Oscorbin, vertically ruled *T* quadrants correspond to fault plane solutions determined by *Fukao and Furumoto* [1975], and horizontally ruled *T* quadrants correspond to centroid moment tensor determined by *Dziewonski et al.* [1985, 1987]. Paleo-stress field horizontal directions deduced from fault set analysis are plotted as convergent (σ_1) or divergent (σ_3) arrows. B is bay, F is fault, GYR is Gyrgylan'i-Ossov fault. (c) Geological map.

Fig. 4. Detailed stratigraphic and lithological section of the west Sakhalin Mountains and the Central Depression at Vakrouchev latitude.

Fig. 5. East-west cross section of Sakhalin, localized in Figure 3c. B is basin, TPF is Tym-Poronaysk fault.

Fig. 6. *P* and *T* axes projection on stereodiagrams for 17 focal mechanisms (lower hemisphere). Seven focal mechanisms of the northern offshore earthquakes are not taken into account as they are not consistent with the other ones. Contours and grids are determined with the right dihedra method.

Fig. 7. Landsat image of the southwestern horn of Sakhalin (localized in Figure 3c) showing the clockwise curvature of the dextral en échelon fold axis in the vicinity of the Tym-Poronaysk fault.

Fig. 8. Compressional structures (drag fold and ramp and flat structures) along the Tym-Poronaysk fault in Upper Cretaceous formations (central Sakhalin).

Fig. 9. Structural interpretation of a mosaic of two SPOT images of the Yuzhno-Sakhalinsk region along the Tym-Poronaysk fault (localized in Figure 3c).

Fig. 10. Structural interpretation of a mosaic of two SPOT images along the Tym-Poronaysk fault (northern region localized in Figure 3c). Same legend as figure 9. F is fault.

Fig. 11. (a) Mosaic of two SPOT images along the Tym-Poronaysk fault (central region localized in Figure 3c) and (b) structural interpretation. Same legend as Figure 9. Thick lines

are fault traces and the main sills are mapped with thin lines. The arrows on the images show the Tym-Poronaysk fault trace. (c) Geological map of the central region after K. F. Sergeyev (unpublished data, 1980) and our new observations. Key shows (1) Maruyama formation and upper Pliocene-Quaternary deposits, (2) Verknedyuska formation, (3) Tcheckhov formation, (4) Kholmsk formation, (5) Gastello formation, (6) Paleogene basal deposits, (7), (8), and (9) Bikov suite, (10) Miocene volcanics, (11) mud volcano, (12) fault and suspected fault (dashed line), (13) fold axis (syncline and anticline, respectively), (14) geological contour and suspected geological contour (dashed line), (15) paleo-stress field direction. The Santonian-Campanian cuesta is shown as the boundary between formations 7 and 8.

Fig. 12. (a) Paleogene basal conglomerate on the E-W road to Boshnyakovo (central Sakhalin), lying unconformably onto Upper Cretaceous formations (to the east). The thickness of the conglomerate is variable and reaches 600 m in some places. (b) Disrupted fold in Neogene Kholmsk formation south of Yuzhno-Sakhalinsk. (c) Sill in almost verticalized Miocene sedimentary beds along the Tym-Poronaysk fault in the Lozovaya river valley (mapped in Figure 11b). Cooling joints are perpendicular to the stratification.

Fig. 13. Cross-sections across the Tym-Poronaysk fault (localized in Figure 11c). TPF is Tym-Poronaysk fault.

Fig. 14. Fault set stereodiagrams (Schmidt projection, lower hemisphere) and deduced paleostress field directions for four sites plotted in Figure 12b. Dashed lines represent bedding planes. Three-branch star is σ_3 . Four-branch star is σ_2 . Five-branch star is σ_1 ($\sigma_1 > \sigma_2 > \sigma_3$).

Fig. 15. Fault set stereodiagrams (lower hemisphere) and deduced paleostress field directions for sites plotted in Figure 3b. Two successive stress fields are observed on sites T3, T4, and T5.

Fig. 16. Detail of the Landsat image of the East Sakhalin Mountains showing three parallel faults bounding Neogene basins.

Fig. 17. (a) Simplified fault pattern in Sakhalin. CF is central fault, LF is Liman fault, PF is Pribrezhnaya fault, TPF is Tym-Poronaysk fault, WSF is West Sakhalin fault. Dashed lines represent fold axes. (b) Fault pattern isolated from the coast lines. West of the Tym-Poronaysk fault, the West Sakhalin Mountains (WSM, dark shaded) behaved as a single block. E-W shortening is taken up by the internal deformation of the block (en échelon folds). East of the Tym-Poronaysk fault, the East Sakhalin Mountains (ESM) behaved as a domino blocks system in a dextral transpressional shear zone. E-W shortening is taken up by

counterclockwise rotation of the blocks and compressional structures along their borders. (c) Simplification of the fault pattern with a domino block model.

Fig. 18. Geological map of Noto Peninsula and Yatsuo basin and fault set measurements in lower and middle Miocene deposits. Strike-slip and normal faults are often associated, paleostress field is transtensional with σ_{Hmax} trending NE.

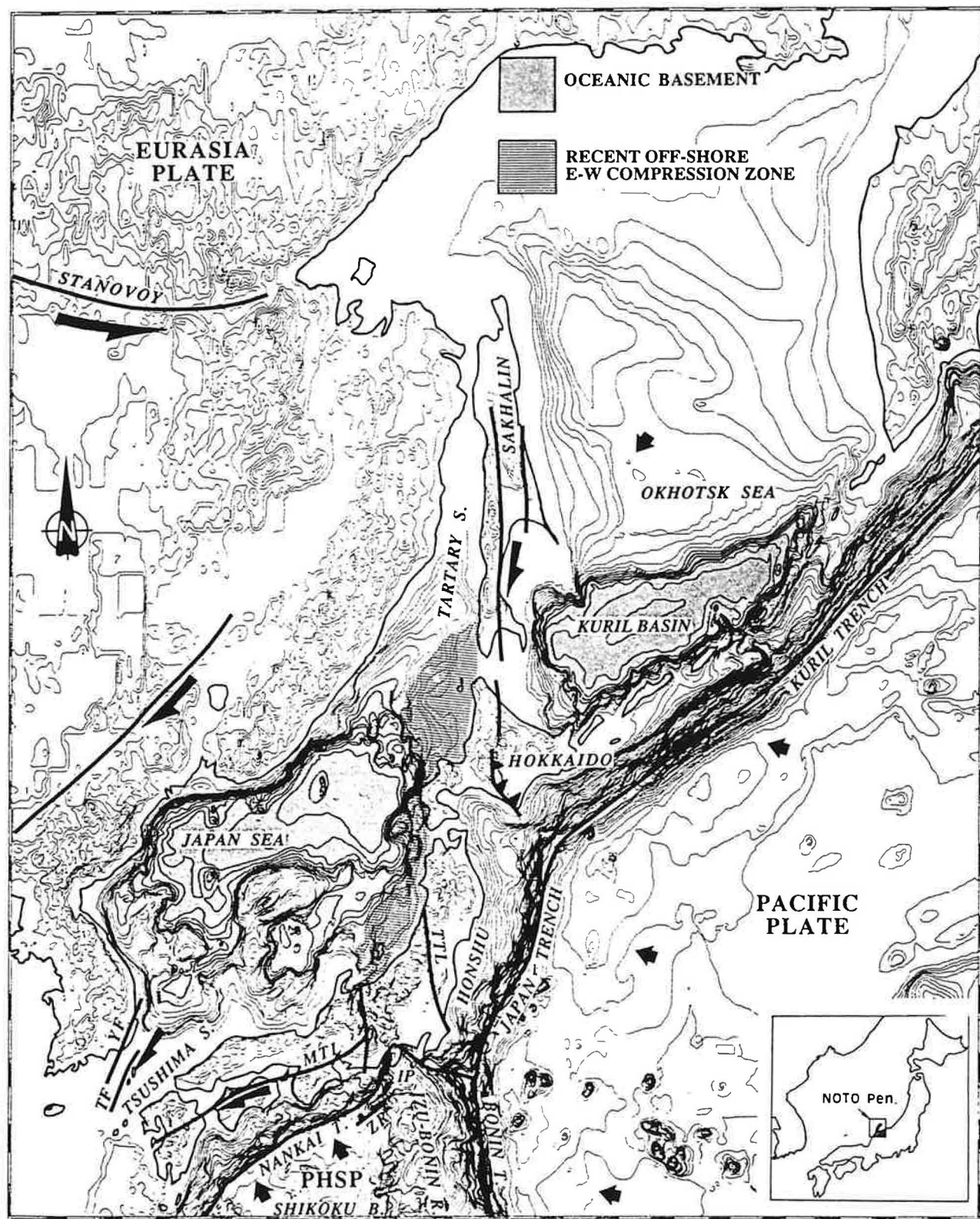
Fig. 19. Simplified model of deformation of Asia (oblique Mercator projection)[after *Jolivet et al.*, 1990]. ATF is Altyn Tagh fault, RRF is Red River fault, and TF is Tanlu fault.

Fig. 20. (a) Present-day geodynamic context of Sakhalin and Japan Sea region. Shaded area represents the oceanic crust of Japan Sea and Kuril Basin. Darker shading shows the zone of active compression of eastern Japan Sea. (b) Same region 20 Ma ago, reconstruction parameters after *Jolivet et al.* [1991] and *Jolivet and Tamaki* [1992]. TPF is Tym-Poronaysk fault, HSZ is Hidaka Shear Zone, MTL is median tectonic line, YBK is Yamato Bank, YB is Yamato Basin, YF is Yangsan fault, TB is Tsushima Basin, and TF is Tsushima fault.

TABLE 1. List of Source Parameter Results for 24 Earthquakes Plotted in Figure 3b.

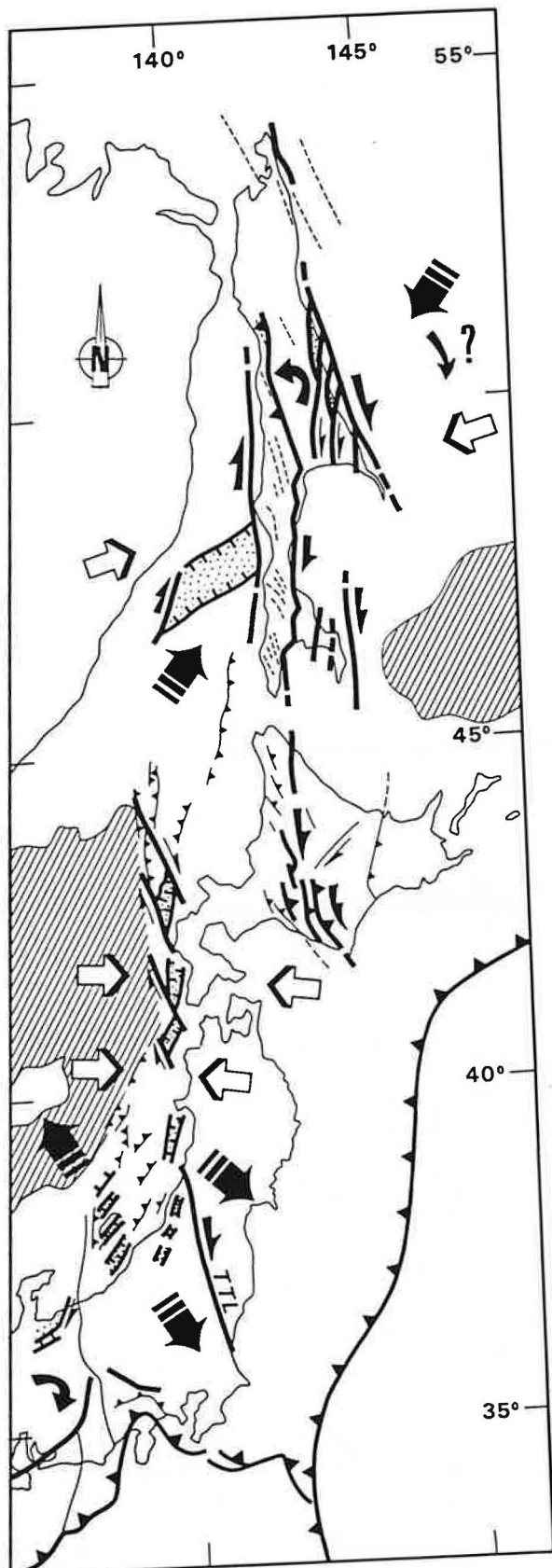
Number	Date	Latitude	Longitude	Depth, km	Magnitude	P Axis	T Axis	Reference
1	March 12, 1962	47.1	143.2	30	4.8	233	38	126 23 1
2	April 7, 1963	53.8	142.7	17	5.0	182	02	272 34 1
3	May 10, 1964	46.6	142.4	13	5.0	301	01	211 28 1
4	Oct. 2, 1964	51.9	143.3	10	5.8	243	50	126 22 1
5	Dec. 24, 1967	54.7	143.6	20	5.5	335	30	245 00 1
6	Dec. 29, 1967	54.7	143.7	20	4.3	238	03	148 17 1
7	Jan. 6, 1970	49.6	142.3	25	5.5	220	26	312 05 1
8	Jan. 6, 1970	49.6	142.4	22	4.7	074	01	169 80 1
9	Jan. 10, 1971	55.1	142.1	20	4.9	220	56	116 11 1
10	Sept. 5, 1971	46.45	141.24	22	7.1	099	06	236 81 3
11	Feb. 6, 1973	49.2	141.9	10	4.7	069	28	175 27 1
12	April 4, 1973	53.9	141.3	20	5.0	025	14	280 50 1
13	Aug. 17, 1974	54.7	144.3	15	5.4	310	02	217 58 1
14	Aug. 17, 1974	55.0	144.0	15	4.2	116	37	216 15 1
15	July 25, 1977	51.8	143.0	10	4.6	294	00	207 73 1
16	July 28, 1979	50.0	142.7	20	5.8	229	01	320 39 1
17	July 28, 1979	49.48	142.41	15		260	06	157 62 2
18	March 14, 1980	52.4	142.2	16	4.8	276	13	019 43 1
19	March 19, 1982	52.3	142.7	5	4.1	302	01	207 70 1
20	March 20, 1982	52.3	142.8	5	4.3	292	03	198 60 1
21	March 17, 1983	51.5	142.4	20	5.2	242	02	336 45 1
22	July 22, 1983	50.3	142.2	20	4.5	103	25	313 62 1
23	Dec. 22, 1984	50.0	142.7	30	5.2	088	38	294 49 1
24	Dec. 22, 1984	50.17	142.79	37.8		084	06	296 83 2

References are (1) L. S. Oscrbin (this study), (2) Dziewonski et al. [1985, 1987], and (3) Fukao and Furumoto [1975].



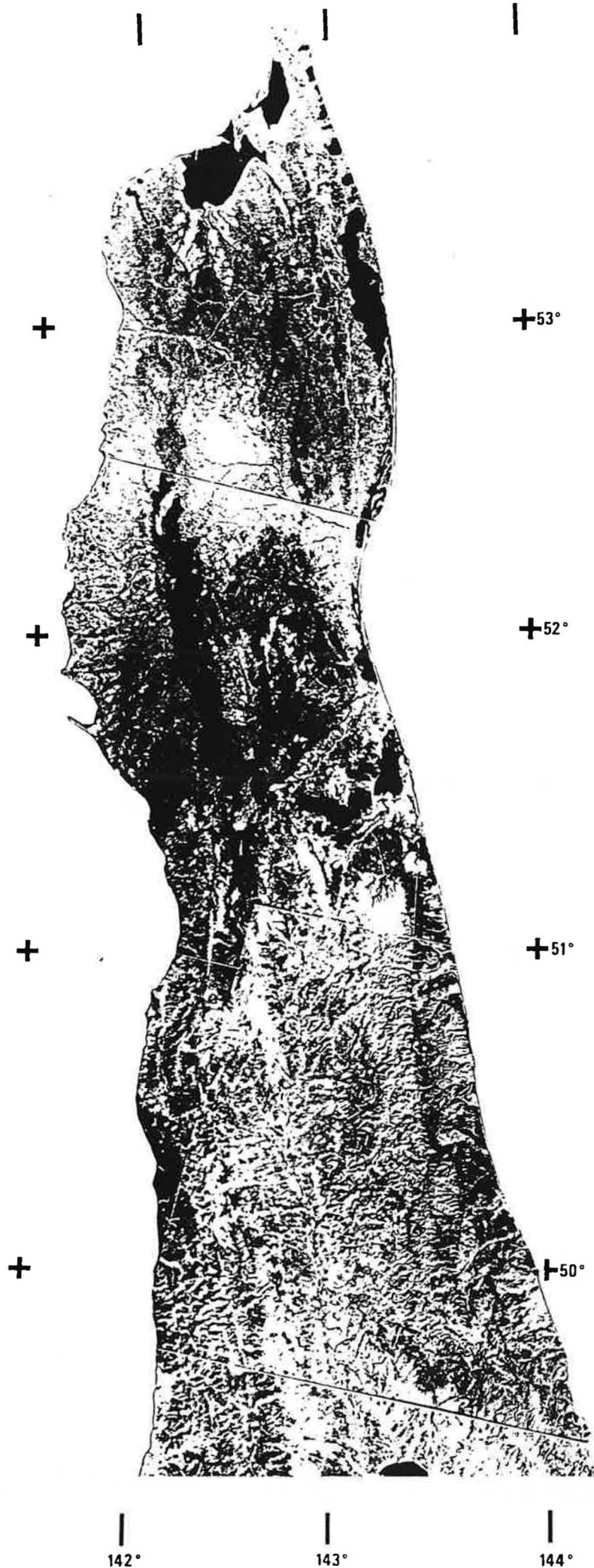
FOURNIER ET AL

FIG 1



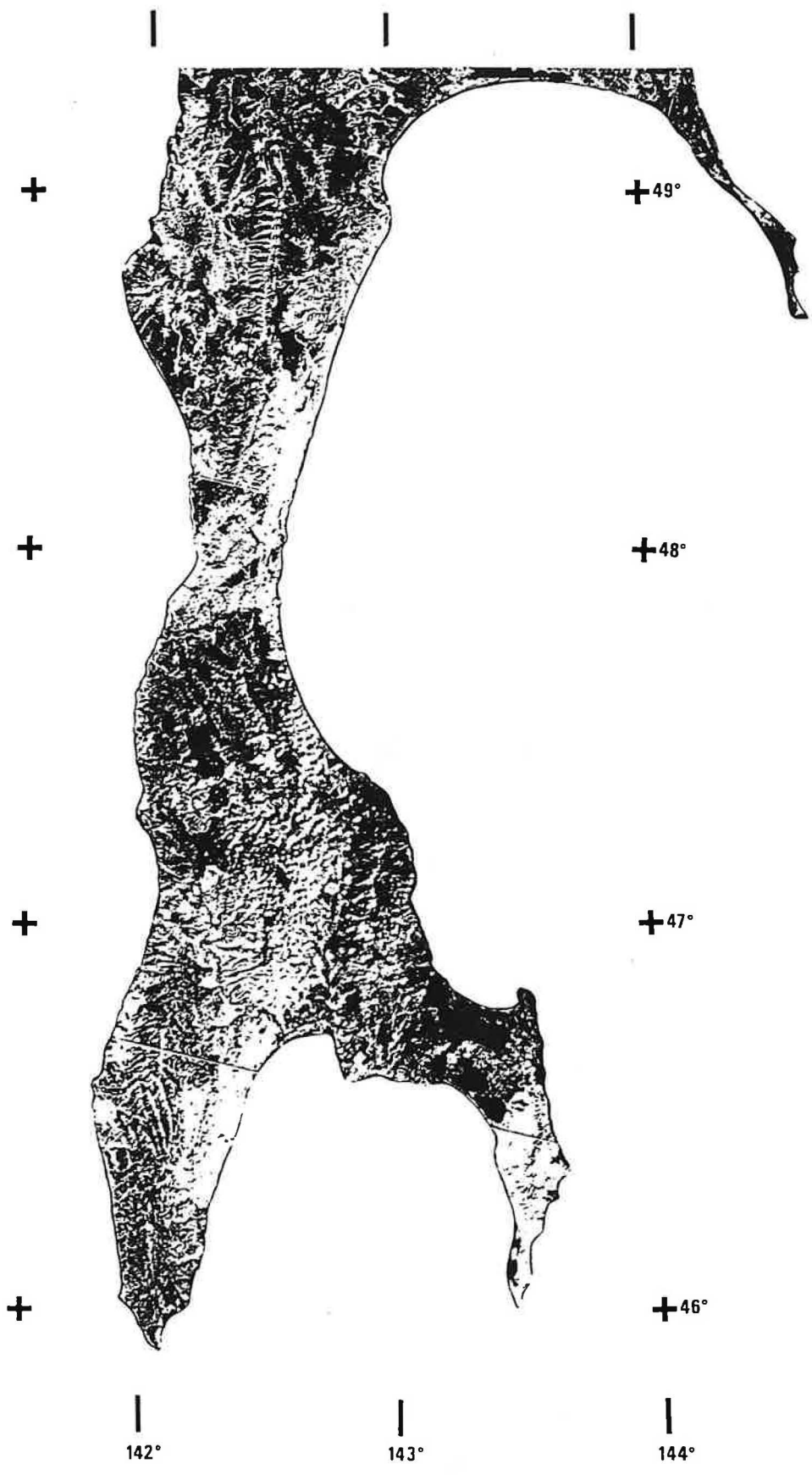
FOURNIER ET AL

FIG 2



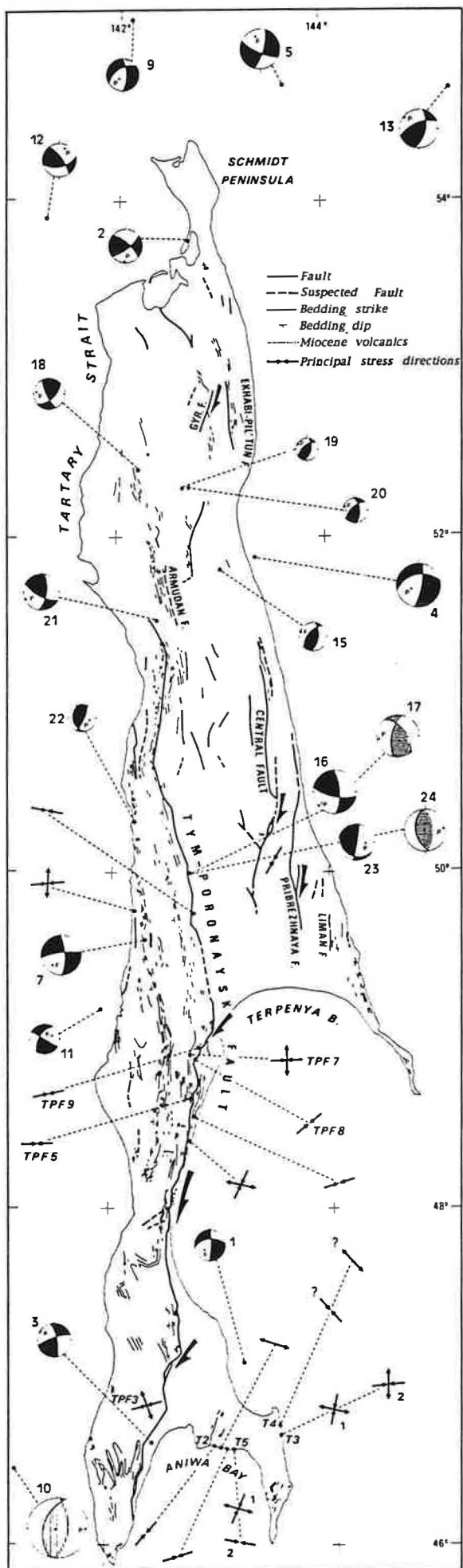
FOURNIER
ET AL

Fig. 3a 1
North



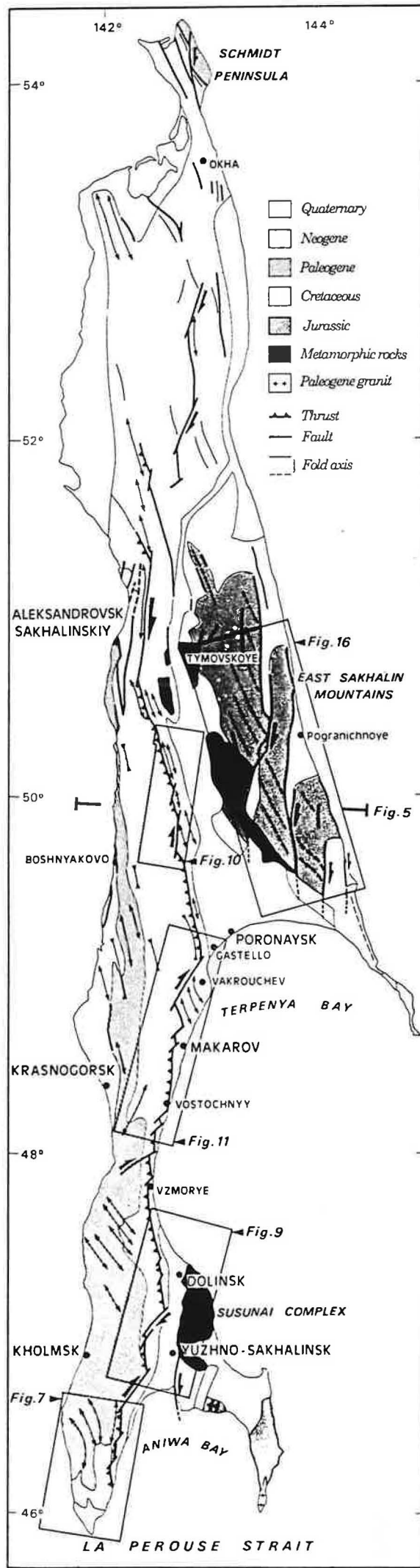
FOURNIER
ET AL

Fig. 3a2
South



FOURNIER ET AL

FIGURE 3b



FOURNIER ET AL.

FIGURE 3 C

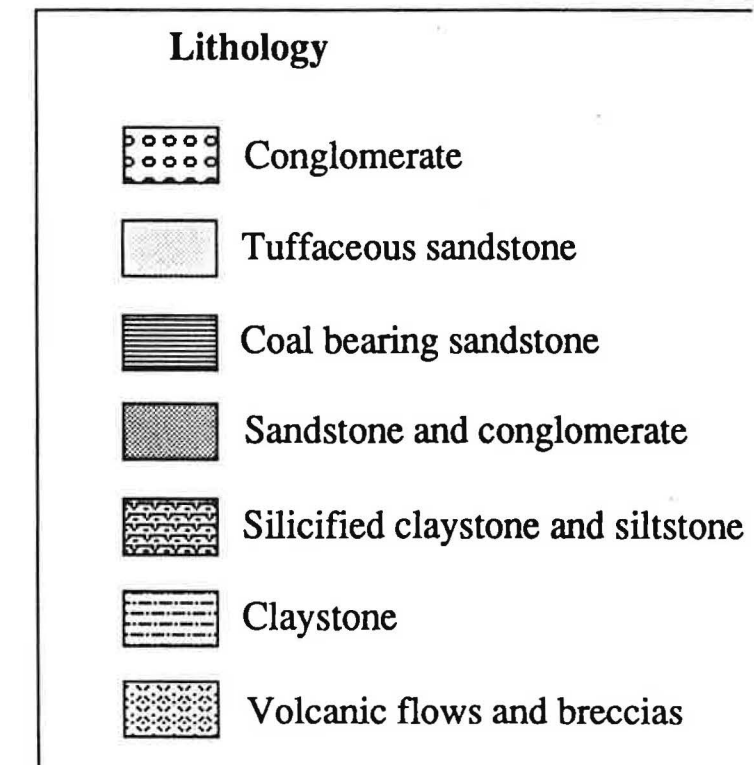
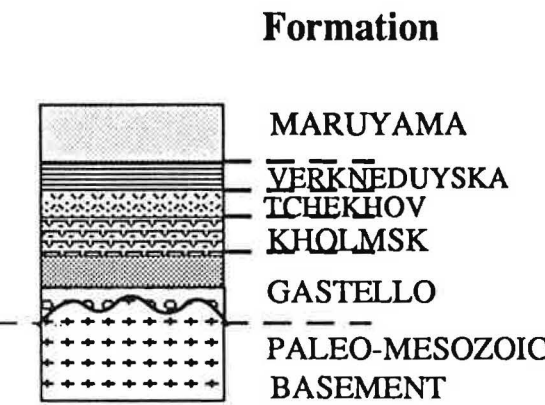
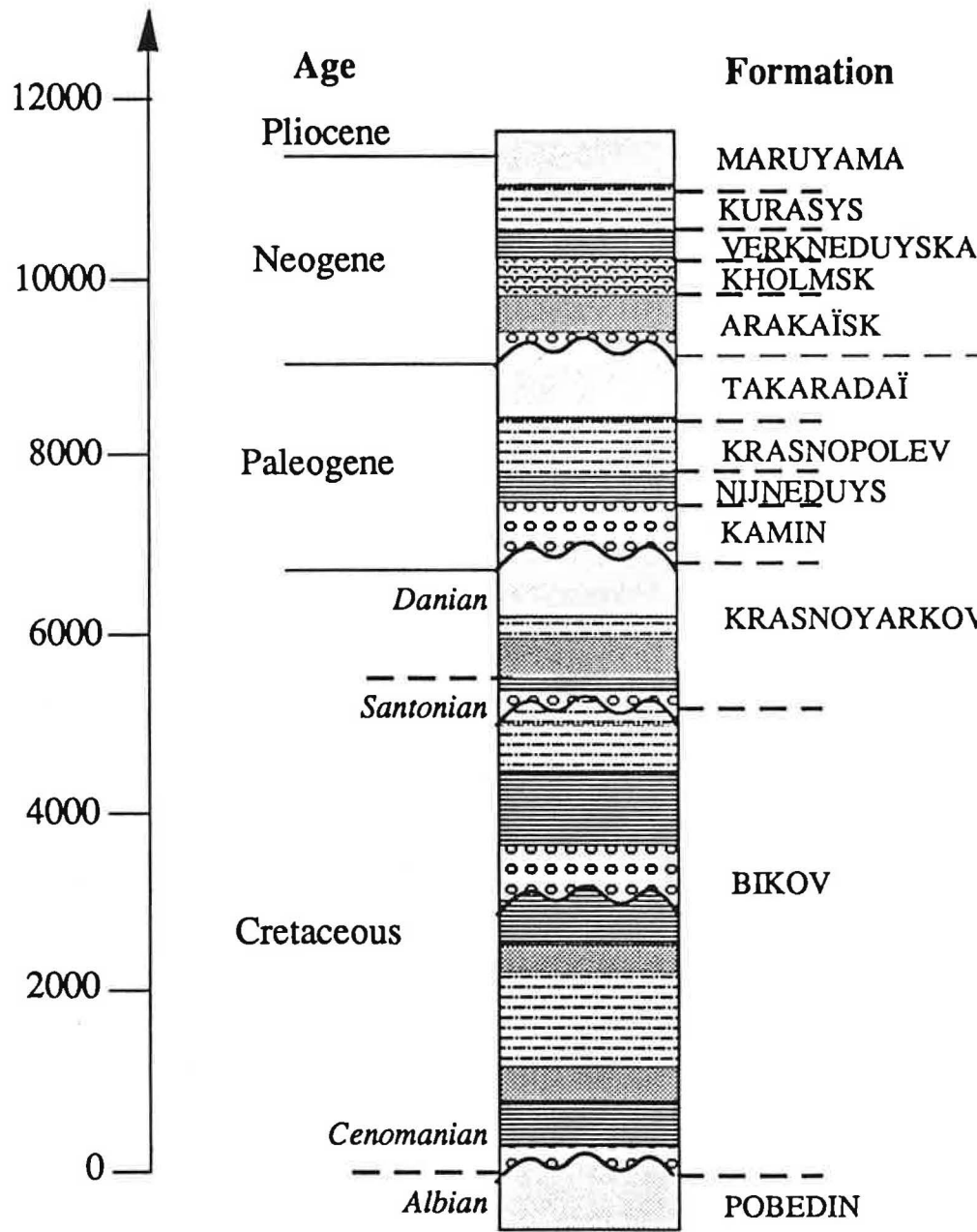
Approximative
thickness (m)

WEST SAKHALIN BASIN

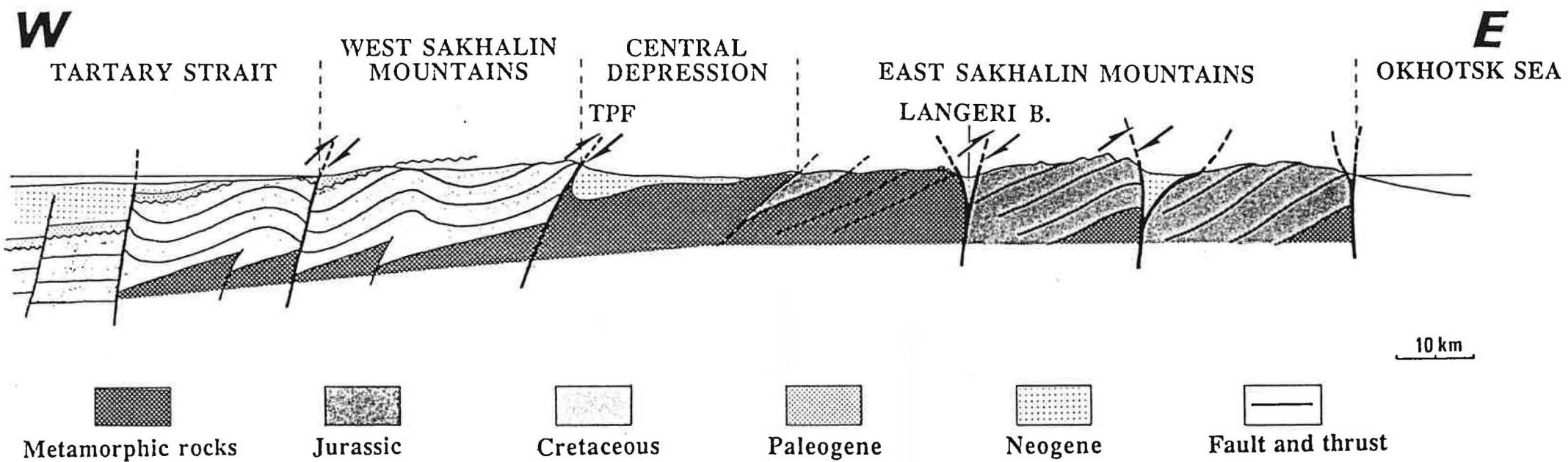
West of the Tym-Poronaysk fault

CENTRAL DEPRESSION

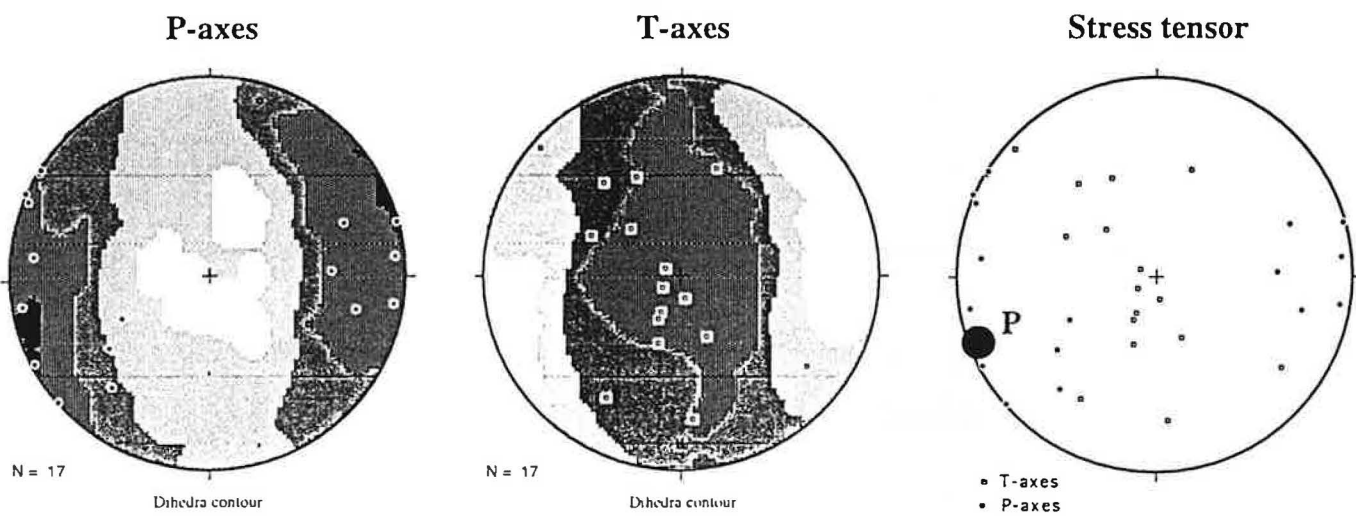
East of the Tym-Poronaysk fault



FOURNIER ET AL
Fig. 4

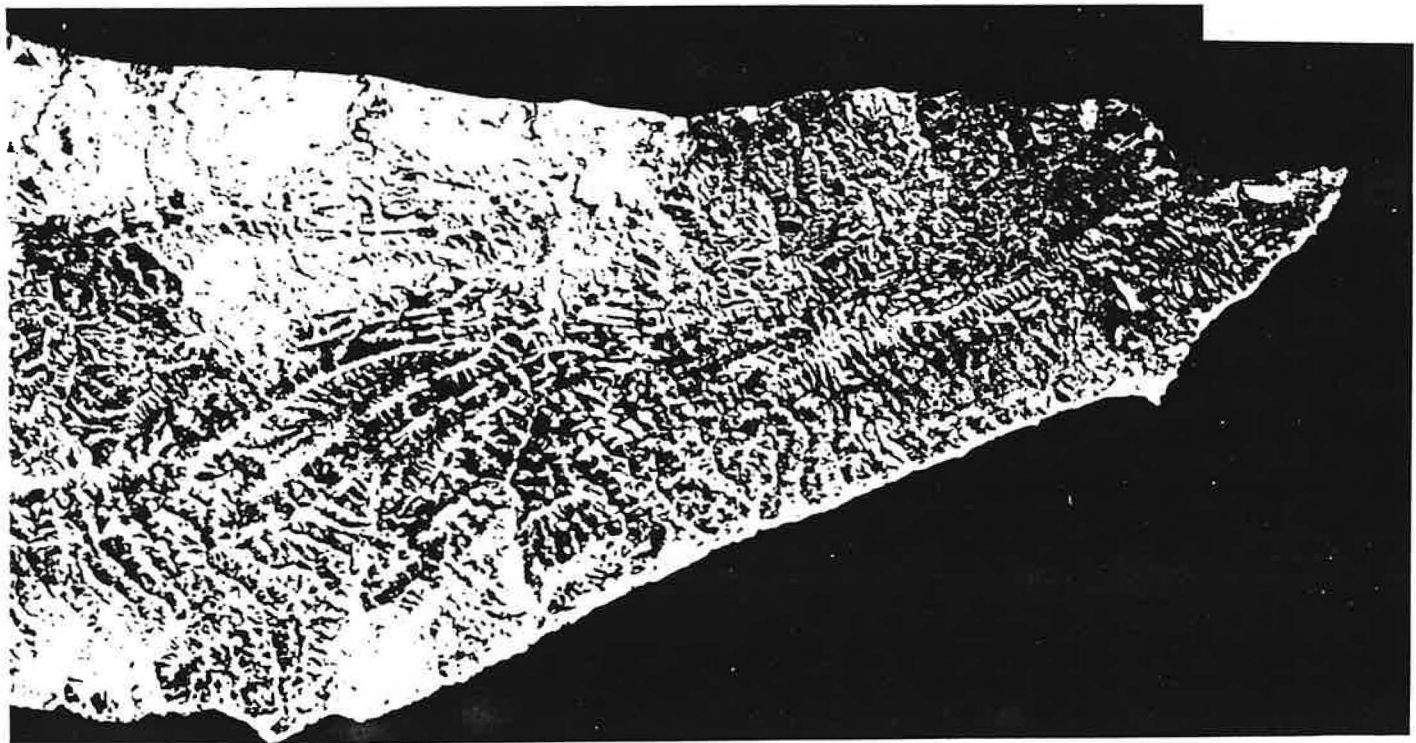
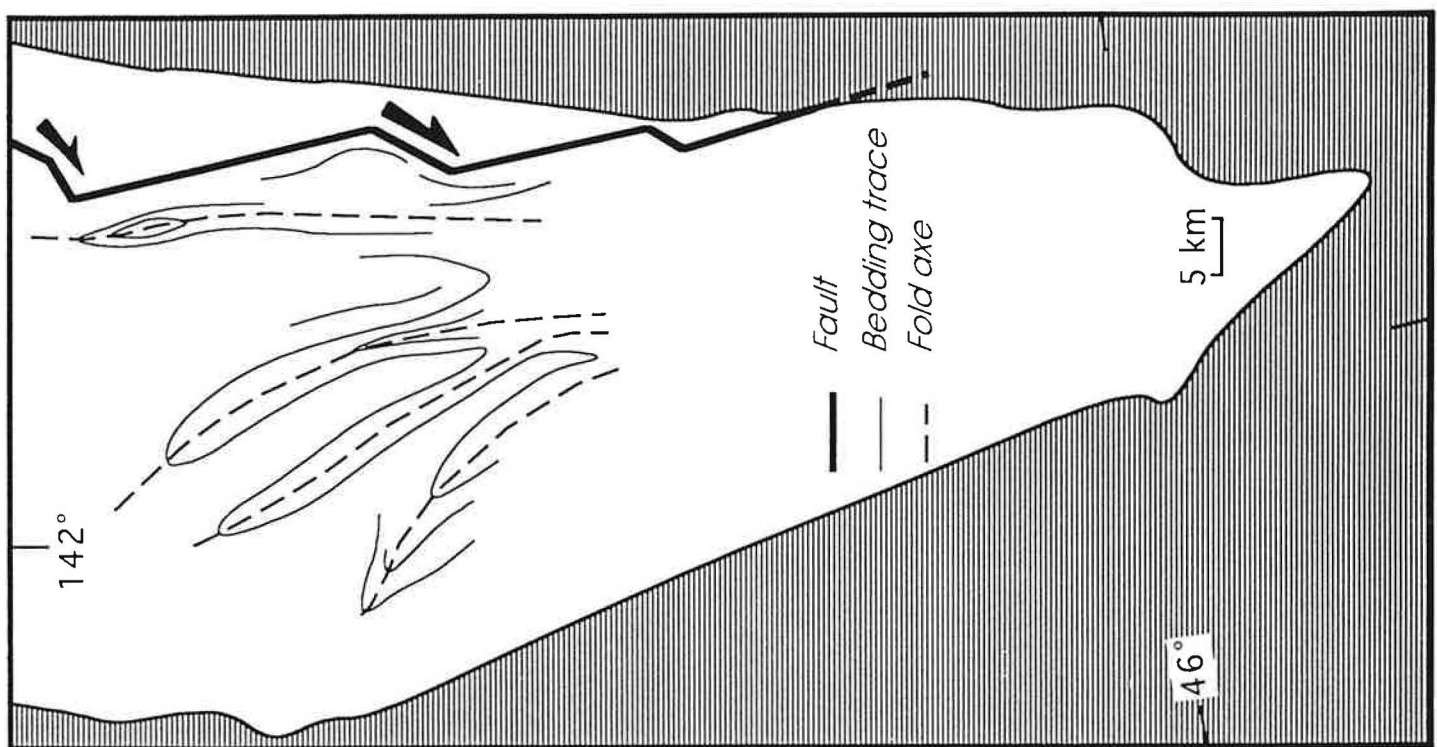


FOURNIER ET AL Fig. 5



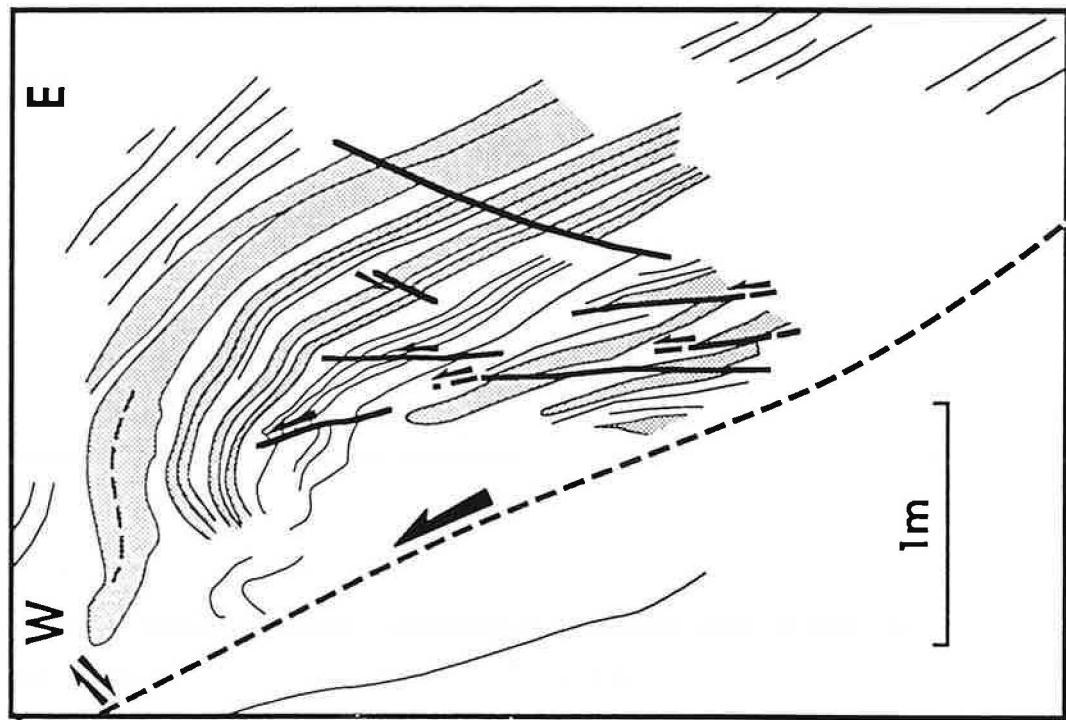
FOURNIER ET AL FIG 6

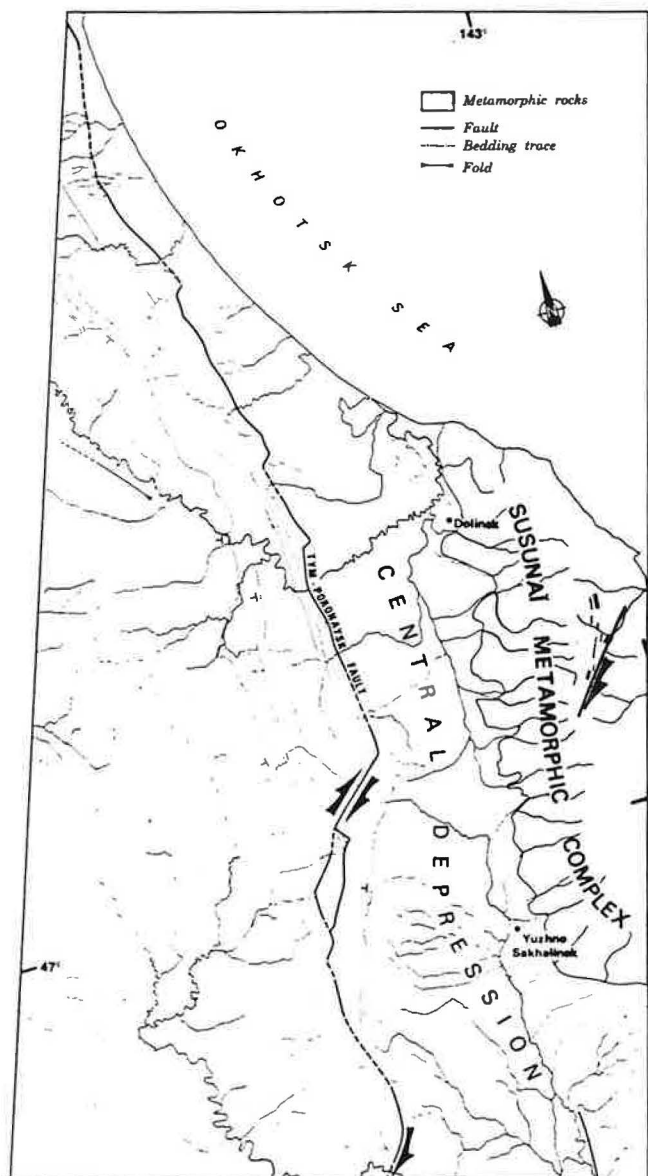
Poirier
et al.
FIG. 7



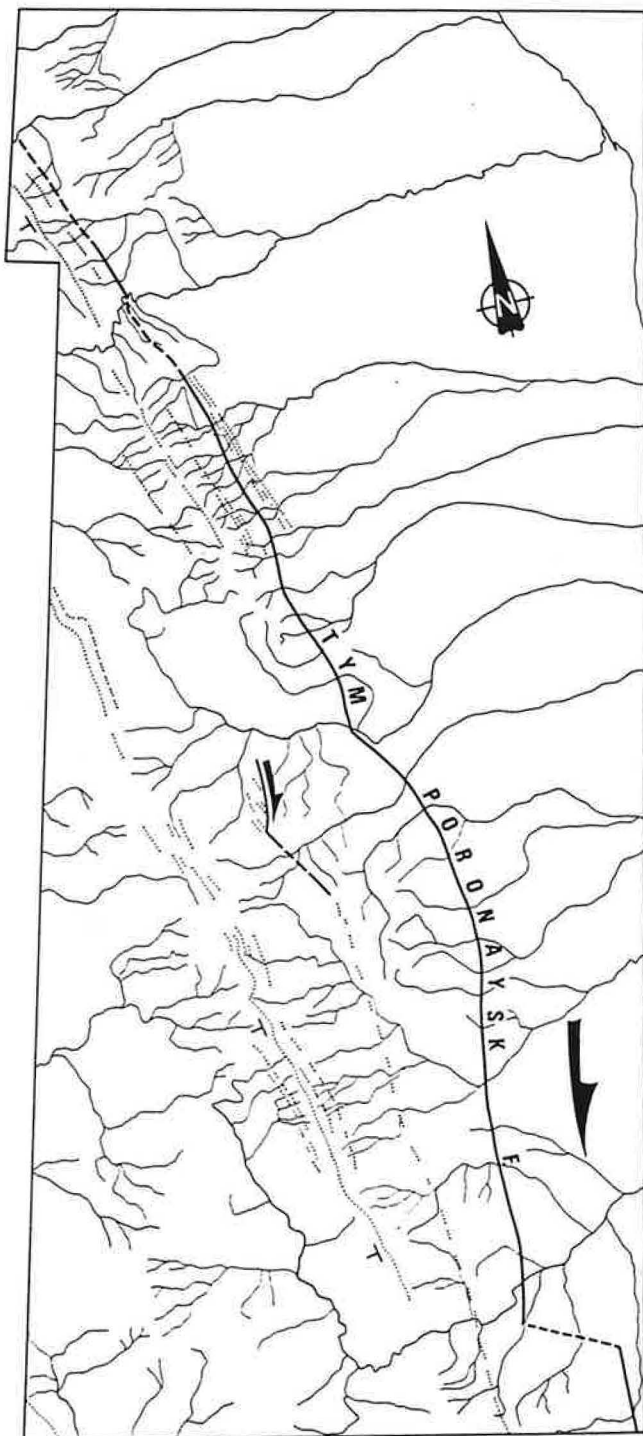
FOURNIER
ET AL.

fig. 8





FOURNIER et al. FIG. 9

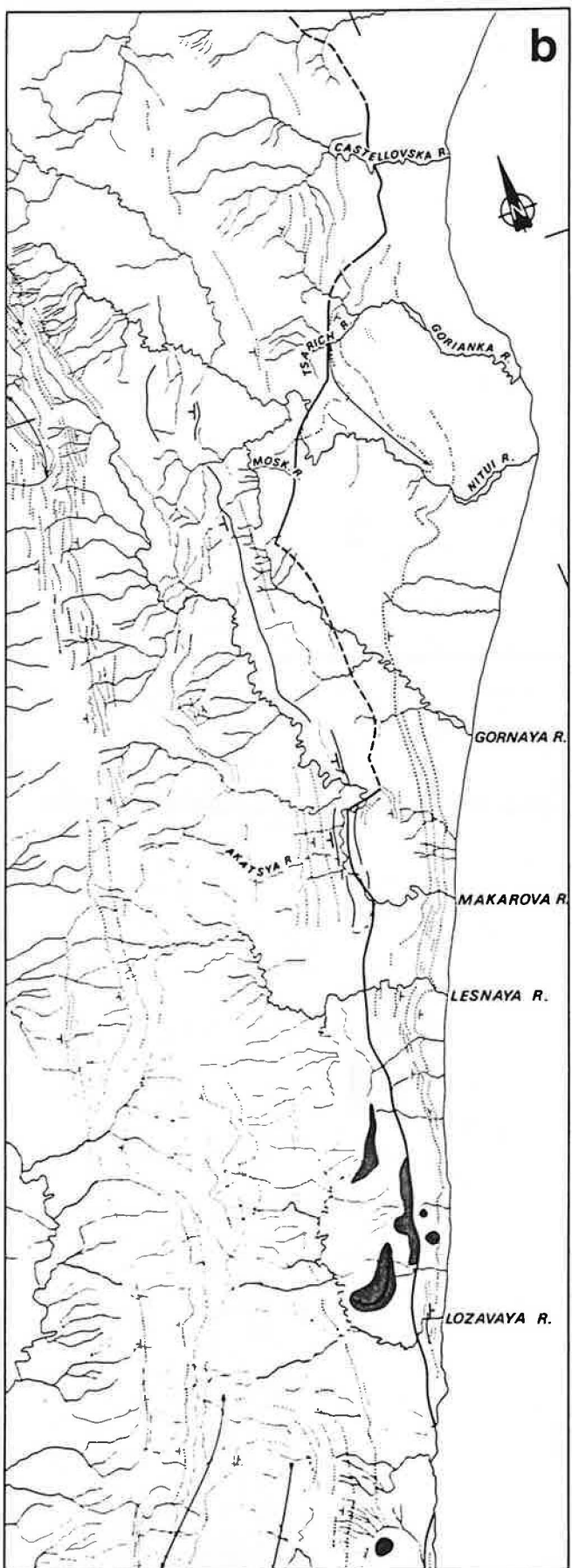


Fournier et al. FIG. 10



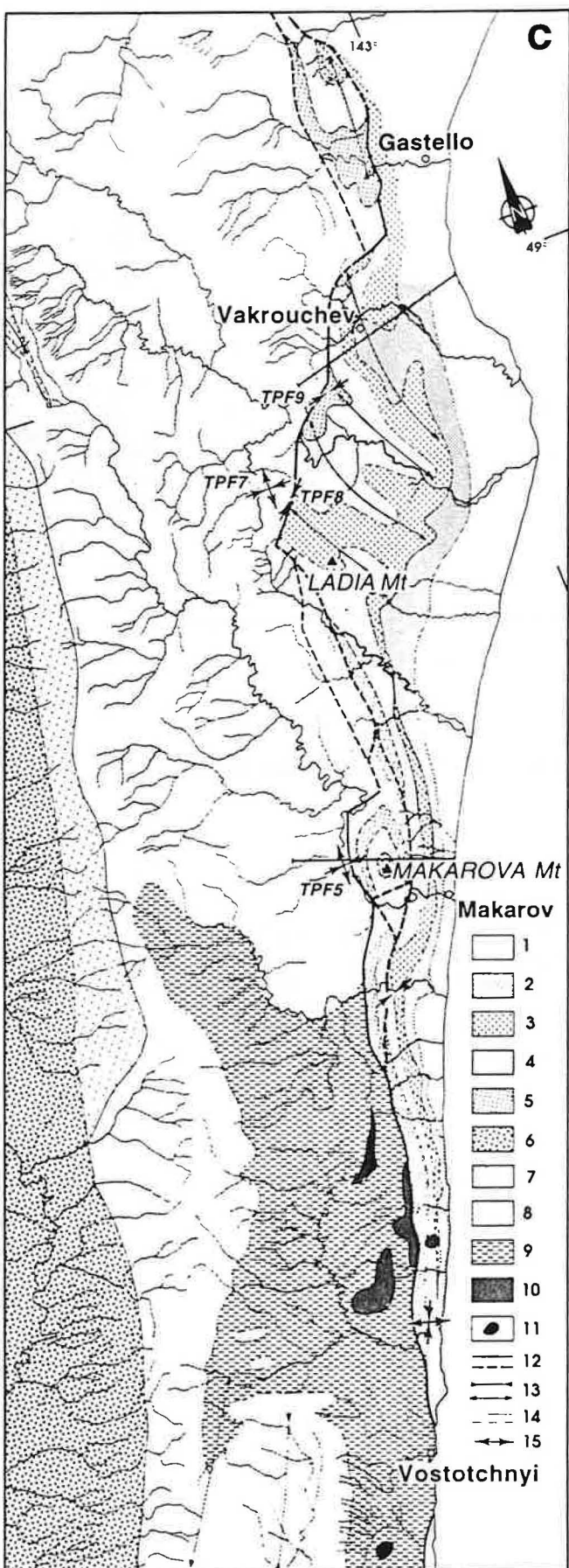
FOURNIER
ET AL

Fig. 11a



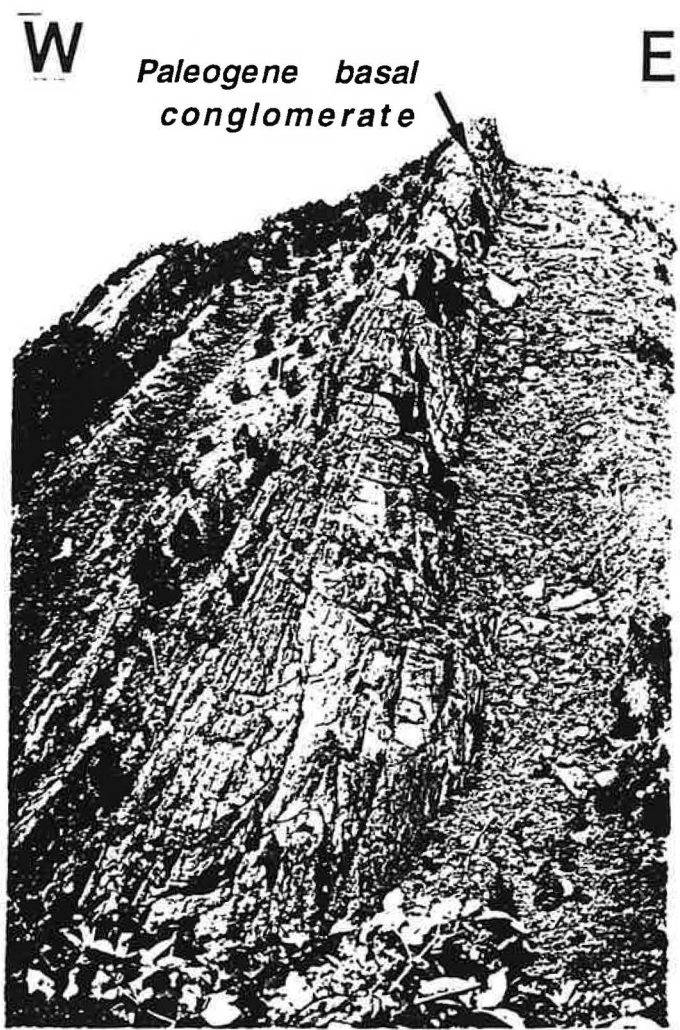
FOURNIER
et al

FIG 11b

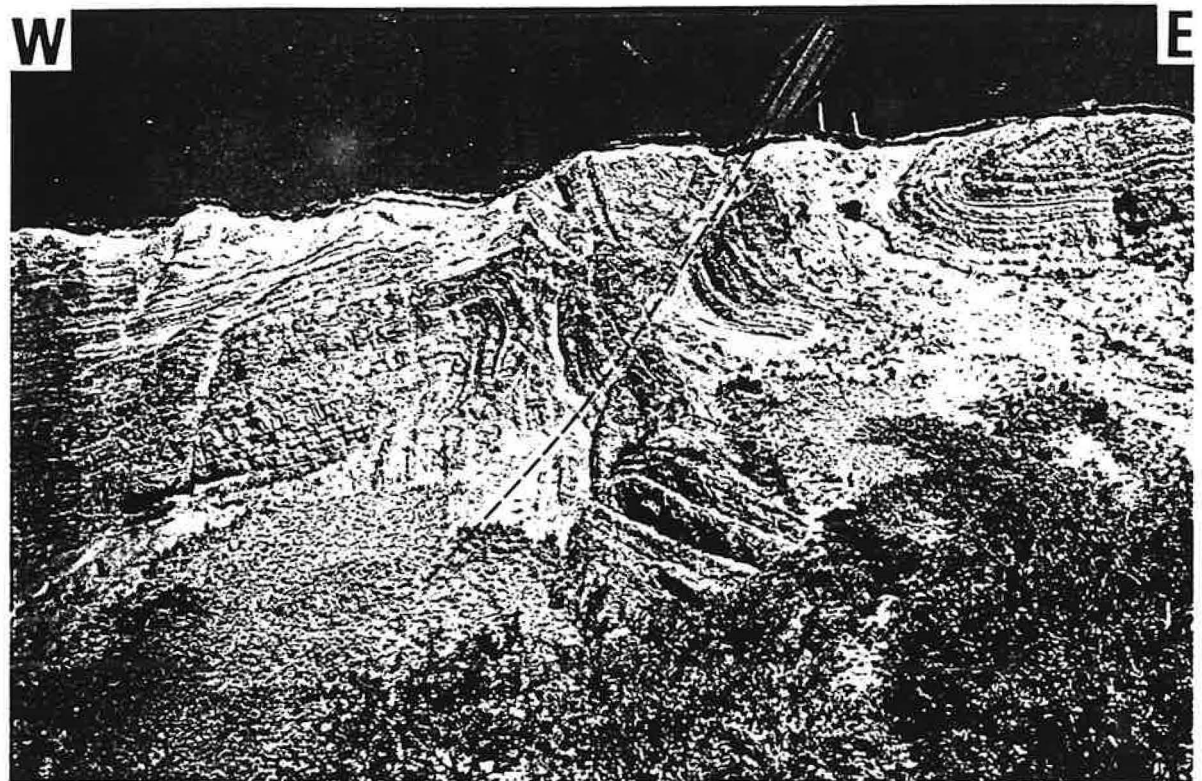


FOURNIER et al

FIG 11c



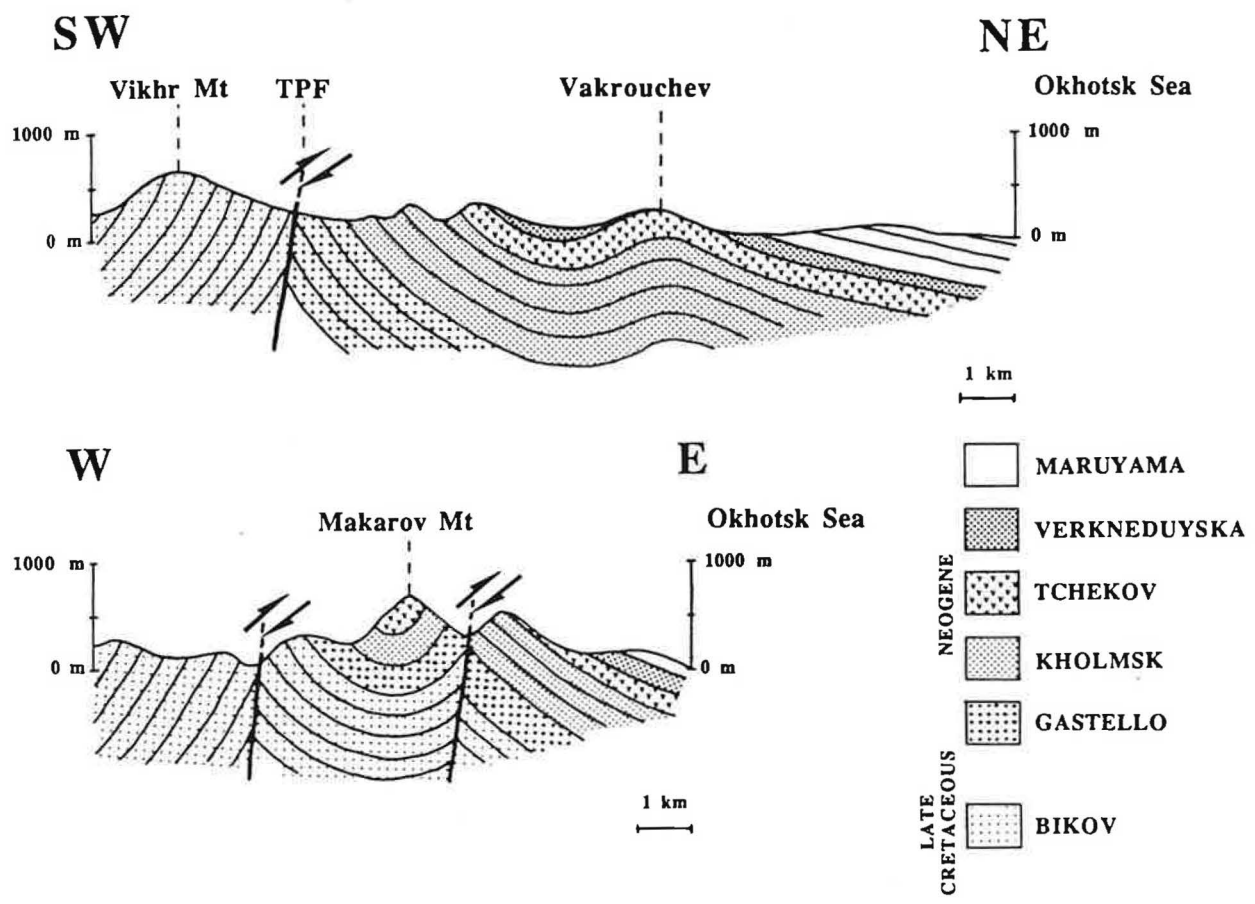
Turner et al fig 12a



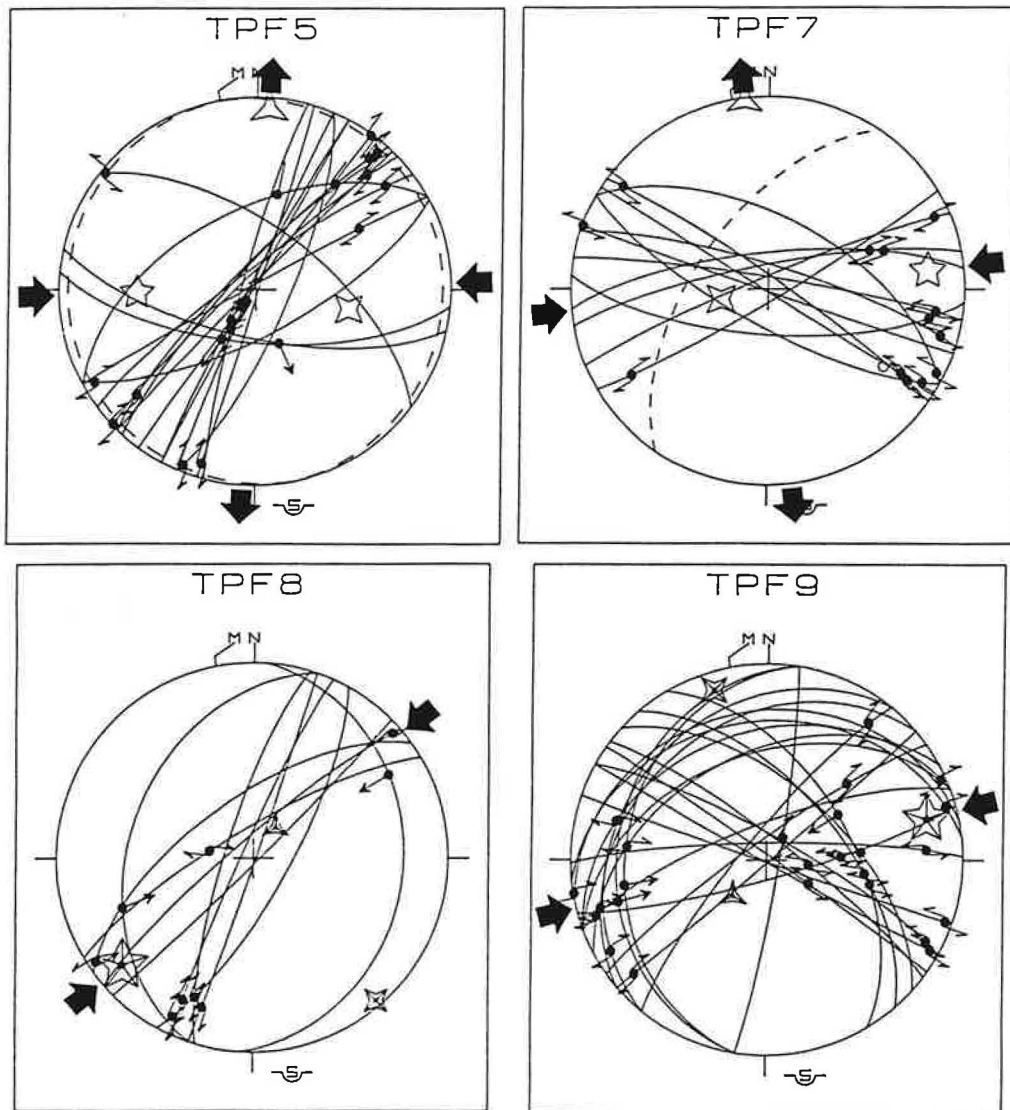
Fournier et al. fig 12b



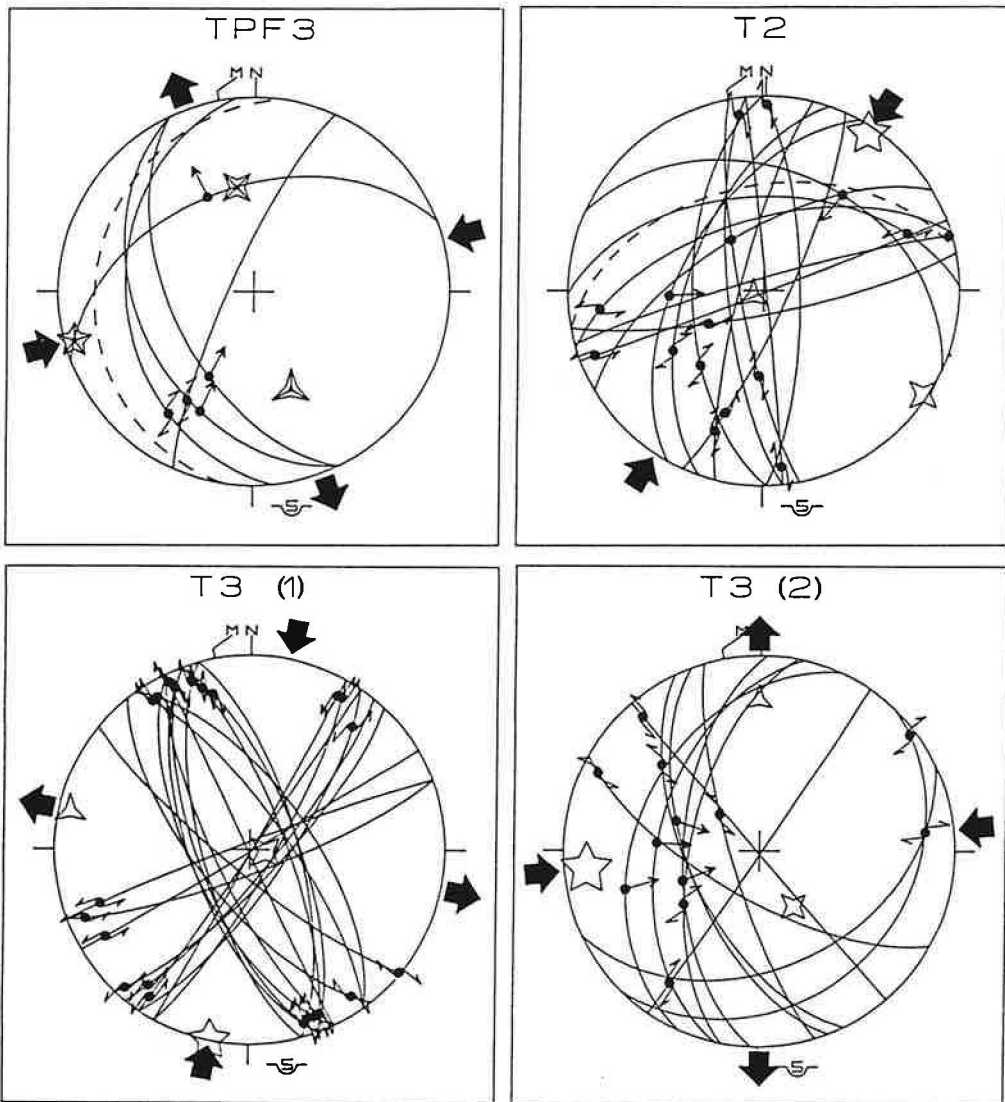
Fournier et al. fig 12c



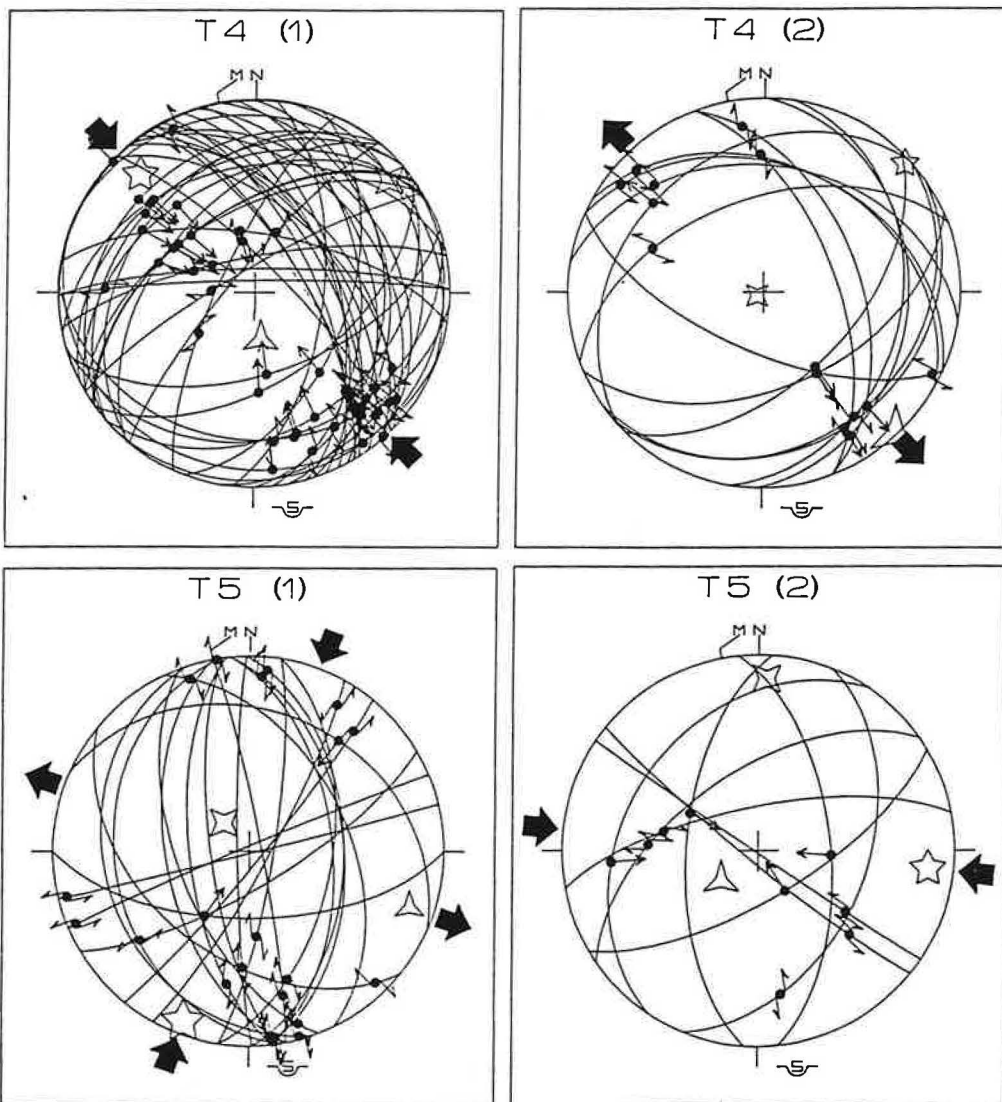
Fournier et al. fig. 13



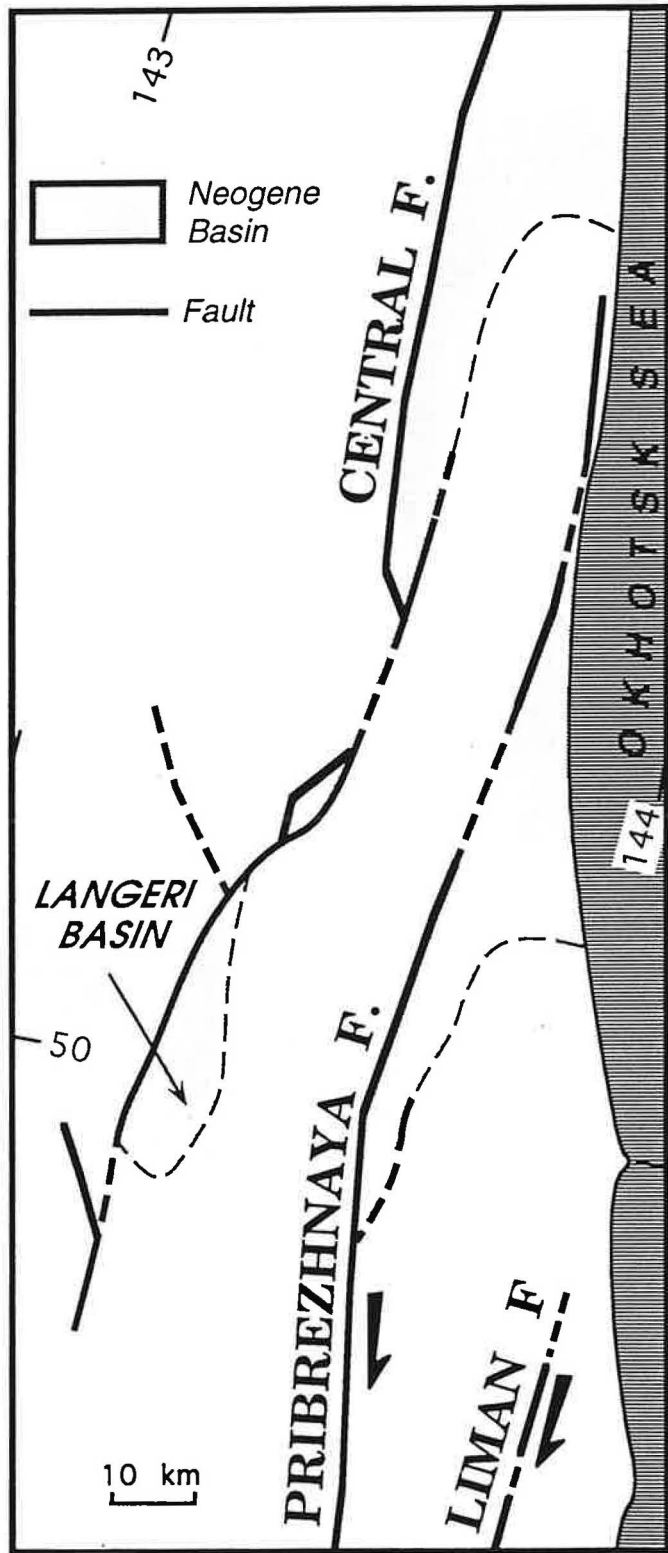
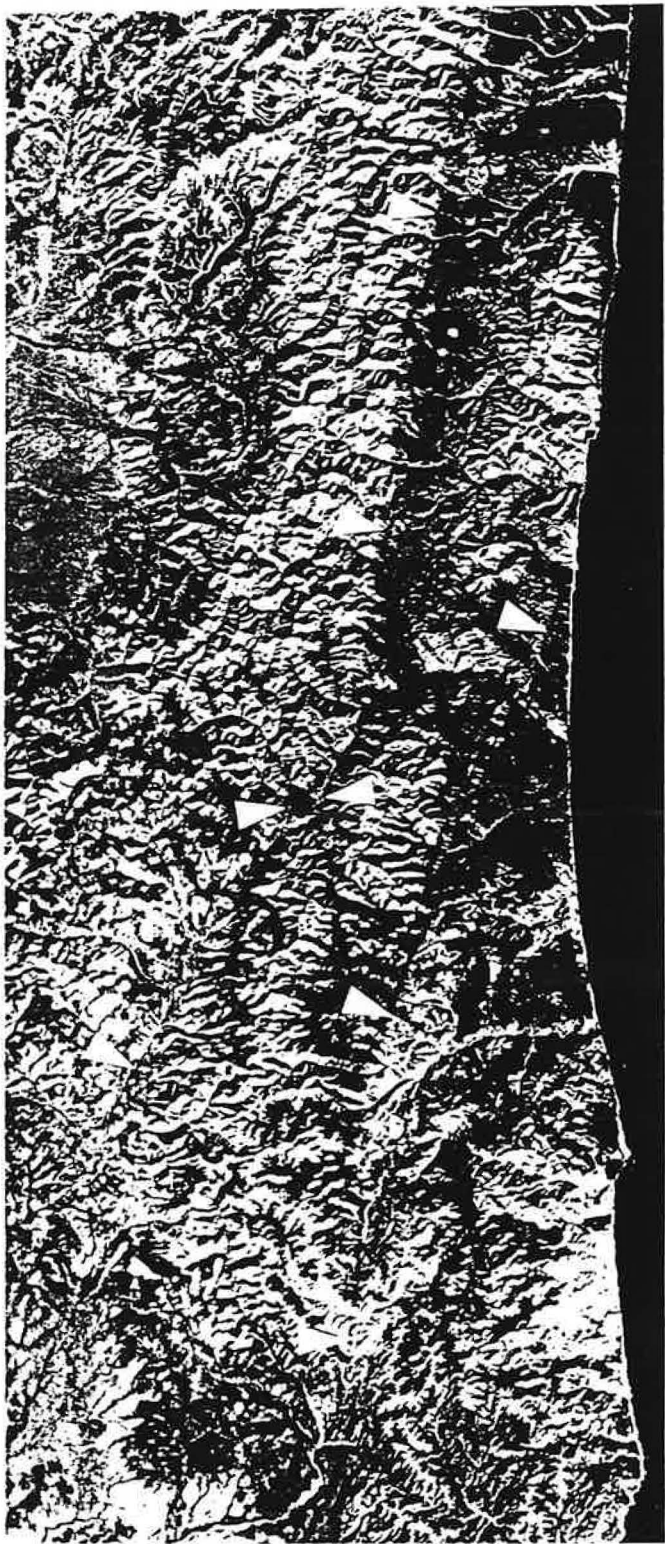
FOURNIER ET AL. FIG. 14



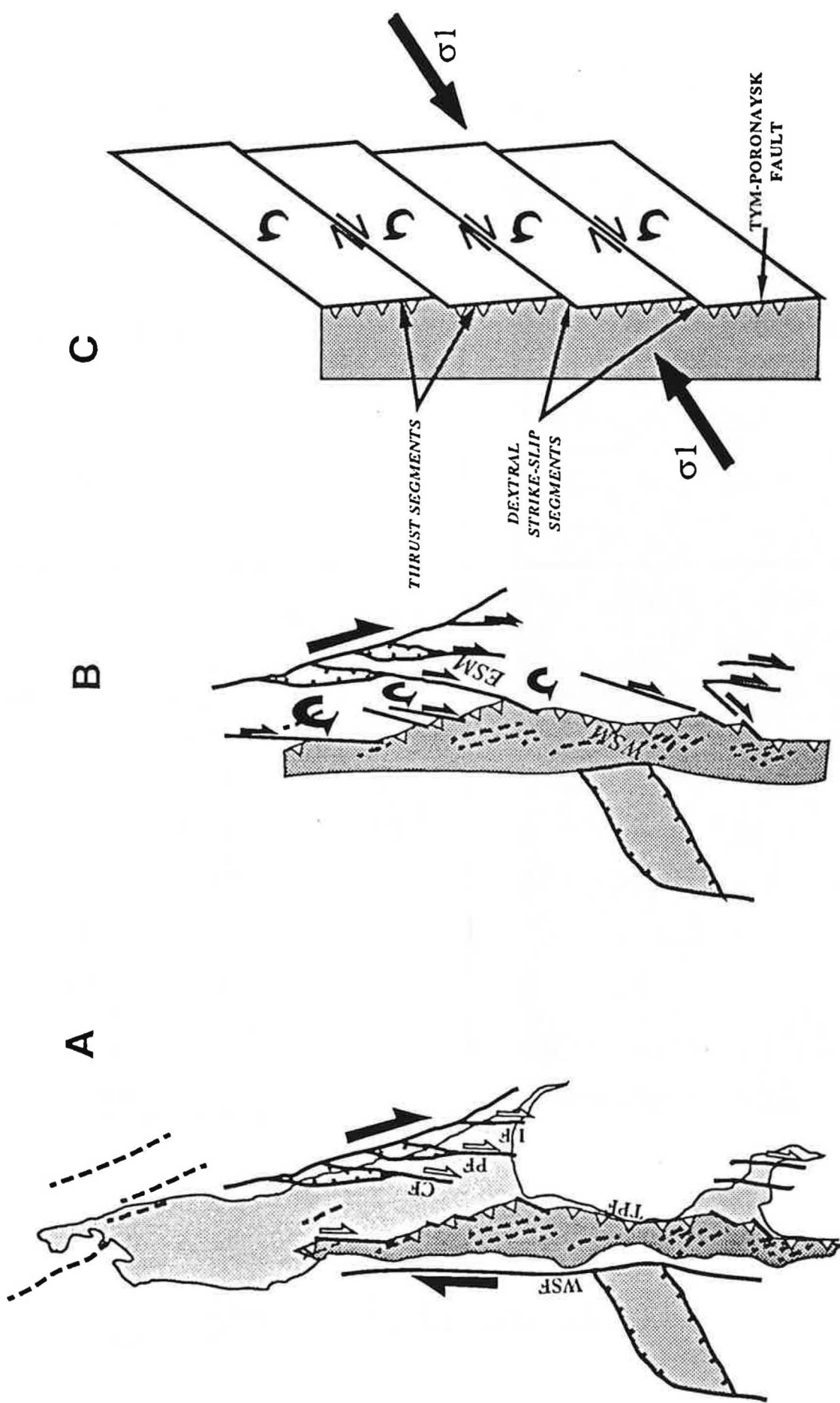
Foreman et al fig 15a

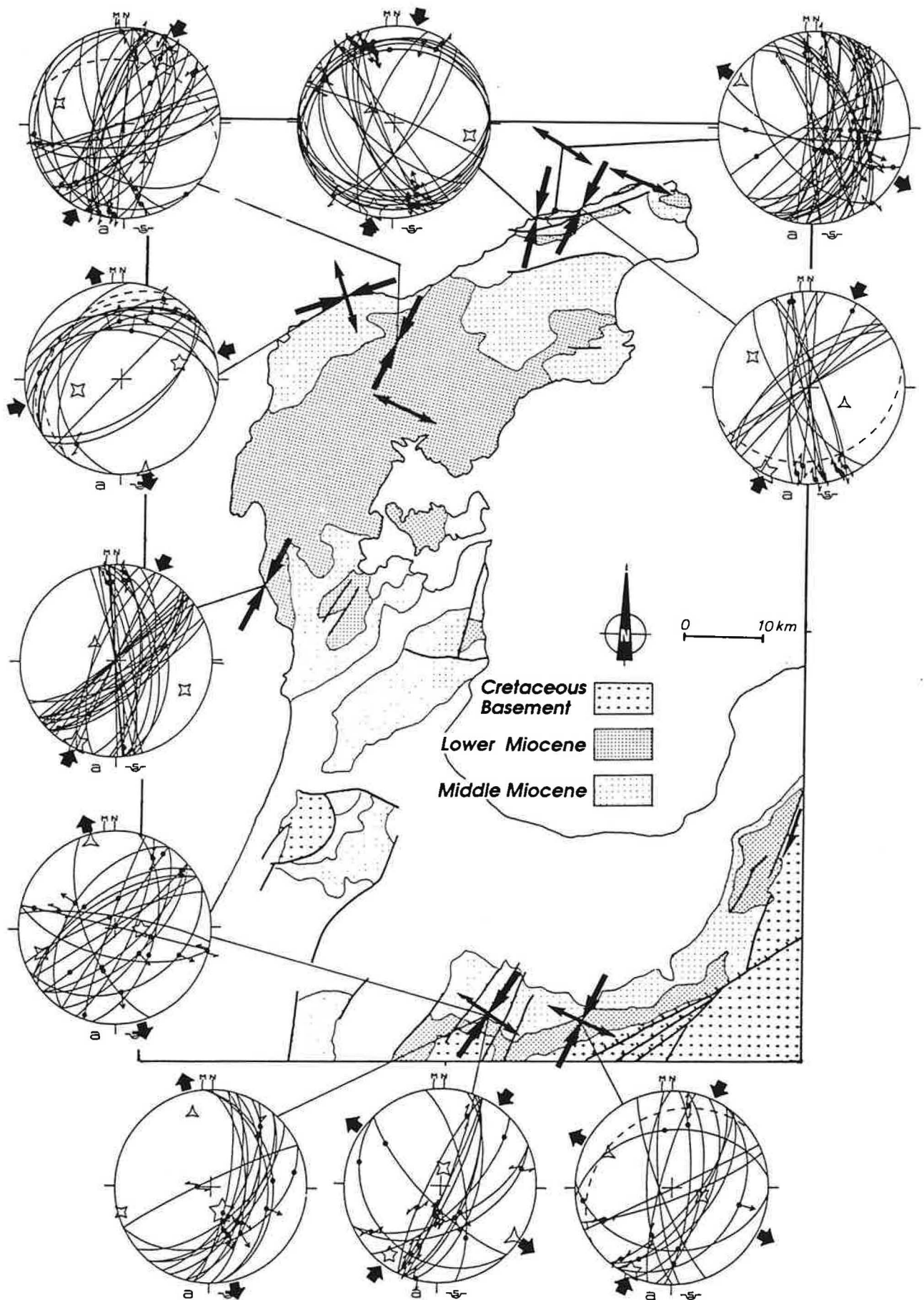


Fournier et al fig. 15b

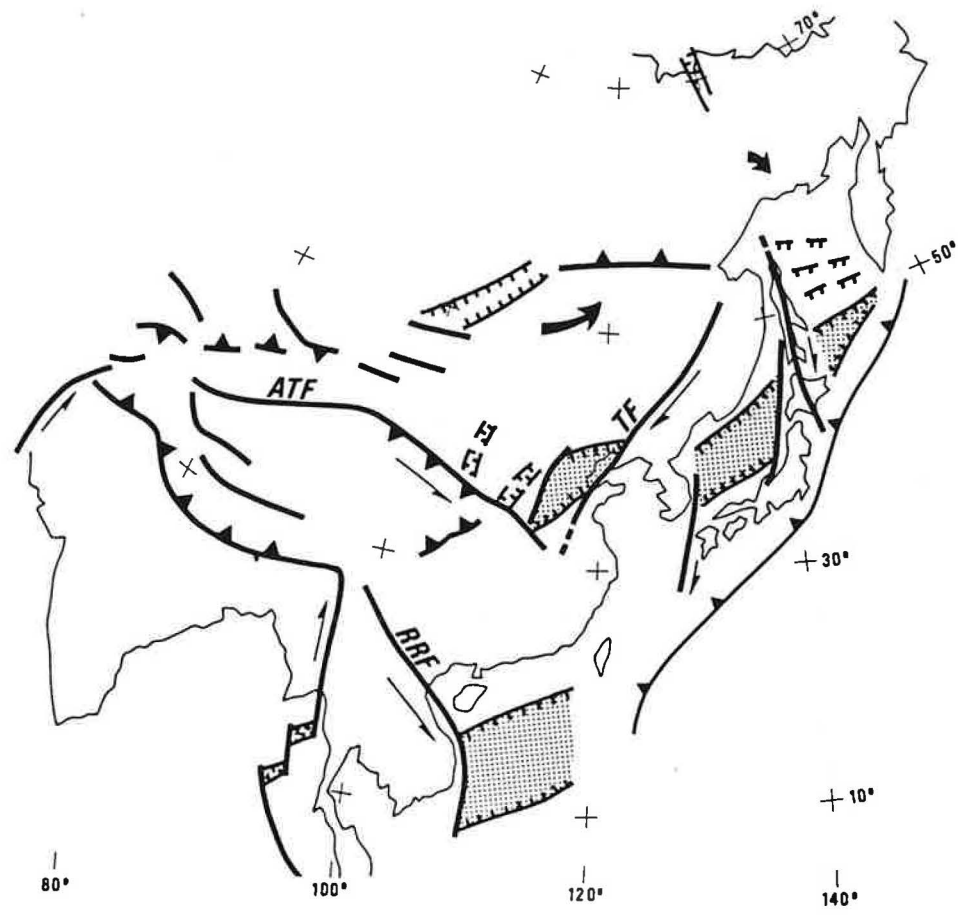


FOURNIER et al. fig. 16





FOURNIER ET AL. FIG. 18

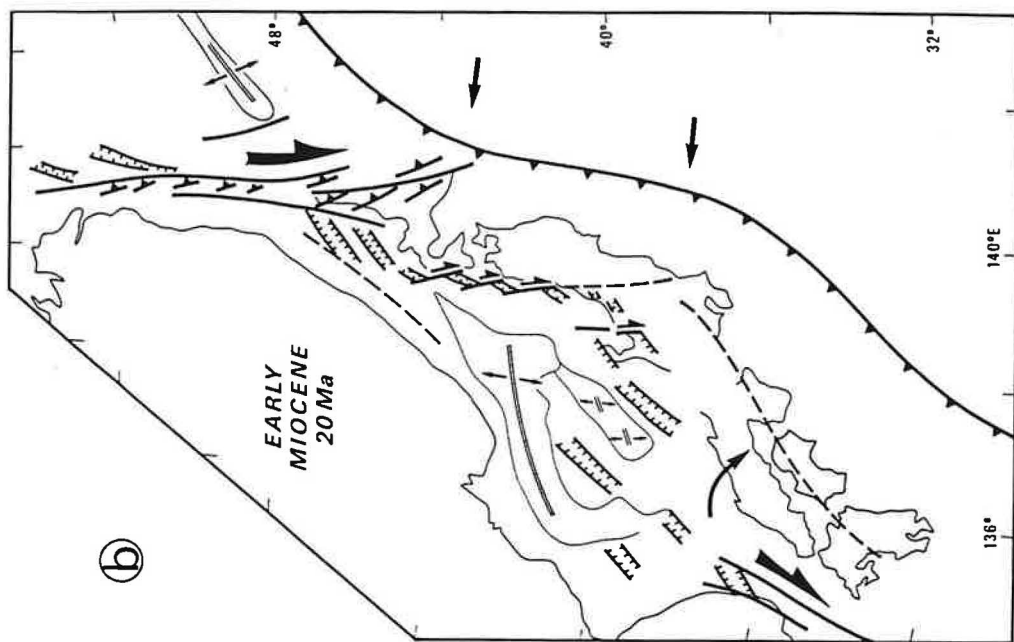


POURNIEZ
~~SOLINET~~ et al FIG 19

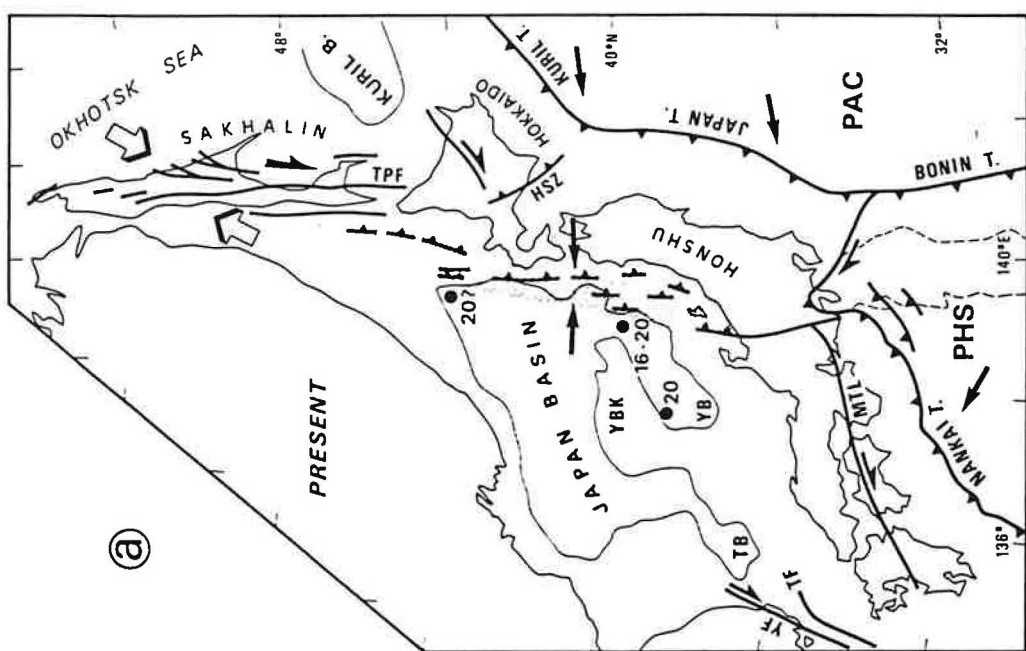
FIG 20

FORWARD

(b)



(a)



II. LA ZONE DÉCROCHANTE DE L'EST DE LA MER DU JAPON : article "Cenozoic intracontinental dextral motion in the Okhotsk-Japan Sea region"
 (Tectonics, 11, 968-977, 1992)

Résumé : Cet article présente une synthèse et une discussion sur l'évolution depuis l'Oligo-Miocène de la déformation le long de la zone décrochante est-mer du Japon, du Japon central jusqu'à Sakhaline.

Le long de la côte ouest du NE Honshu, une série de bassins en échelons dextres de direction NNE-SSO est décrite en mer. Un de ces bassins affleure sur l'île de Sado, il est d'âge Miocène inférieur à moyen, contemporain de l'ouverture de la mer du Japon. Jolivet et al. (1991) décrivent dans les formations Miocène inférieur et moyen de Sado une association de failles normales et décrochantes. Le champ de contraintes qu'ils dérivent de ces failles est à composante extensive NO-SE.

A Hokkaido, la zone d'Hidaka a été déformée par cisaillement dextre dans le faciès amphibolite à l'Oligo-Miocène (Jolivet et Miyashita, 1985). Cette déformation ductile profonde correspond dans les niveaux superficiels à des failles décrochantes et inverses associées, des plis en échelon dextre, et des chevauchements (Jolivet et Huchon, 1989). Le régime de contraintes est transpressif, la direction de compression est NE-SO.

A Sakhaline, la déformation est absorbée depuis le Miocène par des décrochements N-S, associés à des plis en échelons à l'ouest de la faille de Tym-Poronaysk, et à des bassins en échelons dans le socle Paléozoïque-Jurassique à l'est de la faille de Tym-Poronaysk.

La déformation active est purement compressive sur la marge orientale de la mer du Japon où la subduction vers l'est de la mer du Japon sous l'arc japonais est amorcée depuis 1.8 Ma (Tamaki et al., 1992). La transition entre la transtension Miocène et la compression actuelle se situe au Miocène supérieur. La compression est limitée à l'arc japonais et la région arrière-arc à proximité. A Sakhaline, la déformation décrochante Néogène se poursuit actuellement comme le montrent les mécanismes au foyer des séismes. Des mouvements décrochants dextres identiques sont décrits sur la marge coréenne de la mer du Japon (Jun, 1990), et plus loin à l'intérieur du continent asiatique le long de la faille de Tan-Lu. La compression dans l'arc Japonais apparaît donc comme un phénomène localisé qui doit trouver une cause locale. Le régime de subduction de la lithosphère océanique ancienne de la plaque Pacifique n'a pas changé depuis le Miocène, l'extension étant d'ailleurs toujours active au-dessus des fosses d'Izu-Bonin et des Mariannes dans la plaque mer des Philippines (Taylor et al., 1991). Il faut plutôt voir dans la compression un effet de la subduction du jeune (Oligo-Miocène) plancher océanique du bassin de Shikoku sous le Japon sud-ouest, subduction qui a débuté au Miocène moyen ou supérieur, et/ou un effet des collisions successives de l'extrême nord de l'arc des Bonins avec le Japon central depuis le Miocène supérieur.

(collisions de Tanzawa et d'Izu). Le changement de régime de contraintes dans l'arc Japonais coïncide ainsi avec un changement de conditions aux limites le long de la zone de subduction, suggérant un couplage entre la zone de subduction et la région arrière-arc.

Loin de la zone de subduction, la déformation décrochante évolue indépendamment de la subduction, comme à Sakhaline où le même régime transpressif se poursuit depuis le Miocène. Les travaux de Kimura et Tamaki (1986) et Jolivet et al. (1990) suggèrent que cette déformation décrochante est directement liée à la collision Inde-Asie.

CENOZOIC INTRACONTINENTAL DEXTRAL MOTION IN THE OKHOTSK-JAPAN SEA REGION

Laurent Jolivet, Marc Fournier, and Philippe Huchon
Département de Géologie, Ecole Normale Supérieure, Paris, France

Vitali S. Rozhdestvenskiy, Konstantin F. Sergeyev,
and Leonid S. Oscrbin
Institute of Marine Geology and Geophysics, Far East Science Center, Yuzhno-Sakhalinsk, USSR

Abstract. A right-lateral shear zone trending northerly along more than 2000 km is recognized from central Japan to northern Sakhalin. It was active mainly during the Neogene and has accommodated several hundreds of kilometers of displacement. The whole structure of Sakhalin is built on this shear zone. En échelon sigmoidal folds and thrusts, en échelon narrow Miocene basins, and a major discontinuity which is observed along more than 600 km, the Tym-Poronaisk fault, characterize the deformation there. In Hokkaido, en échelon folds and thrusts and a ductile shear zone with high-temperature metamorphism constitute the southern extension of this transpressional shear zone. It continues to the south as a zone of transtensional deformation along the eastern margin of Japan Sea, as en échelon basins and dextral transfer faults observed as far south as Noto peninsula and Yatsuo basin. The style of the shear zone thus evolves from transpressional in the north far from the subduction zone, to transtensional in the south in the back-arc region. Strike-slip motion along this shear zone was primarily responsible for the dextral pull-apart opening of Japan Sea during the early and middle Miocene. Dextral motion is still active in the north along the Tym-Poronaisk fault in Sakhalin as well as on the continental margin of Japan Sea (Korea and Asia mainland). Active E-W compression replaced the dextral motion along the eastern margin of Japan Sea in late Miocene time, and incipient subduction began in the early Quaternary.

INTRODUCTION

A diffuse zone of active deformation with crustal seismicity runs along Sakhalin, between the Amur region and Okhostk Sea (Figure 1). It has led to various interpretations, they are discussed by Jolivet et al. [1990]. Chapman and Solomon [1976], on the basis of a study of several large earthquakes focal mechanisms, concluded that a zone of active compression was perpendicular to the trend of Sakhalin. They assigned this deformation to the motion of North America (NAM hereafter) relative to

Eurasia (EUR hereafter). The rotation pole is located in eastern Siberia; north of it, extension prevails along the Cherskyi ranges, and oceanic spreading is active along the Gakkel-Nansen ridge, which is the northernmost extension of the Mid-Atlantic ridge. Savostin et al. [1983] instead proposed dextral motion between the Okhotsk and Amurian blocks and a kinematic interpretation taking into account the major structures of northeast Asia such as the Stanovoy ranges (see also Savostin and Karasik [1981], and Cook et al. [1986]).

This active zone extends southward in Hokkaido and along the eastern margin of Japan Sea. Large shallow earthquakes occur frequently there (Figures 2 and 3); they are all of reverse fault type with E-W direction of compression [Fukao and Furumoto, 1975]. Nakamura [1983] proposed that it corresponds to the southward extension of the NAM-EUR plate boundary following Chapman and Solomon [1976].

This active zone also corresponds to a domain which has suffered deformation since Oligocene time. Kimura et al. [1983] proposed that dextral oblique collision along the Okhotsk-Amur plate boundary was responsible for the Tertiary structures, such as en échelon folds in Hokkaido and Sakhalin. Jolivet and Miyashita [1985], Jolivet and Huchon [1989], and Jolivet et al. [1990] showed that dextral shear can be recognized along the central belt of Hokkaido (Hidaka Shear Zone) as well as the eastern margin of Japan Sea for lower to middle Miocene time. Lallemand and Jolivet [1985], Kimura and Tamaki [1986], and Jolivet [1986] proposed that this shear zone has been responsible for the dextral pull-apart opening of Japan Sea in Miocene time (Figure 1). Large dextral motions along N-S trending shear zones are usually not taken into account when describing the deformation of Asia except by Kimura and Tamaki [1986], Jolivet [1986], Chen and Nabelek [1988], or Jolivet et al. [1990].

In this paper, we present a synthesis of our studies based upon field surveys along this active zone from central Japan to Sakhalin, Landsat imagery, and focal mechanism of earthquakes. Detailed work will be published separately. A new tectonic map of the entire fault zone is described. We show that in Miocene time, structures located along this 2000-km-long shear zone are compatible with a localized dextral shear zone which evolves from transpressional in the north to transtensional in the south in the back-arc region. We discuss its relation to the opening of the Japan Sea back-arc basin. We also briefly discuss the significance of the dextral motions in the overall deformation of eastern Asia.

GENERAL TECTONIC CONTEXT

In the back-arc region of the Pacific subduction zone, behind the Kuril trench, Sakhalin is a long island extending along some 1000 km between the Okhotsk Sea and the Tartar strait (Figures 1-3). It does not exceed 200 km in width and is as narrow as 30 km at 48°N. It is the northern extension of the

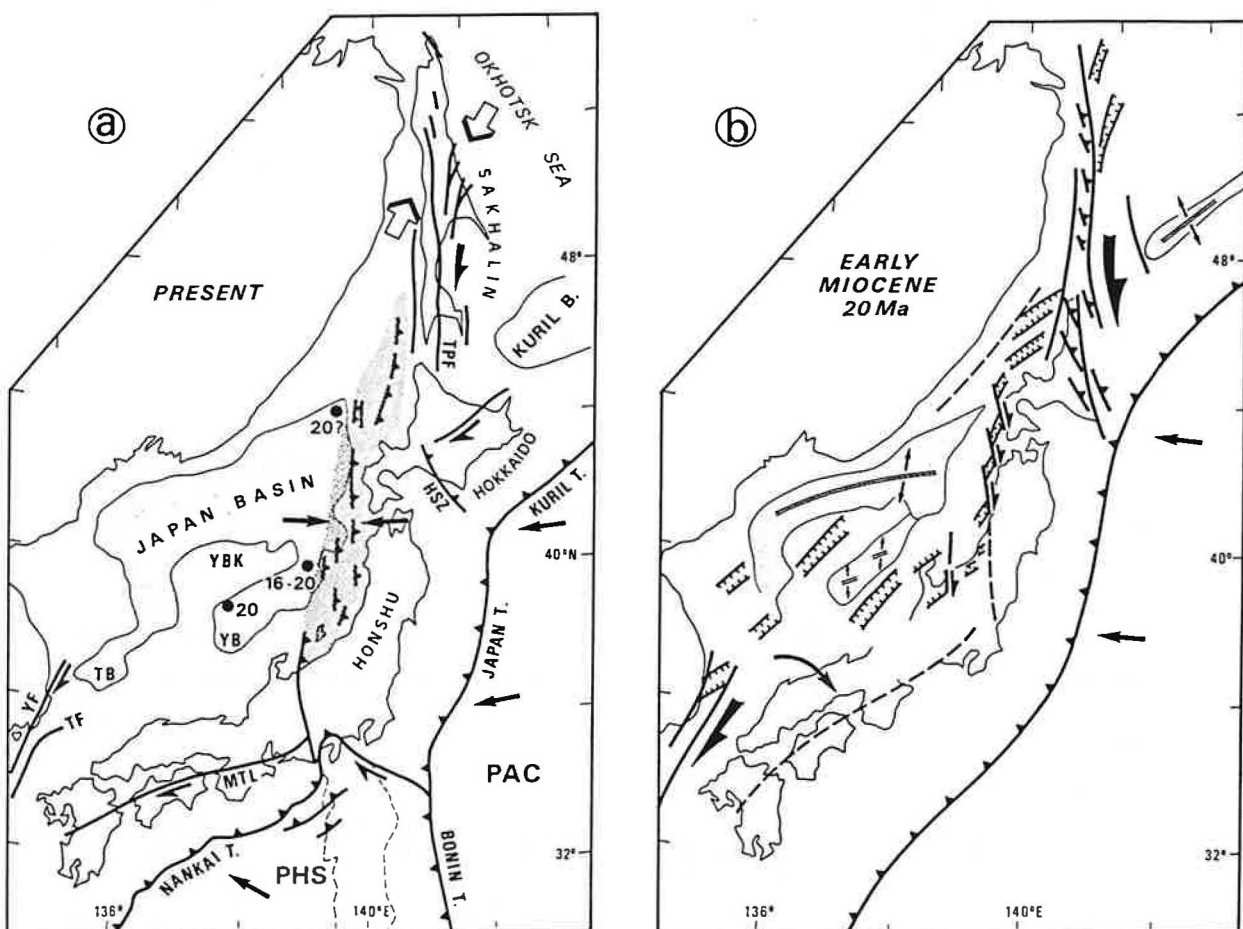


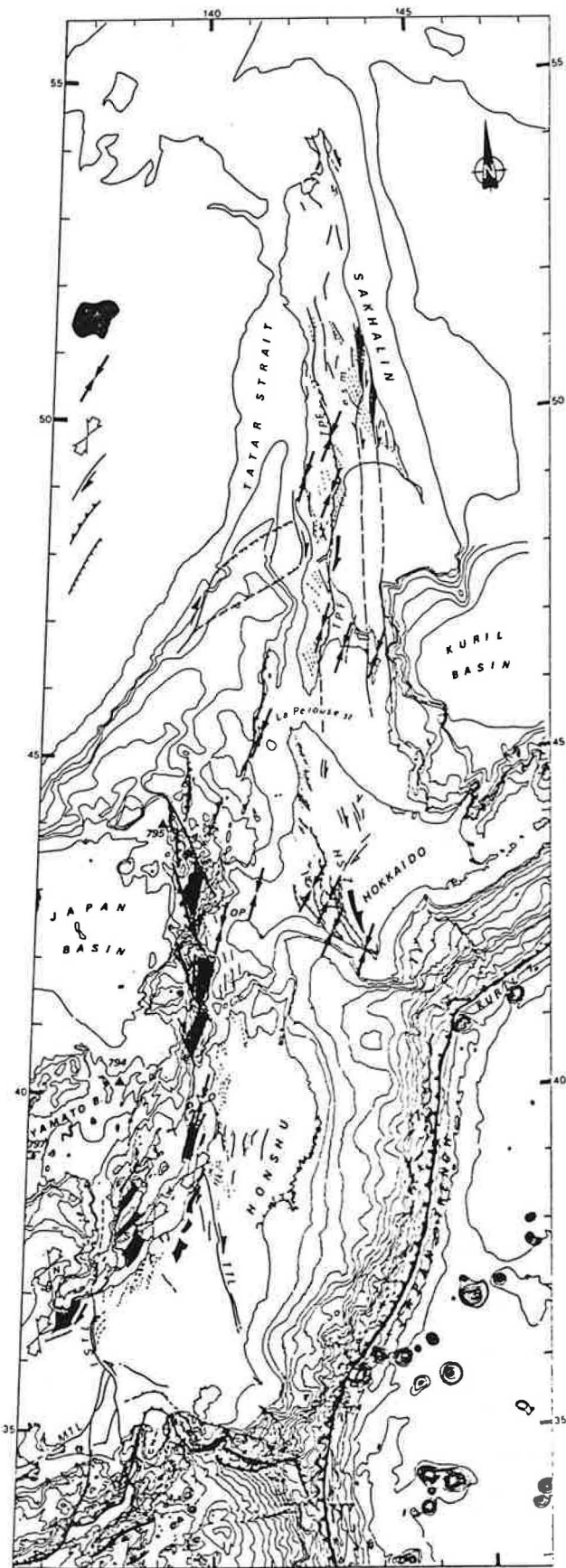
Fig. 1. (a) Present-day geodynamic context of Sakhalin and Japan Sea region. Shaded area represent the oceanic crusts of the Japan Sea and Kuril Basin. Dotted area is the zone of active compression of the eastern Japan Sea. (b) Same region 20 m.y. ago. Reconstruction parameters are after Jolivet et al. [1991] and Jolivet and Tamaki [1992]. Abbreviations are TPF, Tym-Poronaisk fault; HSZ, Hidaka Shear Zone; MTL, Median Tectonic Line; YBK, Yamato Bank; YB, Yamato basin; YF, Yangsan Fault; TB, Tsushima basin; TF, Tsushima fault; PAC, Pacific plate; and PHS, Philippine Sea plate.

central range of Hokkaido in northern Japan. It is separated from the Asian mainland by the shallow water Tartar Strait, which is the northernmost part of the Japan Sea. To the east, the Okhostk Sea has a continental basement cut by numerous faults making submarine ridges and troughs [Margulies et al., 1979; Gnibidenko, 1985]. In the southern part of the Okhostk Sea is the Kuril basin, which is floored with thick Cenozoic sediments and oceanic crust possibly of Miocene age [Kimura and Tamaki, 1985]. To the west the Tartar strait is floored with thinned continental crust cut by N-S trending faults and blanketed by a thick sedimentary cover up to 8 km [Antipov et al., 1980; H. S. Gnibidenko et al., manuscript in preparation, 1992]. Further south, the Japan Sea is divided into three major basins floored with oceanic crust (Japan basin, deeper than 3 km) or highly intruded thinned continental crust (Yamato

and Tsushima basins, deeper than 2 km) [Tamaki, 1985, 1988; Tamaki et al., 1990].

The Kuril trench continues to the south as the Japan trench until its junction with the Bonin trench south of the trench-trench-trench triple junction between the Philippine Sea (PHS hereafter), Pacific (PAC hereafter), and EUR plates [Huchon and Labaume, 1989]. The Pacific plate subducts westward at a velocity of about 10 cm/year [Seno, 1985]. The Philippine Sea plate subducts below southwest Japan at slower rate (4 cm/year) [Ranken et al., 1984; Huchon, 1986].

Active deformation is recorded along the eastern margin of Japan Sea, Hokkaido and Sakhalin as a diffuse seismic zone [Fukao and Furumoto, 1975; Tamaki, 1988]. Deformation is also recorded in the Tsushima strait [Jun, 1990], between Kyushu and Korea, as well as on the continental side of Japan



Sea in the Bohai gulf region along major strike-slip dextral faults [Chen and Nabelek, 1988].

The Japan Sea opened during the early and middle Miocene as was recently shown by the results of Ocean Drilling Program legs 127 and 128, which encountered oceanic crust about 20 m.y. old [Tamaki, 1990; Suyehiro et al., 1990]. Figures 2 and 3 show the position of sites 794, 795 and 797 where oceanic basaltic sills were recovered and dated, with the corresponding ages after Kaneoka et al. [1992].

In the region of the trench-trench-trench triple junction, the Bonin arc collides with central Japan north of the Izu peninsula, and active intraoceanic thrusting occurs south of the Nankai trench along the Zenisu ridge [Le Pichon et al., 1987; Chamot-Rooke and Le Pichon, 1989; Lallemand et al., 1989; Taira et al., 1989]. Between the collision zone and the triple junction, right-lateral motion is active along the Sagami trough. The relative motion of PHS relative to Japan has changed drastically since 2 Ma [Huchon, 1985; Jolivet et al., 1989]. The direction of the PHS-EUR motion vector was more northerly during Neogene and then turned to NW.

We now describe the structures observed along the entire deformed domain from south to north. We distinguish two zones of deformation. One is the eastern margin of Japan Sea sensu stricto (northeast Honshu, west Hokkaido, and offshore until Moneron island west of Sakhalin); the other one is the Central belt of Hokkaido and Sakhalin.

EAST JAPAN SEA

Late Miocene to Present

E-W compression is active along the eastern margin of Japan Sea. The most spectacular evidence is given by frequent large earthquakes and active faults recorded offshore Honshu, Hokkaido, and Sakhalin [Fukao and Furumoto, 1975; Tamaki, 1988]. Figures 2 and 3 show that this zone extends from the Japan Sea coast of central Japan to the west of Sakhalin. Fault plane solutions indicate E-W compression and pure reverse fault mechanisms. These earthquakes are associated with N-S trending active reverse faults. These are associated with the

Fig. 2. Tectonic map of the entire shear zone: 1, oceanic crust; 2, en échelon extensional basins of Miocene age; 3, direction of Miocene maximum compression deduced from fault set analysis; 4, same as for 3 but intermediate compression; 6, strike-slip faults; 7, thrust faults; and 8, normal faults. Abbreviations are esm, East Sakhalin Mountains; OP, Oshima peninsula; O, Oga peninsula; N, Noto peninsula; IZU, Izu peninsula, TPF, Tym-Poronaisk Fault; MTL, Median Tectonic Line; TTL, Tanakura Tectonic Line; ISTL, Itoigawa-Shizuoka Tectonic Line; HSZ, Hidaka Shear Zone, and TTT: trench-trench-trench triple junction of Central Japan.

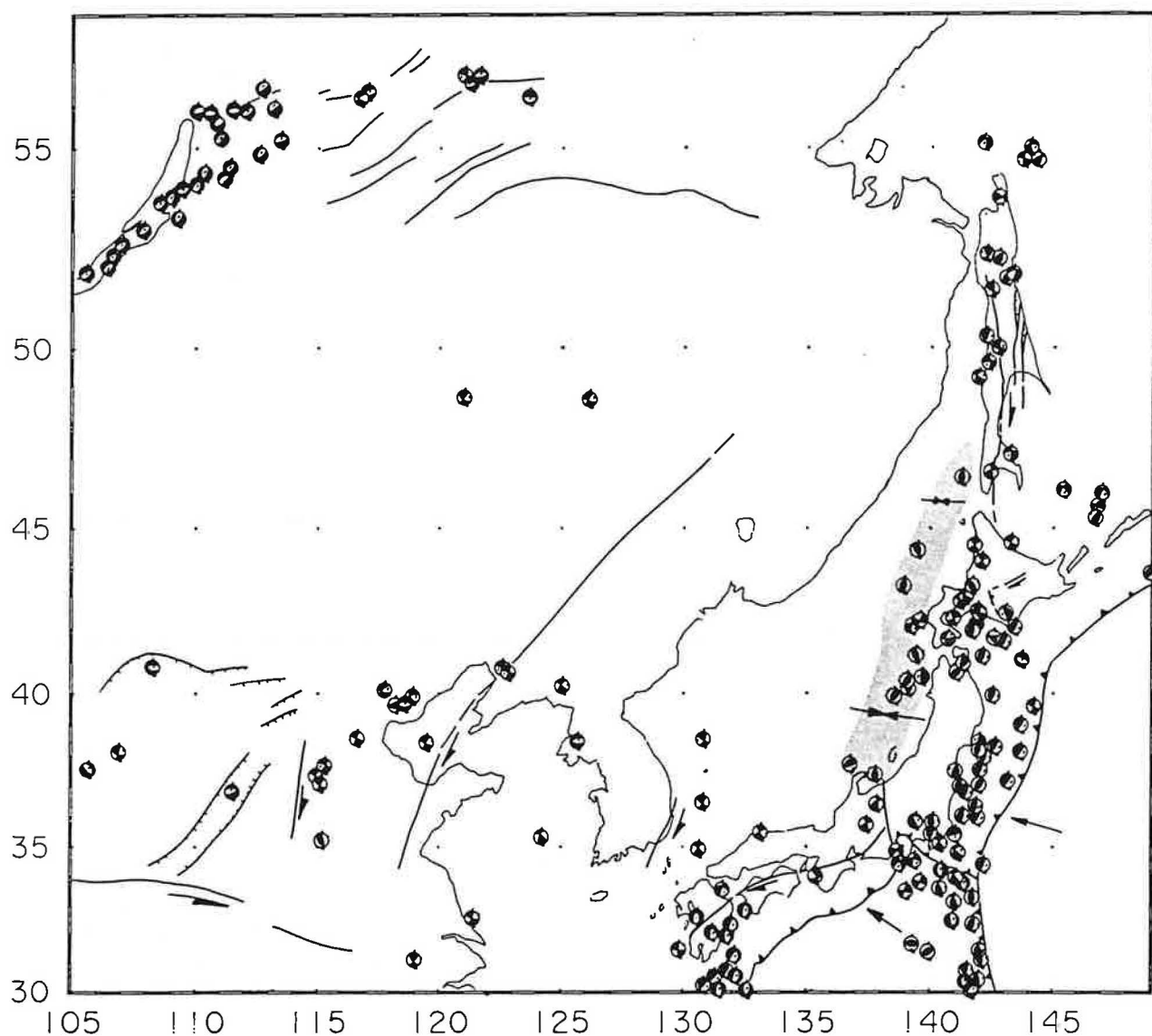


Fig. 3. Compilation of crustal earthquakes focal mechanisms (compressional quadrant in black). After Savostin et al. [1981], Dziewonski et al. [1983], L. S. Oscorbin [unpublished data, 1977], Chen and Nabelek [1988], Jun [1990]. Shaded area represents the zone of E-W compression in the eastern Japan Sea.

reactivation of Neogene en échelon basins [Jolivet et al., 1991]. Active thrust faults uplift narrow ridges of oceanic crust such as the Okushiri ridge [Tamaki, 1988]. Deep drilling on the ridge during ODP leg 127 revealed that the coarse-grained detrital supply stops on the ridge at 1.8 Ma because the ridge was uplifted above the bottom of the basin at this time [Tamaki et al., 1990]. This age is interpreted as the inception of subduction of Japan Sea lithosphere.

Active deformation is observed also onland where Neogene deposits are folded with N-S trending fold axes and thrusts [Amano and Sato, 1989; Sato, 1989]. Early studies of vertical movements of the northeast Honshu arc reveal a period of upheaval

from 5 Ma to the present [Sugi et al., 1983]. The paleostress field inferred from dike orientation changes to E-W compression at 7 Ma [Nakamura and Uyeda, 1980; Takeuchi, 1985]. Neogene subsidence curves on the margins of Japan Sea and at oceanic sites show uplift from 10 Ma to the present [Ingle, 1992]. Observation of fault sets in the Neogene deposits of western Hokkaido and northeast Honshu indicates a change of maximum horizontal compression from NE-SW to E-W between the middle and late Miocene [Jolivet and Huchon, 1989; Yamagishi and Watanabe, 1986; Otsuki, 1989]. The age of beginning of E-W compression can thus be determined to have occurred around 9 Ma.

Early and Middle Miocene Deformation

This active deformation reworks a zone of Miocene transtension. The en échelon geometry of Quaternary compressional basins is not compatible with the present stress field. Because a Miocene graben crops out on Sado island which is parallel to the en échelon basins, it is likely that they all correspond to Miocene extensional basins. Their en échelon position is then compatible with a dextral oblique extension [Jolivet et al., 1991]. A similar geometry is observed onland in the Uetsu district, where fast rifting is observed to have occurred in the early Miocene [Yamaji, 1989; 1990]. In general the age of rifting on the eastern margin of Japan Sea is considered to be early to middle Miocene [Suzuki, 1989; Amano and Sato, 1989]. The age of formation of the oceanic basin offshore NE Honshu has been recently revealed by ODP leg 127: at site 794 and 797 early Miocene (20 Ma to 16 Ma) basalts were recovered as sills interbedded with deep water sediments. Intense basaltic intrusive and extrusive activity, around 15 Ma, is recognized in the Aosawa region onland NE Honshu [Tsuchiya, 1989, 1990].

Fault set analysis indicates that NW-SE extension prevailed with association of normal and strike-slip faults until the end of the middle Miocene in NE Honshu and Sado island [Jolivet et al., 1991]. Additional observations confirm this geometry in the Noto peninsula and Yatsuo basin further south (Figure 3). All fault set data from Sakhalin to Yatsuo basin will be published separately [Fournier et al., paper submitted to Journal of Geophysical Research, 1992]. Right-lateral shear is not restricted to the Japan Sea coastal area, since Cretaceous left-lateral shear zones such as the Tanakura Tectonic Line were reactivated in Miocene time as dextral faults [Koshiya, 1986].

The direction of horizontal maximum compression of Miocene age remains constant from Yatsuo to Rebun island, but it corresponds to σ_2 (intermediate principal stress) in the south and σ_1 in the north. In Rebun island and Hokkaido, NE trending compression prevails with strike-slip and reverse faults [Jolivet and Huchon, 1989].

To summarize, the eastern margin of Japan Sea was the site of dextral oblique extension in early and middle Miocene time. Meanwhile, oceanic spreading was occurring in Yamato and Japan basins. By the end of the middle Miocene a sharp change in stress field occurred. E-W compression took place on the same zone. By the early Quaternary, subduction began, and thrust faults affected the oceanic back-arc region.

HOKKAIDO CENTRAL BELT

Late Miocene to Present Deformation

The N-S trending Hokkaido central belt was built through polyphase evolution from the Mesozoic to the present. A drastic change in the deformation regime occurred at the end of the middle Miocene as

far south as Honshu. Recent evolution is characterized by E-W compression and fast uplift of the metamorphic core of the belt, the Hidaka mountains [Kimura et al., 1983]. Steep N-S trending thrusts separate it from the foreland to the west, where active thrusting affects Pliocene and recent sediments of the Sapporo-Tomakomai depression [Mitani, 1978; Yamagishi and Watanabe, 1986].

Oligocene to Middle Miocene deformation

An older stage of deformation prior to the E-W compression is recognized only in sediments older than late Miocene; reverse and strike-slip faults are associated with this stage [Jolivet and Huchon, 1989]. The maximum horizontal compression trends NE consistently from south to north. This stage is characterized by the formation of NW trending en échelon folds and thrusts in the nonmetamorphic zones [Kimura et al., 1983] and a ductile shear zone (Hidaka Shear Zone) in the metamorphic zone. Jolivet and Miyashita [1985] interpreted this ductile deformation as the result of dextral shear in a deep crustal environment. Jolivet and Huchon [1989] related the en échelon folds and thrusts and the ductile shear zone to a crustal-scale half flower structure built along a transpressional dextral strike-slip crustal fault of Oligocene to middle Miocene age. This interpretation is roughly consistent with that of Kimura et al. [1983] in terms of kinematics (dextral oblique collision). Recent paleomagnetic investigations in Hokkaido confirm this interpretation [Kodama et al., 1990]. The dextral transpression is observed till Rebun island on the Japan Sea margin offshore northernmost Hokkaido. East of the Hokkaido central belt, N-S trending dextral faults are related to the formation of small pull-apart basins in Miocene time [Watanabe and Iwata, 1985; Watanabe, 1988].

SAKHALIN

The Hokkaido central belt extends northward through Sakhalin island. East Sakhalin Mountains is a tectonic map of Sakhalin derived from the existing geological map at 1/1000000 scale, Rozhdestvenskiy [1983, 1986], K. F. Sergeyev (unpublished data, 1990) and our own field observations and Landsat images analysis. The most prominent structure is the Tym-Poronaisk fault, which runs N-S for more than 600 km. Other N-S trending faults are recognized east of the Tym-Poronaisk fault, but they are probably less active. Following Rozhdestvenskiy [1982] and Kimura et al. [1983] we recognize in Sakhalin the same dextral strike-slip deformation already described in Honshu and Hokkaido, but the recent E-W compression does not show obviously in the structures.

Neogene Deformation

Figure 4 summarizes the Cenozoic structures of Sakhalin, and Figure 5 shows the features seen on

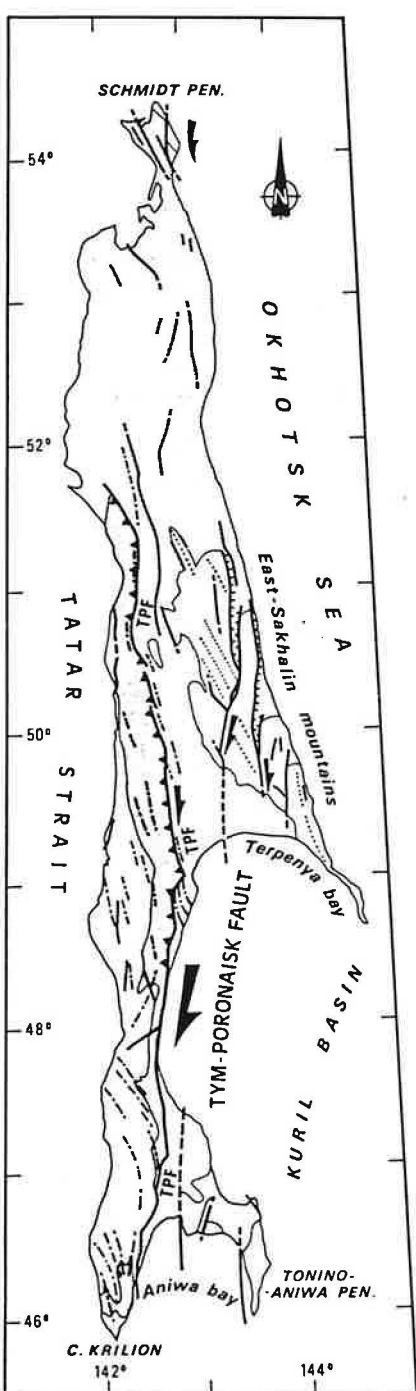


Fig. 4. Tectonic map of Sakhalin after the geological map of Sakhalin, Rozhdestvenskiy [1982], analysis of Landsat images (M. Fournier et al., paper submitted to Journal of Geophysical research, 1992) and K. F. Sergeyev (unpublished data, 1990). Dashed lines are Cenozoic folds axes seen in the Cretaceous to Miocene sediments; dotted lines are axes of postfoliation open folds seen in the Mesozoic metamorphic complex of the Eastern Sakhalin Mountains.

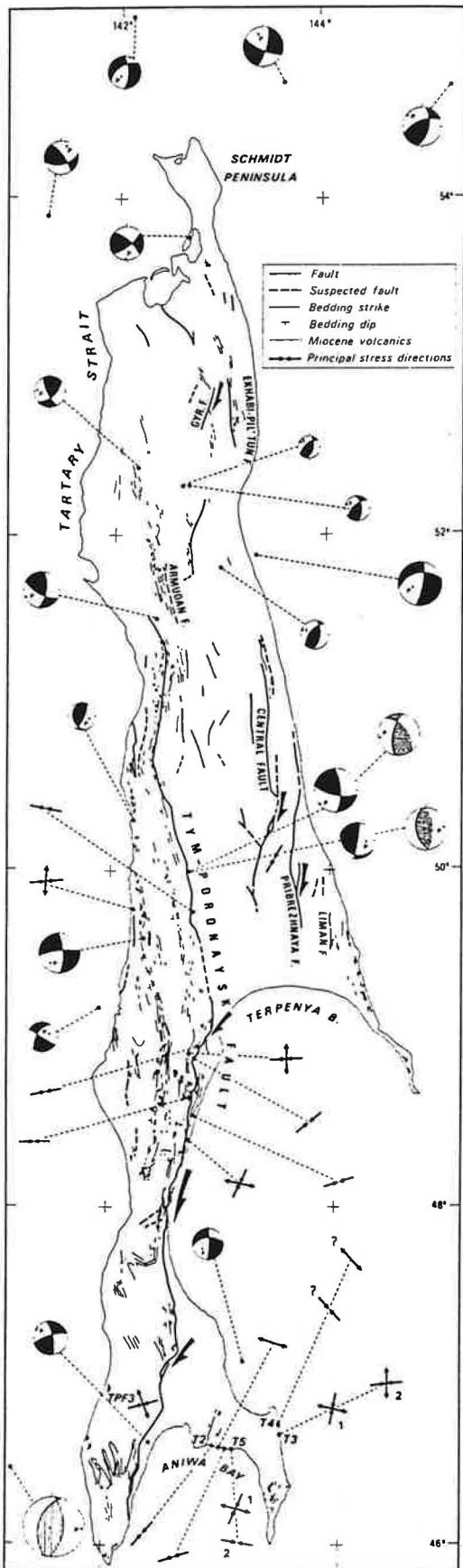
the Landsat mosaic as well as focal mechanisms of shallow earthquakes. The Tym-Poronaisk fault divides Sakhalin in two parts: West Sakhalin Mountains and East Sakhalin Mountains.

The Cenozoic sequence is roughly similar on both sides of the fault. It begins in the upper Oligocene with coarse conglomerate and fines upward into lower Miocene sandstone and middle Miocene siltstone and siliceous claystone [Melnikov, 1987]. The whole sequence is intruded by basic dykes and sills, and basaltic lavas and breccia constitute the end of the middle Miocene. The late Miocene and Pliocene are made of tuffaceous siltstone and sandstone.

The West Sakhalin Mountains represent the northern extension of the central belt of Hokkaido; in general facies are similar to those of the Central Belt though less deep in general [Melnikov, 1987]. The Cretaceous is represented by forearc deposits with abundant terrestrial and volcanic detritus. In the East Sakhalin Mountains, Cenozoic deposits are underlain by a complex system of thrust slices composed of oceanic material of Late Jurassic to Cretaceous age, partly metamorphosed under high-pressure low-temperature conditions [Rozhdestvenskiy, 1986]. G. Kimura et al. (manuscript in preparation, 1992) describe this system as a Cretaceous accretionary complex. It is the northern extension of the Kamuikotan zone of Hokkaido.

West of the fault and immediately east of it, Cretaceous and Cenozoic sediments are folded; the NW trending axes of the folds distributed with a dextral en échelon pattern [Rozhdestvenskiy, 1982; Melnikov, 1987]. The folds axes are curved close to the fault, thus giving a sigmoidal shape compatible with dextral displacement. The fault is a very sharp feature clearly seen on Landsat images. The fault plane itself occurs between Cretaceous sediments or lavas and Miocene sandstones. It is usually a N-S trending vertical plane with horizontal striation and evidence of dextral motion. In the East Sakhalin Mountains, N-S trending steep faults (Central, Pribrezhnaya, and Liman faults) cut through the Mesozoic accretionary complex. They are associated with narrow Miocene sedimentary basins which are arranged en échelon. A small dextral pull-apart basin is seen on Landsat images along the North-Sakhalin fault. Rozhdestvenskiy [1982] shows that the contact between a metamorphic complex and nonmetamorphosed sediments is offset dextrally by 25 km. Dextral offset along N-S trending faults is also observed in Schmidt peninsula in the very north of Sakhalin.

We performed fault set analysis along and around the Tym-Poronaisk fault. All data are compatible with NE trending horizontal compression (Figures 2 and 5). Fault set analysis [Fournier et al., paper submitted to Journal of Geophysical Research, and Figure 5] shows an E-W trending compression at several sites along the fault, it is however always associated with curved fold axes with the dextral en échelon pattern. The direction of compression is



elsewhere NE-trending and always perpendicular to fold axes. E-W compression therefore corresponds to rotated sites and the original direction of compression (Figure 2) was thus NE. This is in good agreement with the trend of fold axes and strike-slip faults.

Our observations of the deformation in the accretionary complex below the Cenozoic deposits of the East Sakhalin Mountains reveal a first stage with layer-parallel shear of probable Mesozoic age [Kimura et al., in prep.] followed by a second stage of upright folding. These folds trend NW and are compatible with the same NE trending compression which gave the en échelon folds of West Sakhalin. We thus attribute these folds also to the Cenozoic stage and the strike-slip motion.

A recent compilation of seismic data allowed H. S. Gribidenko et al. (manuscript in preparation, 1992) to draw a precise isopach map of Cenozoic sediments in the Tartar Strait. One prominent feature is a deep rhombohedral basin (Figure 2) bounded by NS-trending vertical compressional faults and NE trending normal faults and filled with more than 8 km of Cenozoic deposits. The overall shape of the basin and the nature of the faults lead us to the conclusion that it corresponds to a dextral pull-apart. This shows that a large part of the dextral motion was localized in the Tartar Strait.

Active Deformation

Fault plane solutions of earthquakes in Sakhalin (L. S. Oscorbin, unpublished data) show two kinds of mechanisms (Figures 3 and 5), both being

Fig. 5. Map of Sakhalin showing the features seen on the Landsat mosaic after M. Fournier et al. (paper submitted to Journal of Geophysical Research, 1992). Paleo-stress-field horizontal directions deduced from fault set analysis are plotted. Fault plane solutions of superficial earthquakes (depth lower than 30 km) determined by L. S. Oscorbin (T-quadrants in black), and Fukao and Furumoto [1975] (T-quadrants vertically ruled) and centroid moment tensors determined by Dziewonski et al. [1985, 1987] (T-quadrants horizontally ruled) are shown. Radii of focal mechanisms are a function of the magnitude (surface waves) of earthquakes except for Dziewonski et al. [1985, 1987]. Concerning Oscorbin data, we kept the main event only when two focal mechanisms were determined for the same earthquake. The two centroid moment tensors determined by Dziewonski et al. [1985, 1987] correspond to two earthquakes which fault plane solutions have independently been determined by Oscorbin (in order to simplify we indicate only Oscorbin's epicenter locations). P axes are almost similar in each case, and T axes of Dziewonski et al.'s focal mechanisms are steeper so that they indicate compressional motion when Oscorbin's indicate strike-slip motion.

compressional: strike-slip and reverse faults. Several mechanisms located close to the main fault trace are compatible with dextral motion along the fault. Rozhdestvenskiy [1986] describes a change in the stress pattern in Pliocene time from dextral wrench along the Tym-Poronaisk fault to E-W compression. As described above, the fault set analysis does not reveal E-W compression except perhaps in the south, and all structures observed at large scale are compatible with dextral motion. The existence of dextral fault plane solutions lead us to think that dextral wrench is still active in Sakhalin, as already stated by Savostin et al. [1983].

DISCUSSION

From central Japan to the north of Sakhalin, along more than 2000 km, we recognize a narrow domain of strain localization with evidence of dextral motion in Miocene time. It is thus a major feature of the deformation of eastern Asia, and it is worth discussing its evolution with time.

Present-Day Activity

Although E-W compression is obvious in the south, in the back-arc region, with numerous large compressional earthquakes and other compressional features, it is not as clear in the north. Dextral motion is probably still active in Sakhalin, except in the very south (the Moneron earthquake is similar to those off Hokkaido and Honshu and corresponds to the northernmost extension of the East Japan Sea nascent subduction zone).

Miocene Deformation

In the north the strike-slip deformation is transpressional and localized along a very narrow zone, characterized by en échelon folds and thrusts and one major discontinuity, the Tym-Poronaisk fault. Further south it becomes more transpressional in the Hidaka mountains where the shear zone curves toward a more westerly trend. Ductile parts of the shear zone were there uplifted during the dextral shear. This transpressional zone continues in the southwest as a transtensional one along the eastern margin of Japan Sea. It is characterized by en échelon graben and dextral transfer faults which were later reactivated as compressional structures. The dextral shear in Hokkaido and Japan Sea margin ended about 10 m.y. ago and is contemporaneous with the deposition of early to middle Miocene sediments. It is thus exactly contemporaneous with the opening of Japan Sea. Figure 1b shows a reconstruction of the strike-slip shear zone in early Miocene time during an early stage of Japan Sea opening [after Jolivet et al., 1991; Jolivet and Tamaki, 1992]. It is contemporaneous with the rotation of SW Japan deduced from paleomagnetic data [Otofuji et al., 1985]. The dextral shear zone extends to the south as a dextral fault between SW Japan and Korea [Sillitoe, 1977].

Therefore, if the dextral motion is correlated with the Japan Sea opening, several hundred kilometers of dextral displacement are expected. Reconstructions of the pre-opening situation [Jolivet and Tamaki, 1992] show a total offset since 25 Ma of about 400 km. There is no direct evidence concerning the total dextral offset. Only Rozhdestvenskiy [1982] describes a 25-km offset along one fault in the East Sakhalin Mountains. As the deformation is distributed on several major faults the total displacement is most likely much larger. The Tym-Poronaisk, being the major onshore fault, probably accommodated the largest displacement but certainly not more than a few tens of kilometers. So, the largest part of the dextral motion must be taken up along the Tartar Strait where the crust is thinner.

It is noticeable that the dextral shear zone is nowhere compatible with the PAC-EUR relative motion. Furthermore, it extends northward very far from the subduction zone and trends at a large angle to the trench system. It is thus unlikely that it represents a back-arc strike-slip fault such as the Philippine or Sumatra faults which accommodate the obliquity of the motion vector [Huchon and Le Pichon, 1984]. Such obliquity is observed in the Kuril trench at present and is accommodated by a ENE-WSW dextral fault parallel to the Kuril arc, which cuts through eastern Hokkaido [Kimura, 1986]. It is almost perpendicular to the trend of the major dextral shear zone.

The dextral shear zone was turned into a compressional zone in the back-arc region about 10 m.y. ago. This date corresponds to the end of the Japan Sea opening and is slightly younger than the arrival of the triple junction in its present position [Jolivet et al., 1989]. The compression is restricted to the back-arc region north to the central Japan triple junction. Far off the triple junction, either in Sakhalin or in Korea, and also on the continental side of Japan Sea, the deformation is still dextral (Figure 3) [Chen and Nabelek, 1988; Jun, 1990]. South of the triple junction, extension is active in the Bonin arc. This suggests that compression is due to the local plate configuration in the triple junction region and/or the degree of plate coupling along the subduction zone and is not characteristic of the more general tectonic context of eastern Asia. Following Kimura and Tamaki [1986] and Jolivet et al. [1990], we suggest that the Sakhalin-East Japan Sea is one of the major dextral faults created in the Asian continent during the India-Asia collision. Figure 3 shows that other dextral faults which are still active, exist west of it. Chen and Nabelek [1988] showed that dextral motion has been active in the Bohai gulf region along NNE trending faults. Jun [1990] describes focal mechanisms along the Tsushima fault which are compatible with dextral shear. This shear zone reactivated in Miocene time the Mesozoic suture that runs along Hokkaido and Sakhalin. Far from the subduction zone it was, and still is, a transpressional wrench fault, and it turned to a transtensional one in the back-arc region because extensional tectonics was prevailing there. At that time all major back-arc

basins were opening (Japan Sea, Shikoku basin, South China Sea, and possibly Kuril basin), which indicates that extensional conditions were active all along the western Pacific margin behind the subduction zone. The formation of this strike-slip shear zone disturbed the back-arc extension, giving rise to the pull-apart geometry we now observe. Extension in the back-arc region was linked with the mechanics of stress coupling along the subduction zone, and strike-slip with internal deformation of Asia due to collision with India.

REFERENCES

- Amano, K. and H. Saito, Neogene tectonics of the central part of northeast Honshu arc, *Mem. Geol. Soc. Jpn.*, 32, 81-96, 1989.
- Antipov, M.P., V.M. Kovylin, and V.P. Filat'yev, Sedimentary cover of the deep water basins of Tatar strait and the northern part of the sea of Japan, *Int. Geol. Rev.*, 22, 1327-1334, 1980.
- Chamot-Rooke, N., and X. Le Pichon, Zenisu ridge: mechanical model of formation, *Tectonophysics*, 160, 175-194, 1989.
- Chapman M. C., and S. C. Solomon, North American-Eurasian plate boundary in northeast Asia, *J. Geophys. Res.*, 81, 921-930, 1976.
- Chen, W. P. and J. Nabelek, Seismogenic strike-slip faulting and the development of the North China basin, *Tectonics*, 7, 975-989, 1988.
- Cook, D.B., K. Fujita, and C. A. Mac Mullen, Present day plate interactions in northeast Asia: North America, Eurasian and Okhotsk plates, *J. Geodyn.*, 6, 33-51, 1986.
- Dziewonski, A. M., A. Friedman, D. Giardini, and J.H. Woodhouse, Global seismicity of 1982: centroid moment tensor solutions for 308 earthquakes, *Phys. Earth Planet. Int.*, 45, 11-36, 1983.
- Dziewonski, A. M., J. E. Franzen, and J. H. Woodhouse, Centroid-moment tensor solutions for October-December 1984, *Phys. Earth Planet. Int.*, 39, 147-156, 1985.
- Dziewonski, A. M., G. Ekstrom, J. E. Franzen, and J. H. Woodhouse, Global seismicity of 1979: centroid-moment tensor solutions for 524 earthquakes, *Phys. Earth Planet. Int.*, 48, 18-46, 1987.
- Fukao, Y., and M. Furumoto, Mechanisms of large earthquakes along the eastern margin of the Japan sea, *Tectonophysics*, 25, 247-266, 1975.
- Gnibidenko, H. S., The Sea of Okhotsk-Kuril islands ridge and Kuril-Kamchatka trench, in *The Ocean Basins and Margins*, vol. 7A, edited by A.E.N. Naim et al., pp. 377-418, Plenum, New York, 1985.
- Huchon, P., Géodynamique de la zone de collision d'Izu et du point triple du Japon Central, Thèse de Doctorat, Univ. Pierre et Marie Curie, Paris, 414 pp., 1985.
- Huchon, P., Comment on "Kinematics of the Philippine sea plate" by B. Ranken, R. K. Cardwell and D. E. Karig, *Tectonics*, 5, 165-168, 1986.
- Huchon, P., and P. Labaume, Central Japan triple junction: a three-dimensional compression model, *Tectonophysics*, 160, 117-133, 1989.
- Huchon, P. and X. Le Pichon, Sunda strait and Central Sumatra Fault, *Geology*, 12, 668-672, 1984.
- Ingle, J. C., Subsidence of the Japan Sea: evidence from ODP sites and onshore sequences, In *Tamaki, K., Suyehiro, K., Allan, J. et al.*, 1992, *Proc. ODP, Sci. Results*, 127-128, in press, 1992.
- Jolivet, L., America-Eurasia plate boundary in eastern Asia and the opening of marginal basins, *Earth Planet. Sci. Lett.*, 81, 282-288, 1986.
- Jolivet, L., and P. Huchon, Crustal scale strike-slip shear zone in Hokkaido, Northeast Japan, *J. Struct. Geol.*, 11, 509-522, 1989.
- Jolivet, L., and S. Miyashita, The Hidaka Shear Zone (Hokkaido, Japan), genesis during a right-lateral strike slip movement, *Tectonics*, 4, 289-302, 1985.
- Jolivet, L., and K. Tamaki, Neogene kinematics in the Japan sea region and volcanic activity of the northeast Japan arc, In Tamaki, K., Suyehiro, K., Allan, J. et al., 1992, *Proc. ODP, Sci. Results*, 127-128, in press, 1992.
- Jolivet, L., P. Davy, and P. R. Cobbold, Right-lateral shear along the northwest Pacific margin and the India-Eurasia collision, *Tectonics*, 9, 1409-1419, 1990.
- Jolivet, L., P. Huchon, and C. Rangin, Tectonic setting of western Pacific marginal basins, *Tectonophysics*, 160, 23-48, 1989.
- Jolivet, L., P. Huchon, J. P. Brun, N. Chamot-Rooke, X. Le Pichon and J.C. Thomas, Arc deformation and marginal basin opening; Japan Sea as a case study, *J. Geophys. Res.*, 96, 4367-4384, 1991.
- Jun, M. S., Source parameters of shallow intraplate earthquakes in and around the Korean peninsula and their tectonic implication, *Acta Univ. Ups., Comp. Sum. of Uppsala Diss. Fac. Sci.*, 285, 16 pp., 1990.
- Kaneoka, I., Takigami, Y., Takaoka, N., Yamashita, S. and Tamaki, K., 40Ar-39Ar analyses of volcanic rocks drilled from the Japan Sea floor by Legs 127/128, In Tamaki, K., Suyehiro, K., Allan, J. et al., 1992, *Proc. ODP, Sci. Results*, 127-128, in press, 1992.
- Kimura, G., Oblique subduction and collision; forearc tectonics of the Kuril arc, *Geology*, 14, 404-407, 1986.
- Kimura, G., and K. Tamaki, Tectonic framework of the Kuril arc since its initiation, in: *Formation of Active Ocean Margins*, edited by N. Nasu et al., pp. 641-676, Terrapub, Tokyo, 641-676, 1985.
- Kimura, G., and K. Tamaki, Collision, rotation and back arc spreading: the case of the Okhotsk and Japan seas, *Tectonics*, 5, 389-401, 1986.
- Kimura, G., S. Miyashita, and S. Miyasaka, Collision tectonics in Hokkaido and Sakhalin, in *Accretion Tectonics in the Circum-Pacific Regions*, edited by M. Hashimoto and S. Uyeda, pp. 117-128, Terrapub, Tokyo, 1983.
- Kodama, K., T. Takeuchi and T. Ozawa, Paleomagnetism of Early Cretaceous to Neogene deposits in Central Hokkaido, Japan: block rotation caused by strike-slip fault movement (abstract), *Eos Trans. AGU*, 71 (28), 865, 1990.
- Koshiya, S., Tanakura Shear Zone, the deformation process of fault rocks and its kinematics, *J. Geol. Soc. Jpn.*, 92, 15-29, 1986.
- Lallemand, S., and L. Jolivet, Japan Sea, a pull apart basin, *Earth Planet. Sci. Lett.*, 76, 375-389, 1985.
- Lallemand, S., N. Chamot-Rooke, X. Le Pichon, and C. Rangin, Zenisu ridge: a deep intraoceanic thrust related to subduction, off Southwest Japan, *Tectonophysics*, 160, 151-174, 1989.
- Le Pichon, X., J. T. Iiyama, J. Boulègue, J. Charvet, M. Faure, K. Kano, S. Lallemand, H. Okada, C. Rangin, A. Taira, T. Urabe, and S. Uyeda, Nakai trough and Zenisu ridge: a deep sea submersible survey, *Earth Planet. Sci. Lett.*, 83, 285-299, 1987.
- Margulies, L.S., Mudretsov, V.B., Sapozhnikov, B.G., Fedotov, G.D. & Khvelauk, I.I., 1979, Geological structure of the northwestern part of the sea of Okhotsk, *Int. Geol. Rev.*, 22, 1094-1102, 1979.
- Melnikov, O.A., Structure and geodynamics in Hokkaido and Sakhalin, in Russian, *Nauka*, 95 pp., 1987.
- Mitani, K., Changing of the Tertiary sedimentary basins in the western flank of the axial belt of Hokkaido- bearing a significance of the Sunagawa lowland to Umai Hilly belt, *Assoc. Geol. Collab. Jpn. Monogr.* 21, 127-137, 1978.
- Nakamura, K., Possible nascent trench along the eastern Japan sea as the convergent boundary between Eurasia and North American plates (in Japanese with English abstract), *Bull. Earthquake Research Inst. Univ. Tokyo*, 58, 721-732, 1983.
- Nakamura, K. and S. Uyeda, Stress gradient in back arc regions and plate subduction, *J. Geophys. Res.*, 85, 6419-6428, 1980.
- Otofuji, Y., T. Matsuda, and S. Nohda, Paleomagnetic evidences for the Miocene counter clockwise rotation of northeast Japan - rising process of the Japan arc, *Earth Planet. Sci. Lett.*, 75, 265-277, 1985.
- Osaki, K., Reconstruction of Neogene tectonic stress field of Northeast Honshu arc from metalliferous veins, *Mem. Geol. Soc. Jpn.*, 32, 281-304, 1989.
- Ranken, B., R. K. Cardwell, and D. E. Karig, Kinematics of the Philippine sea plate, *Tectonics*, 3, 555-575, 1984.
- Rozhdestvenskiy, V. S., The role of wrench faults in the structure of Sakhalin, *Geotectonics*, 16, 323-332, 1982.

- Rozdestvenskiy, V. S., Evolution of the Sakhalin fold system, *Tectonophysics*, 127, 331-339, 1986.
- Sato, H., Degree of deformation of Late Cenozoic strata in the Northeast Honshu arc, *Mem. Geol. Soc. Jpn.*, 32, 257-268, 1989.
- Savostin, L.A., and A. M. Karasik, Recent plate tectonics of the Arctic basin and of northeastern Asia, *Tectonophysics*, 74, 111-145, 1981.
- Savostin, L., L. Zonenshain, and B. Baranov, Geology and plate tectonics of the Sea of Okhotsk, in: *Geodynamics of the Western Pacific and Indonesian Region*, *Geodyn. Ser.*, vol. 11, W.C.T. Hilde and S. Uyeda, pp. 343-354, AGU, Washington, D.C., 1983.
- Seno, T., Is Northern Honshu a microplate?, *Tectonophysics*, 115, 177-196, 1985.
- Sillito, R. H., Metallogeny of an Andean-type continental margin in South Korea, implications for opening of the Japan Sea, in *Island Arcs, Deep Sea Trenches and Back Arc Basins*, Maurice Ewing Ser., vol. 1, edited by M. Talwani and W.C. Pitman III, pp. 303-310, AGU, Washington, D.C., 1977.
- Sugi, N., K. Chinzei, and S. Uyeda, Vertical crustal movements of northeast Japan since Middle Miocene, in: *Geodynamics of the Western Pacific and Indonesian Region*, *Geodyn. Ser.*, vol. 11, W.C.T. Hilde and S. Uyeda, pp. 317-329, AGU, Washington, D.C., 1983.
- Suyehiro, K., et al., *Proc. Ocean Drilling Program Initial Rep.*, 128, 1990.
- Suzuki, K., On the Late Cenozoic history in the southern part of northeast Honshu in Japan, *Mem. Geol. Soc. Jpn.*, 32, 97-112, 1989.
- Taira, A., H. Tokuyama, and W. Soh, Accretion tectonics and evolution of Japan, In *The Evolution of the Pacific Ocean Margin*, edited by Z. Ben-Avraham, pp. 160-123, Oxford University Press, 100-123, New York, 1989.
- Takeuchi, A., On the episodic vicissitude of tectonic stress field of the Cenozoic northeast Honshu arc, Japan, in *Formation of Active Ocean Margins*, edited by N. Nasu et al., Terrapub, pp. 443-468, Tokyo, 1985.
- Tamaki, K., Two modes of back arc spreading, *Geology*, 13, 475-478, 1985.
- Tamaki, K., Geological structure of the Japan sea and its tectonic implications, *Bull. Geol. Surv. Jpn.*, 39, 269-365, 1988.
- Tamaki, K., *Proc. Ocean Drilling Program Initial Rep.*, 127, 1990.
- Tsuchiya, N., Submarine basalt volcanism of Miocene Aozawa formation in the Akita-Yamagata oil field basin, back-arc region of Northeast Japan, *Mem. Geol. Soc. Jpn.*, 32, 399-408, 1989.
- Tsuchiya, N., Middle Miocene back-arc rift magmatism of basalt in the NE Japan arc, *Bull. Geol. Surv. Jpn.*, 41, 473-505, 1990.
- Watanabe, Y., Deformation structure of the Uenshiri horst in the Hidaka belt, Central Hokkaido, *J. Geol. Soc. Jpn.*, 94, 527-533, 1988.
- Watanabe, Y., and K. Iwata, The age of the Miocene Kamishiyubetsu formation in northern Hokkaido and the basins formed by tectonic movements, *J. Geol. Soc. Jpn.*, 91, 427-430, 1985.
- Yamagishi, H., and Y. Watanabe, Change of stress field of Late Cenozoic Southwest Hokkaido, Japan, - investigation of geologic faults, dykes, ore veins and active faults, *Monogr. Geol. Collab. Jpn.*, 31, 321-332, 1986.
- Yamaji, A., Geology of the Atsumi area and Early Miocene rifting in the Uetsu District, Northeast Japan, *Mem. Geol. Soc. Jpn.*, 32, 305-320, 1989.
- Yamaji, A., Rapid intra-arc rifting in Miocene northeast Japan, *Tectonics*, 9, 365-378, 1990.
-
- M. Fournier, P. Huchon, and L. Jolivet,
Département de Géologie, Ecole Normale Supérieure, 24 Rue Lhomond, 75231 Paris cedex,
France.
- L. S. Osorbin, V. S. Rozdestvenskiy, and
K.F. Sergeyev, Institute of Marine Geology and
Geophysics, Far East Science Center, Yuzhno-Sakhalinsk, USSR.

(Received January 23, 1991;
revised December 18, 1991;
accepted February 10, 1992.)

III. CONCLUSIONS

La marge orientale de la mer du Japon est le siège de mouvements décrochants dextres au Miocène inférieur et moyen, du Japon central jusqu'au nord de Sakhaline. Il en va de même pour la marge occidentale à la même époque. Les déplacements le long des zones décrochantes peuvent être estimés, à partir des reconstructions cinématiques de Jolivet et al. (1991), à environ 400 km sur la marge est de la mer du Japon, et 200 km sur la marge ouest. Un déplacement de 400 km sur la marge orientale correspond à une vitesse de 4 cm/an sur 10 Ma, ou 2,5 cm/an sur 15 Ma. Les mouvements dextres à Sakhaline le long des principaux décrochements n'excèdent jamais quelques dizaines de kilomètres quand ils peuvent être estimés. Jolivet et al. (1992) et Jolivet et Tamaki (1992) suggèrent donc que la déformation décrochante a été principalement accommodée le long de zones de moindre résistance où la croûte est amincie, à savoir sur la marge de la mer du Japon et dans le détroit des Tartares à l'ouest de Sakhaline.

Tamaki et Kobayashi (1988) et Tamaki et al. (1992) suggèrent à partir de l'interprétation des données magnétiques du bassin du Japon que l'océanisation s'est initiée dans la partie est du bassin et s'est propagé vers l'ouest. Cette interprétation explique la forme triangulaire du bassin qui se termine en pointe vers l'ouest. Pour Jolivet et Tamaki (1992), la cassure de la lithosphère et l'océanisation s'initient le long de la zone décrochante est-mer du Japon, vraisemblablement dans la zone de cisaillement et d'étirement maximal (Figure 32). L'absence d'océanisation vraie dans le bassin de Yamato pourrait être attribuée à la diminution du taux de déformation d'est en ouest dans la mer du Japon.

L'étude de la totalité de la zone décrochante est-mer du Japon montre qu'il faut distinguer une composante décrochante de la déformation, représentative de la déformation à l'intérieur du continent asiatique, d'une composante de proximité de la zone de subduction qui varie en fonction des conditions de subduction. Deux explications ont été proposées pour rendre compte de la déformation décrochante continentale, d'une part la collision Inde-Asie, et d'autre part l'extrusion d'une plaque Okhotsk. L'extrusion de la plaque Okhotsk telle qu'elle est proposée par Cook et al. (1986) est un phénomène récent d'âge Pliocène supérieur qui ne peut expliquer les mouvements décrochants contemporains de l'ouverture de la mer du Japon. D'autre part, la définition d'une plaque Okhotsk apparaît problématique en l'absence de sismicité entre la plaque Amour et la frontière des plaques Nord Amérique et Eurasie. Nous ne retenons donc pas cette hypothèse.

Par contre, la géométrie à grande échelle de la déformation en Asie du nord-est est dominée par la collision de l'Inde. Les deux grandes zones de déformation sub-méridiennes du NE asiatique que sont la faille de Tan-Lu (Lu et al., 1983) et la zone décrochante est-mer du Japon, accommodent des mouvements dextres depuis l'Oligocène. Lu et al. (1983)

interprètent l'inversion du sens de mouvement le long de la faille de Tan-Lu, sénestre au Mésozoïque mais dextre ensuite, comme la conséquence de la collision Inde-Asie. La zone N-S de grabens en échelon du Shanxi (est-Ordos), accommode aussi des déplacements dextres depuis le Pliocène (Xu et Ma, 1992), ainsi que la zone décrochante du détroit de Tsushima au Miocène inférieur et moyen. Quant aux zones de déformation sub-latitudinales du NE asiatique, le Qinling Shan, la zone nord-Ordos (bassin de l'Hetao et son prolongement vers l'est), et les Monts Stanovoï, elles accommodent des mouvements décrochants sénestres. Des zones décrochantes conjuguées se dessinent ainsi à grande échelle. Elles sont compatibles avec une direction de contrainte maximum horizontale NE-SO. Cette direction de contrainte peut être attribuée à la collision Inde-Asie.

Nous proposons donc de relier la déformation décrochante en Asie du NE à la collision Inde-Asie.

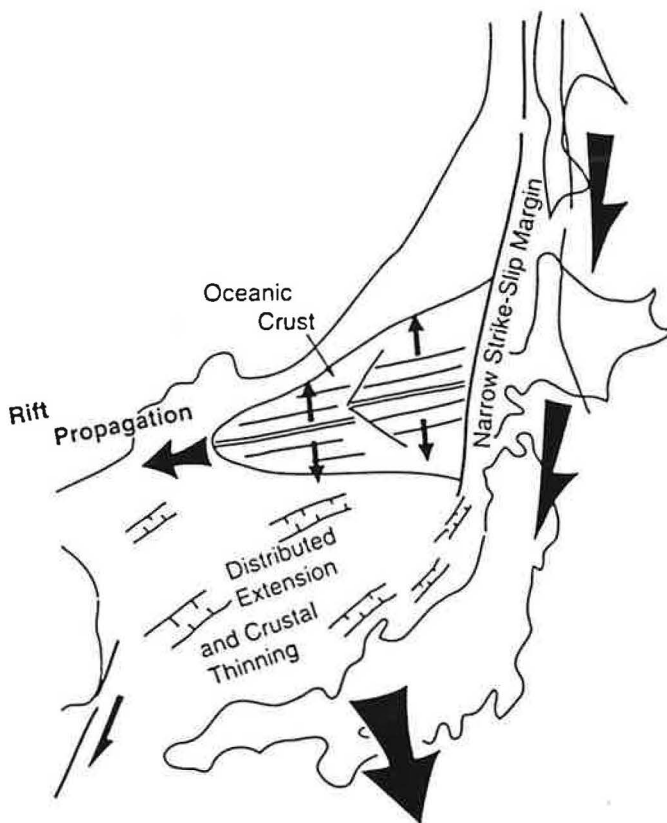
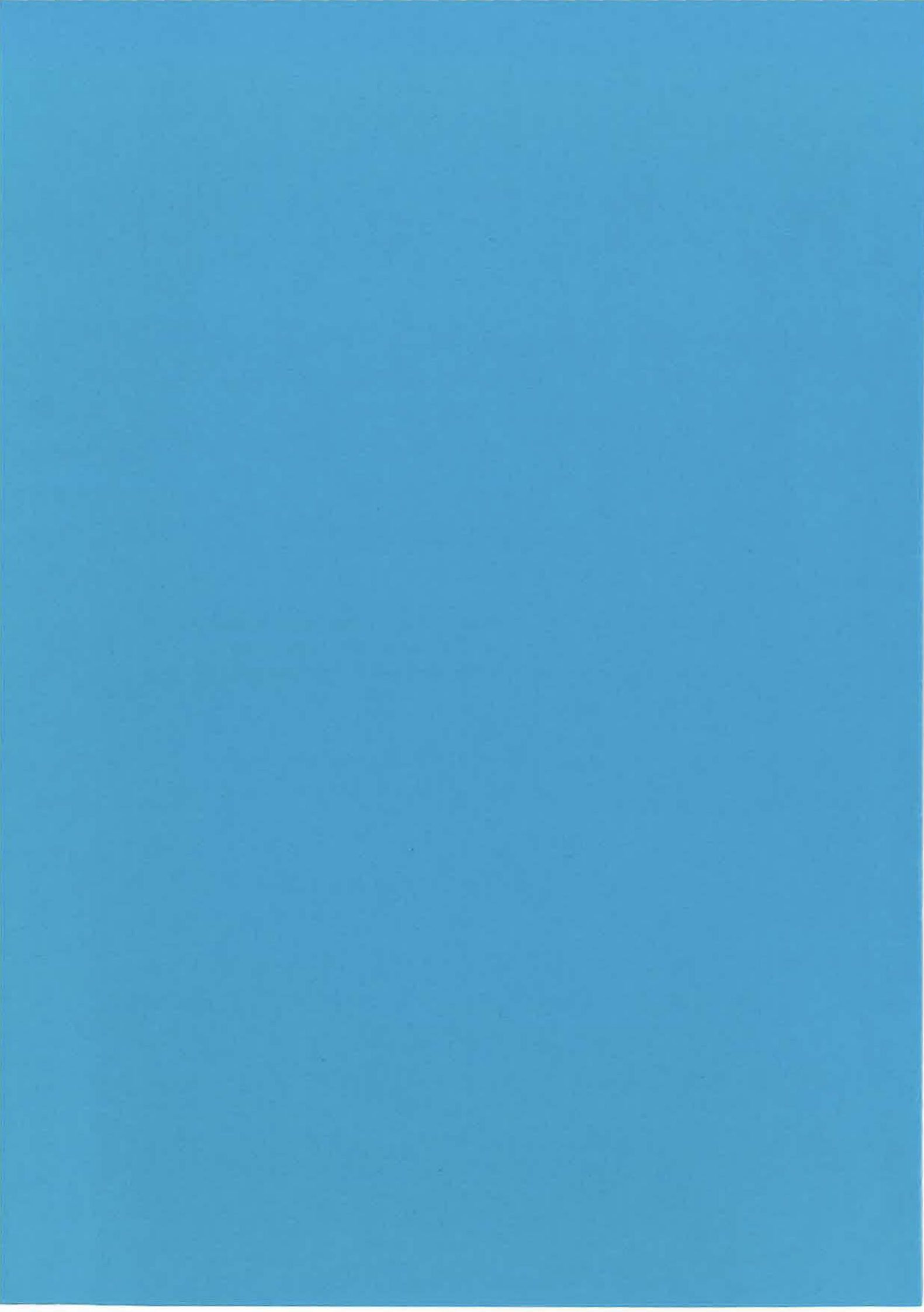


Figure 32. Mécanisme simplifié d'ouverture de la mer du Japon (d'après Tamaki et al., 1992). Extension et amincissement crustal prévalent pendant le stade initial de l'ouverture. L'océanisation est provoquée par la cassure de la lithosphère le long de la marge décrochante et se propage vers l'ouest.

TROISIÈME PARTIE

**CHAMP DE CONTRAINTES ET MÉCANISME DE DÉFORMATION
PENDANT L'OUVERTURE DE LA MER DU JAPON :
COMPATIBILITÉ AVEC LES ROTATIONS PALÉOMAGNÉTIQUES**



TROISIÈME PARTIE
CHAMP DE CONTRAINTES ET MÉCANISME DE DÉFORMATION
PENDANT L'OUVERTURE DE LA MER DU JAPON :
COMPATIBILITÉ AVEC LES ROTATIONS PALÉOMAGNÉTIQUES

I. INTRODUCTION

Cette partie traite de la compatibilité des données paléomagnétiques et des données structurales au Japon et repose sur 2 articles. Le premier est une étude du champ de contraintes Néogène dans le Japon sud-ouest à partir de l'analyse de la fracturation, et du mécanisme de déformation pendant l'ouverture de la mer du Japon. Cette étude complète l'étude du champ de contraintes réalisée par Jolivet et Huchon (1989), Jolivet et al. (1991), et Fournier et al. (1994) le long de la marge est de la mer du Japon. La marge ouest a été étudiée à Tsushima par Fabbri et Charvet (1994) et en Corée du sud par Hwang (1992), la marge nord en Russie restant encore à étudier. Cette étude apporte aussi des informations sur la déformation interne du Japon sud-ouest pendant l'ouverture, qui suggèrent des rotations de blocs à différentes échelles contemporaines des rotations paléomagnétiques.

Le second article présente une synthèse critique des données paléomagnétiques et radiométriques associées sur tout l'ensemble du Japon, données qui sont ensuite reliées au cadre structural de l'ouverture. Cette synthèse débouche sur un modèle d'ouverture en pull-apart intégrant les rotations paléomagnétiques.

II. LES DONNÉES PALÉOMAGNÉTIQUES

Depuis Kawai et al. (1961, 1971), les rotations différentielles du Japon nord-est et sud-ouest il y a environ 15 Ma ont été étudiées par de nombreux auteurs (Sasajima, 1981 ; Otofuji et Matsuda, 1983, 1984 ; Hayashida et Ito, 1984 ; Otofuji et al., 1985, 1987, 1991, 1994 ; Celaya et McCabe, 1987 ; Moreau et al., 1987 ; Itoh, 1988 ; Tosha et Hamano, 1988 ; Yamazaki, 1989 ; Kodama, 1990 ; Hayashida et al., 1991 ; Kodama et al., 1993). La Figure 33, d'après Jolivet et al. (1989), montre l'ensemble des directions paléomagnétiques en fonction de l'âge des roches. Les données les plus récentes concernant le Japon NE (Kodama et al., 1993 ; Otofuji et al., 1994) sont montrées en Figures 34 et 35 (voir aussi la Figure 2 dans l'article qui suit). Les données récentes d'Otofuji et al. (1991) et Hayashida et al. (1991) concernant le Japon sud-ouest n'apportent pas de changements significatifs à la carte de Jolivet et al. (1989). Les données les plus précisément contraintes en âge sont celles d'Otofuji et al. (1991) et d'Hayashida et al. (1991) pour le Japon sud-ouest, qui concluent à une rotation

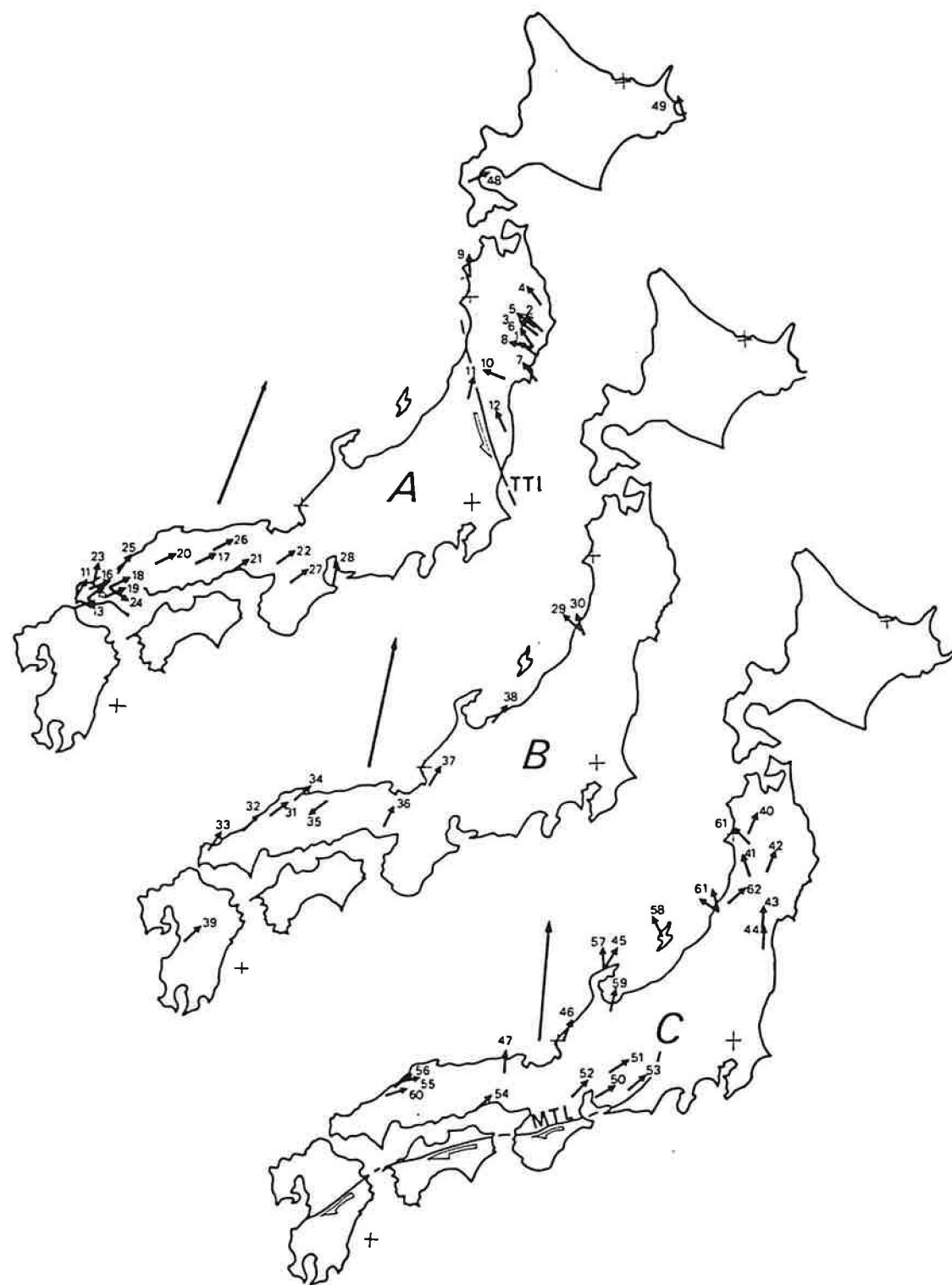


Figure 33. Directions paléomagnétiques au Japon en fonction de l'âge des roches (A: Crétacé supérieur; B: Paléogène; C: Miocène inférieur) (d'après Jolivet et al., 1989).

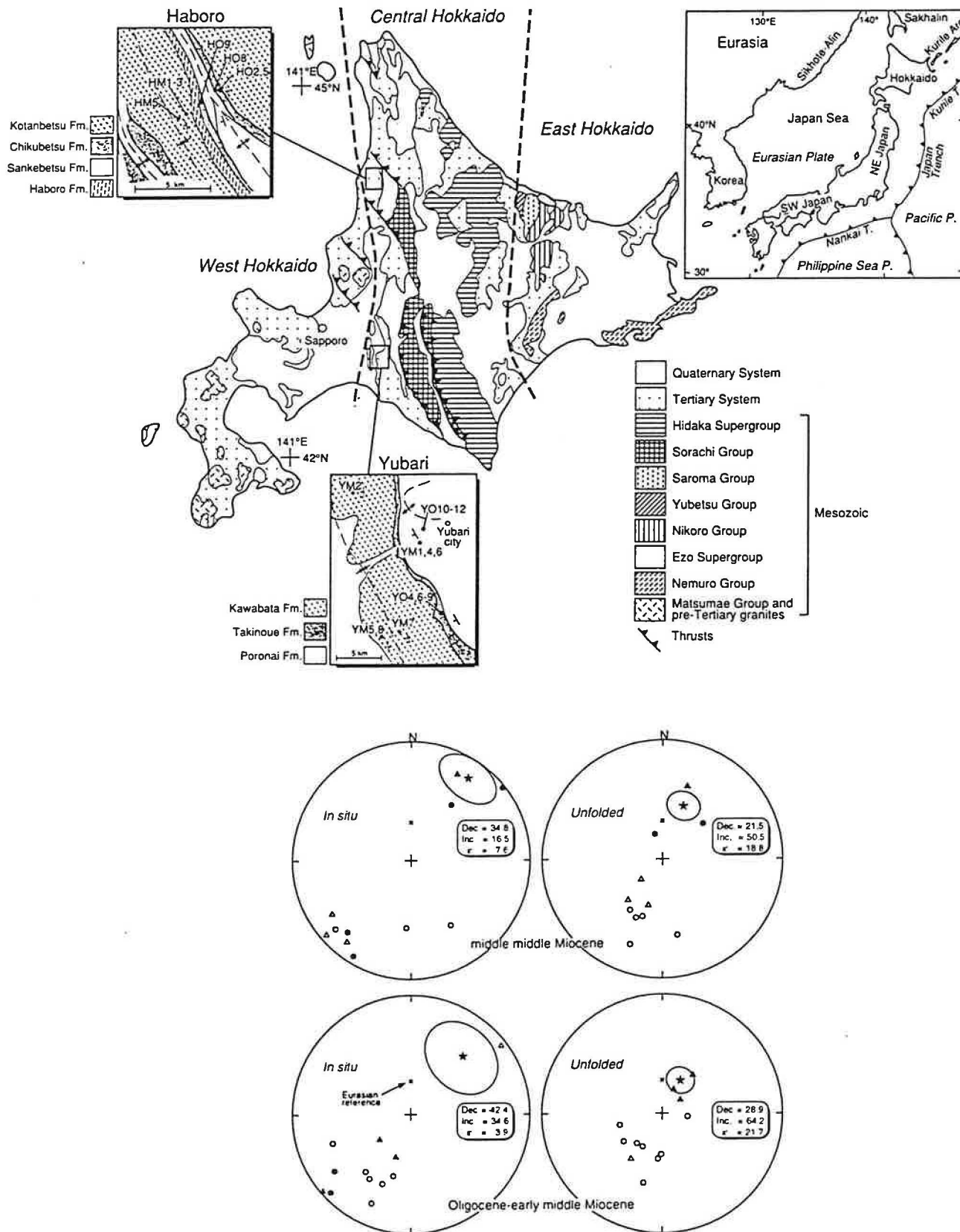


Figure 34. Sites de mesures dans la zone déformation centrale d'Hokkaido et directions paléomagnétiques dans les formations Oligocène-Miocène inférieur ($30^{\circ}\text{E} \pm 21$) et Miocène moyen ($21^{\circ}\text{E} \pm 15$) mettant en évidence des rotations horaires (d'après Kodama et al., 1993).

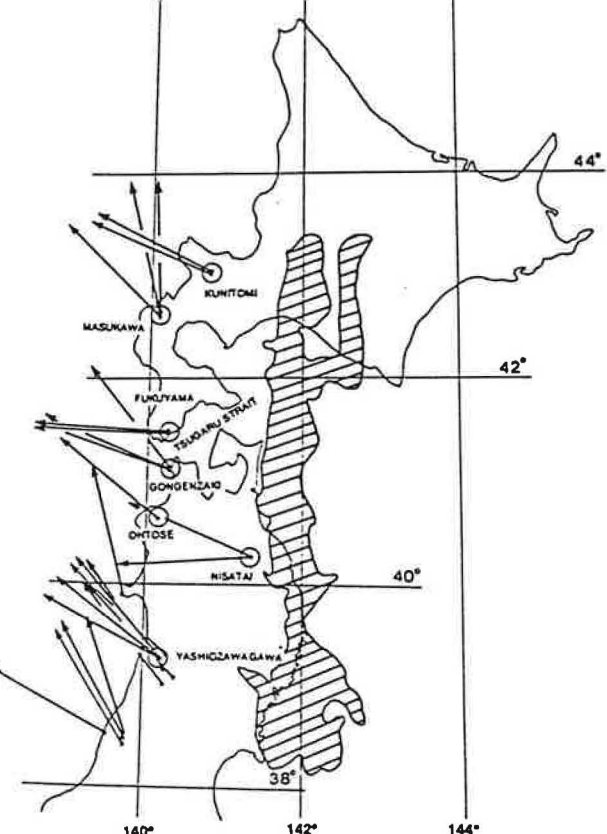


Figure 35. Déclinaisons paléomagnétiques dans les formations oligocène et miocène inférieur du Japon NE (d'après Otofuji et al., 1994).

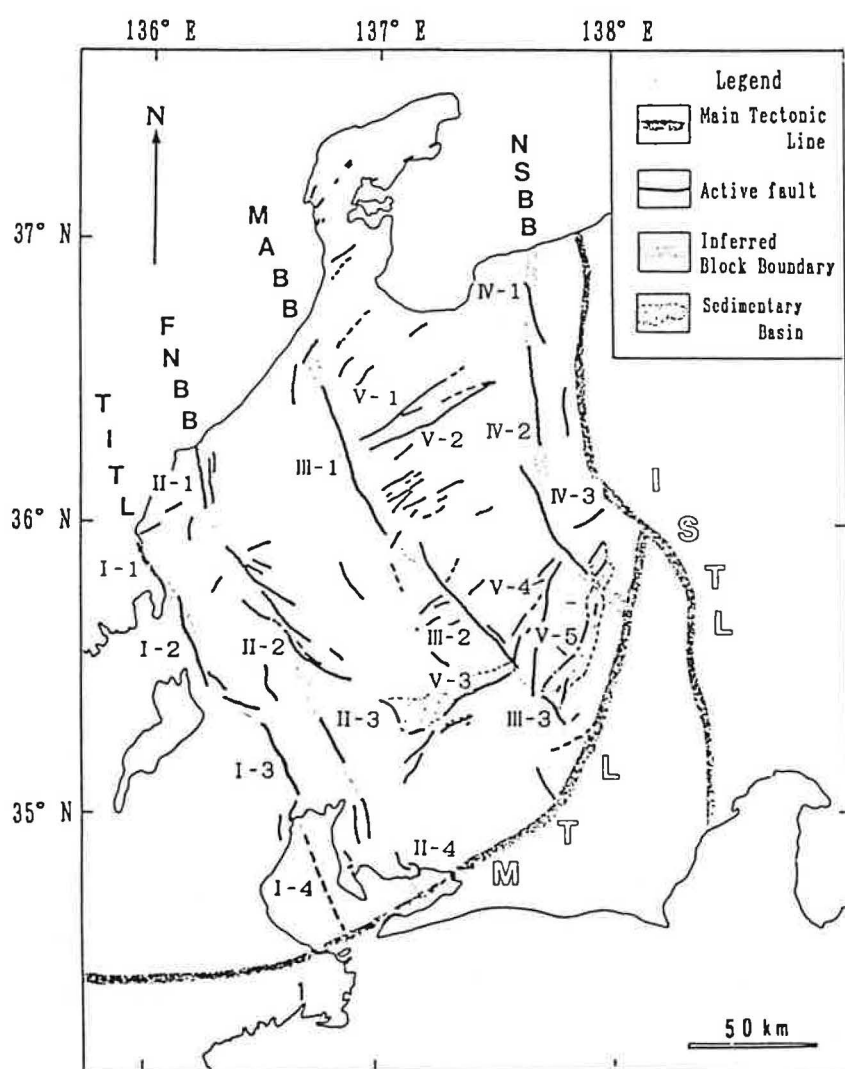


Figure 36. Distribution des failles actives dans le Japon central et structure en blocs proposée par Kanaori et al. (1992).

horaire d'environ 50° entre 16 et 14 Ma, et celles d'Otofuji et al. (1994) pour le Japon nord-est, qui concluent à une rotation anti-horaire d'environ 45° après 17 Ma et aux environs de 15 Ma. Hayashida et al. (1991) ont suggéré que le pôle de rotation du Japon sud-ouest se trouve au centre du Japon sud-ouest, et non plus dans le détroit de Tsushima comme précédemment, afin de rendre compte de la convergence entre la Corée et l'extrémité ouest du Japon sud-ouest et des rotations anti-horaires du détroit de Tsushima (sans que le mécanisme concernant ce dernier point ne soit explicité). Le raccourcissement Japon-Corée étant daté du Miocène supérieur (voir par exemple Fabbri et Charvet, 1994), il ne semble pas justifié que les rotations Miocène moyen en rendent compte.

La plupart des auteurs précédents considèrent les rotations locales comme représentatives des rotation en bloc du Japon SO et du Japon NE et attribuent les rotations à l'ouverture de la mer du Japon. Ils prétendent contraindre ainsi l'âge de l'ouverture connaissant celui des rotations. On l'a vu en introduction, les forages ODP ont indiqué que l'ouverture se place entre 32 et 11 Ma avec une phase d'océanisation dans le bassin du Japon entre 24 et 17 Ma, Tamaki et al. (1992) concluant à une ouverture progressive sur 10 millions d'années plutôt qu'à une ouverture instantanée en moins de 2 millions d'années. Si le calage en temps des rotations paléomagnétiques est correct, il faut conclure à une phase de rotation entre 16 et 14 Ma pendant l'ouverture. L'incompréhension sur ce point avec Otofuji et al. (1994) reste totale puisqu'une des conclusions de leur récent article (p. 515) est la suivante : "Seeing as the recent results of ODP drilling in the Sea of Japan suggest that opening commenced at about 20 Ma, differential rotation of NE Japan and SW Japan is attributable to the opening of the Sea of Japan. The differential rotation of the Japan arc identified from paleomagnetism therefore constrains the timing of the opening of the Sea of Japan". L'argument ne vaut que si l'on convient que "A inclus dans B" implique nécessairement "B inclus dans A".

Un débat attenant aux rotations paléomagnétiques concerne le taux d'ouverture excessivement fort (20 à 50 cm/an ; Otofuji et Matsuda, 1987 ; Otofuji et al., 1991) qu'implique la rotation rigide de 45° du Japon sud-ouest, long d'environ 600 km, en moins de 2 millions d'années. Un moyen d'accommoder des rotations rapides est de distribuer la déformation entre des petits blocs rigides qui tournent simultanément. Un tel modèle de déformation a été proposé par Kanaori (1990) pour le Japon sud-ouest, qu'il a divisé (au nord de la MTL) en une dizaine de blocs rigides limités par des failles ou "des lignes géologiques discrètes" (non continues) telles que des alignements de failles. A partir de la géométrie de failles actives sénestres NNO-SSE, Kanaori et al. (1992) définissent un système de quatre blocs rigides dans le Japon central (Figure 36). La géométrie des blocs rigides pour tout le

Japon sud-ouest proposée par Kanaori (1990) est montrée en Figure 37. Les limites entre les blocs y sont moins évidentes que dans le Japon central.

Deux arguments sont opposés au modèle de blocs rigides. D'une part, les structures anté-ouverture sont linéaires sur près de 600 km au sud de la MTL, et ne sont pas décalées par des limites de blocs éventuels (Otofuji et al., 1994). Notons qu'il n'y a pas dans la littérature de données paléomagnétiques disponibles au sud de la MTL, si ce n'est à Kyushu où des rotations anti-horaires post Miocène supérieur sont documentées (Kodama et al., 1991 ; Kodama et Nakayama, 1993), et que par conséquent c'est toujours au nord de la MTL, là où sont documentées les rotations paléomagnétiques, que des blocs rigides ont été argumentés. L'autre argument opposé à ces blocs insiste sur le fait que les rotations paléomagnétiques sont pratiquement de taux constant dans tout le Japon sud-ouest (Otofuji et al., 1994). Les rotations documentées par Hirooka et al. (1986) et Itoh (1988) dans la partie est du Japon sud-ouest (Japon central) sont cependant significativement plus faibles, voire nulles (cf. Figure 2 dans l'article qui suit), et il est difficile de dire s'il s'agit là de l'effet local et tardif des collisions successives des blocs Tanzawa et Izu, ou de rotations initialement plus faibles. Localement, la géométrie en blocs rigides est en effet bien définie dans le Japon central (Figure 36; Kanaori et al., 1992).

III. CHAMP DE CONTRAINTES ACTUEL

Les cartes des trajectoires de contraintes actuelles déterminées à partir de mécanismes au foyer des séismes (Nakamura et Uyeda, 1980 ; Ishii et al., 1983 ; Tsukahara et Ikeda, 1991 ; Tsukahara et Kobayashi, 1991), de mesures de contraintes in situ (Ishii et al., 1983 ; Tsukahara et Ikeda, 1991 ; Tsukahara et Kobayashi, 1991), et de statistiques sur les directions de dykes (Yamamoto, 1991), sont montrées sur les Figures 38 à 41. La direction de la contrainte maximale horizontale, σ_1 selon Nakamura et Uyeda (1980), est globalement est-ouest dans le Japon nord-est, et ONO-ESE dans le Japon sud-ouest, avec une légère inflexion au sud pour devenir pratiquement perpendiculaire à la fosse de Nankai. La direction de σ_1 est ainsi globalement parallèle à la direction de convergence Pacifique-Eurasie.

Le champ de contraintes compressif E-O s'est mis en place dans le Japon NE au Miocène supérieur (Yamagishi et Watanabe, 1986 ; Jolivet et Huchon, 1989), ce qui coïncide avec le début de soulèvement du Japon NE enregistré il y a 10 Ma (Sugi et al., 1983 ; Ingle, 1992).

La Figure 42, d'après Tsukahara et Ikeda (1991), montre la perturbation du champ de contraintes dans la zone de collision d'Izu. Les zones en pointillés sont les zones où il a été estimé que le champ de contraintes était trop perturbé pour qu'un lissage soit réalisable. La distribution rayonnante des trajectoires de contraintes autour de la zone de collision d'Izu,

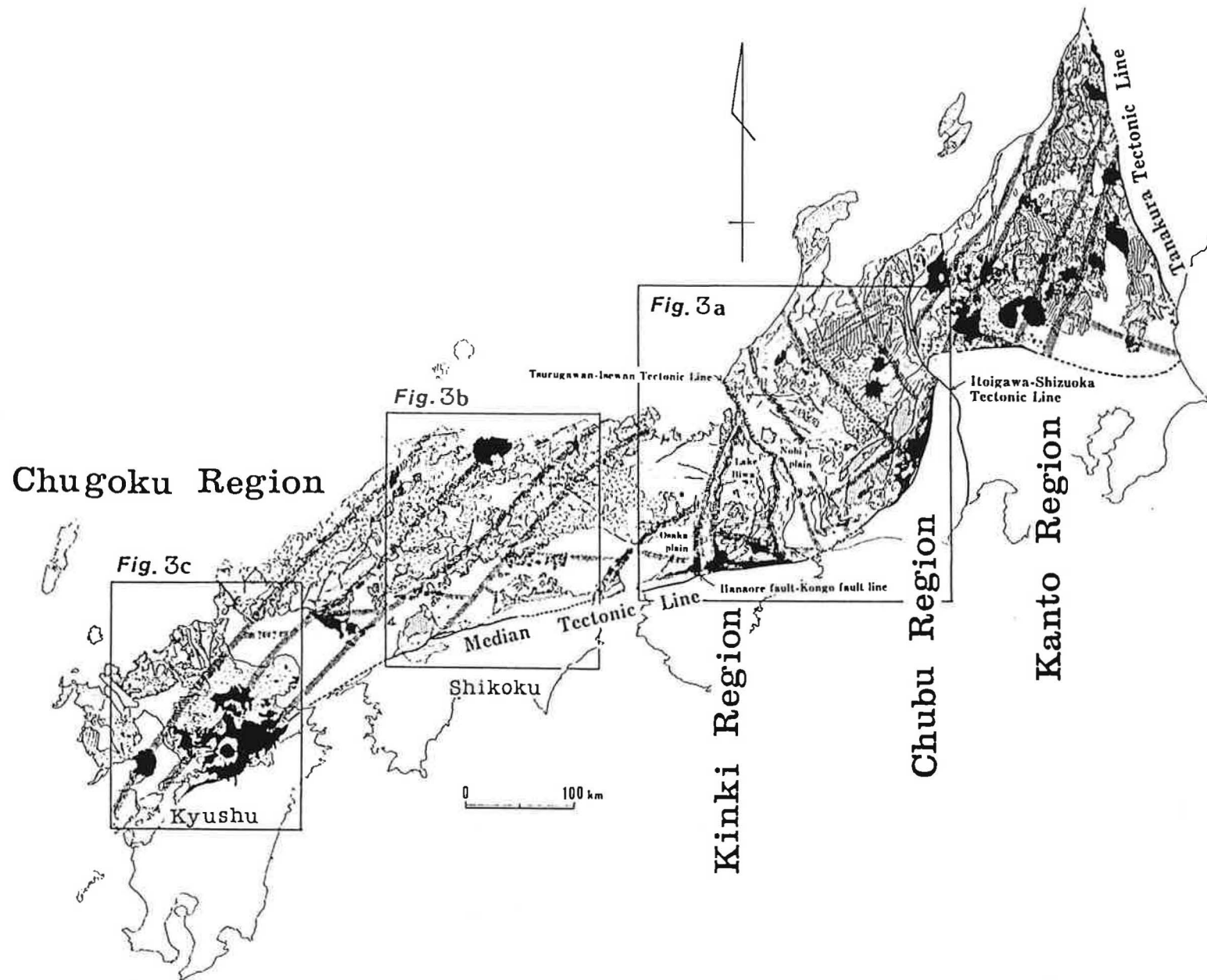


Figure 37. Structure en blocs du Japon sud-ouest interne (nord de la MTL) proposée par Kanaori (1990).

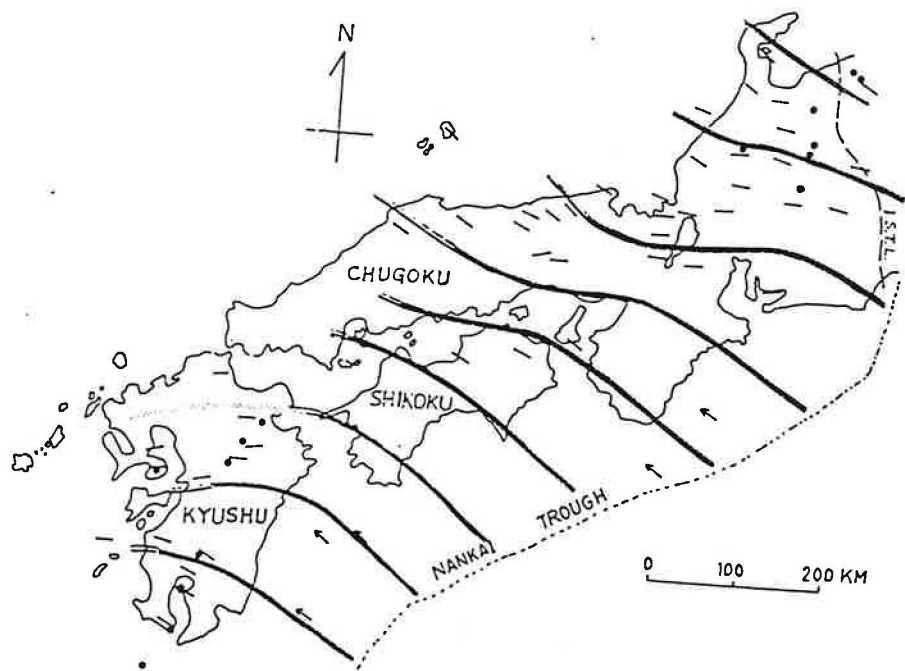
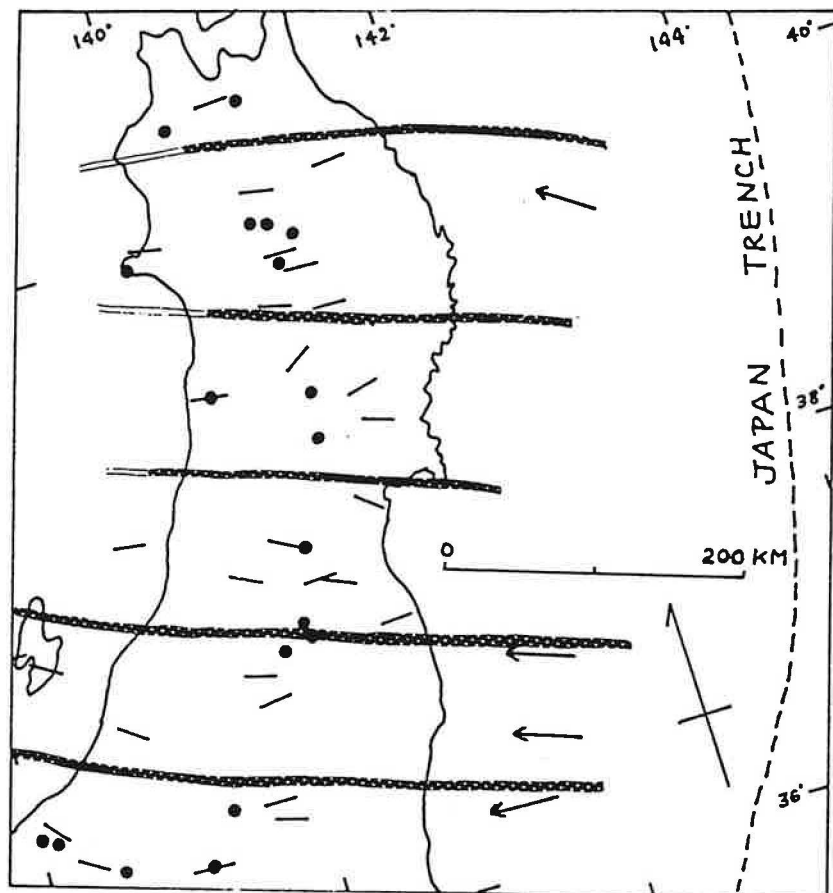


Figure 38. Trajectoires de $\sigma_{H\max}$ dans le Japon NE et SO déterminées à partir des failles actives (d'après Nakamura et Uyeda, 1980). Les lignes noires représentent σ_1 et les lignes pointillées σ_2 .

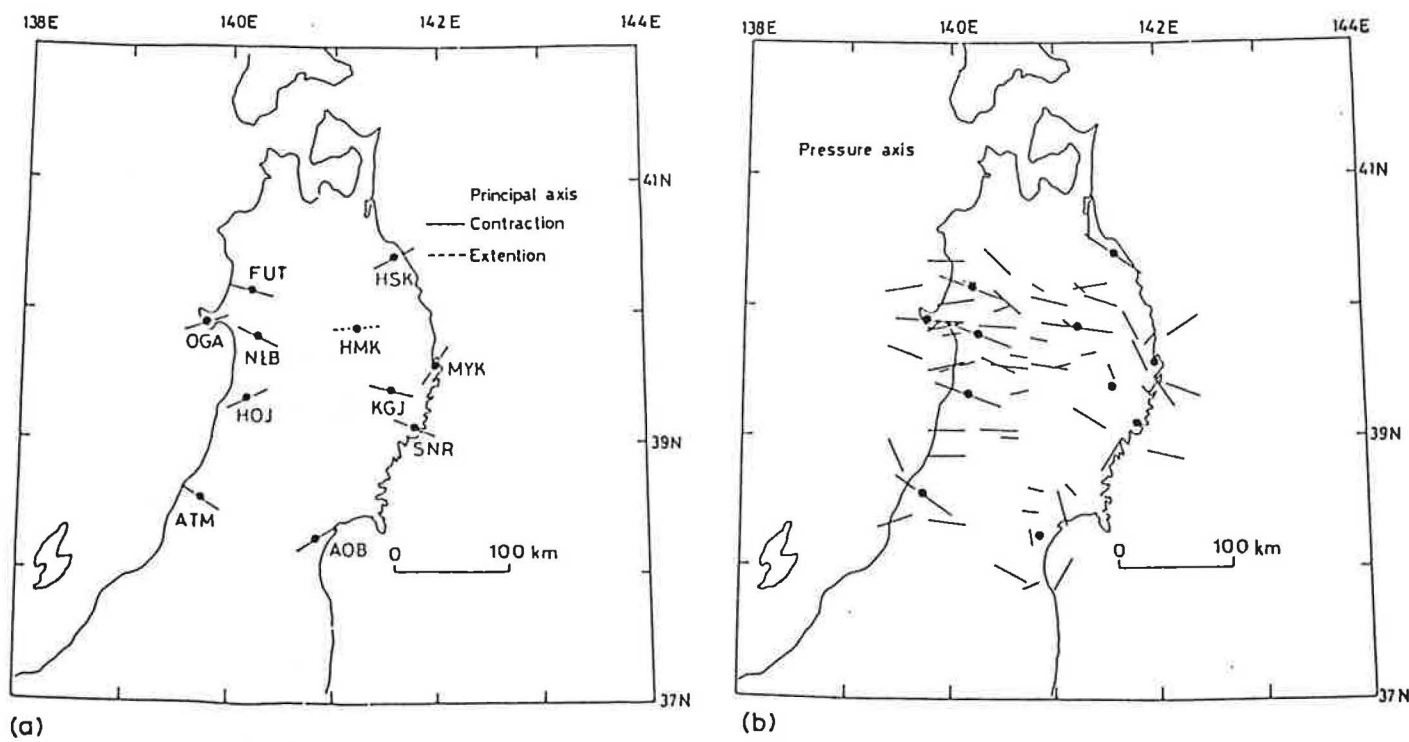


Figure 39. Directions (a) de raccourcissement obtenues à partir de mesures de contraintes in situ et (b) d'axe P de mécanismes au foyer de micro-séismes (d'après Ishii et al., 1983).

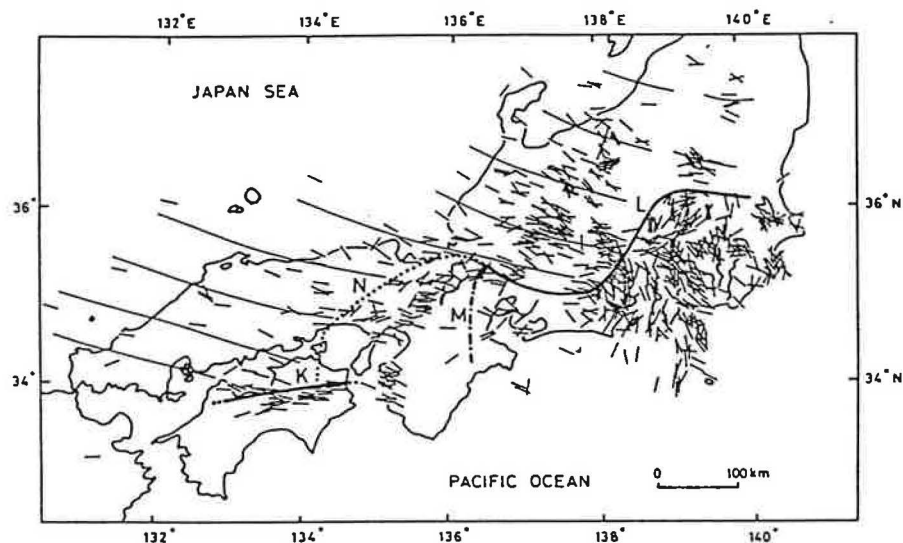


Figure 40. Directions et trajectoires de σ_{Hmax} dans le Japon SO déterminées à partir de mesures in situ et de mécanismes au foyer de séismes (d'après Tsukahara et Kobayashi, 1991).

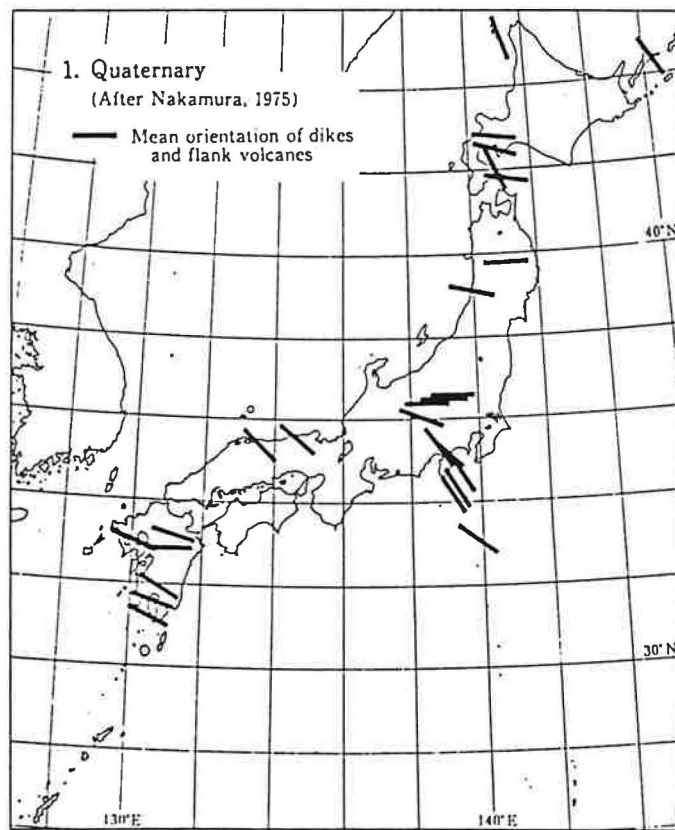
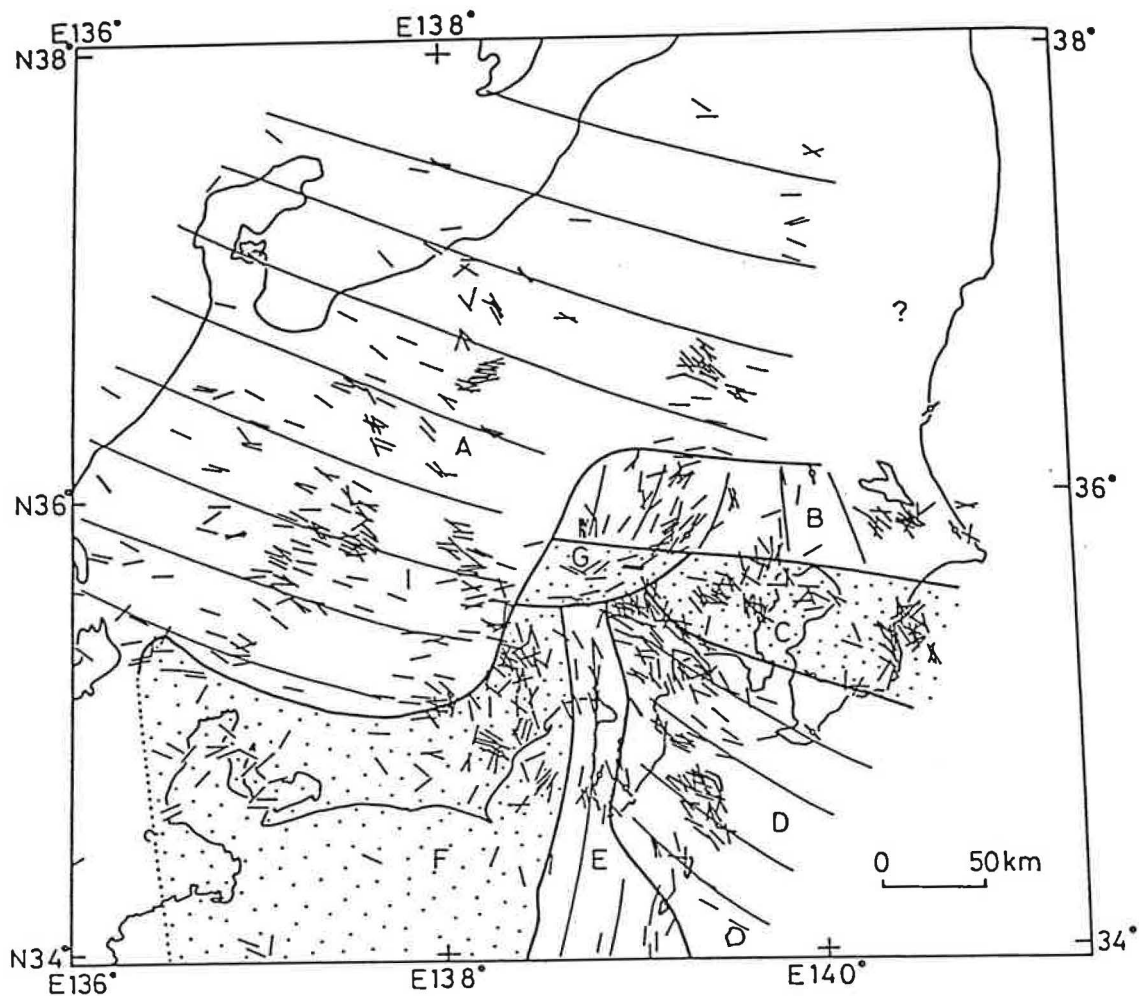


Figure 41. Directions de σ_1 déterminées à partir de statistiques sur les directions de dykes (d'après Yamamoto, 1991).



第2図. 応力区図. 太線: 応力区の境界線. 細線: 各応力区の平均的 σ_{Hmax} 方位の軌跡. 点をつけた区域(応力区 C, F, G)は応力方位の漸移帶.

Figure 42. Directions et trajectoires de σ_{Hmax} dans la zone de collision d'Izu déterminées à partir de mesures in situ et de mécanismes au foyer de séismes (d'après Tsukahara et Ikeda, 1991).

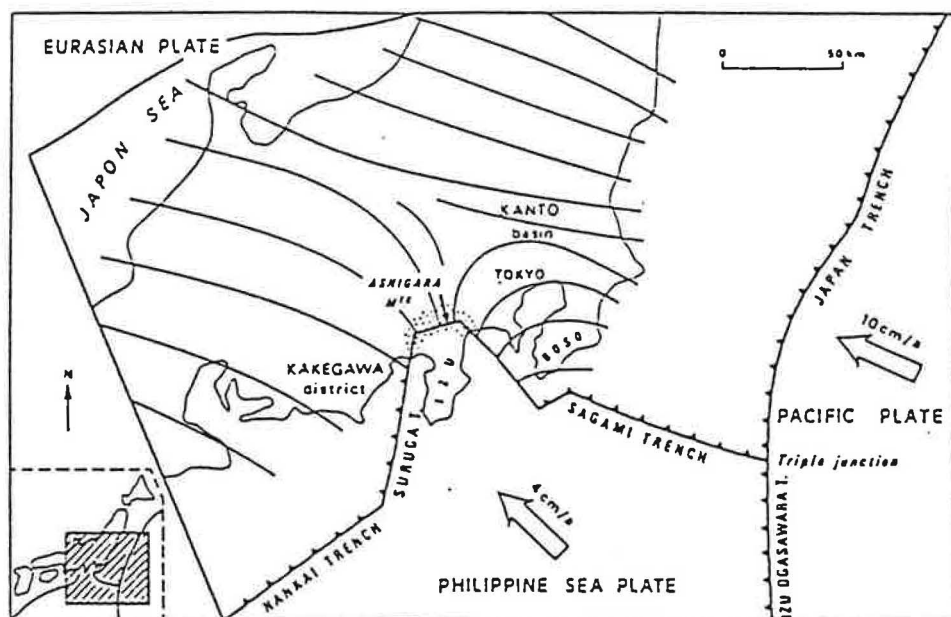


Figure 43. Trajectoires de raccourcissement d'après les données géodésiques, les failles actives, les mesures de contraintes in situ, les dykes volcaniques, et les mécanismes au foyer de séismes superficiels (d'après Huchon, 1986).

telle qu'elle a été calculée par Huchon (1986) à partir de données similaires mais moins nombreuses, est montrée en Figure 43. Ces figures montrent clairement que la perturbation du champ de contraintes est restreinte à la zone de collision d'Izu. D'après la carte du champ de contraintes dans le Japon SO de Nakamura et Uyeda (1980), la même remarque peut s'étendre à toute la fosse de Nankai, les directions de contraintes étant localement perturbées par la fosse. Le couplage entre la plaque mer des Philippines et le Japon sud-ouest au niveau de la zone de subduction de Nankai ou de la zone de collision d'Izu n'affecte donc que localement le champ de contraintes. Nous invoquons généralement l'initiation de la subduction de la plaque mer des Philippines sous le Japon sud-ouest et/ou les collisions successives des blocs Tanzawa et Izu avec le Japon central pour expliquer le changement de régime de contraintes au Miocène supérieur. Les trajectoires de contraintes actuelles suggèrent pourtant que ces deux phénomènes ont peu d'influence sur le champ de contraintes.

IV. CHAMP DE CONTRAINTES NÉOGÈNE ET MÉCANISME DE DÉFORMATION DU JAPON SUD-OUEST : article "*Neogene stress field in SW Japan and mechanism of deformation during Japan Sea opening*"

(soumis à J. Geophys. Res.)

Résumé : Pour comprendre le contexte structural des rotations paléomagnétiques horaires du Japon sud-ouest, nous avons étudié le champ de contraintes Néogène au moyen de l'analyse de la fracturation. Cette étude a été réalisée dans 7 bassins Néogènes, 3 bassins sur la côte de la mer du Japon, et 4 bassins le long de la MTL. Les résultats concernant la péninsule de Noto et le bassin de Yatsuo ont été décrits précédemment (Fournier et al., 1994). Sont présentés ici les résultats concernant les péninsules de Shimane (San'In district) et de Tango sur la côte de la mer du Japon, et les bassins d'Ishizuchi (Shikoku), de Shidara (Japon central), de Chichibu (Monts du Kanto) et de Itsukaichi (Monts du Kanto) le long de la MTL.

Ces résultats sont compilés avec les précédents résultats de Jolivet et Huchon (1989), Jolivet et al. (1991), et Fournier et al. (1994), pour fournir une carte du champ de contraintes Miocène moyen dans tout l'arc japonais. Les directions du champ de contraintes sont remarquablement cohérentes sur toute la côte de la mer du Japon, NE-SO pour la contrainte maximale horizontale, et NO-SE pour la contrainte minimale horizontale. Le champ de contraintes évolue de transpressif à Sakhaline et Hokkaido, à transtensif le long de la côte ouest du NE Honshu, et pratiquement purement extensif le long de la côte nord du Japon sud-ouest. Ces directions du champ de contraintes sont en accord avec celles obtenues par Hwang (1992) en Corée dans le bassin de Pohang, par Charvet et al. (1992) dans la mer du Japon, et par Otsuki (1990) à partir de statistiques sur des directions de veines métallifères. Les statistiques sur les directions de dykes sont aussi discutées.

Ce champ de contraintes est compatible avec la géométrie d'ouverture en pull-apart proposée par Lallemand et Jolivet (1985) et Jolivet et al. (1991), et il est vraisemblable qu'il a prévalu pendant toute la durée de l'ouverture de la mer du Japon. La cohérence des directions du champ de contraintes dans tout le Japon suggère cependant que nous avons échantillonné un champ de contraintes postérieur aux rotations différentielles du Japon NE et du Japon SO, qui se terminent vers 15-14 Ma (Tosha et Hamano, 1988 ; Otofuji et al., 1991, 1994 ; Hayashida et al. 1991 ; Otofuji et al., 1994). Les formations miocènes supérieur n'étant pas affectées par ce champ de contrainte, il doit être d'âge Miocène moyen et correspond à un stade tardif de l'ouverture. La géométrie de l'ouverture suggère qu'il est resté identique pendant toute l'ouverture. La dispersion des données (comme par exemple dans la péninsule de Tango) pourrait d'ailleurs être interprétée comme la conséquence de la rotation progressive du champ de contraintes fossilisé pendant l'ouverture. N'ayant pas suffisamment d'arguments chronologiques pour discuter ce point, nous ne l'avons pas retenu dans l'article.

Le champ de contraintes Miocène moyen mesuré le long de la MTL est extensif et compatible avec un mouvement sénestre à composante normale le long de la faille dans le Japon central, et avec un mouvement purement normal à Shikoku. Le sens de cisaillement sénestre le long de la MTL au Miocène moyen est de signe opposé au sens des rotations horaires contemporaines dans le Japon sud-ouest. Les 2 sens sont compatibles si l'on considère la MTL comme une faille de second ordre accommodant les rotations horaires de blocs rigides à l'intérieur d'une zone de cisaillement dextre d'échelle plus grande. Dans le contexte de l'ouverture de la mer du Japon, cette zone de cisaillement dextre est limitée à l'est par la zone décrochante est-mer du Japon, et à l'ouest par la zone décrochante de Tsushima.

Un mécanisme de déformation du Japon sud-ouest est discuté à partir de la description d'un affleurement dans la formation Miocène inférieur Kuri-Kawai (péninsule de Shimane) qui a subi la rotation horaire du Japon sud-ouest (Otofuji et al., 1991), et où des blocs limités par des décrochements sont observés à trois échelles superposées. Ce type d'observation suggère que des rotations de blocs à différentes échelles sont envisageables. Elles rejoignent le modèle de déformation du Japon sud-ouest proposé par Kanaori (1990), qui comprend une dizaine de blocs rigides tournant dans le sens horaire.

L'ensemble de ces données est synthétisé dans un modèle d'ouverture en pull-apart rendant compte des rotations paléomagnétiques du Japon sud-ouest. L'ouverture de la mer du Japon est replacée dans le contexte de la déformation de l'Asie. A cette échelle, la déformation dextre contemporaine de l'ouverture de la mer du Japon accorde la rotation anti-horaire de grands blocs continentaux à l'intérieur d'une zone de déformation sénestre limitée par le Qinling Shan au sud et les Monts Stanovoï au nord. La rotation anti-horaire du Japon NE est reliée à ce méga-cisaillement sénestre généré par la collision Inde-Asie.

NEogene STRESS FIELD IN SW JAPAN AND MECHANISM OF DEFORMATION DURING THE JAPAN SEA OPENING

MARC FOURNIER AND LAURENT JOLIVET

Laboratoire de Géologie, Ecole Normale Supérieure

24, rue Lhomond, 75231 Paris cedex 05, France

Fax: (33-1) 44 32 20 00

OLIVIER FABBRI

Department of Geology and Mineralogical Sciences, Faculty of Science

Yamaguchi University, Yoshida 1677-1, 753 Yamaguchi, Japan

Fax: 81-839-32-2041

Abstract

The formation of the Japan Sea is well accounted for by a dextral pull apart model involving block rotations between two N-S shear zones. Paleomagnetic data obtained in SW Japan are however in apparent contradiction with this model in terms of timing because they suggest an almost instantaneous opening 15 Ma ago. In order to understand the structural context of the paleomagnetic rotations, we investigated the Neogene stress field of SW Japan by means of fault set analysis. We present results for seven Neogene basins located on the Japan Sea coast and along the Median Tectonic Line (MTL). We computed a mean Middle Miocene stress field for each basin and for the regions previously surveyed by Jolivet and Huchon (1989), Jolivet et al. (1991), and Fournier et al. (1994), and compiled the available stress field data of the Japan Sea region. The results show remarkably consistent stress directions from Sakhalin to western Honshu with the maximum horizontal stress trending NE-SW and the minimum horizontal stress trending NW-SE. We therefore sampled the Middle Miocene stress field post-dating the differential rotations of NE and SW Japan which occurred about 15 Ma ago, that is the stress field corresponding to the last stage of opening of the Japan Sea. The overall geometry suggests that the same stress field likely prevailed during the whole opening. The stress regime changes from transpressional in Sakhalin and Hokkaido, to transtensional on the eastern margin of the Japan Sea, and almost purely extensional on the southern margin. The stress field along the MTL is compatible with left-lateral and normal movements along the fault during the opening of the Japan Sea, which makes it a second order fault rotating between two major dextral shear zones and accommodating clockwise block rotations. Observations in Shimane peninsula show that SW Japan also suffered a distributed deformation with numerous small-scale blocks at the time of fast paleomagnetic rotations. These observations support a model of deformation of SW Japan with block rotations at all

scales. All these results are integrated in a single model of opening of the Japan Sea which accounts for paleomagnetic data.

Introduction

Paleomagnetism is a very efficient tool to study continental deformation provided that the geometry of crustal blocks and the shear zones that bound them are fully understood (e. g., Ron et al., 1984; Luyendyk et al., 1985). The case of the Japan Sea is somewhat controversial because it is uneasy to conciliate marine data showing that the opening occurred between 24 and 11 Ma (Tamaki et al., 1992; Kaneoka et al., 1990) as well as structural data suggesting a progressive pull-apart opening (Lallemand et Jolivet, 1985; Jolivet and Huchon, 1989; Jolivet et al., 1991), with paleomagnetic data supporting an almost instantaneous rigid rotation of about 50° of SW Japan 15 Ma ago (Figure 1) (Otofuji et al., 1991; Hayashida et al., 1991). The pull-apart model which was originally proposed by Lallemand and Jolivet (1985) and refined afterwards (Jolivet et al., 1991; Jolivet and Tamaki, 1992) fits a large amount of data onland and offshore, but abuts against the timing of the paleomagnetic rotations which remains apparently incompatible with the timing of opening. One possibility is that SW Japan did not rotate as a single rigid block and consequently that the rotation is not simply linked with the Japan Sea opening. Paleomagnetic deflections of Lower Miocene rocks in the eastern part of SW Japan are indeed significantly smaller than in the western part (Figure 1) (Itoh, 1988; Hirooka, 1986). SW Japan would then consist of small rigid blocks which underwent differential clockwise (CW) rotations during the opening of the Japan Sea, as suggested by Kanaori (1990), Kodama et al. (1993), and Jolivet et al. (1994).

We thus need to understand the geometry of block rotations in SW Japan. The study of the Neogene stress field from northern Sakhalin to central Honshu (Jolivet and Huchon, 1989; Jolivet et al., 1991; Jolivet et al., 1992; Fournier et al., 1994) by means of analysis of fault slip data (Angelier, 1984) has brought up consistent results over a 2000 km long strike-slip zone, which strongly support the model of pull-apart opening. In this paper, we extend the study to Neogene basins of SW Japan (Figure 2). We present results for two basins located on the Japan Sea coast, the basins of Shimane peninsula and Tango peninsula, and for four basins located along the Median Tectonic Line (MTL) of SW Japan, the basins of Ishizuchi, Shidara, Chichibu, and Itsukaichi. Results for the basins of Noto peninsula, Yatsuo, and Sado, were previously published (Fournier et al., 1994; Jolivet et al., 1991). The basins of Tsu and Muro along the MTL were surveyed without any result because of the lack of outcrops. The ages of formations of the surveyed basins are compiled in Figure 3.

Neogene Basins of the Southern Margin of the Japan Sea

Miocene sediments are distributed along the coast of the Japan Sea in two regions: east of Tottori city and in Tango peninsula, on one hand, and around Shimane peninsula in the San'In

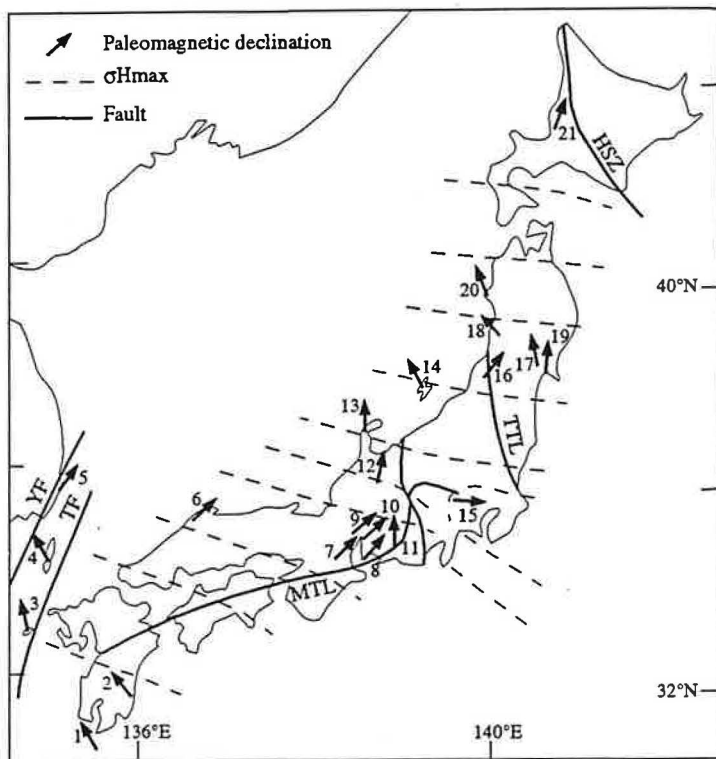


Fig. 1. Neogene paleomagnetic declinations and present-day stress field. HSZ is Hidaka shear zone, MTL is Median Tectonic Line, TF is Tsushima fault, TTL is Tanakura tectonic line, YF is Yangsan fault. Paleomagnetic declinations compiled from: 1-Kodama et al. (1991), 2-Kodama and Nakayama (1993), 3-Ishikawa and Tagami (1991), 4-Ishikawa et al. (1989), 5-Kim et al. (1986), McKabe (pers. comm.), 6-Otofuji et al. (1991), 7-Hayashida and Ito (1984), 8 and 9-Hayashida (1986), 10-Hayashida et al. (1991), 11-Otofuji et al. (1985); 12-Itoh (1988), 13 and 14-Hirooka et al. (1986), 15-Hyodo and Niitsuma (1986), 16, 17, and 18-Otofuji et al.(1985), 19-Yamazaki (1989), 20-Tosha and Hamano (1988), 21-Kodama et al. (1993). The trajectories of present-day $\sigma_{H\max}$ are compiled from Tsukahara and Kobayashi (1991), Tsukahara and Ikeda (1991), Ishii et al. (1983), and Nakamura and Uyeda (1980).

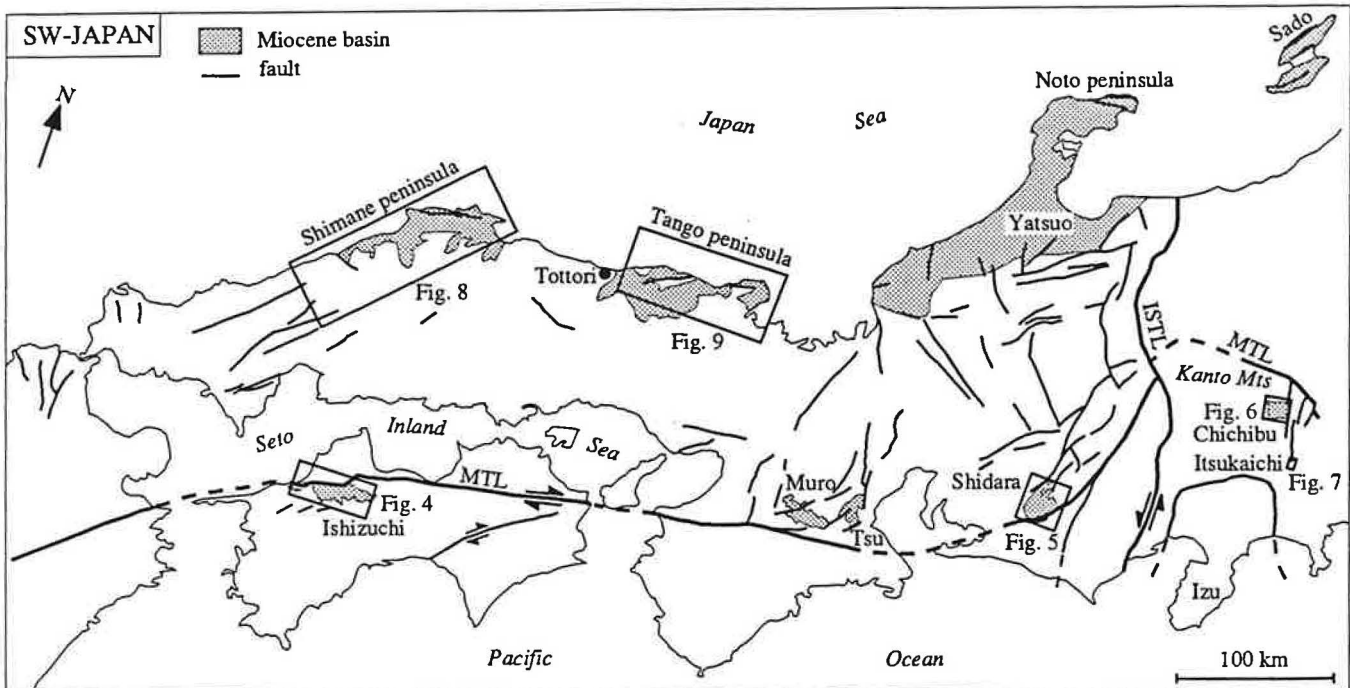


Fig. 2. Miocene basins of SW-Japan.

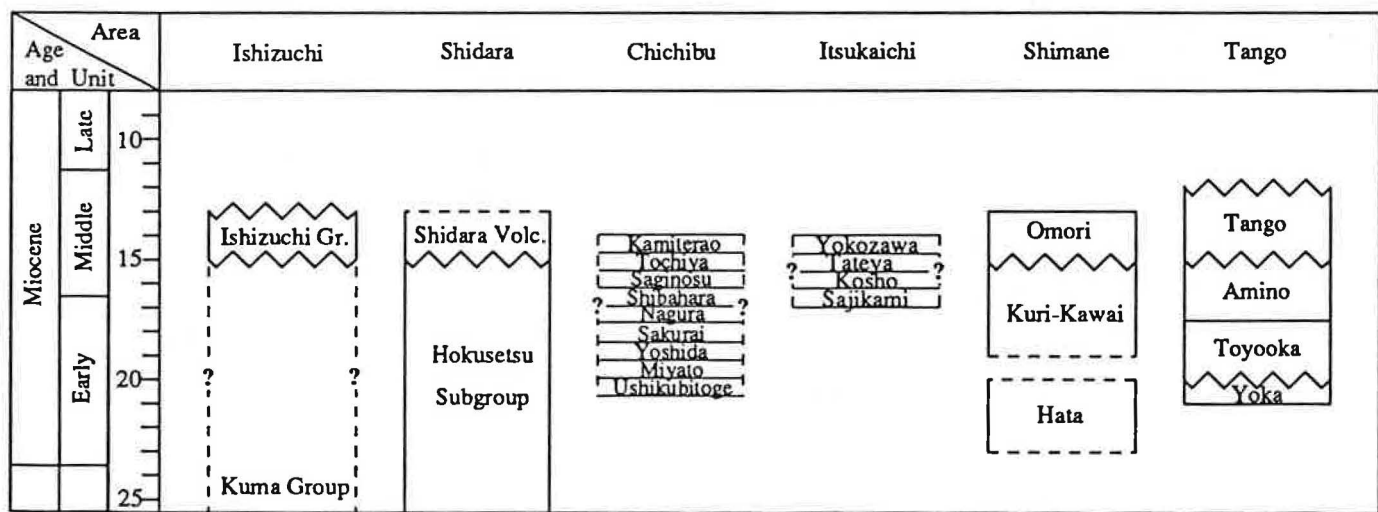


Fig. 3. Age of formations of Miocene basins. After Kano et al. (1991), Arai and Kano (1960) for Chichibu basin, and Irizuki et al. (1990) for Itsukaichi basin.

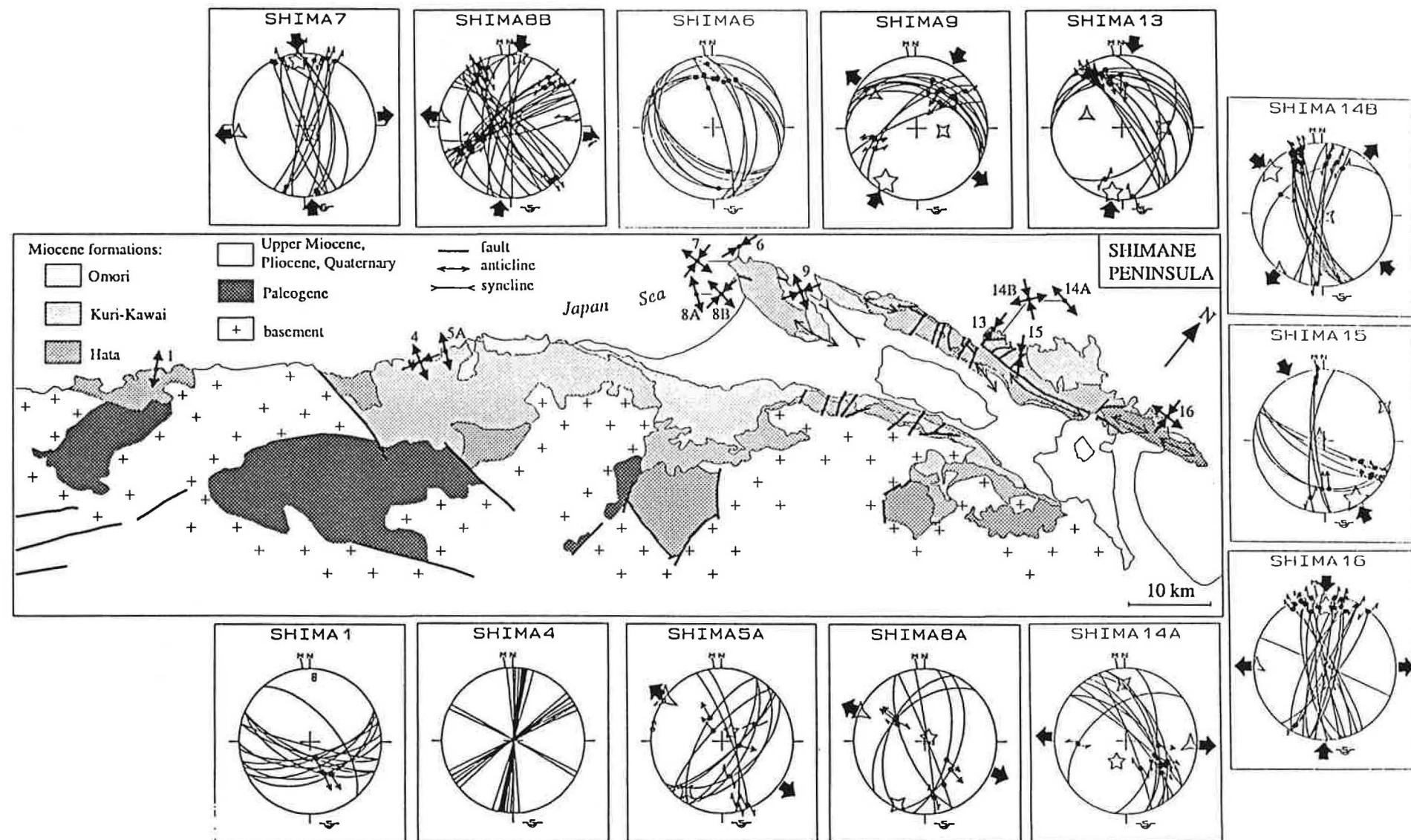


Fig. 4. Stress tensors computed for Shimane peninsula.

district, on the other hand (Figure 2). Data concerning Noto peninsula and Yatsuo basin are described in Fournier et al. (1994).

San'In District (Shimane peninsula)

The lower and middle Miocene deposits of the San'In district are divided in three formations, the Hata, Kuri-Kawai, and Omori formations in ascending order (Figure 3). K-Ar ages were obtained for these formations: 15-19 Ma in the Hata formation (Kano and Yoshida, 1984; Kano and Nakano, 1985), 14-18 Ma in the Kuri-Kawai formation (Otofuji et al., 1991), and 13-16 Ma in the Omori formation (Kano and Yoshida, 1984; Kano et al., 1991; Otofuji et al., 1991). In the northern Shimane peninsula, the Omori formation is intruded by N-trending dikes (Kobayashi, 1979a) with a K-Ar age of 9.3 ± 2.4 Ma (Kano and Yoshida, 1984). The mean paleomagnetic declination is about 60°E in the Hata formation (Otofuji and Matsuda, 1983; 1984), $39^\circ\text{E} \pm 15^\circ$ in the Kuri-Kawai formation (Otofuji et al., 1991), and roughly N-S in the Omori formation (Otofuji et al., 1991).

Fault slip data were measured in the Hata, Kuri-Kawai, and Omori formations and the results are shown in Figure 4. Three categories of sites can be distinguished: purely extensional sites yielding a NW-SE extension (σ_3) (sites 1, 4, 5A, 8A, 14A), transtensional sites with conjugate strike-slip faults yielding a N-S trending $\sigma_{H\max}$ (sites 7, 8B, 16), and compressional sites with reverse faults yielding N-S to NW-SE trending compression (σ_1). The extensional sites are documented in the Hata and Kuri-Kawai formations, the transtensional sites are exclusively documented in shales of the upper part of the Kuri-Kawai formation, and the compressional sites are documented in the Kuri-Kawai and Omori formations, the upper part of the Omori formation being affected by reverse faults. A regional N-S compression is also suggested in Shimane peninsula by large scale E-W trending folds in the middle Miocene formations (Geological Map of Shimane Prefecture, 1982). Similar folds are known offshore and are unconformably overlain by Pliocene sediments (Tanaka and Ogusa, 1981; Yamamoto, 1993). Thus, the N-S compression post-dates the Middle Miocene and predates the Pliocene. The N-S dikes of Late Miocene age in northern Shimane peninsula (Kobayashi, 1979a) are probably coeval with the N-S trending compression. The extensional and transtensional stress fields are not documented in the Omori formation (Middle Miocene) and likely predate it. No relative chronology could be observed in the field between these two stages. Both extensional and transtensional stress fields have directions of extension between E-W and NW-SE.

Data obtained in this region are especially important because it is there that Otofuji et al. (1991) dated with the best precision the CW rotation of SW Japan. The geometry of faulting in the Kuri-Kawai formation, which underwent the CW rotation of SW Japan, suggests block rotations at all scales and will be described in a later section of this paper.

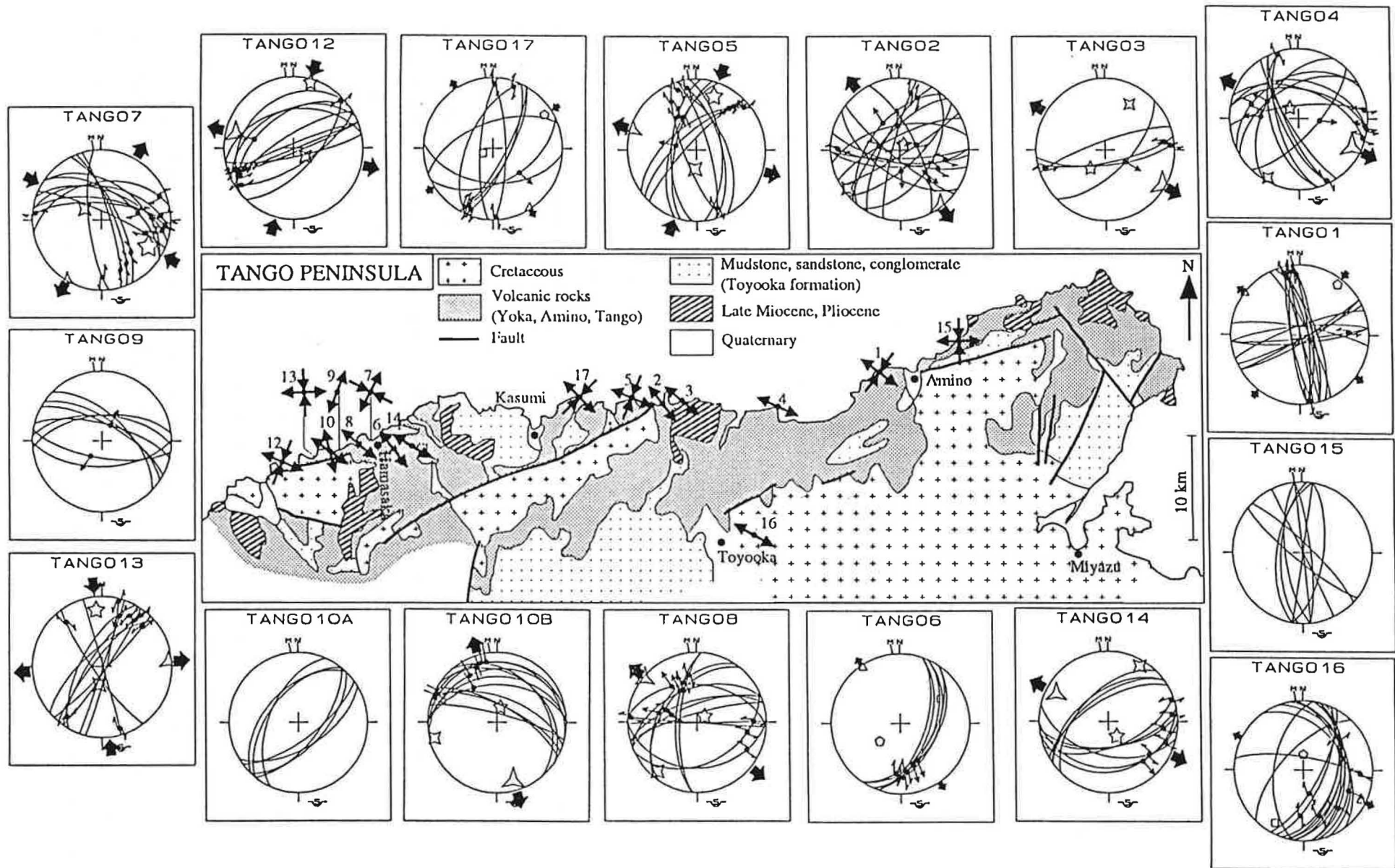


Fig. 5. Stress tensors computed for Tango peninsula.

Tango peninsula area

In the Tango peninsula area (Figure 5), the Miocene system is mainly represented by the Hokutan group which is composed of the Yoka, Toyooka, Amino, and Tango formations in ascending order (Figure 3). The Yoka, Amino, and Tango formations are made of volcanic rocks, and the Toyooka formation mainly consist of sedimentary rocks (conglomerates, sandstones, mudstones). The Yoka and Tango formations are intruded by dikes with K/Ar ages of 19-20 Ma and 14-15 Ma (Tsunakawa et al., 1983; Yamamoto and Hoshizumi, 1988), respectively. The Amino formation, which is unconformably overlain by the Tango formation, records a 15 Ma (K-Ar) episode of silicic volcanism (Yamamoto and Hoshizumi, 1988). The upper Miocene and Pliocene volcanics of Tango peninsula rest unconformably upon the Hokutan group. According to Sasajima (1981), paleomagnetic measurements in the Yoka formation showed no significant rotation. However, according to the coordinates of the sampling site, the age of the sampled rocks is most likely Late Miocene.

Fault slip data were obtained in the volcanics of the Hokutan group because the sedimentary rocks of the Toyooka formation are nearly free from deformation. The results are shown in Figure 5. In the eastern part of the basin, east of Kasumi, the measurements were undertaken in the Amino and Tango formations. The results consistently show a NW-SE extension evidenced by conjugate normal faults. The extensional regime is locally transtensional with conjugated strike-slip faults associated with normal faults. In the western part of the basin, near Hamasaka, we analysed the fracturation in volcanic rocks of the Yoka formation for sites 7, 9, 10A, 10B, 12, 13, and 14, and in volcanic rocks of the Toyooka formation for sites 6 and 8. The NW-SE extension is always documented in the Toyooka formation, and in sites 10A, 10B, 12, and 14 in the Yoka formation. Sub-vertical dikes trending N070E to N090E are observed in sites 12 and 14. These dikes have a trend similar to those described by Kobayashi (1979b) in the Yoka formation and dated of 19-20 Ma (Tsunakawa et al., 1983). In both sites left-lateral strike-slip slickensides were observed on the dike margins and used to compute the extensional stress field. The extension therefore post-dated the emplacement of the dikes. Sites 7 and 9 in the Yoka formation yielded a stress field with a NE-SW extension which is never recorded in the younger formations and may predate the NW-SE extension. Site 13, with conjugate strike-slip faults, documents N-S compression and perpendicular extension. This stress field is similar to that observed in site 15, north of Amino, where N-S trending normal faults and joints are associated with numerous N-S basaltic dikes (Kobayashi, 1979) dated 14-15 Ma (K-Ar; Tsunakawa et al., 1983). This stress field does not differ much from the extensional stress field locally transtensional described above. It might be intermediate between the Early-early Middle NW-SE extension and the Late Miocene N-S compression identified by E-W folds off the coast of Tottori (Yamamoto, 1993).

Stress fields documented in the Tango peninsula area can be related to dike emplacements. The NW-SE extension post-dates the emplacement of E-W to NNE-SSW trending dikes 20 Ma ago. The trend of $\sigma_{H\max}$ seems to have changed from NE-SW to N-S about 14-15 Ma ago when dikes were emplaced in Tango peninsula. The latter stress field did not affect the upper Miocene and Pliocene rocks of Tango peninsula.

Noto Peninsula

The Middle Miocene stress tensors of Noto peninsula and Yatsuo basin have been published in Fournier et al. (1994). Two kinds of tensors were computed for the lower to middle Miocene formations corresponding to an extensional stress field with σ_3 trending NW-SE, and to a transtensional stress field with σ_1 trending NE-SW and σ_3 trending NW-SE. Jolivet et al. (1991) described similar fracturation data in Sado island. There, two successive stages of deformation could be recognised, strike-slip faulting preceding normal faulting. The same chronology likely applies to Noto peninsula and Yatsuo basin, as well as Tango and Shimane peninsulas where we described both extensional and transtensional sites.

Neogene Basins Along the Median Tectonic Line

The MTL is the most prominent dislocation in SW Japan. A major left-lateral strike-slip fault in the Cretaceous and Paleogene (Ichikawa, 1980; Miyata et al., 1980), the MTL is presently active as a right-lateral fault with a slow rate of motion (Okada, 1980, 1992). The sense of motion during the rotation of SW Japan has remained poorly constrained (e.g., Miyata et al., 1980). The only way to constrain it is to study the Neogene basins distributed along the MTL.

Ishizuchi basin

The Tertiary basin of Ishizuchi consists of a detrital sedimentary sequence with conglomerates, sandstones, and mudstones (Kuma Group), covered by Middle Miocene volcanic rocks (Ishizuchi Group) (Figure 3). Since Nagai (1956), all authors consider the Kuma Group as dating of Late Eocene and the contact with the Ishizuchi volcanics as being an unconformity, but tuff layers at the base of the volcanics are locally intercalated with the Kuma Group sandstones suggesting a progressive transition. In the eastern part of the basin, these rocks are intruded by granodioritic stocks dated at 14 Ma (K-Ar, Shibata and Nozawa, 1967; Yoshida, 1984). The E-W trending andesitic dikes of the Kuromori-Toge area (Kobayashi, 1979b) were emplaced at the same period (Yoshida, 1984).

The Ishizuchi basin is bounded to the north by the MTL which puts into contact the upper Cretaceous Izumi Group to the north with the Sanbagawa schists or the Kuma Group to the south (Takahashi, 1986; 1992; Takeshita, 1991). According to Tazaki et al. (1990) the MTL

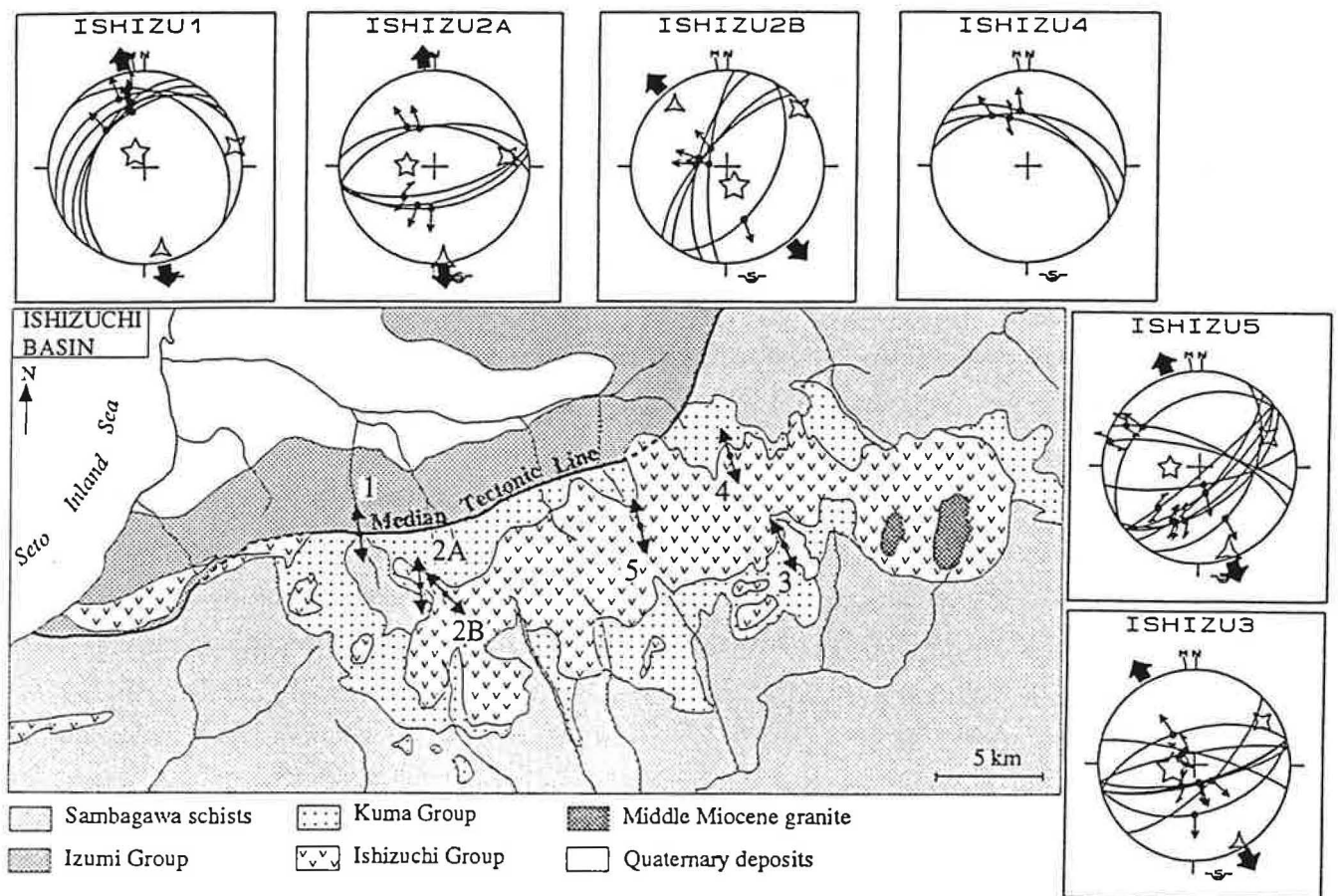


Fig. 6. Stress tensors computed for Ishizuchi basin.

is sealed by the volcanics of the Ishizuchi Group, and andesitic intrusions along it dated 15.1 to 15.4 Ma (K-Ar) are not deformed. Takagi et al. (1992) dated the fault gouge along the MTL, and the youngest K-Ar age they found is 14.7 Ma. From asymmetric shear bands in the fault zone they concluded to a northward motion of the hanging wall, i.e., normal faulting along the MTL. No paleomagnetic data are available for Cenozoic rocks of the Ishizuchi basin. Kodama (1990) provided paleomagnetic data for the nearby upper Cretaceous Izumi Group showing CW rotations of 75°-90°.

Fault measurements were carried out in the Kuma and Ishizuchi Groups, and within the fault zone of the MTL for site 1 (Tobe Thrust type locality) (Figure 6). Normal faulting prevails in all sites. In site 5, normal faults are associated with strike-slip faults with a normal component. No relative chronology has been observed in the field between the two fault systems which are likely synchronous. The volcanics of the Ishizuchi Group are not strongly strained and only five stress tensors could be computed. The results are consistent and show a N-S to NW-SE extension in agreement with the E-W trend of Middle Miocene dikes (Kobayashi, 1979), and compatible with normal faulting along the MTL at the same period (Takagi et al., 1992). This Middle Miocene extensional stress field can be considered to be coeval with the emplacement of the Ishizuchi volcanics.

Shidara basin

Further east along the MTL, the Shidara basin (central Japan) is a cauldron of Miocene age (Kogi, 1983; Takada, 1987a, b). Deposition of tuffaceous sandstones and mudstones in the basin (Hokusetsu subgroup) preceded the emplacement of rhyolitic and dacitic rocks (Shidara volcanics) (Figure 3). These acidic rocks were subsequently intruded by andesitic dikes with K-Ar ages of 16.5-14.9 Ma (Tsunakawa et al., 1983). Paleomagnetism of andesitic dikes, and rhyolitic and dacitic rocks of the central part of the basin yielded N-S declinations (Torii, 1983), showing that no significant rotation occurred in Shidara basin since the emplacement of dikes 15 Ma ago. The Shidara basin is bounded to the south by the MTL marked by granite cataclasites (Ui, 1980).

The present-day trend of the maximum horizontal stress ($\sigma_{H\max}$) in central Japan to the north of the MTL, determined from in-situ measurements and shallow earthquakes focal mechanisms (depth < 35 km), is WNW-ESE (Figure 1) and the perpendicular horizontal component is extensional (Tsukahara and Ikeda, 1991; Mikumo et al., 1988). Active strike-slip faulting prevails in Central Japan (Mikumo et al., 1988; Kanaori et al., 1992). Kanaori et al. (1992) described central Japan as a system of rotating blocks: blocks bounded by ENE-WSW right-lateral faults undergo counterclockwise (CCW) rotations between NNW-SSE left-lateral faults.

Fault slip data equal-area projections and computed paleostress field directions for 12 sites are shown in Figure 7. The measurements were done in Lower Miocene formations (sites 7,

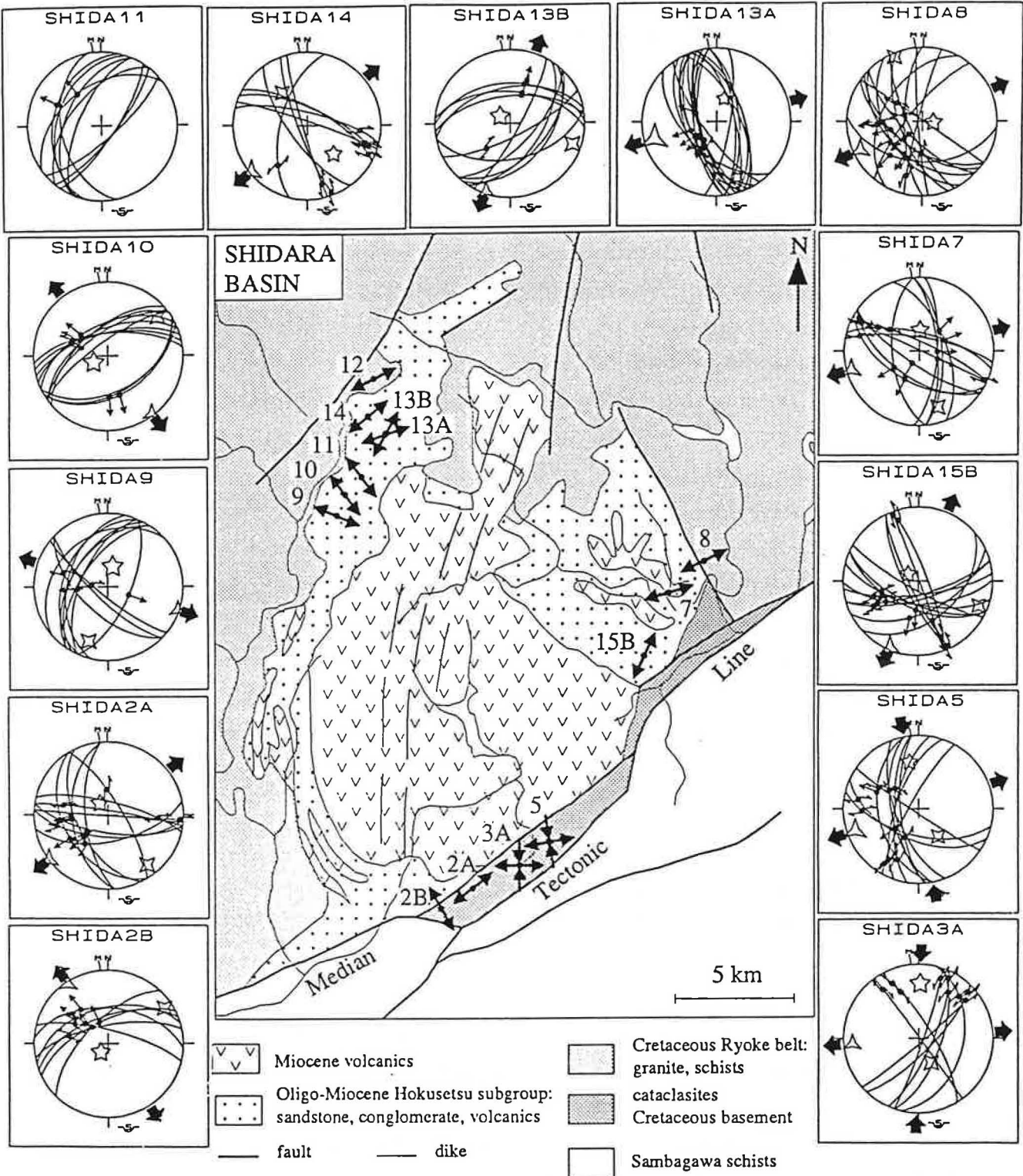


Fig. 7. Stress tensors computed for Shidara basin.

9, 11, 13, 14, 15), in cataclasites along the MTL (sites 2, 3, 5), and in the Cretaceous rocks of the Ryoke belt, granite (site 8) and micaschists (site 12). The Shidara volcanics are seldom faulted and no stress field could be computed from these series. Paleostress fields computed for lower Miocene rocks are consistently extensional, two directions of extension being documented. The more widespread one trends between N045E and N070E, the same direction being obtained in cataclasites along the MTL (site 2A and 5). Normal and strike-slip faults are sometimes associated (site 2A, 5, 7, 8, and 14), both fault systems being compatible with the direction of σ_3 . No relative chronology has been observed in the field between these fault systems. The direction of extension is compatible with the strikes of andesitic dikes in the basin which are N-S over the major part of the basin and change progressively to N020E in the northern part (Kogi, 1983). We then consider that extension is coeval with emplacement of the dikes, i. e., early Middle Miocene in age. The direction of extension is slightly oblique with the trend of the MTL in this region (N050E), and it is compatible with left-lateral strike-slip motion with an extensional component along it. Moreover, the general shape of the cauldron and the orientation of the dike swarm with respect to the MTL are in favour of a left-lateral pull-apart geometry.

Secondly, a NW-SE direction of extension is locally documented in coarse deposits at the base of the Hokusetsu subgroup (sites 9, 10, and 11). In the same area two samples from the Hokusetsu subgroup provided paleomagnetic declinations of 40°E and 70°E (Torii, 1983). Such declinations are representative for Lower Miocene rocks in SW Japan (Otofuji et al., 1985, 1991), which is further confirmed by fission-track ages of the Hokusetsu volcanics of about 32 Ma in this area (Hayashi and Koshimizu, 1992). The NW-SE direction of extension reveals the existence of an early extensional stage presumably of Early Miocene age.

Chichibu basin

The MTL and the external zones of SW Japan are bent in central Japan. This bending is due to the successive collisions of the Tanzawa and Izu blocks of the Philippine Sea Plate (Niitsuma and Matsuda, 1985; Taira et al., 1989). The age of the Tanzawa collision is poorly constrained. Takahashi and Nomura (1989) showed that paleomagnetic declinations of the Chichibu quartzite (6-8 Ma) in the Kanto mountains are not deflected, and dated the Tanzawa collision as Late Miocene or earlier. From paleomagnetic measurements in upper Cretaceous to middle Miocene rocks of central Japan, Itoh (1988) concluded that the bending of external zones of SW Japan took place between 15 and 12 Ma. The Izu collision started during the Quaternary (Huchon and Kitazato, 1984).

The Chichibu basin is a square-shaped basin filled with Neogene sediments as thick as 5 km in its southern part (Arai and Kanno, 1960) and folded in a broad synform with a NE-SW axis. The Neogene deposits unconformably overlie the Mesozoic basement of the Kanto Mountains. The age of the lower formations of the basin is not known, presumably Late

Oligocene-Early Miocene (Arai and Kanno, 1960). Ages of the upper formations are correlated with the planktonic foraminiferal zone N8 of Blow (1969) dating of late Early to early Middle Miocene (Saito and Maiya, 1973), the base of which is dated at 16.3 Ma (Harland et al., 1990). Paleomagnetic declinations measured in the basin show a CW rotation of about 90° of the basin since its formation (Hyodo and Niitsuma, 1986). Hyodo and Niitsuma (1986) attributed this rotation partly to the rotation of SW-Japan during the opening of the Japan Sea (Otofuji and Matsuda, 1987), and partly to the collision of the Tanzawa block in the Middle or Late Miocene.

The present-day stress field deduced from in-situ measurements and focal mechanisms of earthquake shows a $\sigma_{H\max}$ trending NNE-SSW in the Kanto mountains (Figure 1) (Tsukahara and Ikeda, 1991). North of the Kanto mountains, $\sigma_{H\max}$ consistently trends WNW-ESE. The northern boundary of the Kanto mountains coincides with the northern boundary of the zone of stress field perturbation around the Izu collision zone.

We measured sets of faults in sandstones of the lower part of the basin, in the Yoshida, Sakurai, and Nagura formations (Figure 8). We could not compute stress tensors for the upper part of the basin though normal faults were observed in the Saginosu formation. The stereo diagrams are shown after tilt correction of strata. All stress tensors have $\sigma_{H\max}$ trending NE-SW and σ_3 trending NW-SE. Normal faulting prevails in sites 2A, 2B, 4, and 6, and strike-slip faulting prevails in sites 3A, 3B, 5, and 7. Kuwahara (1982) and Sato (1986) described in the Chichibu basin a system of conjugated strike-slip faults similar to that observed in sites 3A, 3B, 5, or 7. With the exception of synsedimentary structures (Latt, 1989), we did not observe any compressional structure (fold or reverse fault) in the basin: the Chichibu basin has been totally preserved from the Tanzawa and Izu collisions.

The age of the stress field measured in the basin is poorly constrained: the fracturation is observed in lower to early middle Miocene formations and it predates the tilting of strata. According to Latt (1989), a first stage of tilting is coeval with the deposition of the upper formations in the basin, which constrains the age of the stress field to early Middle Miocene. It is particularly uneasy to set the age of the stress field with respect to the two successive CW rotations of the Kanto mountains suggested by paleomagnetism (Hyodo and Niitsuma, 1986). As the early Middle Miocene rocks recorded this stress field, it probably post-dates the CW rotation of SW Japan of about 50° at about 15 Ma (Otofuji et al., 1991; Hayashida et al., 1991). By comparison with the early Middle Miocene stress field of Shidara basin, the stress field of Chichibu basin is rotated clockwise by about 50°, and so is the MTL which trends N110E north of the Chichibu basin instead of N050E in Shidara basin. Then, it can be regarded as a fossilised stress field which rotated by about 50° together with the MTL during the Tanzawa collision. The alternative is that the stress field measured in the Chichibu basin is younger than the Tanzawa collision, i. e., younger than 12 m. y. and likely of Late Miocene

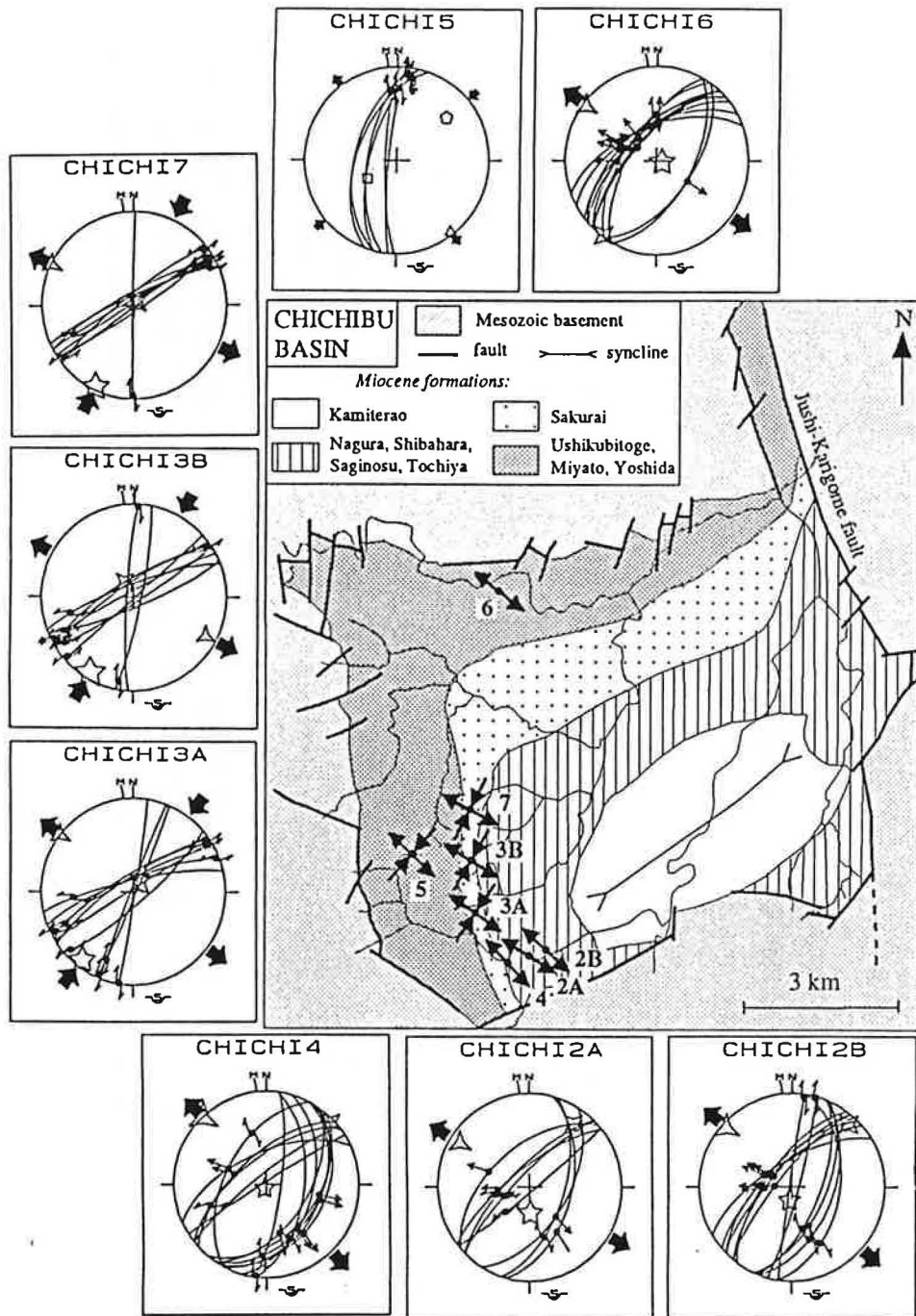


Fig. 8. Stress tensors computed for Chichibu basin.

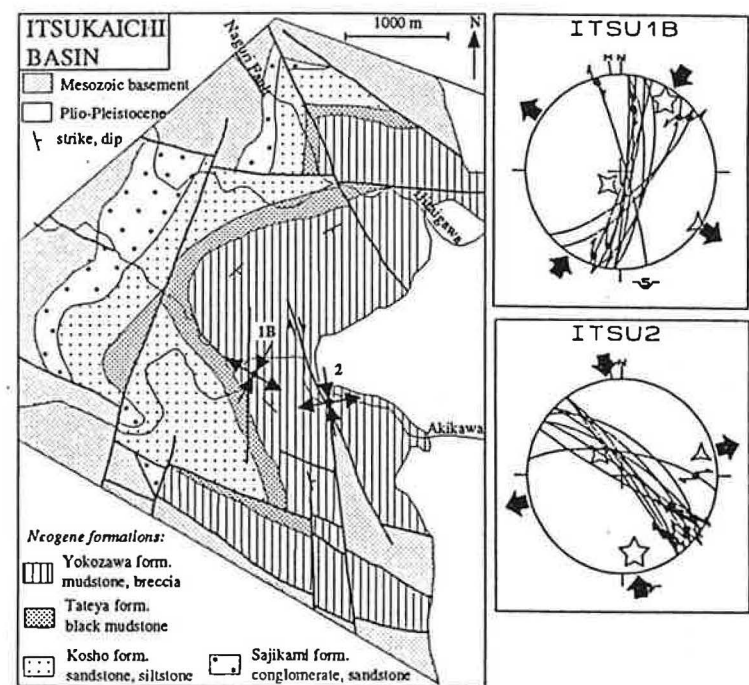


Fig. 9. Stress tensors computed for Itsukaichi basin.

age. It would be the only evidence of extensional deformation of Late Miocene age in the region and this hypothesis can hardly be accepted.

The Chichibu basin is bounded to the east by the NNE-trending Jushi-Karigome fault (Arai and Kanno, 1960) which cuts through the Kanto Mountains and is relayed to the south by the Naguri fault up to Itsukaichi basin. With the observed stress field, these faults are good candidates to accommodate dextral motions, and the Chichibu basin with its square shape might be a dextral pull-apart basin as proposed by Kuwahara (1982). North of the Chichibu basin, the MTL trends N110E. The NW-SE extension documented in the Chichibu basin is slightly oblique with the MTL as in Shidara basin, and it is compatible with left-lateral motion with a normal component along the MTL.

On the northern margin of the Kanto mountains, in the Yorii-Ogawa area, two systems of conjugated strike-slip faults have been described (Kuwahara and Sato, 1981; Kuwahara, 1982). The older one with N-S right-lateral and ENE-WSW left-lateral faults is related to the Early-Middle Miocene stress field with $\sigma_{H\max}$ trending NE-SW and σ_3 trending NW-SE. This is consistent with what we describe in Chichibu basin. The second one with NE-SW right-lateral and NW-SE left-lateral faults is recorded in the middle Miocene Matsuyama Group (Matsumaru and Hayashi, 1980) and is then considered to be Middle-Late Miocene in age. This stress field is similar to the present-day stress field north of the Kanto mountains with $\sigma_{H\max}$ trending WNW-ESE (Tsukahara and Ikeda, 1991) and consistent with the focal mechanism of the west Saitama earthquake (M 7.0) (Abe, 1974).

Itsukaichi basin

The Itsukaichi basin is located on the south-eastern margin of the Kanto Mountains, north of the Izu collision zone. It is filled with Neogene sedimentary deposits up to 2000 m thick. As for Chichibu basin, the age of the basal part of the basin is not known and the upper formation of the basin (Yokozawa formation) is correlated with the early Middle Miocene foraminiferal zone N8 of Blow (1969) (Irizuki et al., 1990) (Figure 3). The basin is folded in a syncline with a WNW-ESE trending axis, and the southern flank of the syncline is locally overturned (Ito, 1989). Plio-Pleistocene deposits unconformably overlie the folded formations. The age of folding is thus constrained between Middle Miocene and Plio-Pleistocene, so that folding can be reasonably attributed to the Tanzawa collision.

The Itsukaichi basin is a small basin (20 km^2) with few outcrops. Three superimposed stress fields were recognised there, but only one could be correctly documented and is shown in Figure 9. It consists of a transtensional stress field with $\sigma_{H\max}$ trending about N-S (sites 1B and 2, no tilt correction), documented along strike-slip faults cutting through the syncline and accommodating right-lateral motions. In site 1B, mudstones of the Yokozawa formations are affected by N020E trending joints post-dating the folding and compatible with the latter stress field. Some joints accommodated right-lateral strike-slip movements. Sato (1986) described a

set of left-lateral strike-slip fault in the Itsukaichi basin consistent with a N-S trending $\sigma_{H\max}$. This stress field is also in agreement with measurements of the present-day stress field in the Kanto mountains (Tsukahara and Ikeda, 1991) and with the recent N-S to NE-SW compression documented along the Izu collision zone in the Ashigara area (Huchon and Kitazato, 1984). It is late with respect to folding, but consistent with the direction of compression during folding. It may correspond to a late compressional stage of the Tanzawa collision of Late Miocene age.

The deformations of the Chichibu and Itsukaichi basins can be compared according to their structural context. The Chichibu basin within the basement of the Kanto mountains was preserved from the Tanzawa and Izu collisions and has fossilised a stress field older than the Tanzawa collision. The Itsukaichi basin on the edge of the Kanto mountains was strained during the Tanzawa collision and recorded superimposed stress fields.

Conclusion

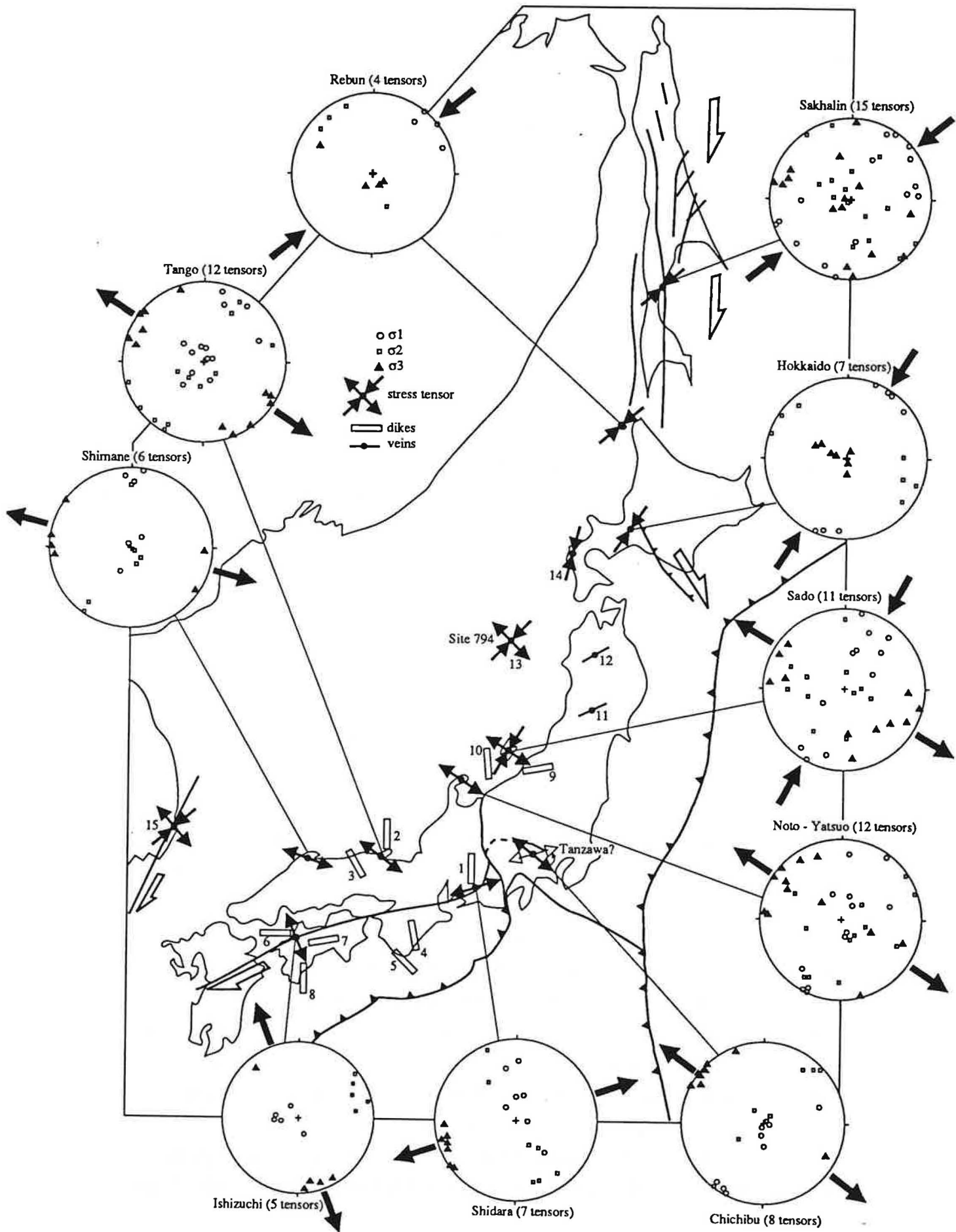
We attribute an early Middle Miocene age to the extensional stress fields measured in Ishizuchi and Shidara basins because of their compatibility with dated dike swarms. The extensional stress field measured in Chichibu basin is likely of the same age by analogy with Shidara basin. These stress fields are compatible with left-lateral and normal motions along the MTL in the eastern part of SW Japan (Shidara and Chichibu basins), and with normal motions only in the western part of SW Japan (Ishizuchi basin). As the dike swarm of Shidara basin did not suffer any rotation since it was emplaced (Otofuji et al., 1985), we consider that the stress fields we measured post-date the CW rotation of SW Japan.

Conclusion

The available data concerning the Early-Middle Miocene stress field in the Japan Sea area are gathered in Figure 10. For each region surveyed by Jolivet and Huchon (1989), Jolivet et al. (1991), Fournier et al. (1994), and this study, we determined a mean stress field from the computed stress tensor (Table 1). The stress field determined from fault analysis in the Tertiary Pohang basin in Korea (Hwang, 1992) and in the Japan Sea during the ODP leg 128 (Charvet et al., 1992) are also plotted, and results of vein and dike strike statistics are shown (Yamagishi and Watanabe, 1986; Otsuki, 1990; Ref. in Table 2).

All along the coasts of the Japan Sea from Sakhalin to western Honshu, the directions of $\sigma_{H\max}$ and $\sigma_{H\min}$ deduced from the analysis of fault slip data are remarkably consistent, NE-SW and NW-SE, respectively. The stress field changes from transpressional in Sakhalin and Hokkaido, to transtensional on the eastern margin of the Japan Sea, and almost purely extensional on its southern margin. The results of vein strike statistics in NE-Japan, of the ODP leg 128, and of fault set analysis in Korea (site 15 in Fig. 10), complete and confirm our

Fig. 10. Middle Miocene stress field in the Japan Sea area. References for dike swarms (1 to 10) are given in Table 2. 11 and 12-Otsuki (1990), 13-Charvet (1992), 14-Yamagishi and Watanabe (1986), 15-Hwang (1992).



results: the directions of the stress field are consistent all along the surveyed margins of the Japan Sea. This stress field is compatible with the overall dextral pull apart geometry described in Lallemand and Jolivet (1985) and Jolivet et al. (1991), and it is likely that it has been active during the whole opening period.

The consistency of the principal directions of the stress field suggests that the stress field did not undergo the CW and CCW rotations of SW and NE Japan in early Middle Miocene time (about 16-14 Ma) (Otofuji, 1991; Hayashida et al. 1991; Tosha and Hamano, 1988), and therefore that we measured the late Middle Miocene stress field coeval with the end of opening of the Japan Sea. As Angelier's method (1984) uses a slip criteria on pre-existing faults, the final stress tensor is generally obtained. Only if the stress regime completely changes, for instance from pure strike-slip to extensional as in Sado, earlier episodes will be recognised. The stress field we measured corresponds to a late stage of opening of the Japan sea and likely prevailed during all the opening of the Japan Sea.

The mean stress fields determined for basins along the MTL are inconsistent with those of the Japan Sea coast, except for Chichibu basin which in fact must be rotated 40° CCW in order to allow a comparison. In the eastern part of SW-Japan, these data suggest a curvature of the trajectories of $\sigma_{H\max}$ close to the MTL, $\sigma_{H\max}$ becoming nearly perpendicular to the MTL. The case of Ishizuchi basin in Shikoku is still different because the MTL was likely a pure normal fault in the early Middle Miocene.

Dike strikes statistics

Neogene stress-field trajectories in SW-Japan were previously determined using dike strike statistics by Kobayashi (1979a, b), Nakamura and Uyeda (1980), Tsunakawa (1986), and Yamamoto (1991). The results can be taken into account if they are in good agreement with fault set measurements.

The results of Nakamura and Uyeda (1980) and Tsunakawa (1986) differ significantly and must be discussed in detail. Tsunakawa (1986) recognised five stages for the evolution of the stress field since the Early Miocene. Stage 3 corresponds to a $\sigma_{H\max}$ trending E-W between 12 and 9 Ma. This stage is defined from data of two sites. The first site in Tango peninsula (site 23b in Tsunakawa (1986)) relies on only one measurement of dike (N120E). According to Kobayashi (1979a), this dike is not representative of the mean direction of dikes in Tango Peninsula which is N-S. The second site is located NW of Matsuyama, Shikoku (site 30 in Tsunakawa (1986)), and is after Tohara (1978). The dikes have an age of 12.6 ± 0.6 Ma (Tatsumi et al., 1980) and their mean direction is N050E, which is hardly consistent with the previous N120E in Tango Peninsula. It is not reasonable to estimate from this single data a stress field for the whole SW Japan during the period 12-9 Ma. Considering that Tsunakawa's stage 3 is poorly constrained and that stages 2 and 4 are similar, we keep only 3 stages for the

stress field evolution, stage 2 with $\sigma_{H\max}$ trending N-S starting from early Middle Miocene (16-15 Ma) and ending in Pliocene. This simplification is in agreement with the evolution of the stress field proposed by Yamamoto (1991) also from dike strike statistics.

As far as SW Honshu is concerned, the stress field maps of Kobayashi (1979b) and Nakamura and Uyeda (1980) for Early and Middle Miocene time (Fig. 7 in Nakamura and Uyeda (1980)) should be restricted to a shorter period. Among the 7 data used to draw the stress field of SW Honshu in Nakamura and Uyeda (1980), two are dubious as they represent non-dated normal faults, south of Shimane Peninsula and in the vicinity of Shidara basin. In the latter area, a dike swarm dated 14-16 Ma by Tsunakawa et al. (1983) actually documents a N-S trending $\sigma_{H\max}$ (Kogi, 1983) when the normal fault which trends N070E is considered to document a N160E trending extension at the same period. Three other data are derived from swarms of dikes in Noto peninsula, SW Kanazawa, and Yoka, which are older than 15 Ma: 16-27 Ma (Shibata et al., 1981), 15-17 Ma (Shibata et al., 1981), and 19.5-20.2 Ma (Tsukunawa et al., 1983), respectively. Another swarm of dikes in eastern Tsuyama is non-dated, and we could not find any reference for the last data located in the vicinity of Osaka. Lastly, recent K-Ar datations showed that the dike swarm of Tango peninsula, used by Kobayashi (1979a) to derive the stress field in Late Miocene, is actually of Middle Miocene age 14.1-15.5 Ma (Tsukanawa et al., 1983). The mean trend of dikes is N-S (Kobayashi, 1979a), which is inconsistent with a $\sigma_{H\max}$ trending N070E as proposed in Nakamura and Uyeda (1980) for the Early-Middle Miocene period. Therefore, the stress field proposed by Nakamura and Uyeda (1980) for the Early and Middle Miocene appears to be the stress field before 16-15 Ma. This stress field is similar to that proposed by Tsunakawa (1986) before 15 Ma.

Dike strike statistics data were recently compiled by Yamamoto (1991) who proposed a 3-stages evolution of the stress field since the Early Miocene in SW-Japan: $\sigma_{H\max}$ trends E-W from 22 to 15 Ma, N-S from 15 to 1.7 Ma, and NW-SE to E-W in the Quaternary. We plotted in Figure 10 only data of dike swarms radiometrically dated of Middle Miocene age (Table 2). These data are locally consistent with fault set analysis data, as in Shidara and Ishizuchi basins. On the Japan Sea coast, the trend of $\sigma_{H\max}$ from dike strike statistics is roughly N-S when it is NE-SW to NNE-SSW from fault set analysis. Dikes can be emplaced along pre-existing fractures not necessarily parallel to $\sigma_{H\max}$ (Delaney et al., 1986). For instance, in a transtensional stress field dikes can be emplaced obliquely to $\sigma_{H\max}$ along conjugated strike-slip faults. In the Niigata region, the dike swarms of Kakudasan and Sado-Ogi (9 and 10 in Figure 10) are of the same age and are perpendicular, N-S and E-W, respectively. Both are consistent with the NE trending $\sigma_{H\max}$ documented by fault analysis (Jolivet et al., 1991).

Mechanism of Deformation of Southwest Japan

Paleomagnetic data of SW Japan support systematically clockwise Miocene rotations with an amplitude decreasing eastward from 50° to 0° (Figure 1). A model of block rotations has been proposed by Kanaori (1990) for the inner belt of SW Japan, which accounts for the disparities of the paleomagnetic rotations. In the following we describe structural data supporting this model.

Block rotations at all scales

Figure 11 shows an outcrop in the Kuri-Kawai formation, at the western extremity of Shimane peninsula in Nakayama (on road 29 to Hironomisaki) and a stereo diagram of the observed fractures. This outcrop corresponds to site 8B in Figure 4. A system of conjugated strike-slip faults is observed, with right-lateral strike-slip faults trending N150E and left-lateral strike-slip faults trending N050E. The N050E left-lateral strike-slip faults are regularly spaced (2 meters) and they have a normal component (Figure 11a). The offset along these faults is of the order of the decimetre. At the metre scale, dextral strike-slip faults trending N-S to N020E accommodate centimetre-scale offsets. These faults are shown in Figure 11b cut by a N050E left-lateral strike-slip fault, and two conjugated strike-slip faults (N050E left-lateral and N010 right-lateral) viewed from above are offsetting N150E joints in Figure 11c. The N010E dextral strike-slip faults bound blocks (about 20 cm large and 2 m long) which likely underwent CCW rotations between the N050E left-lateral strike-slip faults.

The same geometry can be observed at the decimetre scale as illustrated in Figure 11d. Small blocks, about 1 cm large and 10 cm long and bounded by right-lateral faults with minor offsets, rotated between left-lateral faults showing horizontal offsets of about 1 cm.

Thus, the same geometry with rotating blocks is observed at decimetre scale and at metre scale, and it could likely be observed at decametre scale, the N050E left-lateral faults bounding blocks about 2 m large and 10 m long rotating between the N150E right-lateral strike-slip faults, the offsets of which could not be quantified on the outcrop. The overall sense of rotation of such a system of rotating blocks at all scales is determined by the sense of shear along the largest faults.

Similar geometries of deformation have been observed in the region of Tottori in lower to middle Miocene formations. This type of geometry has never been observed in the Late Miocene formations and seems to be characteristic of the Early-Middle Miocene deformation. The Omori formation in Shimane peninsula never shows such distributed deformation involving strike-slip and normal faults, but only folds and reverse faults. There is likely an unconformity at the base of the Omori formation which seals the domino geometry. This observation is of prime importance: Otofuji et al. (1991) showed that the Kuri-Kawai formation suffered the CW rotation characteristic of SW Japan and that the younger Omori

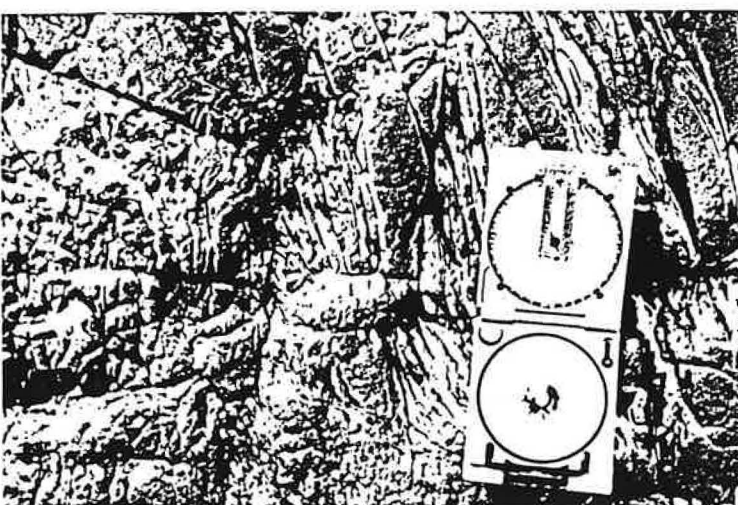
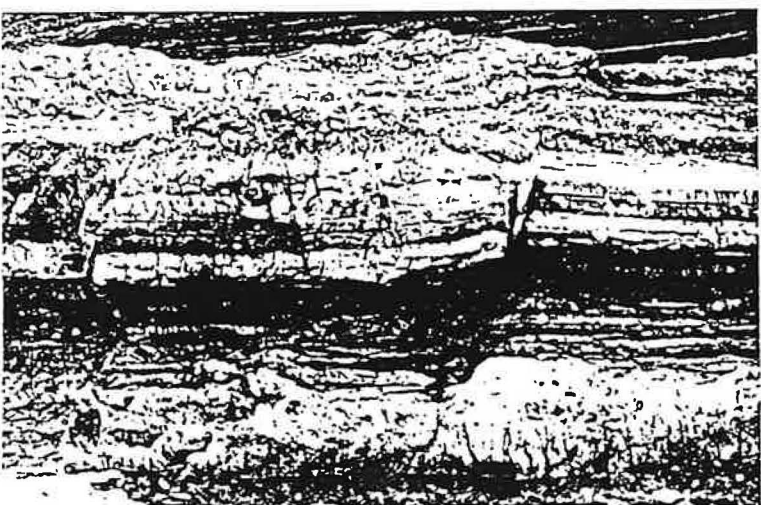
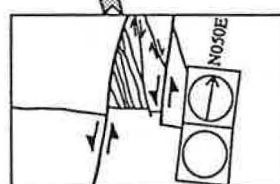
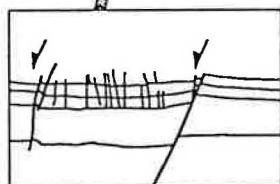
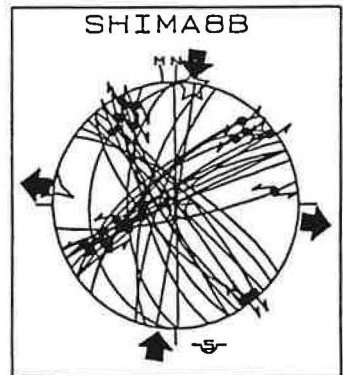
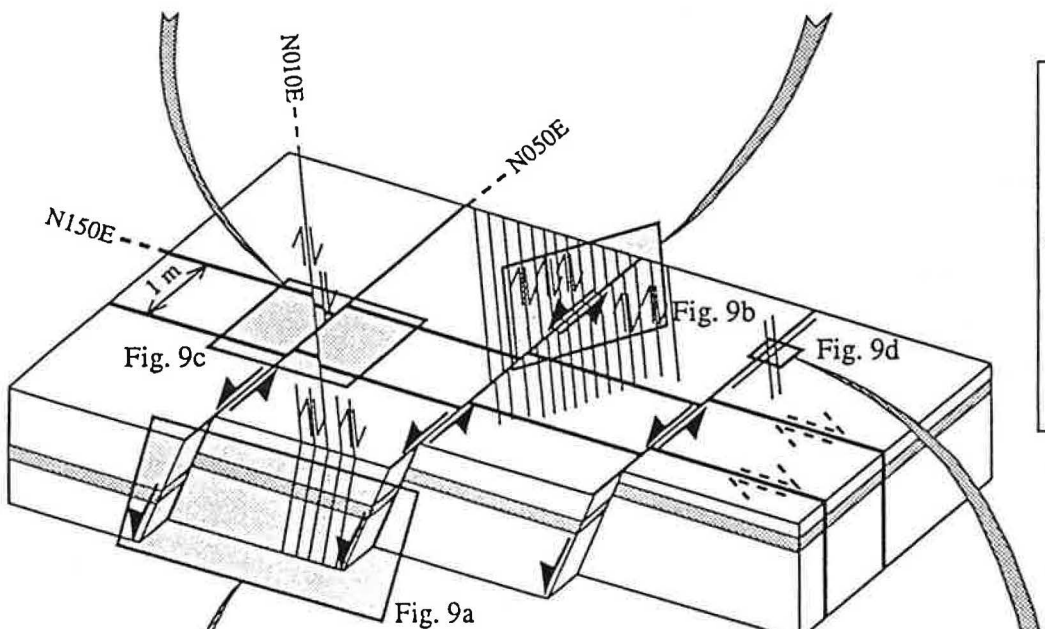
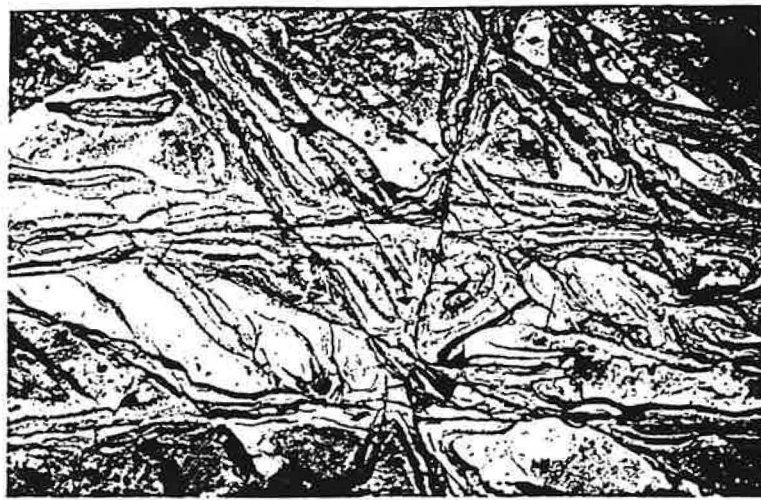


Fig. 11. Detail of an outcrop in the Early-Middle Miocene Kuri-Kawai formation, Shimane peninsula.

formation did not. A temporal link between the paleomagnetic rotations and the domino geometry is strongly suggested by the structural data.

The deformation is distributed at various scales and taken up by differential rotations of rigid blocks. Kanaori (1990) extended this geometry to all SW Japan dividing it in about 10 blocks. Within these blocks smaller blocks could be defined, and so on. Though this geometry is not obvious at the scale of SW Japan because there is not enough major strike-slip faults identified, it is consistent with field observations in the lower to middle Miocene formations.

Median Tectonic Line: a second order fault

The sense of block rotation in a shear zone depends on the sense of shear along the boundaries of the shear zone. In a transtensional context, the sense of rotation of blocks and the sense of shear are similar, i.e., left-lateral shear is associated with CCW rotations and reciprocally. SW Japan underwent CW rotations while the main dislocation (MTL) moved left-laterally. Consequently, the MTL was not a first order strike-slip fault during the opening of the Japan Sea, but more likely a second order fault included in a larger right-lateral shear zone and rotating with SW Japan. This situation is illustrated in Figure 12 with a photograph of the analogue experiments of Jolivet et al. (1991). The experiments investigated the deformation within a right-lateral strike-slip zone, with a two-layers sand-silicone model. The enlargement presented in Figure 12 shows a detail of the dextral transtensional strike-slip zone with rotating dominoes. The dominoes undergo CW rotations accommodated by left-lateral strike-slip faults of second order (between the dominoes). The MTL is likely one of these second order faults, undergoing a CW rotation during the opening of the Japan Sea within the broad right-lateral shear zone delimited to the east by the strike-slip zone of the east Japan Sea margin, and to the west by the strike-slip faults of the Tsushima Strait.

Timing of paleomagnetic rotations

The incompatibility of the apparent instantaneous rotation of SW Japan documented by paleomagnetism and the progressive opening of the Japan Sea has been discussed in Jolivet et al. (1994). In particular, the timing of paleomagnetic rotations proposed by Otofuji et al. (1991) and Hayashida et al. (1991) has been criticised. Jolivet et al. (1994) pointed out that Otofuji et al. (1991) constrained the age of rotation in the San'In district between the average ages of the rotated Kawai formation (16.4 Ma) and the non-rotated Omori formation (14.2 Ma). However, Otofuji et al. (1991) provided two data out of eight in the Kawai formation younger than 14 Ma and with declinations of 29°E and 37°E, respectively, and four data out of fifteen in the Omori formation older than 15 Ma and with declinations from 22°W to 14°E. These data should not be taken into account in computations of average ages. Moreover, Otofuji et al. (1991) and Hayashida et al. (1991) claimed that the rotation of SW Japan

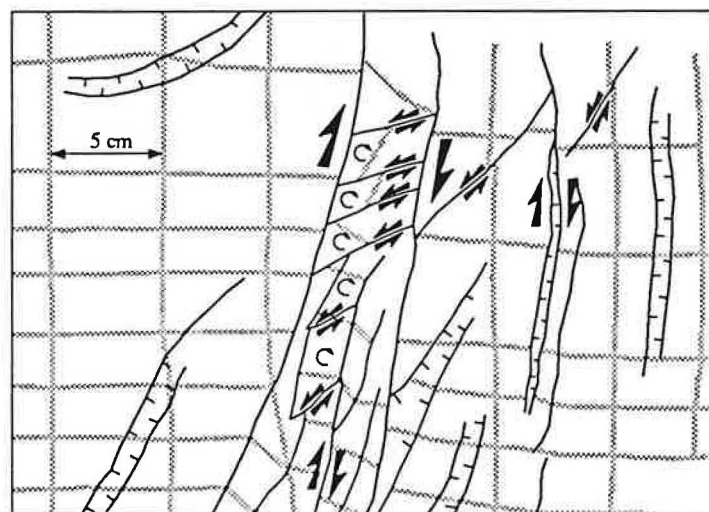
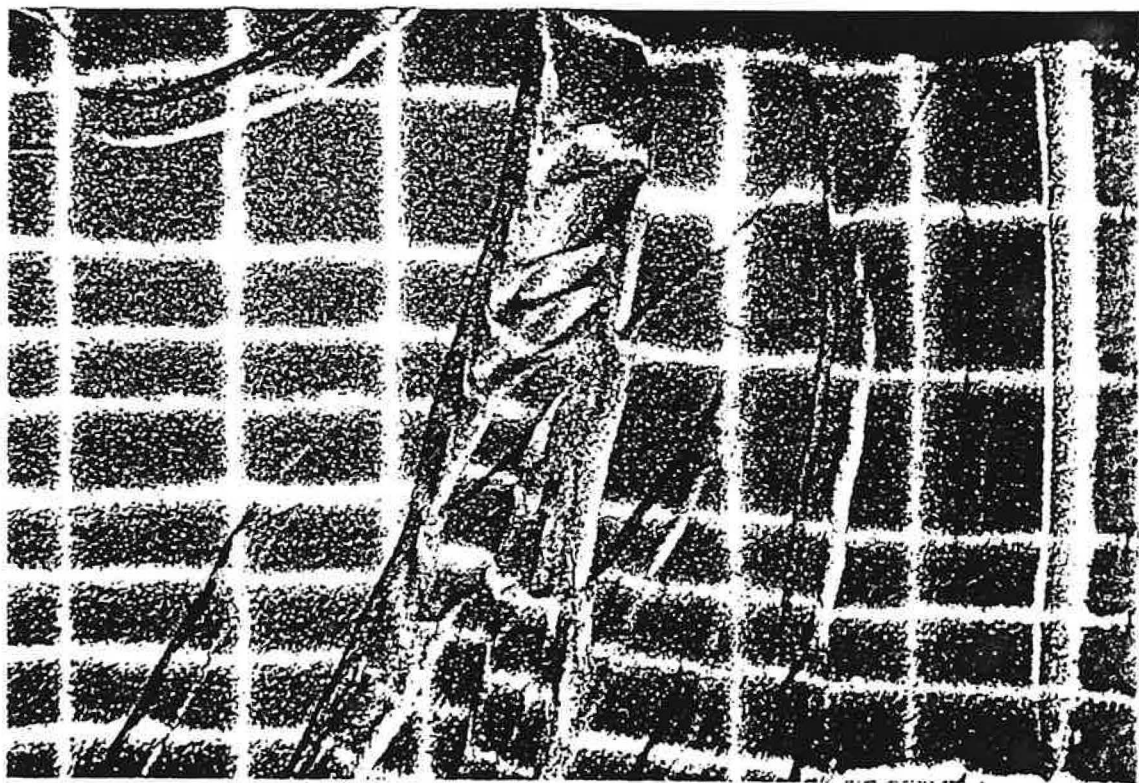


Fig. 12. Detail of a small scale analogue model of a strike-slip zone (Jolivet et al., 1991).

occurred between 16 and 14 Ma, but they also showed that volcanics in Shidara basin dated 16.9-14.5 Ma (K-Ar; Tsunakawa et al., 1983) did not suffer any rotation (Otofuji et al., 1985). Obviously, part of the incompatibility between the timing of paleomagnetic rotations and the opening of the Japan Sea is to be found in the error bars of radiometric data and in the way they are averaged.

Opening of the Japan Sea

A model of opening of the Japan Sea is depicted in Figure 13 after Jolivet et al. (1994). It relies on two major N-S dextral strike-slip zones between which the Japan Sea opened. In SW Japan the deformation is taken up by CW rotations of blocks, accommodated by left-lateral slip along the MTL. Jolivet et al. (1991) proposed reconstructions of the Japan Sea opening. They show that a CCW rotation of 30° of SW Japan about a pole in the Tsushima Strait completely close the Yamato basin and the western part of the Japan Sea. Jolivet et al. (1994) concluded that 30° of rigid rotation is a maximum and that the remaining 20° must be accommodated by the internal deformation of SW Japan.

The data described in this paper and those previously obtained in Sakhalin, Hokkaido, and NE Honshu now provide a set of informations significant at the scale of the Japan Sea and support the dextral pull-apart model. The model of block rotations at various scales agrees with the mechanics of a dextral pull-apart opening suggested by analogue experiments, and also with the sense and partly the timing of paleomagnetic rotations obtained independently.

This model can be integrated in a larger model of the deformation of Asia since the collision of India, as suggested in Jolivet et al. (1990) and shown in Figure 14 from Fournier et al. (in prep). Figure 14 shows an experiment of continental collision with boundary conditions roughly similar to that used in Jolivet et al. (1990) and Davy and Cobbold (1988). A detail of the NE corner of the experiment is shown to illustrate the distribution of dominoes at several scales. First order dominoes rotate CCW by about 15° in a first order left-lateral shear zone which trends NE-SW. This shear zone may be compared to the Pamir-Baikal-Stanovoy deformation zone in Asia, and the dominoes may be compared to continental blocks bounded by right-lateral systems, the en echelons grabens of North China, the Tan-Lu fault, and the Japan Sea strike-slip zone, and rotating between the Qinling Shan and the Stanovoy Ranges. Second order dominoes rotate CW with respect to first order ones inside dextral shear zones which trend N-S. The net CW rotation of the second order dominoes is about 10° in the experiment. SW Japan may be the equivalent of the second order dominoes.

This geometry shows that the complete set of dislocations and the geometry of blocks is needed to interpret paleomagnetic rotations without ambiguity. With such a geometry, the reference for Japanese paleomagnetic sites would be a first order domino system which itself suffered CCW rotations. No data have been so far published to substantiate this hypothesis.

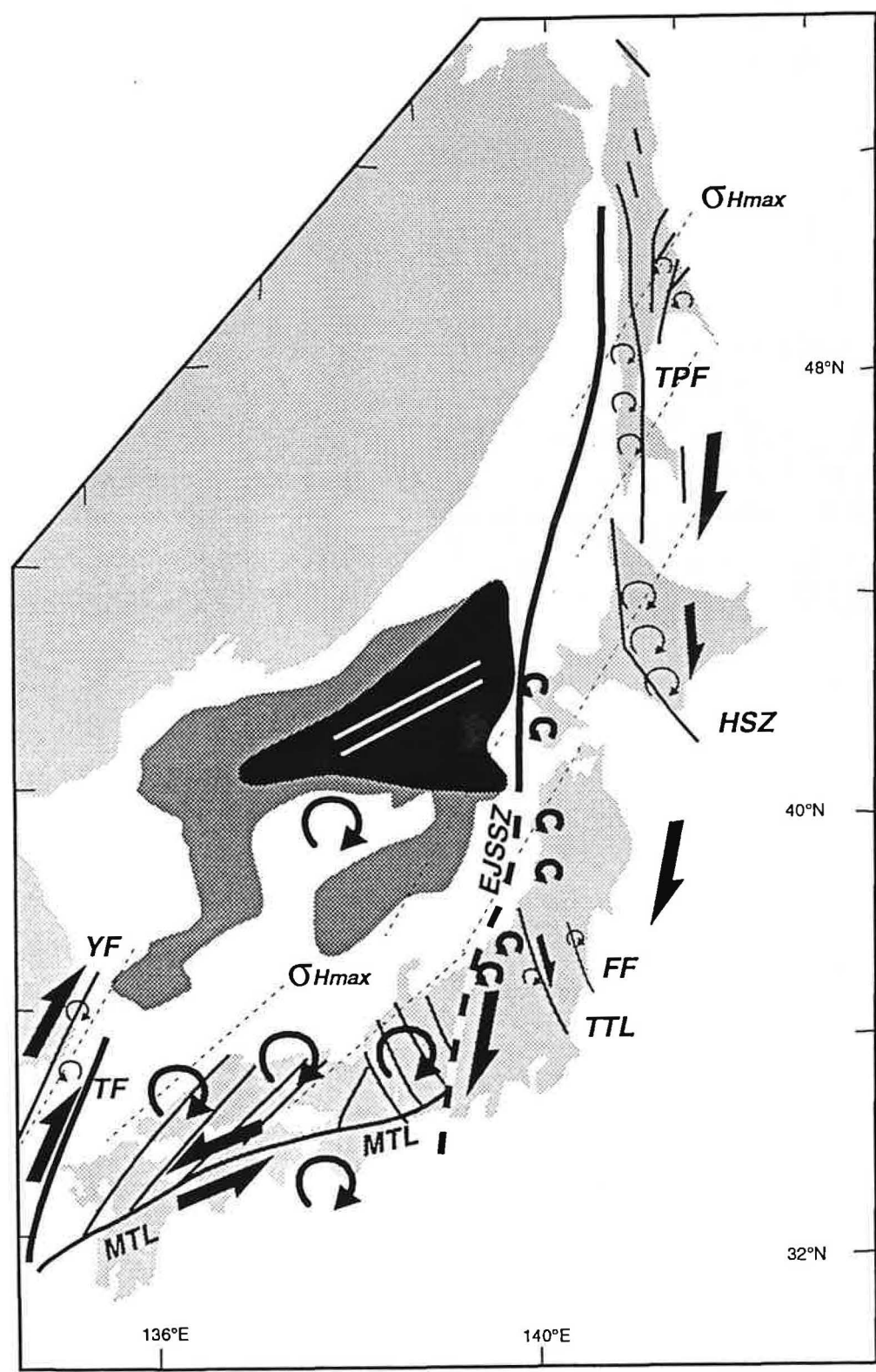


Fig. 13. Model of opening of the Japan Sea (Jolivet et al., 1994). EJSSZ is east Japan Sea shear zone, FF is Futaba fault, HSZ is Hokkaido shear zone, TF is Tsushima fault, TPF is Tym-Poronaysk fault, TTL is Tanakura Tectonic Line, YF is Yangsan fault.

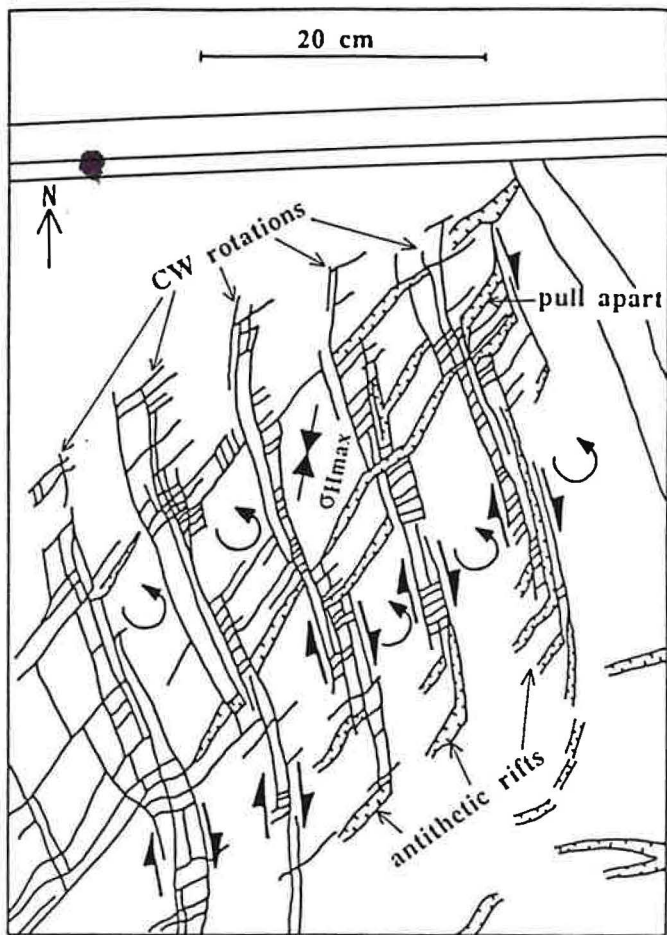
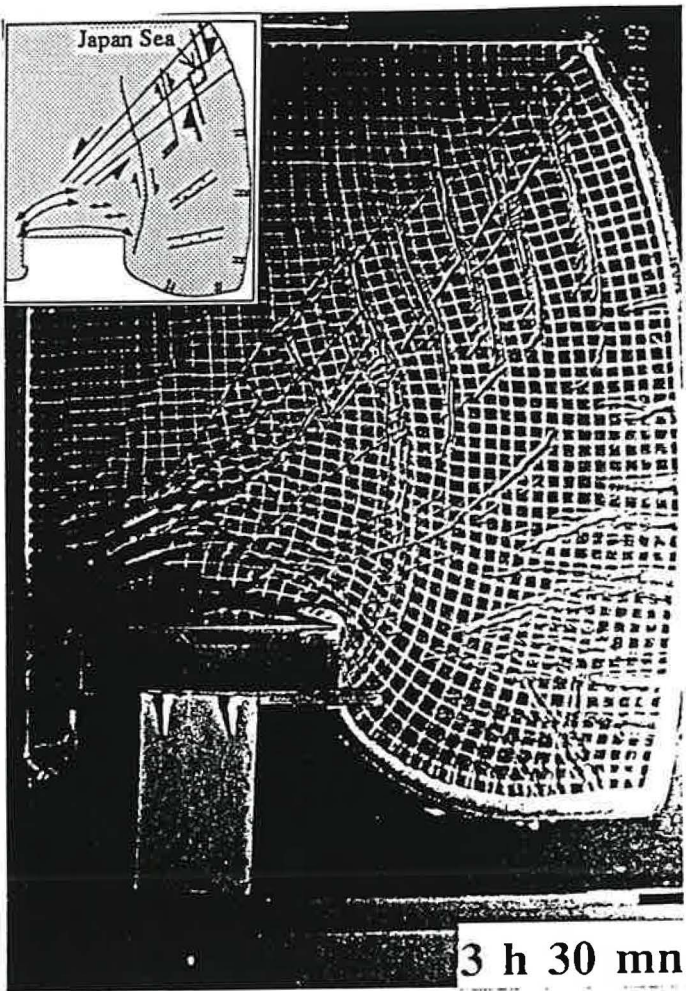


Fig. 14. Analogue model of continental deformation.

How much of this CCW rotation is included in the NE Honshu paleomagnetic data which suggest a CCW rotation between 22 and 15 Ma (Figure 1) (Tosha and Hamano, 1988) is a question worth studying.

Acknowledgements. This work was completed while the first author was in the Ocean Research Institute of the University of Tokyo. We wish to thank K. Kobayashi and K. Tamaki for their help in Japan. We also thank P. Agard and Moe Kyaw Thu for help and discussion during field work.

References

- Abe, K., Seismic displacement and ground motion near a fault: the Saitama earthquake of September 21, 1931, *J. Geophys. Res.*, 79, 4393-4399, 1974.
- Angelier, J., Tectonic analysis of fault slip data sets, *J. Geophys. Res.*, 89, 5835-5848, 1984.
- Arai and Kanno, Tertiary system of the Chichibu basin, Japan, The Japan Society for the Promotion of Science, Tokyo, pp. 396, 1960.
- Blow, W. H., Late Middle Miocene to Recent planktonic foraminiferal biostratigraphy, in Proc. 1st Int. Conf. Planktonic Microfossils, E.J. Brill, Leiden, edited by P. Bronnimann and H. H. Renz, 1, pp. 199-422, 1969.
- Charvet, J., K. Grimm, J. Griffin, L. Jolivet, A. Pouclet, and D. Panis, Structural features in Leg 128 cores: relationship with the tectonic evolution of the Japan Sea, *Proc. Ocean Drill. Program, Sci. Results*, 127/128, 1175-1193, 1992.
- Davy, P., and P. R. Cobbold, Indentation tectonics in nature and experiment. 1. Experiments scaled for gravity, *Bull. Geol. Inst. Univ. Uppsala*, 14, 129-141, 1988.
- Delaney, P. T., D. D. Pollard, J. I. Ziony, and E. H. McKee, Field relations between dikes and joints: emplacement process and paleostress analysis, *J. Geophys. Res.*, 91, 4920-4938, 1986.
- Fournier, M., L. Jolivet, P. Huchon, K. F. Sergeyev and L. S. Oscorbin, Neogene strike-slip faulting in Sakhalin and the Japan Sea opening, *J. Geophys. Res.*, in press.
- Harland, W. B., R. L. Armstrong, A. V. Cox, L. E. Craig, A. G. Smith, and D. G. Smith, A Geologic time scale 1989, Cambridge Univ. Press, pp. 1-263, 1990.
- Hayashi, T., and S. Koshimizu, Fission-track ages of the Shidara Group in the northeast part of the Aichi prefecture and the Eocene molluscs from its lowermost Nagashino formation, *J. Geol. Soc. Jpn.*, 98, 901-904, 1992.
- Hayashida, A., and I. Y. Ito, Paleoposition of southwest Japan at 16 Ma: implication from magnetism of the Miocene Ichishi group, *Earth and Planet. Sci. Lett.*, 68, 335-342, 1984.
- Hayashida, A., Timing of rotational motion of southwest Japan inferred from paleomagnetism of the Setouchi Miocene series, *J. Geomag. Geoelectr.*, 38, 295-310, 1986.
- Hayashida, A., T. Fukui, and M. Torii, Paleomagnetism of the Early Miocene Kani group in southwest Japan and its implication for the opening of the Japan Sea, *Geophys. Res. Lett.*, 18, 1095-1098, 1991.
- Hirooka, K., H. Sakai, T. Takahashi, H. Kinoto, and A. Takeuchi, Tertiary tectonic movement of central Japan inferred from paleomagnetic studies, *J. Geomagn. Geoelectr.*, 38, 311-323, 1986.
- Huchon, P., and H. Kitazato, Collision of the Izu block with central Japan during the Quaternary and geological evolution of the Ishigara area, *Tectonophysics*, 110, 201-210, 1984.

- Hwang, J.-H., L'évolution tectonique post-jurassique de la Corée: apport des reconstitutions de paléocontraintes dans les bassins crétacés méridionaux, Thèse Univ. Paris 6, pp. 301, 1992.
- Hyodo, H., and N. Niitsuma, Tectonic rotation of the Kanto mountains, related with the opening of the Japan Sea and collision of the Tanzawa block since Middle Miocene, *J. Geomag. Geoelectr.*, 38, 335-348, 1986.
- Ichikawa, K., Geohistory of the Median Tectonic Line of southwest Japan, *Mem. Geol. Soc. Jpn.*, 18, 187-210, 1980.
- Ishikawa, N., M. Torii, and K. Koga, Paleomagnetic study of the Tsushima islands, southern margin of the Japan Sea, *J. Geomag. Goelectr.*, 41, 797-811, 1989.
- Ishikawa, N., and T. Tagami, Paleomagnetism and fission-track geochronology on the Goto and Tsushima islands in the Tsushima Strait area: implications for the opening mode of the Japan Sea, *J. Geomag. Geoelectr.*, 43, 229-253, 1991.
- Irizuki, T., M. Takahashi, Y. Tanaka, and M. Oda, Geology and age of the Neogene sedimentary rocks in the Itsukaichi basin, central Japan, *Jour. Geol. Jpn. Soc.*, 9, 759-770, 1990.
- Ishii, H., T. Sato, K. Tachibana, K. Hashimoto, E. Murakami, M. Mishina, S. Miura, K. Sato, A. Takagi, Crustal strain, crustal stress and microearthquake activity in the northeastern Japan arc, *Tectonophysics*, 97, 217-230, 1983.
- Ito, M., The Itsukaichimachi Group: a Middle Miocene strike-slip basin fill in the southeastern margin of the Kanto mountains, central Honshu, Japan, in *Sedimentary Facies in the Active Plate Margin*, ed. A. Taira and F. Masuda, Terrapub, Tokyo, 659-673, 1989.
- Itoh, Y., Differential rotation of the eastern part of Southwest Japan inferred from paleomagnetism of Cretaceous and Neogene rocks, *J. Geophys. Res.*, 93, 3401-3411, 1988.
- Jolivet, L., P. Davy, and P. Cobbold, Right-lateral shear along the northwest Pacific margin and the India-Eurasia collision, *Tectonics*, 9, 1409-1419, 1990.
- Jolivet, L., and P. Huchon, Crustal scale strike-slip deformation in Hokkaido, Northeast Japan, *J. Struct. Geol.*, 11, 509-522, 1989.
- Jolivet, L., P. Huchon, J.P. Brun, N. Chamot-Rooke, X. Le Pichon, and J.C. Thomas, Arc deformation and marginal basin opening, Japan Sea as a case study, *J. Geophys. Res.*, 96, 4367-4384, 1991.
- Jolivet, L., M. Fournier, P. Huchon, V. S. Rozhdestvensky, K. F. Sergeyev, and L. Oscorbin, Cenozoic intracontinental dextral motion in the Okhotsk-Japan Sea region, *Tectonics*, 11, 968-977, 1992.
- Jolivet, L., and K. Tamaki, Neogene kinematics in the Japan Sea region and volcanic activity of the northeast Japan arc, *Proc. ODP, Sci. Results*, 127/128, 1992.
- Jolivet, L., H. Shibuya, and M. Fournier, Paleomagnetic rotations and the Japan Sea opening, submitted to AGU Monograph, 1994.

- Kanaori, Y., Late Mesozoic-Cenozoic strike-slip and block rotation in the inner belt of southwest Japan, *Tectonophysics*, 177, 381-399, 1990.
- Kanaori, Y., S. Kawakami, and K. Yairi, The block structure and Quaternary strike-slip block rotation of central Japan, *Tectonics*, 11, 47-56, 1992.
- Kaneoka, I., K. Notsu, Y. Takigami, K. Fujioka, and H. Sakai, Constraints on the evolution of the Japan Sea based on 39Ar-40Ar ages and Sr isotopic ratios for volcanic rocks of the Yamato seamount chain in the Japan Sea, *Earth Planet. Sci. Lett.*, 97, 211-225, 1990.
- Kano, K., and F. Yoshida, Radiometric age of the Neogene in central eastern Shimane prefecture, Japan, and their implication in stratigraphic correlation, *Bull. Geol. Surv. Japan*, 35, 159-170, 1984.
- Kano, K., and S. Nakano, Stratigraphic correlation of the Neogene in the San'in district, southwest Japan, in the light of radiometric dating, *Bull. Geol. Surv. Japan*, 36, 427-438, 1985.
- Kano, K., H. Kato, Y. Yanagisawa, and F. Yoshida, Stratigraphy and geologic history of the Cenozoic of Japan, Report 274 Geol. Surv. Jpn., pp. 1-114, 1991.
- Kim, K. H., J. K. Won, J. I. Matsuda, K. Nagao, and W. L. Moon, Paleomagnetism and K-Ar age of volcanic rocks from Guryongpo area, Korea, *J. Korean Inst. Mining Geol.*, 19, 231-237, 1986.
- Kobayashi, Y., Late Neogene dike swarms and regional tectonic stress field in the inner belt of southwest Japan, *Bull. Volc. Soc. Jpn.*, 24, 153-168, 1979a.
- Kobayashi, Y., Early and Middle Miocene dike swarms and regional tectonic stress field in the southwest Japan, *Bull. Volc. Soc. Jpn.*, 24, 203-212, 1979b.
- Kodama, K., Magnetostratigraphy of the Izumi Group along the Median Tectonic Line in Shikoku and Awaji islands, southwest Japan, *J. Geol. Soc. Jpn.*, 96, 265-278, 1990.
- Kodama, K., and K. Nakayama, Paleomagnetic evidence for post-Late Miocene intra-arc rotation of south Kyushu, Japan, *Tectonics*, 12, 35-47, 1993.
- Kodama, K., T. Ozawa, K. Inoue, Y. Maeda, and T. Tohru, Paleomagnetism and post-Middle Miocene counter-clockwise rotation of Tanegashima island off Kyushu, Japan, *J. Geomag. Geoelectr.*, 43, 721-740, 1991.
- Kodama, K., T. Takeuchi, and T. Ozawa, Clockwise tectonic rotation of Tertiary sedimentary basins in central Hokkaido, northern Japan, *Geology*, 21, 431-434, 1993.
- Kogi, K., Geology and structure of the Shidara volcanic mass, Aichi prefecture, central Japan, *Jour. Geol. Soc. Jpn.*, 89, 487-500, 1983.
- Kuwahara, T., and T. Sato, Strike-slip fault system of post-Miocene age at the north-eastern margin of the Kanto mountains, central Japan, *Ann. Rep. Inst. Geosci. Univ. Tsukuba*, 7, 46-48, 1981.

- Kuwahara, T., Late Cretaceous to Pliocene fault systems and corresponding regional stress fields in the southern part of northeast Japan, *Sci. Rep. Inst. Geosci. Univ. Tsukuba*, 3, 49-111, 1982.
- Lallemand, S., and L. Jolivet, Japan Sea: A pull apart basin, *Earth Planet. Sci. Lett.*, 76, 375-389, 1985.
- Latt, K. M., Turbidites and related clastic systems in the Tertiary Chichibu basin, central Japan, in *Sedimentary Facies in the Active Plate Margin*, ed. A. Taira and F. Masuda, Terrapub, Tokyo, 421-438, 1989.
- Luyendyk, B. P., M. J. Kamerling, R. R. Terres, and J. S. Hornafius, Simple shear of southern California during Neogene time suggested by paleomagnetic rotations, *J. Geophys. Res.*, 90, 12,454-12,466, 1985.
- Matsumaru, K., and A. Hayashi, Neogene stratigraphy of the eastern marginal areas of Kanto mountains, central Japan, *J. Geol. Soc. Jpn.*, 86, 225-242, 1980.
- Mikumo, T., H. Wada, and M. Koizumi, Seismotectonics of the Hida region, central Honshu, Japan, *Tectonophysics*, 147, 95-119, 1988.
- Miyata, T., H., Ui, and K. Ichikawa, Paleogene left-lateral wrenching on the Median Tectonic Line in southwest Japan, *Mem. Geol. Soc. Jpn.*, 18, 51-68, 1980.
- Nakamura, K., and S. Uyeda, Stress gradient in back arc regions and plate subduction, *J. Geophys. Res.*, 85, 6419-6428, 1980.
- Niitsuma, N., and T. Matsuda, Collision in the south Fossa Magna area, central Japan, *Rec. Progress. Natural Sci. Jpn.*, 10, 41-50, 1985.
- Okada, A., Quaternary faulting along the Median Tectonic Line of southwest Japan, *Mem. Geol. Soc. Jpn.*, 18, 79-108, 1980.
- Okada, A., Proposal of segmentation on the Median Tectonic Line active fault system, *Mem. Geol. Soc. Jpn.*, 40, 15-30, 1992.
- Otofuji, Y., and T. Matsuda, Paleomagnetic evidence for the clockwise rotation of Southwest Japan, *Earth Planet. Sci. Lett.*, 62, 349-359, 1983.
- Otofuji, Y., and T. Matsuda, Timing of rotational motion of Southwest Japan inferred from paleomagnetism, *Earth Planet. Sci. Lett.*, 70, 373-382, 1984.
- Otofuji, Y., A. Hayashida, and M. Torii, When was the Japan Sea opened: paleomagnetic evidence from southwest Japan, in *Formation of active ocean margin*, edited by N. Nasu, S. Uyeda, I. Kushiro, K. Kobayashi, and H. Hagami, 551-556, TERRAPUB, Tokyo, 1985.
- Otofuji, Y., T. Matsuda, and S. Nohda, Paleomagnetic evidence for the Miocene counter-clockwise rotation of Northeast Japan - rifting process of the Japan arc, *Earth Planet. Sci. Lett.*, 75, 265-277, 1985.
- Otofuji, Y., and T. Matsuda, Amount of clockwise rotation of Southwest Japan - fan shape opening of the southwestern part of the Japan Sea, *Earth Planet. Sci. Lett.*, 85, 289-301, 1987.

- Otofuji, Y., T. Itaya, and T. Matsuda, Rapid rotation of southwest Japan - paleomagnetism and K-Ar ages of Miocene volcanic rocks of southwest Japan, *Geophys. J. Int.*, 105, 397-405, 1991.
- Otsuki, K., Neogene tectonic stress fields of northeast Honshu Arc and implications for plate boundary conditions, *Tectonophysics*, 181, 151-164, 1990.
- Ron, H., R. Freund, Z. Garfunkel, and A. Nur, Block rotation by strike-slip faulting: structural and paleomagnetic evidence, *J. Geophys. Res.*, 89, 6256-6270, 1984.
- Saito, T., and S. Maiya, Planktonic Foraminifera of the Nishikurosawa formation, northeast Honshu, Japan, *Trans. Proc. Paleont. Soc. Japan*, 91, 113-125, 1973.
- Sasajima, S., Pre-Neogene paleomagnetism of Japanese island (and vicinities), in *Paleoreconstruction of the Continents*, ed. by M. W. Mc Elhinny and D. A. Valancio, *Geodyn. Series* vol. 2, 1981.
- Sato, T., Fault system in the Kanto Mountains, *Ann. Rep. Inst. geosci. Univ. Tsukuba*, 12, 72-75, 1986.
- Shibata, K., and T. Nozawa, K-Ar ages of granitic rocks from the outer zone of southwest Japan, *Geochem. Jour.*, 1, 131-137, 1967.
- Shibata, K., H. Sato, and M. Nakagawa, K-Ar ages of Neogene volcanic rocks from Noto peninsula, *J. Assoc. Miner. Petrol. Econ. Geol.*, 76, 248-252, 1981.
- Taira, A., H. Tokuyama, and W. Soh, Accretion tectonics and evolution of Japan, in ZviBen-Averaham (ed.), *The Evolution of the Pacific Ocean Margins*, Oxford Univ. Press, NY, Oxford, 100-123, 1989.
- Takada, A., Structure of a cauldron in the Otoge ring complex, Shitara district, Aichi prefecture, central Japan, *J. Geol. Soc. Jpn.*, 93, 107-120, 1987a.
- Takada, A., Development of the Shitara igneous complex, central Japan, and the structure of its cauldrons, *J. Geol. Soc. Jpn.*, 93, 167-184, 1987b.
- Takagi, H., T. Takashita, K. Shibata, S. Uchiumi, and M. Inoue, Middle Miocene normal faulting along the Tobe thrust in western Shikoku, *J. Geol. Soc. Jpn.*, 98, 1069-1072, 1992.
- Takahashi, J., On the Median Tectonic Line in Matsuyama city and the neighbouring areas, Ehime prefecture, Japan, *Mem. Fac. Educ. Ehime Pref.*, Ser. 3, 6, 1-44, 1986.
- Takahashi, J., Faulting history of the Median Tectonic Line in Ehime prefecture, *Mem. Geol. Soc. Jpn.*, 40, 99-112, 1992.
- Takahashi, M., and S. Nomura, Paleomagnetism of the Chichibu quartz diorite - constraints on the time of lateral bending of the Kanto syntaxis, *J. Geomag. Geoelectr.*, 41, 479-489, 1989.
- Takeshita, T., Deformation microstructures in dominantly white-colored rocks distributed along the Tobe thrust of the Median Tectonic Line and their implication, *J. Geol. Soc. Jpn.*, 97, 175-178, 1991.

- Takeuchi, A., Temporal changes of regional stress field and tectonics of sedimentary basin, *J. Geol. Soc. Jpn.*, 87, 737-751, 1981.
- Tamaki, K., K. Suyehiro, J. Allan, M. McWilliams, et al., Tectonic synthesis and implication of Japan Sea ODP drilling, *Proc. Ocean Drill. Program, Sci. Results*, 127/128, 1333-1348, 1992.
- Tanaka, T., and K. Ogusa, Structural movement since Middle Miocene in the off-shore San'in sedimentary basin, the Sea of Japan, *J. geol. Soc. Jpn.*, 87, 725-736, 1981.
- Tatsumi, Y., M. Torii, and K. Ishizaka, On the age of the volcanic activity and the distribution of the Setouchi volcanics rocks, *Bull. Volcanol.* *Soc. Jpn.*, 25, 171-179, 1980.
- Tazaki, K., J. Takahashi, T. Itaya, R. H. Grapes, and N. Kashima, K-Ar ages of the andesites intruding along the Median Tectonic Line in northwestern Shikoku, Japan, *J. Assoc. Miner. Petrol. Econ. Geol.*, 85, 155-160, 1990.
- Tohara, T., Petrological study on Tertiary volcanic rocks and ultramafic inclusions from Matsuyama area, northwestern Shikoku, Master Thesis, Kanazawa Univ., Japan, 1978.
- Torii, M., Paleomagnetism of Miocene rocks in the Setouchi province: evidence for rapid clockwise rotation of southwest Japan in middle Miocene time, Ph. D. Thesis, Kyoto Univ., 1983.
- Tosha, T., and Y. Hamano, Paleomagnetism of Tertiary rocks from the Oga Peninsula and the rotation of northeast Japan, *Tectonics*, 7, 653-662, 1988.
- Tsukahara, H., and R. Ikeda, Crustal stress orientation pattern in the central part of Honshu, Japan, stress provinces and their origins, *Jour. Geol. Soc. Jpn.*, 97, 461-474, 1991.
- Tsukahara H., and Y. Kobayashi, Crustal stress in central and western parts of Honshu, Japan, *J. Seism. Soc. Jpn.*, 44, 221-231, 1991.
- Tsunakawa, H., A. Takeuchi, and K. Amano, K-Ar ages of dikes in southwest Japan, *Geochemical J.*, 17, 265-268, 1983a.
- Tsunakawa, H., A. Takeuchi, and K. Amano, K-Ar ages of dikes in northeast Japan, *Geochemical J.*, 17, 269-275, 1983b.
- Tsunakawa, H., Neogene stress field of the Japanese arc and its relation to igneous activity, *Tectonophysics*, 124, 1-22, 1986.
- Ui, H., Geological structure along the Median Tectonic Line, east of Mikawa-Ono, central Japan, *Mem. Geol. Soc. Jpn.*, 18, 69-78, 1980.
- Yamagishi, H. and Y. Watanabe, Change of stress field in Late Cenozoic, Southwest Hokkaido, Japan, - investigation of geologic faults, dykes, ore veins and active faults, *Monograph Geol. Collabor. Jpn.*, 31, 321-332, 1986.
- Yamamoto, H., Submarine geology and post-opening tectonic movements in the southern region of the Sea of Japan, *Mar. Geol.*, 112, 133-150, 1993.

- Yamamoto, T., and H. Hoshizumi, Stratigraphy of the Neogene system in the Tango peninsula, eastern part of the San-in district, southwest Japan, and associated Middle Miocene volcanism, *Jour. Geol. Soc. Jpn.*, 94, 769-781, 1988.
- Yamamoto, T., Late Cenozoic dike swarms and tectonic stress field in Japan, *Bull. Geol. Surv. Japan*, 42, 131-148, 1991.
- Yamazaki, T., Paleomagnetism of Miocene sedimentary rocks around Matsushima bay, northeast Japan, and its implication for the time of the rotation of northeast Japan, *J. Geomag. Geoelectr.*, 41, 533-548, 1989.
- Yoshida, T., Tertiary Ishizuchi cauldron, southwestern Japan arc: formation by ring fracture subsidence, *J. Geophys. Res.*, 89, 8,502-8,510, 1984.

Table 1. Stress Tensors Plotted in Figure 10.

Site	σ_1	σ_2	σ_3	ϕ	Formation	Age (Ma)
<i>Ishizuchi</i>						
1	328-75	077-05	168-14	0.365	Tobe thrust	14.7
2A	273-66	082-24	174-04	0.560	Ishizuchi	14
2B	158-72	051-06	319-17	0.327	Ishizuchi	14
3	260-71	057-17	149-07	0.212	Kuma	Eoc. - Middle Mioc.
4					Ishizuchi	14
5	268-65	066-24	160-08	0.670	Ishizuchi	
<i>Shidara</i>						
2A	324-74	142-16	233-01	0.610	cataclasites	Cretaceous
2B	221-78	058-12	327-03	0.532	cataclasites	Cretaceous
3A	002-27	153-60	265-13	0.448	cataclasites	Cretaceous
5	349-35	145-52	250-12	0.749	cataclasites	Cretaceous
7	001-67	162-22	254-07	0.569	Hokusetsu	Oligo. - Early Mioc.
8	094-78	336-06	245-10	0.641	Ryoke	
9	014-67	200-23	109-02	0.389	Hokusetsu	
10	245-73	052-17	143-04	0.402	Hokusetsu	
13A	018-64	159-21	255-15	0.931	Hokusetsu	
13B	305-77	109-13	200-04	0.502	Hokusetsu	Oligo. - Early Mioc.
14	138-46	323-43	231-03	0.676	Hokusetsu	Oligo. - Early Mioc.
15B	304-76	112-13	203-03	0.733	Hokusetsu	Oligo. - Early Mioc.
<i>Chichibu</i>						
2A	179-67	036-18	301-13	0.511	Nagara	Early Mioc.
2B	190-78	043-10	312-06	0.689	Nagara	Early Mioc.
3A	217-09	041-81	307-01	0.415	Sakurai	Early Mioc.
3B	210-07	329-75	118-13	0.226	Sakurai	Early Mioc.
4	202-86	046-03	316-02	0.839	Nagara	Early Mioc.
5	073-29	236-60	339-08	0.509	Yoshida	Early Mioc.
6	101-84	217-03	307-06	0.456	Yoshida	Early Mioc.
7	207-03	063-87	297-02	0.365	Sakurai	Early Mioc.
<i>Itsukaichi</i>						
1A	252-10	031-76	160-09	0.501	Yosokawa	Early - Middle Mioc.
1B	033-15	225-75	124-03	0.403	Yosokawa	Early - Middle Mioc.
2	171-21	312-64	075-15	0.286	Yosokawa	Early - Middle Mioc.
<i>Shimane</i>						
1					Hata	15-19
4					Kuri-Kawai	14-18
5A	044-75	216-15	306-02	0.853	Kuri-Kawai	14-18
7	355-11	140-76	263-08	0.424	Kuri-Kawai?	14-18
8A	340-86	214-02	124-03	0.571	Kuri-Kawai	14-18
8B	008-03	144-86	278-03	0.575	Kuri-Kawai	14-18
9	211-14	096-59	308-27	0.166	Omori	13-16
13	189-09	090-42	289-46	0.378	Kuri-Kawai	14-18
14A	205-64	359-23	093-10	0.645	Kuri-Kawai	14-18
14B	309-07	113-83	218-02	0.202	Kuri-Kawai	14-18
15	151-08	061-01	322-82	0.133	Kuri-Kawai	14-18
16	002-18	166-72	270-05	0.418	Kuri-Kawai	14-18
<i>Tango</i>						
1	037-10	226-71	307-01	0.499	Tango	Middle Mioc.
2	042-83	234-07	144-02	0.783	Toyooka	Early Mioc.
3	220-62	029-27	122-04	0.956	Toyooka	Early Mioc.
4	320-74	209-06	117-15	0.940	Tango	Middle Mioc.
5	019-21	184-68	287-05	0.524	Toyooka	
6	228-76	074-13	343-06	0.559	Toyooka	
7	119-23	303-67	210-01	0.277	Yoka	
8	055-79	219-11	310-03	0.698	Toyooka	
10B	013-72	256-08	164-16	0.870	Yoka	Early Mioc.
12	015-06	124-73	284-16	0.854	Yoka	Early Mioc.
13	354-20	190-69	086-05	0.582	Yoka	Early Mioc.
14	151-71	030-10	298-17	0.728	Yoka	Early Mioc.
16	359-72	209-16	117-08	0.543	Tango	Middle Mioc.

17	067-25	252-65	158-02	0,799	Toyooka	Early Mioc.
<i>Noto</i>						
2	342-63	208-19	112-18	0.480	Anamizu	Early Miocene
3	036-06	141-69	304-20	0.188	Anamizu	Early Miocene
5A	159-06	250-10	040-78	0.433	Anamizu	Early Miocene
5B	007-19	156-68	273-11	0.192	Anamizu	Early Miocene
6	039-72	211-18	302-03	0.607	Anamizu	Early Miocene
7	207-02	298-34	114-56	0.114		Middle Miocene
10	022-65	180-23	274-08	0.342	Anamizu	Early Miocene
15	075-38	255-52	165-00	0.597		Middle Miocene
18	206-05	114-23	309-66	0.160	Anamizu	Early Miocene
<i>Yatsuo</i>						
1	206-05	106-63	298-26	0.297	Nirehara	Early Miocene
2	155-76	056-02	325-14	0.846	Iwaine	Early-Middle Mioc.
4	217-24	053-65	310-06	0.701	Iwaina	Early-Middle Mioc.
6	167-71	071-02	340-19	0.290	Kurosedani	Middle Mioc.
<i>Sakhaline</i>						
TPF1	179-40	332-47	077-14	0.712	Bikov	Late Cretaceous
TPF3	252-09	360-62	158-26	0.551	Krasnoyarkov	Late Cretaceous
TPF5	268-39	102-50	004-07	0.657	Bikov	Late Cretaceous
TPF7	086-17	277-72	177-03	0.549	Bikov	Late Cretaceous
TPF8	230-15	139-04	036-75	0.078	Tchekhov	Middle Miocene
TPF9	078-19	346-07	237-69	0.212	Gastello	Early Miocene
TPF10	028-43	175-41	281-17	0.247	Kholmsk	Early Miocene
TPF12	251-04	157-44	345-46	0.231	Tchekov	Middle Miocene
Tonino1	055-12	324-03	222-78	0.492	Naiba	Cretaceous
Tonino2	034-03	123-01	237-86	0.342	Bikov	Late Cretaceous
Tonino3.1	191-01	329-78	281-06	0.738		Cretaceous
Tonino3.2	264-12	093-77	359-23	0.342		Cretaceous
Tonino4.1	316-16	056-10	172-70	0.592		Cretaceous
Tonino4.2	047-03	238-86	137-01	0.986		Cretaceous
Tonino5.1	200-12	313-62	104-24	0.282		Cretaceous
Tonino5.1	097-15	003-15	228-68	0.624		Cretaceous
Tonino6	173-46	034-36	287-21	0.713	Bikov	Late Cretaceous
WSak1	084-30	296-55	182-15	0.806	Kurasy	Late Miocene
ESak1	028-09	140-68	295-20	0.016		Jurassic

Table 2. Mean Trend of Dike Swarms Plotted in Figure 10.

No.	Locality	$\sigma_{H\max}$	Ref.	Age (Ma)	Ref.
1	Shidara	N000-020E	1	14.9-16.5	5
2	Tango	N-S	2	14.1-15.5	5
3	Myoken	N150E	2	13.9-14.6	5
4	Kumano	N170E	1	14	6
5	Shionomisaki	N135E	3	14	6
6	Ishizuchi (Shikoku)	E-W	3	14	6
7	Takaiwa (Shikoku)	N080E	3	14	6
8	Ashizuri (Shikoku)	N-S	1	12.0-14.0	1
9	Kakudasan (Niigata)	N080E	4	11.5-13.6	7
10	Sado Ogi	N005W	4	12	7

References: 1-Tsunakawa (1986), 2-Kobayashi (1979a), 3-Kobayashi (1979b), 4-Takeuchi (1981), 5-Tsunakawa et al. (1983a), 6-Shibata and Nozawa (1967), 7-Tsunakawa (1983b).

V. COMPATIBILITÉ DES DONNÉES PALÉOMAGNÉTIQUES ET STRUCTURALES :
article "*Paleomagnetic rotations and the Japan sea opening*"

(accepté à AGU Monograph, Active Margins and Marginal Basins, A Synthesis of Western Pacific Drilling Results)

Résumé : Cet article discute des deux problèmes liés aux rotations paléomagnétiques pendant l'ouverture de la mer du Japon : le calage en temps des rotations, et la distribution de la déformation et des rotations.

Une synthèse critique de l'ensemble des données paléomagnétiques sur le Japon est d'abord proposée. La rotation du Japon sud-ouest est une rotation rapide entre 16 et 14 Ma (Otofuji et al., 1991 ; Hayashida et al., 1991), et la rotation du Japon nord-est est une rotation lente entre 22 et 15 Ma (Otofuji et al., 1985 ; Toshia et Hamano, 1988 ; Tanaka et al., 1991), antérieure à la rotation du Japon sud-ouest selon Yamazaki (1989). Pour Otofuji et al. (1994) cependant, la plus grande part de la rotation du Japon nord-est (30°) a lieu entre 16 et 14 Ma, comme dans le Japon sud-ouest. La quantité de rotation horaire moyenne dans le Japon sud-ouest depuis le Miocène inférieur varie entre $38,5^\circ$ (Otofuji et al., 1991) et 50° environ (Hayashida et al., 1991) dans la partie ouest, et entre 13° (Itoh, 1988) et 0° (Hirooka et al., 1986) dans la partie est. La quantité de rotation anti-horaire moyenne dans le Japon nord-est depuis le Miocène inférieur varie entre 20° (Toshia et Hamano, 1988) et 45° (Otofuji et al., 1985 ; 1994), la variabilité étant assez grande pour les roches plus vieilles que 17 Ma, 1° à 91° E selon Otofuji et al. (1994).

Les calculs d'âges moyens de formations géologiques sont critiqués. Ces calculs sont réalisés en moyennant des âges radiométriques dispersés dont les barres d'erreur analytique sont faibles. La prise en compte d'âges douteux dans ces calculs est mise en cause. En ce qui concerne l'étude d'Otofuji et al. (1991), les âges les plus jeunes dans les formations ayant subi une rotation ($13,7 \pm 0,3$ Ma) sont nettement plus récents que les âges les plus vieux dans les formations n'ayant pas subi de rotation ($16,2 \pm 1,4$ Ma). Si l'on prend en compte comme Otofuji et al. (1991) ces âges extrêmes dans les calculs d'âges moyens de formations, la durée des rotations est minimisée (entre 16.1 et 14.2 Ma). Si on ne retient pour faire le calcul de l'âge moyen de la formation qui a subi la rotation uniquement les âges de cette formation plus anciens que ceux de la formation qui n'a pas subi la rotation, et inversement, on double la durée des rotations entre 17,1 et 13,0 Ma. Nous pensons que la rapidité des rotations paléomagnétiques est surestimée par les méthodes employées pour déterminer les âges moyens des formations. Ces rotations peuvent s'intégrer sur une plus longue durée dans le processus d'ouverture de la mer du Japon.

Le sens des rotations paléomagnétiques depuis le Miocène inférieur dans les principales zones de déformation à l'est et à l'ouest de la mer du Japon est passé en revue. Les rotations sont systématiquement horaires et compatibles avec les mouvements dextres Miocène dans

les zones de déformation (le long de la Tanakura Tectonic Line (TTL) dans le NE Honshu (Otofuji et al., 1985), dans la partie centrale d'Hokkaido (Kodama et al., 1993), à Sakhaline (Takeuchi et al., 1992), le long de la faille de Yangsan en Corée (Kim et al., 1986)), excepté dans le détroit de Tsushima où les principaux accidents ont rejoué en sénestre au Miocène supérieur et au Pliocène.

A partir d'observations de terrain on montre que le Japon sud-ouest se déforme pendant l'ouverture, et qu'un mécanisme de déformation avec des rotations de blocs à toutes échelles contemporain des rotations paléomagnétiques est envisageable.

Cette synthèse aboutit à un modèle d'ouverture en pull-apart incluant les rotations, et à des reconstructions cinématiques de l'ouverture. Selon ces reconstructions, 30° de rotation rigide sont envisageables pour le Japon sud-ouest, le complément de rotation devant être trouvé localement dans la déformation interne de l'arc.

PALEOMAGNETIC ROTATIONS AND THE JAPAN SEA OPENING

Laurent JOLIVET

Laboratoire de Géologie, Ecole Normale Supérieure
24 rue Lhomond, 75231 Paris cedex 05

Hidetoshi SHIBUYA

Dept. Earth Sciences
University of Osaka Prefecture
Sakai 593, Japon

Marc FOURNIER

Ocean Research Institute
University of Tokyo

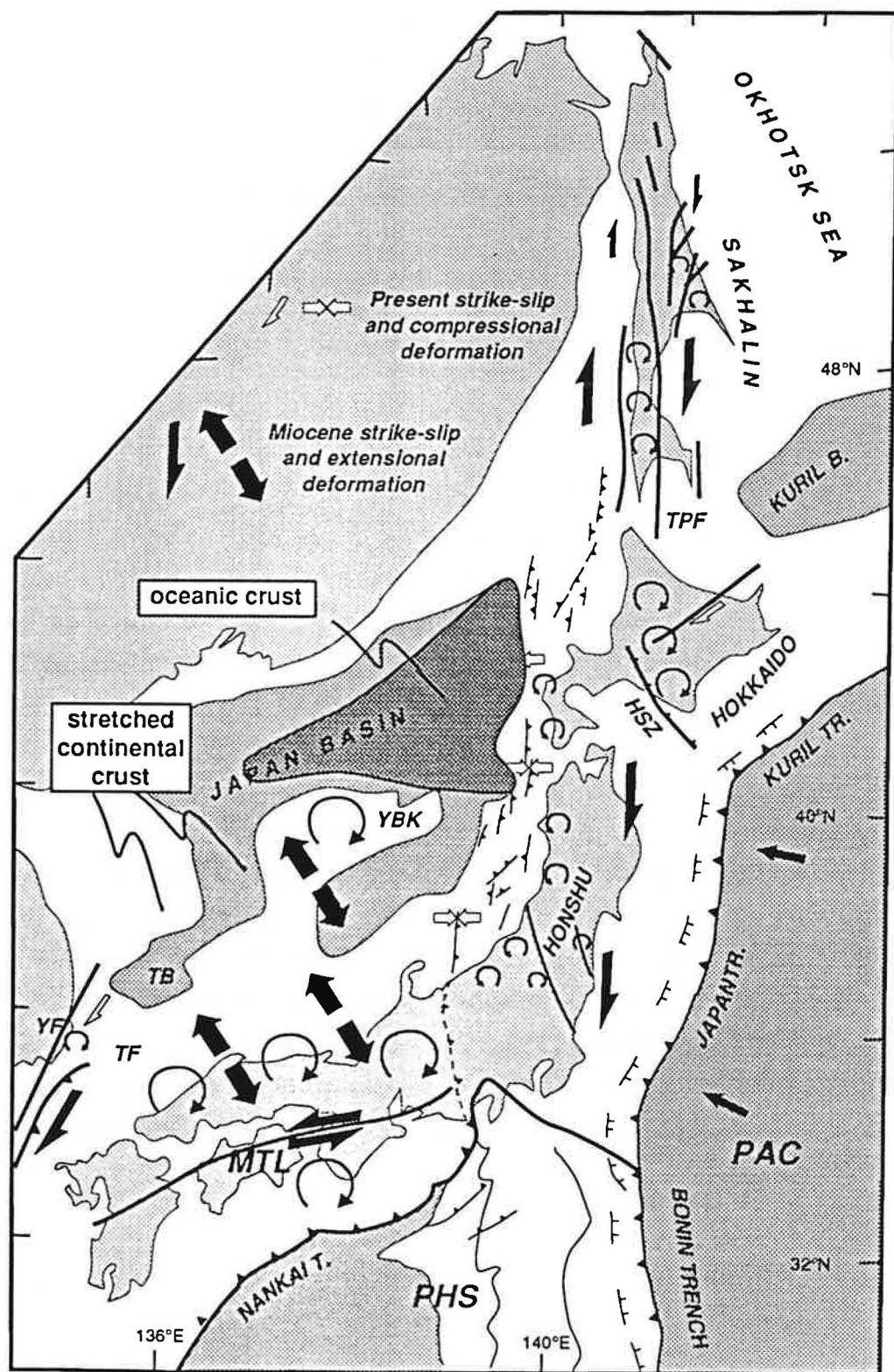
1-15-1 Minami Dai, Nakano Ku, Tokyo 164, Japon
&

Laboratoire de Géologie, Ecole Normale Supérieure
24 rue Lhomond, 75231 Paris cedex 05

Abstract:

The apparent incompatibility of the classical "bar door" opening model of the Japan Sea based on paleomagnetic studies and the pull-apart geometry based on the observation of shear zones in and around Japan is symptomatic of a lack of understanding of the tectonic history of the Japan Sea. After a critical review of paleomagnetic data and a discussion on the possible error bars we present informations concerning the internal strain of the Japan arc during the opening. We show that it is possible to integrate both sets of data in a single model provided that some of the paleomagnetic rotations are due to distributed deformation of SW and NE Japan and not to a rigid body rotation of 600 km long blocks. Rotations occur at all scales and the 50° of CW rotation of SW Japan is the sum of 30° of rotation of SW Japan as a whole and of 20° due to internal deformation. The amount of paleomagnetic rotations are then compatible with the kinematics based on the internal structure of the Japan Sea and the geometry of major dextral shear zones. The rigid body rotation of SW Japan is accommodated by the left-lateral MTL which is a second order fault between the two major dextral shear zones which bound the Japan Sea to the east and to the west. The problem of the apparent instantaneous rotation of SW Japan as opposed to the progressive opening of the Japan Sea is probably due to the way paleomagnetic data and radiometric dates are averaged.

Figure 1: Tectonic map of the Japan Sea area after Jolivet and Tamaki (1992). two successive stress fields are shown (Miocene and Present). Paleomagnetic rotations are indicated. YBK: Yamato Bank, TPF: Tym Poronaisk Fault, TB: Tsushima basin, TF: Tsushima Fault, YF: Yangsan Fault, MTL: Median Tectonic Line, HSZ: Hidaka Shear Zone.



1 Problem setting

The last ten years have seen the development of a debate on the opening mechanism of the Japan Sea (Figure 1). An important breakthrough was made by Otofuji et al. (Otofuji and Matsuda, 1983, 1984, 1987; Otofuji et al., 1985; Otofuji et al., 1991) with their "bar door" opening model based on the observation that SW and NE Japan show consistent easterly and westerly deflected paleomagnetic declinations. The rotation interval was assigned to a very short period, less than 2 Ma long, about 15 Ma ago. The model was that of a double rotation about two nearby poles and a double fan-shaped opening of the Japan Sea. The rigid behaviour of the two continental blocks, each of them being more than 500 km long, implies that oceanic crust formation in the Japan Sea was contemporaneous with the rotation. A very fast opening model was then postulated which implied in turn very fast rates of motion of the rotating blocks.

Based on different grounds, Lallemand and Jolivet (1985) postulated that major dextral strike slip faults guided the opening of the Japan Sea in a pull-apart manner, in opposition with the fan-shaped kinematics of Otofuji et al. Later Jolivet et al. (1989) (Figure 2) Jolivet et al. (1991) and Jolivet and Tamaki (1992) introduced block rotations in the pull-apart model, describing the whole region as a wide dextral shear zone.

Even with these recent adaptations the strike-slip model remains apparently incompatible with paleomagnetic data because it suggests a progressive opening between 25 and 12 Ma (Figure 3), with progressive block rotations instead of instantaneous ones in the fan-shaped model. Most geological and geophysical data, acquired onland as well as offshore show that the Japan Sea did not open instantaneously, and that it was already widely opened 15 Ma ago (Tamaki, 1988; Tamaki et al., 1992). Recent deep sea drilling in several sites in the Japanese waters of the Japan Sea reached the volcanic basement which is everywhere older than 15 Ma, and subsidence curves show a maximum during the Early Miocene (Ingle 1992). Previous geophysical investigations had also shown that heat flow and depth distribution in the basin are compatible with an Early Miocene opening (Tamaki, 1986, 1988).

We start this paper with the assumption that both paleomagnetic data and other geological data are relevant and that the apparent inconsistency is symptomatic of a lack of understanding of the geometry and timing of opening, and we try to reconcile both sets of data in a single model. We first present a critical review of published paleomagnetic data putting the emphasis on the length of error bars. We then present observations on the way the Japan arc deformed during the opening of the Japan Sea and on the geometrical relationships between this deformation and internal structures of the Japan Sea. We emphasise the fact that deformation occurred at various scales, and that distributed strain of the SW Japan and NE Japan blocks might partly explain the observed rotations. We finally propose a geometry of

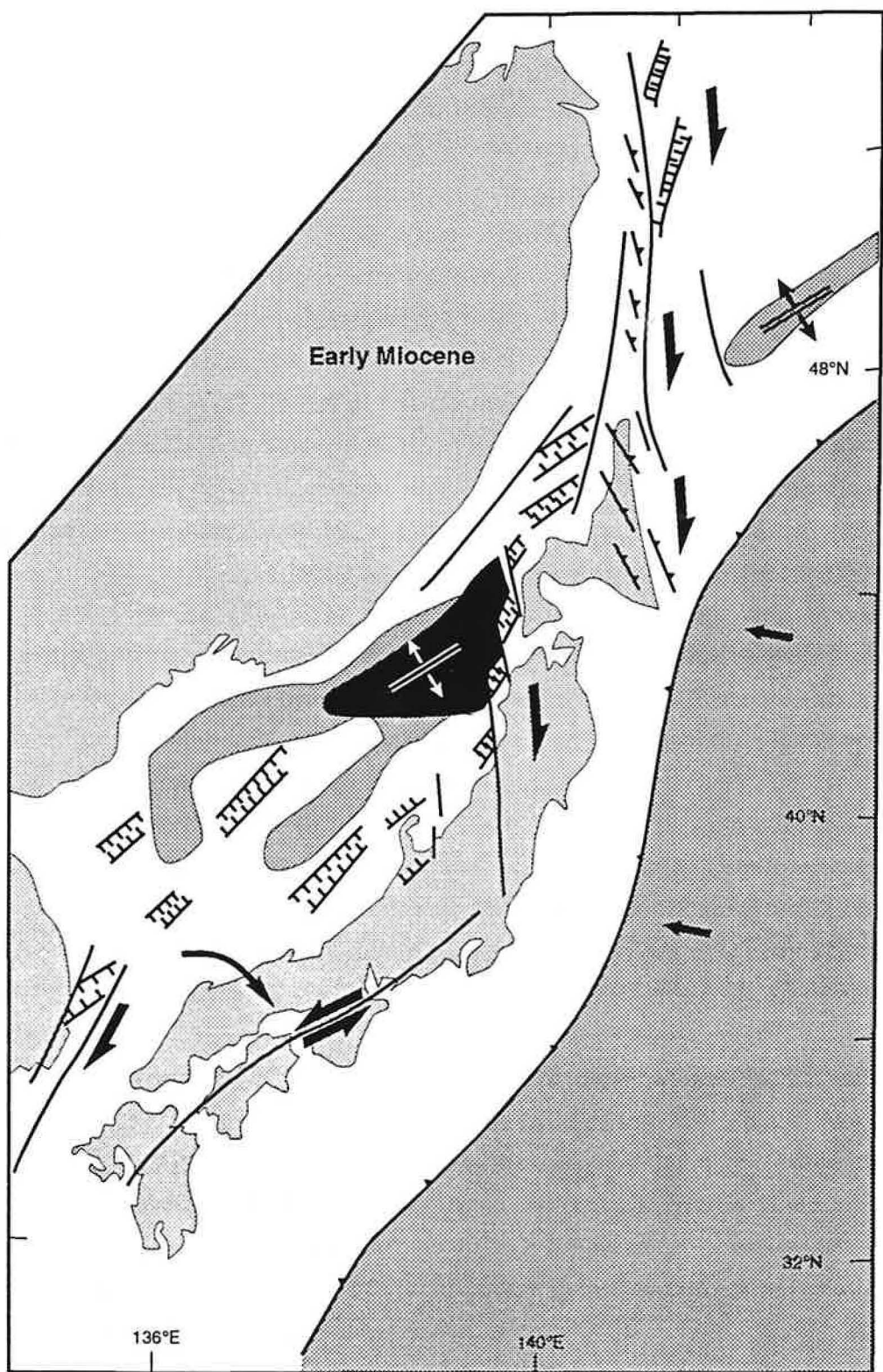


Figure 2: Possible reconstruction of the Japan Sea in the Early Miocene during the opening after Jolivet et al. (1992).

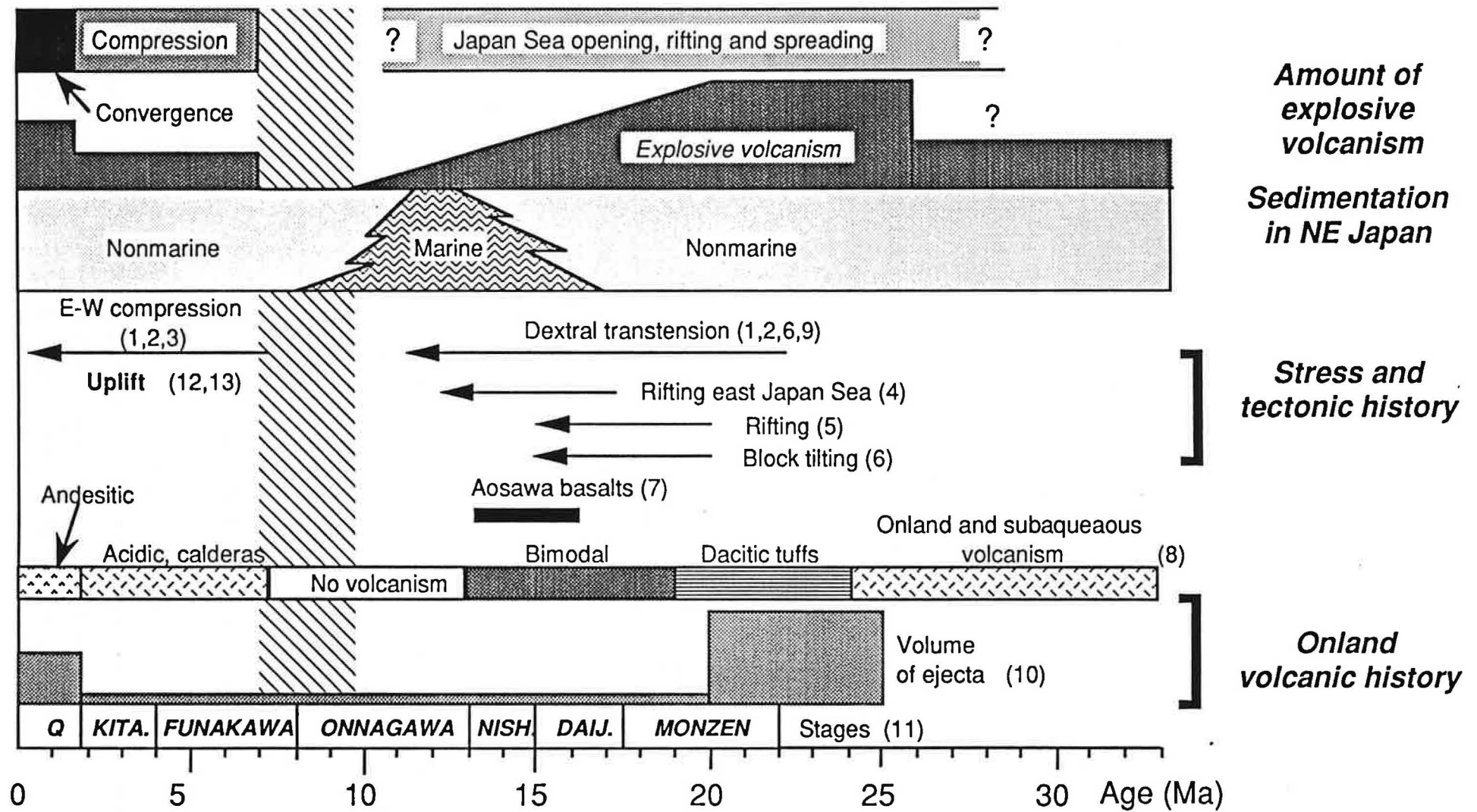


Figure 3: Synthesis of the tectonic and volcanic events in Northeast Honshu after Jolivet and Tamaki (1992): (1) Jolivet and Huchon (1989), (2) Jolivet et al. (1990), (3) Nakamura and Uyeda (1980), (4) Suzuki (1989), (5) Yamaji (1989, 1990), (6) Amano and Sato (1989), (7) Tsuchiya (1989, 1990), (8) Usuta (1989), (9) Otsuki (1989), (10) Sugimura et al. (1963), (11) Fujioka (1986), (12) Sugi et al. (1983), and (13) Iijima and Tada (1990).

opening which partly reconciles both data sets and discuss points which do not fit in this scheme, and possible explanations for these remaining discrepancies.

2 Paleomagnetic constraints

The counterclockwise rotation of NE Japan and the clockwise rotation of SW Japan (Figure 4) were discovered in the early times of paleomagnetism in Japan (Kawai et al., 1961, 1969). Kawai and his colleagues measured remnant magnetisation of granitic rocks in NE and SW Japan. Their material would be considered inappropriate for nowadays standards but these were the only rocks systematically dated in those days which had a strong enough magnetisation for the magnetometer they used.

This work, which was summarised in Kawai et al. (1971), suggested that the Japanese islands had been bent between 120 and 80 Ma. No link was proposed with the opening of the Japan Sea. These results were not easily accepted because the material was not suitable for paleomagnetic tests. Because all samples were Cretaceous in age they all showed normal polarity. Their magnetisation was usually strong and stable enough for the demagnetisation procedures in use in the sixties.

Yaskawa (1979) first proposed a possible correlation between the observed rotations and the opening of the Japan Sea, but the data he gathered did not allow to conclude on the age of rotation.

Although Ito and his colleagues (Ito and Tokieda, 1980; Ito et al., 1980) continue in the same line, it is not until the work of Otofuji and colleagues that the rotation of SW Japan and the opening were linked in the same mechanism and dated as Middle Miocene. The first paper appeared in 1983 (Otofuji and Matsuda, 1983). A thermal demagnetisation technique was applied to acidic volcanic rocks which were not suitable for alternating field demagnetisation because of a slight metasomatism. They also dated the samples and found that the rotation was as young as 20 Ma. Following studies (Otofuji and Matsuda, 1984) on sediments precisely dated by bio- and magnetostratigraphy suggested that the rotation occurred within a short period of time around 15 Ma. Otofuji et al. (1985) later found that the CCW rotation of NE Japan was as young as that of SW Japan. Later works aimed to constrain more precisely the timing and amount of rotation of NE and SW Japan.

2-1 Fast rotation of SW Japan 15 Ma ago

The study which most precisely constrains the timing of rotation was published by Hayashida et al. (1991). They studied sediments of the Setouchi Miocene basins, distributed on the northern side of the Median Tectonic Line, which are dated with biostratigraphic and magnetostratigraphic techniques. Data obtained in the Ichishi basin indicate that the rotation lasted at least until 15.7 Ma. Slightly younger sediments of the Morozaki area, in Blow's N9

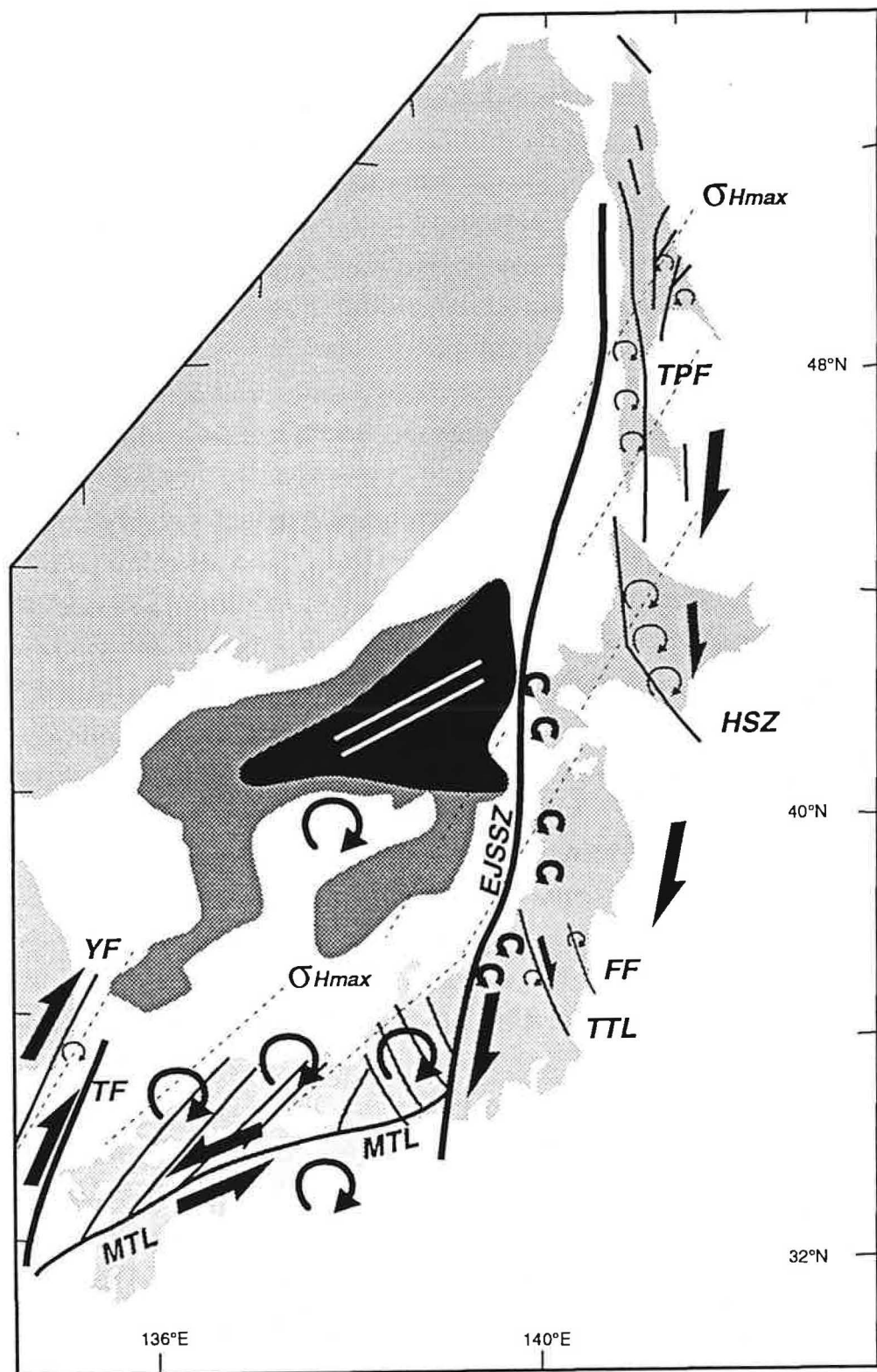


Figure 4: Major faults and sense of block rotations around the Japan Sea. Most rotations are deduced from paleomagnetic studies (see text for references) except for those of NE Sakhalin which are suspected by Fournier et al. (1993) but not demonstrated and of the Yamato Bank which is deduced from Jolivet et al. (1991) kinematics. Also shown is the distribution of crustal blocks suspected by Kanaori (1990) in SW Japan and the direction of the maximum horizontal stress after Jolivet et al. (1991, 1992) and Charvet et al. (1992).

foraminiferal zone (younger than 15 Ma) have smaller clockwise deflections, though the normal polarity leaves opened the possibility that they were recently remagnetized. A very similar chronology is found in the Northern Chubu district (Yatsuo area). Itoh (1988) also concluded to a smaller rotation within the *Denticulopsis Lauta* zone. Both studies found no significant rotation between 20 and 15 Ma. K-Ar dating by Otofuji and Matsuda (1983) suggested that most of the rotation occurred around 15 Ma within a period shorter than can be presently resolved by the available dating techniques.

Some regions of SW Japan nevertheless show different amounts of rotation. The Hokuriku and Chichibu regions are located on both sides of the Median Tectonic Line which makes a sharp bend from an ENE trend to a more northerly direction west of the collision zone of central Japan. The bend is often attributed to the collision of the Izu arc, assuming that the MTL was straight before the collision. The change in rotation angle is consistent with this model which assumes that the whole of SW Japan was first rotated clockwise uniformly, and that later its eastern part was rotated back CCW during the indentation of central Japan by the Izu arc. The rotation angle is calculated for the main part of SW Japan by Otofuji et al. (1985). They selected reliable paleomagnetic data with the following criteria: (1) good age assignment, (2) demagnetisation with both thermal and alternating field techniques, (3) small 95% confidence circle ($<30^\circ$), and (4) data correction for tilt. Fitting a function on the selected data gave a finite rotation of 47° . However the estimation of error is not easy with this method so we tried the conventional direction mean for paleomagnetic data older than 16 Ma adding some recent data (Hayashida et al., 1991; Otofuji et al., 1991). We obtain a rotation angle of $51.0 \pm 6.5^\circ$.

In contrast to NE Japan the rigid rotation of SW Japan as a single block has been widely accepted because of the very limited variations of the paleomagnetic directions and because the geological provinces arranged along the arc south of the MTL are straight and do not show an obvious division into smaller blocks. The only regions with a different trend of magnetisation are located near the collision zone as discussed above. The whole of SW Japan has been sampled for paleomagnetic measurement from the forearc region of the Shimanto belt (Tagami, 1982) to the backarc side near the Japan Sea. It is difficult to divide SW Japan into smaller blocks without violating the apparent simple arrangement of the area.

2-2 Slow rotation of NE Japan between 22 and 15 Ma.

Fewer systematic studies of the paleomagnetism of NE Japan are available in the literature than for SW Japan (Otofuji et al., 1985; Tosha and Hamano, 1986, 1988). These works indicated that a CCW rotation occurred sometime between 22 and 15 Ma. Tosha and Hamano (1986) and Tanaka et al. (1991) showed that the rotation had been completed before 15 Ma. Yamazaki (1989) collected samples from the east coast of Honshu and showed that the Matsushima formation (older than the *Denticulopsis Lauta* zone) has not been rotated.

This result is ascertained by both normal and reverse polarities, though a secondary remagnetization in the present field still is possible. Confusing paleomagnetic results were obtained in the Gongenyama formation 100 km to the north-east. The authors concluded that the rotation was not finished before N9 and N10 Blow's foraminiferal zones. The result is ascertained through the presence of both reverse and normal polarities and a slight improvement of clustering of data after tilt correction. The magnetic direction close to the present field however leaves the possibility of a secondary remagnetization. Several other works also suggest that the rotation occurred before 15 Ma and after 22 Ma. This makes the rotation older than for SW Japan.

The rotation angle is more difficult to determine by comparison to SW Japan. If we take the mean of data with ages between 20 and 40 Ma from Otofuji et al. (1985) and Toshia and Hamano (1988), the declination would be $-44.4 \pm 8.6^\circ$.

2-3 The double rotation model and the opening of the Japan Sea

Despite a less precisely constrained timing of rotation in NE Japan, Otofuji et al. (1985) concluded to a very fast opening of the Japan Sea by rotation of NE and SW Japan about two poles located near the northern and southern ends of the Japan arc in a very short period 15 Ma ago. The almost instantaneous rotation leads to very fast rates of spreading near the hinge between SW and NE Japan (more than 60 cm/year).

Until ODP legs 127 and 128 (Tamaki et al., 1992) there had been no precise dating of oceanic spreading in the Japan Sea. The interval of rifting was rather well constrained by various studies on shore and offshore along the eastern margin in NE Japan but the oceanic basement had never been directly dated. Only in the northern part of the Japan Sea had poorly defined magnetic anomalies been recently discovered (Kobayashi et al., 1988) which suggest an Early Miocene spreading older than the fast rotation of SW Japan. The volcanic basement was penetrated in four sites during the two legs and all results suggest that the Japan Sea was already widely opened when the fast rotation occurred. There is an apparent contradiction between the observed age of opening and paleomagnetic data which suggest rapid rigid rotations of two large blocks.

As we shall see later it is possible to reconcile the amount and sense of paleomagnetic rotations with the observed deformation of the Japan arc, but not the timing of rotation. Do we have to consider that the rotation actually occurred in this short time span, or is it possible that the error on the rotation of SW Japan is larger than usually considered?

Otofuji et al. (1991) give error estimates on the radiometric dating they performed in San'in district. According to them the rotation occurred within a short period of 1.8 ± 1.5 Ma between the non-rotated Omori formation above and the rotated Kawai formation below. The maximum interval for the rotation is then 3.3 Ma which is still shorter than the duration of opening. Ages given for the two formations are means calculated with 8 and 15 different

samples coming from various places in each formation. Is it reasonable to calculate a mean age when the individual ages of samples vary a lot (from 13.7 ± 0.3 to 18.3 ± 0.4 Ma for the Kawai formation)? If the analytical error is small, there is no reason to deny the obtained ages and to prefer a mean value. Lithologic features of the Kawai formation are quite variable and its deposition has apparently lasted longer than supposed by the authors. If the rotation actually occurred in the time interval defined by the two formations, this interval should be defined by the youngest age found in the Kawai formation and the oldest age found in the Omori formation, and not between two mean ages. Furthermore some of the ages obtained in the underlying Kawai formation are younger (13 Ma) than the oldest obtained in the overlying Omori formation. Some of these ages then are not reliable. Why use them to calculate a mean value?

The authors also calculate average VGP's for each formation and give a 95% confidence interval. If block rotations occurred at a small scale, there could be significant local differences between the rotations of each individual sites. What is the meaning of an average VGP in this context? Calculating it, one assumes that the block has rotated rigidly which is not proven a priori. There could thus be an answer to our problem in the way data are treated statistically. If so, many more samples and a much denser sampling procedure is the only way to answer the question of timing and amount of rotation of a complex region; the sampling must also be done in connection with a good structural map where shear zones and other block boundaries are identified. A "statistically rigid" block might be so only because there is no other simple way to consider the numerical data without a priori information on the structure of the concerned region.

An alternative solution is to consider that the observed rotations partly correspond to the internal deformation of the Japan arc. In a classical domino system with a simple geometry crustal blocks rotate by the same amount and it might be impossible to see a difference in the distribution of paleomagnetic rotations between a single rigid block and several dominoes bounded by parallel strike-slip faults. Kanaori (1990) suggested that some of the rotation of SW Japan might be accounted for by rotation of large-scale dominoes (Figure 4).

We shall first see that some paleomagnetic data already show that local rotations occur along major shear zones, and then identify these and the strain regime they imply for the Japan arc.

2-4 Local paleomagnetic rotations along shear zones

NE Japan

There are many reports of paleomagnetic directions anomalous with respect to the rigid rotation model of NE Japan. Otofuji et al. (1985) themselves reported easterly deflected directions from eastern Asahi, which they attributed to the influence of the Tanakura Tectonic

Line (TTL). Oda et al. (1989) observed a 20-30° clockwise rotation south of Sendai city, in the Yanagawa and Takadate area, 15 Ma ago. They attributed these rotations to a drag along the Futaba Fault which runs parallel to the TTL in the Abukuma massif. Regional variations of the declination were already discussed based on data from granitic rocks (Ito and Tokieda, 1986; Kawai et al., 1971). It is thus possible that the rotation did not occur with a single rigid block. The basement of NE Japan is also less continuous than in SW Japan. However the data available do not allow to determine the size and boundaries of rotating blocks.

Tsushima Strait and Korea peninsula

Two sets of paleomagnetic data show local Miocene rotations. One is the clockwise rotation (45°) of the Guryongpo area on the east coast of the Korean Peninsula (Kim et al., 1986) and the second is a counterclockwise rotation of Tsushima island (30°) (Ishikawa et al., 1989). Both regions are located next to large shear zones and the authors attribute these anomalous direction to local strain. It is noteworthy that the two areas rotated in opposite sense despite the fact that they are located on either sides of the same shear zone.

Sakhalin and Hokkaido

Kodama et al. (1992) and Takeuchi et al. (1992) analysed samples from Hokkaido and Sakhalin along the major dextral shear zone which bounds the Japan Sea to the east (East Japan Sea Shear Zone, EJSSZ). In Sakhalin they obtained reliable measurements on the west side of the Tym-Poronaisk Fault which is a major dextral dislocation which runs N-S along more than 600 km (Rozdestvenskiy, 1982). Clockwise rotations are observed consistently in the whole area and the authors conclude to a distributed deformation along the shear zone with a simple domino model. There does not seem to be discrete shear zones dividing crustal blocks west of the Tym-Poronaisk Fault but rather en echelon folds whose axes are curved clockwise near the fault. The dextral rotation can then be explained as well with a more continuous deformation model.

In a recent paper Kodama et al. (1992) describe the results of a sampling campaign in Hokkaido and they show very similar results with dextral rotations which they attribute to the dextral motion along the axial zone of Hokkaido. The dextral rotations seem to last until the early Late Miocene that is later than the end of the Japan Sea opening.

During the Japan Sea opening major strike-slip shear zones were active such as in Central Hokkaido and Sakhalin, and older strike-slip faults such as the MTL or TTL were reactivated. We describe in the following the geometry of deformation of the arc during the opening seen from the view point of the structural geologist and see how it is related to the geometry of opening.

3 Deformation of the Japan arc during the Japan Sea opening

Oceanic crust is distributed only in a restricted area in the northern part of the Japan Sea (Figure 1). Magnetic anomalies identified by Kobayashi et al. (1988) suggest that it dates

back to the Early Miocene. The geometry of anomalies also suggests that the spreading center had been propagating westward during the opening (Tamaki et al., 1992; Jolivet and Tamaki, 1992). This observation is confirmed by the general triangular shape of the area where oceanic crust is distributed with a wide base along the EJSSZ and a tip further west in the Russian waters. In other regions of the Japan Sea, geophysical surveys have shown that no true oceanic crust is present even in deep basins. The seismic velocity structure of the Tsushima and Yamato basin suggest that they are floored by a thinned continental crust intruded by numerous basaltic sills (Tokuyama et al., 1987). True continental crust, similar to that of the Japan arc is found under the Yamato Bank, which has been left over during the southeastward drift of SW Japan. The Japan Sea can thus be divided into two very different regions. The northern part is characterised by the presence of oceanic crust and a very narrow margin on the Japanese side. Little is known on the Siberian side, but bathymetry also suggests a narrow margin. On the other hand the western part of the Japan Sea was formed by distributed intra-continental extension.

3-1 Major dextral strike-slip shear zones

As described in several earlier papers (Lallemand and Jolivet, 1985; Jolivet et al., 1991; Jolivet et al., 1992) the eastern margin of the Japan Sea is paralleled by a major dextral shear zone which trends N-S from the northern tip of Sakhalin to Central Japan (Figures 1 & 2). The most obvious zones of strain localisation within this shear zone are the Hidaka Shear Zone (Central Hokkaido) and the Tym-Poronaisk Fault (central Sakhalin). The Hidaka Shear Zone runs along 200 km in southern Hokkaido and shows a complete crustal section from brittle to ductile structures compatible with a dextral shear with a component of westward thrusting. Further north and west, en echelon folds and thrusts (Kimura et al., 1983) participate to the same dextral shear. Radiometric dating of the high temperature metamorphism contemporaneous with the dextral motion, as well as paleostress tensor analysis in the external domains where biostratigraphy allows to date the successive tectonic events, suggest that the dextral motion has been active from the Late Oligocene to the Middle Miocene (Jolivet and Huchon, 1989). As discussed above, recent paleomagnetic data (Kodama et al., 1993) in Central Hokkaido suggest that it might have lasted longer till the Late Miocene though different interpretations of the same data are still probably possible (see discussion in Jolivet, 1993). The dextral strike-slip motion stopped sometimes in the Late Miocene, and the Hidaka Shear Zone was reworked as a thrust fault, in the hanging wall of which the Hidaka mountains were recently uplifted.

The Tym-Poronaisk Fault (Rozdestvenskiy, 1982) divides the island of Sakhalin in two narrow stripes. The western side shows en echelon folds in Cretaceous and early Cenozoic sediments similar to those of Hokkaido which suggest a component of dextral shear. Tectonic analysis of the Tym-Poronaisk Fault itself shows that it is made of N-S trending strike-slip

segments alternating with NW-SE trending thrust faults. Paleostress analysis near the fault suggest that a transpressional regime has been active during the Miocene until recently; the abrupt change in stress regime seen in Hokkaido is not obvious here though the dextral shear seems less active now (Jolivet et al., 1992, Fournier et al., 1993). The East Sakhalin mountains are cut by several NE-trending dextral strike-slip faults which branch on the Tym-Poronaisk Fault like R-Riedel shears. Counterclockwise rotation of the stripes in-between are expected by Fournier et al. (1993) but no paleomagnetic data are yet available to test this hypothesis. A major N-S trending strike-slip fault runs offshore along the western margin of Sakhalin and it led to the formation of second order pull-apart basins in the Tartar Strait.

The transpressional dextral shear zone of Sakhalin and Hokkaido is more than 1000 km long. It is relayed at the latitude of SW Hokkaido by a narrow zone of transtensional dextral shear parallel to the margin of the Japan Sea. En echelon grabens and dextral strike-slip faults are seen offshore. Paleostress analysis in this region from Oga Peninsula to Sado island, and Noto peninsula (Jolivet et al., 1991, Fournier et al., 1993) show that the direction of the extensional principal stress has been oblique on the margin with a NW-SE trend. It is seen in rocks older than the Late Miocene. It is then replaced by the E-W compression which is active today as attested by the frequent compressional tsunamigenic earthquakes of this side of the Japan arc (Nakamura et al., 1983; Fukao and Furumoto, 1976; DeMets, 1992). This zone of transtensional dextral shear divides the NE Japan arc from the oceanic crust of the northern Japan Sea and has been active during its spreading. The Japan Sea is thus bordered on its eastern side by a major dextral shear zone, more than 2000 km long including the transpressional and the transtensional domains, which was active from the Late Oligocene to the Middle Miocene, and is still active in the north.

A second dextral strike-slip shear zone is known along the south-eastern coast of Korea and in the Tsushima strait (Otsuki and Ehiro, 1978). The NE-trending Yangsan fault offsets the Cretaceous Bulgugsa granites by several tens of kilometres. It also offsets metallogenic belts of Korea, which are then offset again dextrally on the Japanese side of the Tsushima Strait (Sillitoe, 1977). The direction of Early Miocene basaltic dykes intruding the Miocene Pohang basin is compatible with dextral motion along the Yangsan fault (Lee, 1988). Paleostress analysis in the Cretaceous Gyongsan basin and the Miocene Pohang Basin shows two successive stages of dextral motion during the Late Oligocene and Early Miocene (Hwang, 1992). This shear zone was thus active when the Japan Sea was opening.

The geology of Tsushima island is puzzling in this context. It clearly shows en echelon folds and thrusts formed inside a left-lateral shear zone parallel to the dextral one previously described. Recent observations by Fabbri and Charvet (1994) suggest that this compressional deformation occurred more recently than the Japan Sea opening (from 15 Ma onward) and was preceded by a phase of dextral shear. Which is more puzzling is that focal mechanisms of earthquakes in the western part of the Japan Sea (Jun, 1990) are compatible with a mixture of

shortening perpendicular to the Yangsan Fault and dextral strike-slip. Similar mechanisms are seen further inland in the gulf of Bohai (Chen and Nabelek, 1989). The left-lateral event is thus bracketed between two episodes of right-lateral motion.

3-2 Reactivated shear zones

Formed initially as a left-lateral strike-slip fault in the Late Cretaceous and Early Cenozoic the Tanakura Tectonic Line was reactivated as a dextral shear zone during the Miocene (Otsuki and Ehiro, 1978) though the Miocene offset is probably small. Parallel faults cut through the basement of the Abukuma massif such as the Futaba Fault.

The Median Tectonic Line is a very large shear zone which runs E-W between the Inner and Outer zones of SW Japan (Ichikawa, 1989). It was most active during the Late Cretaceous and Early Cenozoic as a left-lateral fault. Ductile deformation is observed on its northern side in the granitoids of the Cretaceous Ryoke Belt. It is active today as a dextral strike-slip shear zone which accommodates the dextral component of the oblique subduction of the Philippine Sea Plate under SW Japan.

Very little is known on the behaviour of the MTL during the Miocene. Jolivet et al. (1989) suggested that it had already reversed its motion for a dextral shear because of the apparent dextral torsion of paleomagnetic direction near the fault. Recent observations of trend of Miocene dykes by Takeshita (1990) on the contrary suggest that it was left-lateral around 15 Ma. Our own recent observations confirm Takeshita's findings. Not only does the trend of Miocene basaltic dikes imply a left-lateral component of motion but also the fault set analysis we performed in Miocene basins distributed along the fault is compatible with this sense of motion (Fournier et al., submitted). No evidence is known for the amount of relative left-lateral displacement during the Miocene

3-3 Distributed deformation in SW Japan

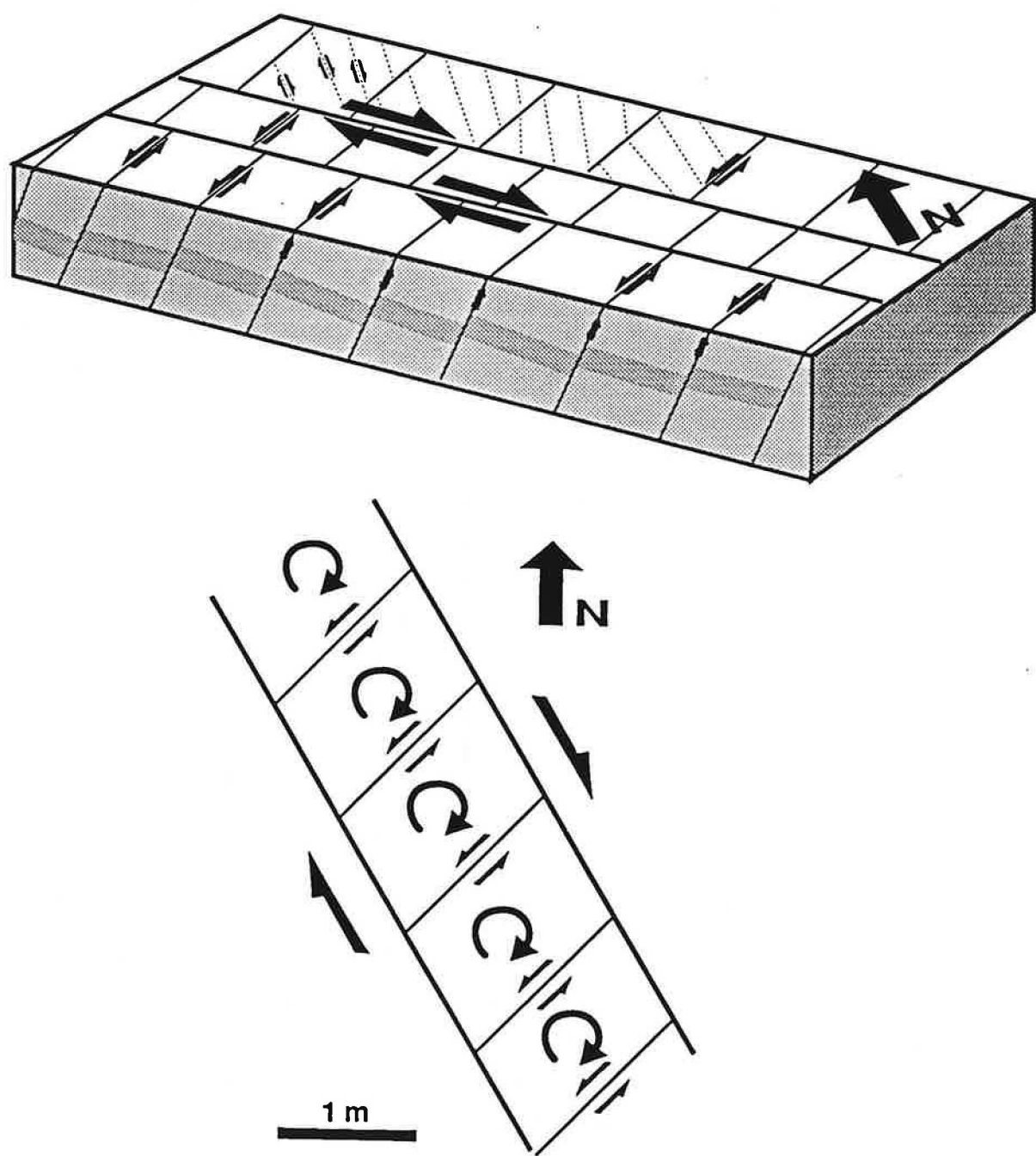
As was said above, the rotations of dominoes can produce an apparently homogenous strain field if only rotations are taken into account and those dominoes not identified. The linearity of the MTL and other boundaries between the belts of SW Japan precludes major internal strain in a first approach. Linearity is however a characteristic of strike-slip shear zones and, because outcrops of SW Japan are far from continuous, some important shear zones bounding dominoes might have been missed by geologists. Already Kanaori (1990) recognised large-scale fault-bounded blocks in SW Japan.

To approach this problem we surveyed the San'in district (central SW Japan on the backarc side) where Otofuji et al (1991) have recognised a fast CW rotation at about 15 Ma. The deformation is very different depending upon the observed stratigraphic level. Miocene strata older than 15 Ma show both normal and strike-slip faults and the inferred direction of extension varies from WNW-ESE to NW-SE. Figure 5 shows the example of a measured site on the western tip of the Shimane peninsula where pure N150E dextral strike-slip faults and

N50E left-lateral and normal faults were observed. The computed stress tensor (Angelier, 1984) (Figure 6) implies a strike-slip regime with σ_1 and σ_3 horizontal. This outcrop is a good example of how the brittle deformation is distributed in the older Miocene strata. Here N150°E dextral strike-slip faults are regularly spaced every 2 meters. These are large fault planes, several tens of meters long. Oblique on this first set is a second one which trends N50°E in average and which corresponds to oblique slip faults with a component of left-lateral slip and a component of normal slip. These planes are also regularly spaced every meter or so and are never longer than 2 or 3 meters. They show normal offsets of 30 cm approximately. The offsets induced by the first set of faults are not seen in the outcrop. Inside the blocks defined by these two sets of faults a third set (N20°E) with very small offsets are observed. These are dextral faults but no striae could be seen. If one consider the two largest sets of faults, they define regularly spaced dominoes and the geometry implies a clockwise rotation (figure 5). Similar outcrops were observed along the coastline of the San'in district with the same regular spacing of faults and several sets with smaller offsets on smaller faults (Fournier et al., submitted). This deformation is characteristic of the Kawai-Kuri and older formations. The Kawai-Kuri formation is dated by Otofuji et al. (1991) as 16.0 ± 1.4 Ma old. Younger formations such as the Omori formation (14.2 ± 0.6 Ma) do not show this deformation. Most of outcrops are little deformed and show only tilting and long wavelength folding which can be attributed to very recent deformation. Only one outcrop in the Omori formation showed a set of faults which indicates a NE-trending compression which could be compatible with the NW-trending extension described above. It could also be the local result of folding and thus have no relation with the older deformation. Except from this outcrop, all formations younger than the Kawai-Kuri formation are little deformed and never show the fault-bounded domino geometry seen below.

According to Otofuji et al. (1991), the Omori formation did not suffer the clockwise rotation observed in the underlying rocks; this allows them to constrain the timing of rotational motion of SW Japan in a very short period about 15 Ma. We see with this example that the rotation was locally accompanied by a strong internal deformation with a domino geometry. Because the outcrops are not continuous enough to draw a complete map of these structures it is impossible to quantify the amount of finite internal deformation of SW Japan. Furthermore the blocks we have seen might be only second or third order blocks within larger ones which are more difficult to see. We can only conclude that some internal deformation of SW Japan occurred during the paleomagnetic rotation and thus that the 50° rotation is only partly rigid. The domino geometry of Kanaori (1990) is a good candidate for a larger scale equivalent of a similar distribution of strain.

Figure 5: Schematic representation of an outcrop in the Kawai-Kuri formation in Shimane Peninsula showing the distribution of strain along the boundaries of small blocks and implying dextral rotation.



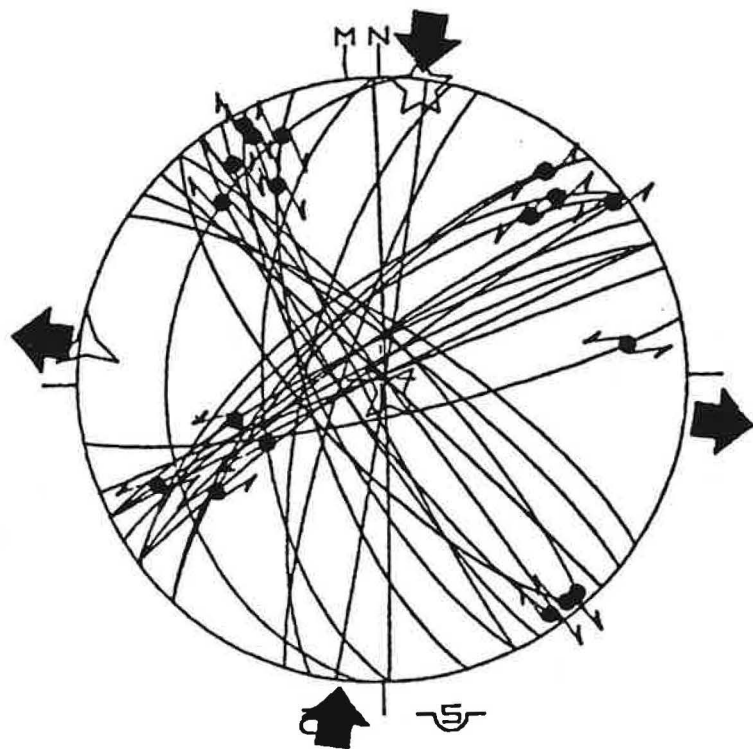


Figure 6: Stress tensor inferred from the faults measured on the outcrop shown in figure 5 with Angelier's method (1984).

4 Strike-slip shear zones and paleomagnetic rotations

Jolivet et al. (1991) used the internal structure of the Japan Sea to close it back to its pre-opening position. One of the constraints was the shape of the northern side of the Yamato Bank which fits reasonably well the 2000 m isobath of a portion of the Siberian coast. This allows them to calculate an approximate pole of rotation which falls in the Tsushima strait. The same authors used the same geometry to rotate back SW Japan to its position before opening and obtained a finite rotation about the same pole of 30° CW. This was based upon the assumption that the Yamato basin was floored with oceanic crust which has been proved wrong afterward (Tamaki et al., 1992). The 30° of rotation completely closes the Yamato basin and the western part of the Japan basin. The presence of highly stretched continental crust instead of oceanic crust is an argument to reduce the finite rotation. However the thickness of the Japan arc crust before the Japan Sea opening is not known precisely enough and it is then impossible to calculate the thinning factor. We shall then consider that 30° of clockwise rigid rotation of SW Japan is a maximum. The remaining 20° must be found in the internal strain we have described above.

The rigid clockwise rotation of SW Japan is compatible with a left-lateral motion along the MTL in a simple domino model. SW Japan inner zones and outer zones can be considered as 600 km long dominoes, bounded by left-lateral E-W cross faults (MTL) and N-S dextral master faults.

To properly close the northern part of the Japan Sea, a 20° CCW rotation was used in Jolivet et al. (1991). This number is similar to what is given by paleomagnetic data for this region.

We can already conclude that, if one accepts that a part of the CW rotation of SW Japan is due to internal strain which is actually observed in the period requested by paleomagnetic results, there is no major conflict between paleomagnetic data and the dextral pull-apart model.

Paleomagnetic studies along the major shear zones have shown that local rotation occur and can be related to the observed deformation in Hokkaido and Sakhalin. Local rotation effects are also observed along less important shear zones such as the Tanakura Tectonic Line.

Reconstructions

The reconstructions shown here (Figure 7) are simplified from those described in Jolivet and Tamaki (1992). The entire Japan Sea is considered as a wide dextral pull-apart zone between two major dextral strike-slip shear zones. The largest one is along the eastern margin of the Japan Sea and in Hokkaido and Sakhalin. A second one divides the Korean peninsula from SW Japan. The 30° of CW rotation of SW Japan accommodate the difference in the

amount of offset on these two shear zones. In the reconstructions 400 km of dextral offset are imposed on the eastern shear zone and only 150 km on the western one. Extension is distributed in the domain of relay between these two shear zones; it eventually localizes at the southern tip of the eastern transpressional domain and finally leads to a complete rupture of the crust and formation of oceanic crust in a triangular zone. The geometry of the oceanic domain is that of a crustal-scale tension crack propagating westward near the end of a strike-slip shear zone. Crustal thinning continues even after the initiation of the spreading center, in the southern part of the Japan Sea. On the reconstructions only the rigid rotations are shown. Local rotations along the major shear zones occur in the meantime. Extension, spreading and strike-slip motion last until the Middle Miocene, and strike-slip motion alone until recent time in the north (Sakhalin). After 10 Ma, a compressional stress field is set on NE Japan and the deformation progressively localizes along the eastern margin where compressional earthquakes are recorded nowadays. This zone has been interpreted as a future subduction zone by Nakamura (1983).

5 Conclusion:

This paper shows that the pull-apart model and the amounts of paleomagnetic rotations of SW and NE Japan are compatible. The left-lateral behaviour of the MTL during the Miocene accommodated the CW rotation of SW Japan between the two major dextral strike-slip faults, one along Sakhalin, Hokkaido and NE Japan, and one between the Korean Peninsula and SW Japan. One has however to accept that a part of the 50° of CW rotation of SW Japan is due to internal deformation of the rotating blocks with second order dominoes. The observation of such distributed brittle deformation in San'in district is in favour of this conclusion.

Local dextral rotations are seen along the major dextral shear zones in Sakhalin and Hokkaido, as well as along the Tanakura Tectonic Line and the Futaba Fault.

This geometry shows that rotations involve blocks of different sizes, major blocks such as SW Japan, smaller blocks along the major shear zones or inside the major blocks as we have seen in San'in district. It is thus most important that the paleomagnetic sampling is made in connection with a precise identification of block boundaries.

The timing of rotation remains difficult to reconcile with other evidences for the age of opening. It is inescapable that the CW rotation of a 600 km block must leave a hole of the size of the Japan Sea, and thus the rotation and the basin formation should have the same age. The evidence for rifting and spreading before the given age for the rotation cannot be ignored. There must then be a problem in the timing of rotation. The discussion of radiometric dating in San'in suggest that the error bar might be much larger than suspected by Otofuji et al. (1991). We suggest that the data be reconsidered without averaging the ages nor the

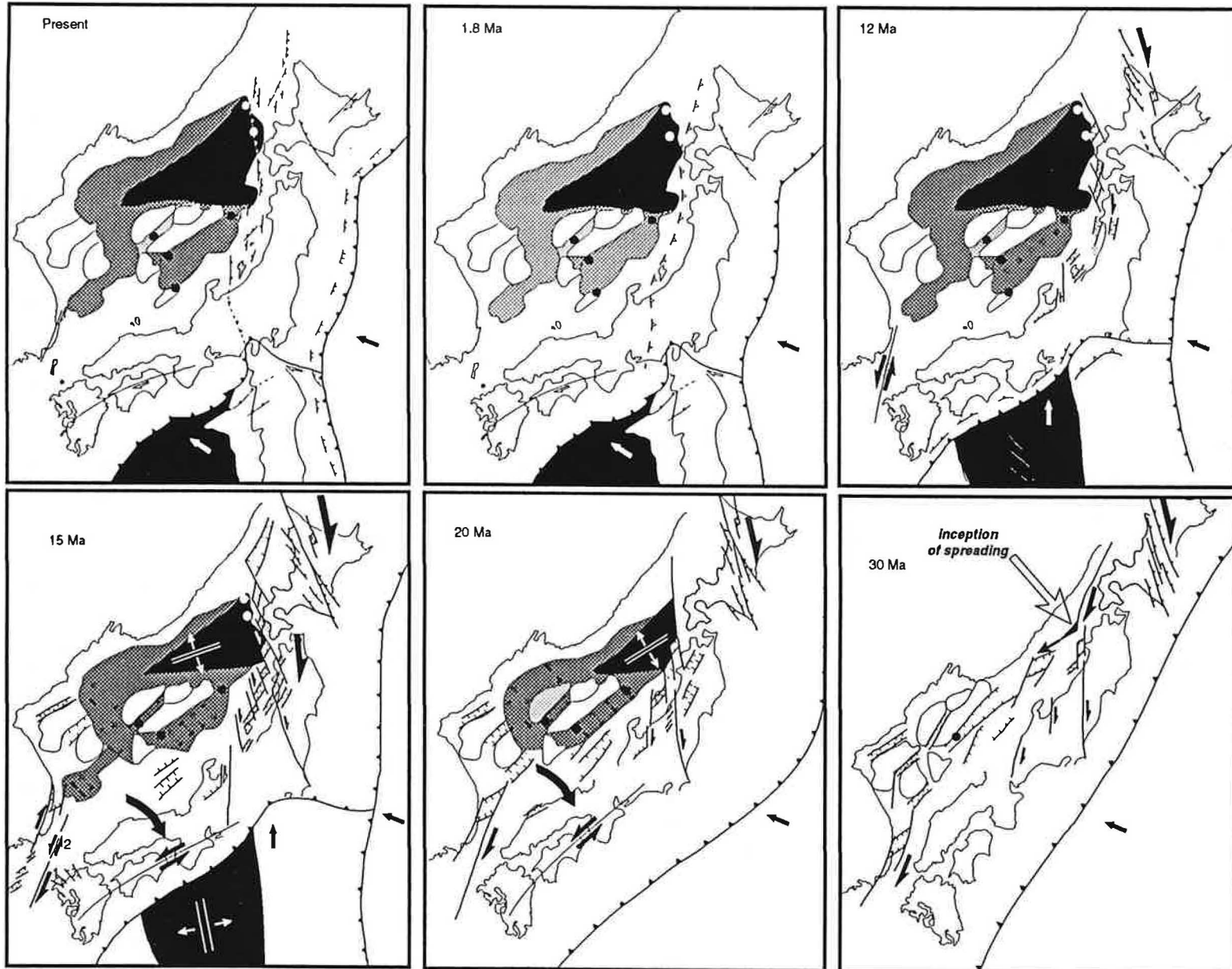


Figure 7: Reconstructions of the Japan Sea evolution from 30 Ma to the Present. Oceanic crust is shown in black and stretched continental crust in grey.

declinations and measurements made on the basis of a structural map showing the possible tectonic boundaries in order to differentiate between first and second order rotations. This job might be difficult to do in Japan because of poor outcropping conditions, but this difficulty must be taken into account when giving uncertainties on the values and ages of rotation.

References

- Amano, K., and Sato, H., Neogene tectonics of the central part of the Northeast Honshu arc. *Mem. Soc. Geol. Jpn.*, 32, 81-96, 1989.
- Angelier, J., 1984, Tectonic analysis of faultslip data sets, *J. Geophys. Res.*, 89, 5835-5848, 1984.
- Charvet, J., Grimm, K., Griffin, J., Jolivet, L. and Pouclet, A., Structural features in ODP leg 128 cores: relationship with the tectonic evolution of the Japan Sea, In Tamaki, K., Suyehiro, K., Allan, J., McWilliams, M. et al., *Proc. ODP, Sci. Results*, 127-128, part 2, 1175-1193, 1992.
- Chen, W.P. & Nabelek, J., Seismogenic strike-slip faulting and the development of the North China basin. *Tectonics*, 7, 975-989, 1988.
- De Mets, C., A test of present-day plate geometries for northeast Asia and Japan, *J. Geophys. Res.*, 12, 17627-17636, 1992.
- Fabbri, O. and Charvet, J., Paleocontraintes et mouvements decrochants dans le détroit de Corée d'après l'exemple des îles Tsushima (Japon Sud-Ouest), *C. R. Acad. Sci. Paris*, submitted, 1993.
- Fournier, M., Jolivet, L., Huchon, P., Rozhdestvensky, V.S., Sergeyev, K. F. and Oscorbin, L., Dextral motion in Sakhalin, and the Japan Sea opening, *J. Geophys. Res.*, in press, 1993.
- Fujioka, K., Synthesis of Neogene explosive volcanism of the Tohoku arc, deduced from the marine tephra drilled around the Japan trench region, Deep Sea Drilling Project Legs 56, 57 and 87B. In Kagami, H., Karig, D. E., and Colbourn, W.T., et al., *Init. Repts. DSDP*, 87: Washington (U.S. Govt. Printing Office), 703-721, 1986.
- Fukao, Y. and Furumoto, M., Mechanisms of large earthquakes along the eastern margin of the Japan sea. *Tectonophysics*, 25, 247-266, 1975.
- Hayashida, A., Fukui, T., and Torii, M., Paleomagnetism of the early Miocene Kano Group in Southwest Japan and its implication for the opening of the Japan Sea. *Geophys. Res. Lett.*, 18:1095-1098, 1991.
- Hwang, J.H., L'évolution tectonique post-Jurassique de la Corée: apport des reconstitutions des paleocontraintes dans les bassins Crétacé méridionaux, Thèse université Pierre et Marie Curie, Paris, 1992..
- Ichikawa, K., Geohistory of the Median Tectonic Line of Southwest Japan. Memoirs of the Geological Society of Japan, 18: 187-212, 1980.
- Iijima, A. and Tada, R., Evolution of Tertiary sedimentary basins of Japan in reference to opening of the Japan Sea, *J. Fac. Sci., Tokyo Univ.*, 22, 121-171, 1990.

- Ingle, C.J., Subsidence of the Japan Sea: stratigraphic evidence from ODP sites and onshore sections, in Tamaki, K., Suyehiro, K., Allan, J., McWilliams, M. et al., *Proc. ODP, Sci. Results, 127/128*: College Station, TX (Ocean Drilling Program), 1197-1218, 1992.
- Ishikawa, N., Torii, M. and Koga, K., Paleomagnetic study of the Tsushima Islands, southern margin of the Japan Sea, *J. Geomag. Geoelectr.*, 41, 797-811, 1989.
- Ito, H. and Tokieda, K., An interpretation of paleomagnetic results from Cretaceous granites in South Korea, *J. Geomag. Geoelectr.*, 32, 275-284, 1980.
- Ito, H. and Tokieda, K., Tilting movements of the Japanese islands inferred from Cretaceous and Early Tertiary paleomagnetic data, *J. Geomag. Geoelectr.*, 38, 361-386, 1986.
- Ito, H., Tokieda, K. and Notsu, Y., A paleomagnetic approach to possible tilting movements of Kitakami mountains and Oshima peninsula of Hokkaido, *Rock Mag. Paleogeophys.*, 7, 113-117, 1980.
- Itoh, Y., Differential rotation of the eastern part of southwest Japan inferred from paleomagnetism of Cretaceous and Neogene rocks. *J. Geophys. Res.*, 93, 3401-3411, 1988.
- Jolivet, L., Comment on "Clockwise tectonic rotation of Tertiary sedimentary basins in central Hokkaido, northern Japan", by K. Kodama, T. Takeuchi and T. Ozawa, *Geology*, 21, 431-434, 1993, *Geology*, in press, 1993.
- Jolivet, L., Ph. Huchon, J.P. Brun, N. Chamot-Rooke, X. Le Pichon & J.C. Thomas, Arc deformation and marginal basin opening, Japan Sea as a case study. *J. Geophys. Res.*, 96, 4367-4384, 1991.
- Jolivet, L. & Huchon, Ph., Crustal scale strike-slip deformation in Hokkaido, Northeast Japan. *J. Struct. Geol.*, 11, 509-522, 1989.
- Jolivet, L., Huchon, Ph. and Rangin, C., Tectonic setting of Western Pacific marginal basins, *Tectonophysics*, 160, 23-47, 1989.
- Jolivet, L., & Tamaki, K., Neogene Kinematics in the Japan Sea region and the volcanic activity of the Northeast Japan arc, in Tamaki, K., Suyehiro, K., Allan, J., McWilliams, M. et al., *Proc. ODP, Sci. Results, 127/128*: College Station, TX (Ocean Drilling Program), 1311-1331, 1992.
- Jolivet, L., Fournier, M., Huchon, P., Rozhdestvenskiy, V. S., Sergeyev, K.F., and Osorbin, L. S., Cenozoic intracontinental dextral motion in the Okhotsk-Japan Sea region, *Tectonics*, 11, 968-977, 1992.
- Jun, M. S., Source parameters of shallow intraplate earthquakes in and around the Korean peninsula and their tectonic implication, *Acta Universitatis Upsaliensis, Comprehensive Summaries of Uppsala Dissertation from the Faculty of Science*, 285, 16 pp., Uppsala, 1990.
- Kanaori, Y., Late Mesozoic - Cenozoic strike-slip and block rotation in the inner belt of Southwest Japan. *Tectonophysics*, 177, 381-399, 1990.

- Kawai, N., Hirooka, K. and Nakajima, T., Paleomagnetic and potassium-argon age informations supporting Cretaceous-Tertiary hypothetic bend of the Main island, Japan, *Palaeogeogr. Palaeoclim. Palaeoecol.*, 6, 277-282, 1969.
- Kawai, N., Ito, H. and Kume, S., Deformation of the Japanese islands as inferred from rock magnetism, *Geophys. J. R. astr. Soc.*, 6, 124-130, 1961.
- Kawai, N., Nakajima, T. and Hirooka, K., The evolution of the island arc of Japan and the formation of granites in the circum Pacific belt. *J. Geomag. Geoelectr.*, 23, 267-293, 1971.
- Kim, K.H., Won, J.K., Matsuda, J., Nagao, K. and Lee, M.W., Paleomagnetism and K-Ar age of volcanic rocks from Guryongpo area, Korea, *J. Kor. inst. Mining Geol.*, 19, 231-237, 1986.
- Kimura G., Miyashita S. and Miyasaka S., Collision tectonics in Hokkaido and Sakhalin, In "*Accretion Tectonics in the Circum Pacific Regions*", M. Hashimoto and S. Uyeda editors, Terrapub, Tokyo, 117-128, 1983.
- Kobayashi, K., Tamaki, K., Nakanishi, M., Isezaki, N., and Sayanagi, K. Complex pseudofault pattern of the Japan Sea - results of detailed geomagnetic survey. *EOS Trans. AGU*, 67:1227, 1988.
- Kodama, K., Takeuchi, T. and Ozawa, T., Clockwise tectonic rotation of Tertiary sedimentary basins in central Hokkaido, northern Japan, *Geology*, 21, 431-434, 1993.
- Lallemand, S. and Jolivet, L., Japan Sea: a pull apart basin. *Earth Planet. Sci. lett.*, 76, 375-389, 1985.
- Lee, J.S., Pétrologie et relations structurales des volcanites Crétacé à Cénozoïques de la Corée du Sud: implications géodynamiques sur la marge est-eurasiatique. Thèse de Doctorat de l'Université d'Orléans, 1988.
- Nakamura, K., Possible nascent trench along the eastern Japan sea as the convergent boundary between Eurasia and North American plates (in Japanese). *Bull. Earthquake Res. Inst.*, 58, 721-732, 1983.
- Nakamura, K., and Uyeda, S., Stress gradient in back arc regions and plate subduction. *J. Geophys. Res.*, 85, 6419-6428, 1980.
- Oda, H., Torii, M. and Hayashida, A., Paleomagnetic study and fission-track dating in Yanagawa and Takadate area, Northeast Japan, *Rock Mag. Paleogeophys.*, 19, 231-237, 1989.
- Otofuji, Y., Itaya, T., and Matsuda, T., Rapid rotation of southwest Japan - paleomagnetism and K-Ar ages of Miocene volcanic rocks of southwest Japan. *Geophys. J. Int.*, 105:397-405, 1991.
- Otofuji, Y. , and Matsuda T., Paleomagnetic evidence for the clockwize rotation of Southwest Japan. *Earth. Planet. Sci. Lett.*, 62, 349-359, 1983.

- Otofuji, Y. , and Matsuda, T., Timing of rotational motion of Southwest Japan inferred from paleomagnetism. *Earth Planet. Sci. Lett.*, 70, 373-382, 1984.
- Otofuji ,Y. , Matsuda T., Amount of clockwise rotation of Southwest Japan - fan shape opening of the southwestern part of the Japan Sea, *Earth Planet. Sci. Lett.*, 85, 289-301, 1987.
- Otofuji, Y. , Matsuda T., and Nohda, S., Paleomagnetic evidences for the Miocene counter clockwise rotation of northeast Japan - rifting process of the Japan arc. *Earth Planet. Sci. Lett.*, 75, 265-277, 1985.
- Otsuki, K., Reconstruction of Neogene tectonic stress field of Northeast Honshu arc from metalliferous veins. *Mem. Soc. Geol. Jpn.*, 32:281-304, 1989.
- Otsuki K. and Ehiro M., Major strike slip faults and their bearing on the spreading of the Japan Sea, *J. Phys. Earth*, supplement issue, 26: 537-555, 1978.
- Rozhdestvenskiy, V.S., The role of wrench faults in the structure of Sakhalin. *Geotectonics*, 16:323-332, 1982.
- Sillitoe, R. H., Metallogeny of an Andean type continental margin in South Korea, implications for opening of the Japan Sea. In M. Talwani, M., and Pitman III, W. C., eds, *Island Arcs, Deep Sea Trenches and Back Arc Basins*, Maurice Ewing Ser. (vol. 1), AGU, Washington, D. C, 303-310, 1977;
- Sugi, N., Chinzei, K., and Uyeda, S., Vertical crustal movements of northeast Japan since middle Miocene. In Hilde, W. C. T., and Uyeda, S., *Geodynamics of the Western Pacific and Indonesian Region*, Geodynamic series, AGU, Washington, 11, 317-329, 1983.
- Sugimura, A., Matsuda, T., Chinzei, K., and Nakamura, K., Quantitative distribution of late Cenozoic volcanic material in Japan. *Bull. Volcanol.*, 26, 125-140, 1963.
- Suzuki, K., On the Late Cenozoic history in the southern part of northeast Honshu in Japan. *Mem. Geol. Soc. Jpn.*, 32, 97-112, 1989.
- Tagami, T., Paleomagnetism and fission-track ages of the Kumano acidic rocks, News of Osaka Micropaleontologists, 9, 23-32, 1982.
- Takeshita, 1990.
- Takeuchi, T., Ozawa, T. and Kodama, K., Paleomagnetism of the Late Cretaceous to Neogene deposits in central Hokkaido, Japan and south Sakhalin of the USSR: multiple rotations caused by transcurrent faults, 29 th International Geological Congress, Kyoto, 24 august-3 september 1992, abstract, 108, 1992.
- Tamaki, K., Age estimation of the Japan sea on the basis of stratigraphy, basement depth and heat flow data. *J. Geomag. Geoelectr.*, 38, 427-446, 1986.
- Tamaki, K., Geological structure of the Japan sea and its tectonic implications. *Bulletin of the Geological Survey of Japan*, 39, 269-365, 1988.
- Tamaki, K., and Kobayashi, K., Geomagnetic anomaly lineation in the Japan Sea, *Marine Sci. Mon.*, 20, 705-710. (in Japanese), 1988.

- Tamaki, K., Suyehiro, K., Allan, J., Ingle, J.C., and Pisciotto, K., Tectonic synthesis and implications of Japan Sea ODP drilling, *Proc. ODP, Sci. Results*, 127/128, College Station, TX (Ocean Drilling Program), 1333-1350, 1992.
- Tanaka, H., Tsunakawa, H., Yamaguchi, H. and Kimura, G., Paleomagnetism of the Shakotan peninsula, West Hokkaido, Japan, *J. Geomag. Geoelectr.*, 43, 277-294, 1991.
- Tokuyama, H., Suyemasu, M., Tamaki, K., Nishiyama, E., Kuramoto, S., Suyehiro, K., Kinoshita, H., and Taira, A., Report on DELP cruises in the Japan Sea, Part III: seismic reflection studies in the Yamato Basin and the Yamato Rise area. *Bull. Earthq. Res. Inst., Univ. Tokyo*, 62, 367-390, 1987.
- Tosha, T. and Hamano, Y., Paleomagnetic study on the dyke swarm in the Oga peninsula, Northeast Honshu island, *J. Geomag. Geoelectr.*, 38, 349-360, 1986.
- Tosha, T., and Hamano, Y., Paleomagnetism of Tertiary rocks from the Oga peninsula and the rotation of northeast Japan. *Tectonics*, 7, 653-662, 1988.
- Tsuchiya, N., Submarine basalt volcanism of Miocene Aosawa formation in the Akita-Yamagata oil field basin, back-arc region of northeast Japan. *Mem. Geol. Soc. Jpn.*, 32, 399-408, 1989.
- Tsuchiya, N., Middle Miocene back-arc rift magmatism of basalt in the Northeast Japan arc. *Bull. Geol. Surv. Jpn.*, 41, 473-505, 1990.
- Usuta, M., Geotectonic history of the southern part of Akita prefecture, Northeast Japan. *Mem. Geol. Soc. Jpn.*, 32, 57-80, 1989.
- Yamaji, A., Geology of Atsumi area and early Miocene rifting in the Uetsu district, northeast Japan. *Mem. geol. Soc. Jpn.*, 32, 305-320, 1989.
- Yamaji, A., Rapid intra-arc rifting in Miocene northeast Japan. *Tectonics*, 9, 365-378, 1990.
- Yamazaki, T., Paleomagnetism of Miocene sedimentary rocks around Matsushima Bay, Northeast Japan and its implication for the time of the rotation of Northeast Japan, *J. Geomag. Geoelectr.*, 41, 533-548, 1989.
- Yaskawa, K. On the paleomagnetic approach to the origin of the Japan Sea, Nihon Kai (Japan Sea), 10, 120-126, 1979, in Japanese.

VI. CONCLUSIONS

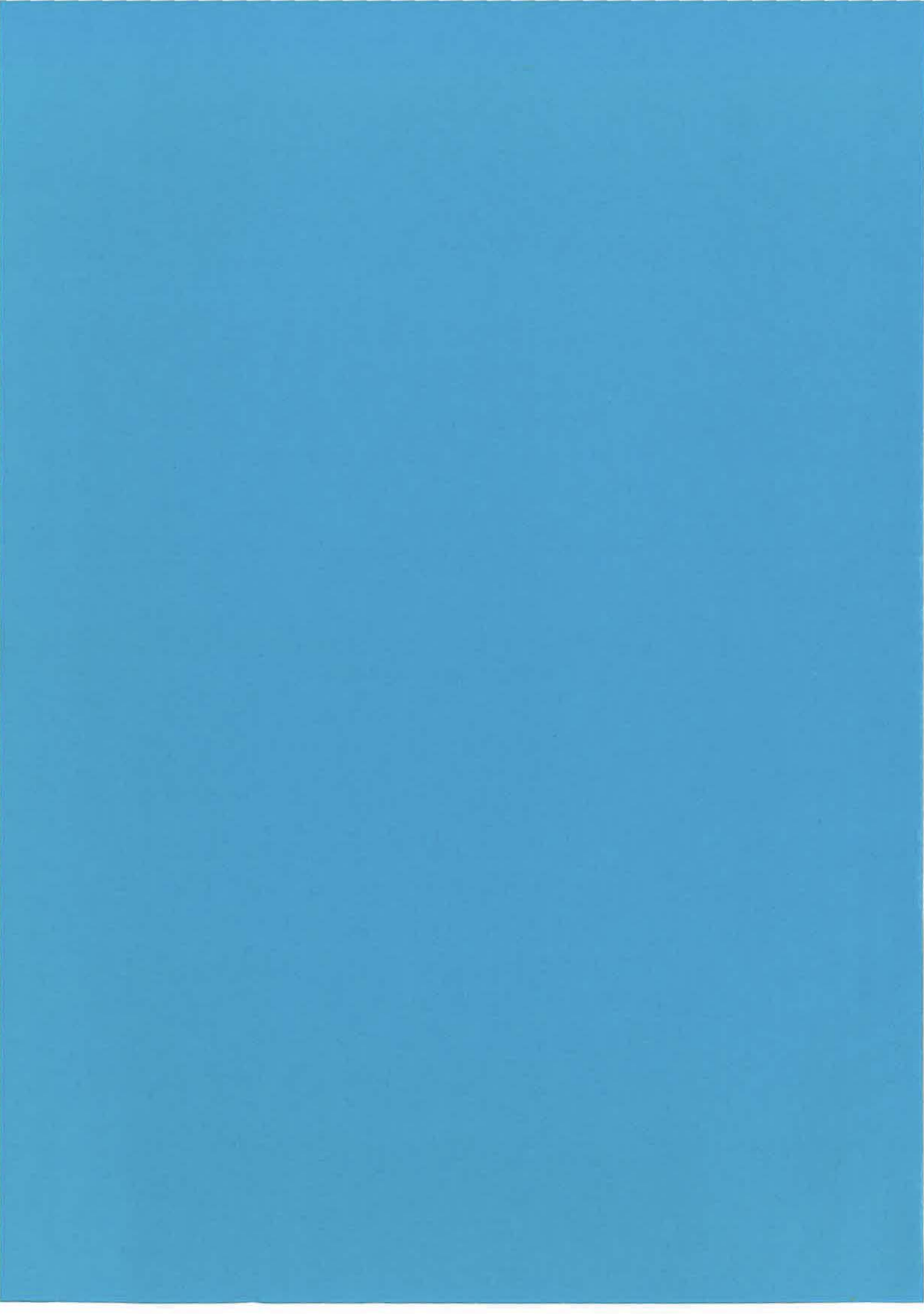
La marge sud de la mer du Japon est extensive au Miocène inférieur et moyen, tandis que les marges est et ouest sont des zones décrochantes dextres. La géométrie d'ouverture en pull-apart est donc acquise.

Un modèle d'ouverture satisfaisant, incluant données structurales et paléomagnétiques est obtenu. La mer du Japon s'ouvre au cœur d'une large zone de cisaillement dextre N-S, limitée à l'est et à l'ouest par deux zones décrochantes majeures. Dans cette zone de cisaillement dextre et le long des décrochements qui la limitent, les blocs tournent dans le sens horaire compatible avec le cisaillement dextre. En ce qui concerne le Japon sud-ouest, une partie de la rotation est susceptible d'être accommodée de façon rigide (d'un seul bloc), l'autre partie devant nécessairement trouver son origine dans la déformation interne de l'arc.

Dans le Japon NE, à l'extérieur des zones de déformation Néogène les roches d'âge Miocène inférieur ont subi une rotation anti-horaire. Il apparaît ainsi que les mouvements dextres dans les zones de déformation accommodent des rotations sénestres de blocs non déformés, vraisemblablement à l'intérieur d'une zone cisaillante sénestre d'échelle plus grande. Comme nous le verrons dans la quatrième partie, cette rotation peut s'expliquer si l'on considère comme Jolivet et al. (1990) qu'à l'échelle de l'Asie la zone de cisaillement dextre de la mer du Japon accorde la rotation anti-horaire de grands blocs continentaux, à l'intérieur d'une zone de cisaillement sénestre qui absorbe le mouvement vers le NE de l'Asie par rapport à la plate-forme russe sous la poussée de l'Inde. Le NE Honshu peut être considéré comme l'un de ces blocs rigides, tournant dans le sens anti-horaire en bordure de la zone de cisaillement dextre de la mer du Japon.

QUATRIÈME PARTIE

**OUVERTURE DE BASSINS MARGINAUX ET DÉFORMATION CONTINENTALE :
APPROCHE ANALOGIQUE**



QUATRIÈME PARTIE

OUVERTURE DE BASSINS MARGINAUX ET DÉFORMATION CONTINENTALE : APPROCHE ANALOGIQUE

I. INTRODUCTION

Nos travaux sur la déformation contemporaine de l'ouverture de la mer du Japon ont montré qu'il faut distinguer une composante décrochante d'affinité continentale, vraisemblablement liée à la collision Inde-Asie, d'une composante extensive proche de la zone de subduction et qui en dépendrait.

Davy et Cobbold (1988) ont réalisé des expériences analogiques qui ont fourni à Jolivet et al. (1990) un modèle reliant l'ouverture des bassins du NE asiatique à la collision Inde-Asie (Figure 29). Dans ces expériences, l'extension dynamique en bordure du modèle n'était pas pris en compte. La bordure est du modèle était libre mais ne se déplaçait que sous l'action de l'indentation. Pour tester l'interaction collision-extension, nous avons repris ces expériences avec un modèle susceptible de s'étaler sous propre poids pour fournir un moteur à l'extension en bordure du modèle.

Les résultats de ces expériences ne concernent pas uniquement l'ouverture des bassins marginaux, mais embrassent la déformation continentale dans son ensemble. C'est pourquoi nous présentons dans le premier chapitre de cette quatrième partie une brève revue de la déformation continentale de l'Asie depuis la collision de l'Inde, où sont en particulier décrits l'extension au Tibet, la déformation dans la zone de cisaillement dextre N-S à l'est du plateau du Tibet, et la déformation dans la zone de cisaillement sénestre Pamir-Stanovoï.

Le second chapitre consiste en un article qui décrit les expériences de modélisation et leurs résultats. En introduction, cet article comprend une revue de la déformation de la marge est-asiatique depuis l'Éocène, qui souligne l'importance de l'extension qui accompagne la collision Inde-Asie.

II. DÉFORMATION DE L'ASIE CONTINENTALE DEPUIS LA COLLISION AVEC L'INDE

A. DÉFORMATION ACTIVE EN ASIE

1. Convergence et extension en Himalaya et au Tibet

a. Cinématique de la convergence en Himalaya

L'Inde remonte vers le nord par rapport à la plate-forme stable de l'Eurasie à la vitesse de 53 mm/an à 90°E (DeMets et al., 1990). L'Himalaya est charrié sur l'Inde au niveau du "Main Boundary Thrust" (MBT) à un taux de 18 ± 7 mm/an (Lyon-Caen et Molnar, 1985 ; Molnar et al., 1987 ; Avouac et Tapponnier, 1993; Figures 44 et 45). L'épaisseur de la croûte augmente progressivement de l'Inde au Tibet en passant de 37-38 km au sud de l'Himalaya (Sharma et al., 1991) à 70 km sous le Tibet (Hirn et al., 1984 ; Zhao et al., 1991 ; Chen et Molnar, 1981 ; Romanowicz, 1982). Le long du MBT les vecteurs glissement des séismes sont orientés de façon radiale, et les axes P des mécanismes au foyer sont perpendiculaires aux contours topographiques (Armijo et al., 1986 ; Baranovski et al., 1984).

b. Cinématique de l'extension

Considérant que l'Inde est rigide, la distribution en éventail des vecteurs glissement implique un taux d'extension E-O de 18 ± 9 mm/an dans le Tibet (Molnar et Lyon-Caen, 1989 ; Armijo et al., 1986). Au sud du Tibet, l'extension active est absorbée par des failles normales N-S distribuées (Armijo et al., 1986 ; Molnar et Chen, 1983 ; Molnar et Tapponnier, 1978 ; Tapponnier et al., 1981). Armijo et al. (1986, 1989) ont montré que l'extension est associée à des mouvements décrochants dextres le long de la zone de failles de Karakorum-Jiali qui court de la faille du Karakorum à l'ouest, jusqu'au nord de la syntaxe est-indienne à l'est (Figure 46). Dans la partie est de la zone de failles de Karakorum-Jiali, Armijo et al. (1989) ont déduit un taux de mouvement holocène de 15 ± 7 mm/an. Ce taux est plus fort (32 mm/an) le long de la faille du Karakorum (cf. Avouac et Tapponnier, 1993). Dans l'est Himalayen, les trajectoires courbes de la déformation mettent en évidence du cisaillement dextre également dans les niveaux ductiles exhumés (Brun et al., 1985). Il n'est pas clair que la zone décrochante dextre se poursuive vers l'est au-delà de la syntaxe est-indienne, le long de la faille Jiali-Po Qu (Armijo et al., 1989) : Holt et al. (1991) fournissent des mécanismes au foyer de séismes le long de la terminaison nord de la faille de Sagaing qui montrent un raccourcissement NE-SO (Figure 47) peu compatible avec le lien extensif entre les failles de Jiali-Po Qu et Sagaing proposé par Armijo et al. (1989) (Figure 48).

Plus loin vers le nord, le plateau du Tibet est affecté par des failles normales et des décrochements conjugués. A l'intérieur du Tibet, aucune faille inverse ni aucun charriage ne

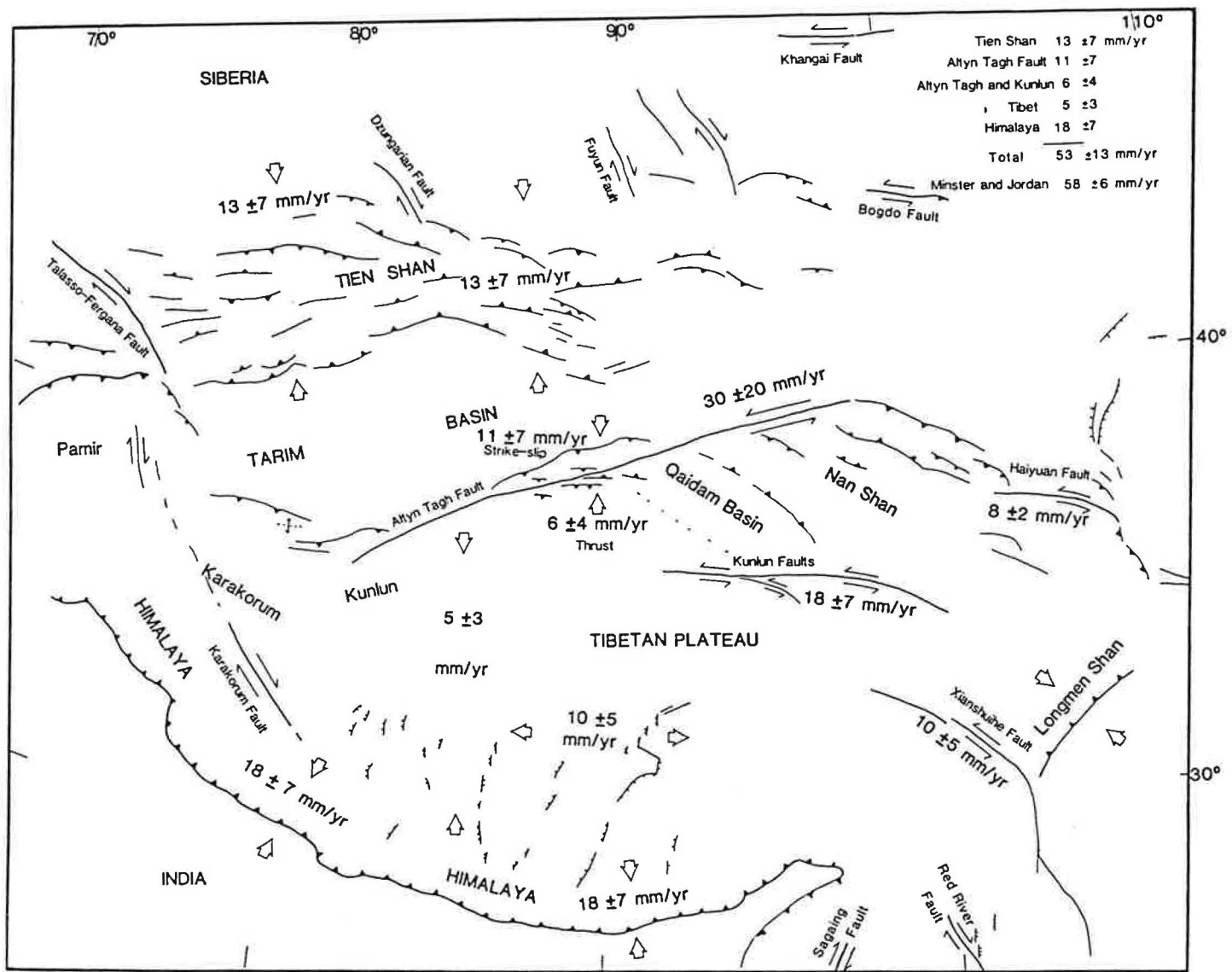


Figure 44. Carte des taux de mouvements le long des failles majeures et des taux de déformation distribuée en Asie centrale (d'après Molnar et al., 1987).

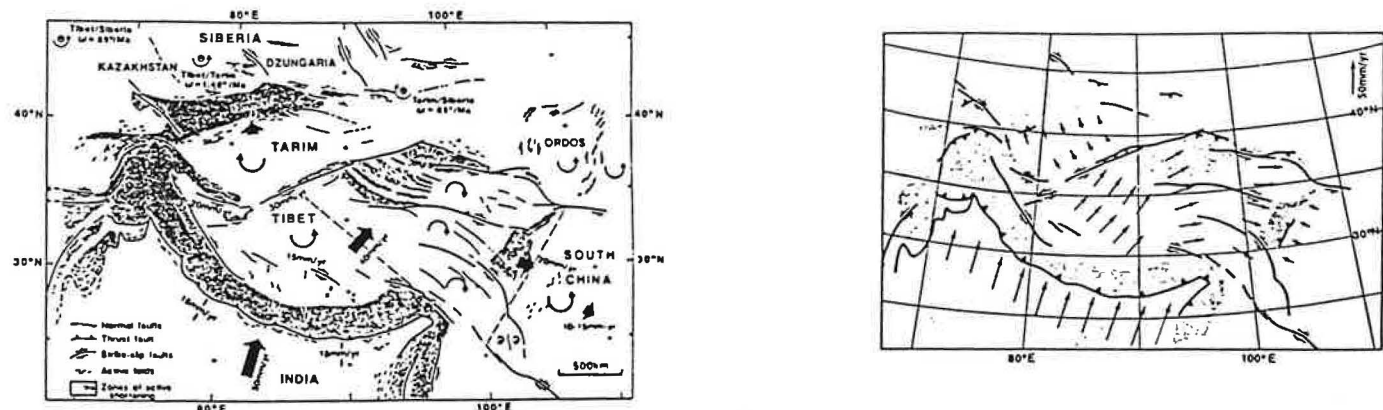


Figure 45. Modèle cinématique et champ de vitesses en Asie centrale par rapport à la Sibérie (d'après Avouac et Tapponnier, 1993).

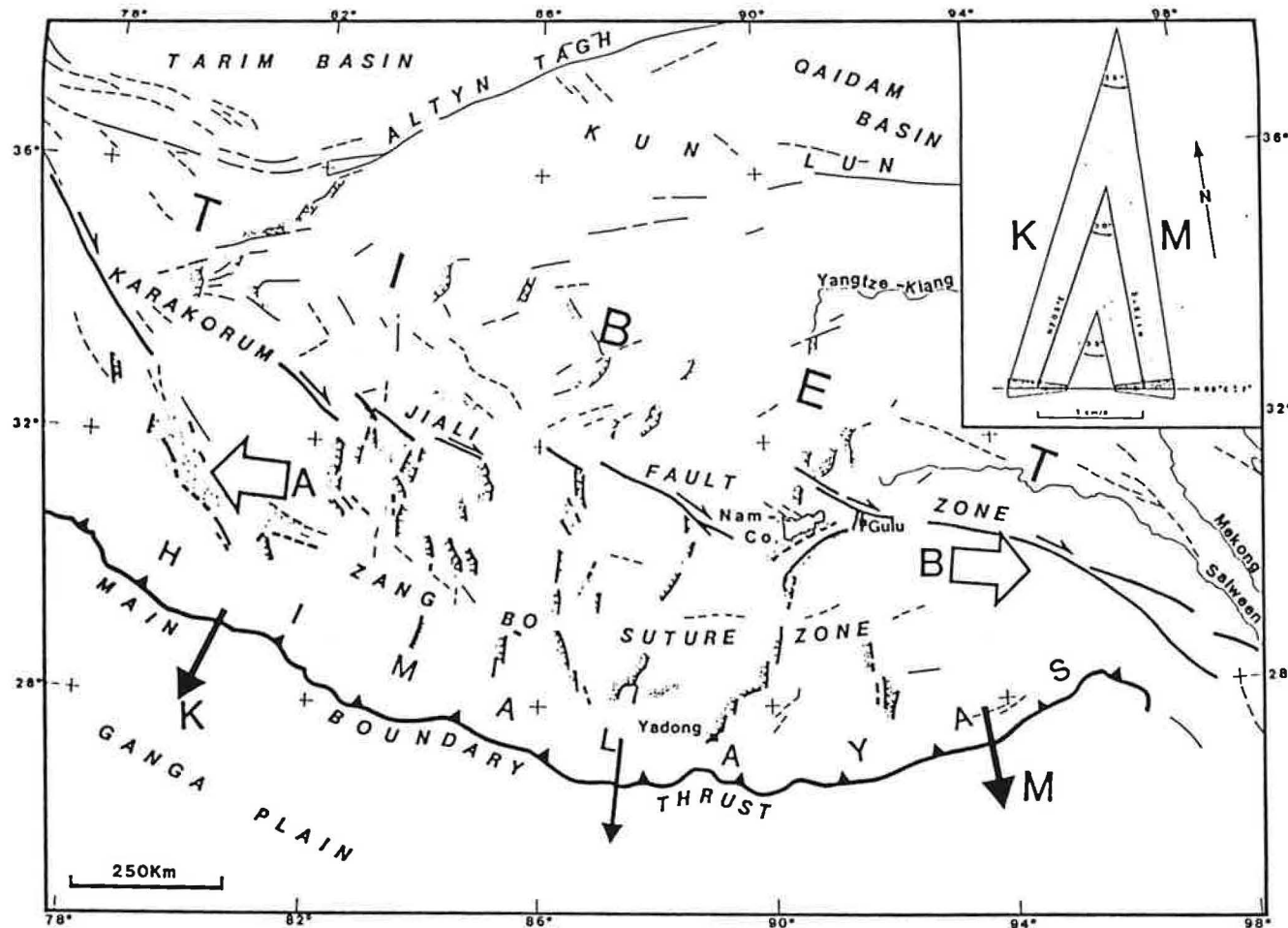


Figure 46. Cinématique des failles actives en Himalaya et dans le sud Tibet (d'après Armijo et al., 1986).

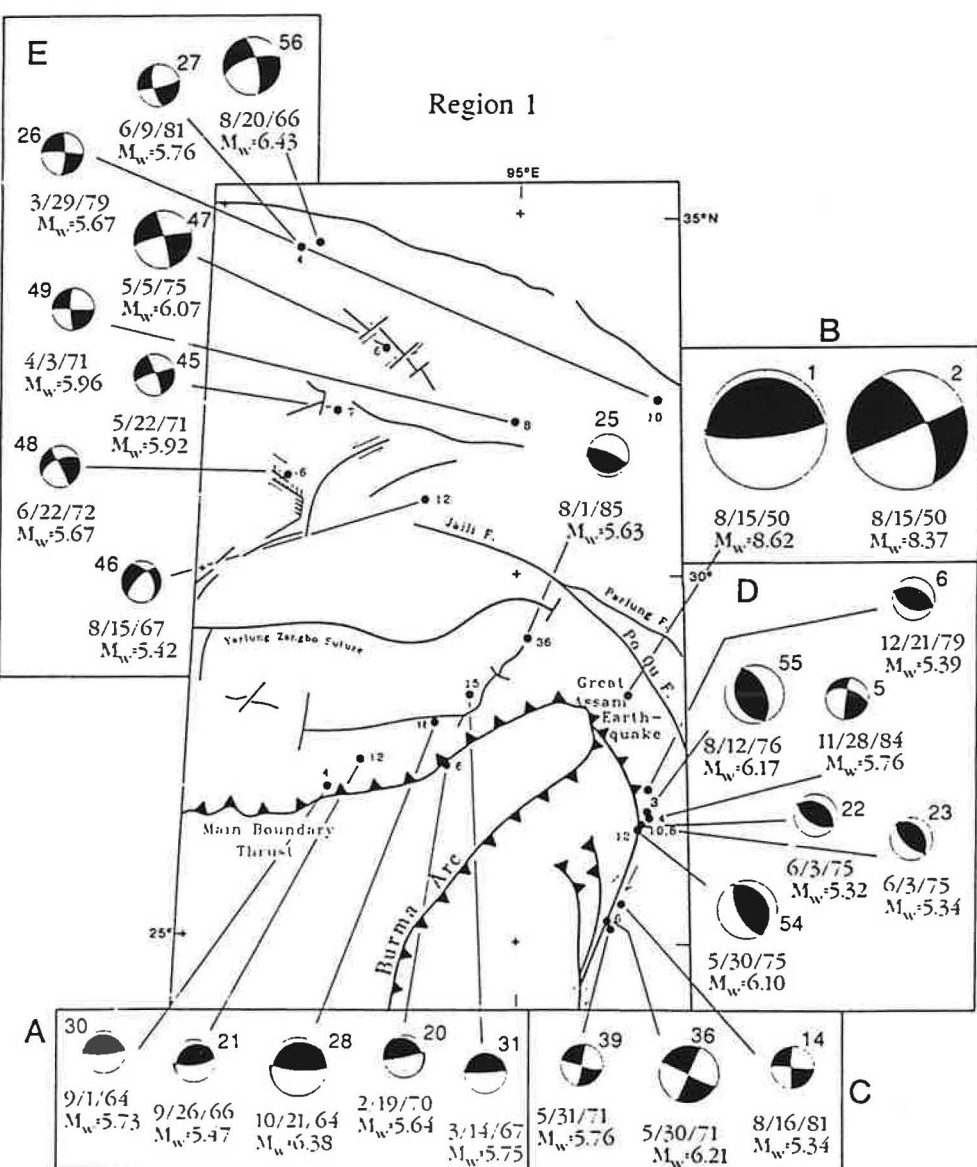


Figure 47. Carte sismotectonique de la syntaxe est-indienne avec des mécanismes au foyer compressif NE-SO sur la terminaison nord de la faille de Sagaing (Holt et al., 1991).

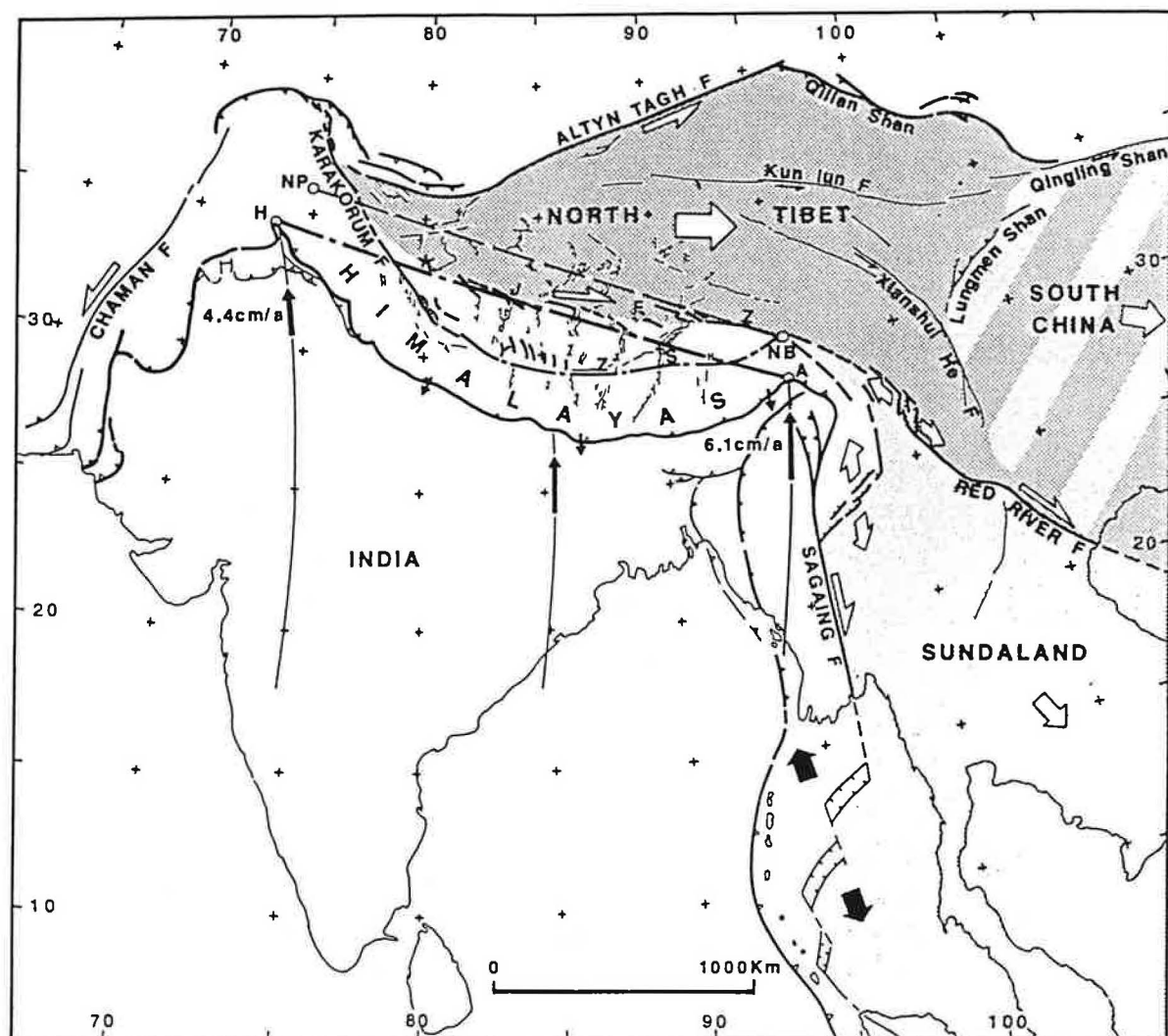


Figure 48. Cinématique de l'extrusion active au Tibet (d'après Armijo et al., 1989).

sont recensés, et une partie du raccourcissement N-S entre l'Inde et l'Asie est absorbé par le jeu des décrochements conjugués (Rotherty et Drury, 1984). Molnar et Chen (1983) ont montré à partir de l'analyse de la sismicité dans le Tibet que l'extension affecte la partie supérieure de la croûte (moins de 15 km), et vraisemblablement aussi le manteau supérieur (Figures 49 et 50) (Chen et al., 1981; Molnar et Lyon-Caen, 1989). La cohérence des directions des axes T des mécanismes au foyer des séismes dans la croûte et le manteau suggère que toute la lithosphère est affectée par l'extension dans un même champ de contraintes. Le fait que la sismicité et les failles sont distribuées sur tout le plateau du Tibet suggère aussi que la déformation est due à l'étalement de la croûte inférieure ductile (Miller, 1992).

c. Poids de la topographie et extension ductile

La topographie et les gradients topographiques jouent un rôle important dans la déformation active du Tibet (Mercier et al., 1987 ; Molnar et Lyon-Caen, 1988, 1989). Molnar et Lyon-Caen (1989) notent que les failles normales et décrochantes prévalent quand on s'élève au-dessus de 5000 m, et que les axes P des mécanismes au foyer sont parallèles aux gradients topographiques tout autour du Tibet, comme le prédisent les modélisations numériques de England et Houseman (1986) de déformation dans une couche mince à comportement visqueux.

Burchfield et Royden (1985) interprètent l'extension Miocène N-S qu'ont mis en évidence Burg et Chen (1984) en Himalaya, comme l'effondrement gravitaire du front topographique entre l'Inde et l'Himalaya. La carte sismotectonique de la Chine (1985) montre que la sismicité suit les gradients topographiques de la bordure est du Tibet (Figure 51).

Considérant que le gradient de pression latérale dans la croûte inférieure ductile dépend du gradient du poids de la topographie (Fleitout et Froidevaux, 1982 ; Bird, 1991), et que les gradients topographiques forts coïncident avec la déformation active au Tibet, il est tentant de relier la déformation dans la croûte cassante à l'étalement dans la croûte inférieure. L'extension a débuté au sud Tibet au Miocène supérieur, après que la croûte eut été épaisse (Mercier et al., 1987). Padd et Kidd (1992) décrivent un décollement extensif d'âge Miocène supérieur qui montre que l'extension était aussi active dans la croûte inférieure à cette époque. La transition entre épaisseissement et extension au Miocène supérieur peut correspondre à l'initiation de "l'extrusion latérale de la croûte inférieure de dessous la topographie grandissante" (Bird, 1991).

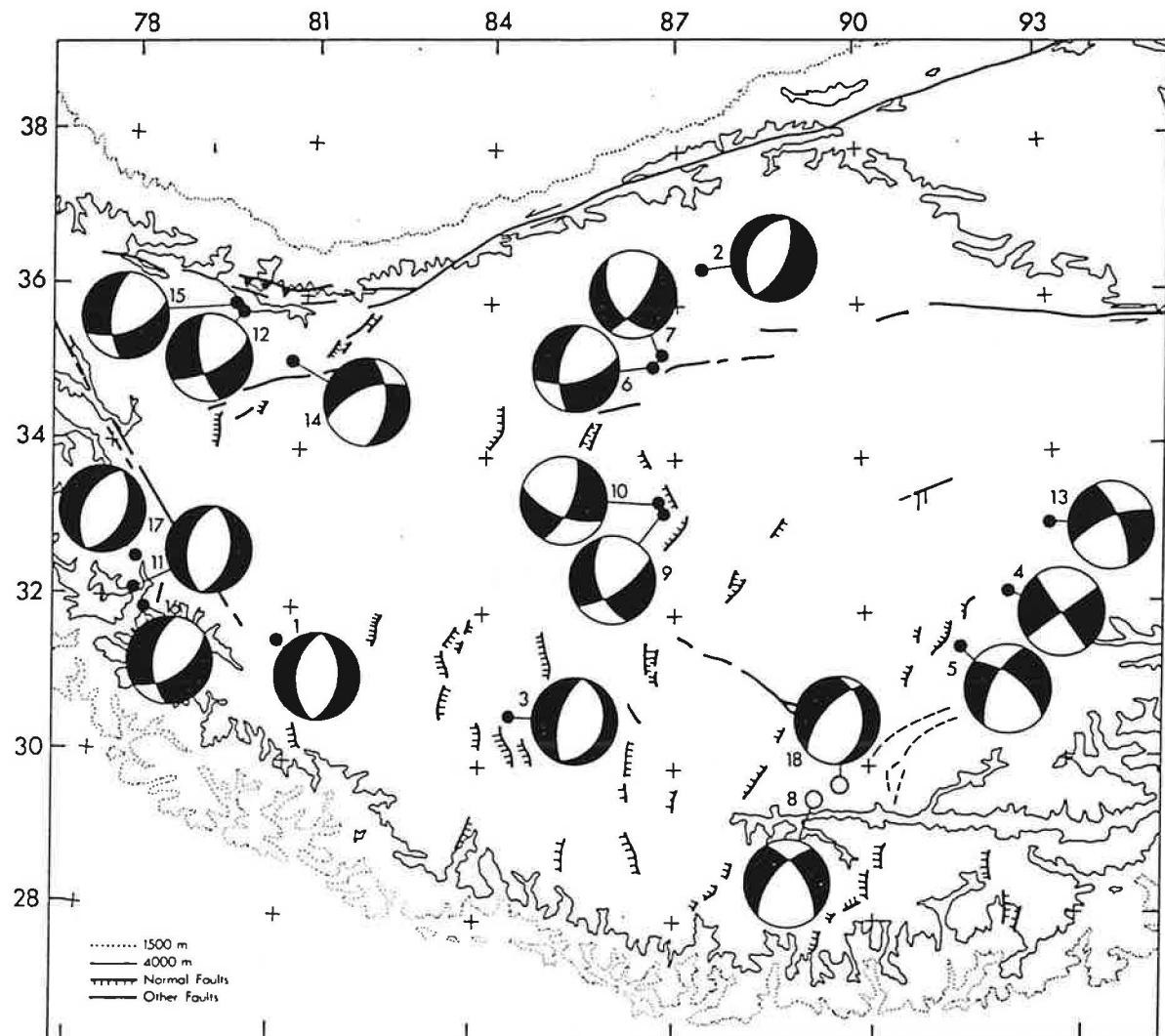
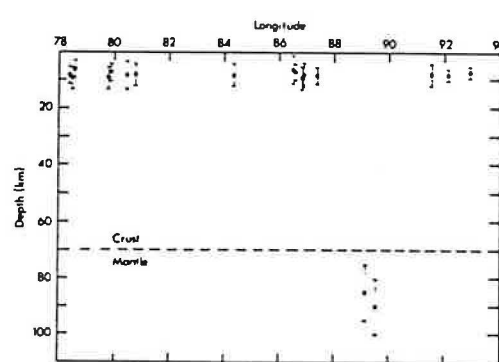
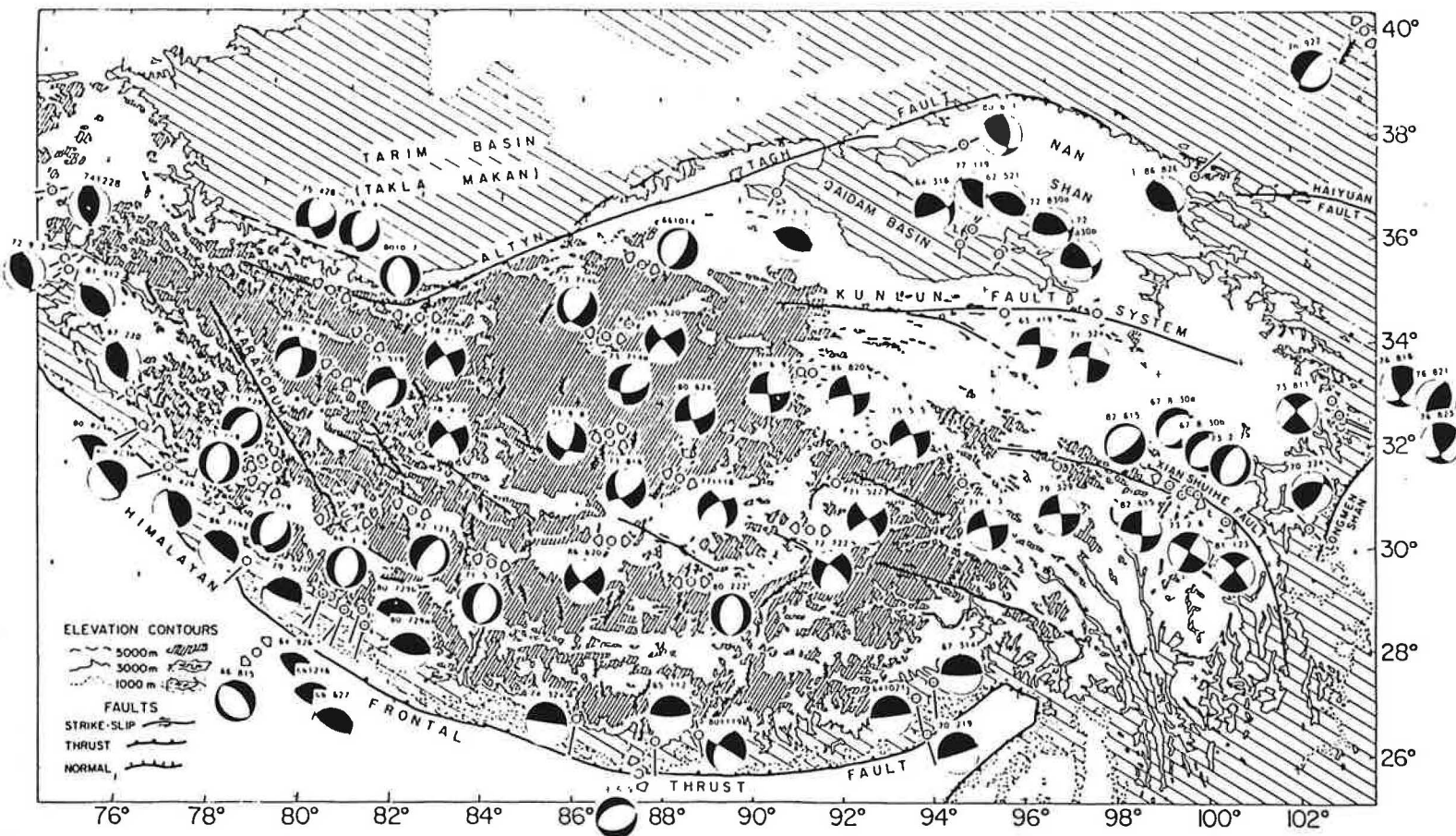


Figure 49. Carte sismotectonique du plateau du Tibet et coupe longitudinale montrant la profondeur des séismes. Les séismes 8 et 18 sont localisés dans le manteau supérieur. Les axes T des séismes sont globalement E-O sur tout le plateau dans la croûte supérieure et le manteau supérieur (d'après Molnar et Chen, 1983).





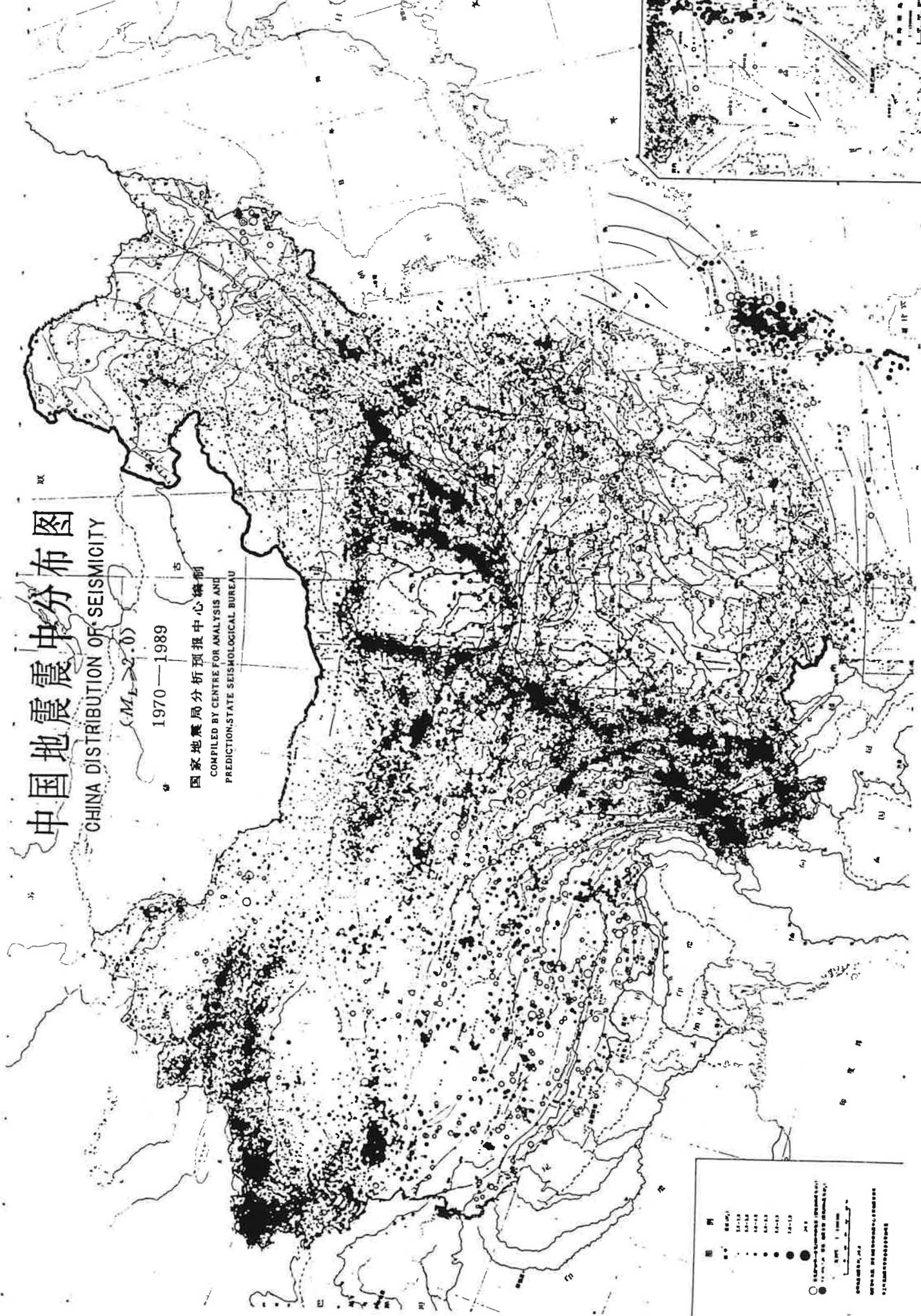


Figure 51. Sismicité en Chine. La sismicité suit les gradients topographiques, excepté au nord du plateau du Tibet le long de la faille de l'Altyn Tagh.

2. Décrochements sénestres et cisaillement dextre N-S à l'est du Tibet

Les mouvements décrochants sénestres prévalent à l'est du plateau Tibétain (Figures 3 et 44) le long de :

- (1) la faille de Xanshuihe à un taux de 15 ± 5 mm/an sur le segment nord-ouest tombant à 5 mm/an sur le segment sud-est (Allen et al., 1991 ; Molnar et Deng, 1984) ;
- (2) le système de failles des Kunlun à un taux de 13 mm/an sur le segment nord et 10 mm/an sur le segment sud (Kidd et Molnar, 1988) ;
- (3) la faille de Haiyuan à un taux de 5 à 10 mm/an (Burchfield et al., 1991) ;
- (4) la faille de Chang Ma à un taux de 5 ± 2 mm/an (Peltzer et al., 1988).

Les failles de Xanshuihe et des Kunlun sont courbes autour de la syntaxe est-indienne et le mouvement sénestre le long de ces failles a pour double effet une rotation autour de la syntaxe et l'extrusion vers l'est du Tibet par rapport à la Chine du nord (Molnar et Lyon-Caen, 1989). Ces failles ne décalent pas de manière significative les contours topographiques du Tibet. Cobbold et Davy (1988), Dewey et al. (1988), Molnar et Lyon-Caen (1989), décrivent la partie est du plateau du Tibet comme une large zone de cisaillement dextre accommodant le mouvement vers le nord du Tibet par rapport à la Chine du sud (Figure 52), et England et Molnar (1990) puis Holt et al. (1991) ont suggéré que les mouvements sénestres le long des principales failles de l'est tibétain accommodaient la rotation horaire de blocs rigides à l'intérieur de cette large zone de cisaillement dextre (Figure 53).

On peut faire quelques remarques concernant ce modèle de cisaillement simple N-S. D'abord, le cisaillement simple est susceptible d'accompagner des taux de rotation diminuant vers le nord, tels qu'ils sont déduits de la déformation active à l'est du Tibet (Holt et al., 1993), à condition que le taux de cisaillement diminue aussi vers le nord, ce qui requiert du raccourcissement N-S à l'intérieur du Tibet qui n'est pas documenté dans la déformation active. D'autre part, un système de blocs limités par des failles courbes (telles que la faille de Xanshuihe) est vraisemblablement instable, dans la mesure où des segments de faille deviennent rapidement mal orientés par rapport au cisaillement général. C'est d'ailleurs le cas d'un segment de la faille de Xanshuihe, nommé faille d'Annighe dans Allen et al. (1982), parfaitement N-S et sénestre à l'intérieur de la zone de cisaillement N-S dextre (voir Figure 55). Pour éviter ce problème, Burchfield et Royden (1991) suggèrent que la zone de cisaillement dextre n'inclut pas la faille d'Annighe et se situe à l'ouest de celle-ci. Notons aussi que dans toutes les expériences analogiques et numériques, les failles ou zones de cisaillement courbes telles que la faille de Xanshuihe qui apparaissent autour du coin NE du poinçon sont systématiquement dextres (Tapponnier et al., 1982 ; Houseman et England, 1986 ; Davy et Cobbond, 1988). Enfin, Nur et al. (1986) ont montré que des rotations excédant 45° requièrent plus d'un jeu de failles qui tournent. Les rotations paléomagnétiques

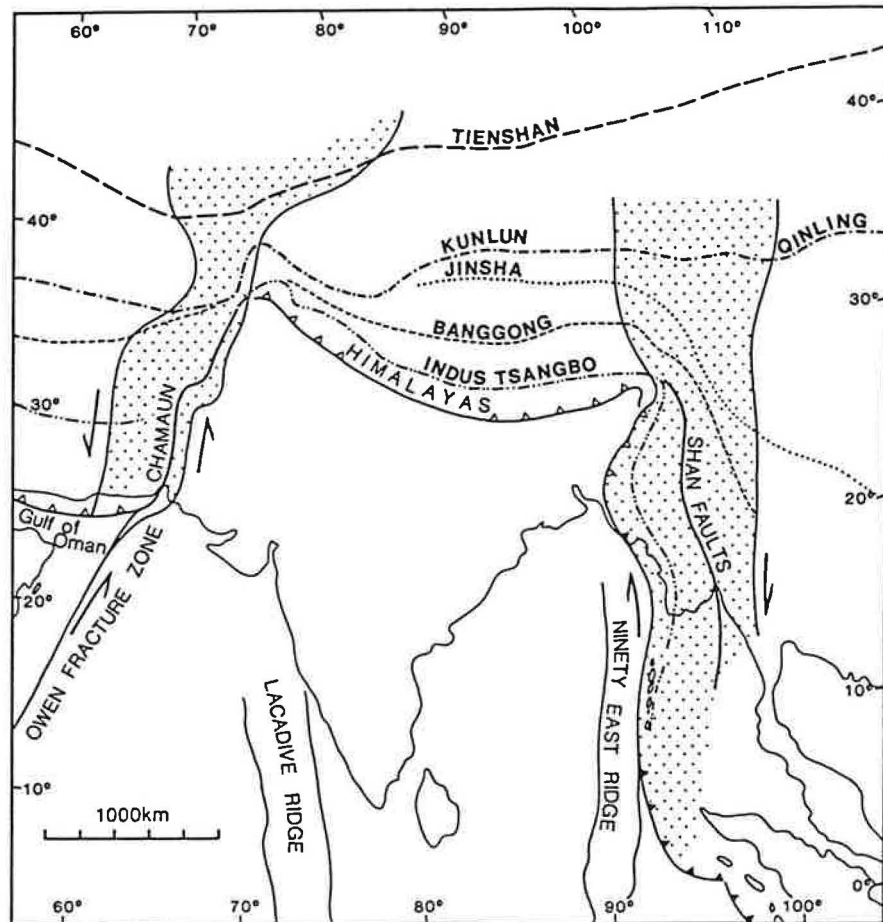


Figure 52. Carte des sutures téthysiennes déformées par la collision Inde-Asie. Deux zones de cisaillement sont représentées de part et d'autre de l'Inde en pointillés (d'après Dewey et al., 1988).

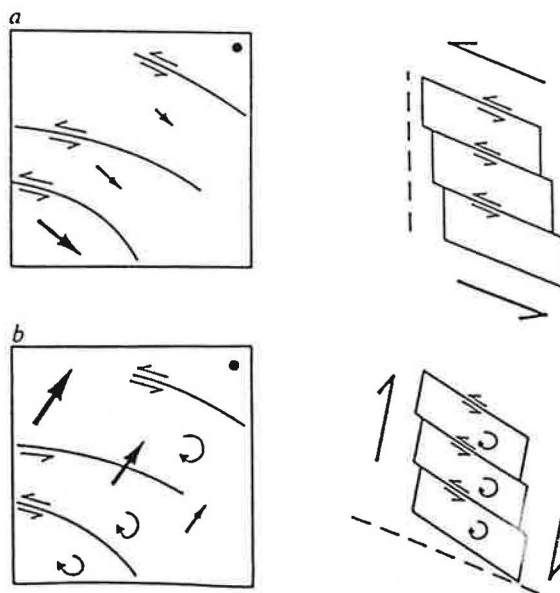


Figure 53. Deux interprétations des failles sénestres de l'est du Tibet et champs de vitesse correspondant: (1) extrusion vers l'est et (2) cisaillement simple N-S accommodé par des rotations de blocs (d'après England et Molnar, 1990).

dépassent 45° à l'est du Tibet (Otofuji et al., 1990) où un seul jeu de failles sénestres est pourtant documenté.

3. Bordures nord et est du plateau du Tibet : extrusion de la Chine du sud ?

La faille de l'Altyn Tagh qui limite au nord-ouest le plateau du Tibet est le siège de mouvements sénestres, peut-être à un taux aussi fort que 30 ± 20 mm/an bien qu'il n'y ait pas eu de gros séisme le long de cette faille depuis 1897 (Molnar et al., 1987; Peltzer et al., 1989). Des chevauchements et des plis sont décrits sur les bordures nord et nord-est du Tibet. Des séismes compressifs le long d'accidents est-ouest sont documentés dans l'Altyn Tagh (Molnar et al., 1987), et, dans le bassin du Qaidam et les régions du Nan Shan et de l'Haiyuan au NE Tibet, des plis et des chevauchements d'orientation NO-SE mettent en évidence un raccourcissement NE-SO (Tapponnier et Molnar, 1977 ; Deng Qidong et al., 1984 ; Meyer, 1991; Burchfield et al., 1991 ; Zhang Peizhen et al., 1991). Cette déformation compressive a débuté au Pliocène dans la région de l'Haiyuan, ce qui suggère que le plateau du Tibet s'étend progressivement vers le nord (Burchfield et al., 1991). Plus loin vers le sud-est, le chevauchement du Longmenshan accommode du raccourcissement NO-SE. Les taux de raccourcissement n'étant pas connu dans la partie est du Tibet, on ne peut pas conclure à l'extrusion vers l'est de la Chine du sud entre la faille du Fleuve Rouge et le Qinling Shan comme le suggèrent Tapponnier et al. (1982 ; 1986) (Figure 54).

Néanmoins, la faille du Fleuve Rouge accommode des mouvements dextres à un taux de 2 à peut-être 5 mm/an (Allen et al., 1984), et des mouvements sénestres Quaternaires sont décrits dans le Qinling Shan (Peltzer et al., 1985 ; Wang, 1987). Molnar et Deng (1984) ont calculé des taux moyens de déformation en Asie à partir des paramètres focaux des séismes les plus importants, et en déduisent que la Chine du sud migre vers l'est par rapport à la Sibérie à une vitesse de 21 mm/an. Holt et al. (1991) ont effectué des calculs identiques à partir des données de 53 séismes dans la région entourant la syntaxe est-indienne. Ils déduisent, à partir des tenseurs de moment des séismes, le champ de vitesse par rapport à la Chine du sud fixe, et calculent que, à 90°E , sont absorbés 38 ± 12 mm/an du mouvement relatif Inde-Chine du sud par des décrochements, des failles normales, et des rotations horaires au Myanmar (ex-Birmanie), dans le Yunnan, et dans l'est Tibétain (Figure 55). Ils ne prennent en compte dans leurs calculs ni les mouvements décrochants dans la partie sud de la faille de Sagaing, ni la totalité des mouvements chevauchants dans l'est Himalayen, qui sont susceptibles d'absorber le reste du mouvement Inde-Chine du sud. Le vecteur vitesse de l'Inde par rapport à la Chine du sud qu'ils calculent montre une légère déviation vers le nord-ouest par rapport au vecteur vitesse Inde-Eurasie du modèle NUVEL-1 (DeMets et al., 1990). Cette déviation peut être due à une composante de raccourcissement NE-SO dans la syntaxe est-indienne, comme ils le suggèrent, et/ou à l'extrusion vers l'est de la Chine du sud par rapport à

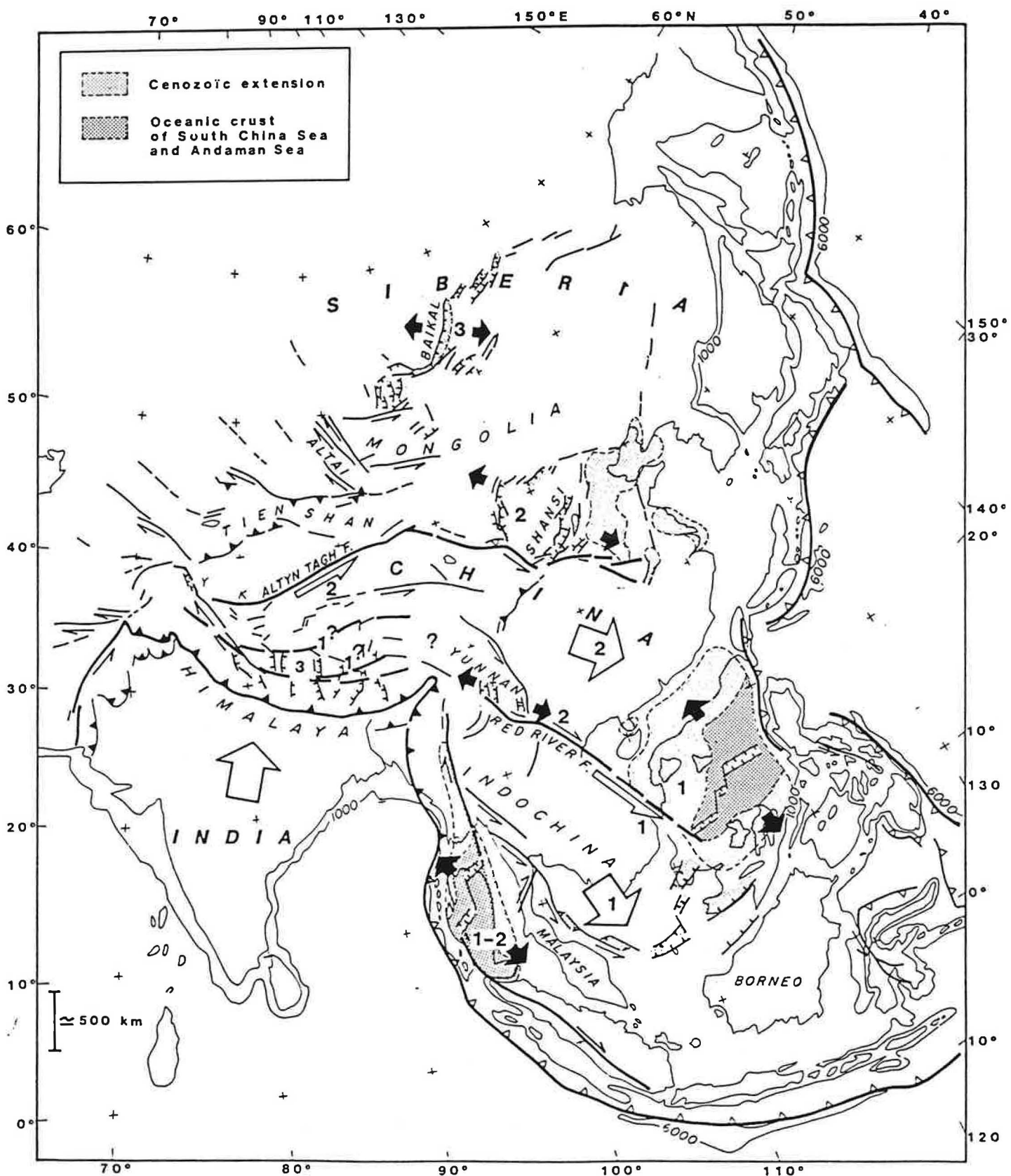


Figure 54. Cinématique de l'extrusion en Asie en 3 phases: 1= 50 à 20 Ma; 2 = 20 à 0 Ma; 3 = actuel et futur
(d'après Tapponnier et al., 1982).

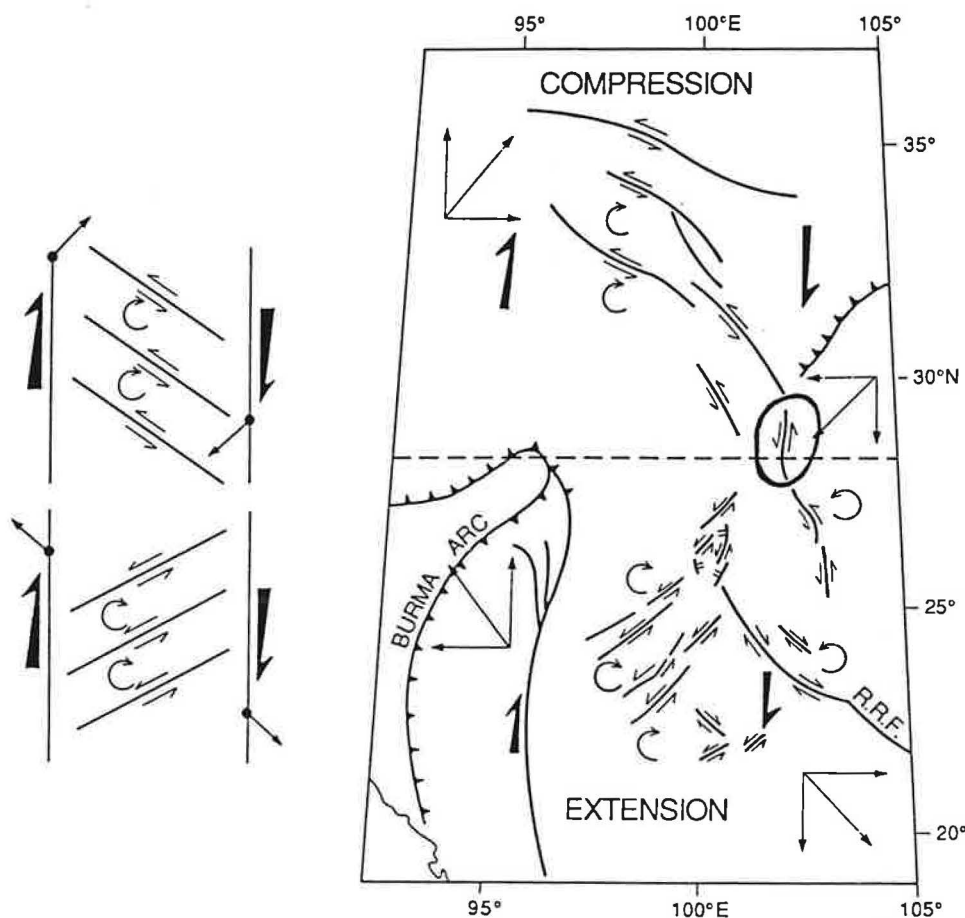


Figure 55. Cisaillement dextre N-S distribué dans la région de la syntaxe est-indienne et de l'est tibétain (d'après Holt et al., 1991). On remarquera le segment N-S de la faille de Xanshuihe (entouré), nommé faille d'Anninghe par Allen et al. (1991), sénestre à l'intérieur de la zone de cisaillement dextre N-S.

l'Eurasie. Il est vrai que si la Chine du Sud était extrudée vers l'est de manière significative, on attendrait de l'extension active en Chine du sud étant donné les directions divergentes des rails de l'extrusion que sont le Qinling Shan et la faille du Fleuve Rouge.

4. La zone de cisaillement sénestre trans-asiatique

A l'ouest de l'Inde, le mouvement relatif Inde-Asie est absorbé par des mouvements sénestres le long de la faille de Chaman, et par des plis et des chevauchements. Cette zone transpressive transfère le mouvement de convergence N-S depuis le prisme d'accrétion du Makhran jusqu'à l'Himalaya pakistanaise, où sont documentés une série de chevauchements courbes (Coward et Butler, 1985) jusqu'au plateau du Pamir. Une large zone de déformation court depuis le Pamir jusqu'aux Monts Stanovoï en Asie du nord-est, à travers le Tien Shan, l'Altai, les Monts Saïan, et la région du Baikal (Figure 56). Des chevauchements est-ouest sont décrits au Tien Shan (Tapponnier et Molnar, 1979 ; Nelson et al., 1987), le taux de raccourcissement N-S à travers le Tien Shan étant estimé à 13 ± 7 mm/an (Molnar et Deng, 1987), et 6 ± 3 mm/an dans le Tien Shan oriental (Avouac et al., 1993). L'Altai est dominé par des décrochements conjugués dont le jeu accommode un raccourcissement NNE-SSO (Tapponnier et Molnar, 1979). Les estimations des taux de raccourcissement finis N-S de Le Pichon et al. (1992), qui prennent en compte uniquement la topographie, montrent que les mêmes taux de raccourcissement finis ont été accommodés dans le Tien Shan et l'Altai. Une série de décrochements dextres de direction NO-SE sont décrits du Tien Shan à l'Altai, pénétrant dans la plate-forme eurasienne stable (Tapponnier et Molnar, 1979 ; Figure 3). Comme l'ont noté Cobbold et Davy (1988), ces décrochements sont susceptibles d'accommoder des rotations anti-horaires de blocs rigides à l'intérieur d'une large zone de cisaillement sénestre NE-SO. Le cisaillement sénestre est d'ailleurs suggéré par l'arrangement en échelon des chaînons montagneux du Tien Shan à l'Altai (Cobbold et Davy, 1988). Plus loin vers le nord-est, le système de rift du Baikal s'ouvre depuis l'Éocène, mais il est actif surtout depuis le Pliocène (Florensov, 1969). Des failles normales NE-SO sont associées à des décrochements sénestres E-O (Tapponnier et Molnar, 1979 ; Zonenshain et Savostin, 1981 ; Deverchère et al., 1991, 1993 ; Hutchinson et al., 1992 ; Sherman, 1992). Dans les Monts Stanovoï, des mouvements sénestres E-O (Parfenoy et al. 1987) et du raccourcissement N-S (Zonenshain et Savostin, 1981) sont décrits.

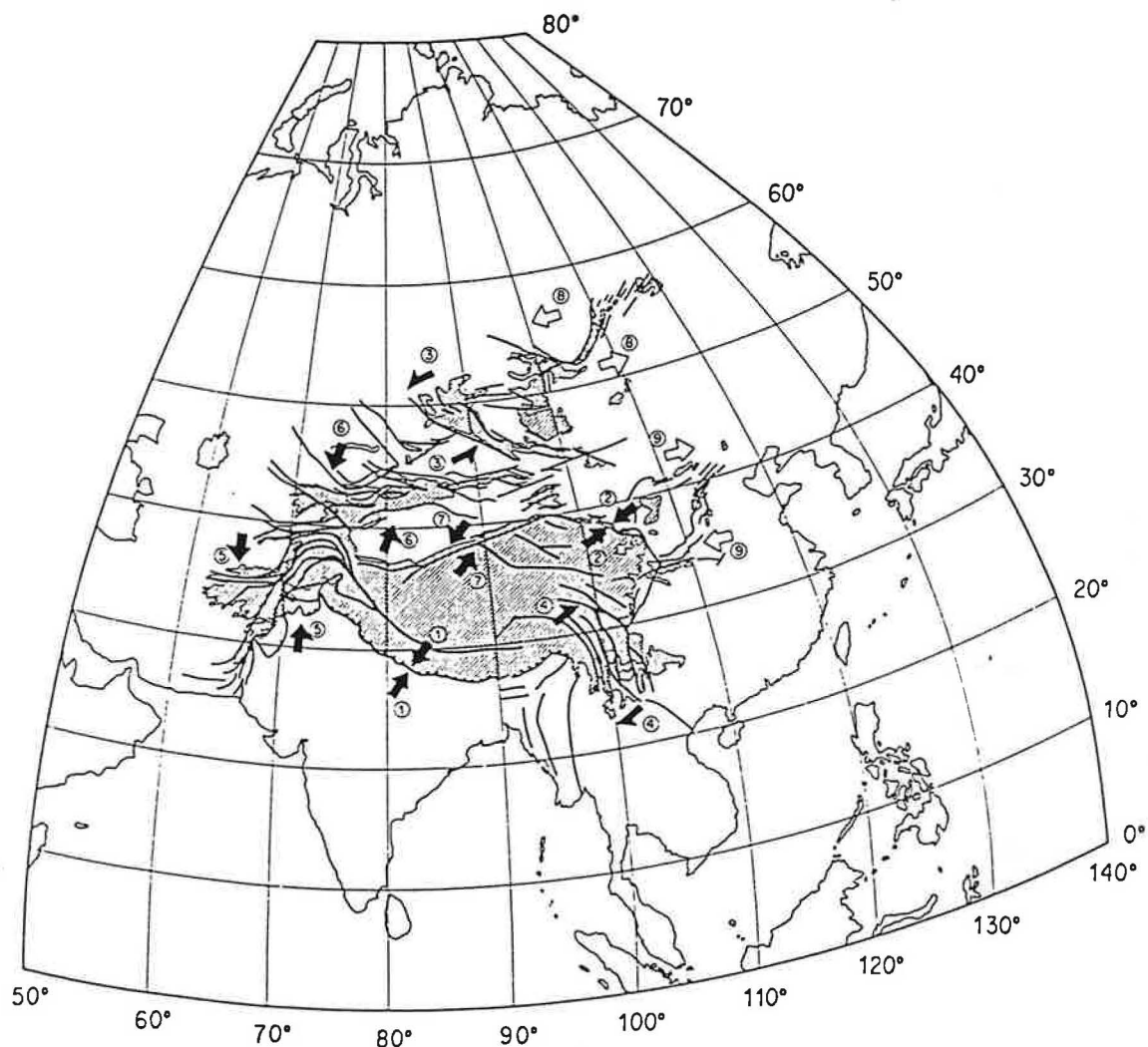


Figure 56. Géométrie de la déformation Cénozoïque en Asie montrant la zone de cisaillement sénestre trans-asiatique Pamir-Tien Shan-Altaï-Baïkal-Stanovoï (d'après Cobbold et Davy, 1988).

B. DEFORMATION FINIE EN ASIE

1. Épaississement

Les données paléomagnétiques montrent que le Tibet a été poussé vers le nord dans l'Asie de 2000 km environ depuis la collision Inde-Asie (Achache et al., 1984 ; Westphal et Pozzi, 1983), alors que la plate-forme eurasienne restait stable (Irving, 1977). La marge indienne a aussi subi un raccourcissement de plusieurs centaines de kilomètres depuis la collision (Besse et al., 1984). Comme le notent Dewey et al. (1988), les sutures téthysiennes en Asie qui ont été déformées pendant la collision sont actuellement incurvées autour de la syntaxe est-indienne et leur courbure diminue quand on va vers le nord, ce qui suggère un amortissement progressif de la déformation depuis le front Himalayen jusqu'à la plate-forme eurasienne. Cette remarque supporte l'idée que la lithosphère continentale se déforme comme un milieu continu et que la plus grande part de la déformation est absorbée au front du poinçon indien par épaississement. Sur le terrain, l'épaississement de la croûte depuis la collision est mis en évidence par des plis, des failles inverses et des chevauchements qui affectent les séries Oligo-Miocène au Tibet (voir par exemple Mercier et al., 1987). Cependant, d'après les calculs de Le Pichon et al. (1992, article en annexe), le raccourcissement calculé par la cinématique n'est pas totalement équilibré par l'excès de masse emmagasiné dans la croûte asiatique épaisse, et une partie significative de la quantité totale de raccourcissement doit être absorbé par extrusion de croûte non épaisse ou perte de croûte inférieure dans le manteau.

2. Extrusion

Tapponnier et al. (1986 ; 1990) et Leloup al. (1993) ont montré que la chaîne métamorphique de l'Ailao Shan, parallèle à la faille du Fleuve Rouge en Chine du sud, a été déformée par cisaillement sénestre dans des conditions de hautes températures avant 23 Ma (Schärer et al., 1990), et qu'elle a accommodé un mouvement fini sénestre substantiel (Lacassin et al., 1993) entre l'Indochine et la Chine du sud. Ils concluent que cette observation démontre la dérive vers l'est de l'Indochine et supporte le modèle d'extrusion proposé par Tapponnier et al. (1982 ; 1986) (Figure 54). On peut cependant estimer que le mouvement sénestre ne fait qu'accorder la rotation horaire de l'Indochine, 20°-30° depuis le Crétacé (Chen et Courtillot, 1989 ; Funahara et al., 1993 ; Yang et Besse, 1994), sous l'effet du cisaillement dextre de toute l'Asie du sud-est provoqué par la remontée de l'Inde vers le nord. Pour un taux de rotation fini donné, le mouvement entre des blocs rigides qui tournent est fonction de la largeur des blocs : plus les blocs sont larges, moins les mouvements sont distribués et plus ils sont grands. Pour un grand bloc continental comme

l'Indochine, large de 500 km entre la faille du Fleuve Rouge et la faille de Wang Chao (ou Mae Ping), on peut s'attendre à des mouvements sénestres significatifs pour accommoder la rotation horaire de 20°-30°.

C. CONCLUSION

Dans la zone de collision, la déformation est plutôt symétrique. De part et d'autre de l'Inde, le cisaillement provoqué par la remontée vers le nord de l'Inde est absorbé le long de failles décrochantes, la faille de Sagaing et la faille de Chaman, et plus au nord il est distribué dans deux larges zones de déformation, la zone de cisaillement dextre de l'est Tibétain et la zone de cisaillement sénestre Pamir-Altaï. L'épaississement est concentré entre ces deux zones de cisaillement.

Si l'on considère l'Asie dans son ensemble, la déformation est cependant nettement asymétrique. Alors que le mouvement de l'Inde est dirigé vers le nord depuis 45 Ma, la topographie produite par la collision s'inscrit dans un triangle basculé vers le NE, ayant pour base l'Inde et pour sommet les Monts Stanovoï (Figure 1). Il est limité au nord-ouest et à l'est par deux zones de cisaillement conjuguées, mais à l'est la zone de cisaillement dextre, qui part de la syntaxe est-indienne, ne dépasse pas la limite nord du bloc Ordos, tandis qu'au nord-ouest la zone de cisaillement sénestre trans-asiatique monte jusqu'aux Monts Stanovoï. Au front de l'Inde, la topographie du Tibet est extrudée vers l'est au-delà de la syntaxe est-indienne. L'Asie du sud-est a aussi été largement affectée par la collision Inde-Asie dans la mesure où elle a subi une rotation de 20°-30° consécutive à la collision. Par comparaison, le Zagros et l'ensemble de l'Eurasie ont été totalement isolés de la collision par la zone de déformation qui débute dans l'océan Indien par la zone de fracture d'Owen, se poursuit à terre par la faille de Chaman, et se prolonge jusqu'au Pamir et aux Monts Stanovoï. L'extension qui a affecté toute la marge est et sud-est asiatique entre l'Éocène et le Miocène moyen s'ajoute à cette asymétrie globale de la déformation directement liée à la collision.

Le concept de conditions aux limites asymétriques et de bordure libre à l'est, mis en pratique par Tapponnier et al. (1982) dans leurs expériences d'indentation, est donc largement justifié par l'asymétrie globale de la déformation en Asie. Dans les nouvelles expériences d'indentation que nous présentons, nous avons pris en compte également une composante d'extension dynamique le long de la bordure libre pour modéliser l'extension de la marge asiatique pendant la collision Inde-Asie.

III. DÉFORMATION CONTINENTALE ET EXTENSION MARGINALE : article "Role of extension during collision tectonics : an analogue experimental approach"

Résumé : Nous avons réalisé de nouvelles expériences d'indentation pour étudier l'interaction collision-extension dans la déformation continentale. Nous utilisons un modèle rhéologique de lithosphère continentale à trois couches (croûte supérieure, croûte inférieure, manteau lithosphérique). L'indentation est réalisée par un poinçon rigide, et l'extension est gouvernée par l'étalement gravitaire du modèle. Ce dispositif est testé pour différentes durées d'extension (étalement avant indentation), différents taux d'extension dans le modèle contrôlés par la présence ou l'absence de confinement latéral, et différentes vitesses d'indentation.

Collision et extension interagissent dans la partie nord-est du modèle. Ce domaine est affecté par des décrochements conjugués produits par l'indentation, sénestres de direction NE-SO et dextres de direction N-S, et par des failles normales. Les grabens réactivent des discontinuités préexistantes (décrochements) et s'ouvrent aussi en terminaison de décrochements dextres, ou en échelon dextres en bordure du modèle.

Dans la partie sud-est du modèle, la déformation est gouvernée par l'extension seule. Les grabens s'ouvrent perpendiculairement à la direction d'étalement du modèle. Aucune faille de type faille du Fleuve Rouge (sénestre, accommodant l'extrusion vers l'est de la partie SE du modèle) n'apparaît dans ces expériences, pas plus qu'il n'en apparaissait dans les expériences de Davy et Cobbold (1988) en l'absence de traction le long de la bordure libre.

La cinématique des mouvements finis peut être décrite par un pôle de rotation situé à l'est de la zone de collision. Ce pôle migre sur une ligne est-ouest en fonction des conditions aux limites : il est proche du poinçon quand la bordure latérale est confinée. Ce pôle est comparé à un pôle situé dans la mer d'Andaman qui décrit correctement un certains nombre de mouvements pendant la déformation de l'Asie.

La relation entre la cinématique finie et les cartes structurales est discutée. Certaines zones de déformation majeures sur les cartes structurales ont un rôle cinématique négligeable. C'est le cas dans les expériences de la zone de cisaillement dextre N-S qui part du bord est du poinçon (équivalent de la zone de cisaillement dextre N-S de l'est du Tibet), et de la faille dextre qui se développe parfois au front du poinçon (équivalente à la zone de failles Karakorum-Jiali).

Enfin, les cartes de variations de surfaces pendant la déformation sont décrites. Le raccourcissement est localisé au front du poinçon, et à l'extrême sud-ouest de la zone de cisaillement sénestre majeure, qui part du bord ouest du poinçon et court vers le NE. Le domaine raccourci au front du poinçon est partiellement extrudé vers l'est. Cette distribution est comparable à la distribution de la topographie en Asie avec d'une part la zone d'épaississement Himalaya-Tibet au front de l'Inde, en partie extrudée au-delà de la syntaxe

est-indienne, et la zone d'épaississement Tien Shan-Altaï dans la partie sud de la zone de déformation sénestre trans-asiatique.

Role of extension during collision tectonics: an analogue experimental approach

MARC FOURNIER,¹ JEAN-CHARLES THOMAS,² LAURENT JOLIVET,¹ AND PHILIPPE DAVY²

¹ Laboratoire de Géologie, Ecole Normale Supérieure, 24 rue Lhomond, 75231 Paris cedex 05, France

FAX: (33 1) 44 32 20 00

² Centre Armorican d'Etude Structurale des Socles, Université de Rennes 1, 35042 Rennes cedex, France

ABSTRACT

We performed analogue experiments of indentation to investigate the influence of extension upon continental deformation in collision context. We used a 3-layers rheological model of continental lithosphere scaled for gravity, resting upon an asthenosphere of low viscosity. The gravity potential of the model is higher than its integrated shear strength, so that it spreads under its own weight and thins. The southern boundary is free, and the eastern boundary is free or weakly confined and always allowing spreading. We study the pattern of deformation for different durations of extension, extension rates, and indentation speeds. The duration of extension is controlled by spreading of the model prior to indentation and the extension rate is controlled by the gravity potential of the model with respect to the eastern boundary. The results of five experiments are discussed. A classical experimental pattern of deformation has been obtained including a thickened zone with an unstrained triangle in front of the indenter, a major left-lateral shear zone trending NE, antithetic N-S trending right-lateral shear zones more or less developed to the east of the indenter, and an extensional domain to the SE. The distribution of deformation is controlled by the preliminary spreading and by the gravity potential of the model. Preliminary spreading accommodated by diffuse normal faulting, distributes the deformation produced by indentation. Part of the early normal faults are reactivated as strike-slip faults. Increasing the gravity potential of the model without preliminary spreading results in an even more diffuse deformation. A dense network of strike-slip faults appears. Variations of the indentation speed have little influence on deformation. The finite displacement field relative to the experimental box can be described with a rotation pole located east of the collision zone. Lateral confinement favours extrusion and spreading toward the southern boundary and brings the pole of finite motions close to the indenter. In the absence of lateral confinement the pole moves eastward. Relations between displacements and faulting are discussed. Major dislocations can have a negligible kinematic role. In the experiments, the main N-S dextral shear zone to the east of the indenter and the

E-W dextral strike-slip fault just in front of the indenter are kinematically insignificant. Spreading is accommodated by opening of grabens along the eastern and southern boundaries. Grabens open perpendicular to the direction of spreading to the SE, and along strike-slip faults to the NE. Maps of strain ellipsoid show that the SE part of the model is strained independently from the collision zone. Grabens opening is driven by spreading only in the south-eastern part of the model, and by indentation and spreading in the north-eastern part. From these results, we discuss the opening of the NE Asian basins. Maps of areal change show that thickening is localised in front of the indenter and at the southern end of the main left-lateral shear zone. In front of the indenter, the thickened zone is extruded eastward. The topography of Asia is compared to areal changes in the experiments.

INTRODUCTION

Numerical and analogue modelling of continental deformation in collision context has been used for the last 20 years to understand the deformation in Asia consecutive to the India-Asia collision (Tapponnier and Molnar, 1976; England and McKenzie, 1982, 1983; Vilote et al., 1982, 1984, 1986; Tapponnier et al., 1982, Houseman and England, 1986, 1993; Davy and Cobbold, 1988). The debate mainly focused on the geometry of deformation around the collision zone and the amount of deformation taken up by thickening and lateral extrusion (Tapponnier et al., 1986; England and Houseman, 1986; Molnar et al., 1987; Cobbold and Davy, 1988; Dewey et al., 1989; England and Molnar, 1990; Holt et al., 1991; Burchfield and Royden, 1991; Le Pichon et al., 1992; Houseman and England, 1993). Far from the collision zone, Asia has also been deformed by extension during the Cenozoic. The whole eastern and south-eastern Asian boundaries were affected by back-arc extension. Models of secondary induced asthenospheric convection (McKenzie, 1969), mass upwelling of the asthenosphere (Karig, 1971), and gravity or eastward asthenospheric flow acting on a dense subducting slab (Molnar and Atwater, 1978; Uyeda and Kanamori, 1979) have been proposed to relate back-arc extension and spreading to the subduction. After Molnar and Tapponnier (1975) and Tapponnier and Molnar (1977; 1979) showed that the whole eastern and south-eastern Asia had been strained by the collision, it has been proposed that the opening of the South China Sea and the Japan Sea was related to the India-Asia collision (Tapponnier et al., 1982; 1986; Kimura and Tamaki, 1986; Jolivet et al., 1990). Extension in Asia is not restricted to margins near the subduction zone, it also prevails inside Asia in the Baikal region since the Oligocene (Tapponnier and Molnar, 1979; Hutchinson et al., 1992; Deverchère et al., 1993) and in northern China since the Eocene (Ma and Wu, 1987). Windley and Allen (1993) proposed that a mantle plume is responsible for the extension in the Baikal region and interacts with the India-Asia collision to drive the deformation in this region. Lastly, extension is also active in Tibet (Molnar and Tapponnier, 1977; Tapponnier et al., 1981; Molnar and Chen, 1983; Armijo et al., 1986, 1989) since the Late Miocene (Mercier et al., 1987; Pan and Kidd, 1992), driven by lateral extrusion of the lower crust from under the growing topography (Bird, 1991), and in the Himalaya (Burg and Chen, 1984; Burchfield and Royden, 1985; Burchfield et al., 1992).

We performed new analogue experiments of indentation to study the role of extension driven by gravity in collision tectonics. Our prime interest is the deformation of continental margins subjected to extension during indentation. In this paper, we present a review of the deformation of the margins of Asia since the India-Asia collision to justify the boundary conditions of our models. We then describe five experiments and their results for varying extension rates, gravity potentials, and indentation speeds. We finally discuss the kinematics and geometry of deformation with respect to boundary conditions, paying attention to

extensional deformation, and compare the deformation of the Asian margins to the experiments.

EXTENSIONAL DEFORMATION OF THE MARGINS OF ASIA DURING THE INDIA-ASIA COLLISION

In the following review, toponymy refers to Figure 1.

Present-day deformation of the Asian margins

SE Asia moves southward with respect to its western and eastern boundaries, the relative motion being taken up along two strike-slip zones. To the west, the dextral strike-slip zone which accommodates the northward motion of India (Patriat and Achache, 1984) and Burma plate (Moore et al., 1980; Chen and Molnar, 1990) includes the Sagaing fault to the north (Curray et al., 1978; Le Dain et al., 1984), the Sumatra and Mentawai faults to the south (Fitch, 1972; Diament et al., 1992), and the Andaman Sea which opens in-between as a pull-apart basin (Curray et al., 1978). To the east, the left-lateral Philippine fault absorbs the strike-slip component of the relative motion between the Philippine Sea Plate and Indonesia (Barrier et al., 1991; Yoshida and Abe, 1992). The convergent component is taken up by shortening in collision zones, the Molucca Sea (McCaffrey et al., 1980; Moore and Silver, 1982), the Philippine archipelago (Marchadier and Rangin, 1989), the Taiwan collision zone (Chingchang et al., 1985), and further north the Izu collision zone in Japan (Matsuda, 1978), and by subduction of the marginal basins of SE Asia, the South China Sea, the Sulu Sea, and the Celebes Sea consumed in the Manilla, Negros, and Cotobato trenches, respectively (Cardwell et al., 1980). Since about 3 Ma the Philippine Sea Plate is also subducting in the Philippine Trench (Cardwell et al., 1980; Rangin et al., 1990).

South of Indonesia, the oceanic crust of the Indo-Australian plate is consumed in the Sunda subduction zone. To the west, the Sunda trench advances southward at a slow rate in the mean hot spot reference frame (Chase, 1978). Active extension parallel to the trench affects the Sunda Strait south of Sumatra (Huchon and Le Pichon, 1984; Harnojo et al., 1991). East of Sumba island, the Australian margin collides with the Banda volcanic arc (Audley-Charles, 1981; McCaffrey, 1988), which provokes the southward subduction of the Banda Sea basin under the Banda arc (Silver et al., 1983; McCaffrey and Nabelek, 1986) and its eastward extrusion together with the Banda arc as they contracts north-south (McCaffrey, 1988; McCaffrey and Abers, 1991).

Northeast of Taiwan, the Okinawa basin opens since Plio-Pleistocene time above the Ryukyu Trench (Eguchi and Uyeda, 1983). The dextral en-echelon pattern of the main grabens within the basin suggests a pull-apart opening (Sibuet et al., 1987; Kuramoto and Konishi, 1989; see also Viallon et al., 1986). Further north, a compressional stress-field

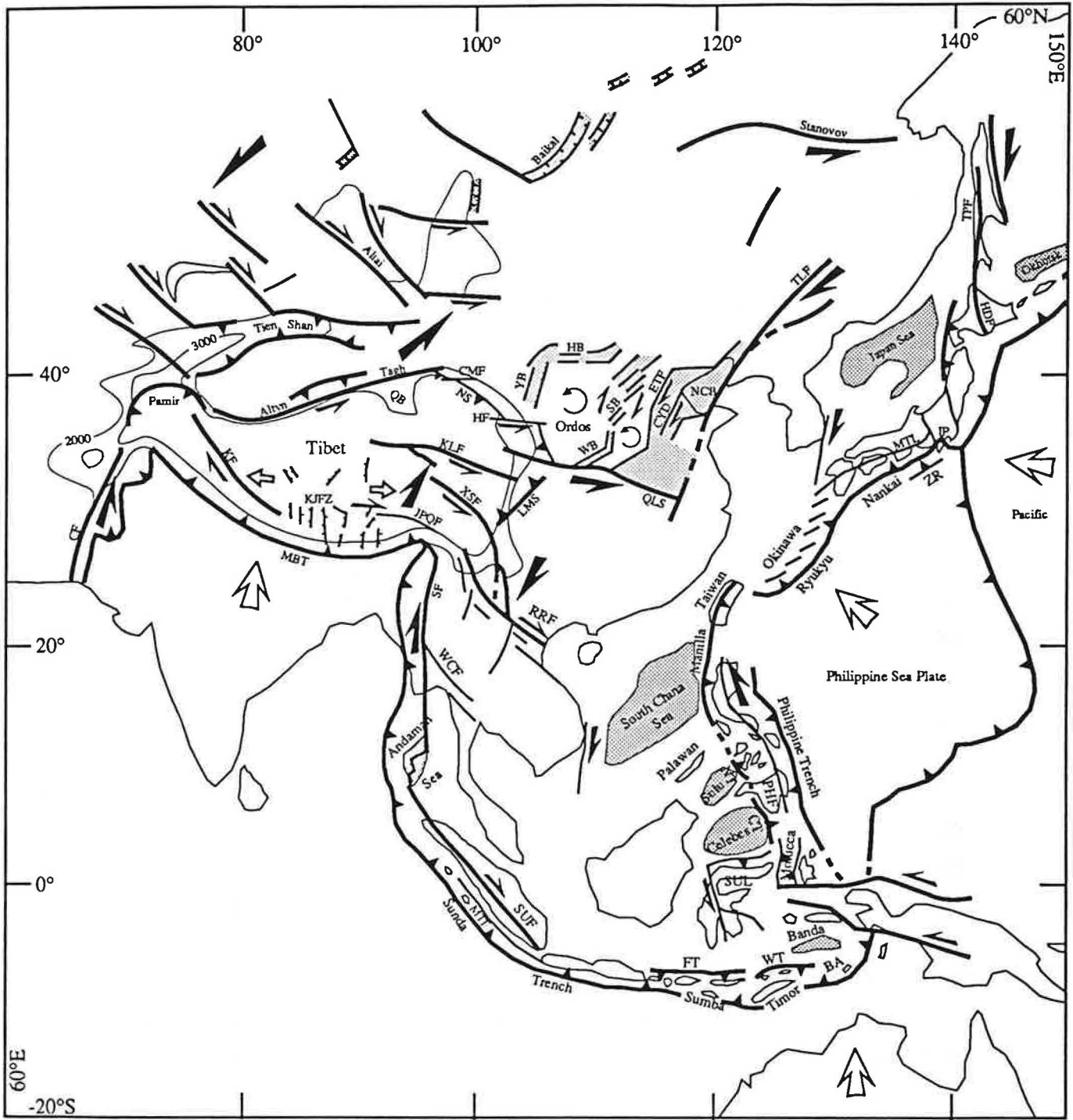


Fig. 1. Simplified structural map of Asia. BA is Banda Arc, BP is Burma Plate, CF is Chaman Fault, CMF is Chang Ma Fault, CT is Cotobato Trench, CXD is Cang Xian-Dongning Fault system, ETF is East Taihang Fault system, FT is Flores Thrust, HB is Hetao Basins, HDF is Hidaka Fault zone, HF is Haiyuan Fault, IP is Izu Peninsula, KF is Karakorum Fault, KJFZ is Karakorum-Jiali Fault Zone, KLF is Kunlun Fault, LMS is Longmen Shan, MBT is Main Boundary Thrust, MTF is Mentawai Fault, MTL is Median Tectonic Line, NCB is North China Basin, NS is Nan Shan, NT is Negros Trench, PHF is Philippine Fault, QB is Qaidam Basin, QLS is Qinling Shan, SB is Shanxi Basins, SF is Sagaing Fault, SUF is Sumatra Fault, SUL is Sulawesi, TLF is Tan-Lu Fault, TPF is Tym-Poronaysk Fault, WCF Wang Chao (or Mae Ping) Fault, WH is Weihe Basin, WT is Wetar Thrust, XSF is Xanshuihe Fault, YB is Yinshuan Basins, ZR is Zenisu Ridge.

perpendicular to the trenches is documented in Japan since the Late Miocene by dike and fault set measurements, earthquake focal mechanisms (Nakamura and Uyeda, 1980; Yamazaki et al., 1985; Yamagishi and Watanabe, 1986; Jolivet and Huchon, 1989; Jolivet et al., 1991), and active E-W contraction detected by interferometry networks (Heki et al., 1990). Crustal shortening is accommodated by thrust faulting in the northern part of the Philippine Sea Plate (Zenisu ridge) (Lallemand et al. 1989; Chamot-Rooke et al., 1989), and along the eastern margin of the Japan Sea which is subducted under the Japan arc (Fukao and Furumoto, 1975; Nakamura, 1983; Tamaki and Honza, 1984). In southwest Japan, the right-lateral Median Tectonic Line (MTL) absorbs the strike-slip component of the oblique subduction of the Philippine Sea Plate at the Nankai trench (Seno, 1977; Ranken et al., 1984; Matsuzaka et al., 1991).

The stress regime changes landward, away from the subduction zone (Nakamura and Uyeda, 1980), strike-slip faulting prevailing in Sakhalin (Jolivet et al., 1992) and in northern China. Sakhalin is a transpressional shear zone since Miocene time, most of the seismicity being related to the N-S trending right-lateral Tym-Poronaysk Fault (Rozhdestvensky, 1982; Fournier et al., 1994). In northern China, Nabelek et al. (1987) showed that active normal faulting and subsidence in the North China Basin are linked with dextral strike-slip faulting along the East Taihang, Cang Xian-Dongning, and Tan-Lu fault systems. Further west, north China experiences active extension around the Ordos block (Tapponnier and Molnar, 1977) in the Yinchuan (Deng Qidong et al., 1984), Weihe (Wang, 1987), and Shanxi graben systems, whereas South China (south of the Qinling Shan) is nearly exempt from active deformation (Seismotectonic Map of China, 1985). The Qinling Shan is a left-lateral fault zone since Pliocene time (Bellier et al., 1988), almost historically inactive. Quaternary left-lateral slip was evidenced by Peltzer et al. (1985) and Wang (1987), but the rate of relative motion between north and south China remains poorly constrained.

Thus, all the eastern boundaries of Asia from the eastern Sunda trench to northern Japan are presently shortened, except above the Ryukyu trench where the Okinawa basin opens. Shortening extends to the whole SE Asian margin where it is essentially taken up by subduction of the Celebes and Sulu Seas. In contrast, northern China evolves independently from the west Pacific subduction zone and undergoes strike-slip and normal faulting.

Extension and opening of marginal basins from Eocene to Miocene

From Eocene to Miocene time south-eastern Asia experienced diffuse extensional deformation. Basins floored with oceanic crust opened: Celebes Sea in the Eocene (Weissel, 1980; Silver et al., 1983; Silver and Rangin, 1991), South China Sea in the Oligocene (Taylor and Hayes, 1980; Briais, 1993), and Sulu Sea in the Early Miocene (Silver and Rangin, 1991). Basin systems in Sumatra, Sunda shelf, Borneo, Gulf of Thailand and Malaysia also opened during the Eocene and Oligocene (Hamilton, 1979; Daly et al., 1991).

The opening of these basins has been related to intra-continental deformation resulting from the India-Asia collision, as for the South China Sea and the Thai and Malay basins (Tapponnier et al., 1982; 1986), and to subduction-related extension, as for the Celebes and Sulu Seas (Rangin et al., 1990).

Further north, the Japan and Okhotsk Seas opened from the Late Oligocene to the Middle Miocene (Tamaki, 1988; Tamaki et al., 1992), and crustal extension is also evidenced during the Paleogene in the Bering Sea (Cooper et al., 1992).

Since Eocene time, northern China experiences distributed extension over the multi-rifted North China Basin (Hellinger et al., 1985; Hong et al., 1985; Chen and Nabelek, 1988; Tian et al., 1992), and in the Hetao, Yinchuan and Weihe graben systems surrounding the Ordos block (Ma and Wu, 1987; Wang, 1987; Bellier et al., 1988). Extension in the Shanxi graben system, east of the Ordos block, was initiated later during the Pliocene (Xu and Ma, 1992). Chen and Nabelek (1988) proposed that the North China Basin opened as a pull-apart basin along the dextral Tan-Lu fault system (Lu et al., 1983; Xu et al., 1987).

The south-eastern and eastern margins of Asia were stretched by back-arc extension until Middle Miocene time. Extension started in SE Asia in the Eocene and in the Japan Sea area in the Late Oligocene. Among all marginal basins of eastern Asia, the opening of the Japan Sea is probably best understood. There is no doubt that opening was associated with right-lateral motions along the mega-shear zone which bounds the Japan Sea to the east, up to northern Sakhalin (Lallemand and Jolivet, 1985; Jolivet and Huchon, 1989; Jolivet et al., 1991, 1992; Tamaki et al., 1992). The stress regime along the shear zone changed from transtensional near the subduction zone to transpressional in its continental portion (Jolivet et al., 1992; Fournier et al. 1994), which led Jolivet et al. (1992) to relate the extensional component of deformation to subduction, and the strike-slip component to continental deformation, i.e., India-Asia collision. Kimura and Tamaki [1986] and Jolivet et al.[1990], putting forward the geometry of the deformation in Asia and small scale analogue modelling, had already related the opening of the Japan Sea to the India-Asia collision. Hence, the Japan Sea appears to be the result of the deformation produced by the India-Asia collision and the subduction. Both driving forces are required to account for the geometry of opening.

Middle Miocene collisions

Collisions of the Philippine Sea Plate and of the Australian margin with SE Asia occurred in the Middle Miocene. In Sulawesi, the Sula and Buton blocks, headlands of the Australian plate, collided first with the north Sulawesi island arc, south easternmost extension of the Asian margin (Hamilton, 1979; Silver et al., 1983; Berry and Grady, 1986; Rangin et al., 1990). An intra-oceanic subduction was subsequently initiated further south. At the same time, convergence and shortening started in SE Asia with the inception of the south-eastward subductions of the Proto South China Sea and the Sulu basin in the Palawan

and south Sulu Sea trenches, respectively (Holloway, 1982; Rangin et al., 1990). During the Pliocene the collision zone was duplicated to the south, in Timor, where the northern Australian margin started to collide with the Banda arc (Audley-Charles, 1981; Milsom and Audley-Charles, 1986; Charlton et al., 1991; Harris, 1991). The deformation front progressed northward and, on the northern edge of the Banda arc, the southward subduction of the Banda Sea basin was initiated along the Flores and Wetar thrusts (Silver et al., 1983). At the same time, the Borneo and Sunda shelf basins experienced a major inversion which started during Miocene time (Daly et al., 1991).

In Japan, the onset of the present-day compressional regime was recorded between 10 Ma and 7 Ma (Tamaki et al., 1992; Jolivet and Tamaki, 1992). It is related to the initiation of the subduction of the young oceanic lithosphere of the Philippine Sea Plate under the Japan arc during the Late Miocene (e.g. Jolivet et al., 1989). The subduction of the Pacific Plate old slab which prevailed before is considered to have acted as a stress-free boundary, with likely a component of trench-pull (Jolivet et al., 1992).

Collisions of Australia and the Philippine Sea Plate with the SE Asian margin in Middle Miocene time ultimately resulted in the present-day compression almost generalised to all the boundaries of Asia. They provoked stopping of opening of marginal basins and beginning of closing. Landward, northern China has not been affected by the changes of stress regime along the subduction zone.

Conclusion

The eastern and south-eastern Asian margins were extended during the first part of the collision of India. The interaction of two driving forces of continental deformation, collision and subduction-related extension, has been invoked to explain the opening of the Japan Sea (Kimura and Tamaki, 1986; Jolivet et al.; 1990; 1992). The continental deformation is responsible through strike-slip faulting for the geometry of opening, and the component of extension required for the opening is provided by the subduction. The Miocene collisions of Australia and of the Philippine Sea Plate with the SE Asian margin provoked a change of boundary conditions: extension and spreading were replaced by compression and shortening.

Since Tapponnier et al. (1982) proposed that the south and east Asian boundaries acted as stress-free boundaries during the collision of India, the most successful modellings of the India-Asia collision in terms of geometry of deformation were performed with passive free boundaries (Tapponnier et al., 1982, Vilote et al., 1982; 1984; 1986; Cohen and Morgan, 1986; Davy and Cobbold, 1988; Peltzer and Tapponnier, 1988; Houseman and England, 1993). So far, the influence of dynamic marginal extension upon continental deformation in context of collision had not been tested by means of models. We performed experiments of indentation with marginal extension to understand to what extent collision

and extension can interact in continental deformation, and to what extent a drastic change of boundary conditions may have an influence on deformation inside the continent.

ANALOGUE MODELLING OF CONTINENTAL DEFORMATION WITH EXTENSION DRIVEN BY GRAVITY

Previous analogue and numerical modellings of continental deformation (Table 1)

Since Argand (1924) and then Molnar and Tapponnier (1975) broadly related the intra-continental deformation in Asia to the India-Eurasia collision, several analogue and numerical modellings of continental deformation were performed. Davy and Cobbold (1988) presented a complete review of these models and we summarise in Table 1 their main characteristics. This section consists in a brief comment of Table 1.

Recent numerical modellings (Houseman and England, 1986; 1993; Villette et al., 1986; Cohen and Morgan, 1986) include buoyancy forces which means that the models thicken in reasonable proportions and thin when the deviatoric stress exceeds the shear strength.

Numerical models assume that the lithosphere can be described as a continuum, local discontinuities being averaged over a scale of about 50-100 km. This assumption deserves a careful testing since faults exist up to several thousand kilometres. As a consequence, structural maps cannot easily be compared to numerical models. On the other hand, lateral stripes of plasticine in the models of Tapponnier et al. (1982) and Peltzer and Tapponnier (1988) provided artificial discontinuities (heterogeneous model in Table 1) along which faults tended to be localised. In particular, the so-interpreted Red River Fault which accommodates the extrusion of Indochina did not appear in the absence of lateral stripes of plasticine (Peltzer and Tapponnier, 1988).

Extrusion can be defined as a component of displacement perpendicular to the direction of indentation, i. e., eastward displacements in the models (Houseman and England, 1993). In the experiments, extrusion is driven by indentation and accommodated by strike-slip faults which transform northward displacements into eastward displacements (lateral expulsion), or it is driven by gravitational spreading and accommodated by extension. Most of the models were tested with a lateral free boundary which inevitably caused lateral extrusion, except under the extreme assumption of plane stress (Villette et al., 1982). On the opposite, a rigid boundary led to crustal thickening in front of the indenter (Houseman and England, 1986; Davy and Cobbold, 1988).

In the first part of this paper, we stated the importance of extensional deformation along the south-eastern and eastern boundaries of Asia during the collision of India. Houseman and England (1993) described numerical experiments with a model including buoyancy forces and with a lithostatic eastern boundary. The deviatoric stress was zero along

the boundary which was allowed to move under the influence of indentation only. Consequently, there was no extension along the eastern margin of the model. Davy and Cobbold (1988) performed analogue experiments with a weakly confined eastern boundary. The deviatoric stress was not zero along the boundary, but the model did not spread because the deviatoric stress was lower than the shear strength of the model. In order to investigate the role of extension during indentation, we built a model of continental lithosphere for which the gravity potential is higher than the integrated shear strength, so that the model can spread provided that boundaries permit it. With such a model, extension always prevails along the free or weakly confined boundaries.

Rheological properties of the model

We used a rheological model of continental lithosphere made of 3 layers resting upon an asthenosphere of glucose syrup (Davy and Cobbold, 1991). The upper crust is assumed to be brittle with a Mohr-Coulomb frictional behaviour and is modelled using dry quartz sand with a negligible cohesion and a frictional angle of about 30°. The lower crust and the upper mantle are modelled with two Newtonian silicone putties (silicone 1 and silicone 2 in Table 2) of different viscosities and densities, higher viscosity and density being used for the upper mantle. The glucose syrup is a Newtonian fluid of low viscosity. Further discussion and justification of the experimental method can be found in Davy and Cobbold (1991). The physical parameters of layers in each experiment are given in Table 2.

Boundary conditions

The southern (lower) boundary of the model is strained by a rigid indenter progressing northward (Figure 2). The northern (upper) and western (lateral left) boundaries of the model are in contact with the rigid experimental box. Along the southern boundary the model is in isostatic equilibrium with the crustless asthenosphere (golden syrup). In the following, this type of boundary will be referred to as "free boundary". The eastern (lateral right) boundary is either free or weakly confined with a five millimetre thick silicone putty layer floating on glucose syrup. This increases the gravity potential of the boundary and slows down lateral spreading of the model. However, whether it is free or weakly confined, the eastern boundary always allows lateral spreading of the model so that its eastern margin is always affected by extension.

Scaling

The experiments are scaled for the normal gravitational field given the physical properties of materials and setting the thickness of a normal crust, about 30 km in nature, to 1.5 cm in the experiments. The initial dimensions of the model are shown in Figure 2. Under the latter conditions, the width of the model (75 cm) represents 1500 km, its length (95 cm)

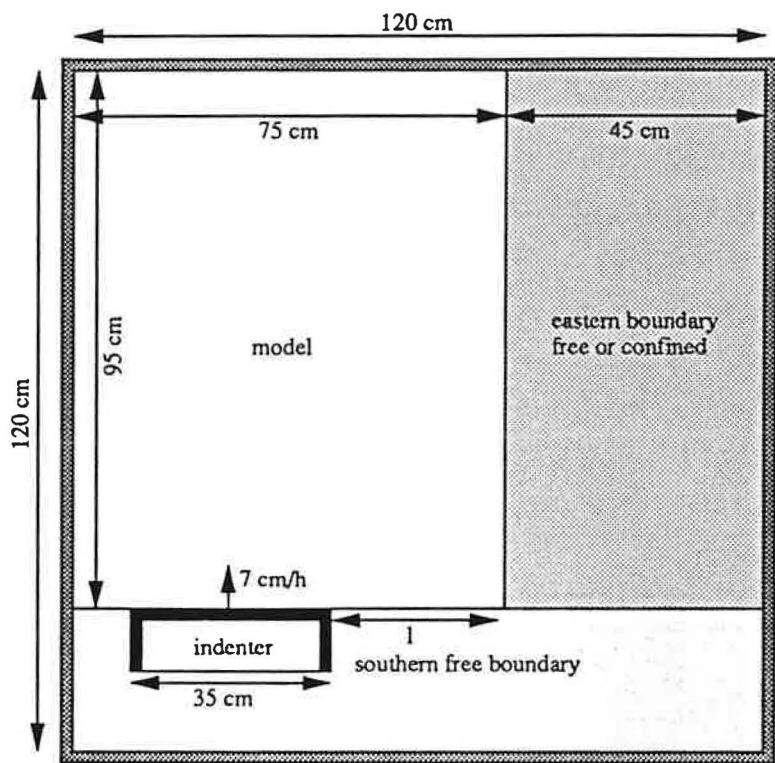


Fig. 2. Experimental device.

represents 1900 km, and the width of the indenter (35 cm) represents 700 km which is about one third of the distance between the syntaxes of India.

The model of lithosphere is in isostatic equilibrium with its southern and eastern boundaries. Two forces compete in the process of gravitational spreading: (I) the deviatoric stress due to topography of the lithosphere relative to the boundary, which favours spreading, and (II) the shear strength of the lithosphere which prevents spreading. Spreading occurs when the gravity potential of the lithosphere relative to the boundary exceeds the integrated shear strength of the lithosphere. The shear strength of the silicone putty is negligible with respect to that of the sand and we assume that the integrated shear strength of the model is a function of the thickness of the brittle crust only. The gravity potential of the model relative to the boundary is a function of the thickness of the (brittle and ductile) crust only, as the density of the lithospheric mantle is similar to that of the asthenosphere in the experiments. Calculations of the magnitude of the gravity potential relative to the integrated shear strength as well as experimental tests suggested that spreading of the model was initiated when the ductile crust was thicker than the brittle crust. We then chose a thickness of 0.5 cm for the brittle crust and a thickness of 1 cm for the ductile crust (Table 2).

Time scales characteristic of deformations produced by indentation or by gravitational spreading could be evaluated. We performed preliminary tests to measure spreading rates in the absence of indentation. The free boundary advanced at a rate of 1 to 2 $\text{cm} \cdot \text{h}^{-1}$ due to spreading, which was equivalent to strain rates of 1 to $2 \cdot 10^{-5} \text{ s}^{-1}$ computed along a line perpendicular to the free boundary. The strain rate produced by indentation is evaluated along a line perpendicular to the indenter between 2 and $6 \cdot 10^{-5} \text{ s}^{-1}$, depending on the speed of the indenter which varied between 6 and $20 \text{ cm} \cdot \text{h}^{-1}$. Thus, time scales of indentation and gravitational spreading are of the same order of magnitude. The two phenomena can interact and be compared to each other.

Varying parameters

Our goal was to study the influence of extension upon deformation. The amount of extension varies with the duration of extension or the extension rate. We studied the deformation pattern for different durations of extension and different extension rates. We controlled the duration of extension by letting the model spread prior to indentation. The model spread for 2h, 1h, and 0h prior to indentation during the experiments 1, 2, and 3 (E1, E2, and E3 thereafter), respectively. We controlled the extension rate in the model by modifying its gravity potential (or extensional potential) with respect to the eastern boundary. This was done by adding or removing lateral confinement. During E1, E2, and E3, the eastern boundary was weakly confined with a five millimetre thick silicone layer (only over the upper 40 cm in E1) which increased the gravity potential of the boundary and reduced the spreading rate of the model. From E3 to E4, we increased the gravity potential of

the model relative to the boundary by removing the confinement. The four first experiments were performed with an almost constant indentation speed, between 5.5 and 7 cm.h⁻¹ (Table 2). From E4 to E5, we increased the indenter speed from 7 to 20 cm.h⁻¹.

Thus, we obtained informations about the role of three parameters during the deformation: duration of extension, extension rate, and indentation speed. We could not perform numerous experiments to test carefully the variations of each parameter, because the large dimensions of the model made it uneasy to build and manipulate. We present the results of five experiments.

Analysis of results

The models were covered by an originally orthogonal grid of lines spaced every two centimetres, drawn with white sand. Deformation of the grid was monitored by photography every 15 minutes. The photographs were used to draw structural maps and to digitise the grid intersections at time-lapse stages for each experiment. The digitised grids provided the finite displacement field for each experiment and were used to compute the strain and rotation tensors in each grid point. We used the second invariant of the strain tensor as an indicator of shear rate (Jaegger and Cook, 1971; Villette et al., 1984, 1986) and we computed maps of shear rate and rate of rigid rotation. We also computed areal change of each grid mesh in order to compare maps of areal changes to topographic maps. However, because we made the assumption that the model was a continuum to compute areas, calculations are inexact especially in areas affected by strike-slip faulting. We therefore provide only simplified maps of areal changes showing features large enough to be significant.

PATTERN OF DEFORMATION WITH RESPECT TO GRAVITATIONAL SPREADING

Common pattern for all experiments

The structural evolution is similar for each experiment. Experiment 3 is shown as an example in Figure 3 with a simplified structural map. Folds and thrust faults first appear in front of the indenter. A left-lateral shear zone running NE is then initiated north of this thickened zone, and an antithetic right-lateral shear zone running north from the eastern edge of the indenter appears afterwards, more or less developed depending on boundary conditions. Grabens open in the SE part of the model defining a large extensional domain. Along the eastern and southern boundaries, grabens form as extrado cracks normal to the boundary. Afterwards, the compressional zone in front of the indenter progressively extends northward, resulting in a triangular zone bounded by folds and thrusts to the south and to the NW, and by smaller folds and/or right-lateral strike-slip faults to the NE. The central part of the triangle remains unstrained and moves rigidly northwards together with the indenter. Further NE, the left-lateral shear zone widens and several antithetic right-lateral shear zones

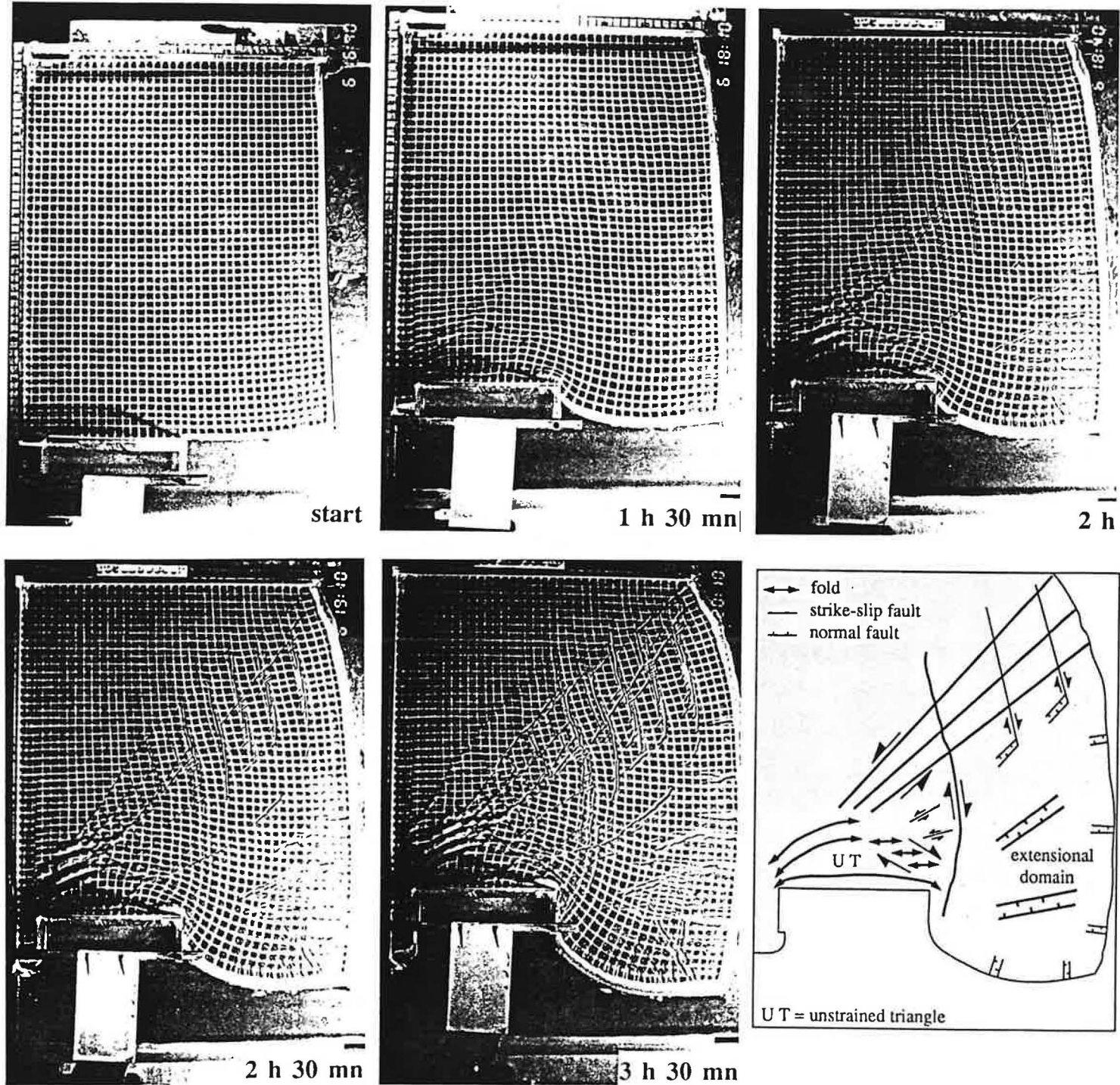


Fig. 3. Successive deformation stages of E3 and interpretative structural map.

appear along it. Grabens open along the right-lateral shear zones. At this stage, the deformation pattern is definitively settled and does not change significantly any longer. The geometry of deformation is very asymmetric because of the free or weakly confined boundary to the east which favours the formation of a major left-lateral shear zone and eastward extrusion. At centimetre scale, sets of conjugate faults are generally observed. Faulting is distributed in a classical way compared with previous numerical and analogue modelling: reverse faulting in front of the indenter, strike-slip faulting in a broad zone heading NE, and normal faulting in the SE part of the model.

Variations of spreading duration

During the first three experiments we progressively reduced the amount of finite extension by reducing duration of spreading prior to indentation. In E1, we let the model spread for 2 hours before starting indentation. The north-eastern boundary was weakly confined with a five millimetre thick silicone putty layer over the upper 40 cm, which favoured south-eastward spreading. Figure 4a shows the model after two hours of spreading plus 45 mn of indentation. Grabens are distributed all over the model except in the NW corner which is not strained, and in the SE corner which suffered almost pure flattening without faulting. For E1, the indenter had been settled in the experimental box before spreading started, which controlled the grabens orientation during preliminary spreading.

A photograph of E1, a structural map, a map of shear rate, and a map of rigid rotations are shown in Figures 4a, b, c and d, respectively, after 2 h 30 mn of indentation following 2 h of preliminary spreading. The structural map shows that deformation is distributed over a wide triangular zone starting from the indenter and pointing to the NE. The south-eastern part of the model behaved almost as a continuum with few faults. Strike-slip faults are distributed symmetrically over the triangular deformation zone: left-lateral on the NW side, and right-lateral on the SE side. An E-W trending right-lateral fault appeared in front of the indenter. The map of shear rate (Figure 4c) confirms that strain is diffuse and shows that the shear rate tends to decrease with the distance to the indenter.

The map of rigid rotations (Figure 4d) is asymmetric. The prominent NE trending stripe of counterclockwise rotations corresponds to the main left-lateral shear zone. Right-lateral shear is diffuse and did not produce significant CW rotations, except along one right-lateral fault zone which cut through the left-lateral shear zone straight ahead the eastern edge of the indenter, nullifying the CCW rotation. The rotations localised along shear zones contrast with the fan shaped distribution of rotations in the SE part of the model.

During E2 and E3 the eastern boundary was entirely confined with a 5 millimetre thick layer of silicone putty. During E2 (Figure 5), the model spread for 1 hour prior to indentation. In Figure 5a the model E2 is shown after 1 h of spreading plus 1 h 30 mn of indentation in order to see the geometry of the extensional structures. Grabens trend NE, and

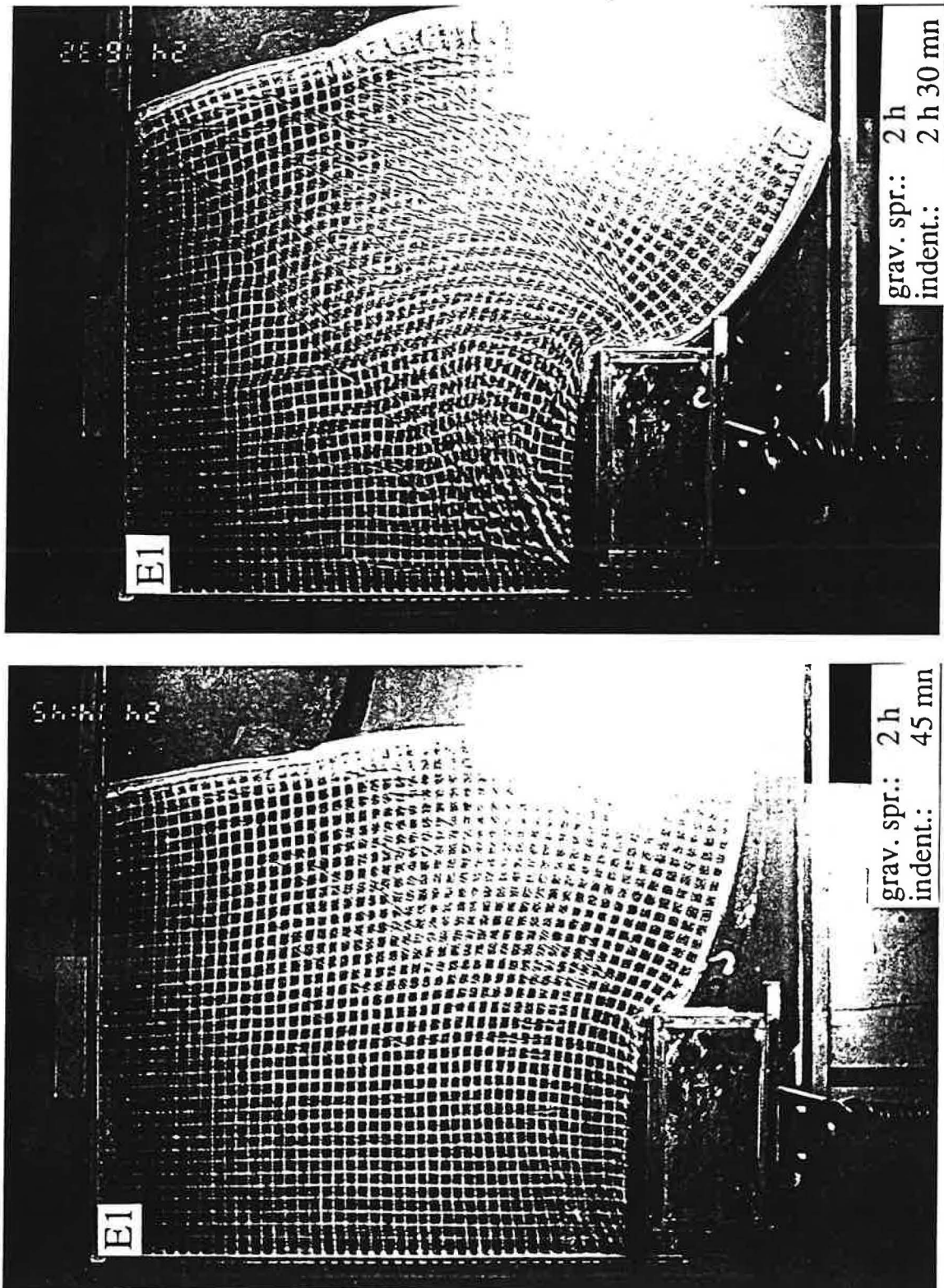
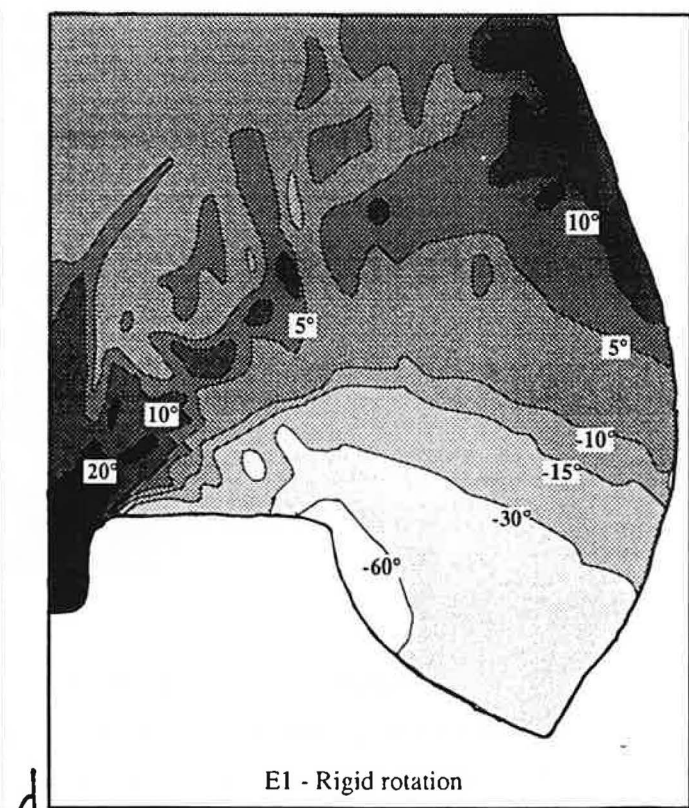
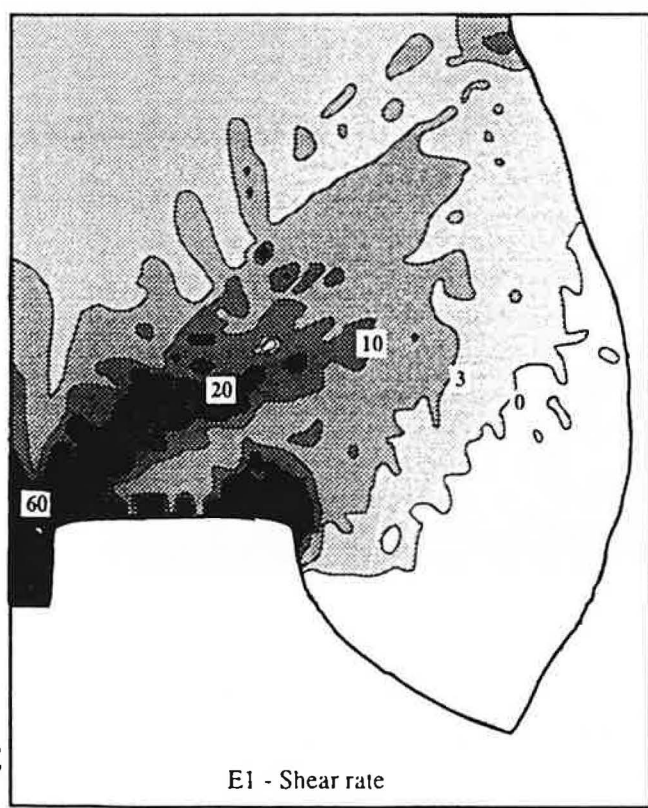
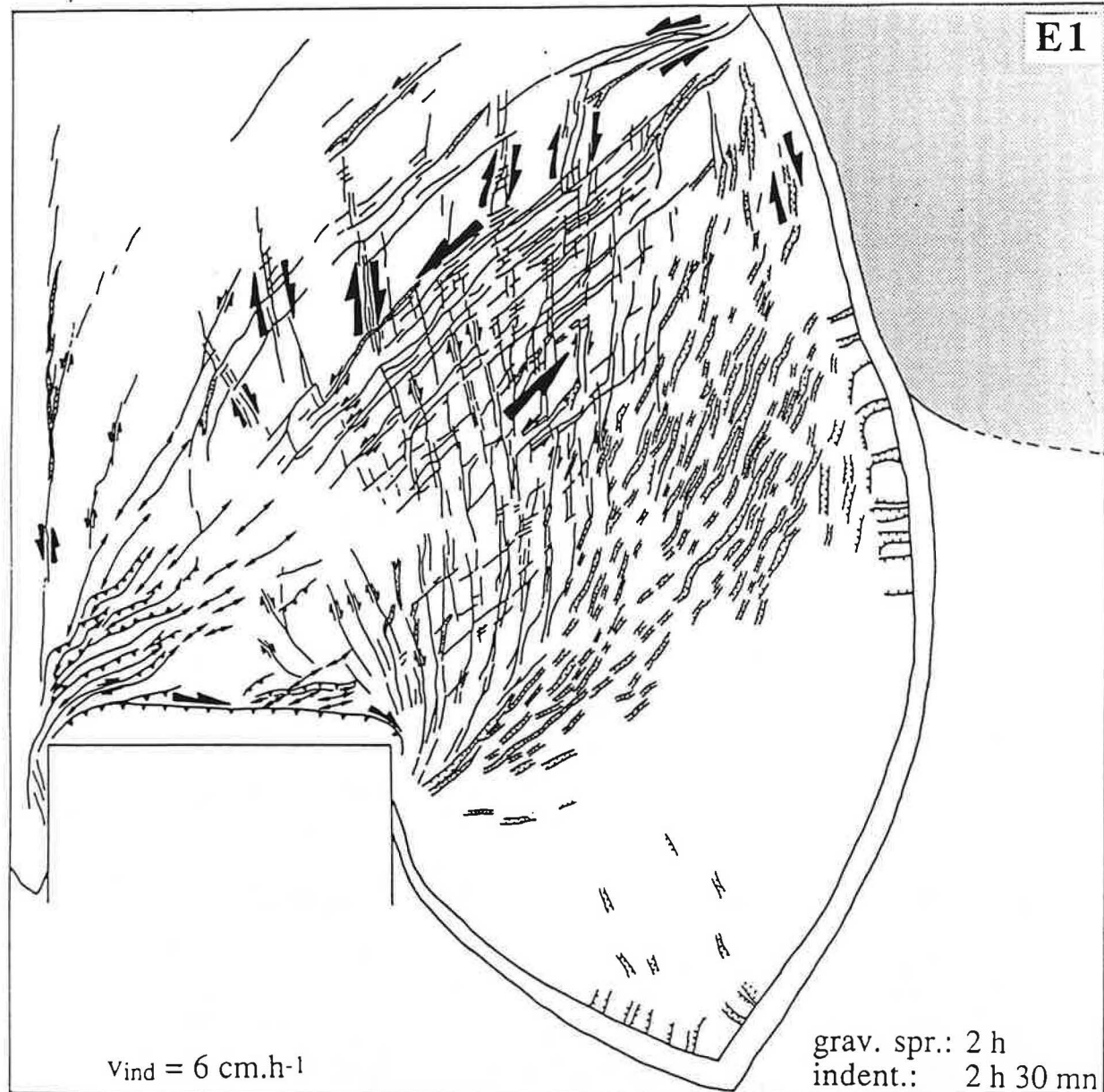


Fig.4. (a) Photographs of E1 after 2 h of preliminary spreading plus 45 mn of indentation, and after 2 h of preliminary spreading plus 2 h 30 mn of indentation, and (b) corresponding structural map. Continuous lines are fault traces which are thrusts (triangle on hanging wall), strike-slip faults, or normal faults (ticks on hanging wall). Folds are continuous lines with arrow at both ends. The dotted area shows the boundary confined with a thin layer of silicone putty. (c) Map of shear rate. (d) Map of rigid rotations. E is experiment. Grav spr is duration of spreading prior to indentation. Indent is the duration of indentation. V_{ind} is velocity of the indenter.



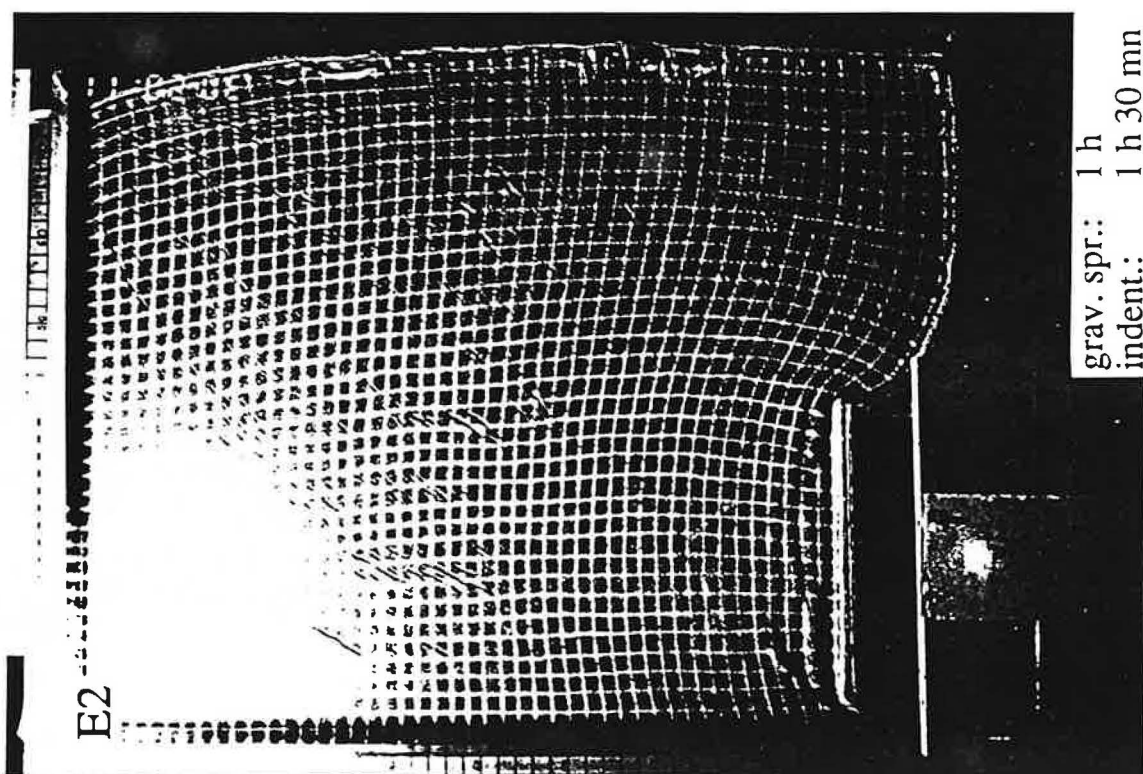
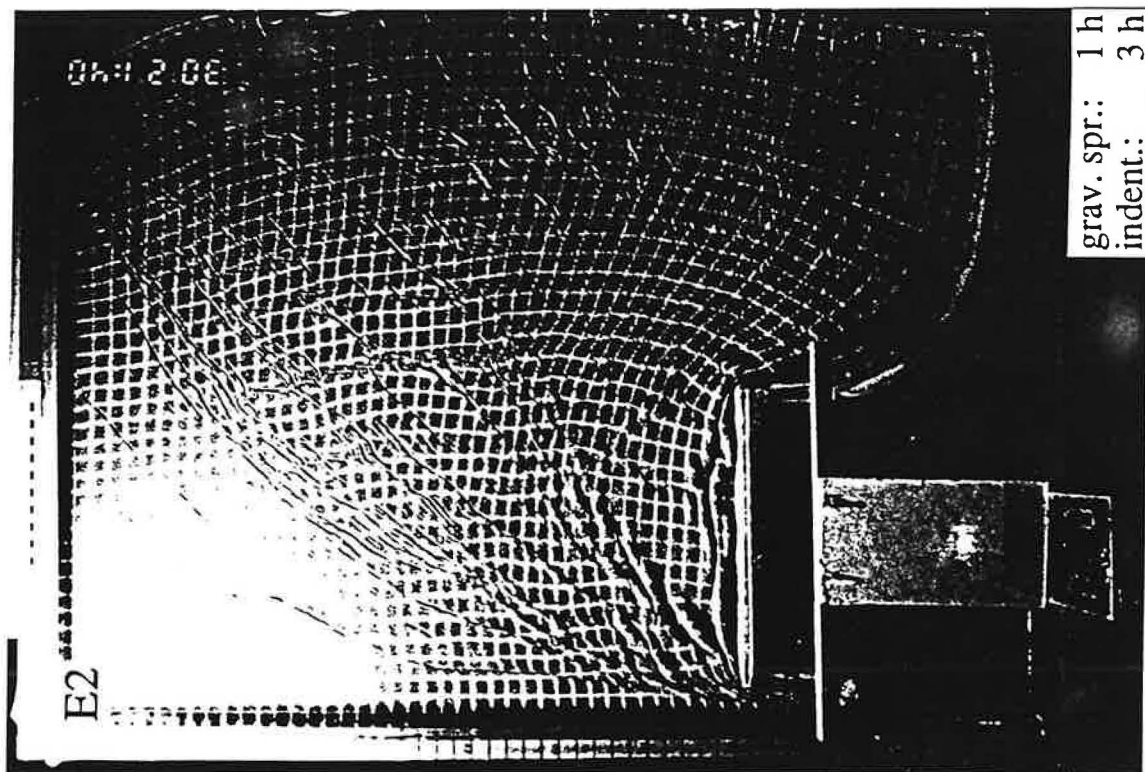
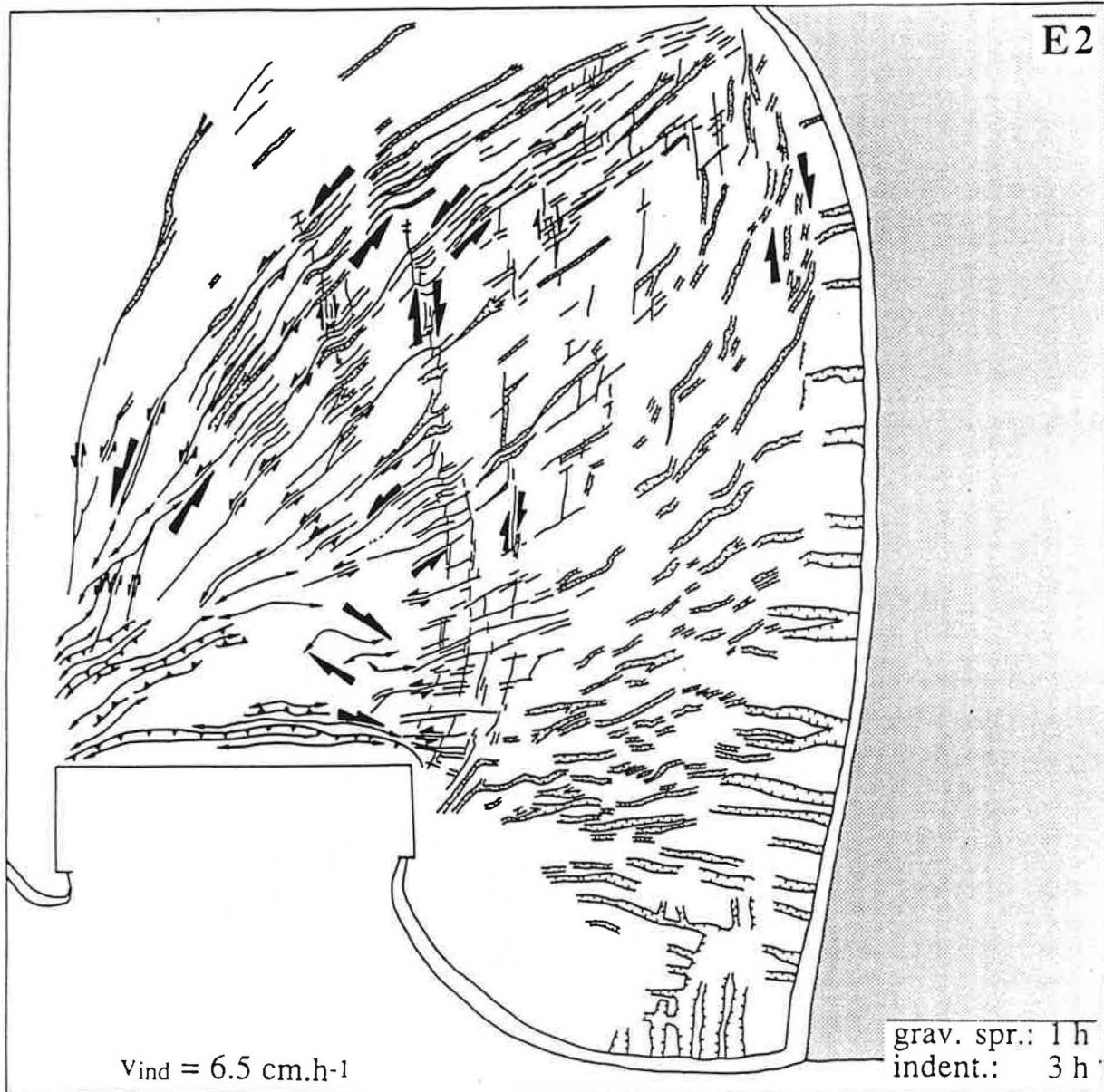
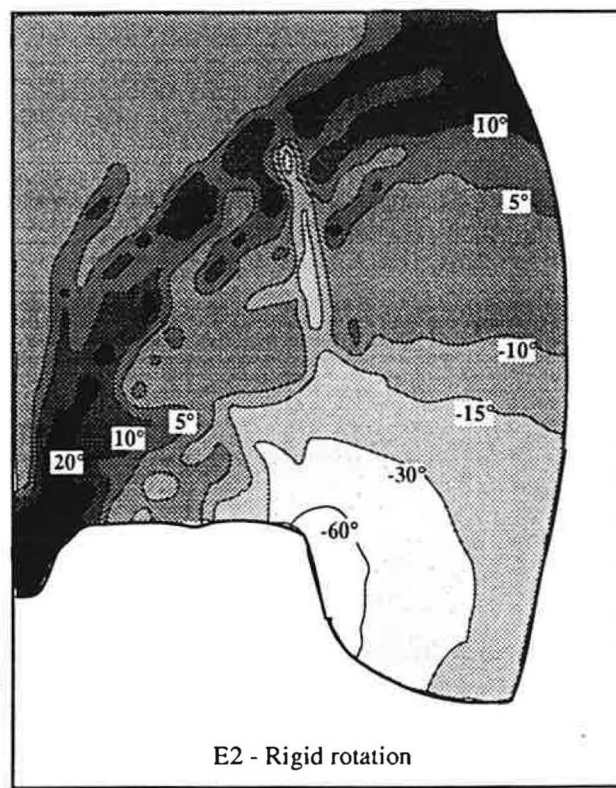
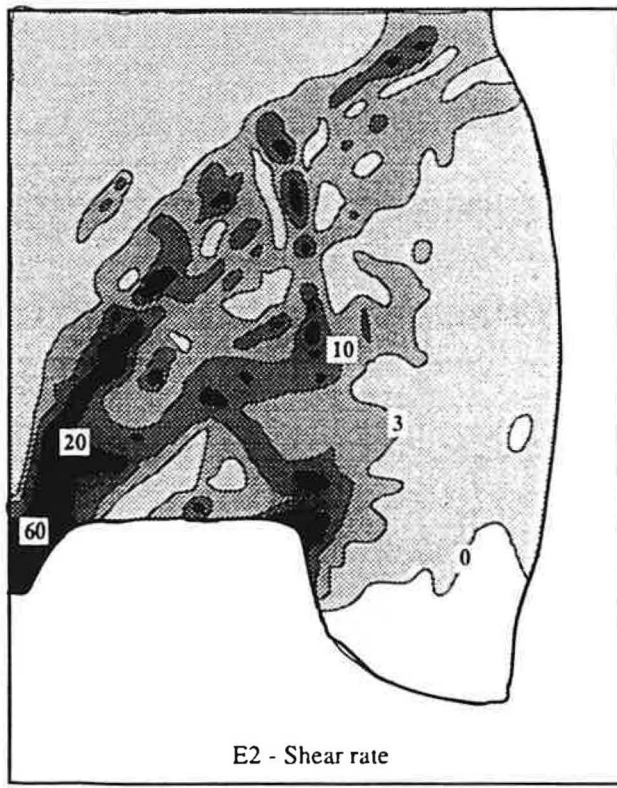


Fig.5. (a) Photographs of E2 after 1 h of preliminary spreading plus 1 h 30 mn of indentation, and after 1 h of preliminary spreading plus 3 h, and (b) corresponding structural map. Same symbols and legend as Fig. 4. (c) Map of shear rate. (d) Map of rigid rotations.

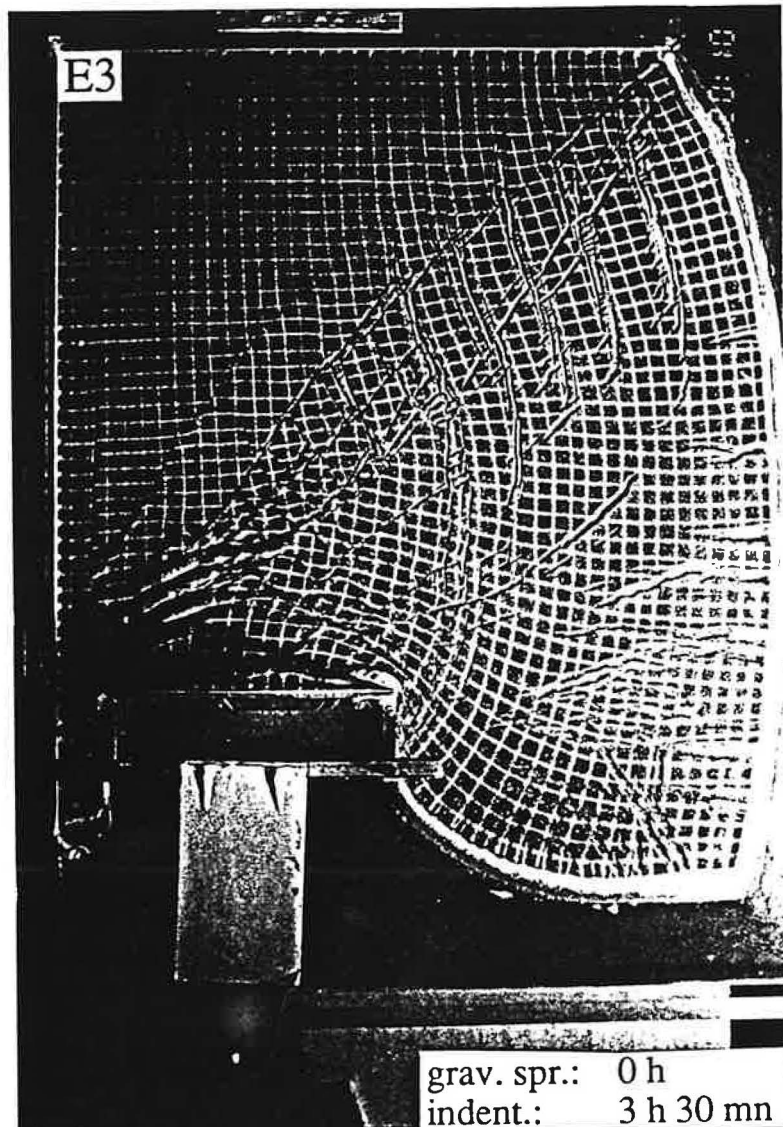


b



c

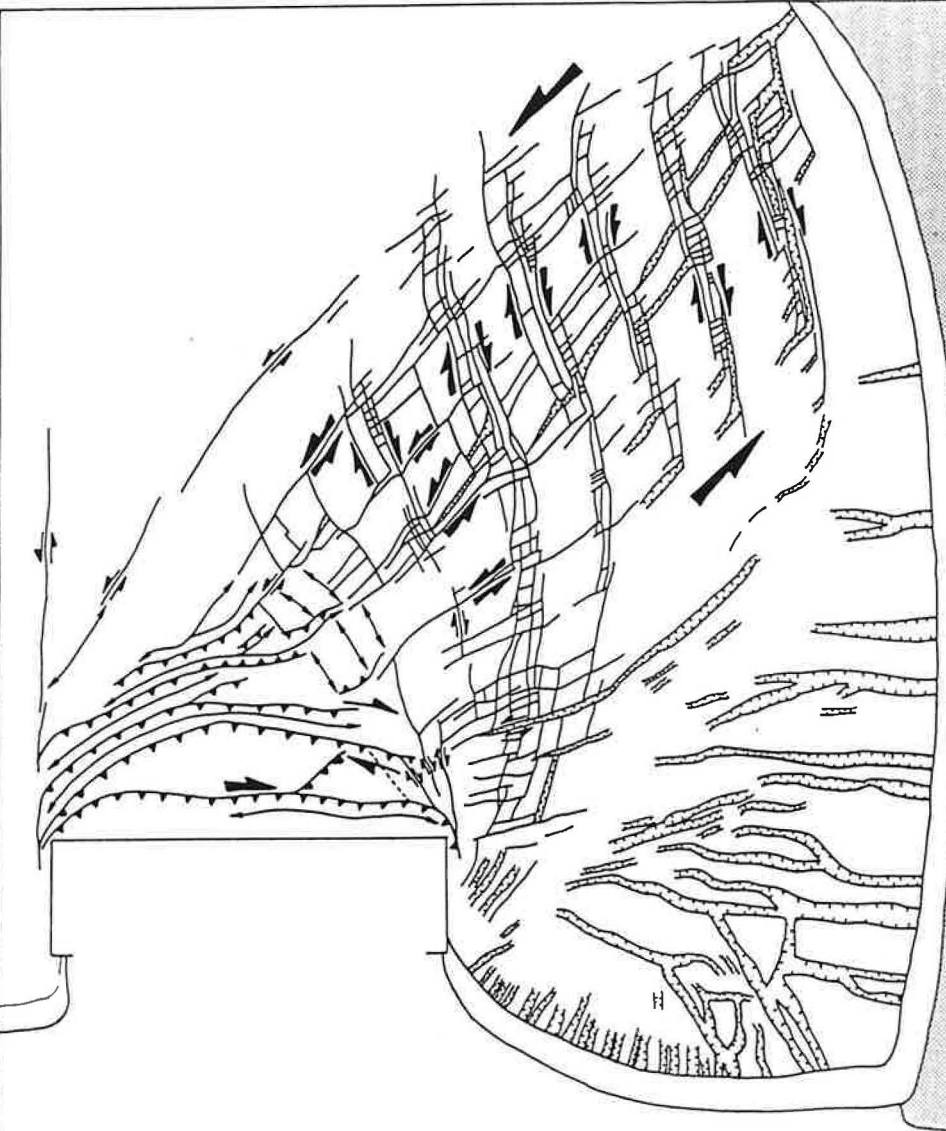
d



grav. spr.: 0 h
indent.: 3 h 30 mn

Fig.6. (a) Photograph of E3 after 3 h 30 mn of indentation (no preliminary spreading), and (b) corresponding structural map. Same symbols and legend as Fig. 4. (c) Map of shear rate. (d) Map of rigid rotations. The successive stages of deformation of E3 are shown in Figure 3.

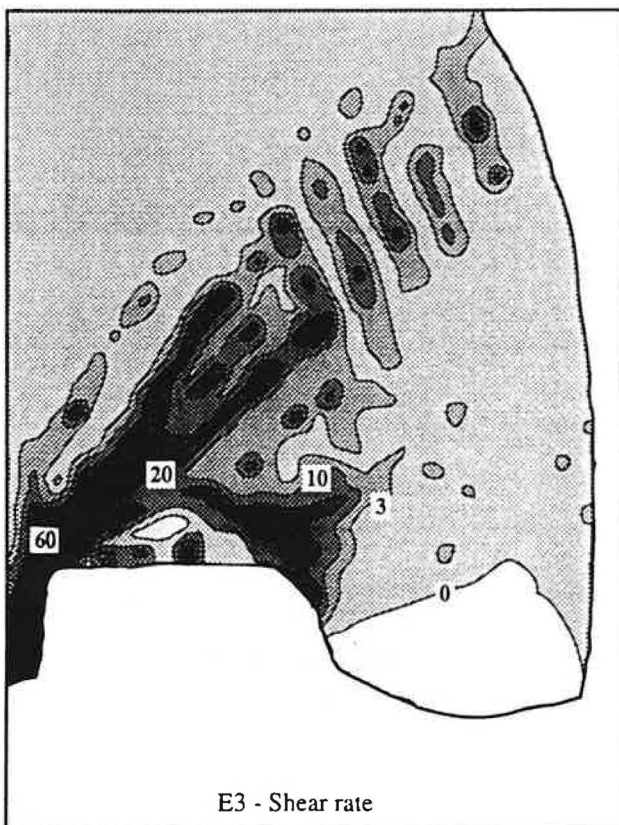
E3



a

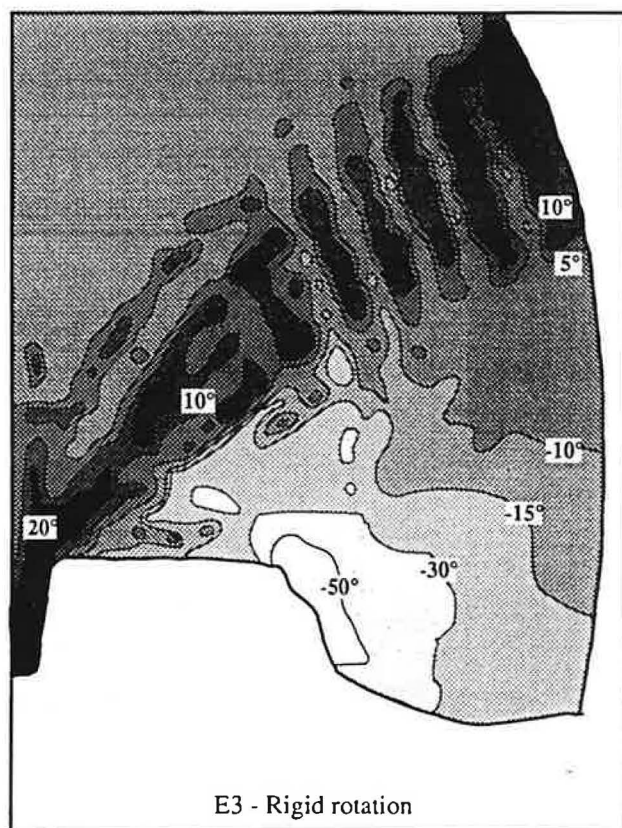
$v_{ind} = 5.5 \text{ cm.h}^{-1}$

indent.: 3 h 30 mn



b

E3 - Shear rate



c

E3 - Rigid rotation

the northernmost lines of grabens are curved toward the NW. After 3 h of indentation, the deformation is less diffuse than in E1, with fewer faults (Figure 5b). The NE trending left-lateral strike-slip faults reactivated some of the pre-existing normal faults. This is particularly clear for the northernmost lines of grabens. Compare to E1, one well differentiated N-S trending right-lateral shear zone appears east of the indenter. It includes minor NE trending left-lateral faults which bound rigid blocks undergoing clockwise rotations in the right-lateral shear zone. Most of the shear is absorbed along two imbricated systems of conjugate shear zones in front of the indenter (Figure 5c). No right-lateral strike-slip fault appears in front of the indenter.

During E3 (Figure 6) indentation and spreading started simultaneously. Deformation is again less diffuse than in E2, with again fewer faults (Figure 6a and b). To the NE, left-lateral shear is accommodated by rotations of blocks bounded by NNW trending right-lateral shear zones. The map of shear rate (Figure 6c) show that right-lateral shear prevails in this area. NE-trending faults accommodate extension rather than left-lateral slip. Figure 7 shows the blocks geometry. Blocks are strained by left-lateral shear and have a sigmoid shape. The finite counterclockwise rotation of the central part of the blocks is 10° to 20° , and the finite clockwise rotation within the right-lateral shear zones locally exceeds 10° (Figure 6d). Left-lateral shear is totally taken up by block rotations and right-lateral shear, provided a slight amount of internal deformation of blocks.

Preliminary spreading is accommodated by normal faulting broadly distributed over the model. The model becomes heterogeneous with diffuse normal faults which tend to distribute the deformation produced by indentation. Preliminary spreading also correspond to a decrease of the gravity potential of the model. Thus, the model is more heterogeneous (with more normal faults), but its gravity potential is lower when the duration of spreading increases. In this first set of experiments, the distribution of deformation is essentially controlled by preliminary spreading. The longer it is, the more diffuse is the final deformation. Moreover, pre-existing normal faults are used as guides for deformation during indentation, the NE-trending faults being reactivated as strike-slip faults. The decrease of gravity potential of the model during preliminary spreading appears to have little influence on deformation.

Influence of the gravity potential on deformation

From E3 to E4 we removed the lateral confinement in order to increase the gravity potential of the model relative to the boundary. The extensional potential of the model is higher and the deformation is highly distributed (Figure 8). In particular, a dense network of conjugate strike-slip faults appeared. The deformation maps of E4 are not shown because they are very similar to that of E5 and show a very diffuse deformation.

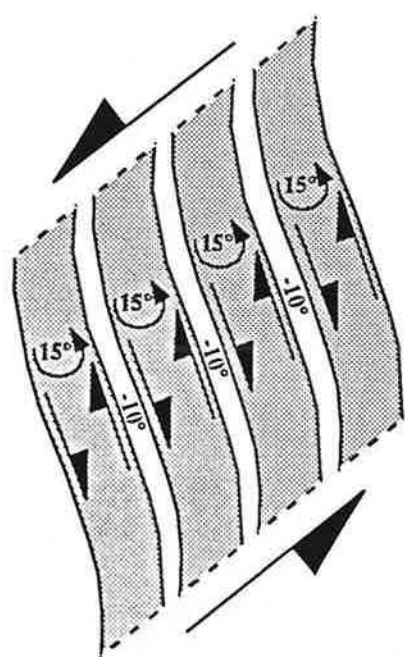


Fig. 7. Mechanism of deformation with block rotations in the NE part of E3.

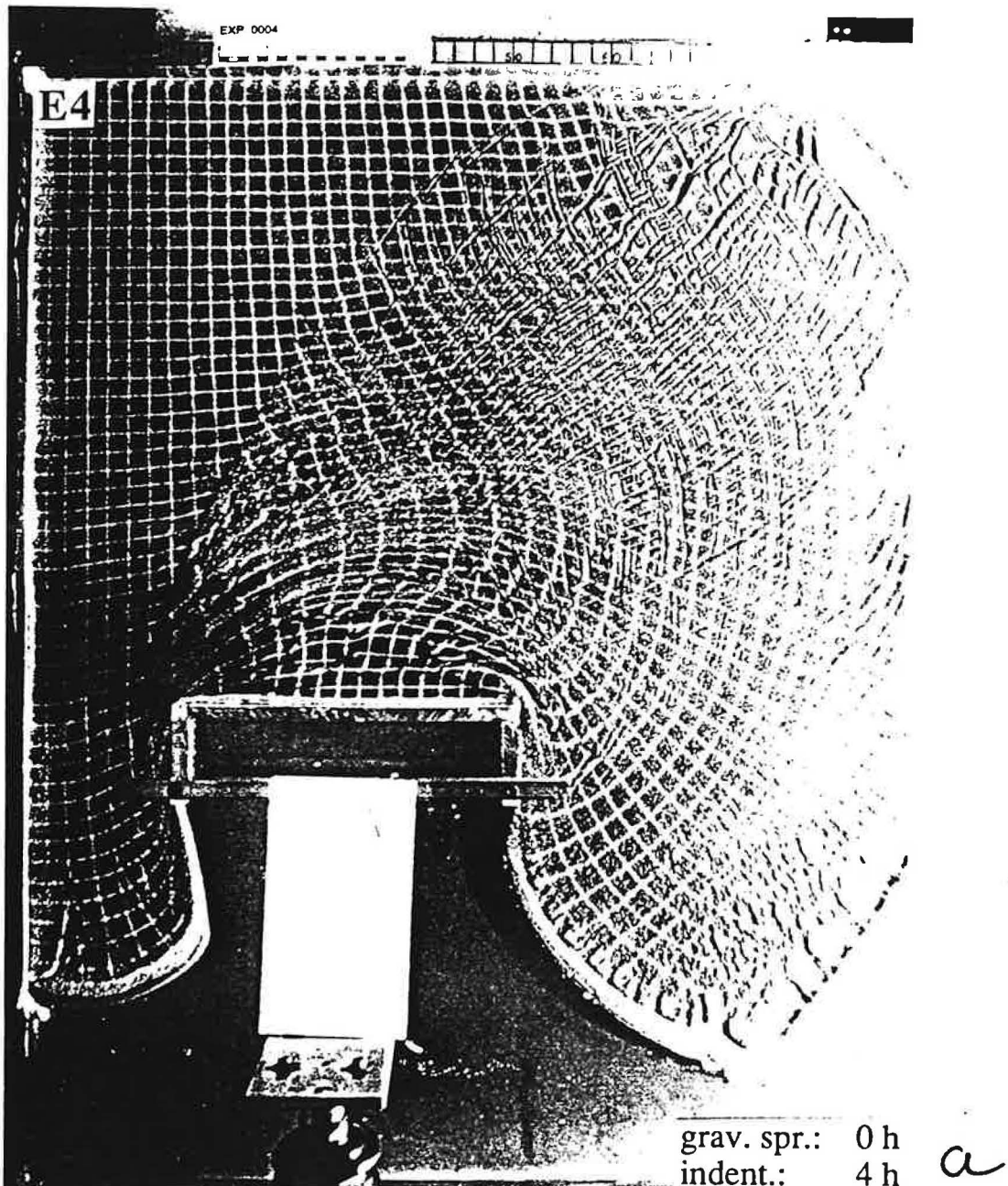
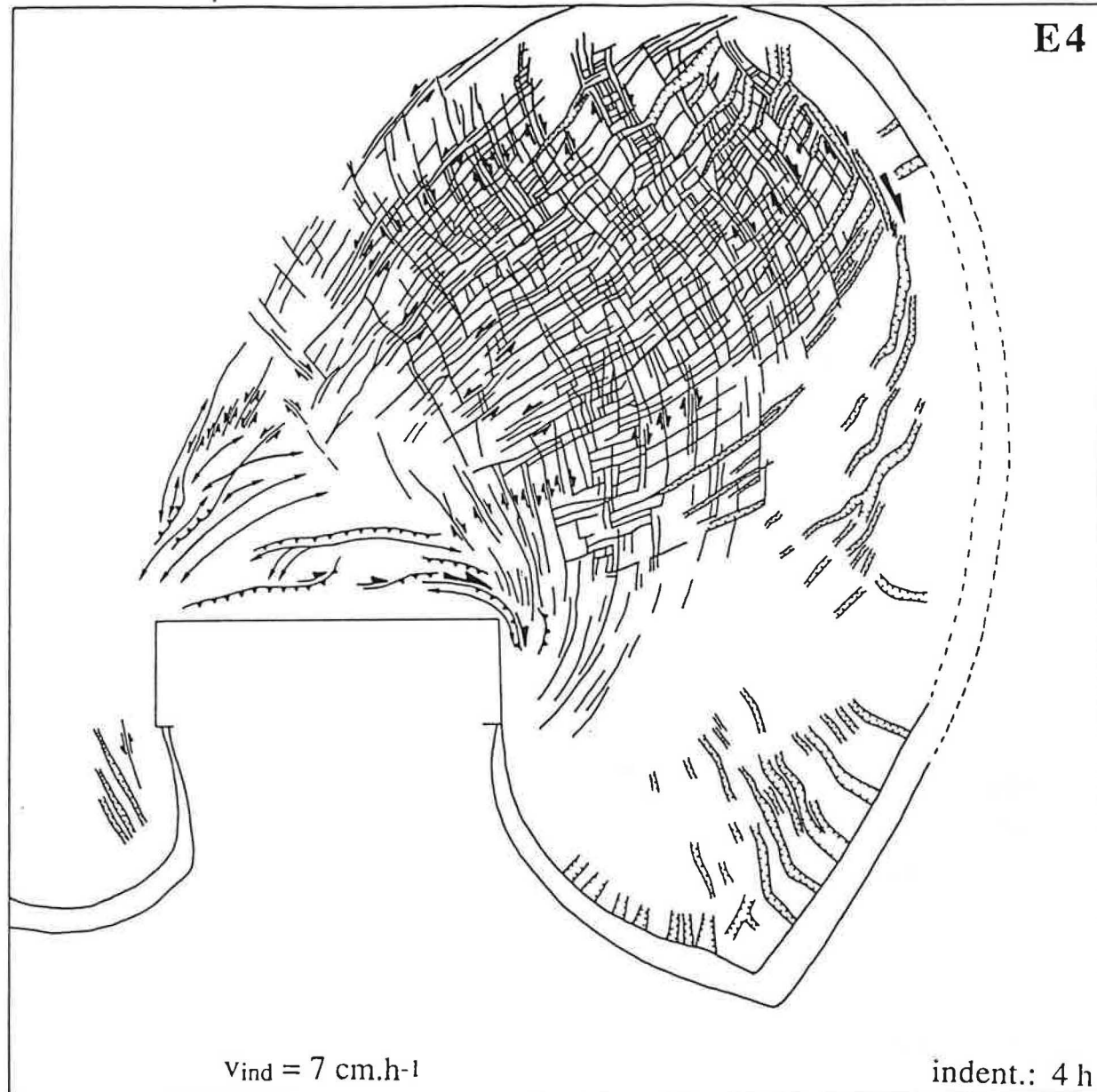


Fig.8. (a) Photograph of E4 after 4 h of indentation (no preliminary spreading), and (b) corresponding structural map. Same symbols and legend as Fig. 4.

E4



b

$v_{ind} = 7 \text{ cm.h}^{-1}$

indent.: 4 h

Increasing the extensional potential of the model by removing the eastern confinement has a similar effect as increasing the duration of preliminary spreading: larger diffusion of the deformation. The pattern of deformation of E4 is yet different from the pattern of deformation of E2 with 1h of preliminary spreading and lateral confinement. Strike-slip faulting is less diffuse in E2 than in E4, and the deformation in E2 is guided by the pre-existing NE trending faults. For similar rates of finite extension, the final deformation tends to be less diffuse for a long-lasting duration of spreading with normal faults reactivated, than for a high spreading rate.

Influence of indentation speed on deformation

From E4 to E5, we increased the indentation speed from 7 cm.h^{-1} to 20 cm.h^{-1} . The results of E5 are shown in Figure 9. The deformation pattern is similar to that of E4. Strain is broadly distributed over the model and no prominent structure appears. A dense network of conjugate strike-slip faults developed, as in E4, with yet fewer faults. Thickening in front of the indenter is more important in E5 because of the higher indentation speed, and grabens are less developed in E5 because it lasted only 1 h 30 mn against 4 h for E4. Hence, a three times faster indentation does not modify significantly the deformation pattern and provokes only a moderate localisation of deformation, unlike the lateral confinement in E3. The deformation is controlled by the high extensional potential of the model rather than by the high strain rate due to the fast indentation speed.

Lateral expulsion and spreading in the experiments

We can have an idea of the component of extrusion due to lateral expulsion (driven by indentation) and the component of extrusion due to spreading (driven by gravity), in studying the variations of the eastward velocity along an originally E-W line. Figure 10a shows the variations of eastward velocities for each experiment along an E-W line of the model originally 20 cm apart from the southern boundary of the model. Figure 10b shows the interpretation of these curves. The eastward velocity is the sum of the spreading velocity and the lateral expulsion velocity. Lateral expulsion being accommodated by diffuse left-lateral shear, the velocity of lateral expulsion increases progressively across the shear zone and is constant east of it. The increase of the spreading velocity is considered to be linear along the E-W line. However, as spreading velocity varies with the topographic load, it is likely higher in front of the indenter where the model is thickened than east of it. Because we measure the spreading rate in the eastern part of the curve, we obtain minimum values for the spreading velocities.

The spreading rate (strain rate to the east of the shear zone), the extrusion rate (strain rate in the shear zone), and the extrusion velocity (eastward velocity at the eastern limit of the shear zone) deduced from the experimental curves are given in Table 3. The velocity of

lateral expulsion is given by the extrusion velocity minus the spreading velocity. Because spreading velocities are minimised, we obtain maximum values for the velocity of lateral expulsion. It is compared in Table 3 with the indentation velocity.

Spreading rate is low in E2 and E3 because of the confined boundary to the east. The spreading rate of E4 and E5 in the absence of confinement is consistent with spreading rates measured during preliminary tests and discussed above (1 to 2.10^{-5} s $^{-1}$). Thus, spreading velocities depend directly on the presence or absence of lateral confinement. About one fourth of the extrusion is taken up by spreading in E2 and E3 (with lateral confinement), and more than one half in E4 (no lateral confinement) with the same indentation velocity. The extrusion rate is low in E3, but it is compensated by the fact that the deformation zone is wide, so that the extrusion velocity is the same as in E2. The velocity of lateral expulsion is similar in the first four experiments with similar indentation velocities. It represents less than one half of the indentation velocity in the first four experiments, and slightly more than one half in E5. According to these data, the velocity of lateral expulsion seems to be related mainly to the indentation velocity and not to boundary conditions.

These calculations give only a crude idea of the nature of extrusion in the experiments. Even in the absence of lateral confinement, one half of the extrusion is taken up by lateral expulsion, the rest being taken up by gravitational spreading. This ratio increases with a confined boundary or with a high indentation velocity. Moreover, the lateral expulsion velocity represents roughly one half of the indentation velocity.

KINEMATICS OF FINITE DEFORMATION

Figure 11 shows the finite displacement field relative to the experimental box for each experiment. The finite displacement field of E1, E2, and E3, can be described with a rotation pole located just east of the zone of impact of the indenter with the model. We verified that the instantaneous displacement fields between successive stages every 30 mn could be described by the same pole. The lateral confinement, even partial in E1, favours southward extrusion and spreading and the result is a return flow east of the indenter. The mean direction of the return flow rotates progressively from N-S in E1 to NW-SE in E3 because of the reduction of the duration of preliminary spreading, which highly contributes to the southward component of the return flow. Vilotte et al. (1982) computed a similar circular displacement field for the case of plane strain with a rigid lateral boundary, the material escaping across the south free boundary.

During E4 and E5 the eastern boundary was free and eastward extrusion prevailed. The rotation pole moves eastward (Figure 11). E5 was fast (1 h 30 mn) because of the high indentation speed, and spreading was low. Consequently, the component of southward spreading was negligible and the displacement field consisted in almost concentric

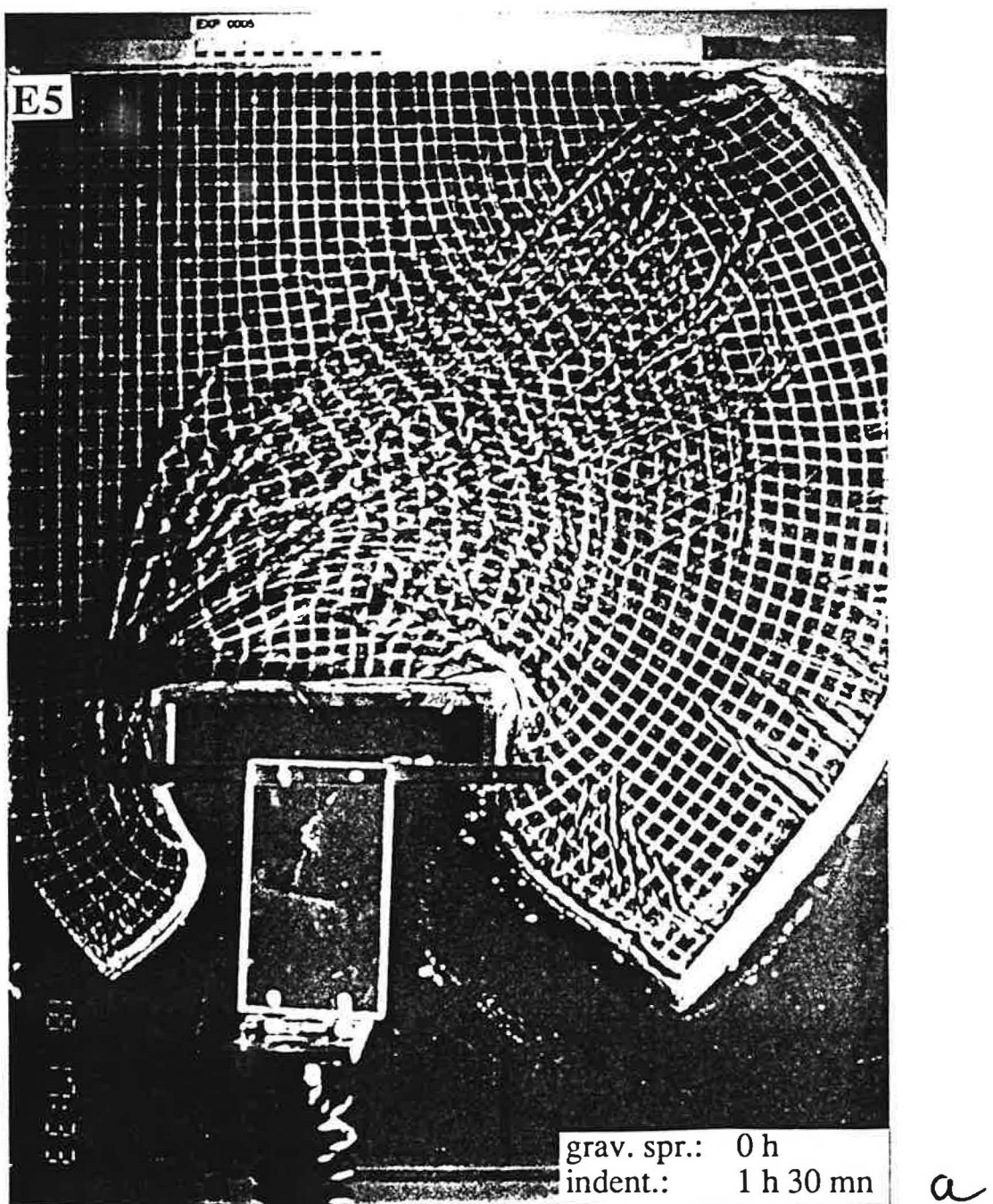
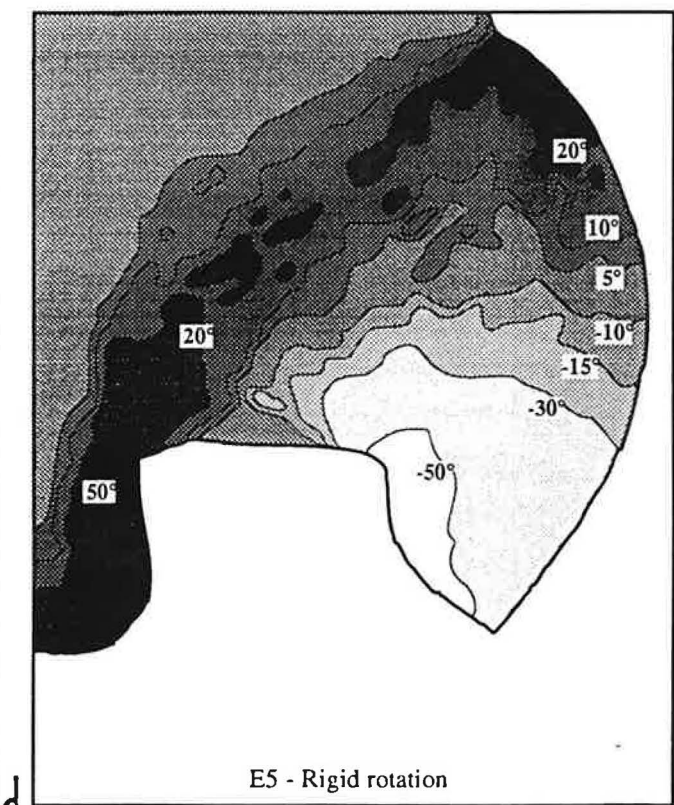
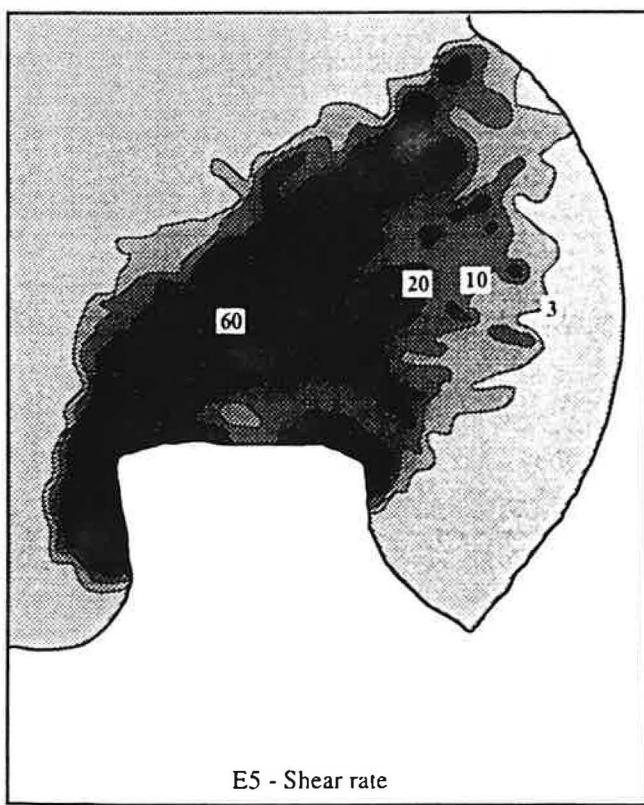
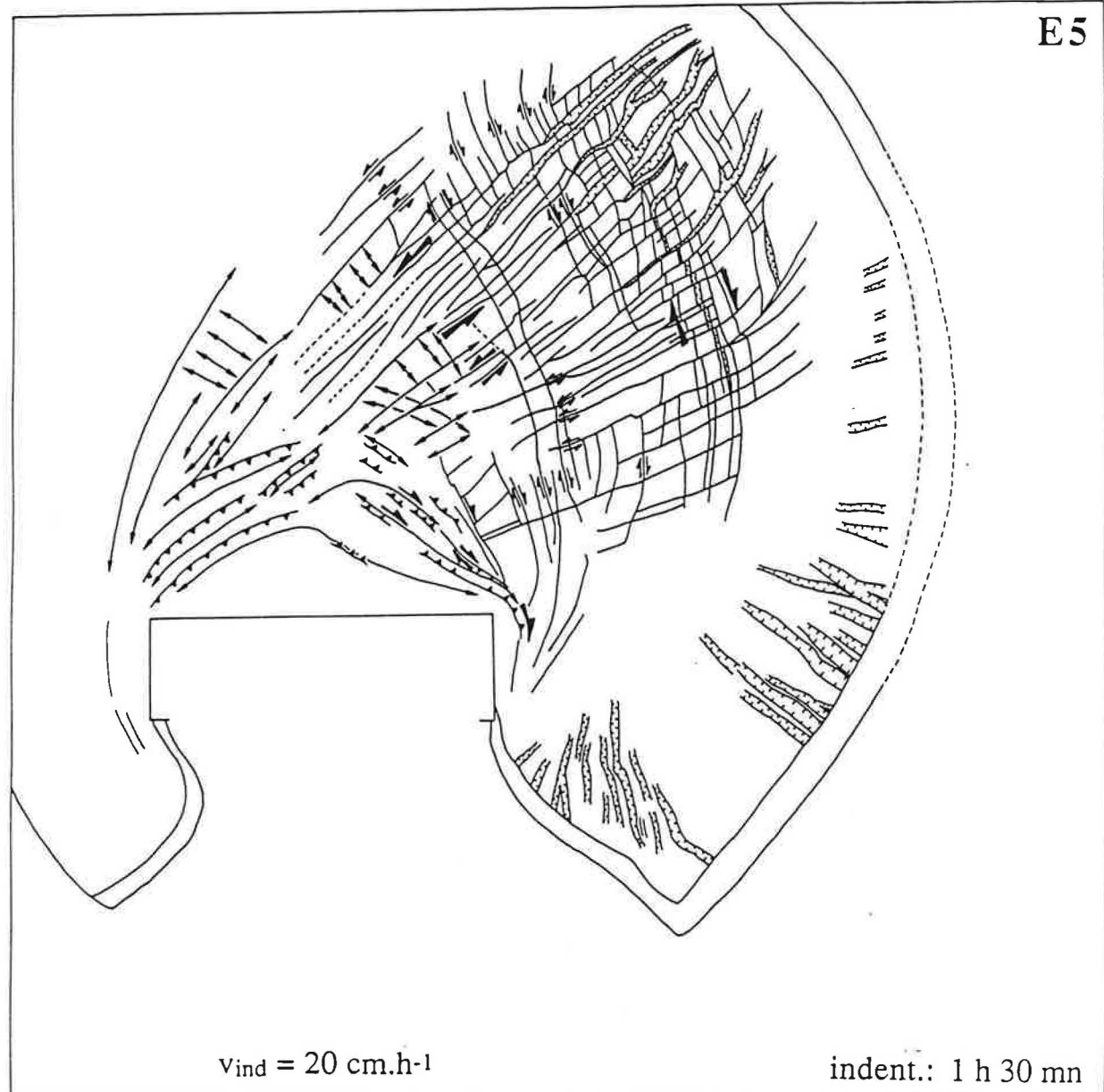


Fig.9. (a) Photograph of E5 after 1 h 30 mn of indentation (preliminary spreading), and (b) corresponding structural map of E5. Same symbols and legend as Fig. 4. (c) Map of shear rate. (d) Map of rigid rotations.

E5



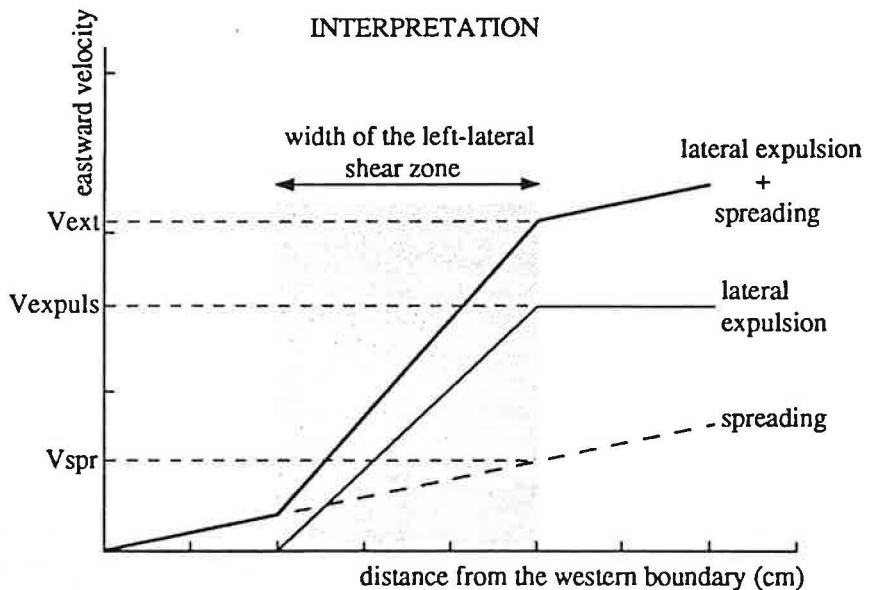
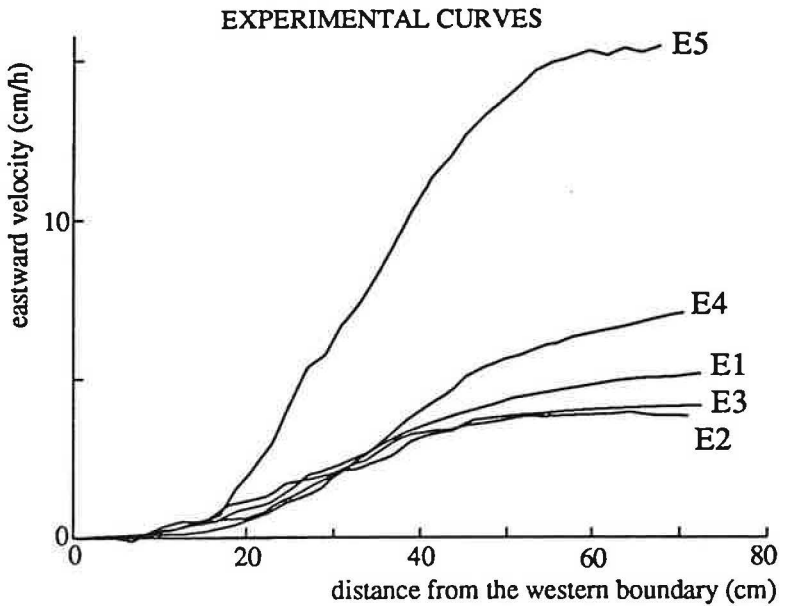


Fig. 10. (a) Curves of eastward velocity along an originally E-W line 20 cm apart from the southern boundary of the model. (b) Eastward velocity (extrusion) is sum of the velocity of lateral expulsion and the spreading velocity. V_{expuls} is velocity of lateral expulsion, V_{extr} is extrusion velocity, V_{spr} is spreading velocity.

trajectories centred on the SE corner of the model. A similar velocity field was computed by Villette et al. (1982) for the case of plain strain with a free lateral boundary. Peltzer and Tapponnier (1988) also obtained similar instantaneous velocity fields with plasticine models. E4 lasted 4h and a substantial return flow appeared east of the indenter because of southward spreading.

Hence, kinematics of finite motions can be described with a rotation pole. The pole is located east of the indenter, its latitude being roughly that of the indenter at the beginning of indentation. Its position depends on boundary conditions. Lateral confinement favours southward spreading and brings the pole close to the indenter. In other words, a rotation pole close to the indenter is symptomatic of a southern boundary less confined than the eastern boundary.

The finite kinematics of Asia since the Eocene is poorly constrained, especially because it is unclear to what extent extrusion took part in the finite deformation. Nevertheless, Le Pichon (1988) noticed that a rotation pole located in the Andaman Sea (13°N - 95°E) fairly well describes finite motions in Asia, as the opening of the South China Sea (see further discussion in Briais et al., 1993), strike-slip motions along the Red River Fault and along the east coast of South Vietnam, and active motions in Tibet (Figure 12). This pole, located east of the collision zone of the eastern Greater Indian Syntaxis with Eurasia, is similar to the rotation poles obtained in E1, E2, or E3. According to the experiments, it is symptomatic of a boundary less free to the east than to the south. Kinematics of the active deformation in central Asia proposed by Avouac and Tapponnier (1993) from rates of motion along faults between four rigid blocks may also be described with a similar pole located in SE Asia. Because we cannot define in the models a rigid block equivalent to South China, the comparison with the velocity field of Asia computed relative to South China from moment tensor of earthquakes (Holt and Haines, 1993) is uneasy.

RELATION BETWEEN DISPLACEMENT AND FAULTING

Displacement fields can be calculated from rates of motion along faults (e.g., Avouac and Tapponnier, 1993). These calculations take into account kinematically significant faults, i.e., major faults with high rates of motion. Two examples from the experiments show that major dislocations may have little influence on displacement fields. The first example is the N-S right-lateral shear zone which develops east of the indenter. This shear zone is well developed in E2 and E3 and accommodates displacements of centimetre scale (Figures 5 and 6). However, the maps of finite motions relative to the experimental box (Figure 11) show that the displacement field is absolutely not disrupted by this shear zone. It accommodates N-S motions negligible with respect to the eastward motions and it is completely drowned in the displacement field. The second example is the right-lateral strike-slip fault which

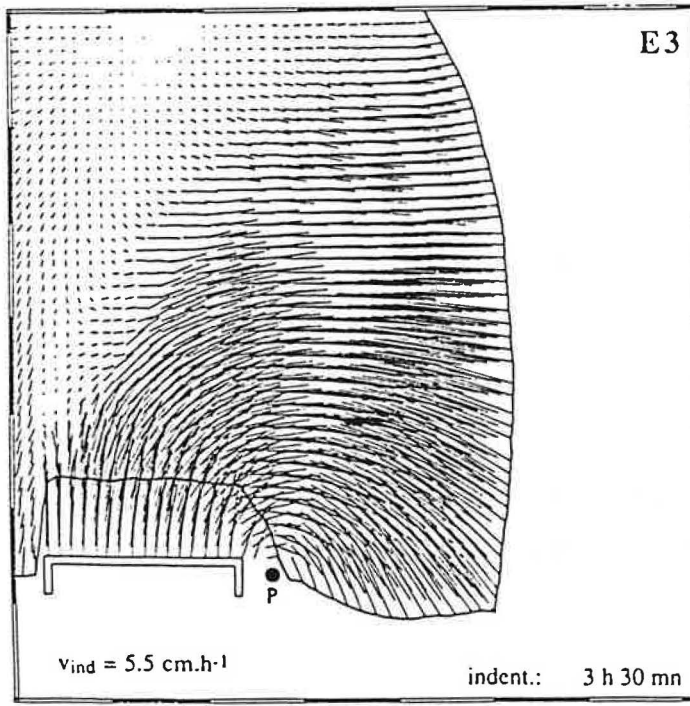
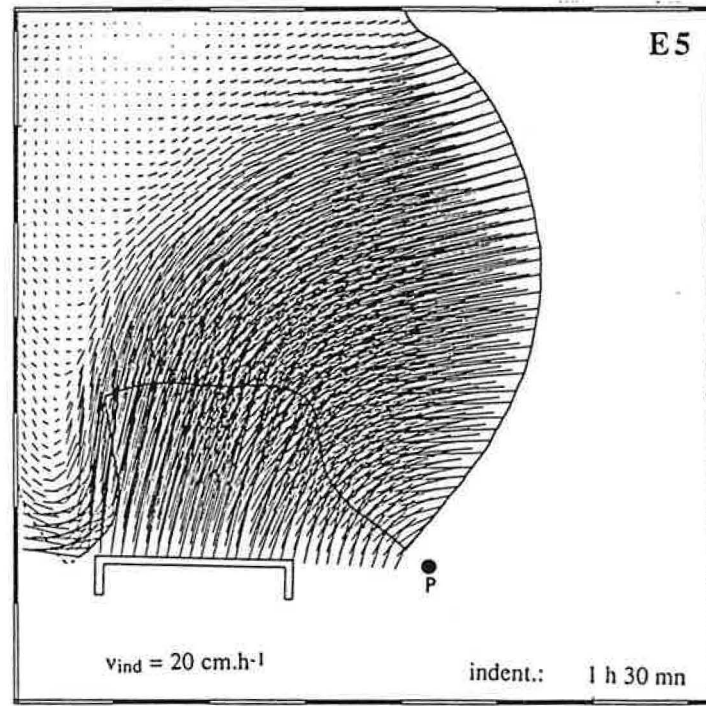
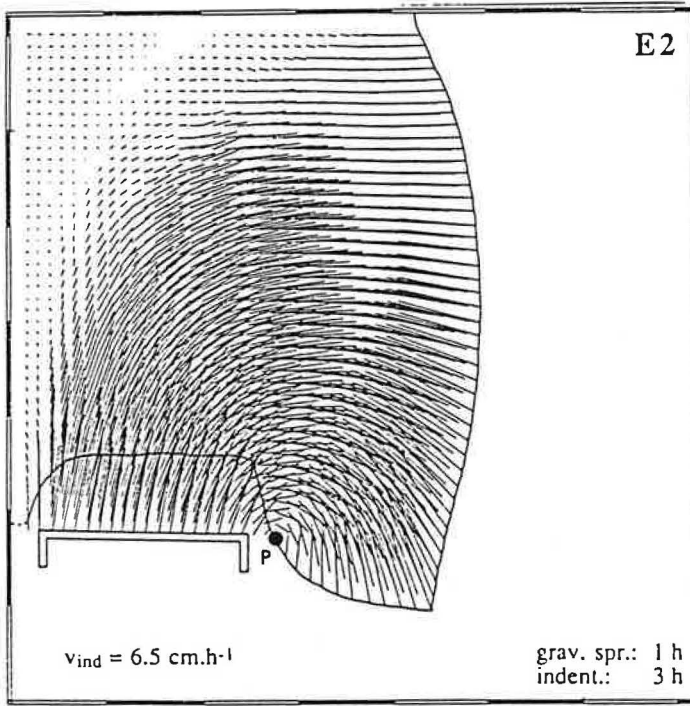
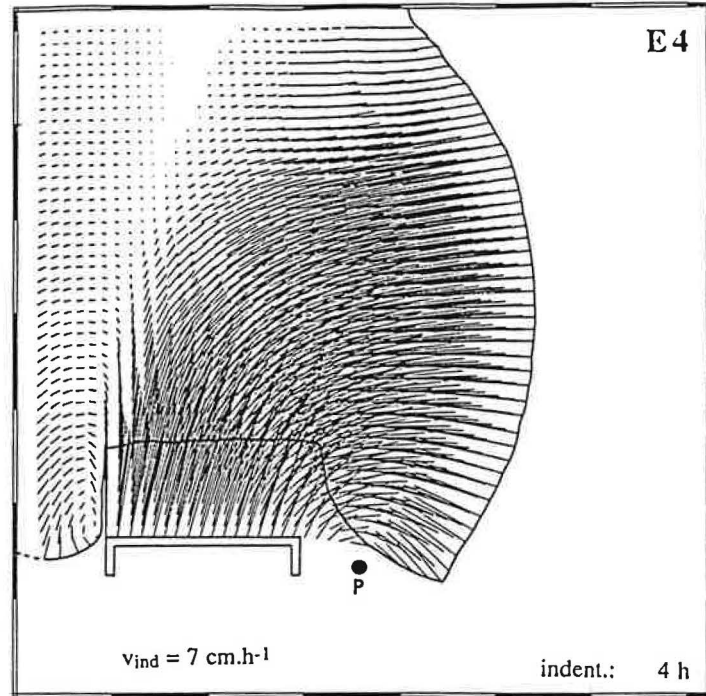
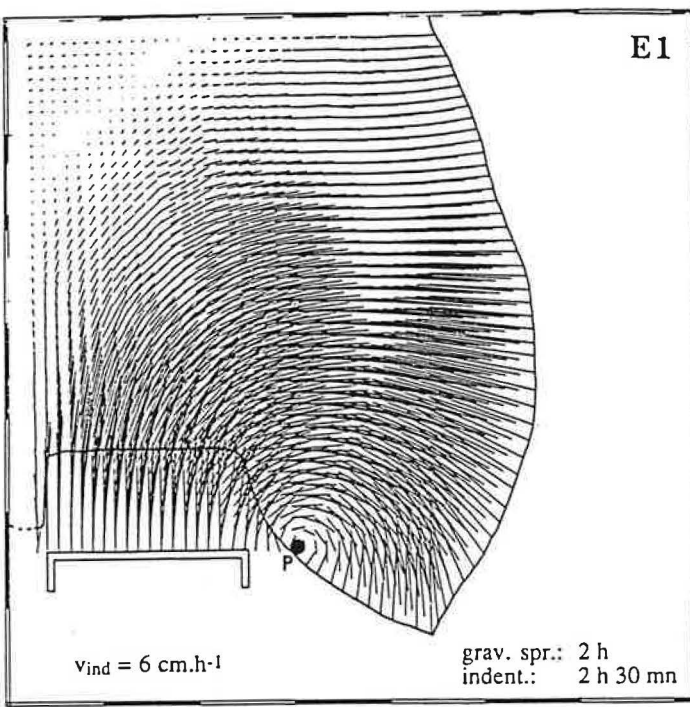


Fig. 11. Finite displacement field relative to the experimental box for each experiment. P is pole of finite motions. Same legend as Fig. 4.

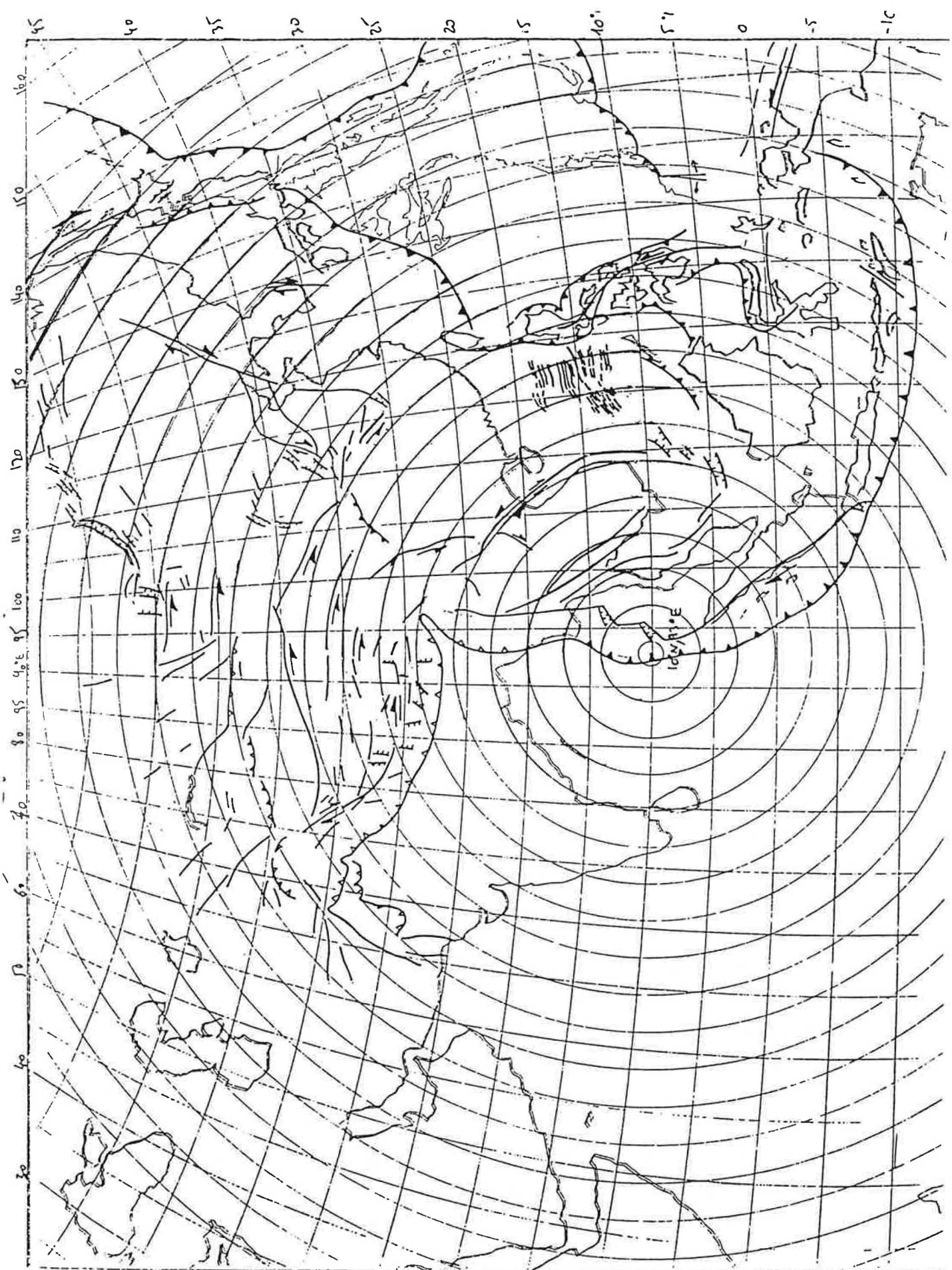


Fig. 12. Deformation of Asia "viewed from" the Adamant Sea pole (10°N , 93°E). Conical Lambert projection (small circles are true circles). Magnetic anomalies of the South China Sea are shown.

develops in front of the indenter and accommodates the extrusion of the unstrained triangle. This fault appears in E1 and E4 only (Figures 4 and 8). Finite motions relative to the indenter are shown in Figure 13 for all the experiments. The presence of the fault in front of the indenter has little influence on the displacement field. The unstrained triangle is always extruded eastward.

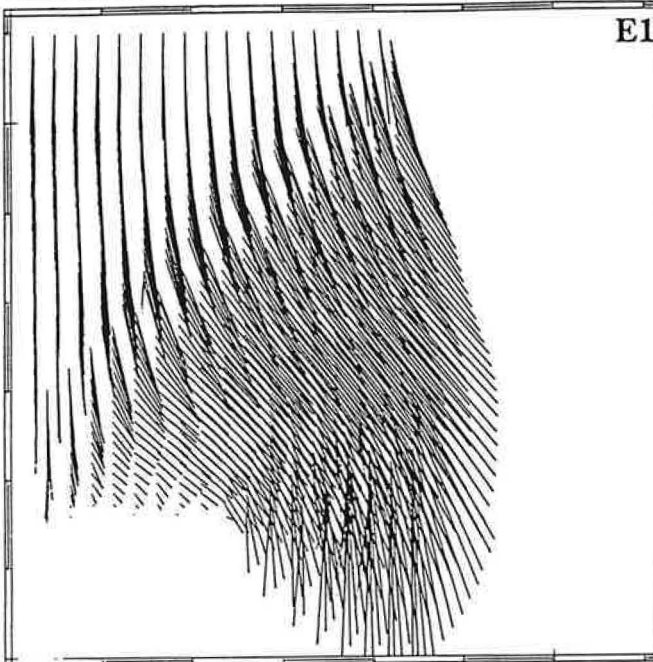
In these examples, motions along faults are negligible with respect to eastward motions due to spreading, shear, and strike-slip faulting. Displacements fields in Figure 11 clearly evidence that the only important structure from kinematics point of view is the NE trending left-lateral shear zone. Calculation of displacement field from rates of motion along faults requires a strong hypothesis on the mechanism of deformation. The experiments show that the choice of faults is also of crucial importance.

OPENING OF MARGINAL BASINS

In this section we discuss the graben formation in the models. We consider the grabens which developed within the model only and do not take into account the extrado cracks along the bent boundaries. In the models E2 and E3, the trends of grabens changes progressively from NE-SW in the north to E-W in the south. A similar evolution from NNE-SSW in the north to NE-SW in the south is observed in E1 and E4. E5 was too fast to allow enough spreading. Trend of grabens depends on the direction of $\sigma_{H\max}$ (maximum horizontal stress) produced by indentation and on the direction of traction produced by gravitational spreading. In Figure 14 we plotted the strain ellipse computed in the horizontal plane for E1, E3, and E5. It was computed in each node of strained grids and its long axis is plotted at each grid point. The arrow indicates the extremity of the axis. The maps show that the trend of the maximum strain in the south-east part of the model is independent from the trend of the maximum strain in the collision zone. Indentation has no influence upon deformation in the SE part of the model, the deformation being only driven by gravitational spreading. The trend of basins in this area is perpendicular to the direction of spreading, i.e., E-W when the east boundary is confined and spreading directed southward (in E2 and E3), and NE-SW when the east boundary is free and spreading directed south-eastward (E1 and E4). In the NE part of the model, the effects of indentation and extension are combined. Figure 15 shows the structural map of the NE part of model E3. The trend of $\sigma_{H\max}$ (N015E) is deduced from the bisecting line between conjugate faults. The geometry of grabens is controlled by the structures produced by indentation, i. e., by conjugate strike-slip faults. Both left-lateral and right-lateral faults localise extension. As already noticed, most of the deformation in this area is taken up by right-lateral shear (Figure 6c). In turns, right-lateral shear is taken up along the shear zones by extensional structures, pull-apart basins or extensional cracks.

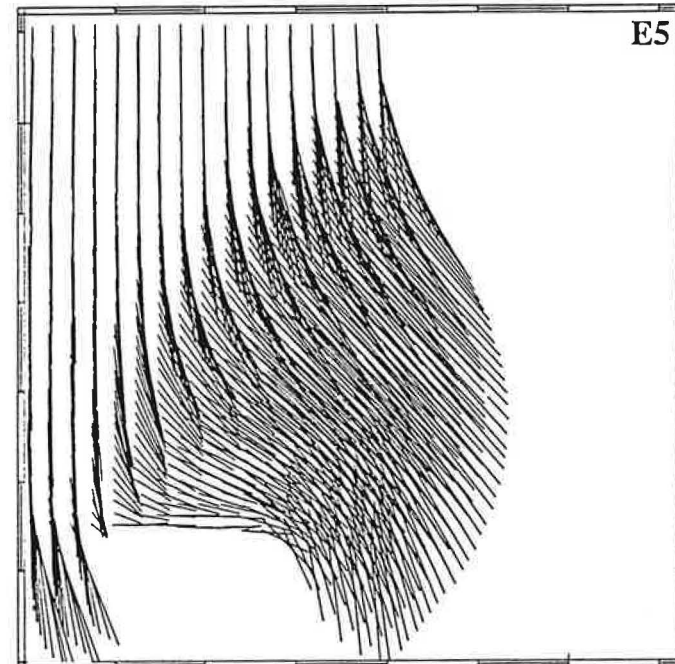
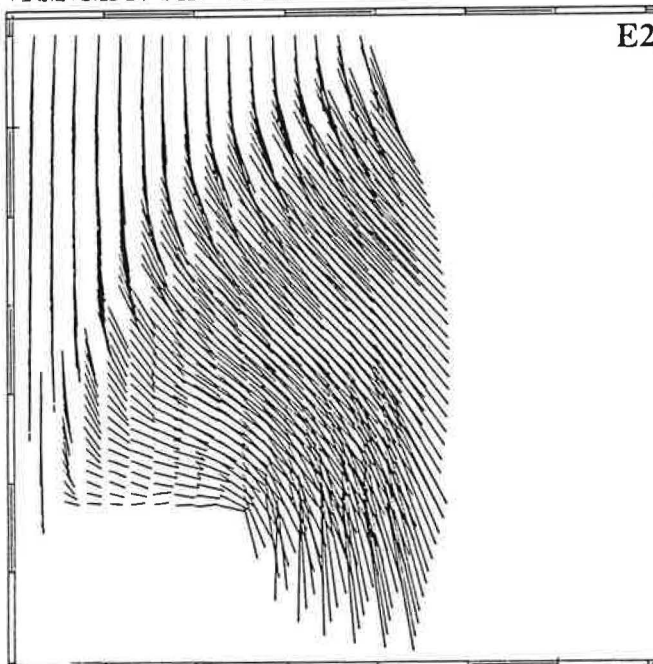
E1

E4



E2

E5



E3

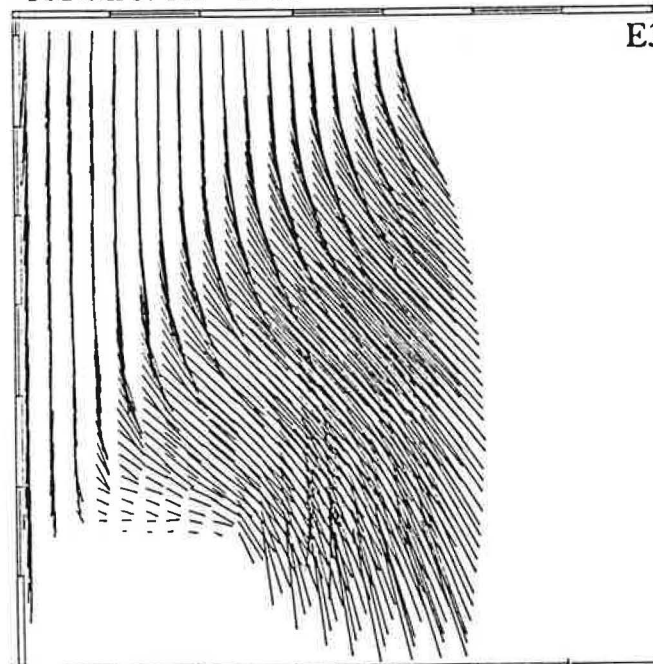


Fig. 13. Finite displacement field relative to the indenter for each experiment.

E1



E3



E5



Fig. 14. Maximum horizontal strain in E1, E3, and E5. The maximum strain axis of the strain ellipse computed in the horizontal plane is plotted in each point. The arrow shows the extremity of the axis.

Jolivet et al. [1990] made similar observations from Davy and Cobbold's [1988] experiments and proposed a model of opening of NE Asian basins (North China Basin and Japan Sea). In their model the convergence between India and Asia is partly taken up along a wide left-lateral shear zone which connects the Pamir to the Stanovoy ranges and evolves from transpression to transtension. In the transtensional domain left-lateral shear is accommodated by rotation of large crustal blocks bounded by right-lateral strike-slip zones, the east Japan Sea shear zone, the Tan-Lu Fault, and en echelon grabens on rims of the Ordos block (Figure 16). E3 reproduces these results and even suggests that left-lateral shear can be totally taken up by right-lateral shear and counterclockwise rotations. The maximum amount of motion accommodated along dextral strike-slip faults during E3 is worth about 2 cm. Given a rigid rotation, shear between rotating blocks increases when it is less distributed, i.e., blocks are wider. For blocks several hundred kilometres wide, one can expect right-lateral motions of the order of 100 km.

No fault equivalent to the Red River Fault ever appears in the experiments and we cannot discuss the opening of the South China Sea in terms of collision-related deformation as in Tapponnier et al. (1982; 1986) and Briais et al. (1993). However, the experiments suggest that the openings of SE Asian marginal basins are controlled by subduction-related extension rather than by collision.

INFLUENCE OF LATERAL CONFINEMENT ON DEFORMATION

In this section we discuss the influence of the lateral confinement on deformation in the SE part of the model. This area is affected by normal faulting only, and studying the distribution of rotations is a good way to describe the deformation. In a brittle medium, rotations about vertical axis are related either to fault slip or to rotation of faults together with fault-bounded blocks. In the experiments, rotations are also due to viscous shear. If rotations due to fault slip can be spectacular (see the maps of E2 and E3), they hardly exceed 20° whereas rotations which affect the SE part of the model can exceed 50° in the absence of strike-slip faults.

Indentation with a south-east free boundary results in the clockwise rotation of the SE part of the model (E1, E4, E5). Similar observations were made by Tapponnier et al. (1982), Vilote et al. (1984), and Davy and Cobbold (1988). The model rotates progressively while the indenter moves northward, the result being the fan-shaped distribution of rotations (E1 and E5) with maximum rotation rates near the indenter. In E1 (in E2 and E3 either) the pole of finite motions is located in the zone of maximum rotation. With respect to this pole which remained fixed during the experiment, all rotations happen to be counterclockwise and motions tend to minimise the rotation of the pole. It is a whirl-like deformation with a higher angular velocity to the centre and lower angular velocities on the edge.

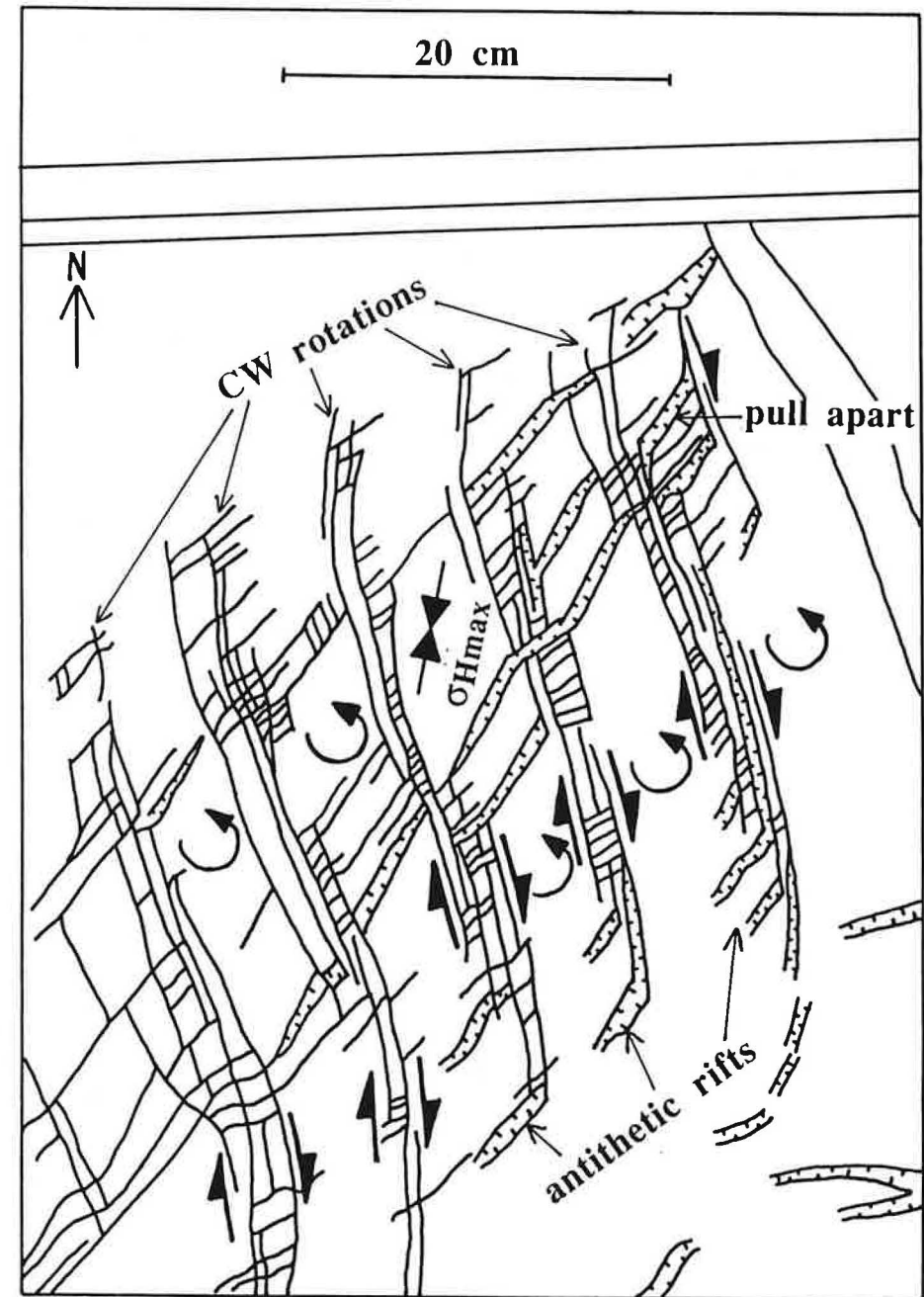
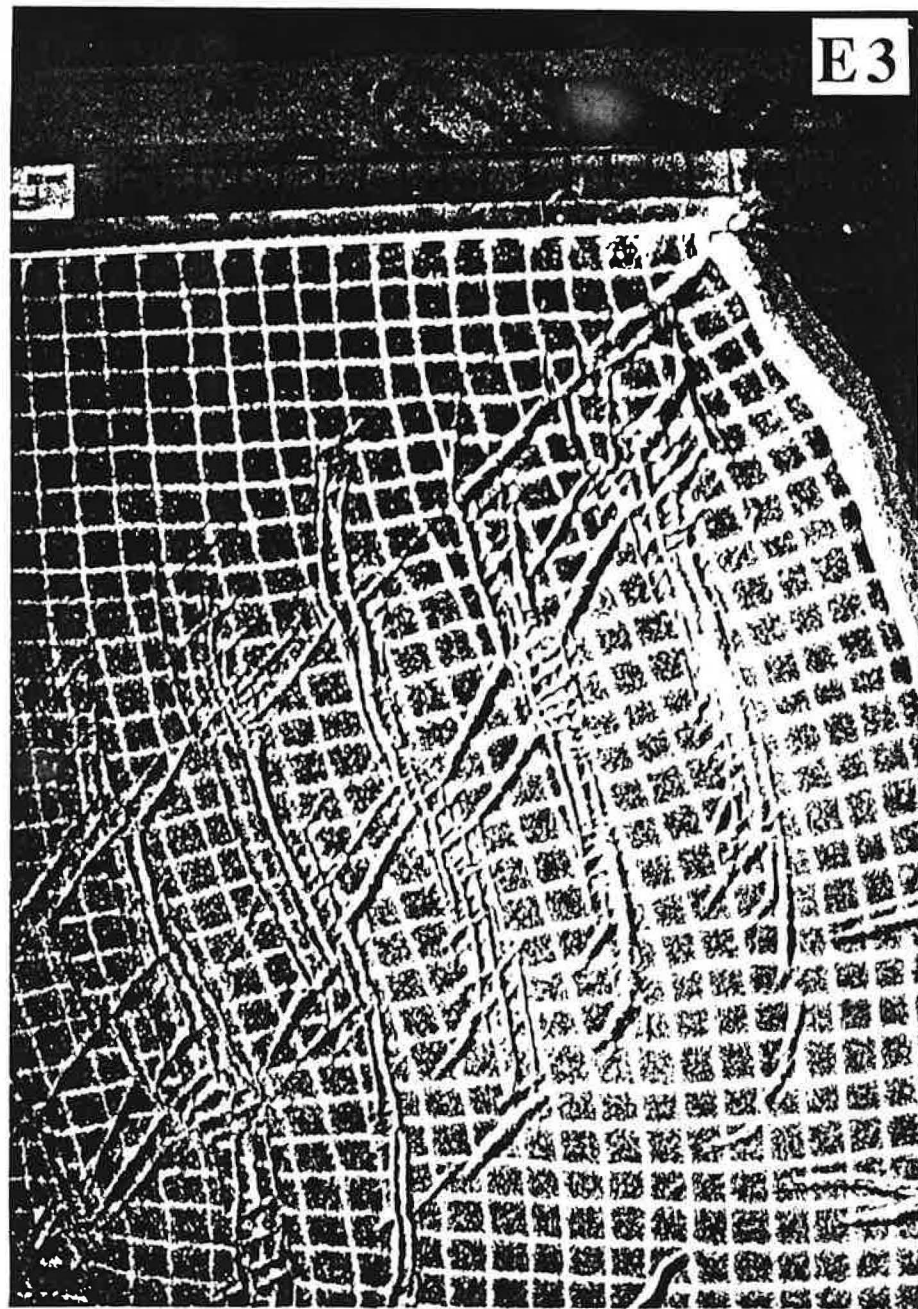


Fig. 15. Detail of the structural map of E3 (Figure 6b) showing grabens opening in the NE part.

When the eastern boundary is confined (E2 and E3), the model is linked to the experimental box by its eastern edge and cannot rotate freely during indentation. In that case, rotations are localised inside the wide N-S trending shear zone east of the indenter. This can be observed on the photograph of E3 in Figure 6a. The originally E-W lines remained E-W after indentation in front of the indenter and on the eastern edge of the model. They are curved east of the indenter inside the right-lateral shear zone. As can be observed on the same photograph, rotations of 15° to 30° computed for the SE corner of the model (Figure 6d) are only due to faster eastward motions in the central part of the eastern boundary than in the southern part, i.e., E-W left-lateral shear.

Thus, by preventing free rotation of the model, lateral confinement modifies the deformation in the SE part of the model. The motion of the indenter relative to the model is taken up by global rotation of the SE part in the absence of lateral confinement, and it is accommodated by N-S shear localised east of the indenter when the eastern boundary is confined. This tends to isolate the deformation of the SE part from that of the collision zone.

The extensional SE Asian boundary of the Oligocene and Early Miocene times likely allowed the rotation of SE Asia as it is documented by paleomagnetism (20°-30° since the Middle Cretaceous) (Achache et al., 1983; Chen and Courtillot; Otofuji et al., 1990; Huang et al., 1992; Funahara et al., 1992). To what extent the Middle Miocene collisions on the SE Asian boundary precluded the rotation of SE Asia and provoked changes in continental deformation far from the subduction zones, is a question worth studying.

AREAL CHANGE AND TOPOGRAPHY OF ASIA

The maps of areal changes can be compared to the topographic map as shortening partly results in thickening and extension in thinning. As remarked before, the maps of areal change are not accurate at small scale and only large scale features can be taken into account. Two simplified maps of areal change are shown in Figure 17 for E1 and E3. The areal change is expressed as the ratio of the final surface to the original surface, in percent. Because we favoured lateral spreading in the experiments, thickening is underestimated and only qualitative observations are valuable. The maps show the asymmetric pattern of the thickened crust in front of the indenter. Thickening occurs at the very front of the indenter and in the southern part of the main left-lateral shear zone. A characteristic triangle of non-thickened crust penetrates from the NE in the thickened area. This asymmetric distribution of thickened crust is symptomatic of the eastern free boundary since the main left-lateral shear zone localises part of the thickening. Another noticeable feature of these maps is the thickened crust extruded eastward past the indenter. Though thickening was quickly resorbed by lateral spreading during the experiments, some thickened crust was extruded.

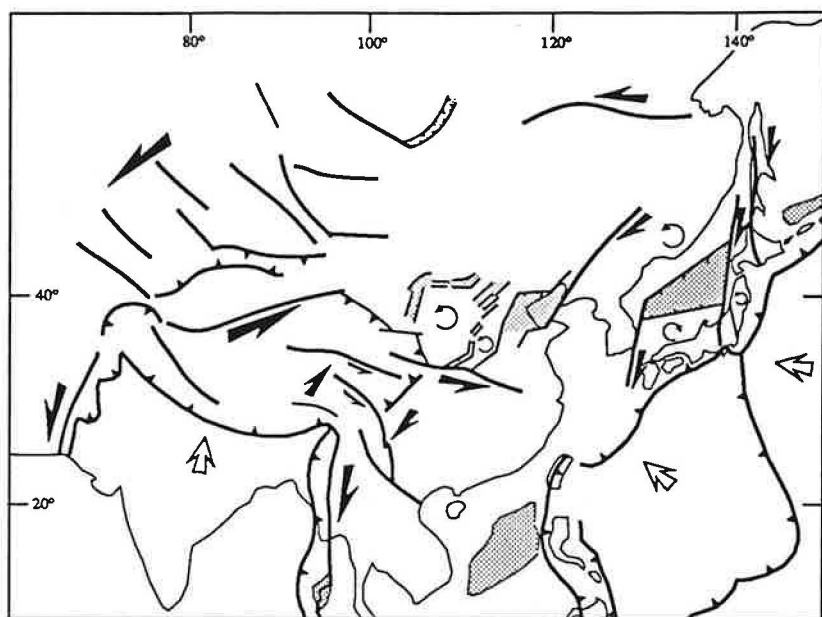


Fig. 16. Mechanism of opening of the NE Asian basins during the India-Asia collision.

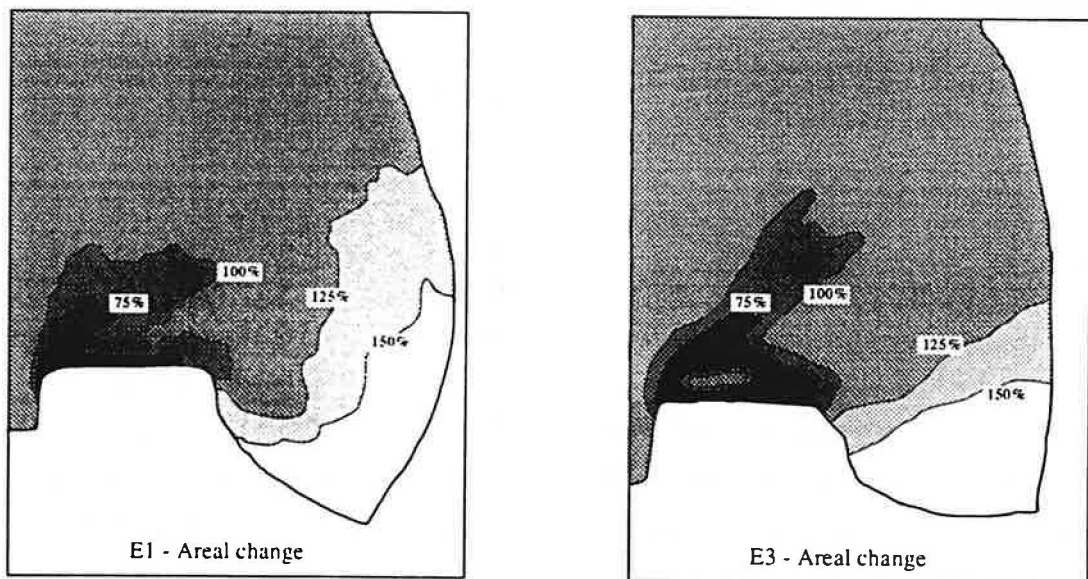


Fig. 17. Maps of areal changes of E1 and E3.

A similar distribution of thickening is observed in Asia (Figure 1). Thickened crust is found in the Tibetan Plateau, and in the Tien Shan and Altai ranges. The Tarim basin being an exotic rigid block, it cannot be regarded as symptomatic of the asymmetry of distribution of thickened crust. However, the same remark does not apply to the almost non-thickened crust which separates the northern Tibet from the Altai ranges and which seems to be equivalent to the non thickened triangle observed on the maps of areal change. Lastly, the topography of Tibet is extruded beyond the eastern Indian syntaxis, as it is in the experiments.

CONCLUSION

We investigated the role of extension driven by gravity during continental deformation produced by collision, by means of analogue models. The deformation pattern we obtained is controlled by duration and rate of gravitational spreading. Spreading prior to indentation, accommodated by widespread normal faulting, provokes the distribution of the deformation during indentation. Part of the NE-trending normal faults are reactivated as left-lateral strike-slip faults. Increasing the gravity potential of the model (i.e., the spreading rate) without preliminary spreading, results in an even more diffuse deformation. The indentation velocity has little influence on the deformation pattern.

The finite displacement field relative to the experimental box can be described with a rotation pole to the east of the indenter. The pole move eastward when lateral confinement is removed. Maps of major faults do not fit well finite displacement fields because some major dislocations accommodate little motions. Formation of grabens is linked with strike-slip faulting produced by indentation in the NE part of the model, but it is driven by gravity only in the SE part.

Deformation in the experiments can be compared to deformation in Asia. The triangular deformation zone pointing toward the NE which appears in front the indenter in the experiments is similar to the triangle of topography over 500 m in Asia pointing toward the Stanovoy ranges. It is bounded to the NE by a wide left-lateral shear zone which can be compared to the Pamir-Tien Shan-Altai-Baikal-Stanovoy deformation zone. Evidences of left-lateral have been described along this deformation zone. From Tien Shan to Altai, left-lateral shear is suggested by the en echelon pattern of mountain ranges (Cobbold and Davy, 1988). In the same region, several right-lateral strike-slip faults which penetrate in the Russian platform have been described (Tapponnier and Molnar, 1979). As pointed out by Cobbold and Davy (1988), these faults likely accommodate counterclockwise rotations of blocks within a wide left-lateral shear zone. In the Baikal region, normal faulting prevails on north-east trending planes, associated with left-lateral slip along E-W faults (Tapponnier and Molnar, 1979; Hutchinson et al., 1992; Deverchère et al., 1993), and further north, active

left-lateral slip along sub latitudinal fault planes is described in the Stanovoy ranges (Parfenoy et al., 1987).

In Asia, topography over 2000 m is found in Himalaya, Tibet, Tien Shan, and Altai, which corresponds to thickened zones in front of the indenter and at the southern end of the left-lateral shear zone in the experiments. In front of the Indian indenter, the topography of the Tibetan plateau is extruded eastward past the eastern Indian syntaxis, as the unstrained triangle in the experiments. To the east of the indenter, the N-S trending dextral shear zone of the experiments can be compared to the huge N-S dextral shear zone in eastern Tibet (England and Molnar, 1990) and/or to the chain of seismicity which bounds the Tibetan plateau to the east, up to the Ordos block (Seismotectonic Map of China, 1985). Lastly, the North China Basin and the Japan Sea opened along dextral strike-slip faults in NE Asia, as grabens in the models to the NE. Therefore, we consider that the experiments reproduce the first order features of the deformation in Asia.

Several origins have been proposed for the extensional deformation in Asia: subduction along the eastern and south-eastern boundaries, collision with India and consecutive deformation of Asia, mantle plume under the Baikal region, and gravity in Tibet. In case of subduction and mantle plume, the high heat flow generated at the base of the crust tend to decrease the integrated shear strength of the crust. This possibly makes it spread toward regions of low stress, e.g., subduction zones. If so, extension along subduction zones and above mantle plumes is driven by gravity, as in regions where the crust is thickened. We do not take into account thermal phenomenons in the experiments. Gravity is used to produce extensional deformation along the boundaries of the model. As discussed above, this experimental assumption is not necessarily unrealistic. The experiments show that gravity and collision-related deformation interact in the NE part of the model, as continental deformation and subduction-related extension interacted in NE Asia during the opening of the Japan Sea. According to the experiments, opening of marginal basins in SE Asia is more likely the result of subduction-related extension only.

References

- Achache, J., V. Courtillot, and J. Besse, Paleomagnetic constraints on the late Cretaceous and Cenozoic tectonics of southeastern Asia, *Earth Planet. Sci. lett.*, 63, 123-136, 1983.
- Argand, E., La tectonique de l'Asie, *Proc. 13th Int. Geol. Congr. Brussels* 1924, 171-372, 1924.
- Armijo, R., P. Tapponnier, J. L. Mercier, and H. Tonglin, Quaternary extension in southern Tibet: field observations and tectonic implications, *J. Geophys. Res.*, 91, 13,803-13,872, 1986.
- Armijo, R., P. Tapponnier, and H. Tonglin, Late Cenozoic right-lateral strike-slip faulting in southern Tibet, *J. Geophys. Res.*, 94, 2787-2838, 1989.
- Audley-Charles, M. G., Geometrical problems and implications of large scale overthrusting in the Banda Arc-Australian margin collision zone, *Spec. Publ. Geol. Soc. Lond.*, 9, 407-416, 1981.
- Avouac, J. P., and P. Tapponnier, Kinematic model of active deformation in central Asia, *Geophys. Res. Lett.*, 20, 895-898, 1993.
- Barrier, E., P. Huchon and M. Aurelio, Philippine fault: a key for Philippine kinematics, *Geology*, 19, 32-35, 1991.
- Bellier, O., J.L. Mercier, P. Vergely, C. Long and C. Ning, Evolution sédimentaire et tectonique du graben cénozoïque de la Wei He (province du Shanxi, Chine du Nord), *Bull. Soc. Géol. France*, 6, 979-994, 1988.
- Berry, R. F., and A. E. Grady, Mesoscopic structures produced by Plio-Pleistocene wrench faulting in S. Sulawesi, Indonesia, *Journal of Structural Geology*, 1986.
- Bird, P., Lateral extrusion of lower crust from under high topography in the isostatic limit, *J. Geophys. Res.*, 96, 10,275-10,286, 1991.
- Briais A., P. Patriat and P. Tapponnier, Updated interpretation of magnetic anomalies and seafloor spreading stages in the South China Sea: implications for the tertiary tectonics of southeast Asia, *J. Geophys. Res.*, 98, 6299-6328, 1993.
- Burchfiel, B. C., and L. H. Royden, North-south extension within the convergent Himalayan region, *Geology*, 679-682, 1985.
- Burchfiel, B. C., and L. H. Royden, Tectonics of Asia 50 years after the death of Emile Argand, *Eclogae Geol. Helv.*, 84, 599-629, 1991.
- Burchfiel, B. C., Chen Zhiliang, K. V. Hodges, Liu Yuping, L. H. Royden, Deng Changrong, Xu Jiene, The south Tibetan detachment system, Himalayan orogen: extension contemporaneous with and parallel to shortening in a collisional mountain belt, *Geol. Soc. Amer. Spec. Pap.*, 269, 1-41, 1992.
- Burg, J. P., and G. M. Chen, Tectonics and structural zonation of southern Tibet, China, *Nature*, 311, 219-223, 1984.

- Cardwell, R. K., B. L. Isacks and D. E. Karig, The spatial distribution of earthquakes, focal mechanism solutions, and subducted lithosphere in the Philippine and northeastern Indonesian islands, in *The Tectonic and Geologic Evolution of Southeast Asian Seas and Islands* edited by D. E. Hayes, *Geophys. Monogr.*, Am. Geophys. Union, 23, 1-35, 1980.
- Chamot-Rooke, N. and X. Le Pichon, Zenisu ridge: mechanical model of formation, *Tectonophysics*, 160, 175-194, 1989.
- Charlton, T. R., A. J. Barber, and S. T. Barkham, The structural evolution of the Timor collision complex, eastern Indonesia, *Journal of Structural Geology*, 13, 489-500, 1991.
- Chase, C. G., Extension behind island arcs and motions relative to hot spots, *J. Geophys. Res.*, 83, 5385-5387, 1978.
- Chen, W.-P., and P. Molnar, Source parameters of earthquakes and intraplate deformation beneath the Shillong Plateau and the Northern Indoburman Ranges, *J. Geophys. Res.*, 95, 12527-12552, 1990.
- Chen, W.-P., and J. Nabelek, Seismogenic strike-slip faulting and the development of the North China basin, *Tectonics*, 7, 975-989, 1988.
- Chingchang, B., C. T. Shyu, J. C. Chen, and S. Boggs, Taiwan: geology, geophysics and marine sediments, in *The Ocean Basins and Margins*, edited by A.E.N. Nairn, F.G. Stehli and S. Uyeda, vol. 7A, 377-418, Plenum Press, New York, 1985.
- Cobbold, P.R. and P. Davy, Indentation tectonics in nature and experiments. 2. Central Asia, *Bulletin of the Geological Institutions of Uppsala*, 14, 143-162, 1988.
- Cohen, S. C., and R. C. Morgan, Intraplate deformation due to continental collisions: a numerical study of deformation in a thin viscous sheet, *Tectonophysics*, 132, 247-259, 1986.
- Cooper, A. K., M. S. Marlow, D. W. Scholl, and A. J. Stevenson, Evidence for Cenozoic crustal extension in the Bering Sea region, *Tectonics*, 11, 719-731, 1992.
- Curry, M. P., D. G. Moore, L. Lawver, F. J. Emmel, R. W. Raitt, M. Henry, and R. Kieckhefer, Tectonics of the Andaman Sea and Burma, *Geological and Geophysical Investigations of Continental Margins*, edited by J. S. Watkins, L. Montadert and P. Dickerson, *Mem. Am. Assoc. Pet. Geol.*, 29, 189-198, 1978.
- Daly, M. C., M. A. Cooper, I. Wilson, D. G. Smith and B. G. D. Hooper, Cenozoic plate tectonics and basin evolution in Indonesia, *Marine and Petroleum Geol.*, 8, 2-21, 1991.
- Davy, P., and P. R. Cobbold, Indentation tectonics in nature and experiment. 1. Experiments scaled for gravity, *Bull. Geol. Inst. Univ. Uppsala*, 14, 129-141, 1988.
- Davy, P., and P. R. Cobbold, Experiments on shortening of a 4-layer model of the continental lithosphere, *Tectonophysics*, 188, 1-25, 1991.
- Deng Qidong, Sung Fengmin, Zhu Shilong, Li Mengluan, Wang Tielin, Zhang Weiqi, B. C. Burchfield, P. Molnar, and Zhang Peizhen, Active faulting and tectonics of the Ningxia-Hui autonomous region, China, *J. Geophys. Res.*, 89, 4427-4445, 1984.

- Deverchère, J., F. Houdry, N. V. Solonenko, A. V. Solonenko, and V. A. Sankov, Seismicity, active faults and stress field of the north Muya region, Baikal rift: new insights on the rheology of extended continental lithosphere, *J. Geophys. Res.*, 98, 19,895-19,912, 1993.
- Dewey, J. F., S. Cande, and W. C. Pitman, Tectonic evolution of the India/Eurasia collision zone, *Eclogae Geol. Helv.*, 82, 717-734, 1989.
- Diament, M., H. Harjono, K. Karta, C. Deplus, D. Dahrin, M. T. Zen, M. Gerard, O. Lassal, A. Martin, and J. Malod, Mentawai fault zone off Sumatra: a new key to the geodynamics of western Indonesia, *Geology*, 20, 259-262, 1992.
- Eguchi, T., and S. Uyeda, Seismotectonics of the Okinawa trough and Ryukyu arc, *Mem. Geol. Soc. China*, 5, 189-210, 1983.
- England, P., and G. Houseman, Finite strain calculations of continental deformation 2. Comparison with the India-Asia collision zone, *J. Geophys. Res.*, 91, 3664-3676, 1986.
- England, P. C., and D. P. McKenzie, A thin viscous sheet model for continental deformation, *Geophys. J. R. Astr. Soc.*, 70, 295-321.
- England, P. C., and D. P. McKenzie, Correction to: a thin viscous sheet model for continental deformation, *Geophys. J. R. Astr. Soc.*, 73, 523-532.
- England, P. and P. Molnar, Right-lateral shear and rotation as the explanation for strike-slip faulting in eastern Tibet, *Nature*, 344, 140-142, 1990.
- Fitch, T. J., Plate convergence, transcurrent faults and internal deformation adjacent to Southeast Asia and the Western Pacific, *J. Geophys. Res.*, 77, 4432-4460, 1972.
- Fournier, M., L. Jolivet, P. Huchon, K. F. Sergeev and L. S. Oscorbin, Neogene strike-slip faulting in Sakhalin and the Japan Sea opening, *J. Geophys. Res.*, 1994.
- Fukao, Y. and M. Furumoto, Mechanisms of large earthquakes along the eastern margin of the Japan sea, *Tectonophysics*, 25, 247-266, 1975.
- Funahara, S., N. Nishiwaki, M. Miki, F. Muruta, Y. Otofugi, and Yi Zhao Wang, Paleomagnetic study of Cretaceous rocks from the Yangtze block, central Yunnan, China: implications for the India-Asia collision, *Earth Planet. Sci. Lett.*, 113, 77-91, 1992.
- Hamilton, W., Tectonics of the Indonesian region, U.S. Geol. Surv. Prof. Paper 1078, pp. 345, 1979.
- Harnojo, H., M. Diament, J. Dubois, and M. Larue, Seismicity of the Sunda Strait: evidence for crustal extension and volcanological implications, *Tectonics*, 10, 17-30, 1991.
- Harris, R.A., Temporal distribution of strain in the active Banda orogen: a reconciliation of rival hypotheses, in: Hall, R., Nichols, G. and C. Rangin, eds., *Orogenesis in action, Journal of southeast Asian earth science*, 5, 1991.
- Hellinger, S. J., K. M. Shedlock, J. G. Sclater and Y. Hong, The Cenozoic evolution of the north China basin, *Tectonics*, 4, 343-358, 1985.

- Heki, K., Y. Takahashi and T. Kondo, Contraction of northeastern Japan: evidence from horizontal displacement of a Japanese station in global very long baseline interferometry networks, *Tectonophysics*, 181, 113-122, 1990.
- Holloway, N. H., The stratigraphy and tectonic relationship of Reed Bank, north Palawan and Mindoro to the Asian mainland and its significance in the evolution of the South China Sea, *Amer. Assoc. Petrol. Bull.*, 66, 1357-1383, 1982.
- Holt, E. H., and A. J. Haines, Velocity field in deforming Asia from the inversion of earthquake-released strains, *Tectonics*, 12, 1-20, 1993.
- Holt, E. H., J. F. Ni, T. C. Wallace, and A. J. Haines, The active tectonics of the eastern Himalayan syntaxis and surrounding regions, *J. Geophys. Res.*, 96, 14595-14632, 1991.
- Hong, Y., K. M. Shedlock, S. J. Hellinger and J. G. Sclater, The North China Basin: an example of a Cenozoic rifted intraplate basin, *Tectonics*, 153-169, 1985.
- Houseman, G., and P. England, Finite strain calculations of continental deformation. 1. Method and general results for convergent zones, *J. Geophys. Res.*, 91, 3651-3663, 1986.
- Houseman, G., and P. England, Crustal thickening versus lateral expulsion in the Indian-Asian continental collision, *J. Geophys. Res.*, 98, 12,233-12,249, 1993
- Huang, K., N. D. Opdyke, J. Li, and X. Peng, Paleomagnetism of Cretaceous rocks from eastern Qiangtang terrane of eastern Tibet, *J. Geophys. Res.*, 97, 1789-1799, 1992.
- Huchon, P., and X. Le Pichon, Sunda strait and central Sumatra fault, *Geology*, 12, 668-672, 1984.
- Hutchinson, D. R., A. J. Golmshtok, L. P. Zonenshain, T. C. Moore, C. A. Scholz, and K. D. Klitgord, Depositional and tectonic framework of the rift basins of lake Baikal from multichannel seismic data, *Geology*, 20,589-592, 1992.
- Jaegger, J. C., and N. G. W. Cook, Fundamentals of rock mechanics, published by Chapman and Hall, London, 515 p., 1971.
- Jolivet, L., P. Davy, and P. Cobbold, Right-lateral shear along the northwest Pacific margin and the India-Eurasia collision, *Tectonics*, 9, 1409-1419, 1990.
- Jolivet, L., and P. Huchon, Crustal scale strike-slip deformation in Hokkaido, Northeast Japan, *J. Struct. Geol.*, 11, 509-522, 1989.
- Jolivet, L., Huchon, P. and Rangin, C., Tectonic setting of Western Pacific marginal basins, *Tectonophysics*, 160, 23-47, 1989.
- Jolivet, L., P. Huchon, J.P. Brun, N. Chamot-Rooke, X. Le Pichon, and J.C. Thomas, Arc deformation and marginal basin opening, Japan Sea as a case study, *J. Geophys. Res.*, 96, 4367-4384, 1991.
- Jolivet, L., M. Fournier, P. Huchon, V. S. Rozhdestvensky, K. F. Sergeyev, and L. Oscorbin, Cenozoic intracontinental dextral motion in the Okhotsk-Japan sea region, *Tectonics*, 11, 968-977, 1992.

- Jolivet, L., and K. Tamaki, Neogene kinematics in the Japan Sea region and volcanic activity of the northeast Japan arc, *Proc. ODP, Sci. Results*, 127/128, 1992.
- Kimura, G. and K. Tamaki, Collision, rotation and back arc spreading: the case of the Okhotsk and Japan seas, *Tectonics*, 5, 389-401, 1986.
- Kuramoto, S., and K. Konishi, The southwest Ryukyu arc is a migrating microplate (forearc silver), *Tectonophysics*, 163, 75-91, 1989.
- Lallemand, S. and L. Jolivet, Japan Sea: a pull apart basin, *Earth Planet. Sci. lett.*, 76, 375-389, 1985.
- Lallemand, S., N. Chamot-Rooke, X. Le Pichon and C. Rangin, Zenisu Ridge a deep intra-oceanic thrust related to subduction off Southwest Japan, *Tectonophysics*, 160, 151-174, 1989.
- Le Dain, A. Y., P Tapponnier, and P. Molnar, Active faulting and tectonics of Burma and surrounding regions, *J. Geophys. Res.*, 89, 453-472, 1984.
- Le Pichon, X., Résumé des cours et travaux, *Annuaire du Collège de France 1987-1988*, 135-144, Collège de France, Paris, 1988.
- Le Pichon, X., M. Fournier, and L. Jolivet, Kinematics, topography, shortening and extrusion in the India-Eurasia collision, *Tectonics*, 1993.
- Lu, H., H. Yu, Y. Ding, and Q. Zhang, Changing stress field in the middle segment of the Tan-Lu fault zone, eastern China, *Tectonophysics*, 98, 253-270, 1983.
- Ma, X., and D. Wu, Cenozoic extensional tectonics in China, *Tectonophysics*, 133, 243-255, 1987.
- Marchadier, Y., and C. Rangin, Passage subduction-collision et tectoniques superposées à l'extremité de la fosse de Manille (Mindoro-Tablas, Philippines), *C. R. Acad. Sci. Paris*, 308, 1715-1720, 1989.
- Matsuda, T., Collision of the Izu-Bonin arc with central Honshu: Cenozoic tectonics of the Fossa Magma, Japan, *Journal of Physics of the Earth*, 26, 409-421, 1978.
- Matsuzaka, S., M. Tobita and Y. Nakahori, Detection of Philippine sea plate motion by very long baseline interferometry, *Geophysical Research Letter*, 18, 1417-1419, 1991.
- McCaffrey, R., E. A. Silver and R. W. Raitt, Crustal structure of the Molucca Sea collision zone, Indonesia, in *The Tectonic and Geologic Evolution of Southeast Asian Seas and Islands* edited by D. E. Hayes, *Geophys. Monogr.*, Am. Geophys. Union, 23, 161-177, 1980.
- McCaffrey, R., and J. Nabelek, Seismological evidence for shallow thrusting north of the Timor Through, *Geophys. J. R. Astron. Soc.*, 85, 365-381, 1986.
- McCaffrey, R., Active tectonics of the eastern Sunda and Banda arc, *J. Geophys. Res.*, 93, 15163-15182, 1988.
- McCaffrey, R., and G. A. Abers, Orogeny in arc-continent collision: the Banda arc and western New Guinea, *Geology*, 19, 563-566, 1991.

- McKenzie, D. P., Speculations on the consequences and causes of plate motions, *Gephys. J. Roy. Astron. Soc.*, 18, 1-32, 1969.
- Mercier, J. L., R. Armijo, P. Tapponnier, E. Carey-Gailhardis, and Han Tong Lin, Change from Late Tertiary compression to Quaternary extension in southern Tibet during the India-Asia collision, *Tectonics*, 6, 275-304, 1987.
- Milsom, J., and M. R. Audley-Charles, Post collisional isostatic adjustment in the southern Banda arc, in: *Collision Tectonics*, Spec. Publ. Geol. Soc. Lon., 19, 353-366, 1986.
- Molnar, P., and P. Tapponnier, Cenozoic tectonics of Asia: Effects of a continental collision, *Science*, 189, 419-425, 1975.
- Molnar, P., and T. Atwater, Interarc spreading and cordilleran tectonics as alternates related to the age of the subducted oceanic lithosphere, *Earth Planet. Sci. Lett.*, 41, 330-340, 1978.
- Molnar, P., Burchfield, B. C., L. K'uangyi, and Z. Ziyun, Geomorphic evidence for active faulting in the Altyn Tagh and northern Tibet and qualitative estimates of its contribution to the convergence of India and Eurasia, *Geology*, 15, 249-253, 1987.
- Moore, G. F., J. R. Curay, D. G. Moore, and D. E. Karig, Variations in geologic structure along the Sunda fore arc, Northeastern Indian Ocean, in: Hayes D. E., Ed., *The tectonic and geologic evolution of southeast Asian seas and islands*, Geophys. Monogr., AGU, Washington, 27, 145-160, 1980.
- Moore, G.F., and E. A. Silver, Collision processes in the northern Molucca sea, The tectonic and geologic evolution of southeast Asian seas and islands, *Geophys. Monogr.*, AGU, 27, 360-372, 1982.
- Nabelek, J., W. P. Chen and H. Ye, The Tangshan earthquake sequence of 1976 and its implications for the evolution of the North China basin, *J. Geophys. Res.*, 92, 12,615-12628, 1987.
- Nakamura, K., Possible nascent trench along the eastern Japan Sea as the convergent boundary between Eurasian and North American plates, *Bul. Earthq. Res. Inst., Univ. Tokyo*, 58, 711-722, 1983 (in Japanese with English abstract).
- Nakamura, K. and S. Uyeda, Stress gradient in back arc regions and plate subduction, *J. Geophys. Res.*, 85, 6419-6428, 1980.
- Otofuji, Y., Y. Inoue, S. Funahara, F. Murata, and X. Zheng, Paleomagnetic study of eastern Tibet-deformation of the Three Rivers region, *Geophys. J. Int.*, 103, 85-94, 1990.
- Pan, Y., and W. S. F. Kidd, Nyainqntanghla shear zone: a late Miocene extensional detachment in the southern Tibetan plateau, *Geology*, 20, 775-778, 1992.
- Parfenoy, L. M., B. M. Koz'Min, V. S. Imayev, and L. A. Savostin, The tectonic character of the Olekma-Stanovoy seismic zone, *Geotectonics*, 21, 560-572, 1987.
- Patriat, P., and J. Achache, Indian-Asia collision chronology has implications for crustal shortening and driving mechanism of plates, *Nature*, 311, 615-621, 1984.

- Peltzer, G., P. Tapponnier, Z. Zhan and Z. Q. Xu, Neogene and Quaternary faulting in and along the Qinling Shan, *Nature*, 317, 500-505, 1985.
- Peltzer, G., and P. Tapponnier, Formation and evolution of strike-slip faults, rifts, and basins during the India-Asia collision: an experimental approach, *J. Geophys. Res.*, 93, 15,085-15,117, 1988.
- Rangin, C., L. Jolivet, M. Pubellier and the Tethys Pacific working group, A simple model for the tectonic evolution of southeast Asia and Indonesia region for the past 43 m.y., *Bull. Soc. Geol. France*, 6, 889-905, 1990.
- Ranken, B., R. K. Cardwell and D. E. Karig, Kinematics of the Philippine sea plate, *Tectonics*, 3, 555-575, 1984.
- Rozhdestvensky, V. S., The role of wrench-faults in the structure of Sakhalin, *Geotectonics*, 16, 323-332, 1982.
- Seismotectonic map of China based on interpretation of satellite images (1: 4.000.000), published by the Earthquake Research Institute, Pekin, 1985.
- Seno, T., The instantaneous rotation vector of the Philippine Sea plate relative to the Eurasian plate, *Tectonophysics*, 42, 209-226, 1977.
- Sibuet, J. C., J. Letouzey, F. Barbier, J. Charvet, J. P. Foucher, T. W. C. Hilde, M. Kimura, C. Ling-Yun, B. Marsset, C. Muller, and J. F. Stephan, Back arc extension in the Okinawa Trough, *J. Geophys. Res.*, 92, 14041-14063, 1987.
- Silver, E. A., R. McCaffrey and R. B. Smith, Collision, rotation, and the initiation of subduction in the evolution of the Sulawesi, Indonesia, *J. Geophys. Res.*, 88, 9407-9418, 1983.
- Silver, E. A., D. Reed, R. McCaffrey, and Y. Joyodiwiryo, Back arc thrusting in the eastern Sunda arc, Indonesia: a consequence of arc-continent collision, *J. Geophys. Res.*, 88, 7429-7448, 1983.
- Silver, E. A., and C. Rangin, Leg 124 tectonic synthesis, *Proceedings of the Ocean Drilling Program, Scientific results*, 124, 3-9, 1991.
- Tamaki, K. and E. Honza, Incipient subduction and obduction along the eastern margin of the Japan sea, *Tectonophysics*, 119, 381-406, 1984.
- Tamaki, K., Geological structure of the Japan sea and its tectonic implications, *Bulletin of the Geological Survey of Japan*, 39, 269-365, 1988.
- Tamaki, K., K. Suyehiro, J. Allan, J. C. Ingle and K. A. Pisciotto, Tectonic synthesis and implications of Japan Sea ODP drilling, *ODP Leg 127/128 Science Volume*, 1992.
- Tapponnier, P. and P. Molnar, Slip-line field theory and large-scale continental tectonics, *Nature*, 264, 319-324, 1976.
- Tapponnier, P., and P. Molnar, Active faulting and tectonics in China, *J. Geophys. Res.*, 82, 2905-2930, 1977.

- Tapponnier, P., and P. Molnar, Active faulting and Cenozoic tectonic of the Tien Shan, Mongolia, and Baykal regions, *J. Geophys. Res.*, 84, 3425-3459, 1979.
- Tapponnier, P., J. L. Mercier, R. Armijo, T. Han, and J. Zhou, Field evidences for active normal faulting in Tibet, *Nature*, 294, 410-414, 1981.
- Tapponnier, P., G. Peltzer, A. Y. Le Dain, R. Armijo, and P. Cobbold, Propagating extrusion tectonics in Asia: new insights from simple experiments with plasticine, *Geology*, 10, 611-616, 1982.
- Tapponnier, P., G. Peltzer, and R. Armijo, On the mechanics of the collision between India and Asia, *Collision tectonics*, edited by Coward M.P. and A. C. Ries, *Geol. Soc. Spec. Pub.*, 19, 115-157, 1986.
- Taylor, B. and D. E. Hayes, The tectonic evolution of the south China basin, in: Hayes D. E., Ed., *The tectonic and geologic evolution of southeast Asian seas and islands*, *Geophys. Monogr.*, AGU, Washington, 27, 89-104, 1980.
- Tian, Z., P. Hang and K. D. Xu, The Mesozoic-Cenozoic east China rift system, *Tectonophysics*, 208, 341-363, 1992.
- Uyeda S. and H. Kanamori, Backarc opening and the mode of subduction, *J. Geophys. Res.*, 84, 1049-1061, 1979.
- Viallon, C., P. Huchon, and E. Barrier, Opening of the Okinawa basin and collision in Taiwan: a retreating trench model with lateral anchoring, *Earth Planet. Sci. lett.*, 80, 145-155, 1986.
- Vilotte, J. P., M. Daignières, and R. Madariaga, Numerical modeling of intraplate deformation: simple mechanical models of continental collision, *J. Geophys. Res.*, 87, 10,709-10,728, 1982.
- Vilotte, J. P., M. Daignieres, R. Madariaga, and O. C. Zienkiewicz, The role of a heterogeneous inclusion during continental collision, *Phys. Earth Planet. Int.*, 36, 236-259, 1984.
- Vilotte, J. P., R. Madariaga, M. Daignieres, and O. C. Zienkiewicz, Numerical study of continental collision: influence of buoyancy forces and an initial stiff inclusion, *Geophys. J. R. Astr. Soc.*, 84, 279-310, 1986.
- Wang, J. M., The Fenwei rift and its recent periodic activity, *Tectonophysics*, 133, 257-275, 1987.
- Weissel, J. K., Evidence for Eocene oceanic crust in the Celebes basin, in: Hayes D. E., Ed., *The tectonic and geologic evolution of southeast Asian seas and islands*, *Geophys. Monogr.*, AGU, Washington, 27, 37-47, 1980.
- Windley, B. F., and M. B. Allen, Mongolian plateau: evidence for a late Cenozoic mantle plume under central Asia, *Geology*, 21, 295-298, 1993.

- Xu, J., G. Zhu, W. Tong, K. Cui, and Q. Liu, Formation and evolution of the Tancheng-Lujiang wrench fault system: a major shear system to the northwest of the Pacific Ocean, *Tectonophysics*, 134, 273-310, 1987.
- Xu, X. and X. Ma, Geodynamics of the Shanxi rift system, *Tectonophysics*, 208, 325-340, 1992.
- Yamagishi, H. and Y. Watanabe, Change of stress field of Late Cenozoic in Southwest Hokkaido, Japan, - investigation of geologic faults, dykes, ore veins and active faults, *Monograph Geol. Collabor. Jpn.*, 31, 321-332, 1986.
- Yamazaki, K., T. Tamura, and I. Kawasaki, Seismogenic stress field of the Japan sea as derived from shallow and small earthquakes, *J. Seismol. Soc. Japan*, 38, 541-558, 1985.
- Yoshida, Y., and K. Abe, Source mechanism of the Luzon, Philippines earthquake of July 16, 1990, *Geophys. Res. Lett.*, 19, 545-548, 1992.

TABLE CAPTIONS

Table 1.

Table 2. Physical properties and thicknesses of the models for 5 experiments. The density of sand is 1.1. The viscosity of silicone 1 and 2 are 5.10^4 Pa.s and 7.10^4 Pa.s, respectively. l is the distance from the western edge of the model to the indenter (see Figure 2).

Table 3. Extrusion and spreading velocities are measured at the eastern limit of the diffuse left-lateral shear zone (Figure 10).

Table 1. Main Properties of Analogue and Numerical Models.

Reference	Thickening	Thinning	Faulting	Heterogeneous model	Extrusion driven by	Comments
<i>Analogue experiments</i>						
Tapponnier et al., 1982 Peltzer and Tapponnier, 1988	-	-	+	+	indentation	Plasticine. Horizontal plane strain.
Davy and Cobbold, 1988	+	-	+	-	indentation	Rheological model scaled for gravity
this study	+	+	+	-	indentation and spreading	Rheological model scaled for gravity Extensional boundary
<i>Numerical experiments</i>						
Tapponnier and Molnar, 1976	-	-	+	-		Horizontal plane strain Instantaneous slip-line fields
Vilotte et al., 1982	-	-	-	-	indentation	Horizontal plane strain
	+	+	-	-	no extrusion	Horizontal plane stress
Vilotte et al., 1984	-	-	-	+	indentation	Horizontal plane strain
Vilotte et al., 1986	+	+	-	±	indentation and spreading	
Houseman and England, 1986	+	+	-	-	no extrusion	Rigid boundary
Cohen and Morgan, 1986	+	+	-	-	indentation	
Houseman and England, 1993	+	+	-	-	indentation	Lithostatic boundary

Table 2. Physical parameters of layers and boundary conditions

Exp. N°	sand	silicone 1		silicone 2		boundary conditions			
		thick ness (cm)	thick ness (cm)	density	thick ness (cm)	density	indentation speed (cm.h ⁻¹)	l (cm)	east boundary
E1	0.5	1	1.14	0.5	1.34	6	35	type 1 (upper 40 cm)	2 h
E2	0.5	1	1.14	0.5	1.34	6.5	35	type 1	1 h
E3	0.5	1	1.14	0.5	1.34	5.5	35	type 1	0 h
E4	0.5	1	1.19	0.5	1.28	7	24	type 2	0 h
E5	0.8	1	1.19	0.5	1.28	20	25	type 2	0 h

Type 1 boundary is confined with a five millimetres thick silicone putty layer. Type 2 boundary is "free boundary".

Table 3. Strain rates and velocities.

Exp N°	Spreading rate (s ⁻¹)	Extrusion rate (s ⁻¹)	Extrusion velocity (cm.h ⁻¹)	Extrusion velocity minus spreading velocity (cm.h ⁻¹)		Indentation velocity (cm.h ⁻¹)
				Extrusion velocity minus spreading velocity (cm.h ⁻¹)	Indentation velocity (cm.h ⁻¹)	
E1	0.89 10 ⁻⁵	3.69 10 ⁻⁵	4.5	2.8	6	
E2	0.63 10 ⁻⁵	3.84 10 ⁻⁵	3.6	2.8	6.5	
E3	0.65 10 ⁻⁵	2.96 10 ⁻⁵	3.7	2.9	5.5	
E4	1.77 10 ⁻⁵	4.88 10 ⁻⁵	6.0	2.7	7	
E5	1.01 10 ⁻⁵	12.41 10 ⁻⁵	15.0	12.9	20	

IV. CONCLUSIONS

Ces expériences montrent que l'interaction collision-extension a lieu dans la partie nord-est du modèle. Le coin sud-est est isolé de la collision et se déforme par extension pure. L'interaction collision-extension se traduit, du point de vue de la déformation, par une association de décrochements et de failles normales. La distribution des décrochements dans la partie NE du modèle varie selon les expériences. Dans les expériences 1 et 2, avec étalement préliminaire, sont surtout représentés des décrochements sénestres NE-SO qui réactivent des failles normales précoces apparues lors de l'étalement préliminaire. Dans les expériences 4 et 5, sans étalement préliminaire ni confinement latéral, un réseau dense de décrochements conjugués apparaît. Dans l'expérience 3, sans étalement préliminaire et un taux d'étalement limité par le confinement latéral, les décrochements dextres N-S prévalent et accommodent la rotation horaire de blocs à l'intérieur d'une zone de cisaillement sénestre.

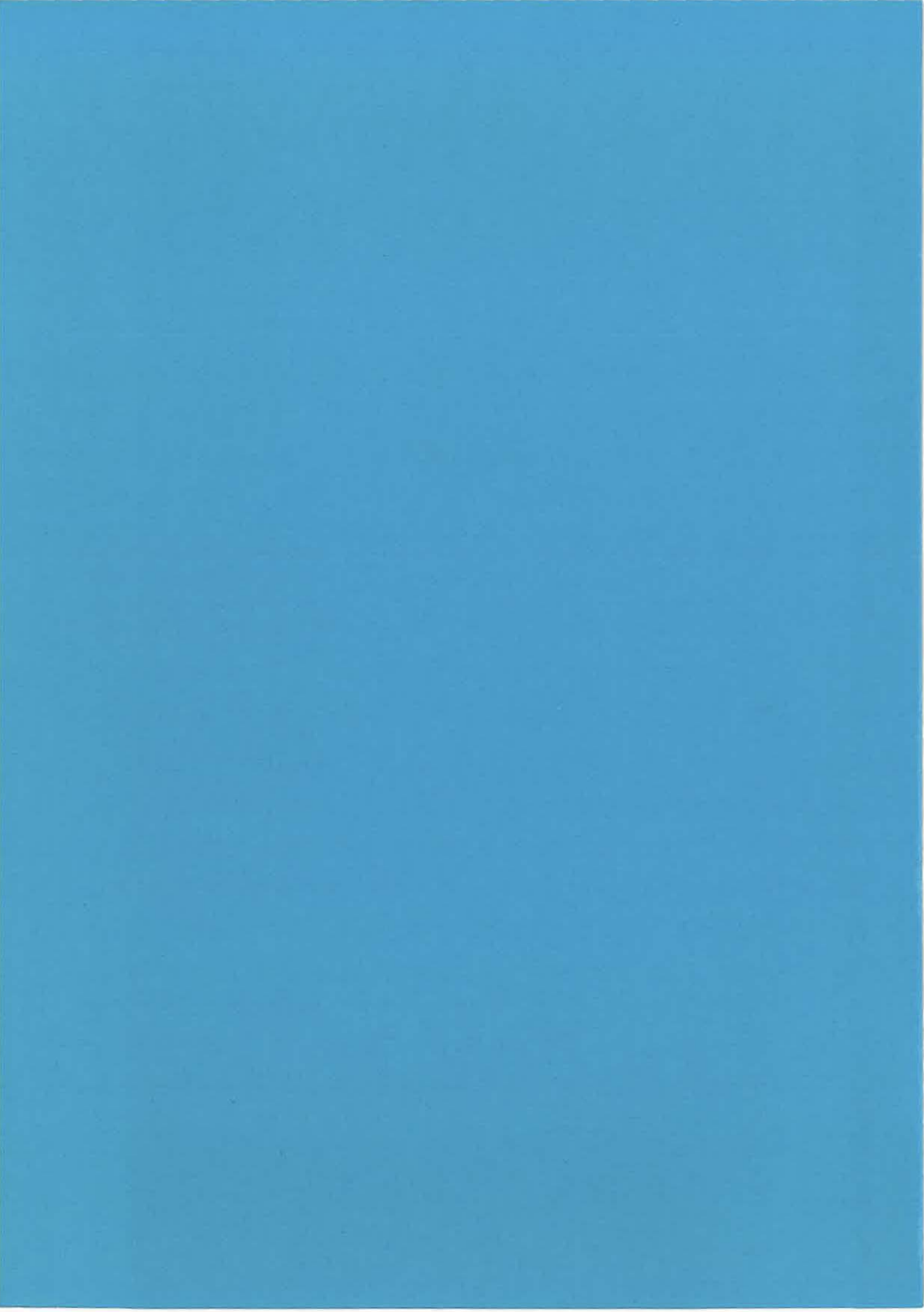
Davy et Cobbold (1988) ont réalisé des expériences similaires avec un modèle de lithosphère qui ne s'étalait pas et qu'ils ont testé avec différents degrés de confinement latéral. Pour proposer leur modèle d'ouverture des bassins d'Asie du nord-est, Jolivet et al. (1990) ont retenu l'expérience de Davy et Cobbold (1988) réalisée avec une bordure latérale libre. Nous avons réalisé des expériences avec un modèle qui s'étale sous son propre poids, que nous avons testé pour différentes durées d'extension et différents taux d'extension. L'expérience 3, dont la géométrie de la déformation est identique à celle de Davy et Cobbold (1988) retenue par Jolivet et al. (1990), correspond à la durée et au taux d'extension minima. Nous obtenons ainsi une géométrie de déformation identique avec un modèle susceptible de s'étaler mais dont les possibilités d'étalement sont limitées au maximum. Cette géométrie correspond en quelque sorte à un intermédiaire entre un modèle "rigide" à bordure libre, et un modèle "plastique" dont l'étalement est limité.

C'est cette géométrie que nous retenons pour la comparer à l'Asie, dans la mesure où c'est elle qui présente le plus de similarités avec la déformation de l'Asie. Lorsqu'on augmente le taux d'extension dans les expériences, la déformation devient en effet très distribuée et difficile à comparer avec la déformation de la lithosphère continentale essentiellement localisée.

Cette géométrie suppose que les mouvements dextres le long des failles sub-méridiennes en Asie du nord-est accommodent la rotation anti-horaire de blocs continentaux dans une large zone de déformation sénestre, qui elle-même accommode le mouvement vers le NE de l'Asie par rapport à la plate-forme russe. De telles rotations de blocs continentaux sont connues dans la région de l'Ordos, et nous estimons qu'elles peuvent être généralisées à toute la région comprise entre le Qinling Shan et les Monts Stanovoï qui sont deux zones de cisaillement sénestres. Nous pensons donc que la plaque Amour est constitué de blocs continentaux bordés par des décrochements dextres qui tournent dans le sens anti-horaire. La

mer du Japon s'est ouverte en bordure de la zone de subduction, le long d'une de ces zones de cisaillement dextre.

SYNTHÈSE



SYNTHÈSE

I. INTRODUCTION

A la suite des travaux sur la déformation décrochante oligo-miocène à Sakhaline (Rozhdestvensky, 1982), Hokkaido (Kimura et al., 1983 ; Jolivet et Miyashita, 1985), sur la marge est de la mer du Japon (Lallemand et Jolivet, 1985), et dans le détroit de Tsushima (Sillitoe, 1977), Lallemand et Jolivet (1985) ont proposé un modèle d'ouverture en pull-apart dextre de la mer du Japon modifié ensuite par Jolivet et al. (1991). Dans ce modèle, la mer du Japon s'ouvre entre deux zones décrochantes dextres N-S, la zone décrochante de Tsushima et la zone décrochante est-mer du Japon. Cette dernière se prolonge vers le nord à l'intérieur du continent asiatique (Sakhaline) où nous sommes allés l'étudier. Il était intéressant en particulier de connaître l'évolution temporelle de la déformation à l'intérieur du continent pour savoir si elle était sous l'influence des changements intervenus au niveau de la zone de subduction.

Parallèlement au modèle de bassin en pull-apart, un modèle d'ouverture en porte à doubles battants a été proposé (Kawai et al., 1971 ; Sasajima, 1981 ; Otofuji et al., 1985, 1991 ; Celaya et McCabe, 1987). Ce modèle repose sur les rotations horaires et anti-horaires mises en évidence par le paléomagnétisme dans le Japon sud-ouest et le Japon nord-est respectivement. Jolivet et al. (1991) ont montré à partir d'expériences analogiques que les rotations horaires dans le Japon sud-ouest étaient compatibles avec le modèle en pull-apart. Le problème posé par ces rotations vient du diachronisme entre leur âge (16-14 Ma dans le Japon sud-ouest ; Otofuji et al., 1991 ; Hayashida et al., 1991) et l'âge de l'océanisation de la mer du Japon déterminé par les forages ODP entre 24 et 17 Ma. Pour comprendre ce problème il est nécessaire de connaître le contexte structural des rotations dans le Japon sud-ouest. Il est donc important de connaître aussi le jeu de la dislocation principale du Japon sud-ouest (MTL) pendant l'ouverture.

Au-delà du problème local (à l'échelle de la mer du Japon) du mécanisme d'ouverture de la mer du Japon, la question du moteur de l'ouverture a été abordée. L'intégration de l'ouverture de la mer du Japon à la déformation de l'Asie consécutive de la collision de l'Inde a été proposée par Kimura et Tamaki (1986) à partir d'une synthèse de la déformation cénozoïque de l'Asie, et par Jolivet et al. (1990) à partir de l'interprétation d'expériences analogiques réalisées par Davy et Cobbold (1988). Ces expériences d'indentation avec bordure libre ne prenaient pas en compte l'extension le long de la bordure libre telle qu'elle est observable en bordure des zones de subduction est-asiatiques. Nous avons donc repris ces expériences en introduisant une composante d'extension dynamique le long de la bordure libre pour tester l'interaction collision-extension dans la déformation.

J'ai donc abordé la problématique de l'ouverture de la mer du Japon dans le cadre de la déformation de l'Asie suivant trois directions. Je me suis intéressé premièrement à la relation entre l'ouverture et la déformation continentale que j'ai étudiée sur le terrain à Sakhaline, deuxièmement à la relation entre la déformation décrochante et les rotations paléomagnétiques que j'ai étudiée sur le terrain dans le Japon sud-ouest, et troisièmement à un modèle d'intégration de l'ouverture de la mer du Japon à la déformation continentale de l'Asie prenant en compte les conditions aux limites extensives induites par la subduction. J'ai mené cette dernière étude au laboratoire de modélisation de l'université de Rennes I en collaboration avec J. C. Thomas, P. Davy et L. Jolivet.

II. MÉCANISME D'OUVERTURE DE LA MER DU JAPON

A. ÉVOLUTION DE LA DÉFORMATION LE LONG DE LA ZONE DÉCROCHANTE EST-MER DU JAPON

1. Stabilité du champ de contraintes et de la déformation à Sakhaline

A Sakhaline, la déformation est absorbée depuis le Miocène par des décrochements N-S, associés à des plis en échelons à l'ouest de la faille de Tym-Poronaysk, et à des bassins en échelons dans le socle Paléozoïque-Jurassique à l'est de la faille (Figures 57 et 58). Le champ de contraintes est transpressif avec une direction de compression NE-SO au Miocène qui évolue vers une orientation ENE-OSO à l'actuel. La déformation décrochante se suit jusqu'à l'extrême nord de Sakhaline dans la péninsule de Schmidt où des failles actives sont observées en surface.

La zone décrochante est-mer du Japon pénètre ainsi profondément sur plus de 1000 km à l'intérieur du continent asiatique. Dans sa portion continentale, le régime de déformation et le régime de contraintes restent pratiquement inchangés depuis le Miocène inférieur.

2. Variabilité du champ de contraintes en bordure de la zone de subduction

a. Hokkaido

La zone centrale d'Hokkaido dans le prolongement sud de la faille de Tym-Poronaysk est à la charnière entre Sakhaline et la subduction Pacifique, c'est à dire sous la double influence de la déformation continentale et de la zone de subduction. A l'Oligocène et au Miocène inférieur et moyen, la déformation y est identique à celle de Sakhaline. Elle est accommodée par une zone de cisaillement ductile dextre dans la zone d'Hidaka et par une association de failles dextres et inverses, de chevauchements, et de plis en échelons dextres dans la croûte supérieure (Figure 58). Le régime de contraintes est transpressif, la direction de

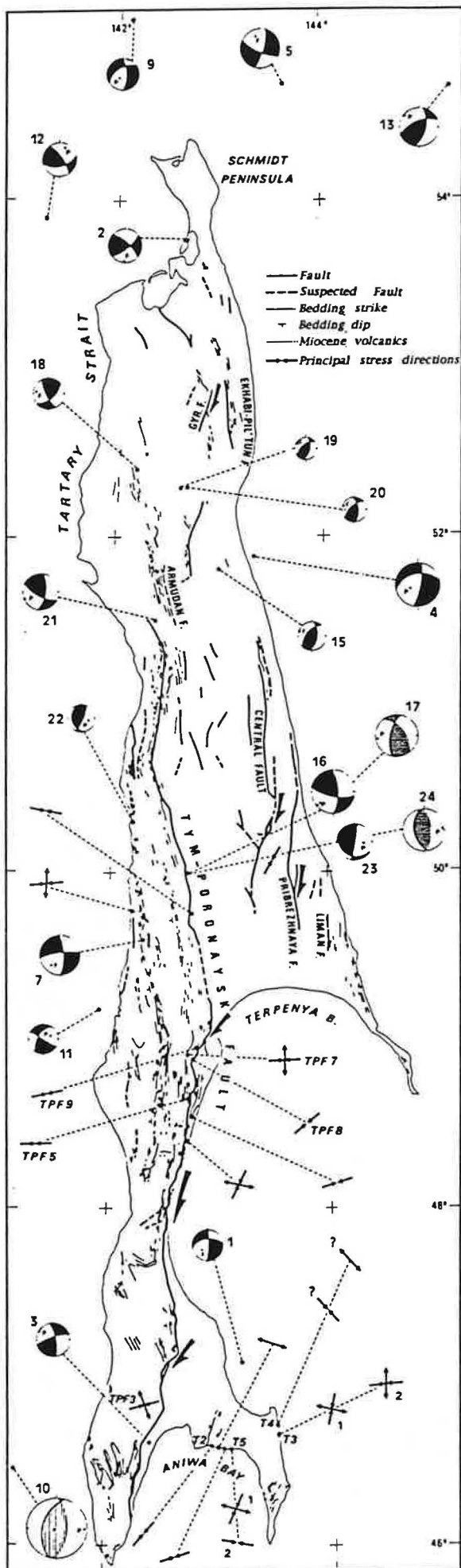


Figure 57. Carte sismotectonique de Sakhaline.

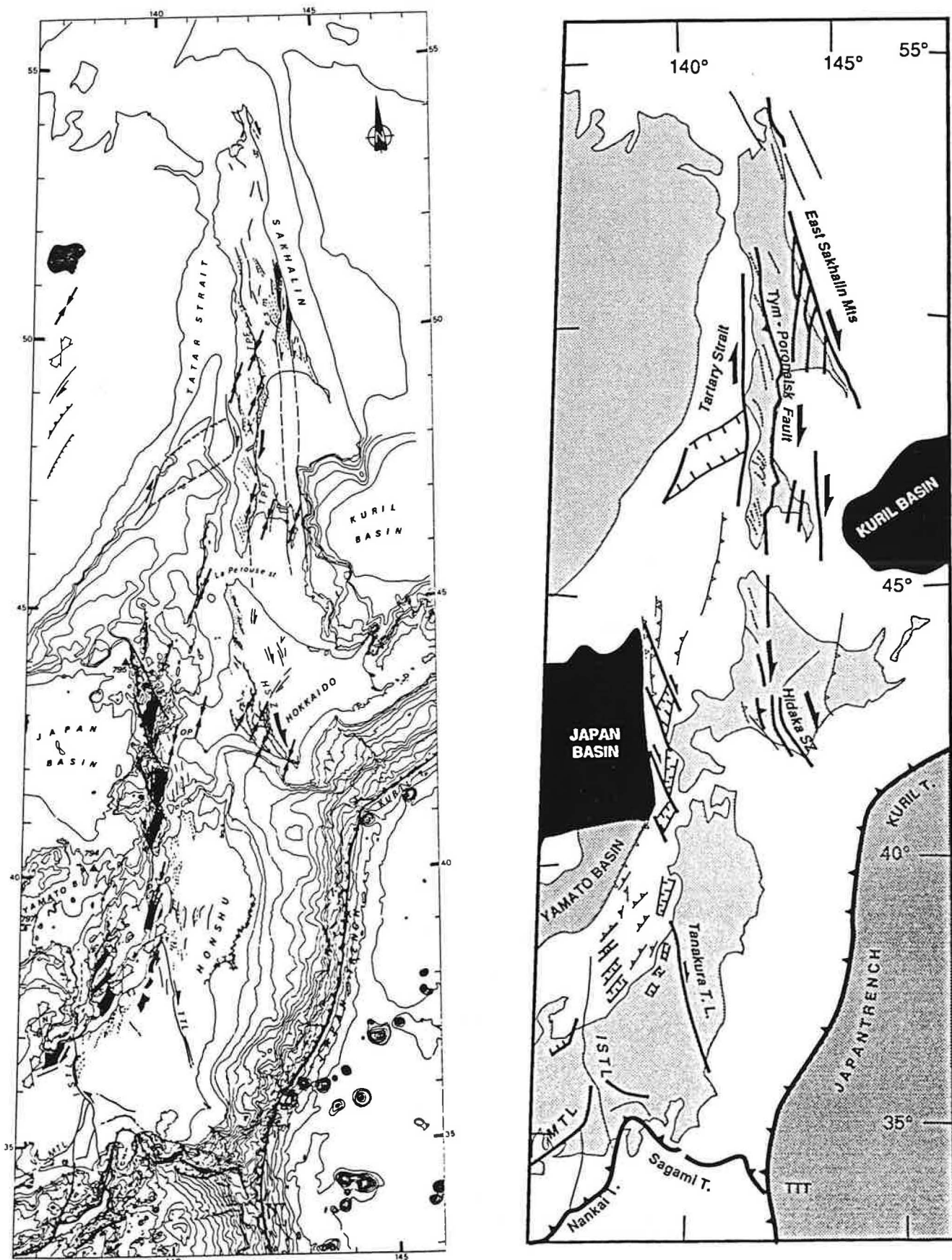


Figure 58. Cartes structurales de la zone décrochante est-mer du Japon. Carte de gauche : les zones ombrées claires représentent la croûte océanique, les zones ombrées foncées les bassins en échelon d'âge Miocène. Les directions de σ_{Hmax} déduites de l'analyse de la fracturation sont montrées. Carte de droite : les structures compressives actuelles sont montrées en traits fins.

compression est NE-SO. A partir du Miocène supérieur le régime de contraintes devient compressif E-O à Hokkaido, comme plus au sud dans le NE Honshu.

b. Honshu

Le champ de contraintes a été étudié uniquement sur la côte ouest du NE Honshu au moyen l'analyse de la fracturation. Il est transtensif pendant le Miocène inférieur et moyen, compatible avec les grabens en échelons dextres du même âge et de direction NNE-SSO décrits en mer (Figure 58). A partir du Miocène supérieur, le champ de contraintes devient compressif E-O, ce qui se traduit tardivement dans la déformation par l'amorce de la subduction vers l'est de la mer du Japon sous le Japon NE au Plio-Pleistocène.

A l'heure actuelle, la même direction de compression E-O à ONO-ESE est documentée dans tout le Japon sud-ouest. L'âge exact de la transition entre le champ de contraintes extensif miocène moyen et la compression actuelle n'est pas connu dans le Japon sud-ouest.

3. Conclusion

La zone décrochante est-mer du Japon sert de guide à l'ouverture en bassin pull-apart de la mer du Japon à l'Oligo-Miocène. La déformation décrochante continentale interagit avec l'extension en bordure de la zone de subduction pour accommoder l'ouverture.

L'ouverture en pull-apart dextre est compatible avec les rotations horaires documentées dans le Japon sud-ouest (Jolivet et al., 1991). Selon Otofuji et al. (1991) et Hayashida et al. (1991) la rotation en bloc du Japon sud-ouest a lieu entre 16 et 14 Ma. Un diachronisme apparaît ainsi entre l'âge des rotations et l'âge de l'océanisation de la mer du Japon (24-17 Ma; Tamaki et al., 1992). Nous sommes donc allés étudier sur le terrain dans le Japon sud-ouest la déformation contemporaine de l'ouverture de la mer du Japon et des rotations.

B. DÉFORMATION DANS LE JAPON SUD-OUEST ET ROTATIONS PALÉOMAGNÉTIQUES

J'ai mené une étude du champ de contraintes contemporain de l'ouverture de la mer du Japon dans le Japon sud-ouest au moyen de l'analyse de la fracturation, d'une part parce que les seules informations disponibles sur le champ de contraintes à cette période reposaient sur des statistiques de directions de dykes, directions dont on sait qu'elles peuvent être influencées par la pré-fracturation de l'encaissant, et d'autre part pour comprendre le contexte structural des rotations paléomagnétiques du Japon sud-ouest.

1. Champ de contraintes Miocène inférieur et moyen dans le Japon sud-ouest

a. Sur la côte de la mer du Japon

L'étude du champ de contraintes a été réalisée dans les péninsules de Shimane, Tango et Noto, et dans le bassin de Yatsuo (Figure 59). Les formations miocènes inférieur et moyen sont affectés par des décrochements conjugués et des failles normales (Figure 60). Ce type de fracturation n'est pas observé dans les formations miocènes supérieur souvent exemptes de déformation (Noto, Tango). A Shimane, les formations miocènes supérieur sont affectés par des failles inverses qui fournissent une direction de compression \pm N-S. Cette compression est exprimée aussi par des plis d'axe E-O.

Les tenseurs de contraintes calculés pour le Miocène inférieur et moyen sur la marge sud de la mer du Japon sont transtensifs ou extensifs avec une direction d'extension moyenne NO-SE à ONO-ESE et une direction de $\sigma_{H\max}$ NE-SO à NNE-SSO (Figure 61). Ces directions principales du champ de contraintes sont identiques à celles déterminées à partir de l'analyse de la fracturation sur la marge est de la mer du Japon et à Hokkaido (Jolivet et Huchon, 1989 ; Jolivet et al., 1991), à Sakhaline (Fournier et al., 1994), et dans le bassin de Pohang en Corée (Hwang, 1992). Charvet et al. (1992) ont déterminé des directions de contraintes identiques sur la marge est de la mer du Japon à partir de l'analyse de la fracturation dans les forages ODP, de même que Yamagishi et Watanabe (1986) et Otsuki (1990) dans le NE Honshu à partir de statistiques sur les directions de veines métallifères et de dykes. Le régime de contraintes est transpressif à Sakhaline et Hokkaido, transtensif sur la marge est de la mer du Japon, et transtensif à purement extensif sur la marge sud. Ce régime de contraintes est en accord avec une ouverture en bassin pull-apart de la mer du Japon.

La cohérence des directions du champ de contraintes oblige à s'interroger sur la rotation du champ de contraintes d'âge Miocène inférieur pendant les rotations différentielles du Japon sud-ouest et du Japon nord-est au Miocène moyen basal. Une certaine dispersion des données pourrait être interprétée comme une indication de cette rotation. Cet aspect est cependant délicat à discuter en l'absence de chronologie relative entre les différents tenseurs. Il est plus probable que nous ayons essentiellement mesuré le champ de contraintes miocène moyen correspondant à un stade tardif de l'ouverture. Étant donnée la géométrie de l'ouverture en pull-apart, le même champ de contraintes a prévalu vraisemblablement pendant toute la durée de l'ouverture.

Ce dernier point reste un problème. Une étude locale et approfondie du champ de contraintes au Miocène inférieur et moyen (comme par exemple dans la péninsule de Tango où les conditions d'affleurement sont correctes) en liaison avec de nouvelles datations radiométriques pourrait peut-être apporter des informations sur l'évolution dans le temps du champ de contraintes pendant l'ouverture.

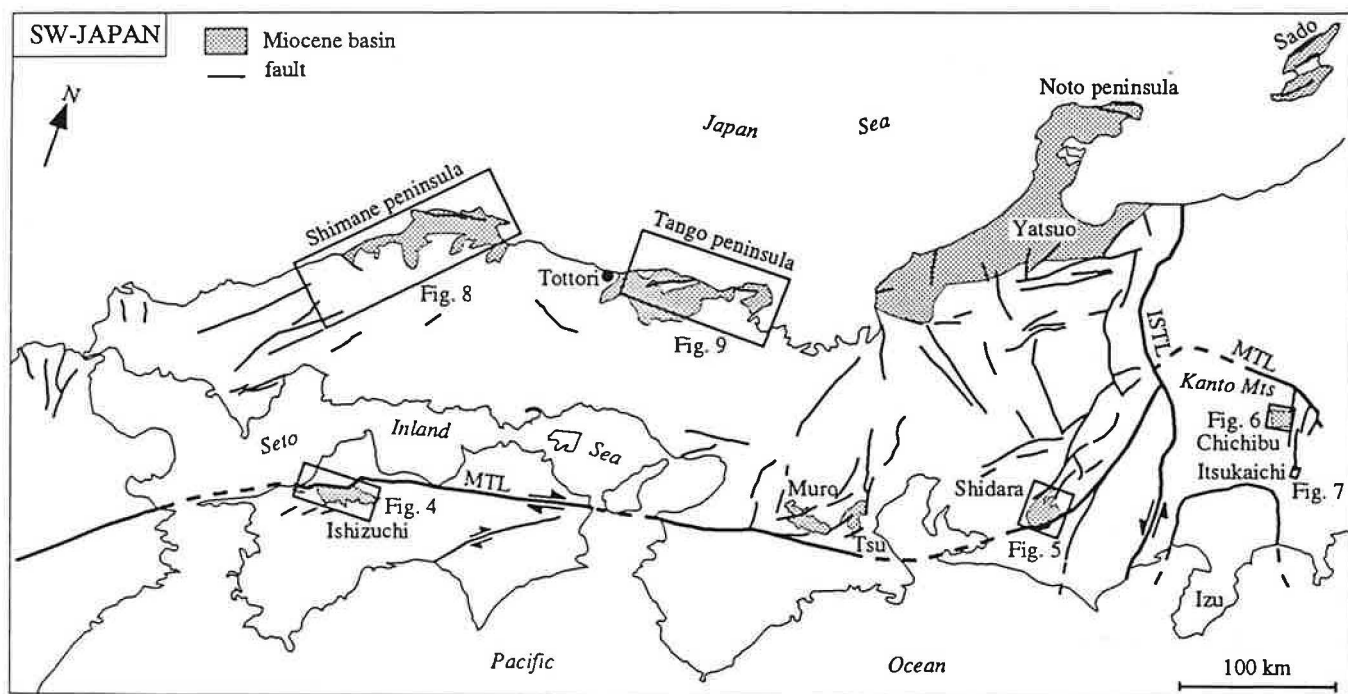
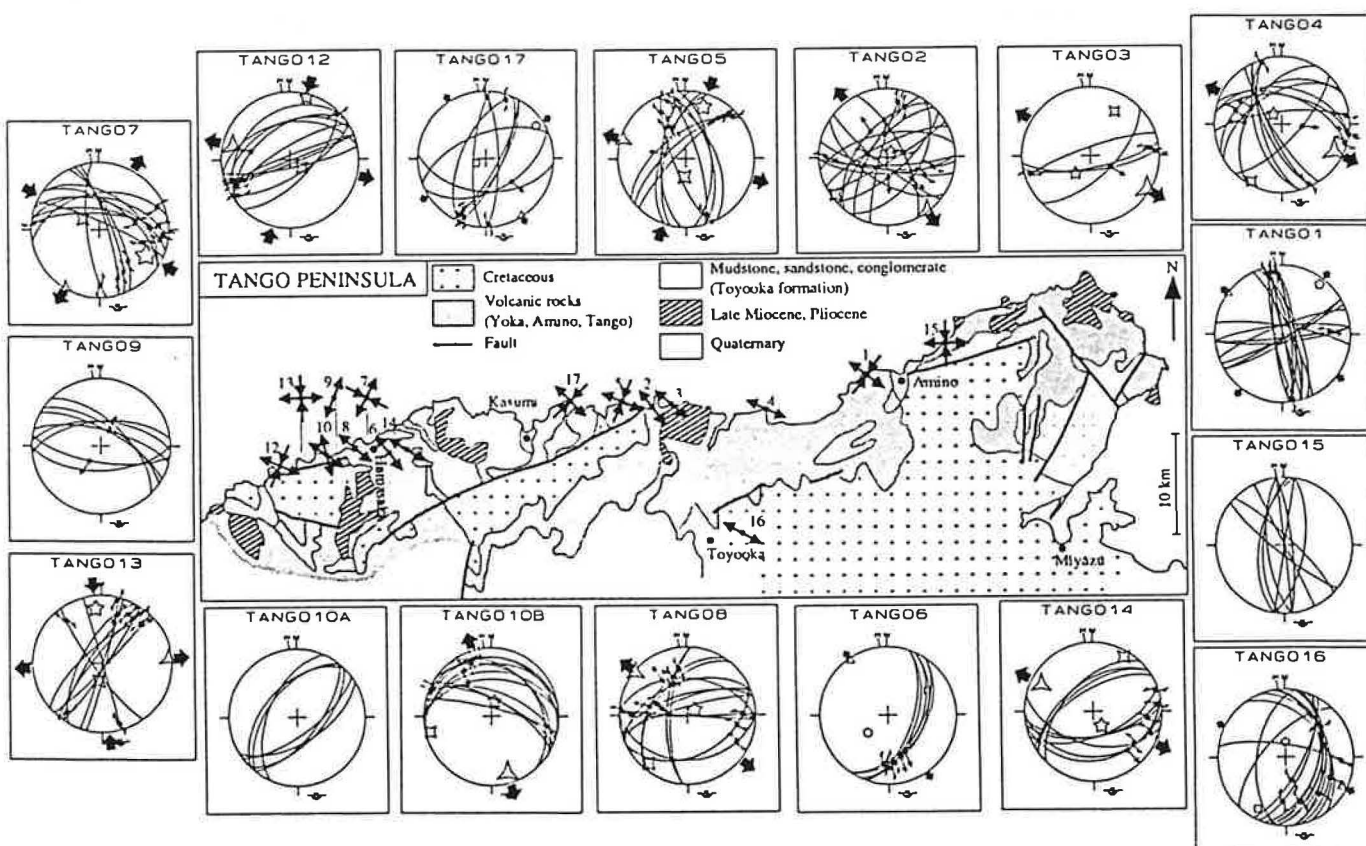
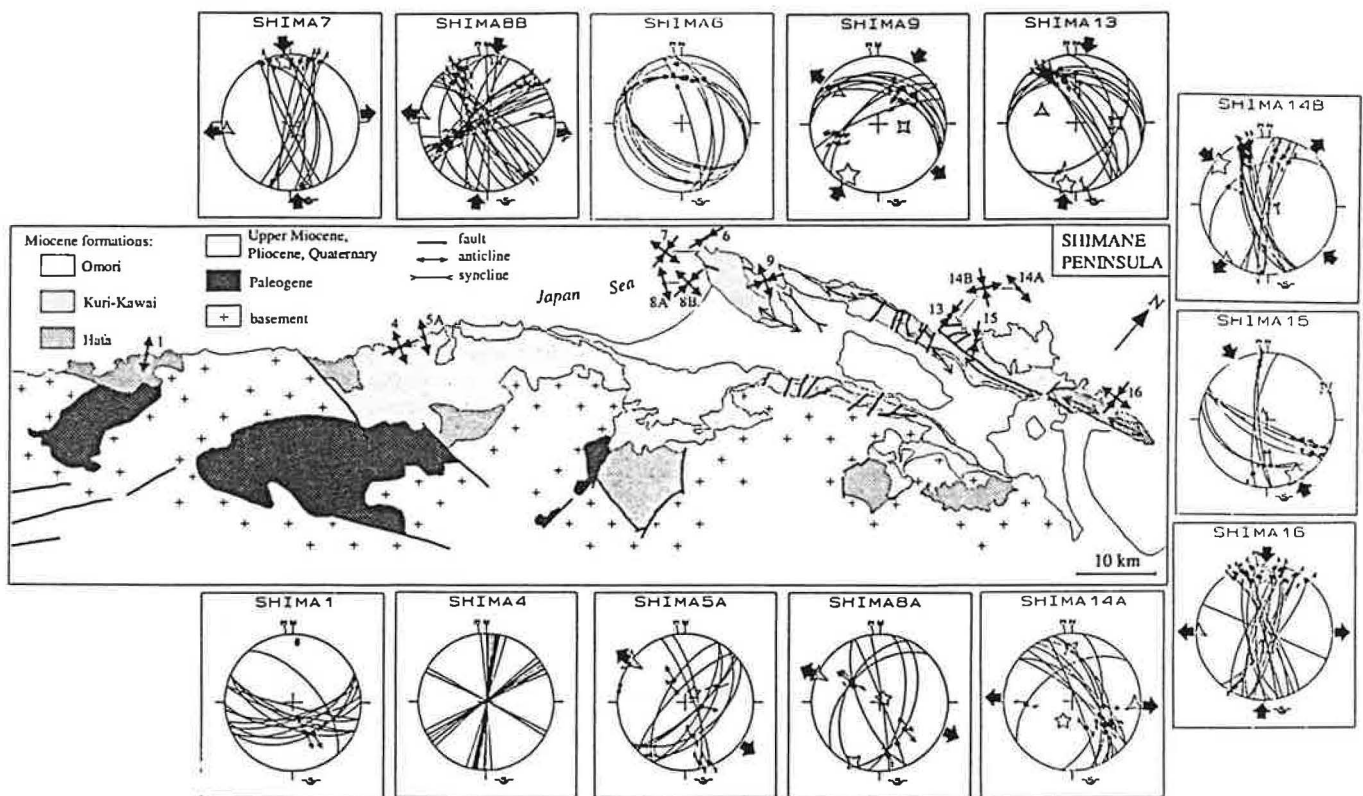


Figure 59. Bassins miocènes du Japon sud-ouest.



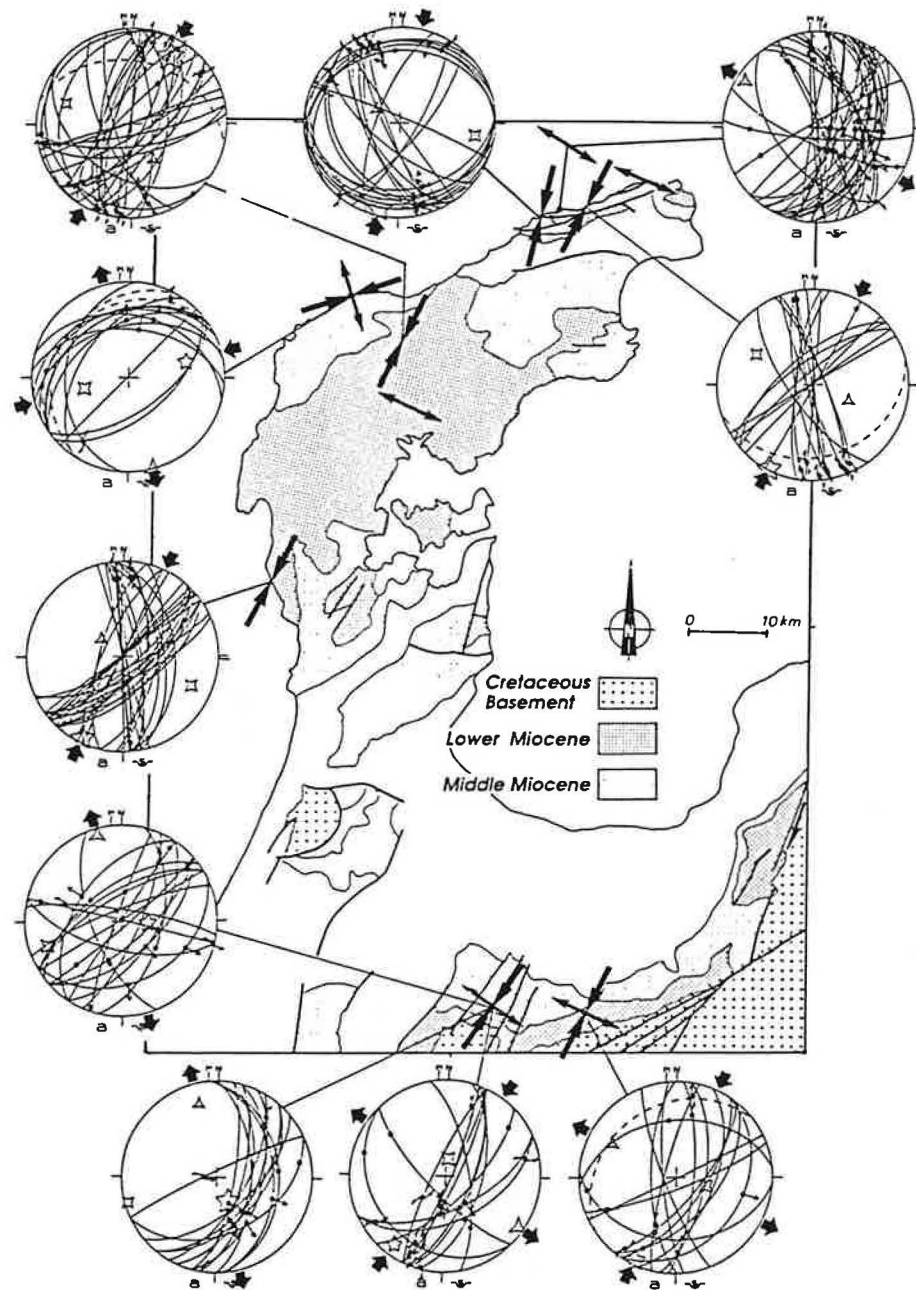
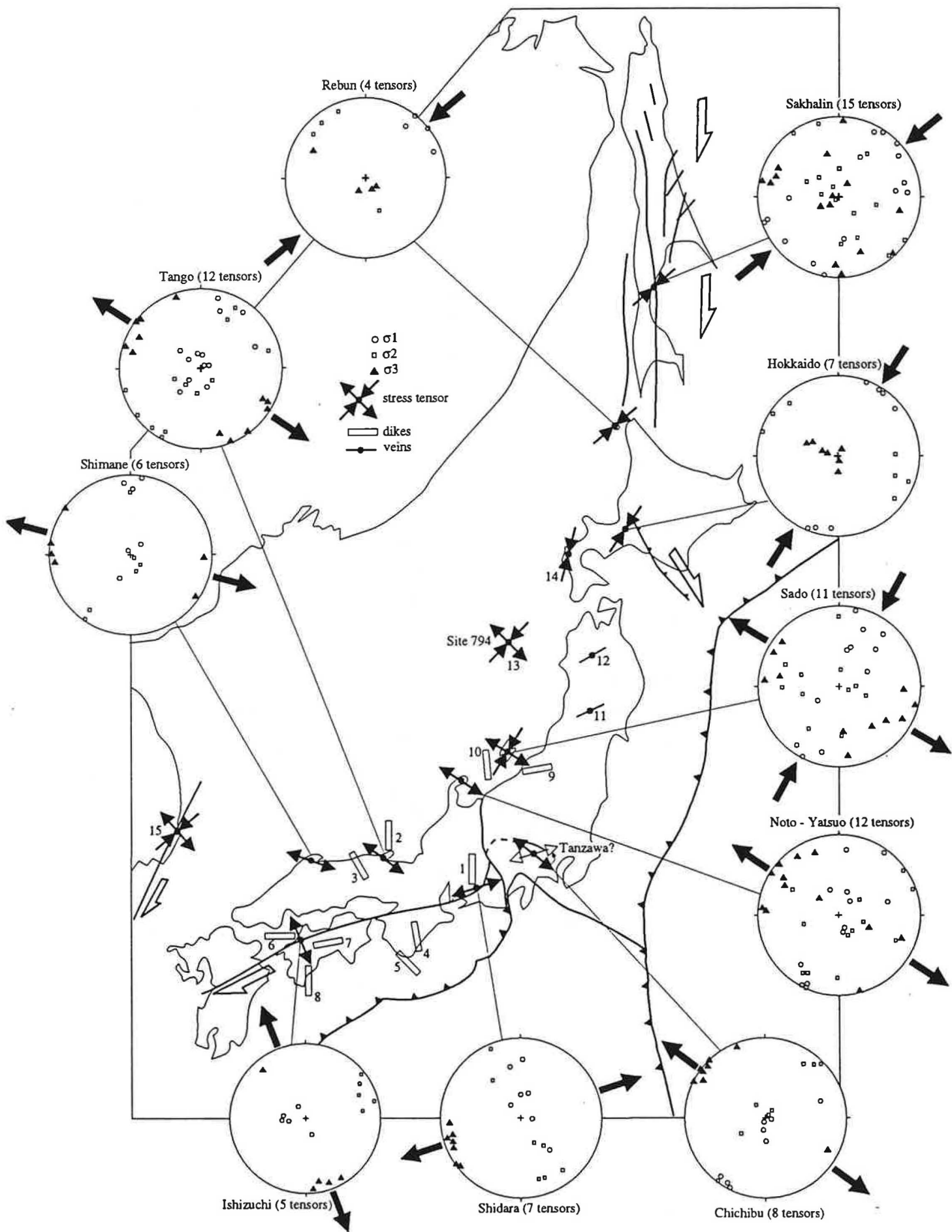


Figure 60. Tenseurs de contraintes dans les péninsules de Shimane, Tango, Noto, et le bassin de Yatsuo.

Figures 61. Tenseurs de contraintes moyens autour de la mer du Japon déduits de l'analyse de la fracturation dans les formations miocènes inférieur et moyen.



b. Le long de la MTL

La MTL est la faille majeure du Japon sud-ouest et pourrait avoir joué un rôle important pendant la rotation. Il est donc essentiel de comprendre son jeu pendant l'ouverture.

Son jeu au Crétacé terminal-Paléogène est à composante décrochante sénestre d'après l'arrangement en échelon des plis et des failles qui affectent le groupe Izumi (Campanien-Maastrichtien) en bordure de la MTL dans le district de Kinki, mais n'affecte pas le groupe Kuma qui s'est déposé entre l'Éocène supérieur et la base du Miocène moyen (Miyata et al., 1980). Son jeu à l'heure actuelle et depuis le Pliocène terminal est à composante décrochante dextre, le taux de mouvement dextre étant estimé à Shikoku dans la partie où le mouvement est le plus rapide à 5 à 10 mm/an à partir du décalage de terrasses quaternaires récentes datées par ^{14}C (Okada, 1980). Il n'y a pratiquement pas de séismicité liée à la MTL et il semble que le dernier gros séisme à avoir ébranlé la MTL est le séisme Keicho en 1596 à Shikoku (Okada, 1992).

Le jeu de la MTL pendant l'ouverture de la mer du Japon est mal connu. Hayashi (1978, cité dans Miyata et al., 1980) aurait montré que la MTL a accommodé un déplacement sénestre de 2 km dans le bassin de Shidara postérieur à la mise en place des dykes andésitiques datés de 15 Ma. Aucun décalage sur la carte géologique du bassin de Shidara ne permet cependant de confirmer cette indication. Sur la base d'orientation de dykes par rapport à la MTL, Takeshita (1990) a aussi proposé que le jeu de la MTL était décrochant sénestre au Miocène. Jolivet et al. (1989) avaient quant à eux interprété l'augmentation vers le sud de la déclinaison dans les roches miocènes inférieur, à l'approche de la MTL, comme une indication de cisaillement dextre pendant l'ouverture de la mer du Japon. L'étude du champ de contraintes néogène que nous avons réalisé le long de la MTL avait donc pour but de déterminer le sens de mouvement de la MTL pendant l'ouverture.

Cette étude s'est avérée difficile, d'une part parce que les bassins néogènes le long de la MTL sont peu nombreux et que les affleurements y sont rares, et d'autre part parce que les résultats ne sont pas aisés à interpréter. Nous avons obtenu des résultats pour 3 bassins (Ishizuchi, Shidara, Chichibu) sur les cinq (les mêmes + Muro et Tsu) que nous avons étudiés (Figure 59). Les tenseurs de contraintes miocènes moyen que nous avons calculés sont pour l'essentiel extensifs et compatibles avec un mouvement sénestre et normal le long de la MTL à Shidara et à Chichibu, et avec un mouvement purement normal à Ishizuchi.

Revenons sur les résultats de Shidara car c'est là que la composante sénestre est la plus évidente. Il faut avoir à l'esprit l'importance du champ de dykes dans ce bassin dont la carte par Kogi (1983) est montrée en Figure 62. Plus d'une centaine de dykes sont cartographiés et les statistiques sur les directions montrent clairement une direction principale N-S dans la partie sud du bassin, évoluant à N020E vers le nord. Dans la partie sud du bassin, les dykes andésitiques se sont mis en place dans un encaissant rhyolitique et dacitique dont j'ai pu vérifier qu'il était massif et pratiquement exempt de failles : les dykes se sont mis en place

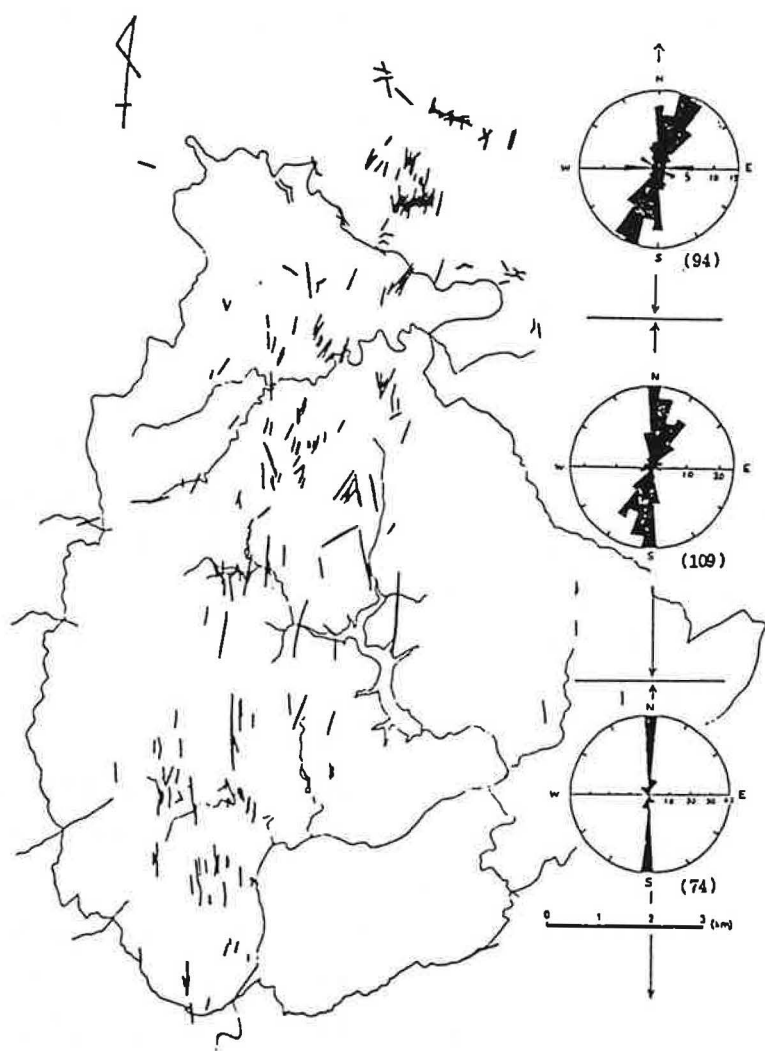


Figure 62. Champ de dykes du bassin de Shidara (d'après Kogi, 1983).

dans un encaissant qui n'était pas pré-fracturé. Il est donc raisonnable d'estimer que les dykes se sont mis en place parallèlement à la direction de la contrainte maximale horizontale, et que celle-ci était donc N-S il y a 15 Ma (âge des dykes, Tsunakawa et al., 1983). Nos données de fracturation sont en accord avec cette direction de $\sigma_{H\max}$ puisqu'elles fournissent une direction d'extension comprise entre NE-SO et E-O. Un tel champ de contraintes est compatible avec un mouvement sénestre et normal le long de la MTL dont la direction est N050°E dans le bassin de Shidara. D'autre part, la géométrie du champ de dykes limité au sud par la MTL et au nord par une faille satellite de la MTL et parallèle à elle, suggère la mise en place en "pull-apart" sénestre du système de dykes entre deux décrochements en relais.

Il nous semble donc légitime d'affirmer à partir de ces arguments de terrain que la MTL a une composante de mouvement sénestre dans sa partie orientale pendant l'ouverture de la mer du Japon.

D'autre part, si l'on considère à grande échelle la rotation horaire de 50° de la MTL avec le Japon SO dans le contexte extensif/transtensif de l'ouverture de la mer du Japon, son jeu ne peut mécaniquement qu'être normal sénestre quelle que soit la cause de la rotation. La Figure 63 montre la modélisation analogique de ce type de déformation rotationnelle dans une zone de cisaillement dextre transtensive. Toutes les failles qui tournent ont une composante sénestre et normale. Les observations de terrain le long de la MTL sont en accord avec ce modèle analogique.

Bien que les données soient peu nombreuses, nous estimons qu'il est possible de considérer que le jeu de la MTL pendant l'ouverture de la mer du Japon est normal sénestre dans sa partie orientale et purement normal dans sa partie occidentale. Le cisaillement sénestre est de sens opposé aux rotations paléomagnétiques horaires dans le Japon sud-ouest. Nous considérons donc la MTL comme une faille de second ordre qui accommode des rotations horaires. Nous proposons de plus, comme on va le discuter maintenant, que ces rotations sont au moins en partie le fait d'un cisaillement dextre du Japon sud-ouest entre les deux zones décrochantes dextres qui bordent la mer du Japon à l'est et à l'ouest.

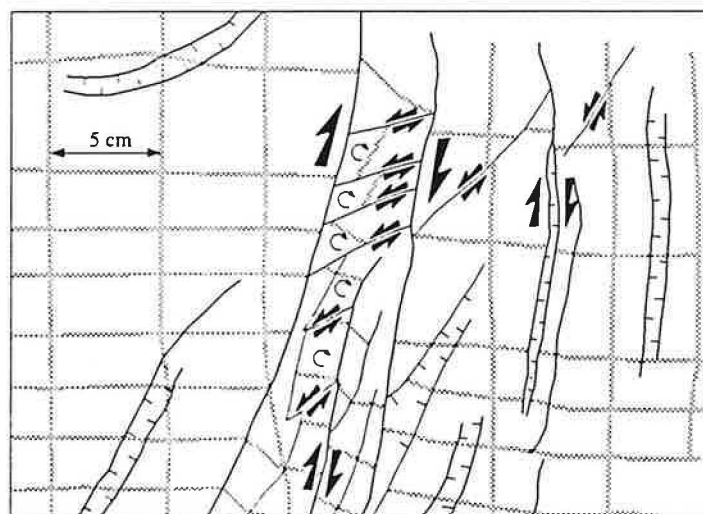
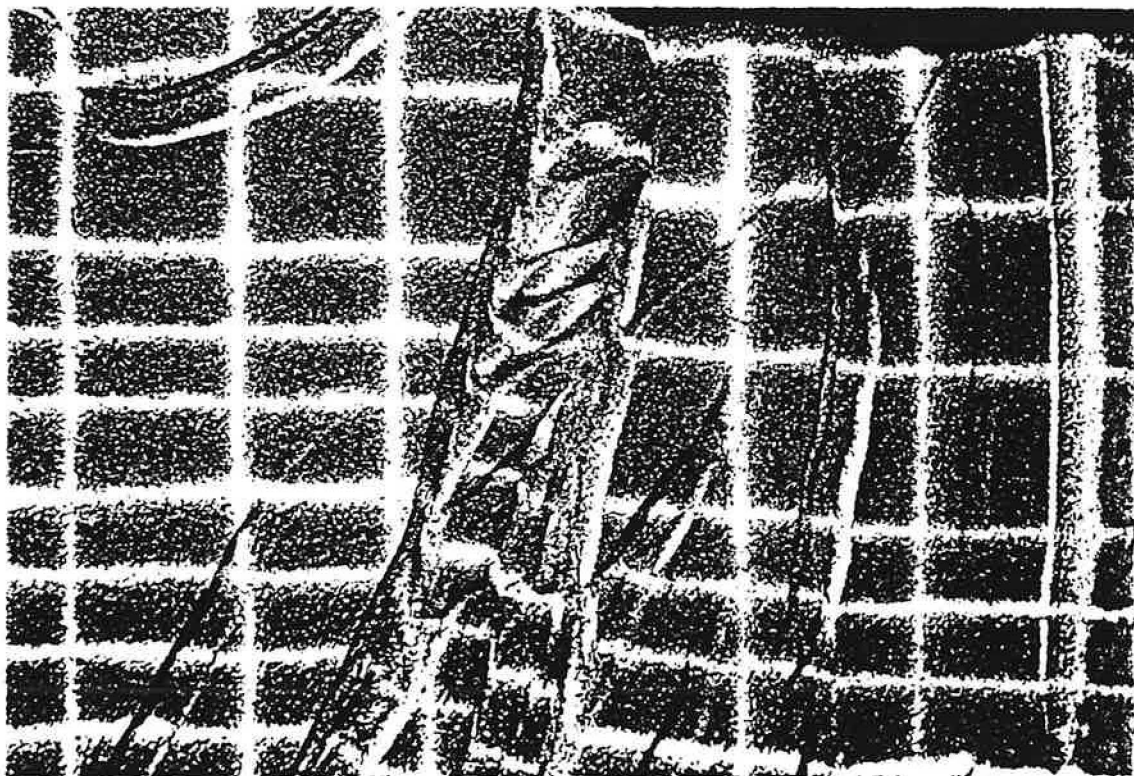


Figure 63. Modélisation analogique de la déformation dans une zone cisaillante dextre.

2. Âge des rotations paléomagnétiques du Japon sud-ouest et ouverture de la mer du Japon

Comme l'ont montré Jolivet et al. (1991), les rotations horaires du Japon SO sont compatibles avec le modèle d'ouverture en bassin pull-apart. Le problème n'est donc pas de nature structurale mais vient du diachronisme entre l'océanisation de la mer du Japon, dont l'âge a été déterminé à l'occasion des forages ODP par datation des basaltes océaniques et des sédiments qui les recouvrent entre 24 et 17 Ma (Tamaki et al., 1992), et l'âge des rotations paléomagnétiques dans le Japon SO contraint entre 16 et 14 Ma (Otofuji et al., 1991 ; Hayashida et al., 1991). Bien avant les forages ODP l'étude des bassins sur les marges et les données de flux de chaleur suggéraient une ouverture plus longue, et plus ancienne que 15 Ma (Tamaki, 1988). Il y a deux façons d'aborder le problème pour tenter d'y apporter une solution.

a. Le diachronisme entre océanisation et rotations est-il réel ?

C'est le problème de la fiabilité des âges de l'océanisation et des rotations. Nous discutons la fiabilité des âges des rotations plutôt que celle des âges ODP, d'une part parce que les âges ODP sont doublements contraints par les datations radiométriques des basaltes et les datations micropaléontologiques des sédiments, et d'autre part parce que les calculs de moyenne réalisés pour contraindre l'âge des rotations paléomagnétiques nous semblent douteux. Nous ne comprenons pas qu'Otofuji et al. (1991) utilisent une donnée aussi jeune que $13,7 \pm 0,3$ Ma pour calculer l'âge moyen d'une formation qui a subi la rotation horaire du Japon SO, en même temps qu'une donnée aussi ancienne que $16,2 \pm 1,4$ Ma pour calculer l'âge moyen d'une formation qui n'a pas subi de rotation. Il nous paraît raisonnable de considérer que les rotations paléomagnétiques se produisent sur un intervalle de temps plus grand que 16-14 Ma, compatible au moins en partie avec l'âge de l'océanisation tel qu'il a été déterminé par les forages ODP.

b. Les rotations paléomagnétiques du Japon sud-ouest sont-elles liées à l'ouverture de la mer du Japon ?

La réponse à cette question est non si les datations sont exactes. Si l'océanisation a eu lieu entre 24 et 17 Ma et les rotations entre 16 et 14 Ma, alors elles n'ont rien à voir. Personne cependant ne se risque à soutenir une chose pareille.

La séparation des deux phénomènes est envisageable si la rotation du Japon SO n'a pas lieu d'un bloc mais qu'elle est absorbée localement par la rotation de petits blocs, sans ouverture d'un grand bassin arrière-arc. Dans cette hypothèse, il était intéressant de connaître le contexte structural des rotations paléomagnétiques dans le Japon sud-ouest.

L'étude structurale a montré que le Japon SO n'est pas exempt de déformation synchrone des rotations paléomagnétiques. La géométrie de la déformation à l'affleurement suggère même que des rotations de systèmes de blocs à différentes échelles sont envisageables et pourraient rendre compte d'une partie au moins des rotations paléomagnétiques. C'est la raison pour laquelle nous estimons qu'une géométrie de blocs telle qu'elle a été proposée par Kanaori (1990) pour le Japon interne n'est pas déraisonnable. Des tels blocs accommodant des rotations importantes sont connus le long de la faille du Levant (Ron et al., 1984) et de la faille de San Andreas (Luyendyk et al., 1985).

Il faut souligner d'autre part que l'argument de la linéarité des structures anté-ouverture au sud de la MTL, souvent avancé à l'encontre d'éventuel blocs (Otofuji et al., 1994 ; voir aussi Faure et Lalevée, 1987), ne vaut qu'au sud de la MTL alors que les blocs ne sont proposés qu'au nord de la MTL (là où sont documentées les rotations paléomagnétiques). Il existe d'ailleurs des décrochements transverses qui recoupent les structures au sud de la MTL, dont la faille de Kaminirogawa-Akuigawa (Murata, 1988 ; Figure 64) à Shikoku est le meilleur exemple. Enfin, il est troublant que, alors que le Japon est l'une des régions au monde les mieux couvertes par le paléomagnétisme, il n'existe aucune donnée publiée au sud de la MTL bien que les formations paléogènes et néogènes ne manquent pas. Ces formations ont-elles tourné autant qu'au nord de la MTL ?

3. Distribution des rotations en fonction de la déformation

Contrairement à ce qui a été longtemps écrit, les rotations paléomagnétiques ne sont pas horaires dans le Japon SO et anti-horaires dans le Japon NE : la distribution des rotations est directement liée au champ de déformation. En première approximation, les rotations sont horaires dans les principales zones de déformation néogènes (Sakhaline, zone centrale d'Hokkaido, Tanakura Tectonic Line, détroit de Tsushima) et anti-horaires dans les blocs non déformés. Il faut bien entendu nuancer ce propos en ce qui concerne le Japon SO. Celui-ci a vraisemblablement tourné (au moins en partie) en bloc dans le sens horaire pendant l'ouverture de la mer du Japon, la propagation de l'océanisation vers l'ouest provoquant nécessairement une rotation horaire (voir les reconstructions de l'ouverture par Jolivet et al. (1991), Figure 27).

On comprend aisément que les zones de déformations soient associées à des rotations horaires puisqu'elles accommodent toutes des mouvements décrochants dextres. Là encore il faut nuancer le propos en ce qui concerne la zone de cisaillement du détroit de Tsushima. Si des rotations horaires sont bien documentées dans les roches oligocènes et miocènes inférieur du bassin de Pohang à proximité de la faille de Yangsan, des rotations anti-horaires de $30^\circ \pm 14^\circ$ ont été obtenues à Tsushima dans des roches intrusives d'âge Miocène moyen (Ishikawa et al., 1989), et aussi à Goto où le taux de rotation reste mal contraint (Ishikawa et Tagami,

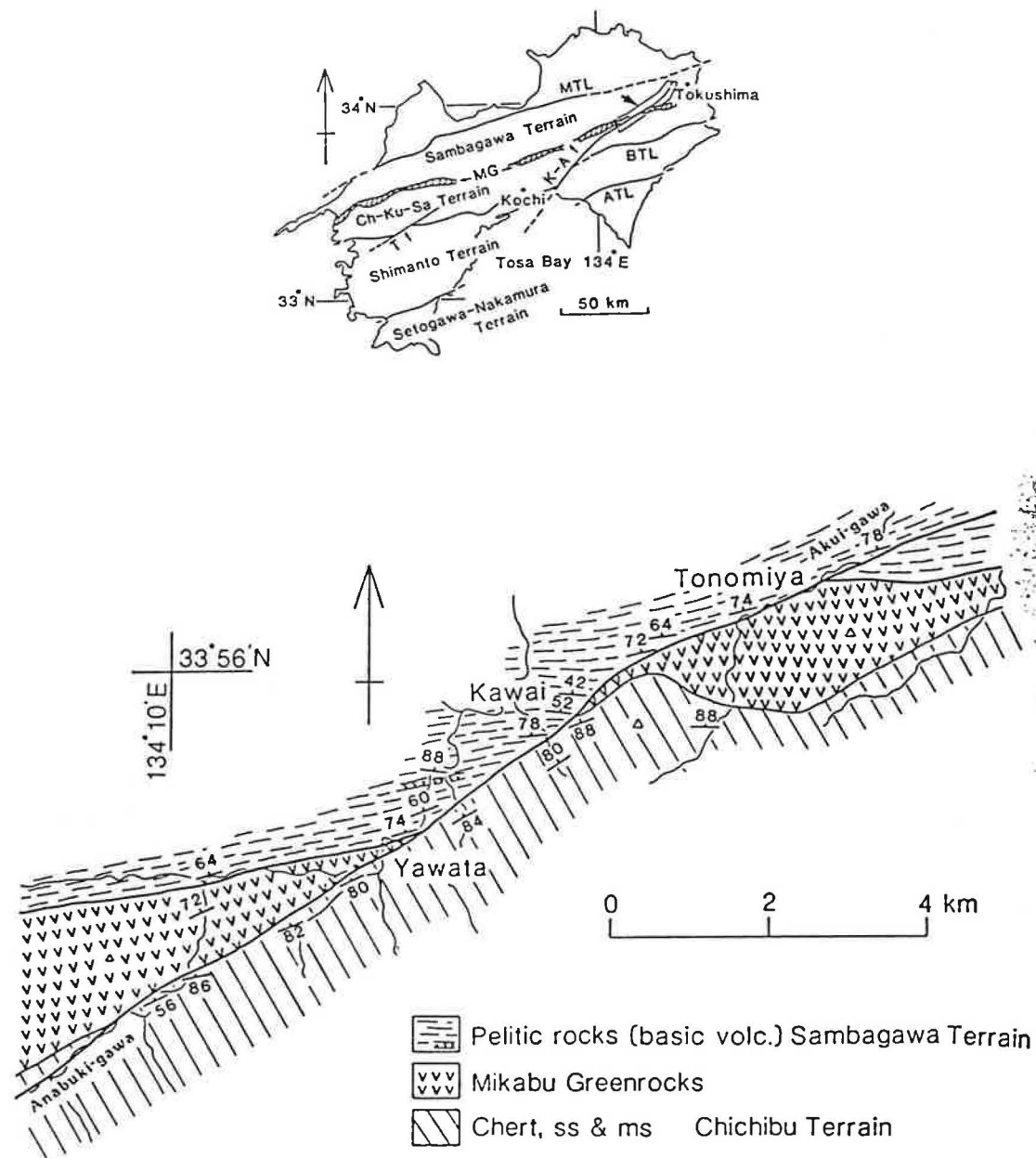


Figure 64. Décalage sénestre des structures rectilignes (Sanbagawa) au sud de la MTL à Shikoku par la faille Kaminirogawa-Akuigawa (Murata, 1988).

1991). La faille de Tsushima ayant rejoué en décrochement sénestre au Miocène supérieur (Fabbri et Charvet, 1994), il est plausible que les rotations anti-horaires sont liées à la déformation tardive.

Il reste à comprendre pourquoi, dans la mesure où toutes les zones de déformation majeures sont dextres et dans la mesure aussi où le champ de contrainte était globalement transtensif pendant l'ouverture, le NE Honshu a tourné dans le sens anti-horaire. Si, en contexte transtensif, des décrochements dextres accommodent la rotation anti-horaire de blocs rigides, alors on peut légitimement envisager une déformation cisaillante sénestre d'échelle supérieure et englobant l'ensemble du système. A l'intérieur d'une zone en cisaillement sénestre des blocs sont en effet susceptibles de tourner dans le sens horaire grâce au jeu de décrochements dextres. Les expériences de modélisation analogique (Davy et Cobbold, 1988; cette étude) fournissent un modèle simple dans ce sens qui relie l'ouverture des bassins du NE asiatique à la collision Inde-Asie.

C. MODÈLE D'OUVERTURE DE LA MER DU JAPON

Pour quelle(s) raison(s) le Japon sud-ouest tourne-t-il ? Est-ce la propagation vers l'ouest de l'océanisation qui provoque la rotation (rotation rigide), ou est-ce le mouvement décrochant dextre le long des marges de la mer du Japon qui provoque un cisaillement dextre général du Japon sud-ouest (déformation distribuée) ?

Les reconstructions de l'ouverture de la mer du Japon proposées par Jolivet et al. (1991) suggèrent que l'ouverture (océanisation incluse) s'accompagne de la rotation horaire de 30° du Japon sud-ouest d'un bloc. Le bassin du Japon est refermé par une rotation horaire de 20°-30° de manière à accolter les contours bathymétriques du banc de Yamato et de la marge nord de la mer du Japon. Encore faut-il que l'âge de l'océanisation et celui des rotations soient compatibles. Nous avons consacré un article (Jolivet et al., p. 169) à montrer qu'ils pouvaient l'être au moins partiellement si les âges des rotations paléomagnétiques étaient calculés différemment. Nous suggérons que les 15° à 20° de rotation restant sont dus au cisaillement dextre du Japon sud-ouest entre les deux zones décrochantes dextres qui bordent la mer du Japon à l'est et à l'ouest. Nous suggérons aussi que cette rotation est absorbée par la déformation interne de l'arc japonais telle qu'elle est documentée sur le terrain, à savoir par des rotations de blocs locales.

Le modèle d'ouverture que nous proposons est présenté en Figure 65. La mer du Japon s'ouvre en bassin pull-apart entre deux zones décrochantes en relais. Pendant la phase initiale de l'ouverture, extension distribuée et amincissement crustal prévalent provocant la formation de bassins (Yamato, Tsushima, Japon) à croûte continentale amincie séparés par des boudins de croûte d'épaisseur normale tels que le banc de Yamato. La mise en place de croûte océanique dans le bassin du Japon débute vers 24 Ma. La cassure initiale de la lithosphère se

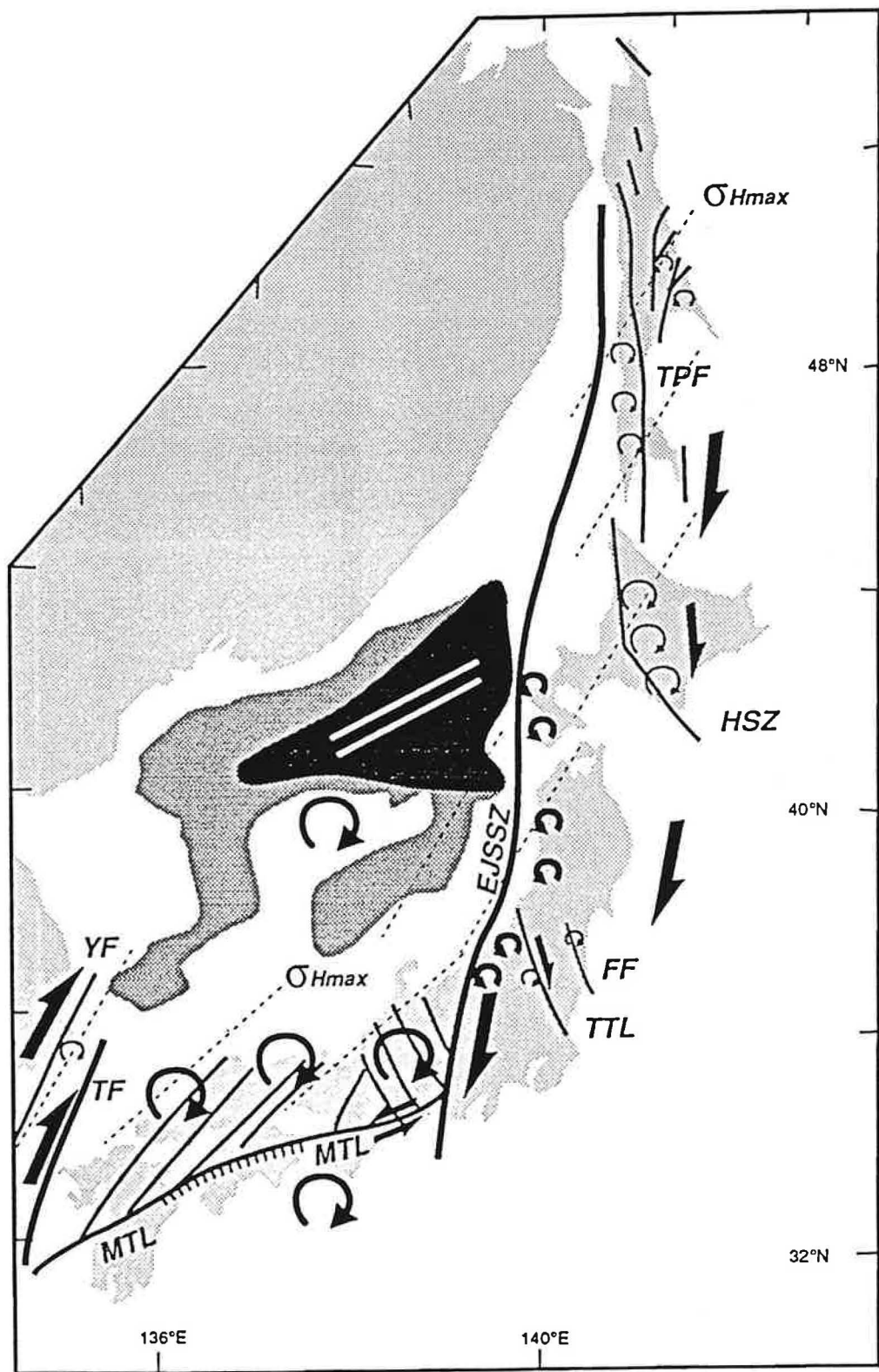


Figure 65. Modèle d'ouverture de la mer du Japon.

produit le long de la marge décrochante orientale, là où le cisaillement et l'étirement sont les plus forts. L'océanisation se propage d'est en ouest provocant nécessairement au sud la rotation horaire du Japon sud-ouest d'environ 30°. Les 15° à 20° de rotation supplémentaires sont attribuées au cisaillement dextre du Japon sud-ouest entre les zones décrochantes bordières de la mer du Japon. Ils sont absorbés par des rotations distribuées. Pendant l'ouverture, la MTL est une faille de second ordre à jeu normal avec localement une composante sénestre qui accommode les rotations. A l'intérieur des zones décrochantes qui limitent à l'est et à l'ouest la mer du Japon, le cisaillement dextre est absorbé dans des zones de déformation localisée où il est associé à des rotations horaires (Sakhaline, zone centrale d'Hokkaido, Tanakura Tectonic Line, faille de Yangsan). A l'intérieur de la zone décrochante est-mer du Japon, les blocs rigides limités par ces zones de cisaillement dextre tournent dans le sens anti-horaire (NE Honshu). Cette distribution des rotations indique que les mouvements dextres accommodent la rotation anti-horaire des blocs rigides. Le modèle d'ouverture de la mer du Japon en relation avec la collision Inde-Asie que nous détaillons ci-après suggère que tout le système de la mer du Japon (mer du Japon et zones de déformation bordières) est inclus dans une zone de cisaillement plus large dont le jeu sénestre est contrôlé par la collision.

Pour tester le modèle de rotations distribuées dans le Japon sud-ouest il faudrait avoir une mesure paléomagnétique au moins dans chacun des blocs tels qu'ils sont proposés par Kanaori(1990), afin d'identifier d'éventuelles rotations différentielles. Les mesures paléomagnétiques sont pour l'heure très groupées, dans le Japon central d'une part, et à l'extrême occidentale du Japon sud-ouest d'autre part (San'In district au sud-ouest de la péninsule de Shimane). Des mesures pourraient facilement être réalisées au moins dans la péninsule de Tango. Comme on l'a dit aussi, des mesures paléomagnétiques au sud de la MTL font défaut. La partie méridionale du Kinki district (au sud d'Osaka) avec des formations miocènes inférieur et moyen semble a priori un bon candidat pour de telles mesures. Il faudrait d'autre part identifier clairement les limites de blocs sur le terrain et étudier la déformation le long de ces limites. Je doute cependant qu'un travail de géologie classique puisse apporter beaucoup d'informations, les affleurements à l'intérieur des terres étant comptés.

III. CAUSES DE L'OUVERTURE DE LA MER DU JAPON : COLLISION ET EXTENSION

A. DÉFORMATION CONTINENTALE EN ASIE DU NORD-EST GOUVERNÉE PAR LES CONDITIONS AUX LIMITES

1. Déformation continentale en Asie du NE et collision

La déformation continentale en Asie du NE est dominée par des décrochements conjugués associés à des bassins en extension (Figure 3). On distingue une famille de décrochements dextres d'orientation plutôt N-S qui comprend la faille de Tan-Lu en bordure du bassin de Chine du nord, le système de grabens en échelon du Shansi, et les zones décrochantes de Tsushima et de l'est de la mer du Japon qui bordent la mer du Japon. Une seconde famille de décrochements sénestres d'orientation plutôt E-O comprend le Qinling Shan associé au graben de la Weihe, et les Monts Stanovoï à l'est des grabens du Baïkal. On remarquera que le système de décrochements dextres est inclus dans la zone de cisaillement sénestre limitée au sud par le Qinling Shan et au nord par les Monts Stanovoï. Les décrochements dextres accommodent donc des rotations anti-horaire de blocs. Deux systèmes de décrochements conjugués accommodent en effet du cisaillement pur sans rotation si les décrochements sont de même échelle, et du cisaillement simple avec des rotations si l'un des systèmes est inclus dans l'autre.

Il ne faut pas sous-estimer l'importance des Stanovoï dans la déformation de l'Asie. La zone des Stanovoï est beaucoup plus active sismiquement que par exemple le Qinling Shan ou la faille de l'Altyn Tagh (Figure 2). Puisqu'il est généralement admis que le bloc Ordos tourne dans le sens anti-horaire par le jeu du mouvement sénestre le long du Qinling Shan, on peut raisonnablement estimer qu'entre la limite nord de l'Ordos et les Stanovoï des blocs continentaux tournent de la même façon, même si leurs limites ne sont pas bien définies. Comme on l'a noté en introduction, la carte topographique de la Figure 1 montre en Asie du NE des gradients topographiques rectilignes de direction NNE-SSO dont la nature géologique est mal connue et qui sont de bons candidats pour d'éventuelles limites de blocs (par comparaison, le bloc Ordos et le système de grabens qui l'entourent sont à peine discernables sur la carte topographique).

La déformation continentale en Asie du NE est donc dominée par le jeu de deux systèmes de décrochements conjugués. La direction de contrainte maximale horizontale qu'implique l'orientation des décrochements est NE-SO. Une telle direction peut être attribuée à la collision Inde-Asie. Si les décrochements sénestres sont en général reliés à la collision (Tapponnier et Molnar, 1979 ; Tapponnier et al., 1982, 1986 ; Peltzer et al., 1985 ; Wang, 1987), les décrochements dextres sont souvent ignorés malgré leur importance. Il n'est cependant pas possible d'expliquer les mouvements dextres par un mécanisme tel que la

subduction (comme pour la faille de Sumatra ou la MTL actuelle), la composante oblique de la subduction n'étant jamais dans le bon sens. Les expériences de Davy et Cobbold (1988) interprétées par Jolivet et al. (1990) fournissent un mécanisme simple pour générer du cisaillement dextre transtensif en relation avec la collision.

2. Influence du régime de subduction sur la déformation

Le régime de subduction de la lithosphère océanique ancienne de la plaque Pacifique n'a pas changé depuis l'Oligocène et l'extension est toujours active au-dessus des fosses d'Izu-Bonin et des Mariannes dans la plaque mer des Philippines.

La subduction de la plaque mer des Philippines sous le Japon sud-ouest débute au Miocène moyen ou supérieur, succédant à la subduction de la plaque Pacifique. La lithosphère océanique qui est subduite est jeune (Oligo-Miocène), son angle de subduction est faible, et elle est porteuse d'aspérités dont les plus significatives sont les blocs de Tanzawa et d'Izu qui entrent en collision depuis le Miocène supérieur avec le Japon central. Charvet et Fabbri (1987) relient aussi la phase Takachiho (Burdigalien) de l'orogenèse Shimanto à la collision ou la subduction difficile de la plaque mer des Philippines sous l'extrémité occidentale du Japon sud-ouest (Figure 66).

La remontée vers le nord de la plaque mer des Philippines et son passage en subduction sous le Japon sud-ouest constitue indéniablement un changement de conditions aux limites au Miocène moyen ou supérieur. Il est tentant de relier ce changement au changement simultané de régime de contraintes dans l'arc japonais et la mise en place du régime compressif E-O. Comme on l'a déjà noté cependant, la direction de compression actuelle E-O à ONO-ESE généralisée à tout l'arc japonais est semblable à la direction de convergence relative Eurasie-Pacifique. D'autre part, la perturbation du champ de contraintes en surface par la subduction de la plaque mer des Philippines et la collision d'Izu reste relativement localisée (Figures 38, 40 et 42). Ces deux remarques suggèrent que le champ de contraintes dans l'arc japonais est indépendant de la subduction de la plaque mer des Philippines.

Le champ de contraintes en surface n'est cependant pas nécessairement représentatif du couplage entre la plaque qui passe en subduction et la plaque supérieure. Les axes P des mécanismes au foyer des séismes plus profonds que 20 km sous Shikoku, considérés comme se produisant à la surface de la plaque plongeante, sont en effet orientés N-S (Yoshioka, 1991 ; Figure 67). Yoshioka (1991) a mené une étude sur le couplage entre la plaque mer des Philippines et l'Eurasie au niveau de la zone de subduction de Nankai au moyen de données géodésiques (taux de déformation en surface). Il conclut de cette étude que le couplage au niveau de la fosse de Nankai est fort par comparaison au couplage Japon NE/Pacifique. La nature du couplage est aussi différente puisqu'il se limite à une région peu profonde dans la fosse de Nankai, région qui correspond à la zone de relaxation des contraintes par les séismes,

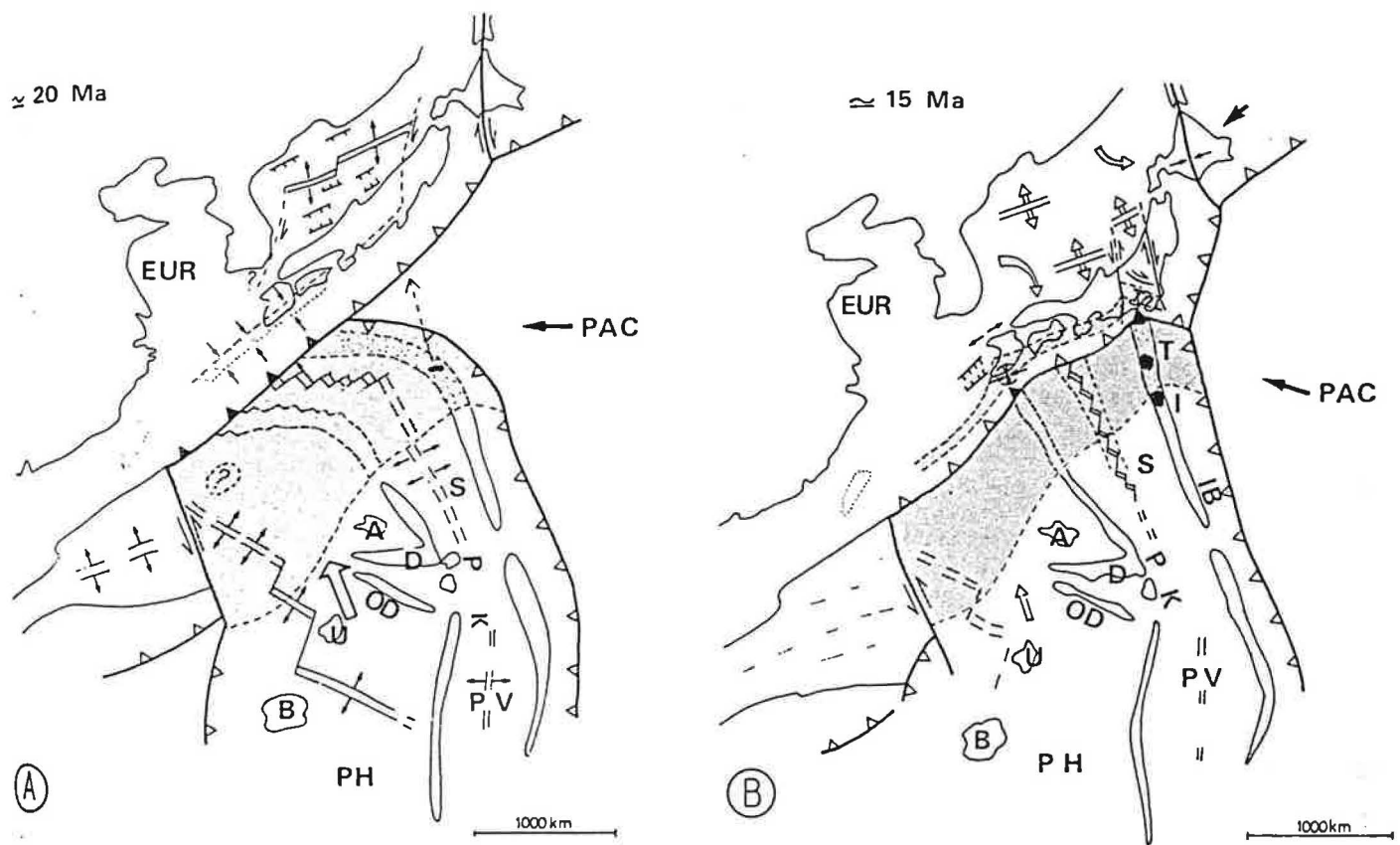


Figure 66. Modèle de l'orogénèse Takachiho dans le Japon sud-ouest pendant la remontée vers le nord de la plaque mer des Philippines. Les triangles vides indiquent la subduction, les triangles pleins la "collision" ou subduction difficile (d'après Charvet et Fabbri, 1987).

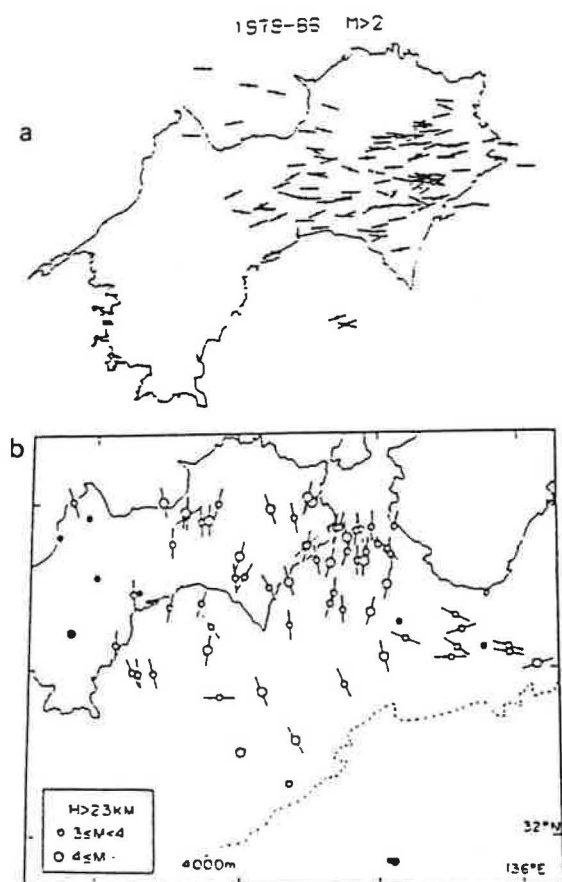


Figure 67. Distribution des axes P des séismes à Shikoku dans la croûte supérieure (en haut) et dans le manteau supérieur (en bas) (d'après Yoshioka, 1991).

tandis que le couplage faible du Japon NE avec la plaque Pacifique semble atteindre la profondeur de 100 km et n'est relaxé par les séismes que dans sa partie supérieure. Yoshioka (1991) conclut aussi que le champ de contraintes crustal à compression E-O ne peut pas être expliqué par le couplage intra-plaque.

Il apparaît donc que :

(1) le couplage plaque mer des Philippines/Japon SO est plus fort que le couplage Pacifique/Japon NE et provoque des déformations de surface à taux forts ($10^{-13}/s$; Yoshioka, 1991). Par analogie avec l'actuel, l'arrivée en subduction de la plaque mer des Philippines au Miocène moyen/supérieur correspond donc à un changement significatif de conditions aux limites. Ce changement est susceptible de provoquer l'arrêt de l'ouverture de la mer du Japon vers 12-10 Ma.

(2) Le couplage ne rend pas compte du champ de contraintes en surface. On ne peut donc pas forcément relier le changement de champ de contraintes au Miocène supérieur avec l'arrivée en subduction de la plaque mer des Philippines.

3. Conclusion

La déformation en Asie du NE est dominée par des décrochements conjugués associés à l'ouverture de bassins et à des rotations de blocs. Il est possible de relier cette déformation à la collision de l'Inde.

En bordure du continent, la déformation est sous l'influence de la subduction. A l'échelle de la zone décrochante est-mer du Japon on distingue une composante décrochante de la déformation, représentative de la déformation continentale et qui ne varie pas depuis le Miocène (Sakhaline), d'une composante qui varie en bordure de la zone de subduction et qui évolue d'extensive (Miocène inférieur et moyen) à compressive (à partir du Miocène supérieur). Cette évolution est synchrone d'un changement de conditions aux limites au niveau de la zone de subduction avec l'arrivée en subduction de la plaque mer des Philippines.

B. INTERACTION COLLISION-EXTENSION : APPROCHE ANALOGIQUE

Davy et Cobbold (1988) ont réalisé des expériences analogiques d'indentation à partir desquelles Jolivet et al. (1990) ont proposé un modèle d'ouverture des bassins du NE asiatique en liaison avec la collision Inde-Asie (Figure 29). Dans ces expériences, la bordure est du modèle est libre et son déplacement gouverné uniquement par l'indentation. Ces expériences ne prennent donc pas en compte l'extension importante qui a affecté toutes les marges E et SE asiatiques de l'Éocène au Miocène moyen, provocant l'ouverture des bassins marginaux au-dessus des zones de subduction. Nous avons décidé de reprendre ces expériences avec un modèle gravitairement instable et susceptible de s'étaler sous son propre poids, de façon à

créer en bordure du modèle une composante d'extension dynamique susceptible de représenter l'effet extensif produit par la subduction.

1. Protocole expérimental

Nous avons utilisé un modèle de lithosphère continentale à trois couches (croûte supérieure, croûte inférieure, manteau lithosphérique) déformé sur sa bordure sud par un poinçon rigide qui progresse vers le nord. L'extension est gouvernée par l'étalement gravitaire du modèle. Le dimensionnement est réalisé de façon à ce que les taux de déformation liés à l'indentation et à l'extension soient du même ordre de grandeur. Les temps caractéristiques des deux phénomènes étant comparables, on peut étudier leur interaction. Ce dispositif est testé pour différentes durées d'extension (étalement avant indentation), différents taux d'extension contrôlés par la présence ou l'absence de confinement latéral, et différentes vitesses d'indentations.

2. Géométrie de la déformation

La géométrie de la déformation est classique par comparaison avec les modélisations numériques et analogiques précédentes (Vilotte et al., 1982, 1984, 1986 ; Tapponnier et al., 1982 ; Houseman et England, 1986, 1993 ; Peltzer et Tapponnier, 1988 ; Davy et Cobbold, 1988). Une zone d'épaississement avec plis et chevauchements apparaît au front du poinçon. Une zone de cisaillement sénestre majeure se développe à partir du coin NO du poinçon vers le NE. Une zone de cisaillement dextre conjuguée se développe depuis le coin NE du poinçon. Cette zone est plus ou moins bien différenciée selon les expériences. Dans la partie NE du modèle la déformation est dominée par des décrochements conjugués et des failles normales. Dans la partie SE, l'extension prévaut.

Le style de la déformation est contrôlé par les conditions aux limites. La distribution de la déformation augmente lorsque la durée ou le taux d'extension augmentent. L'étalement préliminaire accommodé par des failles normales oriente aussi la géométrie de la déformation, les failles normales de direction NE-SO étant préférentiellement réactivées en décrochements sénestres. La vitesse d'indentation n'a par contre pas beaucoup d'influence sur la distribution de la déformation.

3. Cinématique de la déformation et champ de failles dans les expériences

La cinématique des mouvements finis dans les expériences peut être décrite par un pôle de rotation (la déformation est polaire) situé à l'est de la zone de collision (Figure 68). Ce pôle migre sur une ligne est-ouest en fonction des conditions aux limites : il est proche du poinçon quand la bordure latérale est confinée.

La comparaison entre la cinématique finie et le champ de failles dans les expériences montre que certaines failles qui apparaissent comme majeures sur les cartes structurales ont un rôle cinématique négligeable. C'est le cas en particulier de la zone de cisaillement dextre N-S qui part du coin NE du poinçon (équivalent de la zone de cisaillement dextre N-S de l'est du Tibet), et de la faille dextre qui apparaît parfois au front du poinçon (équivalent à la zone de failles Karakorum-Jiali).

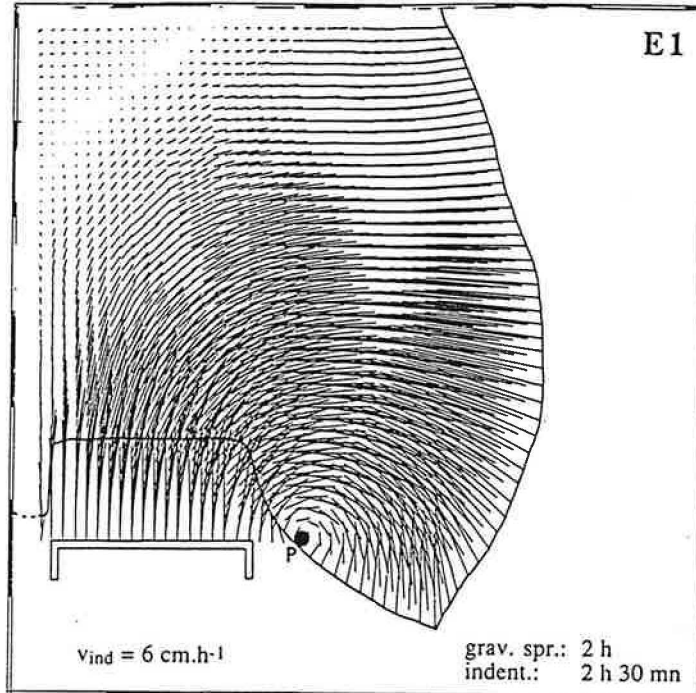
4. Ouverture des bassins marginaux

Ces expériences apportent deux informations en ce qui concerne l'ouverture des grabens en bordure du modèle. Premièrement, les cartes du grand axe de l'ellipse de déformation (dans le plan horizontal) montrent que la déformation est contrôlée par l'indentation dans la plus grande partie du modèle, et qu'elle est contrôlée uniquement par l'extension dans le coin sud-est du modèle. Appliquée à l'Asie, cette observation suggère que l'ouverture des bassins marginaux du NE asiatique est contrôlée par la collision et la subduction (c'est ce qu'on observe pour la mer du Japon), tandis que l'ouverture des bassins du SE asiatique est essentiellement sous le contrôle de la subduction. Ajoutons que l'on n'observe jamais dans nos expériences ni dans celles de Davy et Cobbold (1988) de faille comparable à la faille du Fleuve Rouge accommodant l'extrusion de l'Indochine et l'ouverture de la mer de Chine du sud telles que proposées par Tapponnier et al. (1982) (Figure 54).

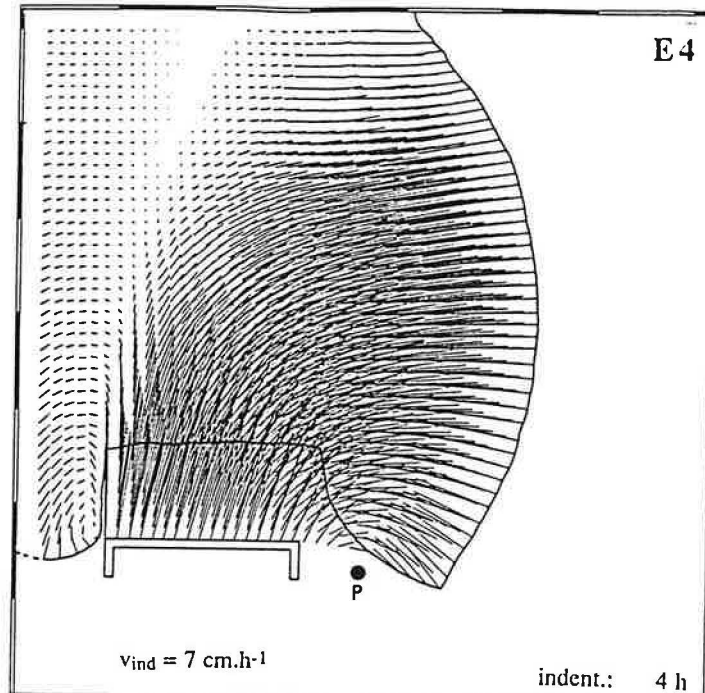
D'autre part, l'expérience E3 (Figure 69) fournit un modèle géométrique d'ouverture des bassins du NE asiatique comparable à celui proposé par Jolivet et al. (1990) (Figure 29). Ce modèle (Figure 70) comprend une large zone de cisaillement sénestre qui se développe à partir du coin NO du poinçon et court vers le NE. Cette zone s'élargit progressivement vers le NE et inclut des zones de cisaillement dextres conjuguées de direction N-S qui accommodent la rotation anti-horaire de blocs rigides. Des grabens s'ouvrent en terminaison de ces zones de cisaillement dextres, comparables aux bassins en pull-apart d'Asie du NE (bassin de Chine du nord, mer du Japon).

La rotation finie anti-horaire des blocs rigides dans les expériences atteint 20° , et à l'intérieur des zones de cisaillement la rotation finie horaire atteint 10° (Figure 29). De telles rotations ne sont pas très éloignées d'une partie de la rotation anti-horaire de 20° du Japon NE telle qu'elle est mesurée par Tosha et Hamano (1988) dans la péninsule d'Oga (bien entendu

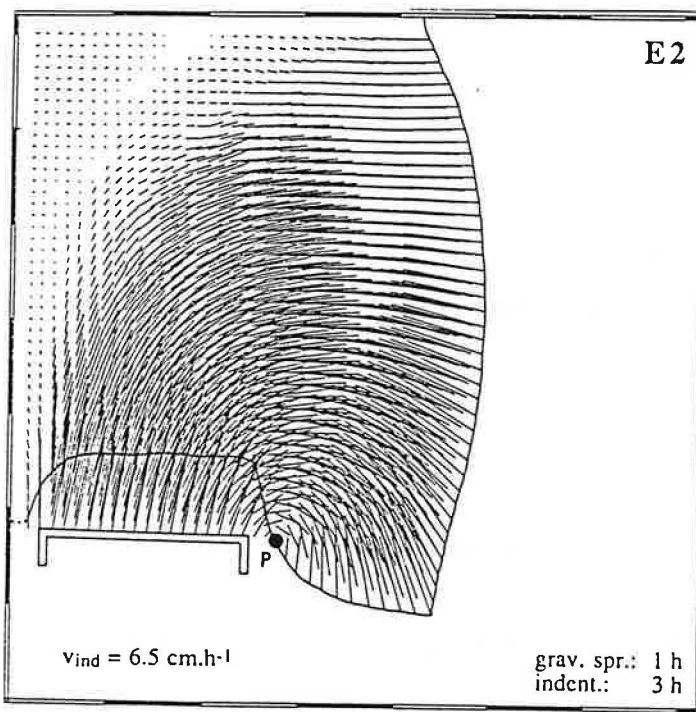
E1



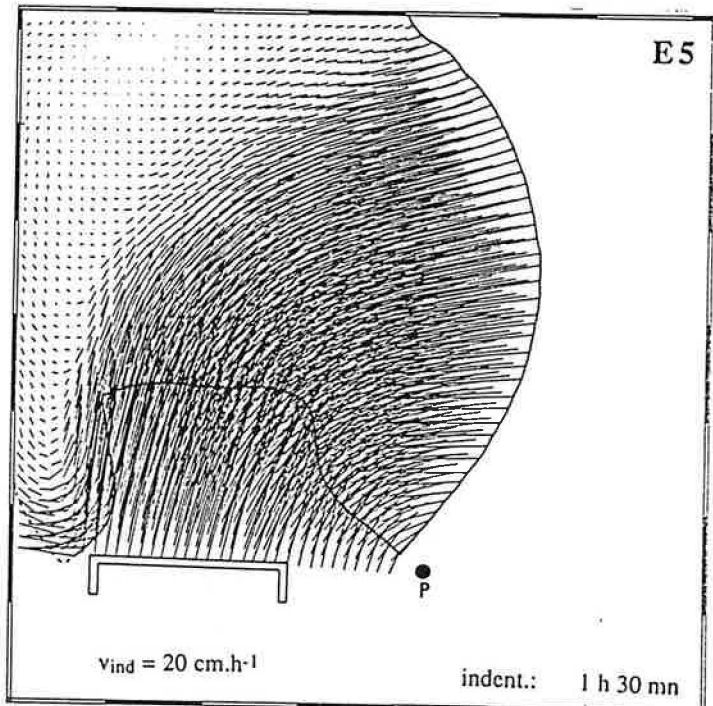
E4



E2



E5



E3

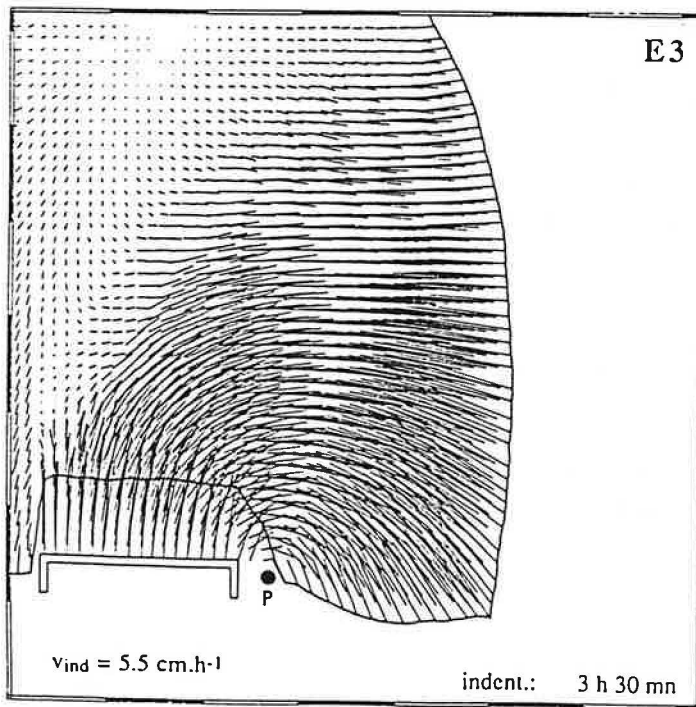


Figure 68. Cinématique des mouvements finis par rapport à la boîte expérimentale pour 5 expériences. La déformation est rotationnelle autour du pôle P.

les rotations mesurées par Otofugi et al. (1994) sont plus élevées, environ 45°), et d'autre part des 15° à 20° de rotation horaire du Japon sud-ouest sous l'effet du cisaillement dextre tel que nous le proposons.

Nous considérons donc que ce modèle est applicable à l'ouverture de la mer du Japon. Bien entendu, il faudrait pour tester ce modèle connaître précisément la géométrie de la déformation en Chine du nord et avoir des données paléomagnétiques. Notons que ce modèle ne prédit pas des rotations importantes: environ 20° de rotation anti-horaire dans les zones non déformées. Quant à la rotation importante du Japon sud-ouest ($45\text{-}50^\circ$), elle nous semble due en grande partie (30°) à l'ouverture asymétrique de la mer du Japon.

IV. CONCLUSION

Trois questions étaient posées au début de ce travail :

(1) Quelle est la relation entre l'ouverture de la mer du Japon et la déformation continentale?

Nous avons montré à Sakhaline que la composante décrochante de la déformation qui régit l'ouverture de la mer du Japon est d'origine continentale, indépendante de la subduction.

(2) Quelles sont les relations entre les mouvements décrochants et les rotations paléomagnétiques?

Nous avons montré que la distribution des rotations est fonction de la déformation. Les rotations sont horaires dans les zones de déformations dextres néogènes. La rotation horaire du Japon sud-ouest nous semble due en partie (30°) à l'ouverture asymétrique de la mer du Japon (propagation de l'océanisation vers l'ouest). Nous proposons que le complément de rotation (15° à 20°) est dû au cisaillement du Japon sud-ouest entre les zones décrochantes dextres bordières de la mer du Japon, et qu'il est absorbé par des rotations distribuées comme le suggère l'observation de la déformation sur le terrain. Pendant l'ouverture de la mer du Japon, la MTL est une faille de second ordre dont le jeu normal avec une composante sénestre dans sa partie orientale accommode les rotations horaires dans le Japon sud-ouest.

Dans le Japon nord-est les rotations sont anti-horaires hors des zones de déformation dextres. Les mouvements dextres accommodent donc la rotation anti-horaire des zones non déformées. Nous suggérons donc que l'ensemble du système mer du Japon est inclus dans une zone de cisaillement sénestre plus large. Les expériences analogiques d'indentation fournissent un modèle pour cette zone de cisaillement sénestre, en relation avec la collision Inde-Asie.

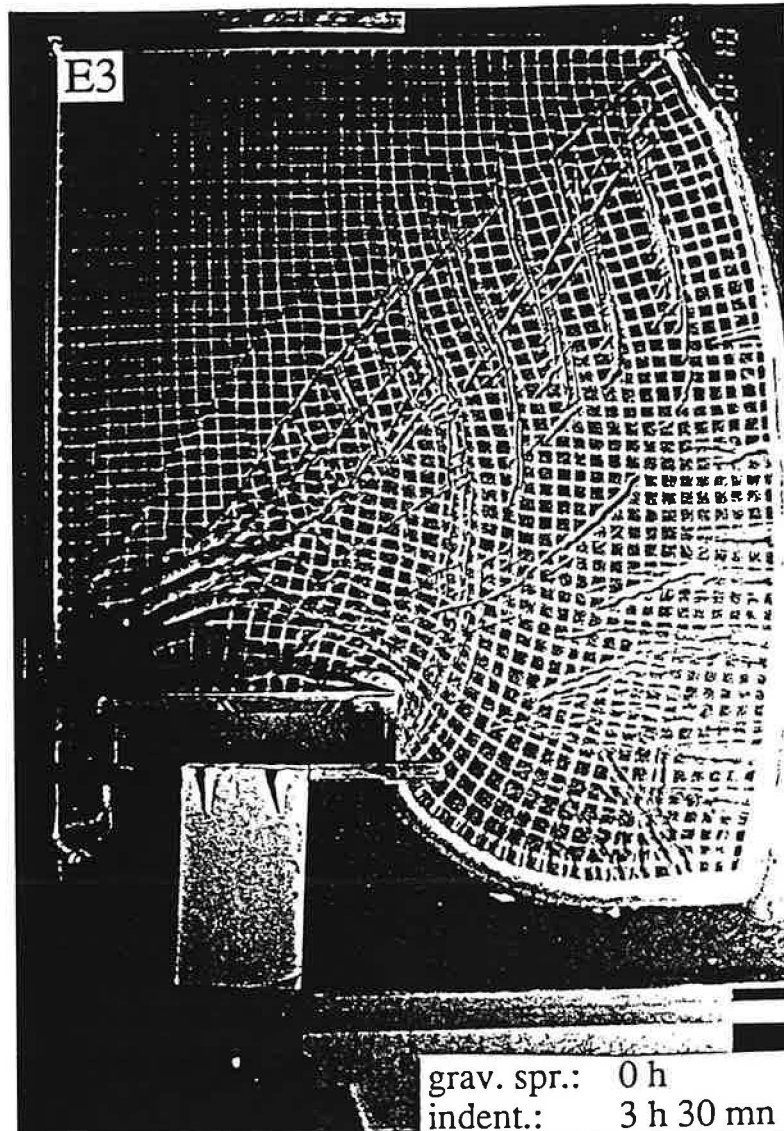
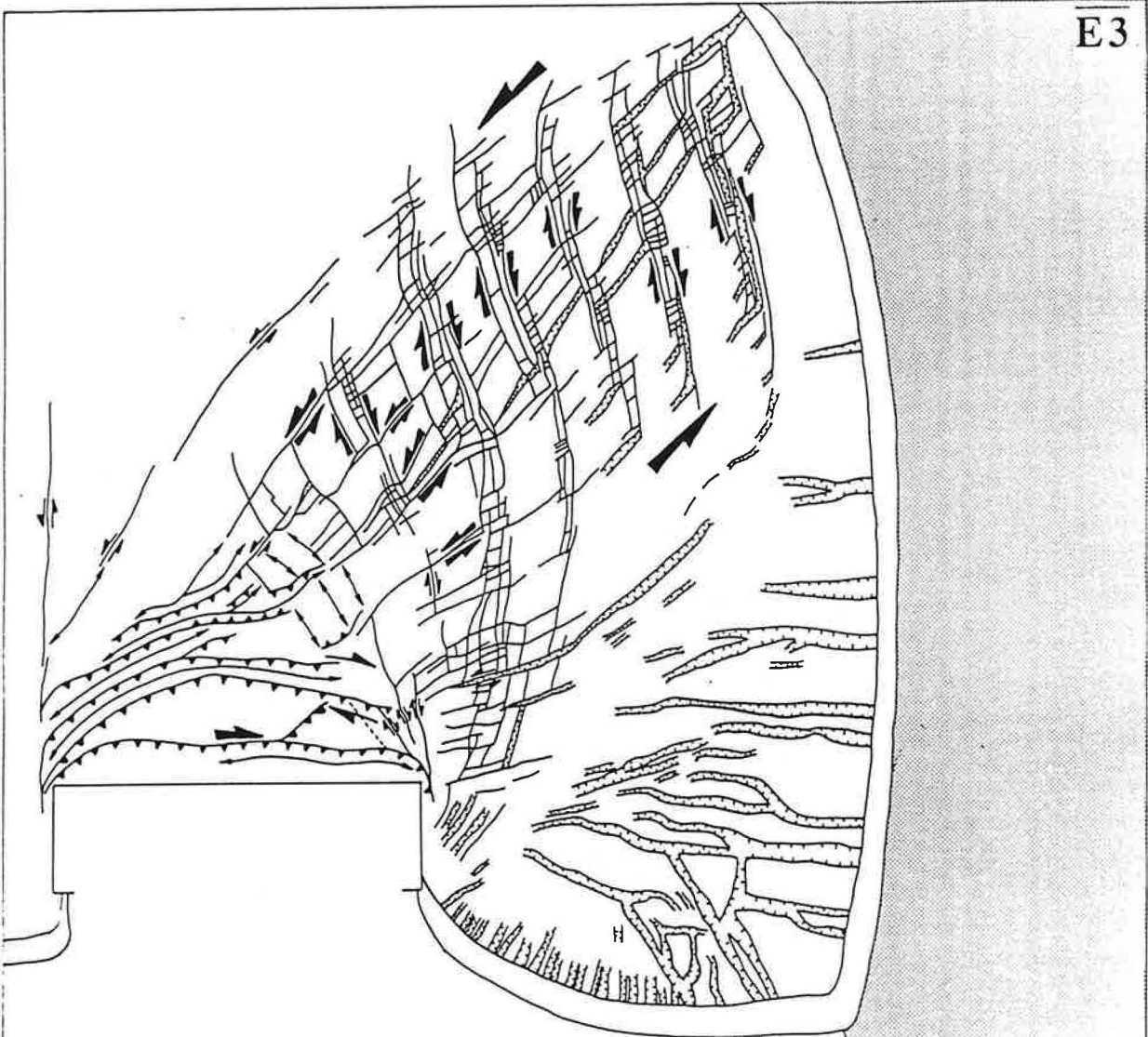


Figure 69. Géométrie de la déformation et cartes des taux de cisaillement et de rotation dans l'expérience E3 (pas d'étalement préliminaire, confinement latéral).

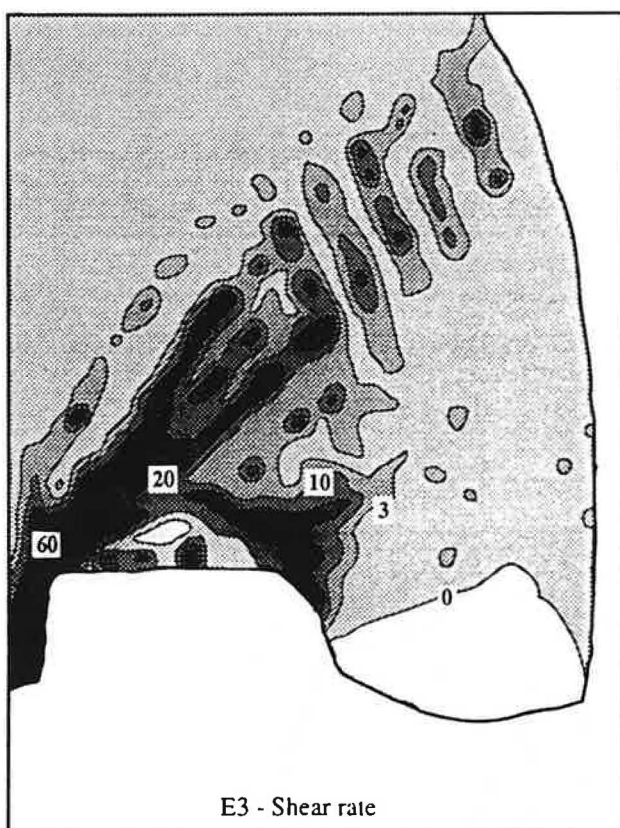
E3



a

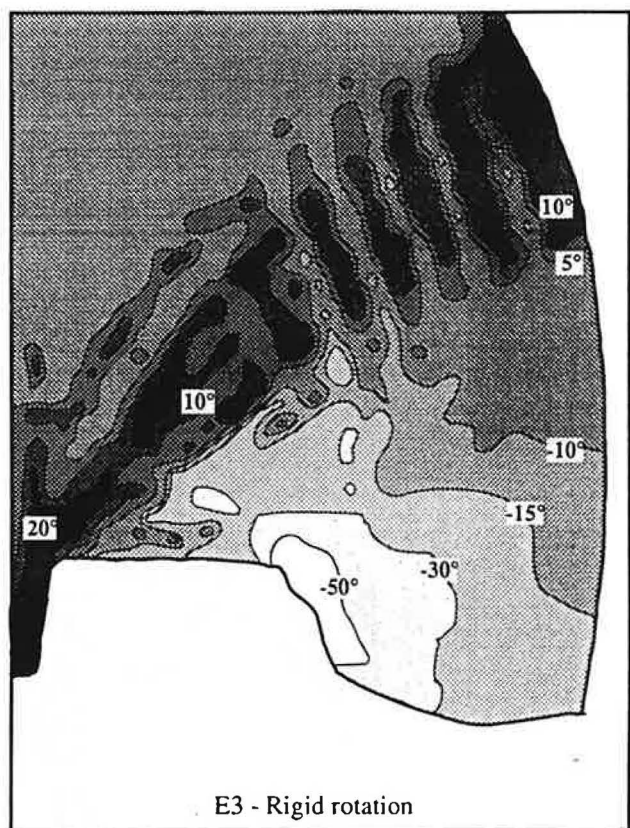
$v_{ind} = 5.5 \text{ cm.h}^{-1}$

indent.: 3 h 30 mn



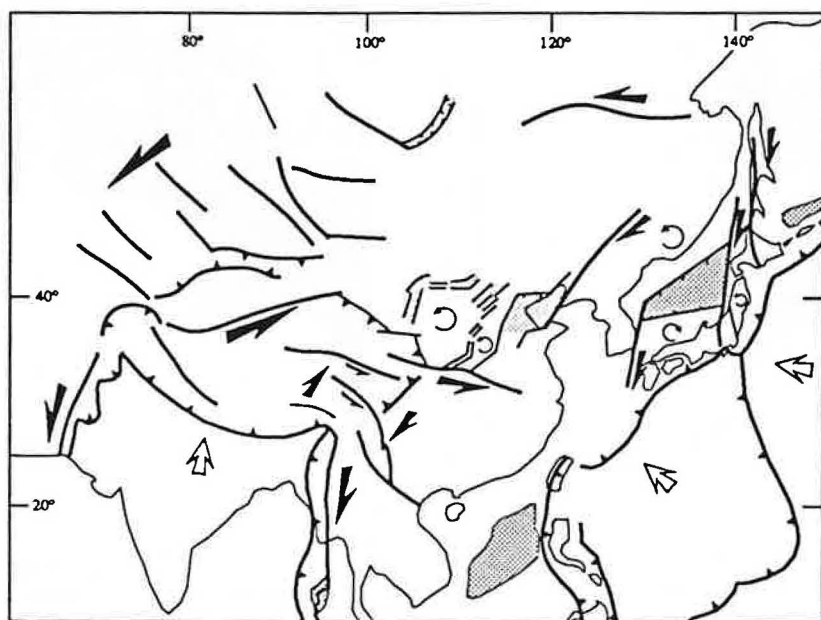
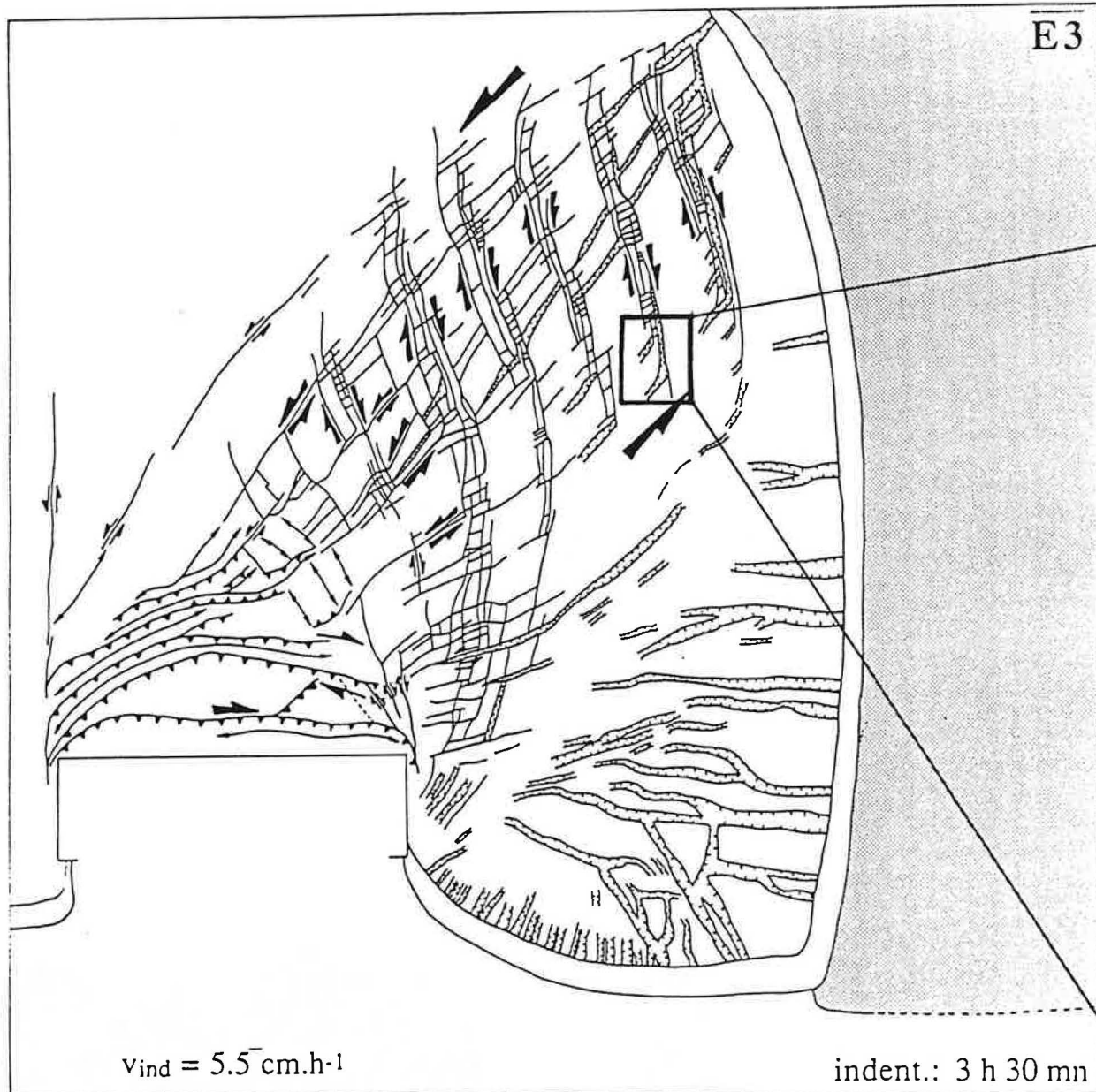
b

E3 - Shear rate



c

E3 - Rigid rotation



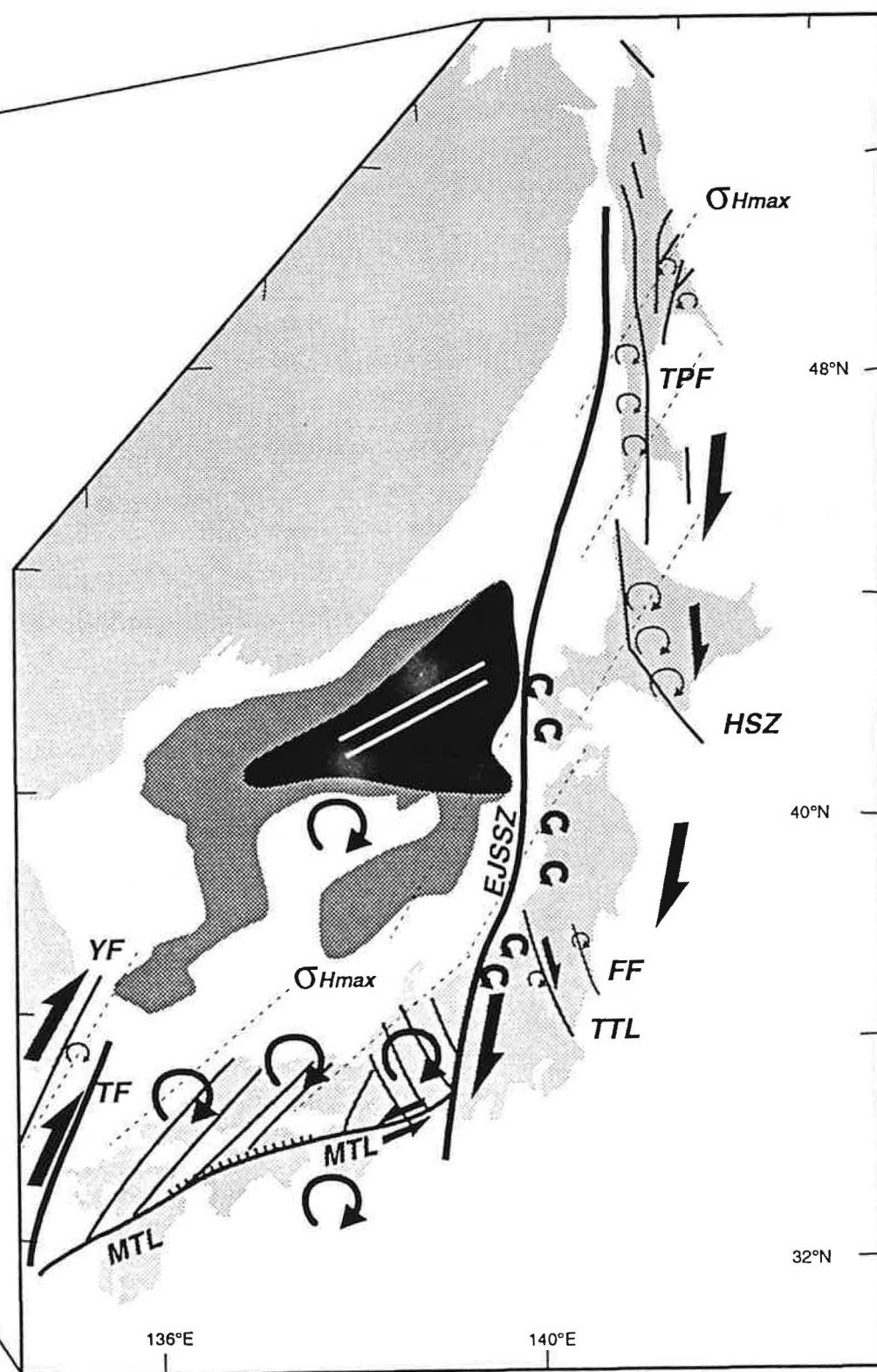


Figure 70. Modèle d'ouverture de la mer du Japon dans le cadre de la déformation de l'Asie.

(3) Quels sont les causes de l'ouverture de la mer du Japon?

Les expériences analogiques que nous avons réalisées suggèrent que l'ouverture de la mer du Japon est contrôlée à la fois par la collision Inde-Asie et par la subduction. Ces expériences fournissent un modèle géométrique simple reliant l'ouverture de la mer du Japon à la collision. Une grande zone de cisaillement sénestre accommode la remontée vers le NE de l'Asie relativement à la plate-forme russe. A l'intérieur de cette zone, des zones décrochantes dextres accommodent l'ouverture de bassins en pull-apart et la rotation anti-horaire de blocs continentaux. La géométrie de la déformation en Asie du NE est compatible avec ce modèle.

On pourrait reprocher à ce modèle d'être un modèle gigogne avec des rotations de blocs emboîtées. Remarquons d'abord qu'il n'y a qu'un seul changement d'échelle dans ce modèle. Il comprend en effet une zone de cisaillement sénestre dans le NE asiatique dans laquelle des blocs continentaux tournent dans le sens anti-horaire, et (changement d'échelle) une zone de déformation dextre (qui accommode la rotation de ces blocs continentaux) à l'intérieur de laquelle la mer du Japon s'ouvre et le Japon SO tourne dans le sens horaire.

La notion de changement d'échelle est à mon sens essentielle pour comprendre les rotations de blocs. Cette notion est très bien illustrée par l'expérience analogique E3 (Figure 69) et son système de blocs qui tournent au NE. Le changement d'échelle est associé à un changement de sens de cisaillement et à un changement de sens de rotation. Il n'y a pas dans ce modèle de grands blocs qui tournent dans un sens, divisés en petits blocs qui tournent dans le sens inverse, divisés eux-mêmes en plus petits blocs qui tournent dans le sens initial, etc... et dont on ne sait jamais dans quel sens les blocs tournent. Ce type de modèles, couramment proposé dans la littérature (voir par exemple le modèle de Kanaori et al. (1990) pour le Japon central), ne me semble pas adapté pour rendre compte de rotations de blocs. Il décrit plutôt des systèmes de décrochements conjugués qui accommodent du cisaillement pur sans rotation.

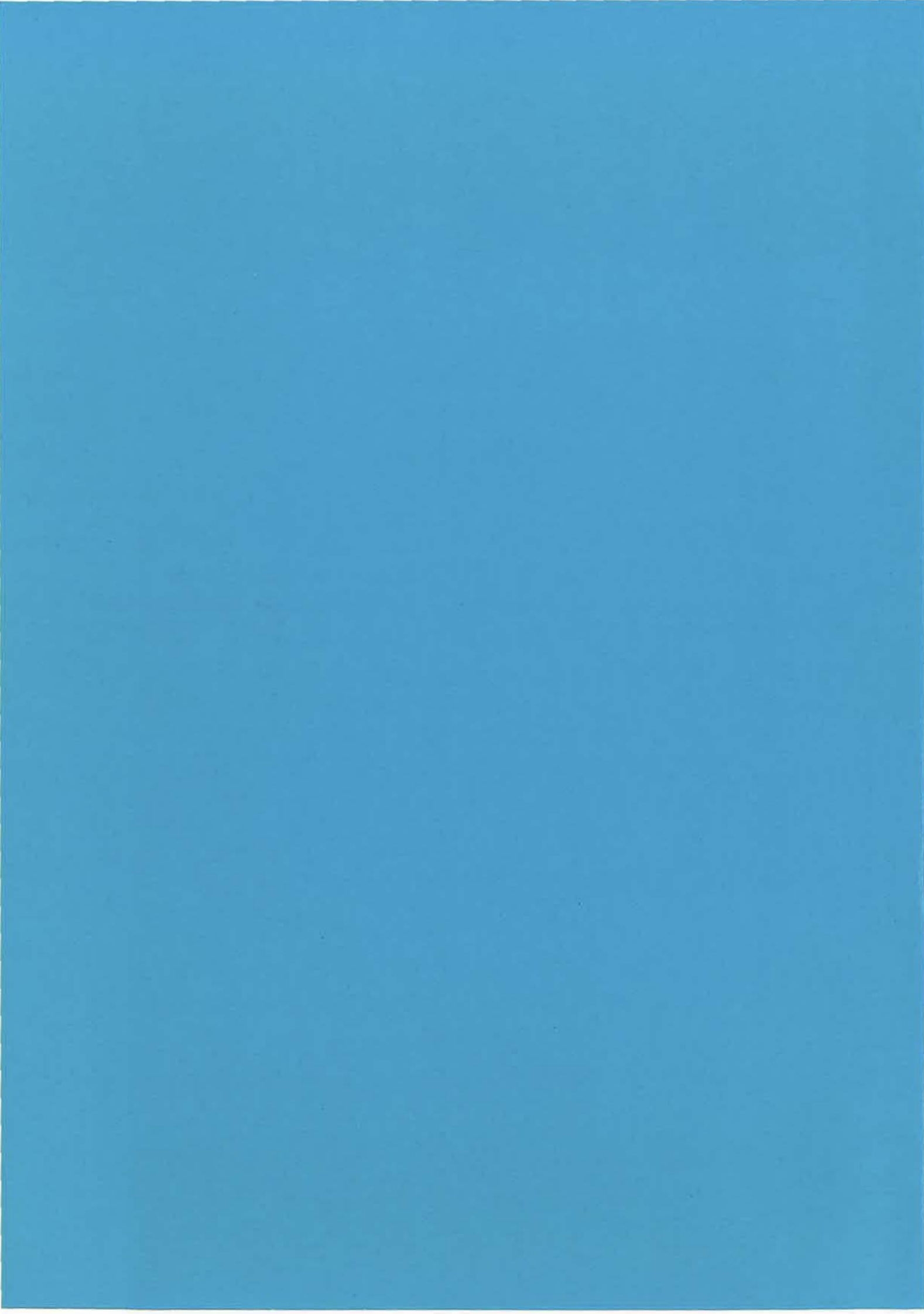
CONCLUSIONS

Nous avons poursuivi l'étude du mécanisme d'ouverture de la mer du Japon dans le Japon sud-ouest et à Sakhaline. Dans ces deux régions la déformation synchrone de l'ouverture est compatible avec un mécanisme d'ouverture en bassin pull-apart. La mer du Japon s'ouvre à l'intérieur d'une zone de cisaillement dextre limitée à l'est et à l'ouest par deux zones décrochantes en relais. Ce mécanisme est en accord avec les rotations paléomagnétiques contemporaines de l'ouverture. Les rotations horaires le long des zones décrochantes Néogène ainsi que dans le Japon sud-ouest inclus dans la zone de cisaillement, sont compatibles avec le sens de cisaillement dextre. La déformation interne du Japon sud-ouest, avec des rotations de blocs à différentes échelles, doit absorber une partie de ces rotations. Le stricte calage en temps des rotations paléomagnétiques est critiqué : celles-ci s'intègrent au processus d'ouverture sur une période de plusieurs millions d'années.

Nous avons suivi vers le nord, à l'intérieur du continent asiatique, la déformation liée à l'ouverture de la mer du Japon, et nous avons montré qu'elle pouvait être géométriquement reliée à la collision Inde-Asie. A partir d'expériences de modélisation analogique, nous proposons un mécanisme qui intègre l'ouverture de la mer du Japon à la déformation de l'Asie. La zone de cisaillement dextre de la mer du Japon accorde la rotation anti-horaire de larges blocs continentaux au sein d'une zone déformation sénestre. Ce cisaillement sénestre décuple l'Asie déformée sous la poussée de l'Inde de la plate-forme eurasienne stable. Dans cette zone de déformation sénestre limitée par le Qinling Shan et les Monts Stanovoï, le Japon NE a subi une rotation anti-horaire de la même façon que le bloc Ordos plus à l'ouest.

"Que dirai-je ? Nous avons interrogé toute l'Asie : elle n'a pas été trop avare de ses dons ; elle nous a parlé d'autres terres, et il y en eu peu qu'elle ne nous ait aidés à mieux voir. Nous sommes venus, au terme, sur ces îles japonaises noblement incurvées et comme penchées sur le secret des flots. Reposons-nous en ces terres bien faites, où chaque matin le soleil levant vient éclairer l'Eurasie. Le Fuji dans l'aurore annonce la gloire du jour. Du fond de l'immensité bleue, les vagues accourent, déferlent et grondent : elles disent la belle fugacité des apparences, le balancement mesuré des choses. Sous nos pieds, des vagues moins agitées se pressent dans la profondeur noire. Loin à l'arrière, jusqu'au cœur du continent, d'autres et d'autres vagues encore, épuisées par le temps, figées dans la splendide torpeur des vieilles chaînes, sont ranimées au prix d'efforts immenses par les lourdes vagues de fond. C'est ainsi qu'ondulent, au cours des âges, les voiles qui cachent le vieux cœur du monde. Elles passent, les vagues, et toutes ensemble content, comme dans les vieux rêves de l'Asie, l'évanescence de l'univers. Que de fois le soleil a lui, que de fois le vent a gémi sur les toundras désolées, sur la morne étendue des taïgas sibériennes, sur les déserts fauves où resplendit le sel de la terre, sur les hautes cimes casquées d'argent, sur les jungles frémissantes, sur les forêts houleuses des tropiques ! Jour après jour, en des temps sans nombre, le spectacle a changé en traits imperceptibles. Sourions à l'illusion d'éternité qui paraît dans ces choses, et pendant que passent tant d'aspects transitoires, écoutons l'hymne antique, ce chant prodigieux des mers qui a salué tant de chaînes montant à la lumière." (dernière page de *La Tectonique de l'Asie*, Argand, 1923).

BIBLIOGRAPHIES



BIBLIOGRAPHIES

- Abe, K., Seismic displacement and ground motion near a fault: the Saitama earthquake of September 21, 1931, *J. Geophys. Res.*, 79, 4393-4399, 1974.
- Achache, J., V. Courtillot, and J. Besse, Paleomagnetic constraints on the late Cretaceous and Cenozoic tectonics of southeastern Asia, *Earth Planet. Sci. Lett.*, 63, 123-136, 1983.
- Achache, J., V. Courtillot, and Zhou Yao Xiu, Paleogeographic and tectonic evolution of southern Tibet since Middle Cretaceous time: new paleomagnetic data and synthesis, *J. Geophys. Res.*, 89, 10,311-10,339, 1984.
- Allen, C. R., L. Zhuoli, Q. Hong, W. Xueze, Z. Huawei, and H. Weishi, Field study of a highly active fault zone: the Xanshuhe fault of southwestern China, *Geol. Soc. Amer. Bull.*, 103, 1178-1199, 1991.
- Allen, C. R., A. R. Gillespie, Han Yuan, K. E. Sieh, Zhang Buchun, and Zhu Chengnan, Red river and associated faults, Yunnan province, China: Quaternary geology, slip rates and seismic hazard, *Geol. Soc. Amer. Bull.*, 95, 686-700, 1984.
- Angelier, J., Tectonic analysis of fault slip data sets, *J. Geophys. Res.*, 89, 5835-5848, 1984.
- Angelier, J., and P. Mechler, Sur une méthode graphique de recherche des contraintes principales également utilisable en tectonique et en sismologie, la méthode des dièdres droits, *Bull. Soc. Géol. France*, 19, 1309-1318, 1977.
- Antipov, M. P., V. M. Kovylin, and V. P. Filat'yev, Sedimentary cover of the deepwater basins of Tatar strait and the northern part of the sea of Japan, *Int. Geol. Rev.*, 22(11), 1327-1334, 1979.
- Arai and Kanno, Tertiary system of the Chichibu basin, Japan, *The Japan Society for the Promotion of Science*, Tokyo, pp. 396, 1960.
- Argand, E., La tectonique de l'Asie, *Proc. 13th Int. Geol. Congr.* Brussels 1924, 171-372, 1924.
- Armijo, R., P. Tapponnier, and H. Tonglin, Late Cenozoic right-lateral strike-slip faulting in southern Tibet, *J. Geophys. Res.*, 94, 2787-2838, 1989.
- Armijo, R., P. Tapponnier, J. L. Mercier, and H. Tonglin, Quaternary extension in southern Tibet: field observations and tectonic implications, *J. Geophys. Res.*, 91, 13,803-13,872, 1986.
- Audley-Charles, M. G., Geometrical problems and implications of large scale overthrusting in the Banda Arc-Australian margin collision zone, *Spec. Publ. Geol. Soc. Lond.*, 9, 407-416, 1981.
- Avouac, J. P., P. Tapponnier, M. Bai, H. You, and G. Wang, Active thrusting and folding along the northern Tien Shan and Late Cenozoic rotation of the Tarim relative to Dzungaria and Kazakhstan, *J. Geophys. Res.*, 98, 6755-6804, 1993.
- Avouac, J. P., and P. Tapponnier, Kinematic model of active deformation in central Asia, *Geophys. Res. Lett.*, 20, 895-898, 1993.
- Baranowski, J., Armbruster, J., Seeber, L., and P. Molnar, Focal depths and fault plane solutions of earthquakes and active tectonics of the Himalaya, *J. Geophys. Res.*, 89, 6918-6928, 1984.
- Barrier, E., P. Huchon and M. Aurelio, Philippine fault: a key for Philippine kinematics, *Geology*, 19, 32-35, 1991.
- Bellier, O., J.L. Mercier, P. Vergely, C. Long and C. Ning, Evolution sédimentaire et tectonique du graben cénozoïque de la Wei He (province du Shanxi, Chine du Nord), *Bull. Soc. Géol. France*, 6, 979-994, 1988.
- Berry, R. F., and A. E. Grady, Mesoscopic structures produced by Plio-Pleistocene wrench faulting in S. Sulawesi, Indonesia, *Journal of Structural Geology*, 1986.
- Besse, J., V. Courtillot, J. P. Pozzi, and Y. X. Zhou, Paleomagnetic estimates of crustal shortening in the Himalayan thrusts and Zangbo suture, *Nature*, 311, 621-626, 1984.
- Bird, P., Lateral extrusion of lower crust from under high topography in the isostatic limit, *J. Geophys. Res.*, 96, 10,275-10,286, 1991.
- Blow, W. H., Late Middle Miocene to Recent planktonic foraminiferal biostratigraphy, in *Proc. 1st Int. Conf. Planktonic Microfossils*, E.J. Brill, Leiden, edited by P. Bronnimann and H. H. Renz, 1, pp. 199-422, 1969.
- Briais A., P. Patriat and P. Tapponnier, Updated interpretation of magnetic anomalies and seafloor spreading stages in the South China Sea: implications for the tertiary tectonics of southeast Asia, *J. Geophys. Res.*, 98, 6299-6328, 1993.
- Brun, J.P., J. P. Burg, and Chen Guo Ming, Strain trajectories above the main central thrust (Himalaya) in southern Tibet, *Nature*, 313, 388-390, 1985.
- Burchfiel, B. C., and L. H. Royden, North-south extension within the convergent Himalayan region, *Geology*, 679-682, 1985.
- Burchfiel, B. C., Zhang Peizhen, Wang Yipeng, Zhang Weiqi, Song Fangmin, Deng Qidong, P. Molnar, and L. Royden, Geology of the Haiyuan fault zone, Ningxia-Hui autonomous region, China, and its relation to the evolution of the northeastern margin of the Tibetan plateau, *Tectonics*, 10, 1091-1110, 1991.
- Burchfiel, B. C., and L. H. Royden, Tectonics of Asia 50 years after the death of Emile Argand, *Eclogae Geol. Helv.*, 84, 599-629, 1991.
- Burchfiel, B. C., Chen Zhiliang, K. V. Hodges, Liu Yuping, L. H. Royden, Deng Changrong, Xu Jiene, The south Tibetan detachment system, Himalayan orogen: extension contemporaneous with and parallel to shortening in a collisional mountain belt, *Geol. Soc. Amer. Spec. Pap.*, 269, 1-41, 1992.
- Burg, J. P., and G. M. Chen, Tectonics and structural zonation of southern Tibet, China, *Nature*, 311, 219-223, 1984.
- Cadet, J. P., et al., Deep scientific dives in the Japan and Kuril trenches, *Earth Planet. Sci. Lett.*, 83, 313-328, 1987a.
- Cadet, J. P., et al., The Japan trench and its juncture with the Kuril trench, cruise results of the Kaiko project, Leg 3, *Earth Planet. Sci. Lett.*, 83, 267-284, 1987b.

- Cardwell, R. K., B. L. Isacks and D. E. Karig, The spatial distribution of earthquakes, focal mechanism solutions, and subducted lithosphere in the Philippine and northeastern Indonesian islands, in *The Tectonic and Geologic Evolution of Southeast Asian Seas and Islands* edited by D. E. Hayes, *Geophys. Monogr.*, Am. Geophys. Union, 23, 1-35, 1980.
- Celaya, M., and R. McCabe, Kinematic model for the opening of the sea of Japan and the bending of the Japanese islands, *Geology*, 15, 53-57, 1987.
- Chamot-Rooke, N., V. Renard, and X. Le Pichon, Magnetic anomalies in the Shikoku basin: a new interpretation, *Earth Planet. Sci. Lett.*, 83, 214-228, 1987.
- Chamot-Rooke, N., and X. Le Pichon, Zenisu ridge: Mechanical model of formation, *Tectonophysics*, 160, 175-194, 1989.
- Chang, K. H., B. G. Woo, J. H. Lee, S. O. Park, Yao, Akira, Cretaceous and Early Cenozoic stratigraphy and history of eastern Kyongsang basin, S. Korea, *J. Geol. Soc. Korea*, 26, 471-487, 1990.
- Chapman, M.C., and S. C. Solomon, North American-Eurasian plate boundary in northeast Asia, *J. Geophys. Res.*, 81, 921-930, 1976.
- Charlton, T. R., A. J. Barber, and S. T. Barkham, The structural evolution of the Timor collision complex, eastern Indonesia, *Journal of Structural Geology*, 13, 489-500, 1991.
- Charvet, J., K. Grimm, J. Griffin, L. Jolivet, A. Pouclet, and D. Panis, Structural features in Leg 128 cores: relationship with the tectonic evolution of the Japan Sea, *Proc. Ocean Drill. Program, Sci. Results*, 127/128, 1175-1193, 1992.
- Chase, C. G., Extension behind island arcs and motion relative to hot-spots, *J. Geophys. Res.*, 83, 5385-5387, 1978.
- Chen, W. P., and J. Nabelek, Seismogenic strike-slip faulting and the development of the North China basin, *Tectonics*, 7, 975-989, 1988.
- Chen, W.-P., J. L. Nabelek, T. J. Fitch, and P. Molnar, An intermediate depth earthquake beneath Tibet: source characteristics of the event of September 14, 1976, *J. Geophys. Res.*, 86, 2863-2876, 1981.
- Chen, W.-P., and P. Molnar, Constraints on the seismic wave velocity structure beneath the Tibetan plateau and their tectonic implications, *J. Geophys. Res.*, 86, 5937-5962, 1981.
- Chen, W.-P., and P. Molnar, Source parameters of earthquakes and intraplate deformation beneath the Shillong Plateau and the Northern Indoburman Ranges, *J. Geophys. Res.*, 95, 12527-12552, 1990.
- Chen, Y., and V. Courtillot, Widespread Cenozoic (?) remagnetization in Thailand and its implications for the India-Asia collision, *Earth Planet. Sci. Lett.*, 93, 113-122, 1989.
- Chingchang, B., C. T. Shyu, J. C. Chen, and S. Boggs, Taiwan: geology, geophysics and marine sediments, in *The Ocean Basins and Margins*, edited by A.E.N. Nairn, F.G. Stehli and S. Uyeda, vol. 7A, 377-418, Plenum Press, New York, 1985.
- Cobbond, P.R. and P. Davy, Indentation tectonics in nature and experiments, 2, Central Asia, *Bull. Geol. Instit. Univ. Uppsala*, 14, 143-162, 1988.
- Cohen, S. C., and R. C. Morgan, Intraplate deformation due to continental collisions: a numerical study of deformation in a thin viscous sheet, *Tectonophysics*, 132, 247-259, 1986.
- Cooper, A. K., M. S. Marlow, D. W. Scholl, and A. J. Stevenson, Evidence for Cenozoic crustal extension in the Bering Sea region, *Tectonics*, 11, 719-731, 1992.
- Cook, D.B., K. Fujita, and C. A. Mac Mullen, Present day plate interactions in northeast Asia: North America, Eurasian and Okhotsk plates, *J. Geodyn.*, 6, 33-51, 1986.
- Coward, M. P., and R. W. H. Butler, Thrust tectonics and the deep structure of the Pakistan Himalaya, *Geology*, 13, 417-420, 1985.
- Curry, M. P., D. G. Moore, L. Lawver, F. J. Emmel, R. W. Raitt, M. Henry, and R. Kieckhefer, Tectonics of the Andaman Sea and Burma, *Geological and Geophysical Investigations of Continental Margins*, edited by J. S. Watkins, L. Montadert, and P. Dickerson, AAPG Mem., 29, 189-198, 1979.
- Daly, M. C., M. A. Cooper, I. Wilson, D. G. Smith and B. G. D. Hooper, Cenozoic plate tectonics and basin evolution in Indonesia, *Marine and Petroleum Geol.*, 8, 2-21, 1991.
- Davis, D., J. Suppe, and F. A. Dahlen, Mechanics of fold-and-thrust belts and accretionary wedges, *J. Geophys. Res.*, 88, 1153-1172, 1983.
- Davy, P., and P. R. Cobbond, Indentation tectonics in nature and experiment. 1. Experiments scaled for gravity, *Bull. Geol. Inst. Univ. Uppsala*, 14, 129-141, 1988.
- Davy, P., and P. R. Cobbond, Experiments on shortening of a 4-layer model of the continental lithosphere, *Tectonophysics*, 188, 1-25, 1991.
- Delaney, P. T., D. D. Pollard, J. I. Ziony, and E. H. McKee, Field relations between dikes and joints: emplacement process and paleostress analysis, *J. Geophys. Res.*, 91, 4920-4938, 1986.
- DeMets, C., R. G. Gordon, D. F. Argus, and S. Stein, Current plate motions, *Geophys. J. Int.*, 101, 425-478, 1990.
- DeMets, C., A test of the present-day plate geometries for northeast Asia and Japan, *J. Geophys. Res.*, 97, 17,627-17,635, 1992.
- Deng Qidong, Sung Fengmin, Zhu Shilong, Li Mengluan, Wang Tielin, Zhang Weiqi, B. C. Burchfield, P. Molnar, and Zhang Peizhen, Active faulting and tectonics of the Ningxia-Hui autonomous region, China, *J. Geophys. Res.*, 89, 4427-4445, 1984.
- Deverchère, J., F. Houdry, M. Diament, N. V. Solonenko, and A. V. Solonenko, Evidence for a seismogenic upper mantle and lower crust in the Baikal rift, *Geophys. Res. Lett.*, 18, 1099-1102, 1991.
- Deverchère, J., F. Houdry, N. V. Solonenko, A. V. Solonenko, and V. A. Sankov, Seismicity, active faults and stress field of the north Muya region, Baikal rift: new insights on the rheology of extended continental lithosphere, *J. Geophys. Res.*, 98, 19,895-19,912, 1993.

- Dewey, J. F., Episodicity, Sequence, and style at convergent plate boundaries, in Stangway, D. W., ed., The continental crust and its mineral deposits: Geol. Assoc. Canada Spec. Pap., 20, 553-573, 1980.
- Dewey, J. F., R. M. Shackleton, Chang Chengfa, and Sun Yiyin, The tectonic evolution of the Tibetan plateau, Phil. Trans. R. Soc. Lond., A 327, 379-413, 1988.
- Dewey, J. F., S. Cande, and W. C. Pitman, Tectonic evolution of the India/Eurasia collision zone, Eclogae Geol. Helv., 82, 717-734, 1989.
- Diament, M., H. Harjono, K. Karta, C. Deplus, D. Dahrin, M. T. Zen, M. Gerard, O. Lassal, A. Martin, and J. Malod, Mentawai fault zone off Sumatra: a new key to the geodynamics of western Indonesia, Geology, 20, 259-262, 1992.
- Dziewonski, A. M., T. A. Chou, and J. H. Woodhouse, Determination of earthquake source parameters from waveform data for studies of global and regional seismicity, J. Geophys. Res., 86, 2825-2852, 1981.
- Dziewonski, A. M., and J. H. Woodhouse, An experiment in systematic study of global seismicity: centroid-moment tensor solutions for 201 moderate and large earthquakes of 1982, J. Geophys. Res., 88, 3247-3271, 1983.
- Dziewonski, A. M., J. E. Franzen, and J. H. Woodhouse, Centroid-moment tensor solutions for October-December 1984, Phys. Earth Planet. Inter., 39, 147-156, 1985.
- Dziewonski, A. M., G. Ekstrom, J. E. Franzen, and J. H. Woodhouse, Global seismicity of 1979: centroid-moment tensor solutions for 524 earthquakes, Phys. Earth Planet. Inter., 48, 18-46, 1987.
- Eguchi, T., and S. Uyeda, Seismotectonics of the Okinawa trough and Ryukyu arc, Mem. Geol. Soc. China, 5, 189-210, 1983.
- England, P. C., and D. P. McKenzie, A thin viscous sheet model for continental deformation, Geophys. J. R. Astr. Soc., 70, 295-321.
- England, P. C., and D. P. McKenzie, Correction to: a thin viscous sheet model for continental deformation, Geophys. J. R. Astr. Soc., 73, 523-532.
- England, P., and G. Houseman, Finite strain calculations of continental deformation 2. Comparison with the India-Asia collision zone, J. Geophys. Res., 91, 3664-3676, 1986.
- England, P. and P. Molnar, Right-lateral shear and rotation as the explanation for strike-slip faulting in eastern Tibet, Nature, 344, 140-142, 1990.
- Fabbri, O., and J. Charvet, Paléocontraintes et mouvements décrochants dans le détroit de Corée d'après l'exemple des îles Tsushima (Japon sud-ouest), C. R. Acad. Sci., Paris, in press, 1994.
- Faure, M., and F. Lalevée, Bent structural trends of Japan: flexural-slip folding related to the Neogene opening of the Sea of Japan, Geology, 15, 49-52, 1987.
- Fitch, T. J., Plate convergence, transcurrent faults and internal deformation adjacent to Southeast Asia and the Western Pacific, J. Geophys. Res., 77, 4432-4460, 1972.
- Fleitout, L., and C. Froidevaux, Tectonics and topography for a lithosphere containing density heterogeneities, Tectonics, 1, 21-56, 1982.
- Florensov, N. A., Rifts of the Baikal mountain region, Tectonophysics, 8, 443-456, 1969.
- Fournier, M., L. Jolivet, B. Goffé, and R. Dubois, Alpine Corsica metamorphic core complex, Tectonics, 10, 1173-1186, 1991.
- Fournier, M., L. Jolivet, P. Huchon, K. F. Sergeev and L. S. Osorbin, Neogene strike-slip faulting in Sakhalin and the Japan Sea opening, J. Geophys. Res., 99, 2701-2725, 1994.
- Fournier, M., L., Jolivet, and O. Fabbri, Neogene stress field in SW Japan and mechanism of deformation during the Japan Sea opening, submitted to J. Geophys. Res.
- Fournier, M., J. C. Thomas, L. Jolivet, and P. Davy, Role of extension during collision tectonics: an analogue experimental approach, submitted to Tectonophysics.
- Fukao, Y. and M. Furumoto, Mechanisms of large earthquakes along the eastern margin of the Japan Sea, Tectonophysics, 25, 247-266, 1975.
- Fukuchi, T., N. Imai, and K. Shimokawa, ESR dating of fault movement using various defect centres in quartz; the case in the western south Fossa Magna, Japan, Earth Planet. Sci. Lett., 78, 121-128, 1986.
- Fujita, K., F. William Cambray, and M. A. Velbel, Tectonics of the Laptev Sea and Moma rift systems, northeast USSR, Mar. Geol., 93, 95-118, 1990.
- Funahara, S., N. Nishiwaki, M. Miki, F. Muruta, Y. Otofuji, and Yi Zhao Wang, Paleomagnetic study of Cretaceous rocks from the Yangtze block, central Yunnan, China: implications for the India-Asia collision, Earth Planet. Sci. Lett., 113, 77-91, 1992.
- Geology of the USSR, vol. 33, Sakhalin Geological Description, 431 pp., Nedra, Moscow, 1970.
- Glatzmaier, G. A., Schubert, G., and D. bercovici, Chaotic subduction-like downflows in a spherical model of convection in the Earth's mantle, Nature, 347, 274-277, 1990.
- Gnibidenko, H.S., The Sea of Okhotsk-Kuril islands ridge and Kuril-Kamchatka trench, in The Ocean Basins and Margins, vol. 7A, edited by A.E.N. Nairn, F.G. Stehli and S. Uyeda, pp. 377-418, Plenum, New York, 1985.
- Gnibidenko, H.S., and A. S. Svarichevsky, Tectonics of the south Okhotsk deep-sea basin, Tectonophysics, 102, 225-244, 1984.
- Hamilton, W., Tectonics of the Indonesian region, U.S. Geol. Surv. Prof. Paper 1078, pp. 345, 1979.
- Harland, W. B., R. L. Armstrong, A. V. Cox, L. E. Craig, A. G. Smith, and D. G. Smith, A Geologic time scale 1989, Cambridge Univ. Press, pp. 1-263, 1990.
- Harnojo, H., M. Diament, J. Dubois, and M. Larue, Seismicity of the Sunda Strait: evidence for crustal extension and volcanological implications, Tectonics, 10, 17-30, 1991.
- Harris, R.A., Temporal distribution of strain in the active Banda orogen: a reconciliation of rival hypotheses, in: Hall, R., Nichols, G. and C. Rangin, eds., Orogenesis in action, Journal of southeast Asian earth science, 5, 1991.

- Hayashi, T., and S. Koshimizu, Fission-track ages of the Shidara Group in the northeast part of the Aichi prefecture and the Eocene molluscs from its lowermost Nagashino formation, *J. Geol. Soc. Jpn.*, 98, 901-904, 1992.
- Hayashi, M., and H. Takagi, Shape fabric of recrystallized quartz in the mylonites along the Median Tectonic Line, southern Nagano prefecture, *J. Geol. Soc. Japan*, 93, 349-359, 1987.
- Hayashida, A., and I. Y. Ito, Paleoposition of southwest Japan at 16 Ma: implication from magnetism of the Miocene Ichishi group, *Earth and Planet. Sci. Lett.*, 68, 335-342, 1984.
- Hayashida, A., Timing of rotational motion of southwest Japan inferred from paleomagnetism of the Setouchi Miocene series, *J. Geomag. Geoelectr.*, 38, 295-310, 1986.
- Hayashida, A., T. Fukui, and M. Torii, Paleomagnetism of the Early Miocene Kani group in southwest Japan and its implication for the opening of the Japan Sea, *Geophys. Res. Lett.*, 18, 1095-1098, 1991.
- Heki, K., Y. Takahashi and T. Kondo, Contraction of northeastern Japan: evidence from horizontal displacement of a Japanese station in global very long baseline interferometry networks, *Tectonophysics*, 181, 113-122, 1990.
- Hellinger, S. J., K. M. Shedlock, J. G. Sclater and Y. Hong, The Cenozoic evolution of the north China basin, *Tectonics*, 4, 343-358, 1985.
- Higashino, T., Metamorphic zones of the Sambagawa metamorphic belt in central Shikoku, Japan, *J. Geol. Soc. Japan*, 96, 703-718, 1990.
- Hikosan Collaborative Research Group, Neogene tectonic history of northern Kyushu, Japan - the Hikosan and its western area -, *J. Geol. Soc. Japan*, 98, 571-586, 1992.
- Hirata, N., Tokuyama, H. and Chung, T. W., 1989. An anomalously thick layering of the crust of the Yamato Basin, Southeastern Sea of Japan, the final stage of back-arc spreading, *Tectonophysics*, 165: 303-314.
- Hirm, A., A. Nercessian, M. Sapin, G. Jobert, Xu Zhong Xin, Gao En Yuan, Lu De Yuan, and Teng Ji Wen, Lhasa block and bordering sutures: a continuation of a 500 km Moho traverse through Tibet, *Nature*, 307, 25-27, 1984.
- Hirooka, K., H. Sakai, T. Takahashi, H. Kinoto, and A. Takeuchi, Tertiary tectonic movement of central Japan inferred from paleomagnetic studies, *J. Geomagn. Geoelectr.*, 38, 311-323, 1986.
- Holloway, N. H., The stratigraphy and tectonic relationship of Reed Bank, north Palawan and Mindoro to the Asian mainland and its significance in the evolution of the South China Sea, *Amer. Assoc. Petrol. Bull.*, 66, 1357-1383, 1982.
- Holt, E. H., and A. J. Haines, Velocity field in deforming Asia from the inversion of earthquake-released strains, *Tectonics*, 12, 1-20, 1993.
- Holt, E. H., J. F. Ni, T. C. Wallace, and A. J. Haines, The active tectonics of the eastern Himalayan syntaxis and surrounding regions, *J. Geophys. Res.*, 96, 14,595-14,632, 1991.
- Hong, Y., K. M. Shedlock, S. J. Hellinger and J. G. Sclater, The North China Basin: an example of a Cenozoic rifted intraplate basin, *Tectonics*, 153-169, 1985.
- Houseman, G., and P. England, Finite strain calculations of continental deformation. 1. Method and general results for convergent zones, *J. Geophys. Res.*, 91, 3651-3663, 1986.
- Houseman, G., and P. England, Crustal thickening versus lateral expulsion in the Indian-Asian continental collision, *J. Geophys. Res.*, 98, 12,233-12,249, 1993
- Huang, K., N. D. Opdyke, J. Li, and X. Peng, Paleomagnetism of Cretaceous rocks from eastern Qiangtang terrane of eastern Tibet, *J. Geophys. Res.*, 97, 1789-1799, 1992.
- Huchon, P., and H. Kitazato, Collision of the Izu block with central Japan during the Quaternary and geological evolution of the Ishigara area, *Tectonophysics*, 110, 201-210, 1984.
- Huchon, P., and X. Le Pichon, Sunda strait and central Sumatra fault, *Geology*, 12, 668-672, 1984.
- Huchon, P., Géodynamique de la zone de collision d'Izu et du point triple du Japon Central, thèse de doctorat, 414 pp., Univ. Pierre et Marie Curie, Paris, 1985.
- Huchon, P., X. Le Pichon, and C. Rangin, Indochina peninsula and the collision of India and Eurasia, *Geology*, 22, 27-30, 1994.
- Hutchinson, D. R., A. J. Golmshtok, L. P. Zonenshain, T. C. Moore, C. A. Scholz, and K. D. Klitgord, Depositional and tectonic framework of the rift basins of lake Baikal from multichannel seismic data, *Geology*, 20,589-592, 1992.
- Hwang, J.-H., L'évolution tectonique post-jurassique de la Corée: apport des reconstitutions de paléocontraintes dans les bassins crétacés méridionaux, Thèse Univ. Paris 6, pp. 301, 1992.
- Hyodo, H., and N. Niitsuma, Tectonic rotation of the Kanto mountains, related with the opening of the Japan Sea and collision of the Tanzawa block since Middle Miocene, *J. Geomagn. Geoelectr.*, 38, 335-348, 1986.
- Ichikawa, K., Geohistory of the Median Tectonic Line of southwest Japan, *Mem. Geol. Soc. Jpn.*, 18, 187-210, 1980.
- Ingle, J. C., Subsidence of the Japan Sea: stratigraphic evidence from ODP sites and onshore sections, edited by Tamaki et al., *Proc. Ocean Drill. Program. Sci. Results*, 127/128, 1197-1218, 1992.
- Irving, E., Drift of the major continental blocks since the Devonian, *Nature*, 270, 304-309, 1977.
- Isezaki, N., A magnetic anomaly map of the Japan sea, *J. Geomagn. Geoelectr.*, 38, 403-410, 1986.
- Ishibashi, K., Specification of soon-to-occur seismic faulting in the Tokai district, Central Japan, based upon seismotectonics, in: *Earthquake Prediction: An International Review*, D. W. Simpson and P. G. Richards, eds., Am. Geophys. Union, Maurice Ewing Ser. 4, 297-332, 1981.
- Ishida, M., Geometry and relative motion of the Philippine Sea plate and Pacific plate beneath the Kanto-Tokai district, Japan, *J. Geophys. Res.*, 97, 489-513, 1992.
- Irizuki, T., M. Takahashi, Y. Tanaka, and M. Oda, Geology and age of the Neogene sedimentary rocks in the Itsukaichi basin, central Japan, *Jour. Geol. Jpn. Soc.*, 9, 759-770, 1990.

- Ishii, H., T. Sato, K. Tachibana, K. Hashimoto, E. Murakami, M. Mishina, S. Miura, K. Sato, A. Takagi, Crustal strain, crustal stress and microearthquake activity in the northeastern Japan arc, *Tectonophysics*, 97, 217-230, 1983.
- Ishikawa, N., M. Torii, and K. Koga, Paleomagnetic study of the Tsushima islands, southern margin of the Japan Sea, *J. Geomag. Geoelectr.*, 41, 797-811, 1989.
- Ishikawa, N., and T. Tagami, Paleomagnetism and fission-track geochronology on the Goto and Tsushima islands in the Tsushima Strait area: implications for the opening mode of the Japan Sea, *J. Geomag. Geoelectr.*, 43, 229-253, 1991.
- Ishikawa, Y., Tectonics in eastern Asia and the seismicity around the Median Tectonic Line, *Mem. Geol. Soc. Japan*, 40, 205-218, 1992.
- Ito, M., The Itsukaichimachi Group: a Middle Miocene strike-slip basin fill in the southeastern margin of the Kanto mountains, central Honshu, Japan, in *Sedimentary Facies in the Active Plate Margin*, ed. A. Taira and F. Masuda, Terrapub, Tokyo, 659-673, 1989.
- Itoh, Y., Differential rotation of the eastern part of Southwest Japan inferred from paleomagnetism of Cretaceous and Neogene rocks, *J. Geophys. Res.*, 93, 3401-3411, 1988.
- Jaeger, J. C., and N. G. W. Cook, *Fundamentals of rock mechanics*, published by Chapman and Hall, London, 515 p., 1971.
- Jolivet, L., America-Eurasia plate boundary in eastern Asia and the opening of marginal basins, *Earth Planet. Sci. Lett.*, 81, 282-288, 1986.
- Jolivet, L., and P. Huchon, Crustal scale strike-slip deformation in Hokkaido, Northeast Japan, *J. Struct. Geol.*, 11, 509-522, 1989.
- Jolivet, L., and S. Miyashita, The Hidaka Shear Zone (Hokkaido, Japan): Genesis during a right-lateral strike slip movement, *Tectonics*, 4, 289-302, 1985.
- Jolivet, L., and K. Tamaki, Neogene kinematics in the Japan Sea region and volcanic activity of the northeast -Japan arc, edited by Tamaki et al., *Proc. Ocean Drill. Program, Sci. Results*, 127/128, 1311-1331, 1992.
- Jolivet, L., P. Huchon, and C. Rangin, Tectonic setting of Western Pacific marginal basins, *Tectonophysics*, 160, 23-47, 1989.
- Jolivet, L., P. Davy, and P. Cobbold, Right-lateral shear along the northwest Pacific margin and the India-Eurasia collision, *Tectonics*, 9, 1409-1419, 1990.
- Jolivet, L., P. Huchon, J.P. Brun, N. Chamot-Rooke, X. Le Pichon, and J.C. Thomas, Arc deformation and marginal basin opening, Japan Sea as a case study, *J. Geophys. Res.*, 96, 4367-4384, 1991.
- Jolivet, L., M. Fournier, P. Huchon, V. S. Rozdestvensky, K. F. Sergeyev, and L. Oscoirbin, Cenozoic intracontinental dextral motion in the Okhotsk-Japan Sea region, *Tectonics*, 11, 968-977, 1992.
- Jolivet, L., H. Shibuya, and M. Fournier, Paleomagnetic rotations and the Japan Sea opening, submitted to AGU Monograph, 1994.
- Jun, M.S., Source parameters of shallow intraplate earthquakes in and around the Korean peninsula and their tectonic implication, *Acta Univ. Ups. Abstr. Uppsala Diss. Fac. Sci.*, 285, Kanaori, Y., Late-Mesozoic-Cenozoic strike-slip and block rotation in the inner belt of Southwest Japan, *Tectonophysics*, 177, 381-399, 1990.
- Kanaori, Y., Late Mesozoic-Cenozoic strike-slip and block rotation in the inner belt of southwest Japan, *Tectonophysics*, 177, 381-399, 1990.
- Kanaori, Y., Y. Endo, K. Yairi, and S. Kawakami, A nested fault system with block rotation caused by left-lateral faulting: the Neodani and Atera faults, central Japan, *Tectonophysics*, 1977, 401-418, 1990.
- Kanaori, Y., S. Kawakami, and K. Yairi, The block structure and Quaternary strike-slip block rotation of central Japan, *Tectonics*, 11, 47-56, 1992.
- Kaneoka, I., K. Notsu, Y. Takigami, K. Fujioka, and H. Sakai, Constraints on the evolution of the Japan Sea based on ^{39}Ar - ^{40}Ar ages and Sr isotopic ratios for volcanic rocks of the Yamato seamount chain in the Japan Sea, *Earth Planet. Sci. Lett.*, 97, 211-225, 1990.
- Kaneoka, I., Y. Takigami, N. Takaoka, S. Yamashita, and K. Tamaki, Ar-Ar analysis of volcanic rocks recovered from the Japan Sea floor: constraints on the age of formation of the Japan Sea, edited by Tamaki et al., *Proc. Ocean Drill. Program, Sci. Results*, 127/128, 819-838, 1992.
- Kano, K., and F. Yoshida, Radiometric age of the Neogene in central eastern Shimane prefecture, Japan, and their implication in stratigraphic correlation, *Bull. Geol. Surv. Japan*, 35, 159-170, 1984.
- Kano, K., and S. Nakano, Stratigraphic correlation of the Neogene in the San'in district, southwest Japan, in the light of radiometric dating, *Bull. Geol. Surv. Japan*, 36, 427-438, 1985.
- Kano, K., Post-Paleogene left-lateral strike-slip motion on the Akaishi Tectonic Line, central Japan, *J. Geol. Soc. Japan*, 94, 629-632, 1988.
- Kano, K., K. Kosaka, A. Murata, and S. Yanai, Intra-arc deformations with vertical rotation axes: the case of the pre-Middle Miocene terranes of Southwest Japan, *Tectonophysics*, 176, 333-354, 1990.
- Kano, K., H. Kato, Y. Yanagisawa, and F. Yoshida, Stratigraphy and geologic history of the Cenozoic of Japan, Report 274 Geol. Surv. Jpn., pp. 1-114, 1991.
- Karasawa, Y., and K. Kano, Formation and deformation process of the slate in the Setogawa Group (the Shimanto belt) of the eastern Akaishi mountains, easternmost southwest Japan, *J. Geol. Soc. Japan*, 98, 761-777, 1992.
- Karig, D. E., Origin and development of marginal basins in the western Pacific, *J. Geophys. Res.*, 84, 6796-6802, 1971.
- Kawai, N., H. Ito, and S. Kume, Deformation of the Japanese islands as inferred from rock magnetism, *Geophys. R. Astr. Soc.*, 6, 124-130, 1961.
- Kawai, N., T. Nakajima, and K. Hirooka, The evolution of the island arc of Japan and the formation of granites in the circum Pacific belt, *J. Geomag. Geoelectr.*, 23, 267-293, 1971.

- Kidd, W. S. F., and P. Molnar, Quaternary and active faulting observed on the 1985 Academia Sinica-Royal Society Geotraverse of Tibet, *Phil. Trans. R. Soc. Lond.*, 327, 337-363, 1988.
- Kim, K. H., J. K. Won, J. I. Matsuda, K. Nagao, and W. L. Moon, Paleomagnetism and K-Ar age of volcanic rocks from Guryongpo area, Korea, *J. Korean Inst. Mining Geol.*, 19, 231-237, 1986.
- Kimura, G., Oblique subduction and collision, forearc tectonics of the Kuril arc, *Geology*, 14, 404-407, 1986.
- Kimura, G., and K. Tamaki, Collision, rotation and back arc spreading: The case of the Okhotsk and Japan Seas, *Tectonics*, 5, 389-401, 1986.
- Kimura, G., S. Miyashita, and S. Miyasaka, in *Collision Tectonics in Hokkaido and Sakhalin, Accretion Tectonics in the Circum Pacific Regions*, edited by M. Hashimoto and S. Uyeda, pp. 117-128, Terrapub, Tokyo, 1983.
- Kimura, G., M. Sakakibara, H. Ofuka, H. Ishizuka, S. Miyashita, M. Okamura, O. A. Melnikov, and V. Lushchenko, A deep section of accretionary complex: Susunai complex in Sakhalin island, northwest Pacific margin, *Isl. Arc*, 1, 166-175, 1992.
- Kobayashi, Y., Late Neogene dike swarms and regional tectonic stress field in the inner belt of southwest Japan, *Bull. Volc. Soc. Jpn.*, 24, 153-168, 1979a.
- Kobayashi, Y., Early and Middle Miocene dike swarms and regional tectonic stress field in the southwest Japan, *Bull. Volc. Soc. Jpn.*, 24, 203-212, 1979b.
- Kodama, K., Magnetostratigraphy of the Izumi Group along the Median Tectonic Line in Shikoku and Awaji islands, southwest Japan, *J. Geol. Soc. Jpn.*, 96, 265-278, 1990.
- Kodama, K., and K. Nakayama, Paleomagnetic evidence for post-Late Miocene intra-arc rotation of south Kyushu, Japan, *Tectonics*, 12, 35-47, 1993.
- Kodama, K., T. Ozawa, K. Inoue, Y. Maeda, and T. Tohru, Paleomagnetism and post-Middle Miocene counter-clockwise rotation of Tanegashima island off Kyushu, Japan, *J. Geomag. Geoelectr.*, 43, 721-740, 1991.
- Kodama, K., T. Takeuchi, and T. Ozawa, Clockwise tectonic rotation of Tertiary sedimentary basins in central Hokkaido, northern Japan, *Geology*, 21, 431-434, 1993.
- Kogi, K., Geology and structure of the Shidara volcanic mass, Aichi prefecture, central Japan, *Jour. Geol. Soc. Jpn.*, 89, 487-500, 1983.
- Koshiya, S., Tanakura Shear Zone, the deformation process of fault rocks and its kinematics, *J. Geol. Soc. Jpn.*, 92, 15-29, 1986.
- Koyama, A., The Shimotsutaki thrust - the bend of the Itoigawa-Shizuoka Tectonic Line, *J. Geol. Soc. Japan*, 94, 257-277, 1988.
- Kuramoto, S., and K. Konishi, The southwest Ryukyu arc is a migrating microplate (forearc silver), *Tectonophysics*, 163, 75-91, 1989.
- Kuwahara, T., and T. Sato, Strike-slip fault system of post-Miocene age at the north-eastern margin of the Kanto mountains, central Japan, *Ann. Rep. Inst. Geosci. Univ. Tsukuba*, 7, 46-48, 1981.
- Kuwahara, T., Late Cretaceous to Pliocene fault systems and corresponding regional stress fields in the southern part of northeast Japan, *Sci. Rep. Inst. Geosci. Univ. Tsukuba*, 3, 49-111, 1982.
- Lacassin, R., P. H. Leloup, and P. Tapponnier, Bounds on strain in large Tertiary shear zones of SE Asia from boudinage restoration, *J. Struct. Geol.*, 15, 677-692, 1993.
- Lallemand, S., and L. Jolivet, Japan Sea: A pull apart basin, *Earth Planet. Sci. Lett.*, 76, 375-389, 1985.
- Lallemand, S., N. Charmot-Rooke, X. Le Pichon, and C. Rangin, Zenisu Ridge: A deep intra-oceanic thrust related to subduction off Southwest Japan, *Tectonophysics*, 160, 151-174, 1989.
- Latt, K. M., Turbidites and related clastic systems in the Tertiary Chichibu basin, central Japan, in *Sedimentary Facies in the Active Plate Margin*, ed. A. Taira and F. Masuda, Terrapub, Tokyo, 421-438, 1989.
- Le Dain, A. Y., P. Tapponnier, and P. Molnar, Active faulting and tectonics of Burma and surrounding regions, *J. Geophys. Res.*, 89, 453-472, 1984.
- Lee, J. S., *Pétrologie et relations structurales des volcanites Crétacé à Cénozoïques de la Corée du Sud, implications géodynamiques sur la marge est-eurasiatique*, Thèse de Doctorat, Université d'Orléans, Orléans, 1989.
- Lee G., J. Besse, V. Courtillot, and R. Montigny, Eastern Asia in the Cretaceous: new paleomagnetic data from south Korea and a new look at Chinese and Japanese data, *J. Geophys. Res.*, 92, 3580-3596, 1987.
- Lee, J.S., and A. Pouclet, Le volcanisme néogène de Pohang (SE Corée), nouvelles contraintes géochronologiques pour l'ouverture de la mer du Japon, *C. R. Acad. Sci. Paris, Ser. 2*, 307, 1405-1411, 1988.
- Leloup, P. H., T. Mark Harrison, F. J. Ryerson, Chen Wenji, Li Qi, P. Tapponnier, and R. Lacassin, Structural, petrological and thermal evolution of a Tertiary ductile strike-slip shear zone, Diancang Shan, Yunnan, *J. Geophys. Res.*, 98, 6715-6743, 1993.
- Le Pichon, X., Résumé des cours et travaux, *Annuaire du Collège de France 1987-1988*, 135-144, Collège de France, Paris, 1988.
- Le Pichon, X., M. Fournier, and L. Jolivet, Kinematics, topography, shortening and extrusion in the India-Eurasia collision, *Tectonics*, 1993.
- Le Pichon, et al., Nankai trough and the fossil Shikoku ridge: Results of Box 6 Kaiko survey, *Earth Planet. Sci. Lett.*, 83, 186-198, 1987.
- Le Pichon, X., K. Kobayashi, et al., Fluid venting activity within the eastern Nankai trough accretionary wedge: A summary of the 1989 Kaiko-Nankai results, *Earth Planet. Sci. Lett.*, 109, 303-318, 1992.
- Lu, H., H. Yu, Y. Ding, and Q. Zhang, Changing stress field in the middle segment of the Tan-Lu fault zone, eastern China, *Tectonophysics*, 98, 253-270, 1983.
- Ludwig, W. J., S. Murauchi, and R. E. Houtz, Sediments and structure of the Japan sea, *Geol. Soc. Am. Bull.*, 86, 651-664, 1975.
- Luyendyk, B. P., M. J. Kamerling, R. R. Terres, and J. S. Hornafius, Simple shear of southern California during Neogene time suggested by paleomagnetic rotations, *J. Geophys. Res.*, 90, 12,454-12,466, 1985.

- Lyon-Caen, H., and P. Molnar, Gravity anomalies, flexure of the Indian plate, and the structure, support and evolution of the Himalaya and Ganga basin, *Tectonics*, 4, 513-538, 1985.
- Ma, X., and D. Wu, Cenozoic extensional tectonics in China, *Tectonophysics*, 133, 243-255, 1987.
- Marchadier, Y., and C. Rangin, Passage subduction-collision et tectoniques superposées à l'extrémité de la fosse de Manille (Mindoro-Tablas, Philippines), *C. R. Acad. Sci. Paris*, 308, 1715-1720, 1989.
- Martinod, J., Instabilités périodiques de la lithosphère, Thesis of Rennes Univ., 182 p., 1991.
- Matsuda, T., Collision of the Izu-Bonin arc with central Honshu: Cenozoic tectonics of the Fossa Magna, Japan, *Journal of Physics of the Earth*, 26, 409-421, 1978.
- Matsumaru, K., and A. Hayashi, Neogene stratigraphy of the eastern marginal areas of Kanto mountains, central Japan, *J. Geol. Soc. Jpn.*, 86, 225-242, 1980.
- Matsuzaka, S., M. Tobita, and Y. Nakahori, Detection of Philippine sea plate motion by very long baseline interferometry, *Geophys. Res. Lett.*, 18, 1417-1419, 1991.
- Mattauer, M., and J. L. Mercier, Microtectonique et grande tectonique, *Mém. hors Sér. Soc. Géol. Fr.*, 10, 141-161, 1980.
- McCaffrey, R., E. A. Silver and R. W. Raitt, Crustal structure of the Molucca Sea collision zone, Indonesia, in *The Tectonic and Geologic Evolution of Southeast Asian Seas and Islands* edited by D. E. Hayes, *Geophys. Monogr.*, Am. Geophys. Union, 23, 161-177, 1980.
- McCaffrey, R., and J. Nabelek, Seismological evidence for shallow thrusting north of the Timor Through, *Geophys. J. R. Astron. Soc.*, 85, 365-381, 1986.
- McCaffrey, R., Active tectonics of the eastern Sunda and Banda arc, *J. Geophys. Res.*, 93, 15163-15182, 1988.
- McCaffrey, R., and G. A. Abers, Orogeny in arc-continent collision: the Banda arc and western New Guinea, *Geology*, 19, 563-566, 1991.
- McKenzie, D. P., Speculations on the consequences and causes of plate motions, *Geophys. J. Roy. Astron. Soc.*, 18, 1-32, 1969.
- McKenzie, D. P., and J. A. Jackson, The relationship between strain rates, crustal thickening, paleomagnetism, finite strain and fault movements within a deforming zone, *Earth Planet. Sci. Lett.*, 65, 182-202, 1983.
- McKenzie, D. P., and J. A. Jackson, A block model of distributed deformation by faulting, *J. Geol. Soc. London*, 143, 349-353, 1986.
- Melnikov, O. A., Structure and Geodynamics of the Hokkaido-Sakhalin Folded Region (in Russian), 94 pp., Nauka, Moscow, 1987.
- Melnikov, O. A., and V. S. Rozhdestvensky, Guide-Book for Geological Excursions on the Southern Part of Sakhalin Island, edited by H. S. Gnibidenko, Yuzhno-Sakhalinsk, 1989.
- Melnikov, O. A., and M. A. Zakharova, Cenozoic Sedimentary and Volcanic-Sedimentary Formations of Sakhalin (in Russian), 242 pp., Nauka, Moscow, 1977.
- Mercier, J. L., R. Armijo, P. Tapponnier, E. Carey-Gailhardis, and Han Tong Lin, Change from Late Tertiary compression to Quaternary extension in southern Tibet during the India-Asia collision, *Tectonics*, 6, 275-304, 1987.
- Meyer, B., Mécanismes des grands tremblements de terre et du raccourcissement crustal oblique au bord nord-est du Tibet, doctorat, Univ. Paris VI, 129 pp., 1991.
- Miki, M., T. Matsuda, and Y. Otofuji, Opening mode of the Okinawa Trough: paleomagnetic evidence from the south Ryukyu arc, *Tectonophysics*, 175, 335-347, 1990.
- Mikumo, T., H. Wada, and M. Koizumi, Seismotectonics of the Hida region, central Honshu, Japan, *Tectonophysics*, 147, 95-119, 1988.
- Miller, G. M., Brittle faulting induced by ductile deformation of a rheologically stratified rock sequence, Badwater Turtleback, Death Valley, California, *Geol. Soc. Amer. Bull.*, 104, 1376-1385, 1992.
- Milsom, J., and M. R. Audley-Charles, Post collisional isostatic adjustment in the southern Banda arc, in: *Collision Tectonics*, Spec. Publ. Geol. Soc. Lon., 19, 353-366, 1986.
- Miyashiro, A., Hot regions and the origin of marginal basins in the western Pacific, *Tectonophysics*, 122, 195-216, 1986.
- Miyata, T., H. Ui, and K. Ichikawa, Paleogene left-lateral wrenching on the Median Tectonic Line in southwest Japan, *Mem. Geol. Soc. Jpn.*, 18, 51-68, 1980.
- Molnar, P., and T. Atwater, Interarc spreading and cordilleran tectonics as alternates related to the age of the subducted oceanic lithosphere, *Earth Planet. Sci. Lett.*, 41, 330-340, 1978.
- Molnar, P., and P. Tapponnier, Cenozoic tectonics of Asia: Effects of a continental collision, *Science*, 189, 419-426, 1975.
- Molnar, P., and P. Tapponnier, Active tectonics of Tibet, *J. Geophys. Res.*, 83, 5361-5375, 1978.
- Molnar, P., and W.-P. Chen, Focal depths and fault plane solutions of earthquakes under the Tibetan plateau, *J. Geophys. Res.*, 88, 1180-1196, 1983.
- Molnar, P., and Deng Quidong, Faulting associated with large earthquakes and the average rate of deformation in central and eastern Asia, *J. Geophys. Res.*, 89, 6203-6227, 1984.
- Molnar, P., Burchfield, B. C., L. K'uangyi, and Z. Ziyun, Geomorphic evidence for active faulting in the Altyn Tagh and northern Tibet and qualitative estimates of its contribution to the convergence of India and Eurasia, *Geology*, 15, 249-253, 1987.
- Molnar, P., and H. Lyon-Caen, Some simple physical aspects of the support, structure, and evolution of mountain belts, *Geol. Soc. Amer. Spec. Pap.*, 218, 179-207, 1988.
- Molnar, P., and H. Lyon-Caen, Fault plane solutions of earthquakes and active tectonics of the Tibetan plateau and its margins, *Geophys. J. Int.*, 99, 123-153, 1989.
- Moore, G. F., J. R. Curray, D. G. Moore, and D. E. Karig, Variations in geologic structure along the Sunda fore arc, Northeastern Indian Ocean, in: Hayes D. E., Ed., *The tectonic and geologic evolution of southeast Asian seas and islands*, *Geophys. Monogr.*, AGU, Washington, 27, 145-160, 1980.

- Moore, G.F., and E. A. Silver, Collision processes in the northern Molucca sea, The tectonic and geologic evolution of southeast Asian seas and islands, *Geophys. Monogr.*, AGU, 27, 360-372, 1982.
- Moreau, M. G., V. Courtillot, and J. Besse, On the possibility of a wide spread remagnetization of pre-Oligocene rocks from Northeast Japan and the Miocene rotational opening of the Japan Sea, *Earth Planet. Sci. Lett.*, 84, 321-338, 1987.
- Murata, A., Conical folds in the Hitoyoshi bending, south Kyushu, formed by the clockwise rotation of the southwest Japan arc, *J. Geol. Soc. Japan*, 93, 91-105, 1987.
- Murata, A., Lateral change of horizontal displacement along the Kaminirogawa-Akuigawa fault in east Shikoku, *J. Geol. Soc. Japan*, 94, 689-695, 1988.
- Nabelek, J., W. P. Chen and H. Ye, The Tangshan earthquake sequence of 1976 and its implications for the evolution of the North China basin, *J. Geophys. Res.*, 92, 12,615-12628, 1987.
- Nakamura, K., Possible nascent trench along the eastern Japan Sea as the convergent boundary between Eurasian and North American plates (in Japanese), *Bull. Earthquake. Res. Inst. Univ. Tokyo*, 58, 711-722, 1983.
- Nakamura, K., and S. Uyeda, Stress gradient in back arc regions and plate subduction, *J. Geophys. Res.*, 85, 6419-6428, 1980.
- Nakanishi, M., K. Tamaki, and K. Kobayashi, Magnetic anomaly lineations from Late Jurassic to Early Cretaceous in the west-central Pacific ocean, *Geophys., J. Int.*, 109, 701-719.
- Nelson, M. R., R. McCaffrey, and P. Molnar, Source parameters for 11 earthquakes in the Tien Shan, Central Asia, determined by P and SH waveform inversion, *J. Geophys. Res.*, 92, 12,629-12,648, 1987.
- Niitsuma, N., and T. Matsuda, Collision in the south Fossa Magna area, central Japan, *Rec. Progress. Natural Sci. Jpn.*, 10, 41-50, 1985.
- Nur, A., H. Ron, and O. Scotti, Fault mechanics and the kinematics of block rotations, *Geology*, 14, 746-749, 1986.
- Okada, A., Quaternary faulting along the Median Tectonic Line of southwest Japan, *Mem. Geol. Soc. Jpn.*, 18, 79-108, 1980.
- Okada, A., Proposal of segmentation on the Median Tectonic Line active fault system, *Mem. Geol. Soc. Jpn.*, 40, 15-30, 1992.
- Osorbin, L. S., Seismicity of the Sakhalin island, in Seismic Regions of the Kuril Islands, Primorja and Priamurjia, edited by S. L. Solovjev, Vladivostok, 1977.
- Oshida, A., Tamaki, K., and M. Kimura, Origin of the magnetic anomalies in the southern Okinawa trough, *J. Geomag. Geoelectr.*, 44, 345-359, 1992.
- Otofuji, Y., and T. Matsuda, Paleomagnetic evidence for the clockwise rotation of Southwest Japan, *Earth Planet. Sci. Lett.*, 62, 349-359, 1983.
- Otofuji, Y., and T. Matsuda, Timing of rotational motion of Southwest Japan inferred from paleomagnetism, *Earth Planet. Sci. Lett.*, 70, 373-382, 1984.
- Otofuji, Y., A. Hayashida, and M. Torii, When was the Japan Sea opened: paleomagnetic evidence from southwest Japan, in Formation of active ocean margin, edited by N. Nasu, S. Uyeda, I. Kushiro, K. Kobayashi, and H. Hagami, 551-556, TERRAPUB, Tokyo, 1985.
- Otofuji, Y., T. Matsuda, and S. Nohda, Paleomagnetic evidence for the Miocene counter-clockwise rotation of Northeast Japan - rifting process of the Japan arc, *Earth Planet. Sci. Lett.*, 75, 265-277, 1985.
- Otofuji, Y., and T. Matsuda, Amount of clockwise rotation of Southwest Japan - fan shape opening of the southwestern part of the Japan Sea, *Earth Planet. Sci. Lett.*, 85, 289-301, 1987.
- Otofuji, Y., Y. Inoue, S. Funahara, F. Murata, and X. Zheng, Paleomagnetic study of eastern Tibet-deformation of the Three Rivers region, *Geophys. J. Int.*, 103, 85-94, 1990.
- Otofuji, Y., T. Itaya, and T. Matsuda, Rapid rotation of southwest Japan - paleomagnetism and K-Ar ages of Miocene volcanic rocks of southwest Japan, *Geophys. J. Int.*, 105, 397-405, 1991.
- Otofuji, Y., A. Kambara, T. Matsuda, and S. Nohda, Counterclockwise rotation of northeast Japan: paleomagnetic evidence for regional extent and timing of rotation, *Earth Planet. Sci. Lett.*, 121, 503-518, 1994.
- Otsuki, K., Reconstruction of Neogene tectonic stress field of Northeast Honshu arc from metalliferous veins, *Mem. Soc. Geol. Jpn.*, 32, 281-304, 1989.
- Otsuki, K., Neogene tectonic stress fields of northeast Honshu Arc and implications for plate boundary conditions, *Tectonophysics*, 181, 151-164, 1990.
- Otsuki, K., and M. Ehiro, Major strike slip faults and their bearing on the spreading of the Japan Sea, *J. Phys. Earth*, 26, suppl., 537-555, 1978.
- Pan, Y., and W. S. F. Kidd, Nyainqntanglha shear zone: a late Miocene extensional detachment in the southern Tibetan plateau, *Geology*, 20, 775-778, 1992.
- Parfenoy, L. M., B. M. Koz'Min, V. S. Imayev, and L. A. Savostin, The tectonic character of the Olekma-Stanovoy seismic zone, *Geotectonics*, 21, 560-572, 1987.
- Patriat, P., and J. Achache, Indian-Asia collision chronology has implications for crustal shortening and driving mechanism of plates, *Nature*, 311, 615-621, 1984.
- Peltzer, G., P. Tapponnier, Z. Zhan and Z. Q. Xu, Neogene and Quaternary faulting in and along the Qinling Shan, *Nature*, 317, 500-505, 1985.
- Peltzer, G., and P. Tapponnier, Formation and evolution of strike-slip faults, rifts, and basins during the India-Asia collision: an experimental approach, *J. Geophys. Res.*, 93, 15,085-15,117, 1988.
- Peltzer, G., P. Tapponnier, Y. Gaudemer, B. Meyer, Guo Shumin, Yin Kelun, Chen Zhitai and Dai Huagung, Offsets of late quaternary morphology, rate of slip, and recurrence of large earthquakes on the Chang Ma fault (Gansu, China), *J. Geophys. Res.*, 93, 7793-7812, 1988.

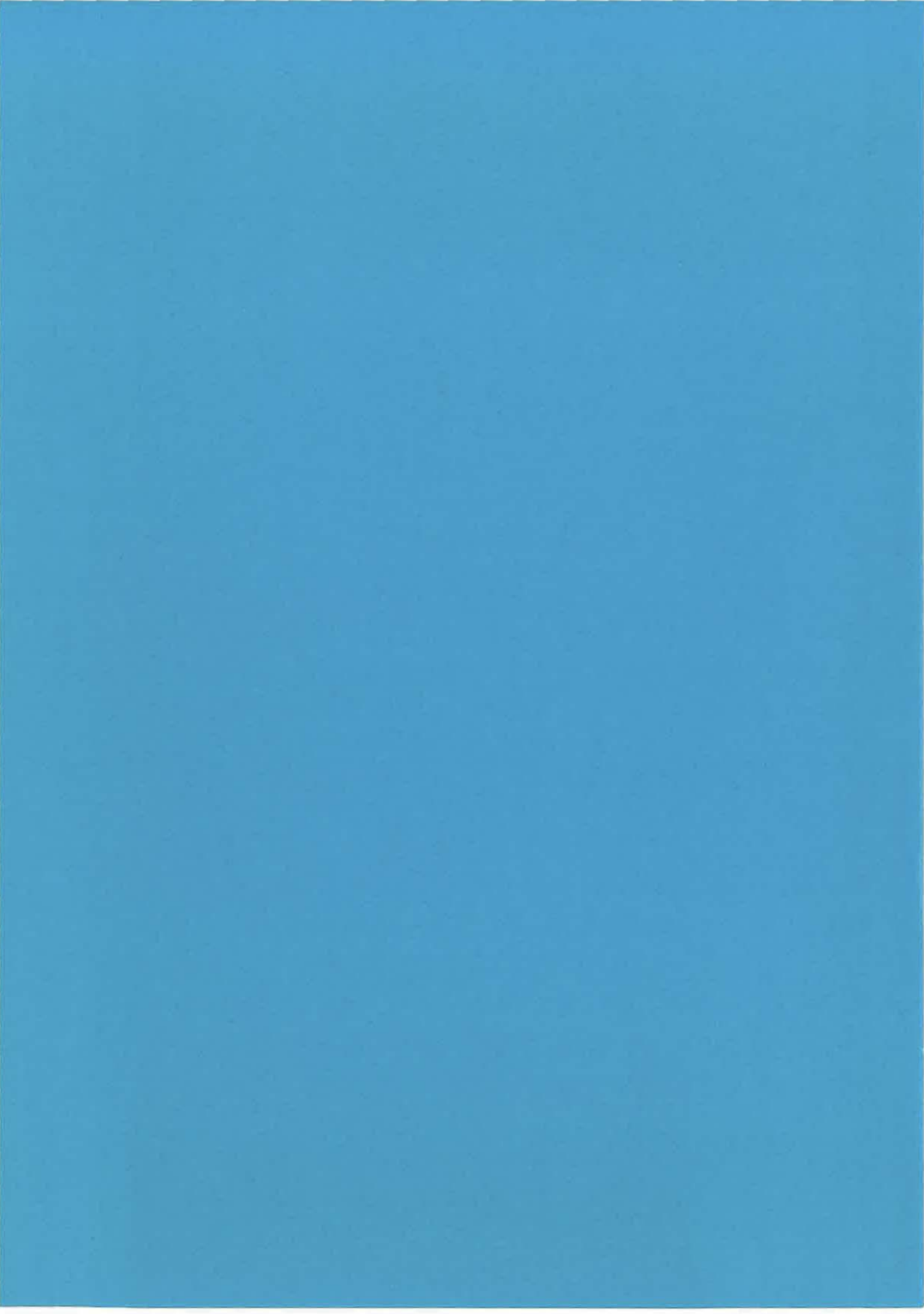
- Peltzer, G., P. Tapponnier, and R. Armijo, Magnitude of Late Quaternary left-lateral displacements along the north edge of Tibet, *Science*, 246, 1285-1289, 1989.
- Pouclet, A., and H. Bellon, Geochemistry and isotopic composition of volcanic rocks from the Yamato basin: hole 294D, Sea of Japan, edited by Tamaki et al., *Proc. Ocean Drill. Program, Sci. Results*, 127/128, 779-790, 1992.
- Pushcharovskiy, Y. M., V. P. Zinkevich, A. O. Mazarovich, A. A. Peyve, Y. N. Raznitsin, A. V. Rikhter, and N. V. Tsukanov, Overthrusts and imbricate structures of the northwestern Pacific margin, *Geotectonics*, 17, 466-477, 1983.
- Rangin, C., L. Jolivet, M. Pubellier and the Tethys Pacific working group, A simple model for the tectonic evolution of southeast Asia and Indonesia region for the past 43 m.y., *Bull. Soc. Geol. France*, 6, 889-905, 1990.
- Ranken, B., R. K. Cardwell and D. E. Karig, Kinematics of the Philippine sea plate, *Tectonics*, 3, 555-575, 1984.
- Riegel, S.A., K. Fujita, B. M. Koz'min, V. S. Imaev, and D. B. Cook, Extrusion tectonics of the Okhotsk plate, northeast Asia, *Geophys. Res. Lett.*, 20, 607-610, 1993.
- Rikhter, A. V., Structure and Tectonic Evolution of Sakhalin in the Mesozoic (in Russian), 90 pp., Nauka, Moscow, 1986.
- Romanowicz, B., Constraints on the structure of the Tibet plateau from pure path phase velocities of Love and Rayleigh waves, *J. Geophys. Res.*, 87, 6865-6883, 1982.
- Ron, H., R. Freund, Z. Garfunkel, and A. Nur, Block rotation by strike slip faulting, structural and paleomagnetic evidence, *J. Geophys. Res.*, 89, 6256-6270, 1984.
- Rotherty, D. A., and S. A. Drury, The Neotectonics of the Tibetan plateau, *Tectonics*, 3, 19-26, 1984.
- Rozhdestvensky, V. S., The role of wrench-faults in the structure of Sakhalin, *Geotectonics*, 16, 323-332, 1982.
- Rozhdestvensky, V. S., Evolution of the Sakhalin fold system, *Tectonophysics*, 127, 331-339, 1986.
- Saito, T., and S. Maiya, Planktonic Foraminifera of the Nishikurosawa formation, northeast Honshu, Japan, *Trans. Proc. Paleont. Soc. Japan*, 91, 113-125, 1973.
- Sasajima, S., Pre-Neogene paleomagnetism of Japanese island (and vicinities), in *Paleoreconstruction of the Continents*, ed. by M. W. Mc Elhinny and D. A. Valancio, *Geodyn. Series* vol. 2, 1981.
- Sato, T., Fault system in the Kanto Mountains, *Ann. Rep. Inst. geosci. Univ. Tsukuba*, 12, 72-75, 1986.
- Savostin, L. A., and A. M. Karasik, Recent plate tectonics of the Arctic basin and of northeastern Asia, *Tectonophysics*, 74, 111-145, 1981.
- Savostin, L., L. Zonenshain, and B. Baranov, Geology and plate tectonics of the Sea of Okhotsk, in *Geodynamics of the Western Pacific-Indonesian Region*, *Geodyn. Ser.*, vol. 11, edited by T. W. C. Hilde and S. Uyeda, pp. 343-354, AGU, Washington, D.C., 1983.
- Schärer, U., P. Tapponnier, R. Lacassin, H. Leloup, Zhong Dalai, and Ji Shaocheng, Intraplate tectonics in Asia: a precise age for large-scale Miocene movement along the Ailao Shan-Red River shear zone, China, *Earth Planet. Sci. Lett.*, 97, 65-77, 1990.
- Scotti, O., A. Nur, and R. Estevez, Distributed deformation and block rotation in three dimensions, *J. Geophys. Res.*, 96, 12,225-12,243, 1991.
- Seismotectonic map of China based on interpretation of satellite images (1: 4.000.000), published by the Earthquake Research Institute, Pekin, 1985.
- Seno, T., The instantaneous rotation vector of the Philippine sea plate relative to the Eurasian plate, *Tectonophysics*, 42, 209-226, 1977.
- Seno, T., and S. Maruyama, Paleogeographic reconstruction and origin of the Philippine Sea, *Tectonophysics*, 102, 53-84, 1984.
- Seno, T., 1985a. Is Northern Honshu a microplate?, *Tectonophysics*, 115: 177-196.
- Seno, T., 1985b. Age of subducting lithosphere and back arc basin formation in the western Pacific since the Middle Tertiary, In: *Formation of Active ocean margins*, edited by N. Nasu et al., Terrapub, Tokyo, 469-481.
- Seno, T., Y. Hamano, and M. Yamano, Basin stretching modelling of Yamato basin, Japan Sea, *Chikyu Extra*, 3, 145-149, 1991.
- Seno, T., S. Stein, and A. E. Gripp, A model for the motion of the Philippine Sea plate consistent with NUVEL-1 and geological data, *J. Geophys. Res.*, 98, 17,941-17,948, 1993.
- Sharma, S. R., A. Sundar, V. K. Rao and D. V. Ramana, Surface heat flow and Ph velocity distribution in peninsular India, *J. Geodyn.*, 13, 67-76, 1991.
- Sherman, S. I., Faults and tectonic stresses of the Baikal rift zone, *Tectonophysics*, 208, 297-307, 1992.
- Shibata, K., and T. Nozawa, K-Ar ages of granitic rocks from the outer zone of southwest Japan, *Geochem. Jour.*, 1, 131-137, 1967.
- Shibata, K., H. Sato, and M. Nakagawa, K-Ar ages of Neogene volcanic rocks from Noto peninsula, *J. Assoc. Miner. Petrol. Econ. Geol.*, 76, 248-252, 1981.
- Shibata, K., and H. Takagi, Isotopic ages and intrafault materials along the Median Tectonic Line - an example in the Bungui-Toge area, Nagano prefecture, *J. Geol. Soc. Japan*, 94, 35-50, 1988.
- Shimizu, I., Ductile deformation in the low-grade part of the Sambagawa metamorphic belt in the northern Kanto mountains, central Japan, *J. Geol. Soc. Japan*, 94, 609-628, 1988.
- Sibuet, J. C., J. Letouzey, F. Barbier, J. Charvet, J. P. Foucher, T. W. C. Hilde, M. Kimura, C. Ling-Yun, B. Marsset, C. Muller, and J. F. Stephan, Back arc extension in the Okinawa Trough, *J. Geophys. Res.*, 92, 14041-14063, 1987.

- Sillitoe, R.H, Metallogeny of an Andean type continental margin in South Korea, implications for opening of the Japan Sea, in Island Arcs, Deep Sea Trenches and Back-Arc Basins, Maurice Ewing Ser. , vol. 1, edited by M. Talwani and W.C. Pitman III, pp. 303-310, AGU, Washington, D.C., 1977.
- Silver, E. A., R. McCaffrey and R. B. Smith, Collision, rotation, and the initiation of subduction in the evolution of the Sulawesi, Indonesia, *J. Geophys. Res.*, 88, 9407-9418, 1983.
- Silver, E. A., D. Reed, R. McCaffrey, and Y. Joyodiwiryo, Back arc thrusting in the eastern Sunda arc, Indonesia: a consequence of arc-continent collision, *J. Geophys. Res.*, 88, 7429-7448, 1983.
- Silver, E. A., and C. Rangin, Leg 124 tectonic synthesis, Proceedings of the Ocean Drilling Program, Scientific results, 124, 3-9, 1991.
- Sleep, N. H., and M. N. Toksoz, Evolution of marginal basins, *Nature*, 33, 548-550, 1971.
- Sugi, N., K. Chinzei and S. Uyeda, Vertical crustal movements of northeast Japan since Middle Miocene, in Geodynamics of the Western Pacific-Indonesian Region, *Geodyn. Ser.*, vol. 11, edited by T. W. C. Hilde and S. Uyeda, pp. 317-329, AGU, Washington, D.C., 1983.
- Tagami, T., N. Lal, R. Sorkhabi, and S. Nishimura, Fission track thermochronologic analysis of the Ryoke belt and the Median Tectonic Line, southwest Japan, *J. Geophys. Res.*, 93, 13,705-13,715, 1988.
- Taira, A., H. Tokuyama, and W. Soh, Accretion tectonics and evolution of Japan, in ZviBen-Averaham (ed.), The Evolution of the Pacific Ocean Margins, Oxford Univ. Press, NY, Oxford, 100-123, 1989.
- Takada, A., Structure of a cauldron in the Otoge ring complex, Shitara district, Aichi prefecture, central Japan, *J. Geol. Soc. Jpn.*, 93, 107-120, 1987a.
- Takada, A., Development of the Shitara igneous complex, central Japan, and the structure of its cauldrons, *J. Geol. Soc. Jpn.*, 93, 167-184, 1987b.
- Takagi, H., T. Takashita, K. Shibata, S. Uchiumi, and M. Inoue, Middle Miocene normal faulting along the Tobe thrust in western Shikoku, *J. Geol. Soc. Jpn.*, 98, 1069-1072, 1992.
- Takahashi, J., On the Median Tectonic Line in Matsuyama city and the neighbouring areas, Ehime prefecture, Japan, *Mem. Fac. Educ. Ehime Pref.*, Ser. 3, 6, 1-44, 1986.
- Takahashi, J., Faulting history of the Median Tectonic Line in Ehime prefecture, *Mem. Geol. Soc. Jpn.*, 40, 99-112, 1992.
- Takahashi, M., and S. Nomura, Paleomagnetism of the Chichibu quartz diorite - constraints on the time of lateral bending of the Kanto syntaxis, *J. Geomag. Geoelectr.*, 41, 479-489, 1989.
- Takeshita, T., Deformation microstructures in dominantly white-colored rocks distributed along the Tobe thrust of the Median Tectonic Line and their implication, *J. Geol. Soc. Jpn.*, 97, 175-178, 1991.
- Takeuchi, A., Temporal changes of regional stress field and tectonics of sedimentary basin, *J. Geol. Soc. Jpn.*, 87, 737-751, 1981.
- Takeuchi, T., T. Ozawa, and K. Kodoma, Paleomagnetism of the late Cretaceous to Neogene deposits in central Hokkaido, Japan and south Sakhalin of the USSR: multiple rotations caused by transcurrent faults, paper presented at 29th International Geological Congress, Jpn. Geol. Soc., Kyoto, 24 August-3 September 1992.
- Tamaki, K., Age estimation of the Japan Sea on the basis of stratigraphy, basement depth and heat flow data, *J. Geomagn. Geoelectr.*, 38, 427-446, 1986.
- Tamaki, K., Geological structure of the Japan Sea and its tectonic implications, *Bull. Geol. Surv. Jpn.*, 39, 269-365, 1988.
- Tamaki, K. and Kobayashi, K., 1988. Geomagnetic anomaly lineation in the Japan Sea, *Mar. Sci. Mon.*, 20: 705-710, (in Japanese).
- Tamaki, K., and E. Honza, Incipient subduction and obduction along the eastern margin of the Japan Sea, *Tectonophysics*, 119, 381-406, 1984.
- Tamaki, K., and E. Honza, Global tectonics and formation of marginal basins: role of the western Pacific, *Episodes*, 14, 224-230, 1991.
- Tamaki, K., K. Suyehiro, J. Allan, M. McWilliams, et al., Tectonic synthesis and implication of Japan Sea ODP drilling, *Proc. Ocean Drill. Program, Sci. Results*, 127/128, 1333-1348, 1992.
- Tanaka, T., and K. Ogusa, Structural movement since Middle Miocene in the off-shore San'in sedimentary basin, the Sea of Japan, *J. geol. Soc. Jpn.*, 87, 725-736, 1981.
- Tanaka, H., and T. Hara, Dextral movement of the Median Tectonic Line before early Miocene as revealed from textures of brittle fault rocks, *J. Geol. Soc. Japan*, 96, 331-334, 1990.
- Tanaka, H., H. Tsunakawa, H. Yamaguchi, and G. Kimura, Paleomagnetism of the Shakotan peninsula, West Hokkaido, Japan, *J. Geomag. Geoelectr.*, 43, 277-294, 1991.
- Tapponnier, P., and P. Molnar, Slip line field theory and large-scale continental tectonics, *Nature*, 264, 319-324, 1976.
- Tapponnier, P., and P. Molnar, Active faulting and tectonics in China, *J. Geophys. Res.*, 82, 2905-2930, 1977.
- Tapponnier, P., and P. Molnar, Active faulting and Cenozoic tectonic of the Tien Shan, Mongolia, and Baykal regions, *J. Geophys. Res.*, 84, 3425-3459, 1979.
- Tapponnier, P., J. L. Mercier, R. Armijo, T. Han, and J. Zhou, Field evidences for active normal faulting in Tibet, *Nature*, 294, 410-414, 1981.
- Tapponnier, P., G. Peltzer, A. Y. Le Dain, and R. Armijo, Propagating extrusion tectonics in Asia: new insights from simple experiments with plasticine, *Geology*, 10, 611-616, 1982.
- Tapponnier, P., G. Peltzer, and R. Armijo, On the mechanics of the collision between India and Asia, Collision tectonics, edited by M. P. Coward and A. C. Ries, *Geol. Soc. Spec. Publ. London*, 19, 115-157, 1986.
- Tapponnier, P., R. Lacassin, P. H. Leloup, U. Shärer, Zhong Dalai, Wu Haiwei, Liu Xiohan, Ji Shaocheng, Zhang Lianshang, and Zhong Jiayou, The Ailao Shan/Red River metamorphic belt: Tertiary left-lateral shear between Indochina and South China, *Nature*, 343, 431-437, 1990.

- Tarakamov, R. Z., and C. U. Kim, Seismofocal zones and geodynamics of the Kuril-Japan region, in: Geodynamics of the Western Pacific-Indonesian Region, *Geodyn. Ser.*, vol. 11, edited by T. W. C. Hilde and S. Uyeda, pp. 223-236, AGU, Washington, D.C., 1983.
- Tatsumi, Y., M. Torii, and K. Ishizaka, On the age of the volcanic activity and the distribution of the Setouchi volcanics rocks, *Bull. Volcanol. Soc. Jpn.*, 25, 171-179, 1980.
- Tatsumi, Y., Otofuji, Y. I., Matsuda, T., and Nohda, S., Opening of the Sea of Japan back-arc basin by asthenospheric injection, *Tectonophysics*, 166, 317-329, 1989.
- Taylor, B. and D. E. Hayes, The tectonic evolution of the south China basin, in: Hayes D. E., Ed., The tectonic and geologic evolution of southeast Asian seas and islands, *Geophys. Monogr.*, AGU, Washington, 27, 89-104, 1980.
- Taylor, B., and G. D. Karner, On the evolution of marginal basins, *Rev. Geophys.*, 21, 1727-1741, 1983.
- Taylor, B., A. Klaus, G.R. Brown, G. F. Moore, Y. Okamura, and F. Murakami, Structural development of Sumisu rift, Izu-Boni arc, *J. Geophys. Res.*, 96, 16,113-16,129, 1991.
- Tazaki, K., J. Takahashi, T. Itaya, R. H. Grapes, and N. Kashima, K-Ar ages of the andesites intruding along the Median Tectonic Line in northwestern Shikoku, Japan, *J. Assoc. Miner. Petrol. Econ. Geol.*, 85, 155-160, 1990.
- Tian, Z., P. Hang and K. D. Xu, The Mesozoic-Cenozoic east China rift system, *Tectonophysics*, 208, 341-363, 1992.
- Tohara, T., Petrological study on Tertiary volcanic rocks and ultramafic inclusions from Matsuyama area, northwestern Shikoku, Master Thesis, Kanazawa Univ., Japan, 1978.
- Torii, M., Paleomagnetism of Miocene rocks in the Setouchi province: evidence for rapid clockwise rotation of southwest Japan in middle Miocene time, Ph. D. Thesis, Kyoto Univ., 1983.
- Tosha, T., and Y. Hamano, Paleomagnetism of Tertiary rocks from the Oga Peninsula and the rotation of northeast Japan, *Tectonics*, 7, 653-662, 1988.
- Tsukahara, H., and R. Ikeda, Crustal stress orientation pattern in the central part of Honshu, Japan, stress provinces and their origins, *Jour. Geol. Soc. Jpn.*, 97, 461-474, 1991.
- Tsukahara H., and Y. Kobayashi, Crustal stress in central and western parts of Honshu, Japan, *J. Seism. Soc. Jpn.*, 44, 221-231, 1991.
- Tsunakawa, H., A. Takeuchi, and K. Amano, K-Ar ages of dikes in southwest Japan, *Geochemical J.*, 17, 265-268, 1983a.
- Tsunakawa, H., A. Takeuchi, and K. Amano, K-Ar ages of dikes in northeast Japan, *Geochemical J.*, 17, 269-275, 1983b.
- Tsunakawa, H., Neogene stress field of the Japanese arc and its relation to igneous activity, *Tectonophysics*, 124, 1-22, 1986.
- Ui, H., Geological structure along the Median Tectonic Line, east of Mikawa-Ono, central Japan, *Mem. Geol. Soc. Jpn.*, 18, 69-78, 1980.
- Uyeda, S., and H. Kanamori, Back arc opening and the mode of subduction, *J. Geophys. Res.*, 84, 1049-1061, 1979.
- Viallon, C., P. Huchon, and E. Barrier, Opening of the Okinawa basin and collision in Taiwan: a retreating trench model with lateral anchoring, *Earth Planet. Sci. lett.*, 80, 145-155, 1986.
- Vilotte, J. P., M. Daignières, and R. Madariaga, Numerical modeling of intraplate deformation: simple mechanical models of continental collision, *J. Geophys. Res.*, 87, 10,709-10,728, 1982.
- Vilotte, J. P., M. Daignieres, R. Madariaga, and O. C. Zienkiewicz, The role of a heterogeneous inclusion during continental collision, *Phys. Earth Planet. Int.*, 36, 236-259, 1984.
- Vilotte, J. P., R. Madariaga, M. Daignieres, and O. C. Zienkiewicz, Numerical study of continental collision: influence of buoyancy forces and an initial stiff inclusion, *Geophys. J. R. Astr. Soc.*, 84, 279-310, 1986.
- Von Huene, R., and S. Lallemand, Tectonic erosion of the Japan and Peru convergent margins, *Geol. Soc. Am. Bull.*, 102, 704-720, 1990.
- Wang, J. M., The Fenwei rift and its recent periodic activity, *Tectonophysics*, 133, 257-275, 1987.
- Weissel, J. K., Evidence for Eocene oceanic crust in the Celebes basin, in: Hayes D. E., Ed., The tectonic and geologic evolution of southeast Asian seas and islands, *Geophys. Monogr.*, AGU, Washington, 27, 37-47, 1980.
- Westphal, M., and J. P. Pozzi, Paleomagnetic and plate tectonics constraints on the movement of Tibet, *Tectonophysics*, 98, 1-10, 1983.
- Xu, J., G. Zhu, W. Tong, K. Cui, and Q. Liu, Formation and evolution of the Tancheng-Lujiang wrench fault system: a major shear system to the northwest of the Pacific Ocean, *Tectonophysics*, 134, 273-310, 1987.
- Xu, X. and X. Ma, Geodynamics of the Shanxi rift system, *Tectonophysics*, 208, 325-340, 1992.
- Yamagishi, H. and Y. Watanabe, Change of stress field in Late Cenozoic, Southwest Hokkaido, Japan, - investigation of geologic faults, dykes, ore veins and active faults, *Monograph Geol. Collabor. Jpn.*, 31, 321-332, 1986.
- Yamaji, A., Rapid intra-arc rifting in Miocene Northeast Japan, *Tectonics*, 9, 365-378, 1990.
- Yamamoto, H., Submarine geology and post-opening tectonic movements in the southern region of the Sea of Japan, *Mar. Geol.*, 112, 133-150, 1993.
- Yamamoto, T., and H. Hoshizumi, Stratigraphy of the Neogene system in the Tango peninsula, eastern part of the San-in district, southwest Japan, and associated Middle Miocene volcanism, *Jour. Geol. Soc. Jpn.*, 94, 769-781, 1988.
- Yamamoto, T., Late Cenozoic dike swarms and tectonic stress field in Japan, *Bull. Geol. Surv. Japan*, 42, 131-148, 1991.
- Yamazaki, T., Paleomagnetism of Miocene sedimentary rocks around Matsushima bay, northeast Japan, and its implication for the time of the rotation of northeast Japan, *J. Geomag. Geoelectr.*, 41, 533-548, 1989.

- Yamazaki, K., T. Tamura, and I. Kawasaki, Seismogenic stress field of the Japan sea as derived from shallow and small earthquakes, *J. Seismol. Soc. Japan*, 38, 541-558, 1985.
- Yang., Z., and J. Besse, Paleomagnetic study of Permian and Mesozoic sediments from northern Thailand supports the extrusion model for Indochina, submitted to *JGR*, 1994.
- Yoshida, T., Tertiary Ishizuchi cauldron, southwestern Japan arc: formation by ring fracture subsidence, *J. Geophys. Res.*, 89, 8,502-8,510, 1984.
- Yoshida, Y., and K. Abe, Source mechanism of the Luzon, Philippines earthquake of July 16, 1990, *Geophys. Res. Lett.*, 19, 545-548, 1992.
- Yoshioka, S., The interplate coupling and stress accumulation process of large earthquakes along the Nankai trough, southwest Japan, derived from geodetic and seismic data, *Phys. Earth Planet. Int.*, 66, 214-243, 1991.
- Yoshioka, S., T. Yabuki, T. Sagiyama, T. Tada, and M. Matsu'ura, Interplate coupling and relative plate motion in the Tokai district, central Japan, deduced from geodetic data inversion using ABIC, *Geophys. J. Int.*, 113, 607-621, 1993.
- Zakharov, V. K., and G. G. Yakushko, Modern vertical crustal movement in southern Sakhalin as determined by repeated surveying, *Dokl. Akad. Nauk SSSR, Engl. Transl.*, 207, 45, 1972.
- Zanyukov, V. N., The central Sakhalin fault and its role in the tectonic evolution of the island (in Russian), *Dokl. Akad. Nauk SSSR*, 196, 913-916, 1971.
- Zhang Peizhen, B. C. Burchfield, P. Molnar, Zhang Weiqi, Jiao Dechen, Deng Qidong, Wang Yipeng, L. Royden and Song Fangmin, Amount and style of late Cenozoic deformation in the Liupan Shan area, Ningxia autonomous region, China, *Tectonics*, 10, 1111-1129, 1991.
- Zhao, W. L., and W. J. Morgan, Uplift of Tibetan plateau, *Tectonics*, 4, 359-369, 1985.
- Zhao, Y. A., D. V., Helmberger, and D. G. Harkrider, Shear velocity structure of the crust and upper mantle beneath the Tibetan plateau and southeastern China, *Geophys. J. Int.*, 105, 713-730, 1991.
- Zoback, M. L., First- and second-order patterns of stress in the lithosphere: the world stress map project, *J. Geophys. Res.*, 97, 11,703-11,728, 1992.
- Zonenshain, L.P., and L.A. Savostin, Geodynamics of the Baikal rift zone and plate tectonics of Asia, *Tectonophysics*, 76, 1-45, 1981.
- Zonenshain, L. P., M. I. Kuzmin, and L. M. Natapov, Geology of the USSR: A plate-tectonic synthesis, in *Geodyn. Ser.*, vol. 21, edited by B. M. Page, pp. 242, AGU, Washington, D. C., 1990.

ANNEXE 1



KINEMATICS, TOPOGRAPHY, SHORTENING, AND EXTRUSION IN THE INDIA-EURASIA COLLISION

Xavier Le Pichon, Marc Fournier, and Laurent Jolivet
 Laboratoire de Géologie, Département Terre-Atmosphère-Océan, Ecole Normale Supérieure, Paris, France

Abstract. We examine the problem of partitioning between shortening and extrusion in the India-Asia collision since 45 Ma. We compute the amount of shortening expected from the kinematics of India's motion with respect to Eurasia, using the reconstruction at collision time to put bounds on the possible amounts of surface loss within Greater India and within Eurasia. We then compute the amounts of surface loss corresponding to the thickened crust of Tibet and of the Himalayas, assuming conservation of continental crust. The spatial distribution of the topography reveals a large systematic deficit of crustal thickening distributed rather uniformly west of the eastern syntaxis but an excess of shortening east of it. This distribution indicates an important eastward crustal mass transfer. However, the excess mass east of the eastern syntaxis does not account for more than one third to one half of the deficit west of the eastern syntaxis. The deficit may be accounted either by loss of lower crust into the mantle, for example through massive eclogitization, or by lateral extrusion of nonthickened crust. A mass budget of the crust of the Himalayas indicates that lower crust has not been conserved there, but the deficit is so large that local loss in the mantle is unlikely to be the unique cause of the deficit. Alternatively, following Zhao and Morgan [1985], lower crust may have been transferred below the Tibetan crust. We conclude that a combination of possible transfer of lower crust to the mantle by eclogitization and lateral extrusion has to account for a minimum of one third and a maximum of one half of the total amount of shortening between India and Asia since 45 Ma. This conclusion leaves open the possibility that the partitioning between extrusion and loss of lower crust into the mantle on the one hand and shortening on the other hand has significantly changed during the 45 m.y. history of the collision.

INTRODUCTION

The indentation of India has resulted in deformation distributed over a vast area of the Asian continent. A major unresolved problem concerns the quantitative partitioning of the deformation between shortening (through thickening) and extrusion [e.g., Tapponnier et al., 1986; Dewey et al., 1989]. In this

paper, we compute the amount of surface shortening expected from the kinematics of India with respect to Asia since collision and use the reconstruction at collision time to put bounds on the amounts of shortening within Greater India and within Asia. We compare these estimates to the amount of surface shortening implied by the topography of Asia around India, in order to determine the relative amounts of shortening and extrusion and to discuss their spatial distribution.

SHORTENING BETWEEN INDIA AND EURASIA FROM PLATE KINEMATICS

Patriat and Achache [1984] derived fairly precise relative motions of India with respect to Eurasia using the detailed Indian Ocean magnetic data published by Patriat [1983]. Since this paper, several reconstructions of the motion of India with respect to Eurasia have been published [e.g., Besse and Courtillot, 1988; Dewey et al., 1989]. Although all solutions indicate a dramatic slowdown of the northward relative motion of India and some reorientations of the motion from anomalies 24 to 30, significant differences still exist because the reconstructions require summing the motions of three ridge plate boundaries with relatively large uncertainties. However, the amounts of shortening obtained with these different solutions are not significantly different for our purpose. We will demonstrate this by comparing the solution we use with the solution published by Dewey et al. [1989].

We have chosen the kinematic parameters of Besse and Courtillot [1988] for anomalies 6 and 21. Anomaly 6 is given as 23 Ma in the Harland et al. [1982] scale they adopt. We choose instead to adopt the more recent scale of Kent and Gradstein [1986] which gives an age of 20.5 Ma. Similarly, for anomaly 21, we use an age of 49 Ma instead of 48.5.

We adopt the pole given by De Mets et al. [1990] for the present motion of India with respect to Asia (see Table 1). This pole takes into account shortening between India and Australia along the eastern equatorial Indian Ocean. We assume that this shortening started 7 m.y. ago as indicated by the dating of a widespread unconformity marking the onset of deformation [Leg 116 Shipboard Scientific Party, 1987]. Royer and Chang's [1991] kinematic study suggests that the deformation may have started earlier, between anomalies 5 (10.5 Ma) and 6 (20.5 Ma), but the available geologic evidence does not confirm this hypothesis.

Discussions of the amount of shortening absorbed within the India-Eurasia collision are generally made in terms of linear motion. However, the shortening is obviously at least partly redistributed in a rather complex way, and we consequently need areal estimates of shortening [Zhao and Morgan, 1985]. The rate of surface shortening along a portion of boundary AB is

$$\dot{S}_{AB} = \int_A^B \vec{v} \cdot \hat{n} ds$$

TABLE 1. India-Eurasia Relative Rotations

Rotation Pole				
Age, Ma	North	East	Angle	Reference
0-7	24.4°	17.7°	3.7°	1
7-20.5	16.7°	38.9°	10.0°	2
20.5-49	14.4°	35.0°	19.7°	3

References are 1, De Mets et al. [1990]; 2, anomaly 6 [Besse and Courtillot, 1988]; and 3, anomaly 21 [Besse and Courtillot, 1988].

where \vec{v} is the relative velocity across this boundary and \hat{n} is the unit vector normal to the boundary. But

$$\vec{v} \cdot \hat{n} ds = \omega R^2 \cos \varphi d\varphi$$

where φ is the Eulerian latitude, R the radius of the Earth, and ω the rate of rotation. Thus

$$\dot{S}_{AB} = \omega R^2 (\sin \varphi_B - \sin \varphi_A)$$

and only depends on the Eulerian latitude of the two extremities of boundary considered. For a finite length of time t ,

$$\Delta S_{AB} = \dot{S}_{AB} \cdot t$$

Thus ΔS_{AB} is independent of the actual shape of the portion of boundary between points A and B.

We compute the amount of shortening between the western (point A) and eastern (point B) syntaxes (Figure 1). Point C, close to Karachi (25°N, 66°E), and D, close to Rangoon (16°N, 97°E), mark the southern limits of the western and eastern limbs (Figure 1). The eastern limb is transform and there is no significant shortening across it, whereas some shortening, which we compute, occurs along the western limb (between point C and point A). Table 1 gives the parameters of reconstruction. Tables 2, 3, and 4 give the main results of the computations. Figure 1 shows the path of India relative to Eurasia in its present position.

Collision Time

As mentioned earlier, all kinematic solutions reveal a major slowdown and some reorientation of the relative motion between anomalies 24 (56 Ma) and 20 (46 Ma). Besse and Courtillot [1988] showed that paleomagnetic data also indicate a rather sharp slowdown of the meridional component of convergence between India and Eurasia sometime between 55 and 40 Ma.

Although the kinematic uncertainties are still too large to choose unambiguously a collision time within this 55-40 Ma window, one can get some indirect estimates of the collision time from the now well-understood kinematics of the Central Indian

Ocean Ridge which was situated directly south of India and presumably was most affected by any change in the "absolute" motion of India. Patriat [1983] had shown that this ridge was affected by a major reorganization between anomalies 20 and 18 (46 and 43 Ma) and that a sharp slowdown of the opening rate from 16 to 10 cm yr⁻¹ occurred earlier, between anomalies 22 and 21 (51 and 49 Ma). The less detailed but more constrained analysis of Royer and Sandwell [1991] confirms these results. The spreading velocity is very stable at 5-6 cm yr⁻¹ after anomaly 18 (43 Ma). The only significant reorganization of spreading occurs between anomalies 20 and 18 (46 and 43 Ma). Thus the conclusion of Dewey et al. [1989] that the main collision occurred near 45 Ma seems quite reasonable from a kinematic point of view and we adopt it.

Geologic evidence indicates that the northern Tethys margin was an Andean type margin with active shortening in Upper Cretaceous time. Volcanic activity continued into lower Eocene [Mercier et al., 1987; Searle et al., 1987]. Ophiolites were obducted onto this margin in Upper Cretaceous time (the Xigaze ophiolites) in the main part of the range [Mercier et al., 1987]. Farther to the west, ophiolites were obducted on the southern margin sometime in early Paleocene [Searle et al., 1987] at a time when India was situated very far from Asia. According to Mercier et al. [1987, p. 277] "the first deformations which clearly demonstrate that an India-Asia collision occurred took place subsequent to early Eocene time". This is the time at which neritic limestones, present both on the northern and southern margins, are deformed and the whole belt emerges. Conglomerates are then deposited in the Zang Po suture zone on top of a presumably trench melange [Searle et al., 1987]. Thus, although some evidence of tectonic activity, possibly due to collision with offshore arcs, exists on the Asian margin since Upper Cretaceous time, the geologic evidence suggests that true continental collision occurred in middle Eocene time, near 45 Ma, and was active along the whole boundary at the latest by the end of Eocene (37 Ma).

Treloar and Coward [1991] argue that the collision occurred first in the western syntaxis, near 55-50 Ma and then at about 45 Ma in the main part of the range. There is little geologic evidence indicating significant differences in timing of orogeny between these two

zones (see the compilation of Searle et al. [1987]) and the main argument in favor of this hypothesis comes from the present diamond shape of India and the fact that the eastern syntaxis was situated 1300

km farther south than the western one at collision time. We will come back to this point later when discussing the former configurations of Greater India and Asia.

Shortening Since 45 Ma

Tables 2 to 4 summarize the main results of our kinematic analysis. The total distances traveled by the western syntaxis (point A) and eastern syntaxis (point B) since 45 Ma are 2150 km and 2860 km, respectively, corresponding to average velocities of 48 and 64 mm yr⁻¹. The velocities were very stable until 7 Ma and then decreased somewhat (Table 2).

However, we are more interested in shortening distances perpendicular to the boundary. The distance components at A and B, perpendicular to the great circle joining A to B, are reduced to 1850 km and 2600 km, respectively.

The shortening velocity is constant before 7 Ma at 40 mm yr⁻¹ near A and 60 mm yr⁻¹ near B (Table 3). There is thus a 50% increase in shortening velocity over the 2180 km AB distance. The obliquity of the motion with AB (the angle between the motion vector and the perpendicular to AB) is about 30° in the west and 20° in the east. This means that the obliquity with the arcuate mountain belt was about 50°–60° in the west but fairly small in the east.

A 20° clockwise rotation of the motion vectors occurred 7 m.y. ago [De Mets et al., 1990] with the formation of the equatorial Indian Ocean deformation zone. As a result, the obliquity between great circle AB and the motion vectors disappeared at this time (Table 2). Since 7 Ma, the Indian indentor has moved perpendicular to AB and the significant dextral component of motion along AB which existed previously has disappeared. The shortening velocity slightly increased at point A to 45 mm yr⁻¹ but decreased at point B to 55 mm yr⁻¹. Consequently, there is now only a 20% difference in shortening velocity between A and B compared to 50% prior to 7 Ma.

The total amount of surface elimination across AB since 45 Ma is 5×10^6 km² (Table 4), about twice the present surface of Tibet as noted by Zhao and Morgan [1985]. Across the western limb, between A and C, the surface elimination since 45 Ma is 1.8×10^6 km². The rate of surface elimination across AB since 45 Ma has been quite constant at 1.1×10^5 km² m.y.⁻¹ corresponding to an average shortening velocity of 51 mm yr⁻¹. The rate of surface elimination across AC was 0.43×10^5 km² m.y.⁻¹ prior to 7 Ma and decreased to 0.28 after 7 Ma, corresponding to velocities of 36 and 23 mm yr⁻¹, respectively. This sharp decrease 7 m.y. ago is due to the 20° rotation of the motion vectors at this time.

To conclude, the total amount of surface eliminated since 45 Ma, if collision was indeed complete at this time, is 6.8×10^6 km². The rate of elimination was constant through AB although a 35° to 25° right lateral obliquity disappeared 7 m.y. ago.

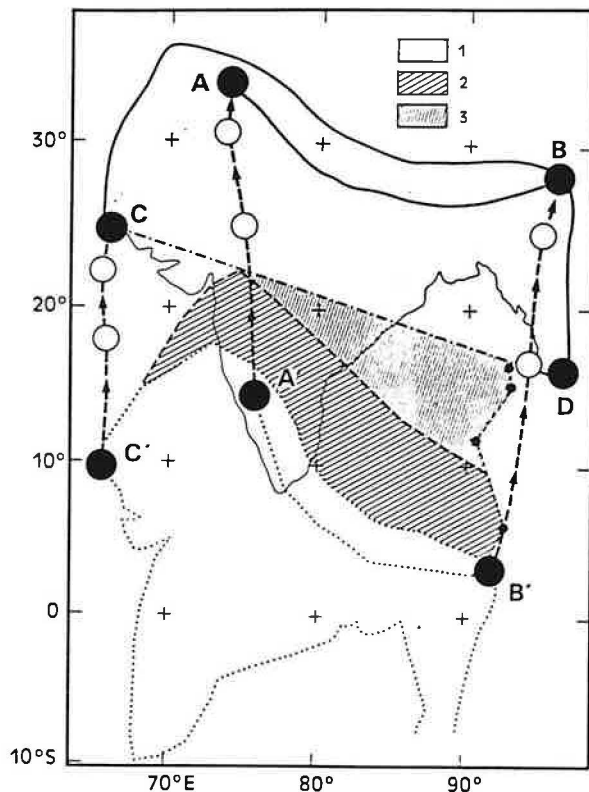


Fig. 1. Kinematics of India with respect to Eurasia since 45 Ma according to the parameters of Table 1. The position of India is shown 45 m.y. ago (A'B'C') and today (ABCD) in Eurasian coordinates. A and B correspond respectively to the western and eastern syntaxes of the Himalayas. C (near Karachi) and D (near Rangoon) define the approximate southern limits of the western and eastern branches of the transform-collision belts. Intermediate positions of ABC are shown at 20.5 Ma (anomaly 6) and 7 Ma by open circles. The outline of the Himalayas is taken along the Main Boundary Thrust to the south and the Indus Suture to the north. The eastward limit of northern Greater India at 45 Ma is shown by a dashed line joining small solid circles [after Powell et al., 1988]. It defines the maximum extent of Greater India. The minimum extent is based on estimates of shortening in the Himalayas. The minimum extent of former Asia is obtained by joining C to D. The maximum extent of former Asia would have extended southward to the minimum extent of Greater India. Note the probable presence of an oceanic gap northwest of A'C'. Patterns are 1, surface lost by Asia; 2, minimal surface lost by Greater India; and 3, maximum surface lost by Greater India.

The rate of elimination significantly decreased 7 m.y. ago through BC as the left lateral obliquity increased from about 35° to 55° .

Former Configuration of Greater India and of the Asian Southern Boundary

To derive the figure of $6.8 \times 10^6 \text{ km}^2$ of surface elimination, we have assumed that the whole boundary CAB was in collision 45 m.y. ago and that consequently there was no oceanic space left between India and Asia along this boundary. We mentioned earlier that Treloar and Coward [1991] have proposed that collision occurred a few millions years earlier near A than near B. This hypothesis poses the question of the former shapes of the northern border

of India and the southern border of Asia. It has been the subject of a large amount of debate summarized by Treloar and Coward [1991].

Figure 1 shows that India has penetrated within the Asian continent a distance of about 1250 km. As noted by Tapponnier et al. [1986], it is unlikely that India exactly docked within a preexisting indentation in Asia. Let us assume that this "hole" is indeed the result of Asian shortening and that consequently the boundary of Asia was along great circle CD. This crude assumption probably gives a minimum estimate of the Asian shortening, that is, $3.45 \times 10^6 \text{ km}^2$ (note that in this paper we integrate exactly the surfaces enclosed by the boundaries as given in the figures). This shortening may have resulted from crustal shortening and (or) lateral expulsion.

TABLE 2. Distance Traveled by Point and Average Velocity

Age, Ma	A		B		C	
	Distance	Velocity	Distance	Velocity	Distance	Velocity
0-7	314	45	385	55	284	41
7-20.5	651	48	898	67	500	37
20.5-45	1185	48	1574	64	934	38
0-45	2149	48	2857	64	1718	38

Point A refers to western syntaxis (33.5°N , 74°E), point B refers to eastern syntaxis (28°N , 96°E), and point C refers to the southern end of western limb (25°N , 66°E). Distance is in kilometers; average velocity is in millimeters per year.

TABLE 3. Velocity Azimuth, Obliquity, and Shortening Velocity

Age, Ma	A			B			C		
	V	O	S	V	O	S	V	O	S
0-7	5	5	45	17	-5	55	11	63	18
7-20.5	-13	33	40	4	24	61	-6	35	30
20.5-45	0	35	40	12	26	58	+6	30	33

V is velocity azimuth in degrees east; O is obliquity in degrees measured with respect to perpendicular to AB for A and B, positive to the west and to perpendicular to BC for C, positive to the north; S is shortening velocity in millimeters per year and equals velocity \times cos (obliquity).

TABLE 4. Surface Loss and Rate of Surface Loss

	0-7 Ma		7-20.5 Ma		20.5-45 Ma		0-45 Ma	
	Loss	Rate	Loss	Rate	Loss	Rate	Loss	Rate
A B	7.7	1.1	15.5	1.15	27.3	1.11	50.5	1.12
B C	2.0	0.28	5.8	0.43	10.6	0.44	18.4	0.41

Surface loss is in unit of 10^5 km^2 ; rate is in unit of $10^5 \text{ km}^2 \text{ m.y.}^{-1}$ through great circles AB and BC, respectively.

The distances between the positions of A and B 45 m.y. ago (A' and B' in Figure 1) and this assumed Asian boundary are then 600 and 1300 km, respectively. Coward et al. [1987] have measured a minimum amount of shortening of about 500 km near A in the Western Himalayas. Thus India should be extended by at least 500 km to the north near A'. Dewey et al. [1989] believe that as much as 1000 km may have been absorbed by shortening of Indian crust within the Himalayas. Molnar [1987], following Lyon-Caen and Molnar [1985], has estimated the post-Oligocene average Himalayan rate of shortening near 75° - 80° E at 18 ± 7 mm yr $^{-1}$ or 450 ± 175 km since 25 m.y. ago. Using the same rate, the shortening since 45 Ma would be 810 ± 315 km. We take the minimum amount shortening within the Himalayas as 600 km. Then, this minimum configuration of Greater India implies that about 20×10^5 km 2 have since disappeared by shortening or underplating. In this configuration, initiation of collision occurred 45 m.y. ago near A' with the minimal Asian configuration discussed above. However, near B', there was still a 700 km oceanic gap.

Powell et al. [1988] have argued that one can get some fairly precise information on the actual shape of the eastern Greater India configuration from the original fit of this margin with Australia. The fit they propose indicates that at the level of the present Himalayas, India could not extend to the east of the present 95° E longitude. Veevers and Powell [1979] argued further that the present structure of the Australian margin suggests that Greater India extended as far north as the Cape Range Fracture Zone, on the Australian eastern margin, corresponding to 40° N, 93.5° E in present India coordinates. This point is now situated on the northernmost boundary of Tibet and would imply that Greater India extended 1300 km north of the Indus Suture Zone near the eastern syntaxis. Figure 1 shows this eastern boundary of Greater India according to Powell et al. [1988]. The corresponding surface of Greater India beyond the Indus Suture Zone is 25.8×10^5 km 2 . This maximal configuration of Greater India would have achieved full collision 45 m.y. ago with the minimal former configuration of Asia shown in Figure 1.

We have seen that collision should be complete by the end of middle Eocene, some 42 m.y. ago because no neritic limestones were deposited on the Indian shelf beyond this date and because there is no more significant change in the Indian ocean spreading pattern after anomaly 18 (43 Ma). A 3 m.y. difference corresponds to a northward Indian motion of 180 km. However, collision is probably tectonically significant when the distance between the edges of the two shelves is less than 200-300 km. For example, compressive tectonics already effect the mantle in the Mediterranean Sea between Crete and Libya, which are about 300 km apart [Taymaz et al., 1991], and by the time the space is reduced to 100 km, there might be very little if any sea left there. Consequently, a maximum oceanic gap of about 300

km may have existed near B' 45 m.y. ago, and the remaining 400 km left open by the minimal configurations for Greater India and former Asia must be filled either by Indian crust, as in the solution of Powell et al. [1988] or by Asian crust, as in the solution of Tappognier et al. [1986] and Dewey et al. [1989].

In these latter two papers, the southern boundary of Asia is drawn between point C in Figure 1 and the Mentawai islands near 5° S, 100° E. The corresponding surface of Asia which has disappeared by shortening or expulsion is then 5.25×10^6 km 2 . However, with this configuration, the minimal Greater India would have begun its collision with Asia about 55 m.y. ago which is too early by 10 million years. Consequently the southern boundary of India must have been much closer to the minimal configuration chosen in Figure 1.

As a result, the range of possibilities to achieve full collision 45 m.y. ago along AB is relatively small. The total surface loss is $68-69 \times 10^5$ km 2 (see Table 4), but about 10% (6.5×10^5 km 2) correspond to oceanic space in front of B'C' on the western border of India. Consequently, about 62×10^5 km 2 of continental shortening should be given by a combination of Greater India surface shortening north of the Indus Suture Zone and Asian shortening. As argued above, this figure could be slightly reduced because collision might not have been complete everywhere between A and B 45 m.y. ago and because, if Powell et al. [1988] are correct, the eastern boundary of Greater India in its northern portion was situated to the east of flow line B'B (see Figure 1).

We conclude that the total amount of continental shortening and (or) expulsion since 45 Ma lies somewhere between 57×10^5 km 2 and 62×10^5 km 2 with 11.5×10^5 km 2 across AC and the balance across AB. We conclude further that Asian shortening has been between 34.5×10^5 km 2 and 42×10^5 km 2 and Greater Indian shortening between 20×10^5 km 2 and 25.8×10^5 km 2 . The ratio of Greater India versus total shortening varies between 30 and 45%.

The estimates of total continental shortening are fairly robust as they mostly depend on the initiation time of collision along the Himalayas (45 ± 2 Ma) because the kinematics of India relative motion are sufficiently well known. This will now be demonstrated by comparing our solution to the one proposed by Dewey et al. [1989].

Comparison With the Solution Proposed by Dewey et al. [1989]

We have made the same computations using the kinematic solution proposed by Dewey et al. [1989]. Dewey et al. use the Haq et al. [1987] chronology, which puts anomaly 20 at 44.7 Ma instead of 46.2 Ma in the scale of Kent and Gradstein [1986]. Using their chronology, the surface shortening across AB since 45 Ma is 5.2×10^6 km 2 and is 5×10^6 km 2 if

we use the Kent and Gradstein scale. Thus the surface shortening in both solutions is the same provided we use the same time scale.

The total distances traveled by A and B with respect to Asia since 45 Ma are 2290 and 3040 km in the Dewey et al. solution compared to 2150 and 2860 in our solution. The small differences result from a more complex and detailed path for the Dewey et al. solution as they have five intermediate positions of India between 45 Ma and now compared to two in our solution. However, their resulting velocities show abrupt changes at anomaly 8 (30% decrease), anomaly 5 (5% increase), and anomaly 3 (30% decrease again) which may simply reflect excessive detail in their kinematic solution. Note that the figures given here are different from the ones published by Dewey et al., which appear to be inexact.

Concerning the partitioning between shortening within Asia and shortening of the northern extension of Greater India, Dewey et al. [1989] limit India to the north to the Main Boundary Thrust in their reconstruction. They should have added to India the present width of the Himalayas (250 to 300 km) plus the shortening of the Himalayas which they consider to be about 1000 km. Then, the northern boundary of Greater India would have lain 1200 to 1300 km further north than drawn on their reconstructions and collision with the former configuration of Asia they adopt would have occurred much too early as discussed above.

Position of Southern Tibet From Paleomagnetic Data

The range of former Asian configurations previously considered acceptable indicates about 1250 km to 1900 km of latitudinal shortening between southern Tibet and Asia at the longitude of Lhasa. Achache et al. [1984] obtained a paleolatitude near Lhasa for Aptian-Albian (Takena formation) of $12.5^{\circ}\text{N} \pm 3^{\circ}$. A similar paleolatitude was found for Western Tibet for the same period [Chen et al., 1991]. Using the 110-100 Ma average paleomagnetic pole of Eurasia of Besse and Courtillot (1991), the latitudinal shortening between southeastern Tibet and Asia is 1300 km and between Southern Tibet and Asia 1500 which fits our conclusions. On the other hand, the Paleocene pole proposed by Achache et al. [1984] gives a larger 2000 to 2500 km amount of latitudinal shortening between southern Tibet and Asia since 60-50 Ma. This larger shortening is beyond the range of permissible Asian shortening given by our reconstruction. However, as pointed out by Achache et al., this result would have implied a relative latitudinal southward motion of Tibet with respect to Asia between 110-100 Ma and 60-50 Ma, at a time when the northern Lhasa block was already firmly accreted to Northern Tibet [Chang et al., 1986].

TOPOGRAPHY OF ASIA AND SHORTENING

We now investigate whether the Asian topography around India can account for the surface loss

computed in the previous section, assuming that the volume of crust is conserved and that its density is unchanged. We estimate quantitatively the distribution of topography using theETOPO 5 data base which gives an average altitude for each $5' \times 5'$ rectangle. Figure 2 shows the areas over which these estimates have been made. Zone 1 includes Tibet and the Himalayas but extends somewhat beyond the base of the steep slope. The area of $4.1 \times 10^6 \text{ km}^2$ thus is larger than the actual area of high plateau which explains the relatively small average elevation of 3.63 km. Zone 2 includes other regions of compressive tectonics considered to be related to the indentation of Asia. We have excluded to the east regions of extension and anomalously thin lithosphere in eastern China, around Shan Xi [Ma et al., 1984; Ma and Wu, 1987] and in Mongolia, southwest and south of the Baikal [Zorin et al., 1990]. Zone 3, finally, includes the western limb, west of 71°E .

Qualitative Description

Figure 3 shows 10 topographic profiles located in Figure 2 and oriented $N10^{\circ}\text{E}$, parallel to the present motion vector. The topography over India and to the north in Siberia is small. The average altitude of India south of the Himalayas is about 400 m, and the average altitude of the Siberia plain east of the Baikal region is less than 250 m.

The Tibet massif stands out clearly but cannot be differentiated from the Himalayas. Both have the same base altitude of about 5000 m as was noted by Bird [1978]. Several authors [Tapponnier and Molnar, 1976; Bird, 1978; England and Houseman, 1986; Zhao and Morgan, 1985; Molnar and Lyon-Caen, 1988] have discussed the formation of the uniform altitude of this high-standing plateau and have shown that it involves lateral spreading, most probably within the lower crust [Bird, 1991]. That lateral spreading occurs is suggested by the fact that the Tibetan Plateau extends about 600 km to the southeast beyond the eastern syntaxis [Dewey et al., 1989](see Figure 2 and profile 7 in Figure 3).

Finally, the width of the Tibetan Plateau increases from about 400 km (profiles 1 and 2) to 1100 (profiles 5 and 6) in a relatively smooth fashion from the western to the eastern syntaxis. This is a 175% increase whereas the increase in total kinematic shortening computed in the previous section is only about 40%. If Tibet is indeed the result of crustal shortening and (or) underthrusting, then there must be a drastic redistribution toward the east of the crust north of the indenter. Note, however, that because of the counterclockwise rotation of India (see Figure 1), the western syntaxis has migrated westward about 300 km with respect to Asia, this motion probably being absorbed in dextral faults such as the Karakorum fault [e.g., Armijo et al., 1986, 1989]. This westward migration of the western syntaxis does not agree with the hypothesis of Treloar and Coward [1991], who propose that the western syntaxis, which first indented Asia, was locked into

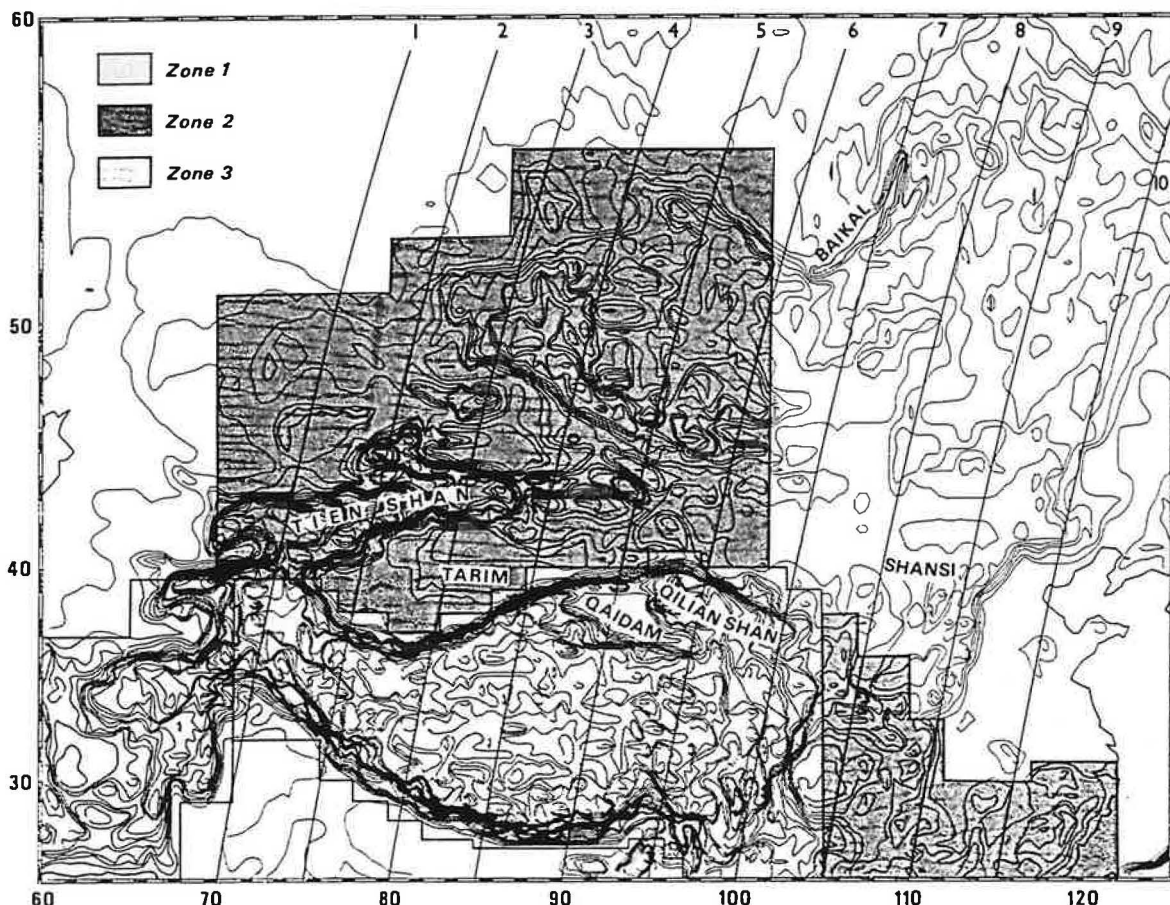


Fig. 2. Base topographic map used for the estimates of volume of topography after the ETOPO5 data base. Contours are every 200 m. A different pattern identifies the three zones: zone 1, Tibet; zone 2, west of 71°E; and zone 3 to the north and east. Locations of the 10 topographic profiles shown in Figure 3 are indicated.

its collision position. It could account on the other hand for a small part of the sharp westward decrease in width of Tibet.

To the north, two massifs stand out clearly, the Tien Shan (profiles 1 to 3) and the Altaï (profiles 3 to 6). That these massifs are related to the Indian indentation is now well established [Molnar and Tapponnier, 1975; Tapponnier and Molnar, 1976, 1977]. The Tien Shan could be considered as a northward extension of Tibet beyond the undeformed and apparently quite rigid Tarim basin (Figure 2 and profile 3 in Figure 3). In the same way, but on a smaller scale, the Qilian Shan appears to be a northward extension of Tibet beyond the small Qaidam basin (Figure 2 and profiles 5 and 6). The Altaï, on the other hand, has a different structure as it is dominated by strike-slip faulting resulting in a net NNE crustal shortening [Tapponnier and Molnar, 1979].

We exclude from our consideration northeastern China and Mongolia east of the Altaï massif because they are regions affected by extension and because the lithosphere is abnormally thin there, as discussed

above. Consequently, their average 1000 m elevation there may be due, at least in part, to the presence of a hotter mantle below.

Quantitative Description

That the topography discussed above is mostly the result of crustal thickening is beyond doubt. The thickness of crust from India to Tibet increases from 37-38 km south of the Himalayas [e.g., Sharma et al., 1991] to up to 75 km below Tibet [Hirn et al., 1984]. The average thickness of the Tibet crust is 70 km (Zhao et al., 1991) for an average topographic elevation of 5 km. The crust is about 35 km thick in southeastern China [Zhao et al., 1991]. A generalized isopach crustal thickness map of China based on gravity data is in agreement with these seismological determinations [e.g., Tan Tong Kie, 1987]. We can consequently assume a simple linear relationship between anomalous crustal thickness ΔT and topographic elevation h :

$$h = \Delta T/7$$

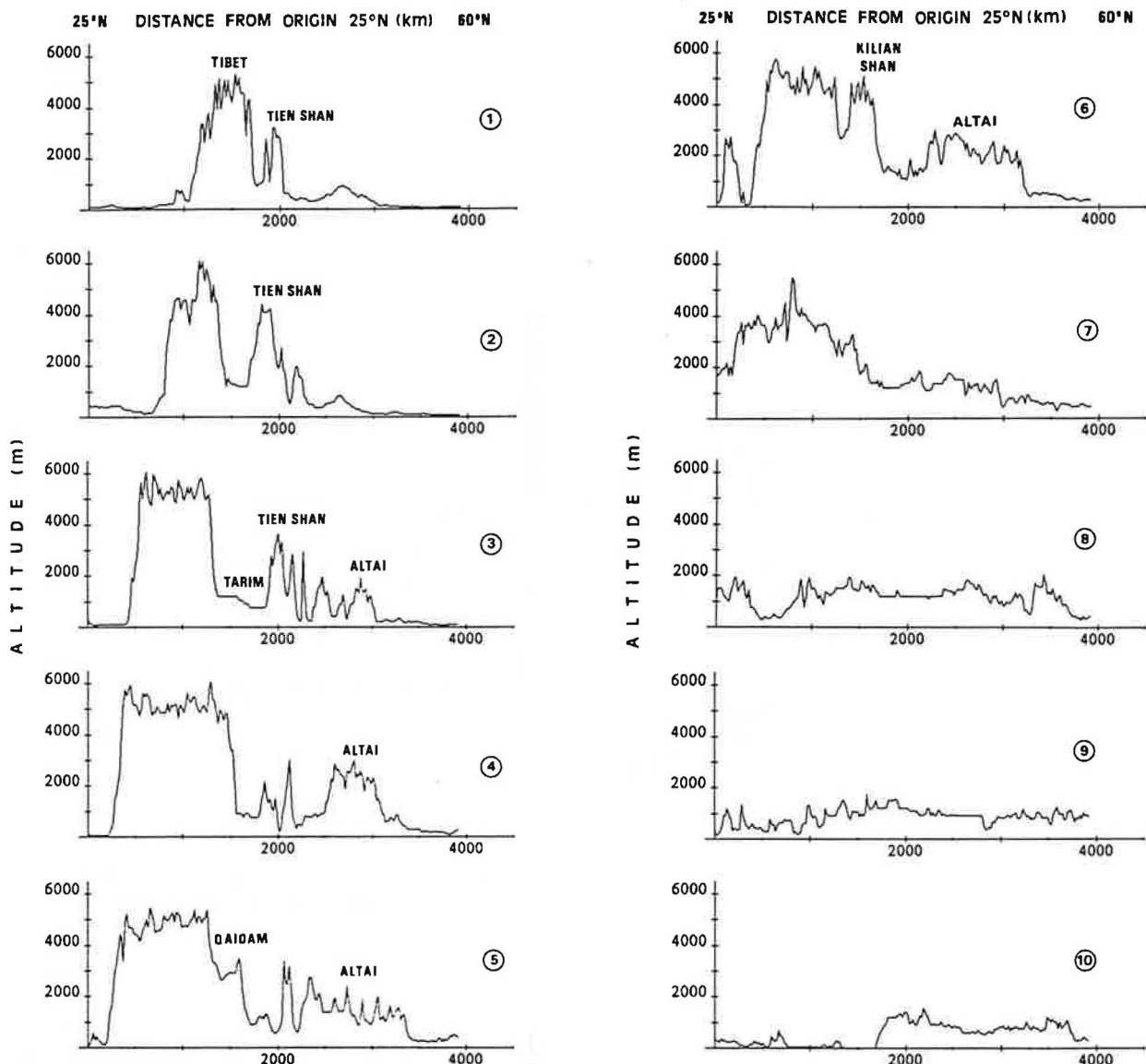


Fig. 3. Ten topographic profiles located in Figure 2 shown with a vertical exaggeration of 200. Note the low elevation in India to the south and Siberia to the north, the eastward widening of Tibet, and the progressive transfer of topography from Tien Shan to the west to Altai to the east. Note also the eastward extension of Tibet to profile 7, beyond the eastern Himalayan syntaxis, whereas the Altai topography does not extend that far eastward. Finally, note the relatively uniform 1000 m altitude of the profiles east of profile 7 in regions mostly dominated by extension.

where $\Delta T = (T - 35)$ km is the excess crustal thickness over 35 km, the adopted thickness for 0 elevation. This relationship gives a thickness of 38 km for India (elevation 400 m) and 70 km for Tibet (elevation 5 km) in agreement with the data.

With this relation, the cross-sectional surface S of the topography above sea level along a profile can be converted in the length of shortening ΔL which would have produced it, assuming plane strain shortening along the profile. We have

$$\Delta L = S/5$$

In the same way, the volume V of the topography above sea level within a given area can be converted in the surface elimination ΔA necessary to produce it. We have

$$\Delta A = V/5$$

In the following, the statistics we give along profiles are in kilometers of length of shortening. We do this because square kilometers of surface

topography along a profile are difficult to relate simply to crustal shortening. However, although our estimates of surface S are exact, the conversion in ΔL is only as valid as the assumptions we make. We will discuss the validity of these assumptions later.

Figure 4 shows estimates of equivalent linear shortening obtained along longitudinal profiles every 5°. The estimates are made over zone 1 (Tibet, middle curve) and zone 2 (Altaï, Tien Shan and South China, lower curve) (see Figure 2 for the localization of the zones). The equivalent shortening increases linearly from 71°E to 90°E from 600 to 1800 km. Then there is a relatively sharp drop to 1500 km at 95°E due to the Qaidam basin, an increase again to a maximum of nearly 2000 km near 98°E, and finally a very steep drop to less than 400 km beyond 105°E.

Two obvious characteristics of this distribution should be noted. First, there is a broad maximum extending east of the eastern syntaxis between 90° and 100°E. It is 3 times larger than the value at the western syntaxis. Second, there is a regular linear increase in the amount of shortening from west to east. This strongly asymmetrical distribution is different from the one expected if linear shortening in front of the indenter were exactly related to its relative motion. Then, one would expect a 40% sinusoidal increase from 71° to 95°E and an abrupt decrease beyond these two points instead of the 200% linear

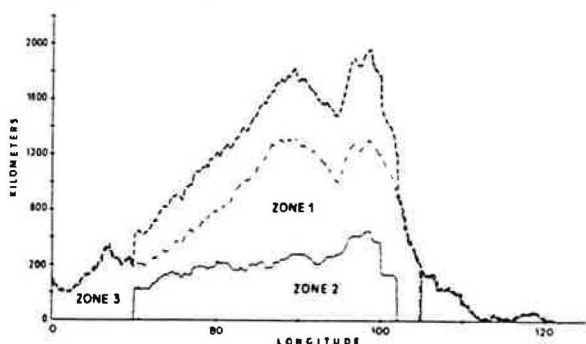


Fig. 4. Equivalent linear shortening in kilometers versus longitude computed for each N-S profile in zone 2 (lower curve), zone 1 (Tibet, middle curve), and combined zones 1, 2, and 3 (upper curve). The shortening is assumed to be purely N-S. There is no correction for nonzero 45 Ma elevation and post-45 Ma erosion. See text for discussion.

increase and the extension of the maximum east of 95°E.

Consider now the shortening corresponding to the excess crust outside of Tibet, in zone 2 (lower curve on Figure 4), essentially within the Tien Shan and Altaï massifs. It increases relatively regularly from about 250-270 to a maximum of 500-600 near 98°E. Beyond 100°E, the sharp drop results from the exclusion of regions of thin lithosphere and extension. However, even if one included these regions, the curve would continue to decrease progressively. Thus the maximum, north of Tibet, is centered at the same longitude as for Tibet. The increase from west to east is also approximately linear and in a ratio of about 2. Finally, the transition between Tien Shan and Altaï (see Figure 2) is impossible to detect in Figure 4. Thus there is a progressive shift in topography from Tien Shan to Altaï across the overlap region.

Table 5 gives the volumes of topography over the three areas. The total amount of $23 \times 10^6 \text{ km}^3$ is identical to the value found by England and Houseman [1986] over a similar area. Table 6 gives the corresponding surface of shortening assuming a zero topography base level prior to collision. With the relation adopted above, the surface in square kilometers is 0.2 of the volume in cubic kilometers. Three millions square kilometers of surface elimination are stored in the crust of Tibet compared to 1.2 km^2 in zone 2 north of Tibet and 0.35 km^2 in zone 3 for a total of $4.55 \times 10^6 \text{ km}^2$. Thus two thirds of the excess crust due to shortening is stored within Tibet and one fourth north of it in Tien Shan and Altaï. This total figure of $4.55 \times 10^6 \text{ km}^2$ should be compared to the 5.7×10^6 to $6.2 \times 10^6 \text{ km}^2$ surface elimination obtained from kinematic considerations in the first section.

England and Houseman [1986] used a more complex relation between topography and crustal thickness which takes into account isostatic balance to the base of the lithosphere. They use two extreme cases. In a first one, their solution gives a 25.3 km crust for zero elevation and 64 km for 5 km elevation. This solution does not fit the Asian data. In a second one, they obtain 34.5 and 71.5 km, respectively, which are close to the values we choose. Thus their second solution best fits the present Asian data and gives results close to ours.

Effects of Preexisting Topography and Erosion

However, we need to discuss the limitations of the rather drastic hypothesis we made to convert

TABLE 5. Volumes of Topography

	Zone 1	Zone 2	Zone 3	Total
Surface area (10^6 km^2)	4.13	5.24	1.30	10.67
Average altitude (km)	3.63	1.17	1.29	2.14
Volume (10^6 km^3)	15.00	6.12	1.68	22.80

topography into surface loss because we have ignored any preexisting topography and we have also ignored erosion. These two effects act in opposite directions, and we now try to estimate them.

The present base level of topography in India, to the south, is about 400 m and in Siberia, to the north, about 250 m as discussed above. Thus one should use a minimum base level of 250 to 400 m. However, one might expect a somewhat higher elevation in the center of the former continent. Yet, to the north of Tibet, in Tien Shan and Altaï, the topography is considered to have been a peneplain until late Oligocene, presumably as in the Siberian plains today [Zonenshain and Savostin, 1981]. Thus we assume a base level of 500 m (corresponding to a crustal thickness of 38.5 km) in zone 2. We do the same for zone 3.

Tibet was subaerial 45 m.y. ago as the last marine sediments deposited there are Mid-Cretaceous [e.g., Mercier et al., 1987]. We mentioned earlier that an Andean type margin was active on its southern margin during Upper Cretaceous and that volcanic activity continued until the collision. However, the Paleocene-Eocene volcanics were deposited on an erosion surface, and the climate was warm, wet subtropical to tropical [Mercier et al., 1987]. It is considered that the altitude was definitely less than 1000 m [e.g., Dewey et al., 1988]. In northern Tibet, Paleogene red beds indicate an arid subtropical climate believed to correspond to a low altitude. One could then conclude that the average altitude was 1000 m or smaller to the south and a few hundreds of meters to the north. Thus the average altitude of Tibet was possibly more than 500 but most probably less than 1000 m. This conclusion is more conservative than that of most previous authors [e.g., England and Houseman, 1986; Mercier et al., 1987; Dewey et al., 1989], who assumed an average elevation equal or smaller than 500 m for Tibet prior to collision.

Table 6 shows estimates corrected for a 500 m base level in zones 2 and 3 and for both a 500 m and a 1000 m base level in zone 1. The total area loss then decreases by 30 to 40% with respect to the zero base level case. Note that the computations have been made assuming local shortening of the crust. Slightly larger figures would be obtained for underthrusting by a normal thickness crust.

We next consider the effect of erosion. Most of the debris of the Himalayan chain lies within the Bengal and Indus fans and within the Ganga basin. Tibet itself has not been affected by a large amount of erosion [Zhao and Morgan, 1985; England and Houseman, 1986]. Copeland and Harrison [1990] estimate 1.5×10^7 to 2.0×10^7 km³ of sediments to be present in the Bengal fan. The map of post-Eocene sediments in the Bengal fan published by Curray [1991] appears to indicate a value close to 1.25×10^7 km³. There is about one fifth that amount in the Indus fan and about 10^6 km³ in the Ganga basin [Lyon-Caen and Molnar, 1983]. Thus a total of 19×10^6 to 25×10^6 km³ of sediments appears to be now present in these fans and basin. Taking into account a 10% decrease in density of the sediments with respect to whole rocks [Lyon-Caen and Molnar, 1983], this amount could be produced by the erosion of 0.45×10^6 to 0.60×10^6 km² of a 38.5 km thick crust. We assume that an additional amount equivalent to 0.10×10^6 to 0.15×10^6 km² of surface loss fills the Neogene basins north of Tibet. Then, the total amount of surface loss corresponding to the eroded sediments is about 0.6×10^6 to 0.75×10^6 km². We have ignored sediments from the Himalayas now stored within the Makran accretionary prism and within the Indo-Burman ranges. On the other hand, the estimate of Copeland and Harrison [1990] appears quite high compared to the latest estimate by Curray [1991]. Thus we estimate that the amount of erosion is unlikely to be significantly larger than the estimate we give.

Table 6 then shows that the corrected total amount of surface loss varies from 5.1×10^6 to 5.3×10^6 km² for zero base level (highly unlikely), to 3.2×10^6 to 3.4×10^6 for 500 m base level for zones 2 and 3 and 1000 m base level for zone 1. For the preferred case of 500 m base level everywhere, we obtain 3.75×10^6 to 3.95×10^6 km² to be compared to 5.7×10^6 to 6.2×10^6 computed from kinematic considerations. Consequently, even in the highest and unrealistic zero base level estimate, there is still a deficit of 10% between the shortening stored in the topography and the kinematic shortening.

TABLE 6. Area Loss Corresponding to Excess Crust

	Zone 1	Zone 2	Zone 3	Total	Total + Erosion
Zero base level	3.00	1.22	0.34	4.56	5.1-5.3
500 m base level (all zones)*	2.35	0.64	0.19	3.18	3.75-3.95
500 m (II, III)*	1.81	0.64	0.19	2.64	3.20-3.40
1000 m (I) [#]					

Area loss is in unit of 10^6 km².

* Crust is 38.5 km thick for 500 m topography.

Crust is 42 km thick for 1000 m topography.

Depending on the base level chosen, somewhere between 500 m everywhere and 1000 m in Tibet, the deficit is 1.75×10^6 to 3.00×10^6 km 2 . To account for this deficit without extrusion, Dewey et al. [1989] have proposed that the continental crust entering the Himalayan collision zone during the early collision (upper Eocene to perhaps Oligocene) was much thinner than the present 38.5 km crust. If this were true, the deficit can indeed be reduced and even altogether eliminated. However, if the shortened upper Eocene to Oligocene crust was very thin, the expected paleo-water depth would be at least 1 to 2 km. However, we have seen that there is no evidence of marine sediments older than 45 Ma in the Himalayas and that the 45 Ma marine sediments were deposited in shallow seas. We thus assume that both Indian and Tibetan crusts implicated in the collision were subaerial and consequently of "normal" thickness at times later than 45 Ma. The computed deficit presumably corresponds to lateral extrusion or to crust transferred to the mantle by eclogitization.

Longitudinal Variation in Deficit

We may try to go further and estimate the deficit as a function of longitude comparing the estimates of equivalent total linear shortening (shown in Figure 4) to the estimates of kinematic shortening made in the first section. We correct for erosion and distribute the 0.75×10^6 km 2 corresponding area lost between 65° and 105° E adding uniformly 200 km to the profiles between 72.5° and 102.5° E but only 100 km west and east of these longitudes. Figure 5 shows this comparison both for the unlikely 0 m base level, which is an absolute maximum, and for the most probable 500 m base level, considered most likely.

There is a fairly uniform deficit of 600 km (0 m base level) to 950 km (500 m base level) west of 96° E and a large excess to the east of it. The amount of the eastern excess shortening is 75% of the western rather uniform deficit in the first case but only 33% in the second one. A simple interpretation is that the western deficit of 600 to 950 km has been transferred east of the eastern syntaxis. Part of this transfer resulted in eastward growth of Tibet, but the main part (probably about two thirds) corresponded to net lateral extrusion of continental crust. However, we still have to consider more closely the difficult problem of the amount of shortening absorbed in the Himalayas.

SHORTENING IN THE HIMALAYAS

Between 74° and 96° E, the Himalayas are limited by two concentric small circles, a southern one along the Main Boundary Thrust and a northern one along the Indus Suture Zone [e.g., Crawford, 1982, quoted in Klootwijk et al., 1985]. A best fit gives a center of the small circles near 42° N, 89° E. The average distance between the circles is 2.4° (265 km) and the length of the arc is 2400 km. The surface of the Himalayas between 74° and 96° E is then $5.9 \times$

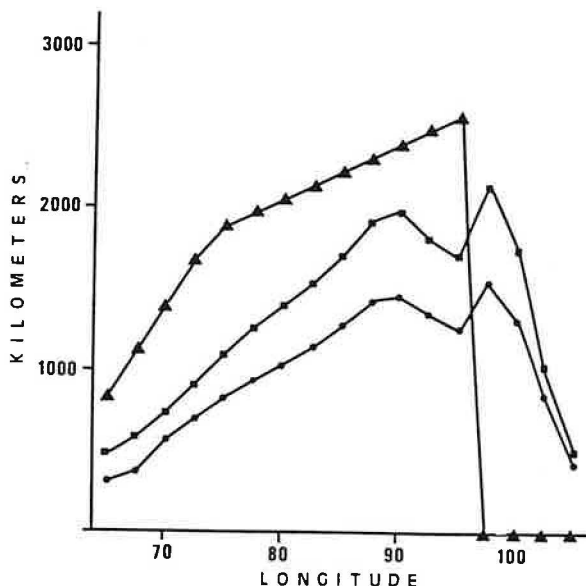


Fig. 5. The equivalent linear shortening as in Figure 4 is shown here corrected for erosion and for the 45 Ma topographic base level. It is compared to the expected linear shortening from kinematics (upper curve with triangles). Two cases are shown for two different topographic base levels at 45 Ma: the 0 m case (curve with squares) and the 500 m one (curve with small circles). See text for discussion.

10^5 km 2 . West of 74° E and east of 96° E, we estimate an additional 2×10^5 km 2 of surface for a total of 7.9×10^5 km 2 . Half of the chain is at Tibet altitude, the other half shows an increase from 500 to 5000 m. Thus the average altitude is 3.85 km.

The excess topography above 500 m is equivalent to a surface loss of 4.8×10^5 km 2 . We have to take into account the additional 18×10^6 to 24×10^6 km 3 of sediments stored in the plains and fans which come almost entirely from the erosion of the Himalayas. This represents 23 to 30 km of average erosion over the whole chain. Then, the surface loss is approximately doubled to 10^6 km 2 . This is equivalent to 300-350 km of average linear shortening. Consequently, as noted by Lyon-Caen and Molnar [1983], if the crust involved in the shortening of the Himalayas has been conserved within the chain, except for the part eroded, it is impossible to account for more than about 350 km of shortening.

Lyon-Caen and Molnar [1985] have used drill hole results in the Ganga plain to determine a rate of underthrusting of $10\text{-}15$ mm yr $^{-1}$ in the last 10-20 m.y. between 76° E and 81° E. Molnar [1987], taking into account 5 mm yr $^{-1}$ of probable strain within the belt itself increased the estimate to 18 ± 7 mm yr $^{-1}$ which is in the upper range of our estimate and

equivalent to 810 ± 315 km since 45 Ma as discussed earlier. If the crust involved in the shortening has been conserved within the mountain belt (except for erosion), the total shortening barely accounts for the last 20 m.y. and no pre-Miocene crust would be preserved in the present belt. This does not appear to be acceptable.

This difficulty led Dewey et al. [1989] to assume that a great part of the crust involved in Himalayas shortening was quite thin. We stated earlier that we cannot accept this solution because there is no evidence for marine sediments older than middle Eocene. However, another possibility is that only the upper part of the crust has been conserved within the mountain belt. Butler [1986] has indeed argued that the crust involved in the structure of the mountain belt is mostly upper crust. The palinspastic reconstruction of Coward et al. [1987] clearly shows the small thickness of preserved crust. Coward et al. [1987] assume that lower crust is somehow decoupled and transferred further north. In the same way, Zhao and Morgan [1985] assumed that the ductile lower crust is injected at depth below Tibet. Alternatively, part of the lower crust might be transferred to the mantle by eclogitization.

In any case, if only the brittle upper 20 km of crust are still preserved within the Himalayas [Le Pichon et al., 1988], the amount of shortening is increased to about 2.5×10^6 to 2.75×10^6 km 2 . The estimates of Greater India made earlier require between 2.0×10^6 and 2.5×10^6 km 2 of shortening. These figures correspond to an average thickness of preserved crust between 20 and 25 km out of the original 38.5 km. The corresponding average velocity of shortening along the Himalayas since 45 Ma is 15 to 18.5 mm yr $^{-1}$.

We conclude that, as an average, only the upper 20 to 25 km of Indian crust involved in the shortening within the Himalayas have been preserved in the mountain belt and that the lower portion of crust has been either transferred to the mantle or fed into Tibetan crust [Butler, 1986; Le Pichon et al., 1988]. The amount of lower crust involved is very large, about 5×10^7 km 3 . It is unlikely that such a large amount would have entirely disappeared below the relatively narrow belt. This solution would imply that the hidden roots of the Himalayas extend to 140 km depth. If the missing lower crust has been entirely transferred below Tibet [Zhao and Morgan, 1985], then about half of the topography of Tibet would be due to this process and half would be due to local shortening. In any case, it is difficult to escape the conclusion that the amount of surface loss in the Himalayas since 45 Ma is 2×10^6 to 2.5×10^6 km 2 . This amount implies an average linear shortening of 600 to 850 km, in fair agreement with the post-Oligocene average 18 ± 7 mm yr $^{-1}$ rate of shortening obtained by Molnar [1987] and with the seismic rate of underthrusting of 18 mm yr $^{-1}$ (with a large uncertainty) obtained by Molnar and Deng [1984].

CONCLUSIONS

Because the collision of Tibet with India is constrained by the reorganization of the kinematics of the Indian Ocean and by the geology of Himalayas and Tibet to have been completed at the end of middle Eocene, 45 m.y. ago, the total amount of continental surface lost between India and Eurasia can be estimated fairly precisely. Taking into account some oceanic space which probably existed 45 m.y. ago west of the Chaman fault (northwest of India), the total surface loss has to be less than 68×10^5 but more than 57×10^5 km 2 and probably lies between 57×10^5 and 62×10^5 km 2 . Most of this, 45×10^5 to 50×10^5 km 2 , occurred between the two syntaxes of the Himalayas; the balance was absorbed northwest of India west of the Chaman fault.

The total linear shortening increases from 1850 to 2600 km from the western to the eastern syntaxis. The rate of surface loss through the Himalayas was quite constant at 1.1×10^5 km 2 m.y. $^{-1}$ during these 45 m.y. in spite of an abrupt 20° clockwise reorientation of India's path 7 m.y. ago which eliminated the previous dextral component of motion.

To achieve full collision 45 m.y. ago along the Himalayas, it is necessary to assume between 35×10^5 and 42×10^5 km 2 of Asian surface loss and between 20×10^5 and 26×10^5 km 2 of Greater India surface loss. The amount of Asian surface loss corresponds to 1250 to 1900 km of longitudinal shortening between southern Tibet and Asia at the longitude of Lhasa. The ratio of Greater India surface loss to total surface loss varies between 30 and 45% for the two extreme solutions. Consequently, both Greater India shortening and Asian shortening are significant, the second one being, however, larger than the first one.

The distribution of crustal thickness in Asia, based on seismological measurements in India, southeastern China, and Tibet appears to have a simple linear relationship with altitude. Each kilometer increase in altitude corresponds to a 7 km increase in crustal thickness. The zero elevation crustal thickness is about 35 km. Using this simple relationship, we convert volumes of topography into surface loss assuming that crust is globally conserved during shortening. We estimate total area loss. We also estimate equivalent linear shortening along N-S profiles (assuming plane strain shortening along the profile) to examine the E-W distribution of shortening. The estimates are corrected for preexisting topography and erosion.

The amount of area loss corresponding to the topography is between 33×10^5 and 52×10^5 km 2 with a most probable value of 39×10^5 km 2 to be compared to the 57×10^5 to 62×10^5 km 2 of expected continental surface loss. The high value of 52×10^5 km 2 is highly unlikely as it assumes everywhere no preexisting topography (0 m altitude) 45 m.y. ago. We conclude that there is a deficit of 18×10^5 to 30×10^5 km 2 of shortening which must be

explained by lateral extrusion of crust and (or) by loss of lower crust into the mantle. We have excluded the alternative solution of anomalously thin Indian crust proposed by Dewey et al. [1989] because it would imply a significant depth of water during upper Eocene and lower Oligocene for which there is no evidence.

An important additional conclusion is that the deficit is distributed rather uniformly west of 95°E (the eastern syntaxis). Everything happens as if 600 to 950 km of linear shortening (depending on the solution chosen) had been transferred elsewhere. Part of this transfer can indeed be found in the excess topography between 95° and 105°E, but this excess topography cannot account for more than one third to one half of the deficit.

A budget of the volume of crust in the Himalayas indicates that the present crust of the Himalayas plus the eroded sediments cannot account for more than 10^6 km^2 of shortening of normal thickness crust or about 350 km of linear shortening as previously concluded by Lyon-Caen and Molnar [1983]. Butler [1986] has proposed that lower crust is not generally found in the belt. If this is correct, then the Himalayas can account for the $2 \times 10^6 \text{ km}^2$ (or more) of shortening proposed in this paper, in agreement with the post-Oligocene average rate of shortening [Lyon-Caen and Molnar, 1985; Molnar, 1987].

This conclusion could be taken as evidence that crust has not been conserved and that large amounts of crust have disappeared in the mantle [Le Pichon et al., 1988]. We prefer the hypothesis proposed by Zhao and Morgan [1985] that at least part of the lower crust missing has been transferred north of the Himalayas below Tibet and contributes to its general elevation. If all of the missing Himalayan lower crust has been transferred below Tibet, half of the elevation of Tibet would be due to local shortening and half to northward migration of Indian lower crust. That large scale migration of lower crust occurs is indicated by the relative uniformity of the

height of the Tibetan plateau as pointed out by Zhao and Morgan [1985] and Bird [1991] among others.

In any case, we believe that we have established that one third to one half of the continental surface loss due to collision between India and Asia has not resulted in crustal thickening and the associated topography and must have been accounted by an unknown combination of lateral extrusion and loss of crust in the mantle. If crust is conserved, lateral extrusion accounts for a maximum of one third to one half of the total amount of shortening between India and Asia since 45 Ma. This conclusion would be compatible with the proposals of Tapponnier and his coworkers [e.g., Tapponnier et al., 1986]. Alternatively, if a significant part of the lower crust has been eclogitized, the amount of extrusion could be reduced to as little as 10%, the minimum amount compatible with the eastward transfer of Tibetan crust. This conclusion leaves open the possibility that the partitioning between extrusion, shortening, and loss of lower crust into the mantle has significantly changed during the 45 m.y. history of the collision. For example, the Indonesian southward facing subduction zone was adjacent to the Indian indenter during the early collision, whereas they are now separated by more than 2000 km. In addition, Australia has been colliding with this subduction zone since upper Miocene. Clearly, lateral extrusion with southward migration of the Indian subduction zone must have been much easier during upper Eocene and Oligocene than since upper Miocene.

Acknowledgments. This paper had its origin in lectures given by the first author in College de France. We thank Nicolas Chamot-Rooke and Jean-Michel Gaulier for help in processing data and for discussions as well as Claude Rangin, Philippe Huchon, and Pierre Henry. We thank John Dewey, Peter Bird, and Kevin Burke for their reviews. John Dewey and Peter Bird insisted on the importance of eclogitization in the quantitative budget.

REFERENCES

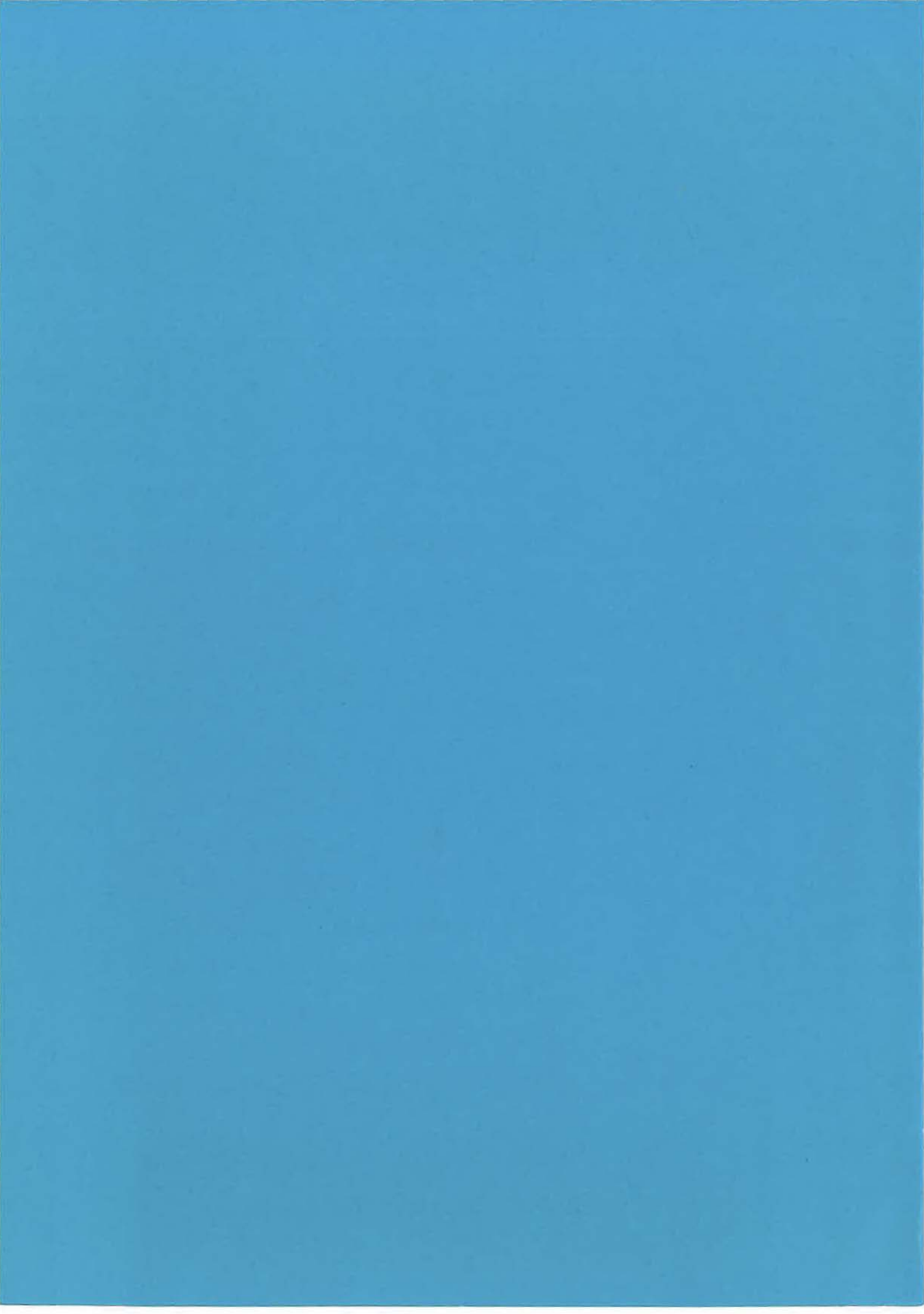
- Achache, J., V. Courtillot, and Y. Xiu, Paleogeographic and tectonic evolution of southern Tibet since middle Cretaceous time: New paleomagnetic data and synthesis, *J. Geophys. Res.*, 89, 10311-10339, 1984.
- Armijo, R., P. Tapponnier, J.L. Mercier, and H. T. Lin, Quaternary extension in Southern Tibet: Field observations and tectonic implications, *J. Geophys. Res.*, 91, 13803-13872, 1986.
- Armijo, R., P. Tapponnier, and H. Tonglin, Late Cenozoic right-lateral strike-slip faulting in Southern Tibet, *J. Geophys. Res.*, 94, 2787-2838, 1989.
- Besse, J., and V. Courtillot, Paleogeographic maps of the continents bordering the Indian Ocean since the Early Jurassic, *J. Geophys. Res.*, 93, 11791-11808, 1988.
- Besse, J., and V. Courtillot, Revised and synthetic apparent polar wander paths of the African, Eurasian, North American and Indian plates, and time polar wander since 200 Ma, *J. Geophys. Res.*, 96, 4029-4050, 1991.
- Bird, P., Initiation of intracontinental subduction in the Himalaya, *J. Geophys. Res.*, 83, 4975-4987, 1978.
- Bird, P., Lateral extension of lower crust from under high topography in the isostatic limit, *J. Geophys. Res.*, 96, 10275-10286, 1991.
- Butler, R.W.H., Thrust tectonics, deep structure and crustal subductions in the Alps and Himalaya, *J. G. Soc. London*, 143, 857-873, 1986.
- Chang, C., et al., Preliminary conclusions of the Royal Society and Academia Sinica 1985 geotraverse of Tibet, *Nature*, 323, 501-507, 1986.
- Chen, Y., J.P. Cogné, L. Bourjot, P. Tapponnier, V. Courtillot, and X. Zhu, Cretaceous paleomagnetic results from Western Tibet and tectonic implications (abstract), *Eos Trans. AGU*, 72, 103, 1991.
- Copeland, P., and T. M. Harrison, Episodic rapid uplift in the Himalaya revealed by the 40Ar/39Ar analysis of the detrital K-feldspar and muscovite, Bengal fan, *Geology*, 18, 354-357, 1990.
- Coward, M.P., R.W.H. Butler, M. A. Khan, and J. Kimpe, The tectonic history of Kohistan and its implications for Himalayan structure, *J. G. Soc. London*, 144, 377-391, 1987.
- Curry, J.R., Possible greenschist metamorphism at the base of a 22-km sedimentary section, Bay of Bengal, *Geology*, 19, 1097-1100, 1991.
- De Mets, C., R.G. Gordon, D.F. Argus, and S. Stein, Current plate motions, *Geophys. J. Int.*, 101, 425-478, 1990.
- Dewey, J.F., R.M. Shackleton, C. Chengfa, and S. Yiyin, The tectonic evolution of the Tibetan plateau, *Philos. Trans. R. Soc. London Ser. A*, 327, 379-413, 1988.
- Dewey, J.F., S. Cande and W.C. Pitman, Tectonic evolution of the India-Eurasia

- collision zone, *Eclogae Geol. Helv.*, 82, 717-734, 1989.
- England, P., and G. Houseman, Finite strain calculations of continental deformation.2, Comparison with the India-Asia collision zone, *J. Geophys. Res.*, 91, 3664-3676, 1986.
- Hao, B.V., J. Hardenbol, and P.R. Vail, Chronology of fluctuating sea levels since the Triassic, *Science*, 235, 1156-1167, 1987.
- Harland, W.B., A.V. Cox, P.G. Llewellyn, C.A.G. Pickton, A.G. Smith, and R. Walters, *A Geologic Time Scale*, 131 pp., Cambridge University Press, New York, 1982.
- Hirn, A., et al., Lhasa block and bordering sutures: a continuation of a 500 Km Moho traverse through Tibet, *Nature*, 307, 25-27, 1984.
- Kent, D.V., and F.M. Gradstein, A Jurassic to recent chronology, in *The Geology of North America*, vol. M, *The Western Atlantic Region*, edited by P.R. Vogt and B.E. Tucholke, pp. 45-50, Geological Society of America, Boulder, Colo., 1986.
- Kie, T. T., Geodynamic and tectonic evolution of the Panxi Rift, *Tectonophysics*, 133, 287-304, 1987.
- Klootwijk, C.T., P.J. Conaghan, and C. Mc. A. Powell, The Himalayan arc, large scale continental subduction, oroclinal bending and back arc-spreading, *Earth Planet. Sci. Lett.*, 75, 167-183, 1985.
- Le Pichon, X., F. Bergerat, and M.J. Roulet, Plate kinematics and tectonics leading to the Alpine belt formation: a new analysis, *Spec. Pap. Geol. Soc. Am.*, 218, 111-131, 1988.
- Leg 116 Shipboard Scientific Party, Collision in the Indian Ocean, *Nature*, 330, 519-521, 1987.
- Lyon-Caen, H., and P. Molnar, Constraints on the structure of the Himalaya from an analysis of gravity anomalies and a flexural model of the lithosphere, *J. Geophys. Res.*, 88, 8171-8191, 1983.
- Lyon-Caen, H., and P. Molnar, Gravity anomalies, flexure of the Indian plate, and the structure, support and evolution of the Himalaya and Ganga Basin, *Tectonics*, 4, 513-538, 1985.
- Ma, X., and D. Wu, Cenozoic extensional tectonics in China, *Tectonophysics*, 133, 243-255, 1987.
- Ma, X., G. Liu, and J. Su, The structure and dynamics of the continental lithosphere in north-northwest China, *Ann. Geophys.*, 2, 611-620, 1984.
- Mercier, J.L., R. Armijo, P. Tapponnier, E. Carey-Gailhardis, and T.L. Han, Change from Late Tertiary compression to Quaternary extension in Southern Tibet during the India-Asia collision, *Tectonics*, 6, 275-304, 1987.
- Molnar, P., Inversion of profiles of uplift rates for the geometry of dip-slip faults at depth, with examples from the Alps and the Himalaya, *Ann. Geophys.*, 5, 663-670, 1987.
- Molnar, P., and Q. Deng, Faulting associated with large earthquakes and the average rate of deformation in Central and Eastern Asia, *J. Geophys. Res.*, 89, 6203-6227, 1984.
- Molnar, P., and H. Lyon-Caen, Some simple aspects of the support, structure and evolution of mountain belts, *Spec. Pap. Geol. Soc. Am.*, 218, 179-207, 1988.
- Molnar, P., and P. Tapponnier, Cenozoic Tectonics of Asia: effects of a continental collision, *Science*, 189, 419-426, 1975.
- Patriat, P., Reconstitution de l'évolution du système de dorsales de l'Océan Indien par les méthodes de la cinématique des plaques, Thèse d'état, 308 pp., Univ. Paris 7, Paris, 1983.
- Patriat, P., and J. Achache, Indian-Asia collision chronology has implications for crustal shortening and driving mechanisms of plates, *Nature*, 311, 615-621, 1984.
- Powell, C.M.A., S.A. Roots, and J.J. Veevers, Pre-breakup and continental extension in East Gondwanaland and the early opening of the Eastern Indian Ocean, *Tectonophysics*, 155, 261-283, 1988.
- Royer, J.R., and T. Chang, Evidence for relative motions between the Indian and Australian Plates during the last 20 m.y. from plate tectonic reconstructions: Implications for the deformation of the Indian-Australian plate, *J. Geophys. Res.*, 96, 11779-11802, 1991.
- Royer, J.Y., and D.T. Sandwell, Evolution of the Eastern Indian Ocean since the Late Cretaceous: Constraints from Geosat altimetry, *J. Geophys. Res.*, 94, 13755-13782, 1989.
- Searle, M.P., et al., The closing of Tethys and the tectonics of the Himalaya, *Geol. Soc. Am. Bull.*, 98, 678-701, 1987.
- Sharma, S.R., A. Sundar, V.K. Rao, and D.V. Ramana, Surface heat flow and P_n velocity distribution in Peninsular India, *J. Geodyn.*, 13, 67-76, 1991.
- Tapponnier, P., and P. Molnar, Slip-line field theory and large scale continental tectonics, *Nature*, 264, 319-324, 1976.
- Tapponnier, P., and P. Molnar, Active faulting and tectonics in China, *J. Geophys. Res.*, 82, 2905-2930, 1977.
- Tapponnier, P., and P. Molnar, Active faulting and Cenozoic tectonics of the Tien Shan, Mongolia and Baikal regions, *J. Geophys. Res.*, 84, 3425-3459, 1979.
- Tapponnier, P., G. Peltzer and R. Armijo, On the mechanisms of the collision between India and Asia, *Geol. Soc. Spec. Publ. London*, 19, 115-157, 1986.
- Taymaz, T., J. Jackson, and D. McKenzie, Active tectonics of the north and central Aegean Sea, *Geophys. J. Int.*, 106, 433-490, 1991.
- Treloar, P.J., and M.P. Coward, Indian Plate motion and shape: constraints on the geometry of the Himalayan orogen, *Tectonophysics*, 191, 189-198, 1991.
- Veevers, J.J., and C. Powell, Sedimentary wedge progradation from transform faulted continental rim: Southern Exmouth Plateau, Western Australia, *AAPG Bull.*, 63, 2088-2096, 1979.
- Zhao, W.L., and W.J. Morgan, Uplift of Tibetan Plateau, *Tectonics*, 4, 359-369, 1985.
- Zhao, L.S., D.V. Helmberger, and D.G. Harkrider, Shear velocity structure of the crust and upper mantle beneath the Tibetan plateau and southeastern China, *Geophys. J. Int.*, 105, 713-730, 1991.
- Zorin, Y.A., M.R. Novoselova, E.K. Turutanov, and V.M. Kozhevnikov, Structure of the lithosphere of the Mongolian-Siberian mountainous province, *J. Geodyn.*, II, 327-342, 1990.
- Zonenshain, L.P., and L.A. Savostin, Geodynamics of the Baikal Rift zone and plate tectonics of Asia, *Tectonophysics*, 76, 1-45, 1981.

M. Fournier, L. Jolivet, and X. Le Pichon, Laboratoire de Géologie, Département Terre-Atmosphère-Océan, Ecole Normale Supérieure, 24, rue Lhomond, 75231 Paris cedex 05, France.

(Received November 27, 1991; revised May 15, 1992; accepted June 26, 1992.)

ANNEXE 2



ALPINE CORSICA METAMORPHIC CORE COMPLEX

Marc Fournier, Laurent Jolivet and Bruno Goffé
Laboratoire de Géologie, Ecole Normale Supérieure,
Paris

Roland Dubois
Laboratoire de Géologie structurale, Université Paris
Sud, Orsay, France

Abstract. Alpine Corsica is an example where superficial nonmetamorphic allochthonous units rest upon a highly strained metamorphic complex. Early ductile deformation under high pressure-low temperature (HP-LT) conditions is due to the westward thrusting of oceanic material onto a continental basement as shown by previous studies. New thermobarometric estimates yield minimal peak HP-LT metamorphism conditions of 11 kbar at 400°C. The early deformation is overprinted by a ductile deformation with an eastward sense of shear postdating or contemporaneous with mineral recrystallizations in the greenschist facies conditions. Early compressive thrust contacts are reworked as east dipping ductile normal faults and the less competent units display only eastward shear criteria. The upper units are affected by an extensional brittle deformation, and east dipping brittle normal faults bound to the west the early to middle Miocene Saint-Florent half-graben. The greenschist metamorphic event lasted until 33 Ma, which is contemporaneous with the beginning of the extension in the Liguro-Provençal basin. We interpret the second deformation stage as the result of a ductile extension following the overthickening of the crust due to the westward thrusting. Extension reduces the thickness of the crust so that upper units free from early P-T conditions are brought into close contact with a HP-LT metamorphic core complex. The geometry of the late extension is controlled by that of the early compressive thrust.

INTRODUCTION

During the extension process which gave birth to the Liguro-Provençal basin and the Tyrrhenian Sea from Oligocene to present, Corsica and Sardinia were left as a stretched continental crust remnant. Crustal thickness in Corsica is about 30 km [Hirn and Sapin, 1976; Morelli et al., 1977], that of a normal continental crust. However Alpine Corsica is part of the western Alps nappe stack, and geological data show that the crust was about 50 km thick in late Eocene time. The crustal thickness had thus been considerably reduced afterwards. Extension and erosion are the two likely processes to reduce this

thickness. We describe in this paper the deformation related to the extension process.

Alpine Corsica is an example where superficial nonmetamorphic allochthonous units affected by brittle deformation rest upon a highly strained high pressure-low temperature (HP-LT) metamorphic complex, the Schistes Lustrés nappe. This broadscale structure is that of a metamorphic core complex similar to those described in the Basin and Range or Franciscan provinces [Coney and Harms, 1984; Malavieille, 1987; Platt, 1986; Lister and Davis, 1989] or in the Cycladic area [Lister et al., 1984]. In these classical examples the contact between the upper brittle plate and the lower ductile plate is interpreted as a detachment fault formed during extension. Malavieille [1987] described in the Basin and Range the superimposition of a ductile extensional deformation onto an earlier compressional one.

Observations of the deformation and contemporaneous metamorphic recrystallizations in the Bastia area in Corsica allow us to distinguish two main successive stages of ductile noncoaxial deformation with opposite sense of shear. The Schistes Lustrés nappe, a tectonic stack of metasediments (schistes lustrés sensu stricto), metamorphic oceanic slices, and serpentized peridotites, was first thrust westward onto the continental basement of western Corsica under HP-LT conditions [Mattauer and Proust, 1975]. This early deformation has been described in detail by Mattauer and Proust [1975, 1976 a] and Mattauer et al. [1977, 1981], Faure and Malavieille [1981], Malavieille [1982], and Warburton [1986]. The age of this deformation is still under discussion. New thermobarometric estimates of the HP-LT metamorphic conditions in the Schistes Lustrés nappe are given in this paper. We use them to restore P-T paths for the nappe.

We show that this early stage was followed by a second deformation with eastward sense of shear which is partly contemporaneous and partly subsequent to greenschist facies parageneses in the Schistes Lustrés nappe. Such eastward kinematic indicators had already been described in Alpine Corsica [Amaudric du Chaffaut, 1982; Jacquet, 1983; Warburton, 1986; Jourdan, 1988] and had been usually considered as evidence for a backthrust stage. However, several lines of evidences show that this deformation is the result of ductile extension coeval with brittle extension in the upper plate. The last thermal event is 35-33 m.y. old [Maluski, 1977; work of H. Maluski, as discussed by Jourdan, 1988], which is contemporaneous with the beginning of the rifting in the Liguro-Provençal basin [Burtus, 1984; Boillot et al., 1984]. The unconformable early Miocene limestone of Saint-Florent was deposited in an asymmetric westdipping graben. Furthermore, the sharp metamorphic contrast between the superficial Balagne-Nebbio-Macinaggio units and the intensively strained HP-LT metamorphic complex (Schistes Lustrés nappe and Tenda massif) suggests that the contact between them is a large detachment fault. We

interpret this late deformation event as a ductile extension, and we suggest that Alpine Corsica is a metamorphic core complex risen by extensional processes [Wernicke and Burchfield, 1982].

GEOLOGIC SETTING

Corsica island is located between two Cenozoic oceanic basins, the Liguro-Provençal basin to the west and the Tyrrhenian Sea to the east. In the northeast, Alpine Corsica is separated from western crystalline Corsica by a late, vertical N-S fault with a strike-slip component (Figure 1). Two main features characterize the geology of Alpine Corsica. The first one is the crustal-scale thrust of oceanic material (the Schistes Lustrés nappe) onto the European continental margin represented by the Tenda massif on Figure 2 (see location of the cross section on Figure 1). The westward obduction in a simple shear context was responsible for the penetrative ductile deformation and associated HP-LT metamorphism within the thrust stack and at the top of the Tenda massif [Mattauer and Proust, 1975, 1976a, b; Mattauer et al., 1981; Faure and Malavieille, 1981; Malaveille, 1982; Jacquet, 1983]. Similar obduction-related HP-LT metamorphism is described in Oman [Goffé et al., 1988]. The core of the Tenda massif consists of unstrained Paleozoic granitoids; metamorphism and deformation increase towards the thrust contact as described by Mattauer and Proust [1975], Jacquet [1983], Gibbons and Horak [1984] and affect the Paleozoic and the Mesozoic (Santo-Pietro di Tenda sequence [Caron, 1977]) cover of the Tenda massif. Low-grade HP-LT assemblages (crossite + epidote [Gibbons and Horak, 1984]) are found in the upper part of the shear zone. A shear zone with blue amphiboles was also observed at the base of the massif with evidence of westward thrusting [Jourdan, 1988].

The Schistes Lustrés nappe is composed of several thrust slices folded in the Cap Corse-Castagniccia late antiform (Figure 1). Five principal units can be recognized. From base to top, they are (Figures 1 and 2): 1, the Castagniccia calcschists unit that crops out both in the Castagniccia and the Cap Corse areas; 2, the lower ophiolitic unit with lenses of eclogites [Autran, 1964; Essene, 1969; Caron et al., 1981; Péquignot, 1984; Harris, 1984; Caron and Péquignot, 1986; Lahondère, 1988; Lahondère and Caby, 1989]; 3, the Inzecca calcschists unit; 4, the Oletta-Serra di Pigno gneisses and their assumed sedimentary cover similar to the Santo-Pietro di Tenda sequence [Caron and Delcey, 1979; Mattauer et al., 1981]; 5, the upper ophiolitic unit composed of serpentinites and metamorphosed basic rocks. The calcschists (Schistes Lustrés sensu stricto) are interpreted as the sedimentary cover of the ophiolites of probable Jurassic to Early Cretaceous age [Caron, 1977; De Wever et al., 1987]. Note that the contact between the "Inzecca schists" and the "Castagniccia schists" of Caron [1977] (also carte géologique de la France a 1/250000: Corse, 1980) is included in our Inzecca schists unit as the metamorphism is similar

on both sides. Detailed geological maps resulting from field surveys in the Bastia area and in the Golo valley are presented in Figures 3 and 4. Several E-W cross sections (Figure 5, see location of the sections in Figure 3; see Durand-Delga [1978] for a cross section of the Golo valley; see also Dallan and Puccinelli [1987]) show the structure of the Schistes Lustrés nappe. The Castagniccia schists crop out in the Golo valley and are overlain by the lower ophiolitic unit with a thick glaucophanitic sequence at

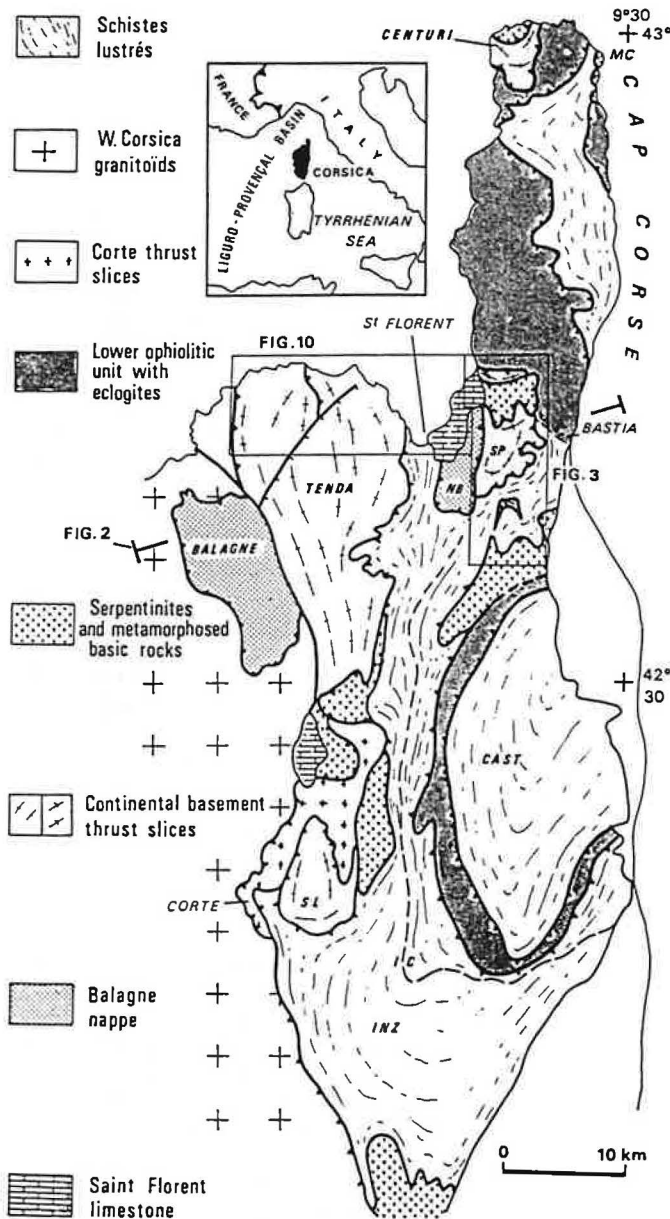


Fig. 1. Simplified tectonic map of Alpine Corsica [after Jolivet et al., 1990]. Abbreviations are CAST, Castagniccia; INZ, Inzecca; MC, Macinaggio; NB, Nebbio; SL, Santa Lucia; and SP, Serra di Pigno. The dotted line within the calcschists represents the contact between the Castagniccia (C) and the Inzecca (I) units of Caron [1977].

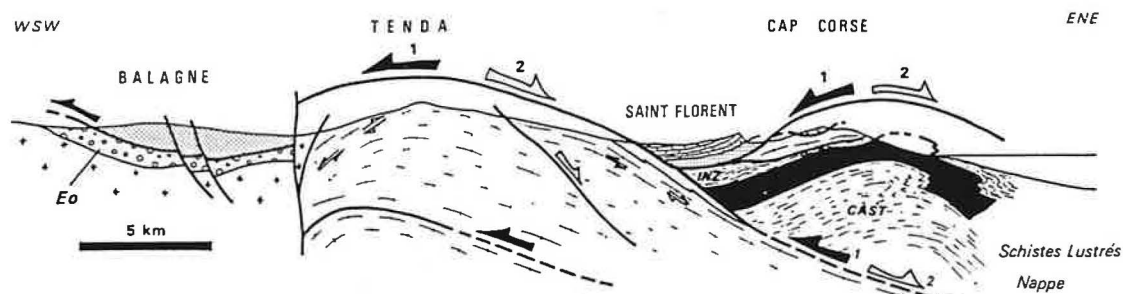


Fig. 2. Synthetic E-W cross section of the Cap Corse in the Bastia area [after Jolivet et al., 1990] (see location of the cross section in Figure 1). Solid arrows indicate the early westward compressional event (HP-LT); open arrows indicate the late eastward extensional event. For abbreviations see Figure 1. EO is Eocene autochthonous sediments.

its base (Figure 5d) covered by ophiolitic material (peridotites and serpentinites, metagabbros, fine-grained glaucophanites and prasinites) associated with schists and gneisses. The Inzecca schists, including ophiolitic slices, cover this ophiolitic unit. The Oletta-Serra di Pigno orthogneisses (Figures 5a and 5b) and their sedimentary cover lay either on the Inzecca schists or on eclogites farther north [Guiraud, 1982; Lahondère, 1988]. The upper ophiolitic unit is superimposed on this stack of tectonic slices. The tectonic contacts are parallel to the main blueschist foliation which is contemporaneous with the thrusting. A similar section is found in the north of Cap Corse near Centuri, where a slice of gneisses is tectonically included between ophiolitic thrust sheets [Malavieille, 1982; Guiraud, 1982].

The second characteristic of the geology of Alpine Corsica is the superimposition of a nonmetamorphic and poorly strained superficial nappe upon the HP-LT metamorphic complex of the Schistes Lustrés nappe. The material of the superficial nappe of Ligurian affinity is found in the Balagne, Nebbio, and Macinaggio klippe. It was emplaced onto a terrigenous basin (upper Lutetian) as observed in Balagne [Mattauer and Proust, 1975; Jourdan, 1988]. This last horizontal movement has been correlated to the 33 Ma thermal event in the Tenda upper shear zone by Jourdan [1988].

The early Miocene Saint-Florent limestone lies unconformably on the Schistes Lustrés nappe and the Nebbio klippe. It is folded in a broad asymmetric syncline whose western limb is covered with horizontal conglomeratic deposits.

In the following, we first present new data on the metamorphism and derive P-T paths for the Schistes Lustrés nappe and then describe the characteristics of the associated deformation with an emphasis on the late stage.

P-T PATHS IN THE SCHISTES LUSTRES NAPPE

Stability Fields of Mineral Assemblages in the Lower Ophiolitic Unit (Lancône Valley)

Thin sections in blueschists of the Lancône valley (Figure 5d) show clasts of glaucophane, epidote, sphene, +/- garnet (65% almandine, 27% grossular,

4% pyrope, 4% spessartine), and +/- lawsonite included in a late foliation with chlorite, albite, +/- actinolite, +/- quartz. The albite-chlorite assemblage crystallizes in asymmetric pressure shadows around garnet, epidote, and lawsonite, or overprint the earlier HP-LT foliation with blue amphiboles which is preserved in the core of the unit. Sphene is a very early phase included in lawsonite or garnet. Lawsonite can also be included in garnet.

The stability fields of mineral assemblages are given by the phase diagrams computed by Evans [1990] with the program Geo-calc written by Brown et al. [1988], for rocks containing epidote and sodic amphibole and rocks containing assemblages characteristic of neighboring metamorphic facies. According to chemical analysis, we used the phase diagram computed for an intermediate pole between glaucophane and ferroglaucophane. The early lawsonite-glaucophane assemblage characterizes the lawsonite blueschist facies (LBS) delineated in Figure 6a. Referring to Massonne and Schreyer [1987], a curve of minimal pressure (curve 1 in Figure 6a) is obtained with the phengites (atomic Si content from 3.473 to 3.548 per formula unit) from garnet-bearing calcschists tectonically associated with ophiolitic rocks (Figure 5d). Postdating the formation of lawsonite and garnet, epidote crystallized under the epidote blueschist facies (EBS) conditions, following the a or b reactions. The albite-chlorite late assemblage may have appeared following reaction c; it is symptomatic of the retrogression of the HP-LT assemblages in the greenschist facies. The study of titanium phase also allowed us to constrain the retrograde evolution. As remarked before, sphene is an early phase in these rocks, and rutile is never observed. The lawsonite-sphene stability field has been computed with Geo-calc, using the thermodynamic data base of Berman [1988] ($X(CO_2) < 0.1\%$ not to destabilize lawsonite). As sphene is not destabilized, the way back to surface conditions is constrained by its stability limit (curve 2 in Figure 6a).

Thus the minimal peak P-T conditions for the glaucophane schists of the Lancône Valley are 11 kbar and 400°C. Previous estimates of blueschist P-T conditions made on the same kind of rocks of the Schistes Lustrés nappe with other thermobarometers

are given in figure 6b [Harris, 1984; Gibbons et al., 1986; Lahondère, 1988], and Harris' P-T path for Cap Corse units is indicated. We also added estimates for the eclogites associated with the basal ophiolitic unit [Caron et al., 1981; Guiraud, 1982; Harris, 1984; Lahondère, 1988].

The Schists Units

The Castagniccia and Inzecca calcschists frequently contain the Fe-carpholite-lawsonite-rutile assemblage characteristic of HP-LT conditions (Figure 7). The presence of carpholite is significant for the retrograde

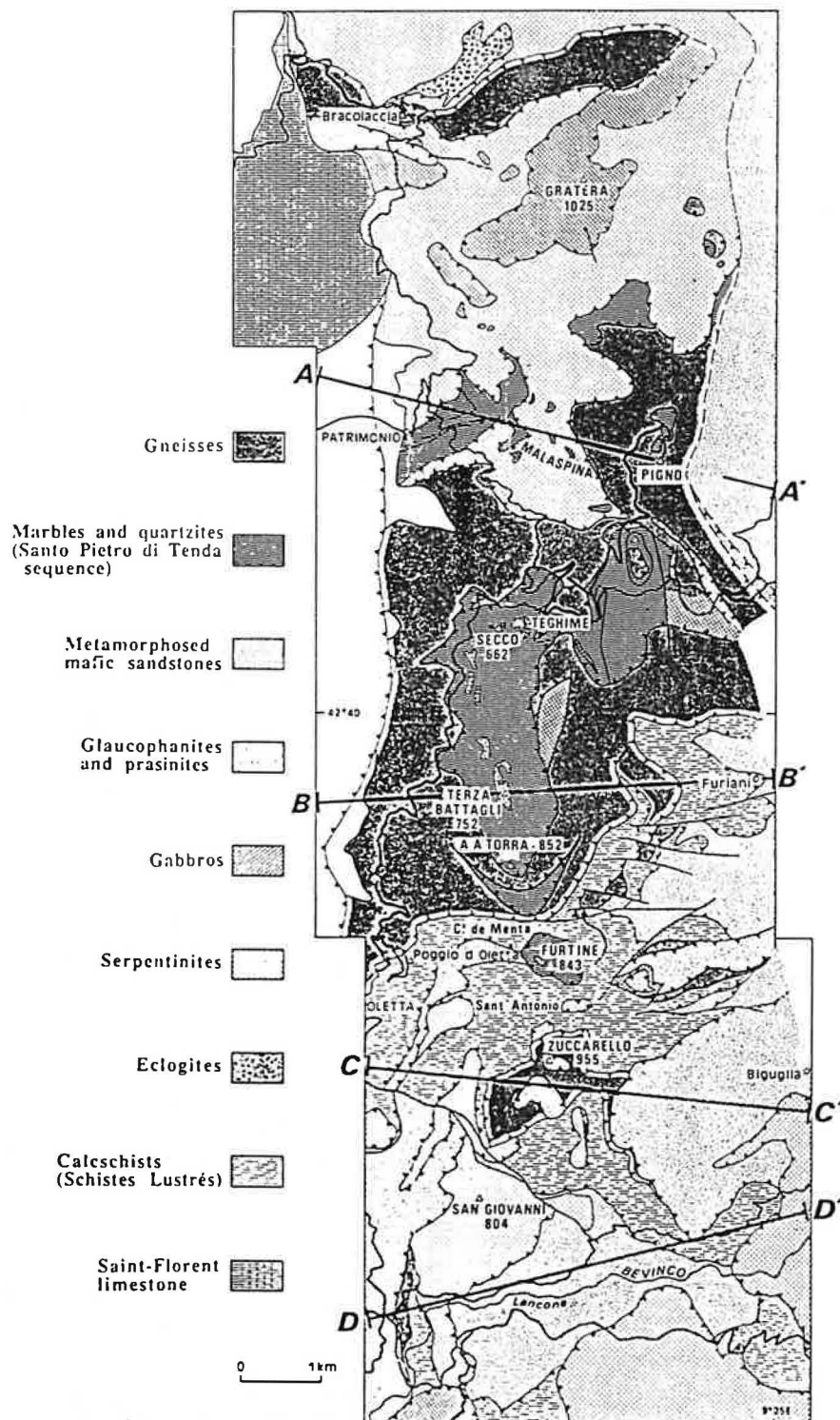


Fig. 3. Geological map of the Bastia-Lancône area.

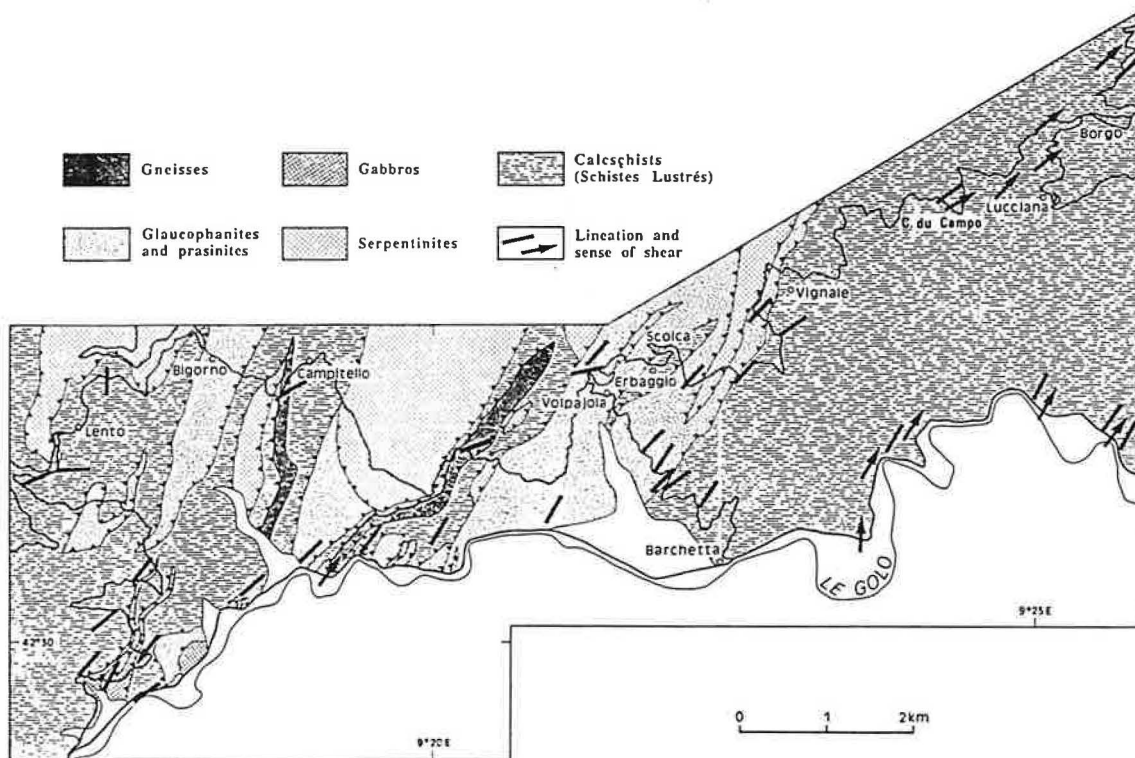


Fig. 4. Geological and structural map of the Golo valley.

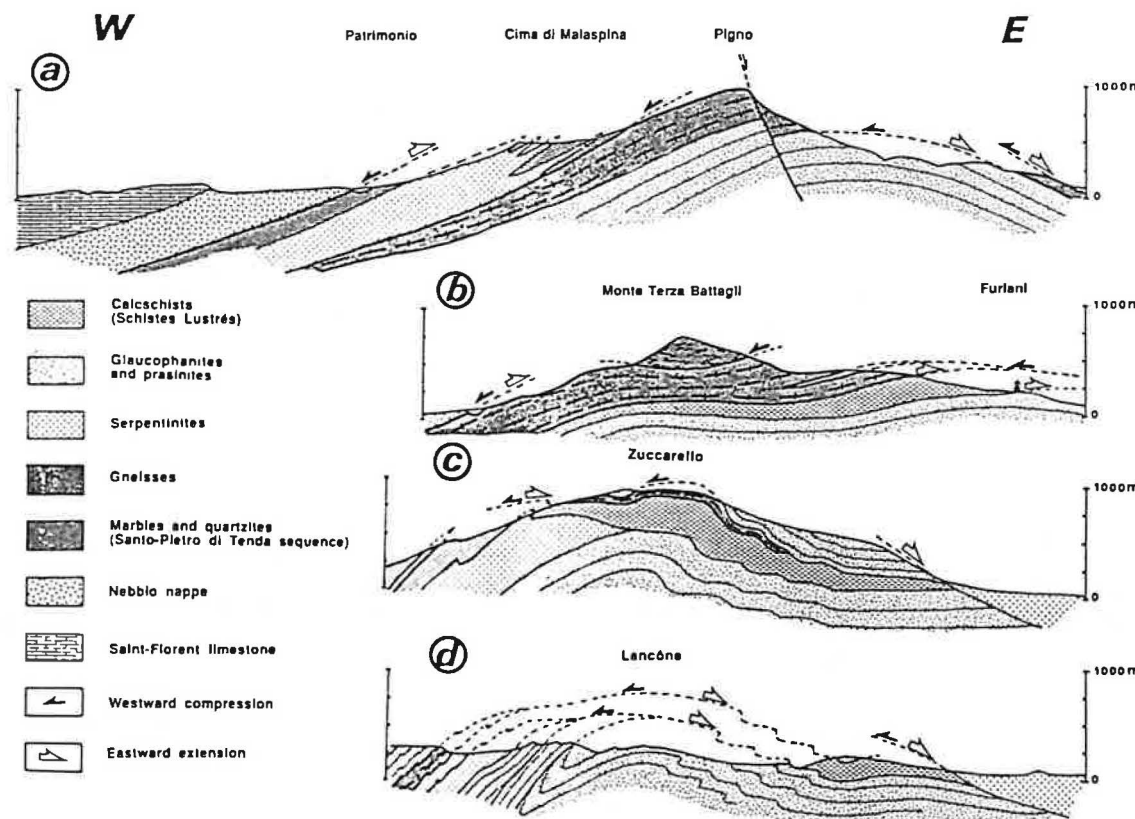


Fig. 5. E-W cross sections of the Bastia-Lancône area (see location in Figure 3). (a) Serra di Pigno cross section, (b) Monte Terza Battagli-Furiani cross section, (c) Zuccarello cross section, (d) the Lancône valley.

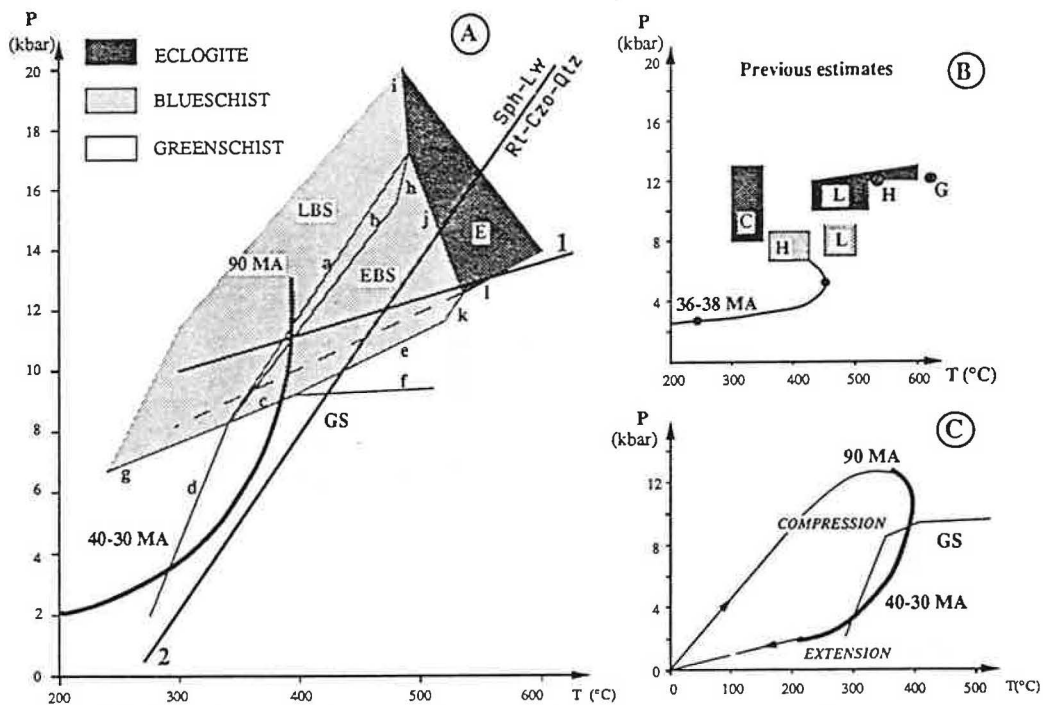


Fig. 6. P-T path in the Schistes Lustrés nappe. (a) P-T path for the Lancône glaucophanites (after calculations of Evans [1990]), E, eclogites; EBS, epidote-blueschist; GS, greenschist; LBS, lawsonite-blueschist. Reaction list (assemblages on the left are stable on the higher-pressure side): a, lawsonite (Lw) + jadeite (Jd) + tremolite (Tr) = clinzoisoite (Czo) + glaucophane (Gln) + quartz (Qtz) + H₂O (W); b, Lw + Gln = paragonite (Pg) + Czo + chlorite (Chl) + Qtz + W; c, Gln + Czo + Qtz + W = albite (Ab) + Chl + Tr; d, pumpellyite (Pmp) + Chl + Qtz = Czo + Tr + W; e, Gln + Czo + Qtz + W = Ab + Pg + Tr; f, Pg + Tr + W = Ab + Czo + Chl + Qtz; g, Lw + Gln = Pmp + Chl + Ab + Qtz + W; i, Jd + diopside (Di) + pyrope (Prp) + Qtz + W = Gln + Lws; j, Jd + Di + Prp + Qtz + W = Gln + Czo; k, Czo + Qtz = Ab + Prp + Tr + W; l, Jd + Qtz = Ab; 1, Si content of phengites = 3.47 [after Massonne and Schreyer, 1987]; 2, Sphene (Sph) + 3 Lw = Qtz + Rutile (Rt) + 2 Czo + 5 W. (b) Previous estimates for eclogites and blueschists P-T conditions: C, Caron et al. [1981]; G, Guiraud [1982]; H, Harris [1984]; L, Lahondère [1988]. P-T path for Cap Corse blueschists after Harris [1984]. (c) Synthetic P-T path for Lancône glaucophanites included in the basal ophiolitic unit. GS is greenschist.

evolution [Goffé, 1984; Goffé and Velde, 1984; Goffé and Chopin, 1986]: carpholite is rapidly destabilized when temperature increases and albite appears. That is the case further north in the Cap Corse where carpholite is never preserved: retrograde evolution increases toward the north. Moreover, chloritoid is never observed associated with carpholite in the studied area and Pequignot [1984] signaled very rare occurrences of chloritoid in schists further to the south. Therefore the retrograde path of the Castagniccia and Inzecca calcschists (curve A in Figure 7) does not cross the Fe-chloritoid stability field and is constrained by the equilibrium Fe-carpholite = Fe-chloritoid + quartz + H₂O (curve 4 computed with Geo-calc [Brown et al., 1988] using thermodynamical data from O. Vidal, B. Goffé and T. Theye (manuscript in preparation, 1991) for an Mg-carpholite having an activity of 0.6). The Serra di Pigno calcschists included in the sedimentary cover of the Oletta-Serra di Pigno gneisses also contain

relics of carpholite in quartz, and the gneisses provide relics of jadeite. Minimal peak P-T conditions can thus be estimated for these units (Figure 7): because of the presence of Fe-carpholite and absence of Fe-chloritoid the temperature can not have exceeded 350°C. The equilibrium albite = jadeite + quartz constrains the pressure (about 11 kbar at 350°C).

The calcschists included in the basal ophiolitic unit do not provide carpholite and contain garnet, sphene and lawsonite often destabilized in epidote. The lawsonite-sphene stability field with presence of calcite has been computed with Geo-Calc [Brown et al., 1988; Figure 7]. It is limited by the curves 5 (calcite + quartz + rutile = sphene + CO₂) and 6 (sphene + 3 lawsonite = rutile + 2 clinzoisoite + quartz + 5 H₂O) that constrained the way back to surface conditions. The calcschists belonging to the basal ophiolitic unit suffered higher temperature (400°C at least) than the Castagniccia and Inzecca calcschists. Their retrograde evolution (curve B in

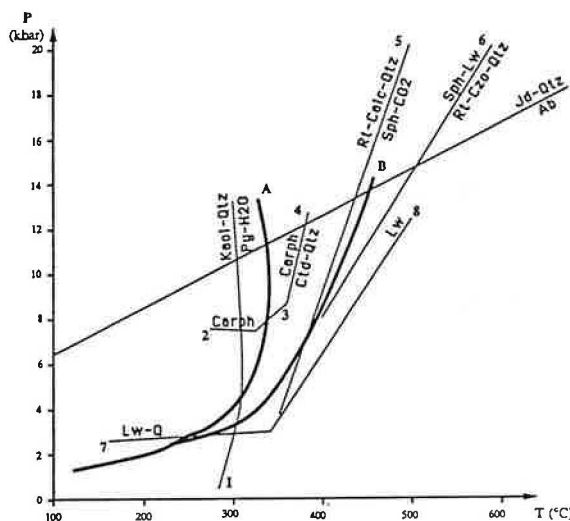


Fig. 7. Stability fields of calcschists assemblages [after Goffé et al., 1988]. A, P-T path for calcschists units; B, P-T path for schists included in the basal ophiolitic unit; 1, kaolinite (Kaol) + Qtz = pyrophyllite (Py) + H₂O; 2, carpholite (Carph) = sudoite + Qtz; 3, Carph + Qtz = Chl + Pyr + H₂O; 4, Carph = chloritoid (Ctd) + Qtz + H₂O; 5, Rt + calcite (Calc) + Qtz = Sph + CO₂; 6, Sph + 3 Lw = Rt + 2 Czo + Qtz + 5 H₂O; 7, Lw + Qtz = laumontite; 8, Lw = zoisite + margarite + Qtz + H₂O.

Figure 7) is similar to that of the associated basic rocks (see Figure 6a).

P-T-t Paths

The Upper Jurassic units display the alpine HP-LT metamorphism and the associated intense deformation, whereas dated Eocene sediments are always less strained [Mattauer and Proust, 1975; Amaudric du Chaffaut, 1982]. Radiochronologic determinations give a mid-Cretaceous age (105 ± 8 Ma, whole rock Rb-Sr [Cohen et al., 1981]; 90 Ma, Ar-Ar on glaucophane] Maluski, 1977]) for the HP-LT metamorphism, and an upper Eocene-early Oligocene age (around 42 Ma, fission tracks on zircon and apatite [Carpena et al., 1979]; 34.4 ± 1 Ma, Ar-Ar on phengites, [Maluski, 1977]; 33 Ma, work of H. Maluski as discussed by Jourdan [1988]) for the late greenschist metamorphism. Actually, recent structural studies of the eastern edge of crystalline Corsica and its autochthonous Eocene cover suggest an Eocene age for the Alpine deformation and the HP-LT associated metamorphism [Bézert and Caby, 1988; Egal and Caron, 1988; Egal, 1989]. Obviously no precise history of the P-T evolution of the Alpine Corsica units can be expected without new radiochronologic determinations on significant metamorphic minerals.

The preceding informations are synthetized in Figure 6c, where a P-T-t path for the basal ophiolitic unit is presented (based on the study of the Lancône glaucophane schists and calcschists belonging to the

basal ophiolitic unit). The P-T prograde evolution is constrained by the HP metamorphic climax, 11 kbar and 400°C at least. Higher values are obtained considering the eclogitic lenses associated with the ophiolitic unit (see Figure 6b). The prograde evolution follows an HP-LT gradient, about 10°C per kilometer, characteristic of the underthrusting of cold units. The retrograde evolution is characterized by a pressure drop at an almost constant temperature in a cold gradient, before a rather warm gradient (about 30°–35°/km). The Castagniccia and Inzecca calcschists followed a similar evolution at lower temperature. These units were lately put into close contact which determined the metamorphic contrast between the "rather hot" basal ophiolitic unit and the "rather cold" Castagniccia and Inzecca units.

DEFORMATION AND STRUCTURAL EVOLUTION

Finite Deformation

The main fabrics in the metamorphic complex are the HP-LT penetrative foliation and the associated stretching lineation [Mattauer et al., 1977; Faure and Malavieille, 1981; Mattauer et al., 1981; Malavieille, 1982] folded in a broad anticline, the Cap Corse-Castagniccia antiform. The stretching lineation is defined by quartz rodding in quartzites and calcschists, stretching and microcrystalline boudinage of amphiboles, epidote and albite in the of pillow lavas, mineral crystallizations in pressure shadows (quartz, albite, amphiboles). Stretching is also expressed by boudins of metamorphosed mafic sandstones levels intercalated with quartzites in the Oletta cover (Figure 8). A crenulation lineation, parallel to the stretching lineation, is sometimes observed in the calcschists, in the gneisses and in the glaucophanites. These lineations are oriented E-W to NE-SW (Figures 4 and 9). As the regional foliation is penetrative and homogeneous, the foliation plane contains the principal X and Y axes of the deformation, and the X axis is parallel to the stretching lineation. Our observation of gneisses

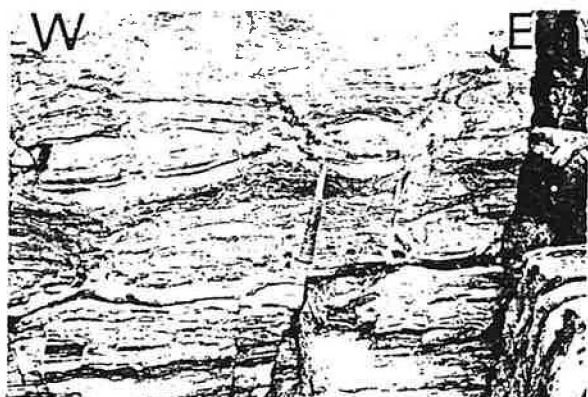


Fig. 8. Boudins of mafic sandstones metamorphosed into quartzites in the Oletta-Serra di Pigno cover (near Monte a a Torra, section b, Figure 3).

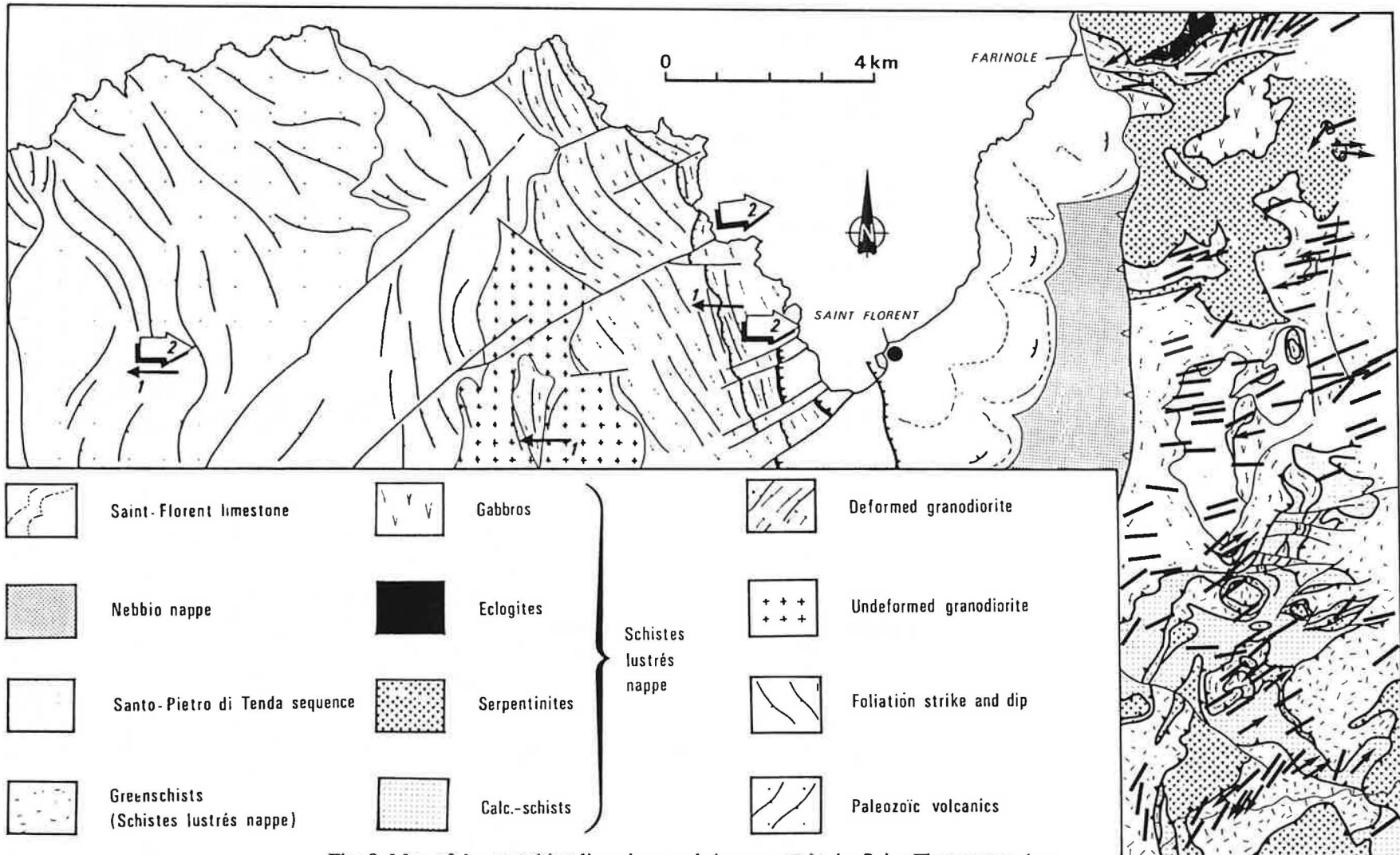


Fig. 9. Map of the stretching lineations and shear sense in the Saint-Florent area (see location in Figure 1), after Jolivet et al. [1990], Malavieille [1982], Jacquet [1983], and Jourdan [1988]. The black bars represent the direction of the stretching lineation in the Schistes Lustrés nappe, with an arrow when the sense of shear is known. Large arrows stand for the average direction of lineation in the Tenda massif after Jacquet [1983] and Jourdan [1988]. The direction of the arrow indicates the sense of shear.

shows that the stretching is intense in the X-Z planes and almost nonexistent in the Y-Z planes, so that the deformation ellipsoid has a cigar shape characteristic of the stretching and/or constriction.

The foliation is axial planar to isoclinal sheath folds (P1) whose axes are parallel to the E-W stretching lineation [Faure and Malavieille, 1980]. The foliation and the early tectonic contacts are folded by eastward vergent folds with N40° axes [Malavieille, 1982]. Lastly, all these structures are refolded by the Cap Corse-Castagniccia antiform.

The Lancône glaucophanites suffered a late brittle extensional deformation expressed by vertical fracture planes trending N100° to N130°, associated with conjugate en échelon cracks.

Noncoaxial Deformation

Observations of deformation in the X-Z section often reveals opposite senses of shear. They can correspond either to a compound component of flattening along the Z axis perpendicular to the foliation or to two successive stages. They are in fact associated with different metamorphic paragenesis: top-to-the-west (westward) shear criteria are associated with HP-LT mineral assemblages while top-to-the-east (eastward) shear criteria are contemporaneous or subsequent to greenschist

assemblages. They are therefore due to two separable successive deformation stages.

Kinematic indicators associated with HP minerals show westward shear sense [Mattauer et al., 1981]. Indicators of shear sense include asymmetric strain shadows around plagioclases in gneisses, pyroxenes in gabbro, and oblique shear planes in gneisses (Figure 10a) and glaucophanites (Figure 10b).

Late kinematic indicators are associated with greenschist paragenesis or postdate them. The whole Castagniccia calcschists unit shows predominant eastward shear planes (Figure 11a), sometimes associated with late en échelon cracks (Figure 11b). The same shear planes are observed in similar calcschists in the Cap Corse near Erbalunga (Figure 11c). Asymmetric quartz lenses confirm this eastward sense of shear (Figure 11d). Plurimetric en échelon cracks associated with an eastward flat shear plane are also observed in the Golo Valley (Figure 11e). The eastward shear planes predate the formation of the Cap Corse-Castagniccia antiform as shown by the evolution of their dip across the Castagniccia dome.

Eastward shear planes are also observed along the major early thrust contacts. At the top of the Tenda massif, the Paleozoic cover displays eastward shear criteria (Figures 12a and 12b) [Jourdan, 1988]. A thermal event contemporaneous with the activation of these planes reset the rejuvenated phengites to 33 Ma (work of H. Maluski, as discussed in Jourdan [1988]). Similarly, the sedimentary cover of the Oletta-Serra di Pigno basement displays eastward shear criteria very near its basal contact (Figure 12c).

In the Lancône gorges, the partly retrogressed glaucophanites show asymmetric strain shadows around garnets with albite crystallized during the retrogression of HP assemblages in the greenschist facies, indicating eastward shear senses (Figure 13a). Moreover, eastward shear planes cut through late albite crystals overprinting the earlier foliation (Figure 13b). Thus the eastward shear stage began during the greenschist metamorphic episode (crystallization of albite and rejuvenation of phengites) and continued after albite crystallization. The final stage gave brittle structures such as en échelon tension cracks.

Data showing brittle extensional deformation affecting the upper units are presented by Jolivet et al. [1991]. Extensional deformation is spectacularly well expressed in the Macinaggio klippe at the contact between the upper unit and the lower HP-LT metamorphic unit. Parallel east dipping normal faults separate tilted blocks just above the detachment plane showing E-W striations. Such a structure is compatible with an eastward sense of shear along the detachment.

Conclusion

Two main deformation stages with opposite senses of shear, associated with two successive metamorphic episodes are distinguished in Alpine Corsica. The first one, contemporaneous with HP-LT metamorphism, corresponds to the westward thrusting of the Schistes Lustres nappe onto the

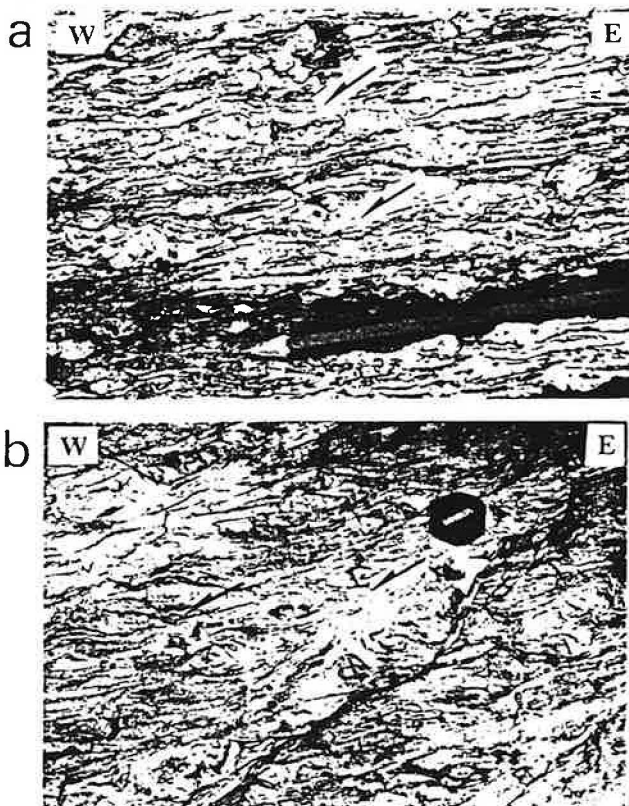


Fig. 10. C' shear planes indicating westward sense of shear in (a) the Zuccarello gneisses (section c, Figure 3) and (b) the Lancône glaucophanite (section d, Figure 3).

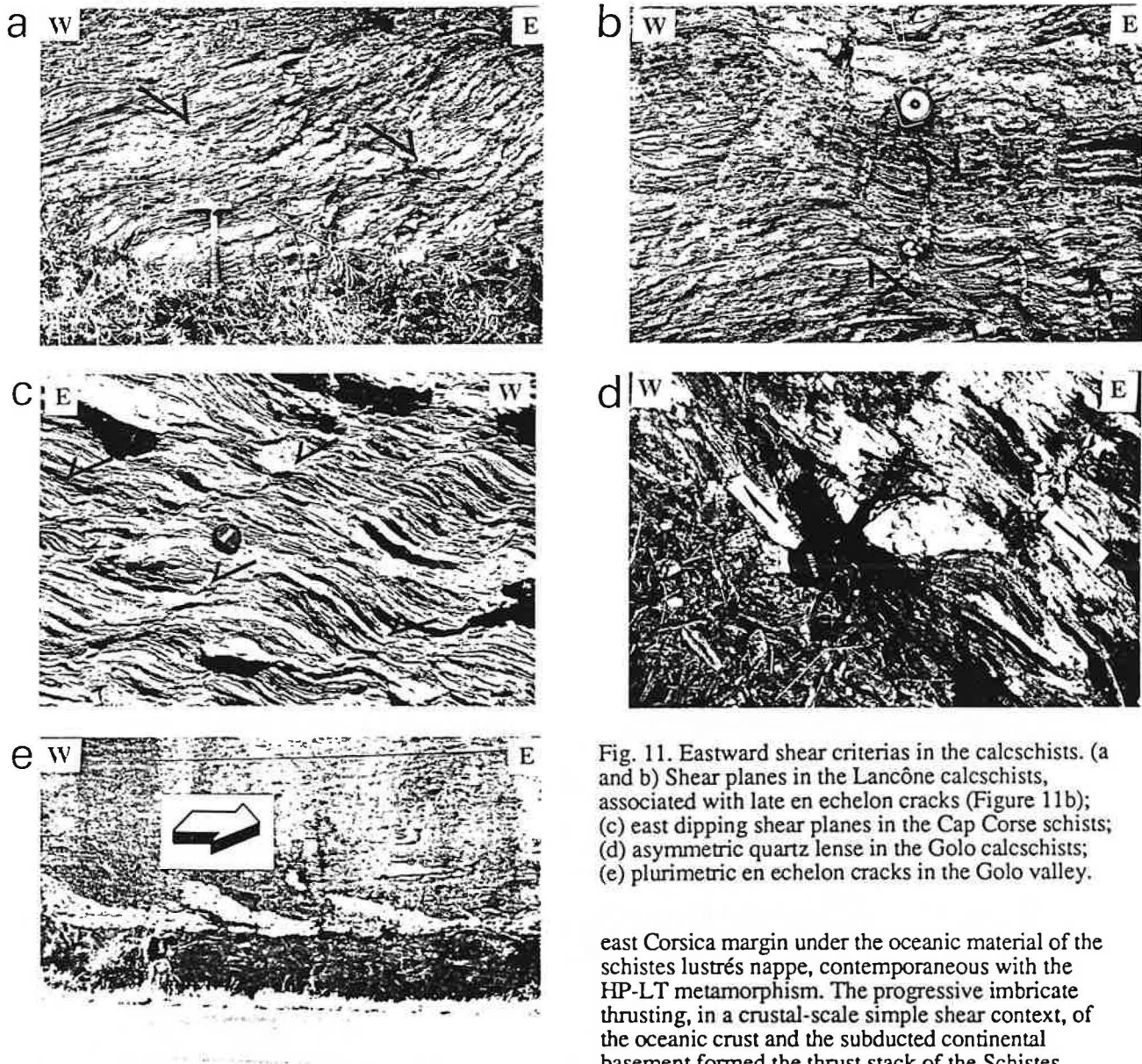


Fig. 11. Eastward shear criterias in the calc-schists. (a and b) Shear planes in the Lancône calc-schists, associated with late en echelon cracks (Figure 11b); (c) east dipping shear planes in the Cap Corse schists; (d) asymmetric quartz lense in the Golo calc-schists; (e) plurimetric en echelon cracks in the Golo valley.

Tenda basement. The regional foliation, stretching lineation and synfolial folds (P1) are associated with this event. The second ductile deformation stage is recorded by 32-33 Ma (early Oligocene) isotopic ages; it started during the greenschist metamorphic episode and continued afterwards. The deformation is mainly concentrated along the major thrust contacts and within the less competent units such as the schists, and shows unequivocal eastward sense of shear. The formation of the Cap Corse-Castagniccia antiform follows this deformation stage.

DISCUSSION

Mattauer and Proust [1976a, b] and Mattauer et al. [1981] first proposed the eastward subduction of the

east Corsica margin under the oceanic material of the schistes lustrés nappe, contemporaneous with the HP-LT metamorphism. The progressive imbricate thrusting, in a crustal-scale simple shear context, of the oceanic crust and the subducted continental basement formed the thrust stack of the Schistes Lustrés nappe. A late backthrust stage associated with greenschist metamorphism after the main westward thrusting has been proposed by various authors [Mattauer and Proust, 1975; Warburton, 1986] (see cross section in Figure 14). However, the HP-LT paragenesis of the Oletta-Serra di Pigno gneisses (jadeite) characterizes a higher metamorphic grade than in the Tenda massif. Thus Warburton's cross section must be discussed.

Petrological and structural data show the collision of the east Corsica stable margin and the adjacent oceanic basin during Alpine times. This shortening occurred in an HP-LT gradient related to the underthrusting of cold European units under an Adria plate mostly exposed in the Balagne nappe, an oceanic crust totally free from HP-LT paragenesis and its sedimentary cover resting upon upper Eocene autochthonous sediments. Thermobarometric estimates

of the HP-LT metamorphism in the Schistes Lustrés nappe show that the material was underthrust to depths of about 30–40 km. Thus the continental crust became at least 40 km thick and stored gravitational potential energy [Molnar and Lyon-Caen, 1988].

Retrograde metamorphic paths of the Schistes Lustrés nappe first follow a HP-LT gradient constrained by the lawsonite stability equilibrium,

showing that convergence continued after the maximum burial. The retrogression of the HP mineral associations in the greenschist facies began during the middle Eocene (43.7+2 Ma [Carpéna et al., 1979]) and went on until the early Oligocene (33 Ma, data of H. Maluski, as discussed by Jourdan [1988]). The eastward shear deformation started at that time. Though active in the entire thickness of the

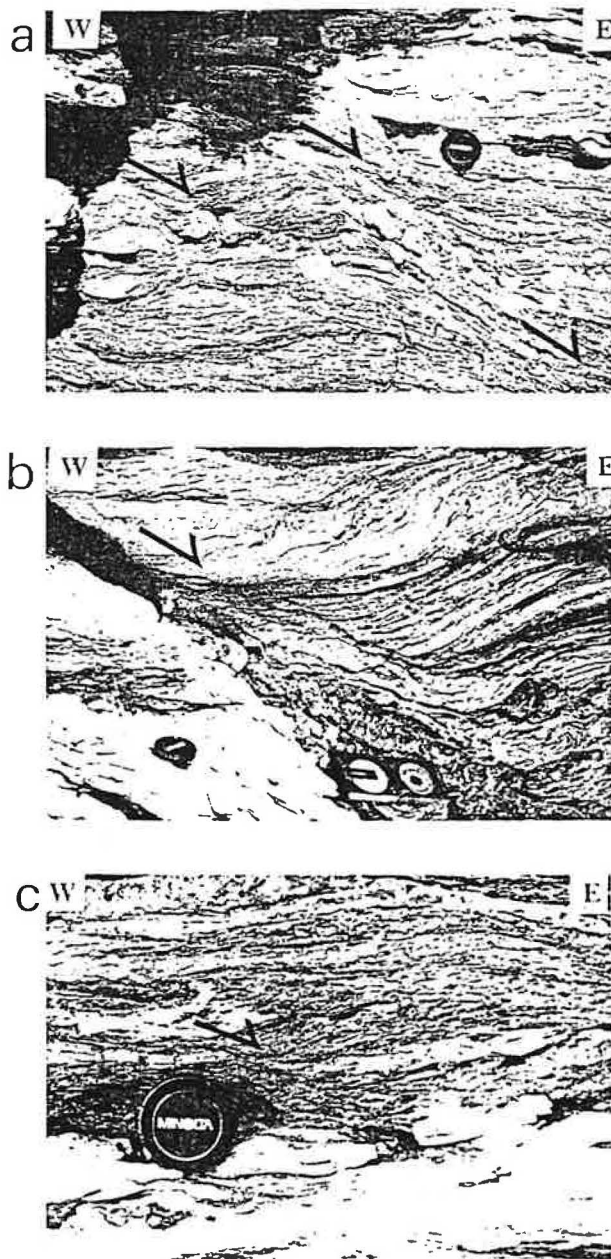


Fig. 12. Eastward shear criteria superposed along the main early thrust contacts. (a and b) Shear planes in the Paleozoic cover of the Tenda massif (west coast of the Saint-Florent gulf); (c) eastward shear plane in the Oletta-Serra di Pigno cover very near the contact with the gneisses.

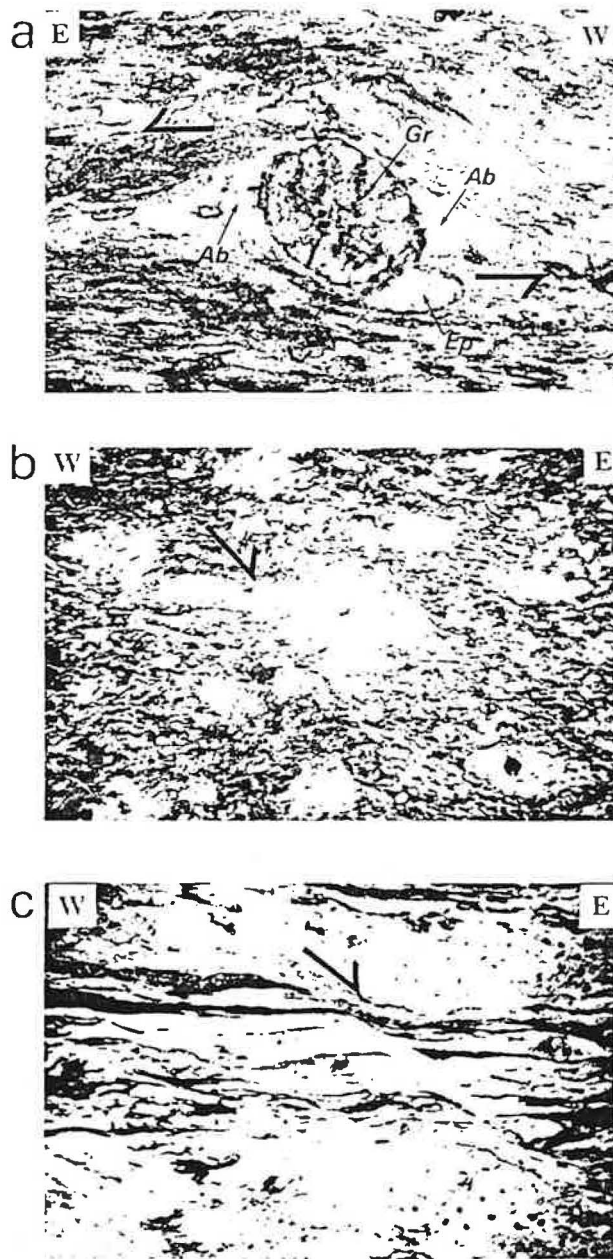


Fig. 13. Microscopic eastward shear criteria. (a) late albite crystallizing in asymmetric pressure shadows around garnet in the Lancône glaucophanites; (b) late albite crystal overprinting the earlier HP-BT foliation cut by eastward shear plane; (c) shear planes in the Cap Corse calcschist.

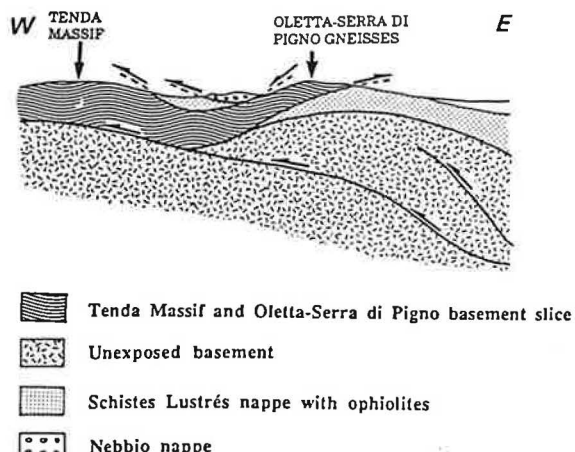


Fig. 14. E-W cross section of the Cap Corse in the Bastia area, after Warburton [1986].

thrust stack, it was essentially localized along the major preceding thrust contacts and within the less competent units. In particular, the eastward dipping thrust contact of the Schistes Lustrés nappe was reactivated toward the east as a ductile normal fault (Figure 2).

At the same time, the Corsica block drifted away from the European continent during the opening of the Liguro-Provençal basin. The rifting started in Oligocene time (35-30 Ma), and ended during the Aquitanian (24-23 Ma) relayed by the drifting until 21-19 Ma [Burrus, 1984; Boillot et al., 1984; Réhault et al., 1984]. On the east side of Corsica, the Tyrrhenian Sea opened during the late Miocene: after an early rifting episode in Oligocene-Miocene time [Boillot et al., 1984], a second stage of rifting started in the late Tortonian (7 Ma) and ceased during the Messinian; the drifting took place during the Pliocene in the south [Kastens and Mascle, 1988].

The Saint-Florent Miocene limestone was deposited from the Burdigalian to the Tortonian [Orszag-Sperber and Pilot, 1976; Dallan and Puccinelli, 1986]. It is gently folded in a strongly asymmetric syncline (the major part of the Miocene basin is west dipping) and is limited toward the west by the east dipping shear zone at the top of the Tenda massif. This syncline is tilted toward the west and may be a half-graben settled above an east-dipping normal fault, parallel to the thrust contact between the Tenda massif and the Schistes Lustrés nappe. The formation of the Cap Corse-Castagniccia antiform may be consecutive to the motion of this normal fault as a rollover antiform.

It is therefore reasonable to relate the post-Eocene deformation in Alpine Corsica to an extensional event that began during the early Oligocene (33 Ma) with the eastward ductile shear partly associated with and partly subsequent to the end of the greenschist overprint, and which continued until the Miocene (tilt of the Saint-Florent limestone and rifting of the Tyrrhenian sea). Extension was driven by the gravitational potential energy accumulated during the obduction and crustal thickening. Superficial brittle

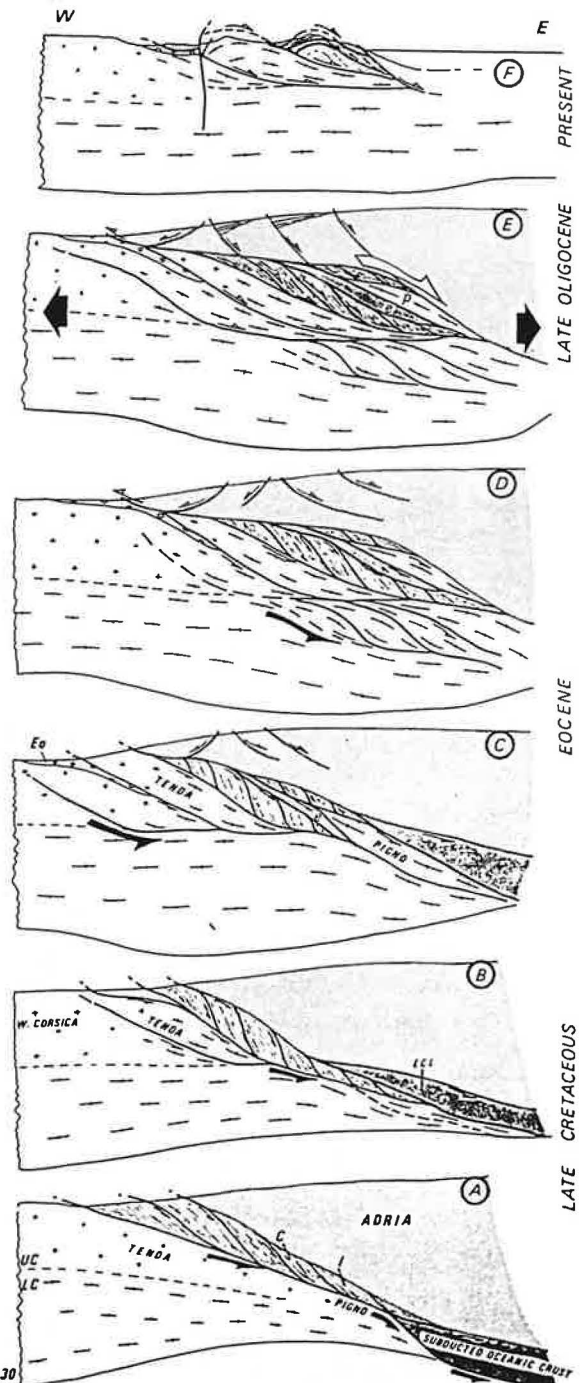


Fig. 15. Evolution scheme along the cross section of Figure 2 from the early compression in HP-LT gradient to the recent extension (explanation in text). Abbreviations are I, Inzecca, C, Castagniccia, ECL, eclogites, UC, upper crust, LC, lower crust, and eoc, eocene. (a and b), Late Cretaceous; (c and d), Eocene; (e and f), late Oligocene to Present.

normal faulting associated at depth with ductile normal faulting accommodated the crustal thinning: the lower continental crust is dragged out from beneath the superficial units.

In Figure 15 a six-stage model of the tectonometamorphic evolution in Alpine Corsica since Late Cretaceous is presented. Four major units are differentiated: (1) the continental margin of the European plate (western Corsica, Tenda Massif, Serra di Pigno gneisses) (2) the Castagniccia and Inzecca units made of the sedimentary cover of the oceanic crust (Schistes Lustrés) integrating tectonic slices of peridotites and oceanic crust, (3) the lower ophiolitic unit made essentially of oceanic rocks (partly eclogites) including small amount of schists and gneisses, and (4) the Adria plate (Balagne-Nebbio nappe). The oceanic crust of the Ligurian Tethys, its sedimentary cover, and the continental margin of the European plate are first underthrust eastward under the Adria plate (Figures 15a-15c). This cold material suffered at depth a HP-LT metamorphism. More deeply buried rocks, oceanic crust and associated schists and gneisses, were metamorphosed under eclogite facies conditions (low-grade). The Castagniccia and Inzecca units, partially blocked during the subduction process, suffered only medium-grade blueschist facies conditions. The Tenda Massif, lately involved in the subduction process, suffered low-grade blueschist facies conditions. Imbricate thrusting propagated toward the west within the slab, progressively adding tectonic slices to the accretionary complex. The major décollement lately isolated the Tenda massif from western Corsica. Once included in the accretionary complex, the tectonic units went up in an HP-LT geotherm preserving the HP-LT assemblages. During this episode the crust thickened to at least 40 km thick.

The extension started first in the thickest part of the stack where the vertical stress overcomes the horizontal stress due to convergence, and the thickening continues more westward (Figure 15d) as

suggested by Molnar and Lyon-Caen [1988]. The Balagne nappe glided into the Eocene sedimentation basin. Convergence ceased during Oligocene time, and was replaced by extension. The geotherm relaxed and rose up progressively so that late greenschist assemblages crystallized simultaneously with the eastward shear. Particularly, the main thrust contact between the Schistes Lustrés nappe and the Tenda Massif was reworked eastward as a ductile normal fault. At shallower depth, continuous brittle extension associated with erosion reduced the thickness of the upper crust (Figures 15e and 15f). The Eastward motion above the main contact continued as a brittle normal fault, forming a half-graben in which the Saint-Florent limestone was deposited during Miocene time. The formation of the Cap Corse-Castagniccia as a hanging wall roll-over antiform is related to this motion. A similar mechanism might explain the formation of the Tenda antiform.

Similar evolutions characterize other metamorphic core complexes as in the North American Cordillera [Coney and Harms, 1984; Malavieille, 1987] or the Aegean Sea [Lister et al., 1984]. We propose here a model of crustal thinning in an extensional (brittle and ductile) context, following a compressional thickening by underthrusting. The asymmetry of the ductile extension is controlled by the asymmetry of the structure as strain is essentially localized along the early eastdipping thrust planes. If the basal contact of the Balagne nappe is considered to be the main detachment, considerable extensional deformation affected its footwall. The simple shear is here distributed through the entire thickness of the Late Cretaceous-early Cenozoic nappe stack.

Acknowledgments The authors wish to thank Ahmet Collaku for help and discussion during field work.

REFERENCES

- Amaudric du Chaffaut, S., *Les unités alpines de la marge orientale du massif cristallin corse*, 133 pp., Travaux du laboratoire de géologie n°15, presses de l'école normale supérieure, Paris, 1982.
- Autran, M.A., Description de l'association jadéite + quartz et des paragénèses minérales associées dans les schistes lustrés de Sant' Andrea di Cotone, *Bull. Soc. Fr. Mineral. Cristallogr.*, 87, 43-44, 1964.
- Berman, R. G., Internally consistent thermodynamic data for minerals in the system Na₂O-K₂O-CaO-MgO-FeO-Fe₂O₃-Al₂O₃-SiO₂-H₂O-CO₂, *J. Petrol.*, 29, 445-552, 1988.
- Bézert, P., and R. Caby, Sur l'âge post-bartonien des événements tectono-métamorphiques alpins en bordure orientale de la Corse cristalline (Nord de Corse), *Bull. Soc. Géol. Fr.*, IV, 6, 965-971, 1988.
- Boillot, G., M. Lemoine, L. Montadert, and B. Bijou-Duval, *Les marges continentales actuelles et fossiles autour de la France*, 342 pp., Masson, Paris, 1984.
- Brown, T. H., R. G. Berman, and E. H. Perkins, Geo-Calc: software package for calculation and display of pressure-temperature-composition phase diagrams using an IBM or compatible personal computer, *Comput. Geosci.*, 14, 279-289, 1988.
- Burrus, J., Contribution to a geodynamic synthesis of the Provençal basin (north-western Mediterranean), *Mar. Geol.*, 55, 247-269, 1984.
- Caron J.M., Lithostratigraphie et tectonique des schistes lustrés dans les Alpes cottiennes septentrionales et en Corse orientale, Thèse de doctorat d'état, 326 pp., Univ. Strasbourg Sc. Géol. Mémo. n°48, Strasbourg, 1977.
- Caron, J.M., and R. Delcey, Lithostratigraphie des schistes lustrés corses: diversité des séries post-ophiolitiques, *C. R. Acad. Sci. Paris*, 288, 1525-1528, 1979.
- Caron, J.M., and G. Pequignot, The transition between blueschist and lawsonite-bearing eclogites based on observations from Corsican metabasalts, *Lithos*, 19, 205-218, 1986.
- Caron, J.M., J. R. Kienast, and C. Triboulet, High pressure-low temperature metamorphism and polyphase Alpine deformation at Sant' Andrea di Cotone (Eastern Corsica, France), *Tectonophysics*, 78, 419-451, 1981.
- Carpén, J., D. Maihè, C. W. Naeser, and G. Poupeau, Sur la datation par traces de fission d'une phase tectonique d'âge Eocène supérieur en Corse, *C. R. Acad. Sci. Paris*, 289, 829-832, 1979.
- Cohen, C. R., R. A. Schweickert, and A. Leroy Odom, Age of emplacement of the schistes lustrés nappes, alpine Corsica, *Tectonophysics*, 73, 267-283, 1981.
- Coney, P.J., and T. A. Harms, Cordilleran metamorphic core complexes: Cenozoic extensional relics of Mesozoic compression, *Geology*, 12, 550-554, 1984.
- Dallan, L., and A. Puccinelli, Geologia della regione del Nebbio (Corsica settentrionale), *Boll. Soc. Geol. Ital.*, 105, 405-414, 1986.
- Dallan, L., and A. Puccinelli, Il quadro geologico e strutturale della regione tra Bastia e St. Florent (Corsica settentrionale), *Atti Soc. Toscana Sci. Nat. Pisa Mem.*, 44, 77-88, 1987.
- De Wever, P., T. Danielian, M. Durand-Delga, F. Cordey, and N. Kito, Datations des radiolarites post-ophiolitiques de Corse alpine à l'aide des radiolaires, *C. R. Acad. Sci. Paris*, 305, 893-900, 1987.
- Durand-Delga, M., *Corse - Guides Géologiques Régionaux*, 152 pp., Masson, Paris, 1978.
- Egal, E., Tectonique de l'Eocène en Corse, Thèse de doctorat d'état, 133 pp., Lyon, 1989.
- Egal, E., and J. M. Caron, Tectonique polyphasée dans l'Eocène autochtone à la bordure ouest de la nappe de Balagne (Corse), *Bull. Soc. Géol. Fr.*, IV, 2, 315-321, 1988.
- Essene, E.J., Relatively pure jadeite from a siliceous Corsican gneiss, *Earth Planet. Sci. Lett.*, 5, 270-272, 1969.
- Evans, B. W., Phase relations in epidote-blueschists, *Lithos*, 25, 3-23, 1990.
- Faure, M., and J. Malavieille, Les plis en fourreau du cisaillement ductile: le charriage ophiolitique Corse dans la région de Bastia, *Bull. Soc. Géol. Fr.*, 23, 335-343, 1981.
- Gibbons, W., and J. Horak, Alpine metamorphism of Hercynian hornblende granodiorite beneath the blueschist facies Schistes Lustrés nappe of NE Corsica, *J. Metamorph. Geol.*, 2, 95-113, 1984.
- Gibbons, W., C. Waters, and J. Warburton, The

- blueschist facies schistes lustrés of Alpine Corsica: a review, *Mem. Geol. Soc. Am.*, 164, 301-311, 1986.
- Goffé, B., Le faciès carpholite chloritoïde dans la couverture briançonnaise des Alpes Ligures: un témoin de l'histoire tectono-métamorphique régionale, *Mem. Soc. Geol. Ital.*, 28, 461-479, 1984.
- Goffé, B., and C. Chopin, High pressure metamorphism in the western Alps: zoneography of metapelites, chronology and consequences, *Schweiz. Mineral. Petrog. Mitt.*, 66, 41-52, 1986.
- Goffé, B., and B. Velde, Contrasted metamorphic evolution in thrusted cover units of the Briançonnais zone (French Alps): a model for the conservation of HP-LT metamorphic assemblages, *Earth Planet. Sci. Lett.*, 68, 351-360, 1984.
- Goffé, B., A. Michard, J. R. Kienast, and O. Le Mer, A case of ecdension-related high-pressure, low-temperature metamorphism in upper crustal nappes, Arabian continental margin, Oman: P-T paths and kinematic interpretation, *Tectonophysics*, 151, 363-386, 1988.
- Guiraud, M., Géothermométrie du faciès schistes verts à glaucophanes, modélisation et application (Afghanistan, Pakistan, Corse, Bohème), Thèse de troisième cycle, Montpellier, 1982.
- Harris, L., Déformations et déplacements dans la chaîne alpine : l'exemple des schistes lustrés du Cap Corse, Thèse de doctorat de 3ème cycle, 307 pp., Rennes, 1984.
- Hirn, A., and M. Sapin, La croûte terrestre sous la Corse: données sismiques, *Bull. Soc. Géol. Fr.*, 18, 1195-1199, 1976.
- Jacquet, M., Evolution structurale et pétrographique de la partie nord du massif du Tenda (Corse), Thèse de troisième cycle, Université Paris VII, 1983.
- Jolivet, L., R. Dubois, M. Fournier, B. Goffé, A. Michard and C. Jourdan, Ductile extension in alpine Corsica, *Geology*, 18, 1007-1010, 1990.
- Jolivet, L., J. M. Daniel and M. Fournier, Geometry and kinematics of extension in Alpine Corsica, *Earth Planet. Sci. Lett.*, in press, 1991.
- Jourdan, C., Balagne orientale et massif du Tende (Corse septentrionale). Etude structurale, interprétation des accidents et des déformations, reconstructions géodynamiques, Thèse, 246 pp., Université Paris Sud, Orsay, 1988.
- Kastens, K., and J. Mascle, ODP Leg 107 in the Tyrrhenian Sea: insights into passive margin and back-arc basin evolution, *Geol. Soc. Am. Bull.*, 100, 1140-1156, 1988.
- Lahondère, D., Le métamorphisme éclogitique dans les orthogneiss et les métabasites ophiolitiques de la région de Farinoli (Corse), *Bull. Soc. Géol. Fr.*, 4, 579-586, 1988.
- Lahondère, D., and R. Caby, Les métaconglomérats polygéniques des "Schistes Lustrés" de la vallée du Golo (Corse alpine): signification paléogéographique et conséquences tectoniques, *C. R. Acad. Sci. Paris*, 309, 727-732, 1989.
- Lister, G.S., and G. Davis, The origin of metamorphic core complexes and detachment faults formed during Tertiary continental extension in the northern Colorado River region, U.S.A., *J. Struct. Geol.*, 11, 65-94, 1989.
- Lister, G.S., G. Banga, and A. Feenstra, Metamorphic core complexes of cordilleran type in the Cyclades, Aegean Sea, Greece, *Geology*, 12, 221-225, 1984.
- Malavieille, J., Etude tectonique et microtectonique de la déformation ductile dans de grands chevauchements crustaux : exemple des Alpes franco italiennes et de la Corse, Thèse de doctorat de 3ème cycle, 117 pp., Université des Sciences et Techniques du Languedoc, Montpellier, 1982.
- Malavieille, J., Extensional shearing deformation and kilometer-scale "a"-type folds in the cordilleran metamorphic core complex (Raft River Mountains, northwestern Utah), *Tectonics*, 6, 423-448, 1987.
- Maluski, H., Application de la méthode 40Ar - 39Ar aux minéraux des roches cristallines perturbées par des événements thermiques et tectoniques en Corse, Thèse de doctorat d'état, Université des Sciences et Techniques du Languedoc, 113 pp., Montpellier, 1977.
- Massonne, H.J., and W. Schreyer, Phenomite geobarometry based on the limiting assemblage with K-feldspar, phlogopite, and quartz, *Contrib. Mineral. Petrol.*, 96, 212-224, 1987.
- Mattauer, M., and F. Proust, Données nouvelles sur l'évolution structurale de la Corse alpine, *C. R. Acad. Sci. Paris*, 281, 1681-1684, 1975.
- Mattauer, M., and F. Proust, Sur quelques problèmes généraux de la chaîne alpine en Corse, *Bull. Soc. Géol. Fr.*, 18, 1177-1178, 1976a.
- Mattauer, M., and F. Proust, La Corse Alpine: un modèle de génèse du métamorphisme haute pression par subduction de croûte continentale sous du matériel océanique, *C. R. Acad. Sci. Paris*, 282, 1249-1252, 1976b.
- Mattauer, M., and F. Proust, and A. Eichencopar, Linéations "A" et mécanisme de cisaillement simple liés au chevauchement de la nappe des Schistes Lustrés en Corse, *Bull. Soc. Géol. Fr.*, 14, 841-847, 1977.
- Mattauer, M., M. Faure, and J. Malavieille, Transverse lineation and large scale structures related to alpine obduction in Corsica, *J. Struct. Geol.*, 3, 401-409, 1981.
- Molnar, P., and H. Lyon-Caen, Some simple physical aspects of the support, structure, and evolution of mountain belts, *Spec. Pap. Geol. Soc. Am.*, 218, 179-207, 1988.
- Morelli, C., P. Gieze, M. T. Carrozo, B. Colombe, I. Guerra, A. Hirn, A. Letz, R. Nicolich, C. Prodehl, C. Reichert, M. Rover, M. Sapin, S. Scarascia and P. Wigger, Crustal and upper mantle structure of the Northern Apennines, the Ligurian sea, and Corsica, derived from seismic and gravimetric data, *Boll. Geofis. Teor. Appl.*, 75-76, 199-260, 1977.
- Orszag-Sperber, F., and M. D. Pilot, Grands traits du Néogène de Corse, *Bull. Soc. Géol. Fr.*, 18, 1183-1187, 1976.
- Pequignot, G., Métamorphisme et tectonique dans les schistes lustrés à l'est de Corse (Corse), Thèse de doctorat de 3ème cycle, 171 pp., Université Claude Bernard, Lyon, 1984.
- Platt, J. P., Dynamics of orogenic wedges and the uplift of high-pressure metamorphic rocks, *Geol. Soc. Am. Bull.*, 97, 1037-1053, 1986.
- Réhault, J.P., G. Boillot, and A. Mauffret, The Western Mediterranean basin geological evolution, *Mar. Geol.*, 55, 447-477, 1984.
- Warburton, J., The ophiolite-bearing Schistes Lustrés nappe in Alpine Corsica: a model for the emplacement of ophiolites that have suffered HP/LT metamorphism, *Mem. Geol. Soc. Am.*, 164, 313-331, 1986.
- Wernicke, B., and B. C. Burchfiel, Modes of extensional tectonics, *J. Struct. Geol.*, 4, 105-115, 1982.
- M. Fournier, B. Goffé, and L. Jolivet, Laboratoire de Géologie, Ecole normale supérieure, 24 rue Lhomond, 75231 Paris Cedex 05, France. R. Dubois, Laboratoire de Géologie Structurale, Université Paris Sud, Orsay, Bat. 504, 91405 Orsay Cedex, France.

(Received March 10, 1990;
revised March 20, 1991;
accepted March 22, 1991.)



